FACULDADE DE FARMÁCIA
UNIVERSIDADE DO PORTO

Diana Duarte de Sousa

STUDYING EXTRACELLULAR VESICLES FROM P-GLYCOPROTEIN OVEREXPRESSING MULTIDRUG RESISTANT CELLS: NEW INSIGHTS INTO THEIR CARGO AND MECHANISMS OF RELEASE

Tese do 3º Ciclo de Estudos Conducente ao Grau de Doutoramento em Ciências Farmacêuticas – Especialidade de Biologia Celular e Molecular, apresentada à Faculdade de Farmácia da Universidade do Porto

Trabalho realizado sob a orientação da **Prof. Doutora Maria Helena Vasconcelos Meehan** [Professora Auxiliar da Faculdade de Farmácia da Universidade do Porto e Group Leader no Instituto de Investigação e Inovação em Saúde (i3S) e Instituto de Patologia e Imunologia Molecular da Universidade do Porto (IPATIMUP)]

e co-orientação da **Doutora Raquel Torres Lima** [Investigadora no Instituto de Investigação e Inovação em Saúde (i3S) e Instituto de Patologia e Imunologia Molecular da Universidade do Porto (IPATIMUP) e Professora Afiliada da Faculdade de Medicina da Universidade do Porto]

Abril 2019

DE ACORDO COM A LEGISLAÇÃO EM VIGOR, NÃO É PERMITIDA A REPRODUÇÃO DE QUALQUER PARTE DESTA TESE.

The candidate performed the experimental work with a doctoral fellowship (SFRH/BD/98054/2013) supported by the “Fundação para a Ciência e a Tecnologia”.The i3S/ IPATIMUP (Portugal) provided the facilities and logistical supports.The experimental research performed in this work has received financial support from the project NORTE-01-0145-FEDER-000029, supported by Norte Portugal Regional Programme (NORTE 2020), under the PORTUGAL 2020 Partnership Agreement, through the European Regional Development Fund (ERDF).

















AUTHORS DECLARATION

Under the terms of the “Decreto-lei nº 216/92, de 13 de Outubro”, is hereby declared that the author afforded a major contribution to the conceptual design and technical execution of the work, interpretation of the results and manuscript preparation of the published articles included in this dissertation.

Under the terms of the same “Decreto-lei”, is hereby declared that the following original articles/communications were prepared in the scope of this dissertation.

Scientific Publications

Articles in international peer-reviewed journals

Review article:

Diana Sousa, Raquel T. Lima, M. Helena Vasconcelos (2015) “Intercellular transfer of cancer drug resistance traits by extracellular vesicles”. Trends Mol Med., 21 (10): 595-608

Research articles:

Diana Sousa, Rune Matthiesen, Raquel T. Lima, M. Helena Vasconcelos. “Deep sequencing analysis reveals distinctive non-coding RNAs when comparing tumour multidrug resistant cells and extracellular vesicles with drug-sensitive counterparts”.
Submitted for publication (in Cancers)

Diana Sousa, Raquel T. Lima, Vanessa Lopes-Rodrigues, Esperanza González, Félix Royo, Juan M. Falcón-Pérez, M. Helena Vasconcelos. “Multidrug Resistant cells have different ability to release and capture EVs than their sensitive counterparts: impact of endocytic pathway alterations”
Under revision (in Journal of Extracellular Vesicles)

Raquel T. Lima*, **Diana Sousa***, Ana M. Paiva, Andreia Palmeira, João Barbosa, Madalena Pedro, Madalena M. Pinto, Emília Sousa, and M. Helena Vasconcelos. (2016) "Modulation of Autophagy by a Thioxanthone Decreases the Viability of Melanoma Cells" Molecules 21, pii: E1343. 595

***** These authors have equally contributed to the work

Abstract published in international periodicals with referees

Diana Sousa, Raquel T. Lima, Vanessa Lopes-Rodrigues, Felix Royo, Juan M. Falcón-Pérez and M. Helena Vasconcelos. (2017) "Is the dissemination of cancer multidrug resistance phenotype influenced by the shedding of Extracellular Vesicles by resistant tumor cells?" Journal of Cancer Science and Therapy, 2017, 9:6 (Suppl)

Communications

Oral Communications

30th-31st January 2019- COST ACTION 17104 –STRATAGEM "New diagnostic and therapeutic tools against multidrug resistant tumours", Turin, Italy:
Diana Sousa, Vanessa Lopes-Rodrigues, Cristina P.R. Xavier, Hugo R. Caires and M. Helena Vasconcelos. "Horizontal transfer of MDR traits by extracellular vesicles: implications for diagnosis and treatment of MDR cancers".
Presented by M.H. Vasconcelos

23rd March 2017- 1st Euskadi Workshop on Exosomes in Bilbao, Spain:
Diana Sousa, Raquel T. Lima, Vanessa Lopes-Rodrigues, Esperanza González, Felix Royo, Juan M. Falcón-Pérez, M. Helena Vasconcelos. "Understanding the role of Extracellular Vesicles in the transfer of Multidrug Resistant traits".
Presented by **Diana Sousa**

1st March 2016 - COST ME-HaD Training Course on Extracellular vesicles, Ioannina, Greece:
Diana Sousa, Vanessa Lopes-Rodrigues, Raquel T. Lima, M. Helena Vasconcelos (2016). "Transfer of cancer drug resistance traits by Extracellular Vesicles"
Presented by **Diana Sousa**

Poster Communications

Diana Sousa#, Raquel T. Lima, Vanessa Lopes-Rodrigues, Felix Royo, Juan M. Falcón-Pérez, M. Helena Vasconcelos. (2018) "Understanding mechanisms of release and internalization of Extracellular Vesicles by multidrug resistant and drug-sensitive cells." i3S Scientific Retreat, Póvoa de Varzim, Portugal

Diana Sousa#, Raquel T. Lima, Vanessa Lopes-Rodrigues, Felix Royo, Juan M. Falcón-Pérez, M. Helena Vasconcelos. (2018) "Influence of Extracellular Vesicles to the acquisition of MDR phenotype by tumor cells." 1st Meeting in Vesicular Biology, Coimbra, Portugal

Diana Sousa#, Raquel T. Lima, Vanessa Lopes-Rodrigues, Felix Royo, Juan M. Falcón-Pérez, M. Helena Vasconcelos. (2017) "Is the dissemination of cancer multidrug resistance phenotype influenced by the shedding of Extracellular Vesicles by resistant tumor cells?" 19th Euro Congress on Cancer Science and Therapy, Lisbon, Portugal

Diana Sousa#, Raquel T. Lima, Vanessa Lopes-Rodrigues, Felix Royo, Juan M. Falcón-Pérez, M. Helena Vasconcelos. (2016) "Extracellular Vesicles in the dissemination of cancer multidrug resistance." i3S Scientific Retreat, Póvoa de Varzim, Portugal

Diana Sousa, Vanessa Lopes-Rodrigues#, Raquel T. Lima, M. Helena Vasconcelos. (2015) "Transfer of Drug Resistance by extracellular vesicles shed by tumor cells." First Iberian Meeting on Extracellular Vesicles, Porto, Portugal

#presenting author

“Nas grandes batalhas da vida, o primeiro passo para a vitória é o desejo de vencer.”

Mahatma Gandhi

AGRADECIMENTOS/ACKNOWLEDGMENTS

A realização deste trabalho não teria sido possível sem o apoio de uma série de pessoas a quem eu agradeço profundamente.

À minha orientadora Prof. Helena Vasconcelos, o meu primeiro agradecimento. Primeiro, por me ter recebido no seu grupo e por me ter proporcionado a oportunidade de crescer como profissional e como ser humano. Identifiquei-me logo no início com a forma de trabalhar e de estar na ciência. Muito obrigada pelo apoio e motivação, por ter estado sempre presente, pelas discussões produtivas e por todos os ensinamentos. Obrigada ainda por ter confiado em mim e aos poucos me ter deixado crescer, dando-me a independência necessária a este processo de aprendizagem.

À minha co-orientadora Raquel Lima, o meu obrigado. Quando cheguei ao IPATIMUP tiveste a generosidade de me ensinar. Ensinar de facto. Estares comigo, partilhares o teu conhecimento, as tuas dicas, a tua forma de trabalhar. E essa forma acompanha-me até hoje. Para além disso, ao longo de toda esta jornada estiveste sempre presente para me motivar e incentivar quando achei que não iria ser possível, ou para me elucidares à última da hora sobre problemas existenciais. Obrigada pela tua amizade e dedicação ao longo destes anos.

Ao Professor Sobrinho Simões, na qualidade de director do IPATIMUP (durante parte do meu doutoramento) agradeço ter-me permitido realizar este trabalho no seu Instituto.

Ao Professor António Barbosa, na qualidade de director do i3S, ter-me permitido realizar este trabalho no Instituto que dirige.

À Fundação para a Ciência e Tecnologia, agradeço o apoio financeiro concedido ao longo destes quatro anos.

To JuanMa, thank you for giving me the opportunity of working in your lab. It exceeded completely my expectations! Thank you so much for sharing all your knowledge and for all your support and guidance.

To Rune, for the bioinformatics analysis and for your patience and availability in receiving me to clarify all my doubts.

To Justyna, for the encouragement and critical discussions. For all the time working together no matter the hours, which always end with funny situations! Thank you so much for your honest friendship and for being my home away from home.

To Espe and Felix for all the teaching, patience and good moments. You are really examples of the kind of scientist I would like to be.

Aos CDRs Mariana, Cristina, Hugo e Pedro obrigada pelos momentos de boa disposição e descontracção que temos no laboratório, essenciais principalmente nesta fase final de stress maior.

A todos os elementos do grupo da Maria e da Prof. Perpétua, pelo bom ambiente e descontracção com que partilhamos o laboratório.

À Alexandra, Inês, Joana, André, Débora, Tamara e Sara, obrigada pela partilha de conhecimentos e pelos bons momentos juntos. Joaninha, um obrigado especial! Foste uma querida numa fase muito especial da minha vida. Não sei o que teria feito sem o teu apoio e suporte. Xana, obrigada por te continuares a preocupar e mesmo estando um “pouquinho” mais longe, continuares tão interessada e sempre pronta a ajudar. És de facto, uma menina especial.

À Vanessa, Filipa, Daniela, Catarina e Hugo Seca. Sinto muita nostalgia do tempo em que todos partilhávamos a bancada. O companheirismo, a entre-ajuda e a amizade sincera dessa altura ensinaram-me muito! Apesar da vida (e do Mundo! ☺) nos ter fisicamente separado, estão todos num cantinho mesmo muito especial do meu coração. Quando a "vida e o Mundo" nos voltar a juntar, tenho a certeza que parecerá que só passaram 2 dias ☺. Minha querida Catarina, um especial obrigado! Pelos conselhos, pelo suporte, e pelas palavras de incentivo. Os últimos tempos não foram fáceis mas estiveste sempre lá com tua serenidade a acalmar "as tropas".

Às minhas queridas e querido "happy nerds" Diana, Ana, Gi, Raquel, Isabel, Mi, Margarida, Zé Pedro e Mariana. Acho que há momentos na vida únicos, que não se voltam a repetir. O nosso encontro foi um deles. É verdade que foi a ciência que nos apresentou mas foi o tempo que fortaleceu a nossa amizade. Obrigada pelos momentos únicos, de tão boa disposição e verdadeira amizade que me ajudaram a "aguentar" o barco. Sinto um enorme orgulho em acompanhar as vossas conquistas, pessoais e profissionais. Sei que de facto, aconteça o que acontecer, vocês estão lá. E eu também estarei, sempre.

Às minhas queridissimas Cecil, Eva e Telma, muito obrigada pelo vosso apoio, por ouvirem os meus desabafos e inseguranças e por no final de tudo verificarmos que a vida é mesmo fabulosa e que temos de a aproveitar! Desculpem o meu estado "tesis eremitus" dos últimos meses mas temos a vida toda para compensar! ☺

Aos meus amigos/padrinhos/cunhados/compadres (o que mais?) Filipa, Ginie, Daniela, Bruno, Vasco, João Miguel e Carlos muito obrigada, por existirem na minha vida e por sem se aperceberem, me ajudarem a desanuviar, a carregar energias e a sentir que a vida é mesmo para ser vivida rodeada de quem nos faz sentir bem. E estar convosco faz-me sentir muito bem! Obrigada ainda ao Pedrinho, Dinis, Simão, Benjamin, Margarida, Olívia e Gonçalinho pela felicidade tão sincera que me dão!

Aos meus sogros, Fátima e João, obrigada pelo exemplo de perseverança e união que nos dão. Pela família tão bonita que construimos e que me enche o coração!

À minha família, em especial à Avó Ana e Avó Mercêdes pelas experiências que me transmitem e pelo amor que me dão! Ao avô Gusto e avô Sousa por me guiarem sempre!

Aos meus pais, por estarem sempre lá, desde sempre. Por me darem segurança, carinho, valores e acima de tudo muito Amor. Um Amor que sinto só de olhar. Nesta fase em particular, tenho de vos agradecer do fundo do coração todo o apoio emocional e logístico que me permitiu terminar esta fase. Vocês foram absolutamente essenciais em tudo. Sem vocês não teria sido possível! São um orgulho para mim e são, sem dúvida, os melhores pais do Mundo!

Aos eternos amores da minha vida João, Vicente e Gabriel.

Ao João, por tudo! É mesmo por tudo! Primeiro, pela pessoa que és, que me continua a apaixonar e a conquistar passados todos estes anos. Obrigada pelo teu Amor, por não me deixares ir abaixo e me dares perspectiva e confiança. Este objectivo superado não é meu, é nosso! E claro, obrigada pela família absolutamente fabulosa que construímos. Acho mesmo que somos os pais com a maior sorte do mundo pois temos os melhores filhos do mundo!

Aos meus queridos Gabriel e Vicente, obrigada por despertarem em mim sentimentos que desconhecia por completo até vos ter! Obrigada pelos vossos sorrisos e gargalhadas cúmplices que me aquecem o coração e pelo vosso miminho que me enche a alma! O meu maior objectivo é, e será sempre, estar sempre aqui para vos apoiar e amar!

ABSTRACT

Multidrug resistance (MDR) is one of the main limitations of cancer treatment. MDR is defined as a phenomenon by which tumour cells develop cross-resistance to several drugs. Overexpression of drug-efflux pumps, particularly P-glycoprotein (P-gp), is a major cause of MDR. In addition, interesting findings show that alterations in autophagy may be associated with tumour MDR. Therefore, inhibitors of MDR, including inhibitors of P-gp, may have an effect on cellular autophagy. However, little is known about this possibility. Although four generations of P-gp inhibitors were developed and showed promising results *in* vitro, they failed to be used in the clinic due to toxicity. Moreover, to date there is no clinically used minimally-invasive method to diagnose and predict MDR, based on biomarkers.

Interestingly, Extracellular Vesicles (EVs) may be mediators of horizontal transfer or MDR phenotype between MDR (donor) cells and drug-sensitive (recipient) cells. EVs are lipid bilayer-enclosed extracellular structures which do not replicate. The processes involved in the release and capture of EVs by MDR and drug-sensitive counterparts are not fully understood. Further knowledge on these processes may contribute to identifying targets to overcome the horizontal transfer of MDR. Importantly, EVs are found in biological fluids. Since their cargo includes components of the donor cells, EVs may be a source of biomarkers. Notably, P-gp was already found in the cargo of EVs released by drug-resistant cells from different tumour models, possibly being responsible for MDR dissemination. A full characterization of the RNAs present in the cargo of EVs from pairs of MDR and drug-sensitive cells may contribute to identifying biomarkers of MDR.

Thus, the aims of the present work were to: i) identify putative biomarkers of MDR in P-gp-overexpressing tumour cells and their EVs; ii) understand the mechanisms involved in the release of EVs by P-gp overexpressing MDR cells and their uptake by drug-sensitive counterparts; iii) investigate the mechanism of action, particularly on autophagy, of a small molecule previously known to have anti-tumour and anti-P-gp dual activity. To accomplish this, in the majority of the studies here presented, two pairs of cell lines from two different tumour models [chronic myeloid leukaemia (CML) and non-small cell lung cancer (NSCLC)] were used, consisting of a drug-sensitive cell line and its MDR (P-gp overexpressing) counterpart.

First, a deep sequence analysis of the RNA content from these cell lines and from their EVs, was carried out. Our results showed distinctive transcripts on MDR cells and their EVs, when compared with drug-sensitive counterparts. Indeed, results from the comparison of MDR and drug-sensitive counterpart cellular RNA allowed identification of 6 transcripts with identically altered expression in the MDR NSCLC and CML tumour cells. In addition, two pseudogenes (a novel pseudogene and RNA 5.8S ribosomal pseudogene 2) were

found increased in the EVs released by MDR cells from both tumour models. Moreover, our findings showed that NSCLC MDR cells and their EVs harbour distinctive transcripts from their drug-sensitive counterparts. We found a signature constituted by 6 microRNAs (miR-204-5p, miR-139-5p, miR-29c-5p, miR-551b-3p, miR-29b-2-5p, miR-204-3p) with increased levels in the NSCLC MDR cells and in their EVs.

Moreover, the mechanisms involved in the release and uptake of EVs by MDR (P-gp overexpressing) cells and their drug-sensitive counterparts were also investigated. MDR cells were shown to release more EVs than their drug-sensitive counterparts and drug-sensitive cells were shown to have higher uptake of EVs than their MDR counterparts. In addition, we found that distinct regulation of the endocytic pathway between drug-sensitive and MDR cells may influence this different ability to release and capture EVs. Moreover, manipulation of the recycling pathway influenced the response of drug-sensitive cells to doxorubicin treatment.

Finally, the modulation of autophagy by a small molecule, previously shown to have dual anti-tumour and P-gp inhibitory activities, was investigated. Our results showed that treatment of melanoma cells with the GI_{50} concentration of this molecule induced the accumulation of autophagic structures. Moreover, an increase in LC3-II levels was also observed, being reverted by an early stage autophagy-inhibitor but further increased by a late-stage autophagy inhibitor. Importantly, an early stage autophagy-inhibitor reverted the effect of this molecule on cellular viability, showing the involvement of autophagy modulation in its mechanism of action.

In conclusion, the results presented in this thesis reinforce the important role of EVs in MDR associated with P-gp overexpression. Our most relevant findings showed that MDR cells and their EVs have distinctive transcripts, particularly non-coding RNAs, when compared with drug-sensitive counterparts. These may be further investigated (in future work) as putative MDR biomarkers. Furthermore, we found that P-gp overexpressing MDR cells and their drug-sensitive counterparts have different abilities to release and capture EVs. Importantly, we showed that regulation of the endocytic pathway is involved in those mechanisms. Increasing knowledge about the players involved in the release and capture of EVs, by pairs of MDR and drug-sensitive counterpart cells, may contribute to identifying targets to overcome the horizontal transfer of MDR. Finally, the results obtained in the present work also add new insights into the study of P-gp inhibitors and contributed to the understanding of the controversial role of autophagy in cancer. The molecule studied may serve as a lead compound for the development of autophagy modulators with antitumour activity.

Keywords: Tumour Multidrug Resistance; P-glycoprotein; Extracellular Vesicles; Autophagy

RESUMO

A resistência a múltiplos fármacos (RMF) é uma das principais limitações do tratamento do cancro. A RMF define-se como um fenómeno em que as células tumorais desenvolvem resistência a vários fármacos. A sobre-expressão de bombas de efluxo de fármacos, particularmente da glicoproteína-P (P-gp), é uma das principais causas de RMF. Para além disso, descobertas interessantes mostram que alterações a nível da autofagia podem estar associadas à RMF no cancro. Por isso, inibidores de RMF, incluindo inibidores da P-gp, podem ter um efeito a nível da autofagia. No entanto, pouco se sabe sobre esta possibilidade. Já foram desenvolvidas quatro gerações de inibidores da P-gp que mostraram resultados promissores *in vitro*, contudo, estes fármacos não foram posteriormente utilizados na clínica pois revelaram toxicidade. É ainda importante referir que, até ao momento, ainda não foi desenvolvido um método minimamente invasivo para diagnosticar e prever a RMF, baseado no estudo de biomarcadores.

Curiosamente, as Vesículas Extracelulares (VEs) podem ser mediadores de transferência horizontal do fenótipo RMF, entre células RMF (dadoras) e células sensíveis a fármacos (receptoras). As VEs são estruturas extracelulares com uma bicamada lipídica fechada, que não se replicam. Os processos envolvidos na libertação e captura de VEs por células RMF e células sensíveis a fármacos não são totalmente compreendidos. Um conhecimento mais profundo sobre estes processos pode contribuir para a identificação de alvos para combater a transferência horizontal de RMF. Importa referir que as VEs podem ser encontradas em fluidos biológicos. Como o seu conteúdo inclui componentes das células dadoras, as VEs podem ser uma fonte de biomarcadores. De facto, a P-gp já foi detectada no conteúdo das VEs libertadas por células resistentes a fármacos de diferentes modelos tumorais, possivelmente sendo responsável pela disseminação da RMF. Uma caracterização completa dos RNAs presentes no conteúdo das VEs provenientes de pares de células RMF e células sensíveis a fármacos, pode contribuir para a identificação de biomarcadores de RMF.

Desta forma, os objetivos do presente trabalho foram: i) identificar biomarcadores putativos de RMF em células tumorais com sobre-expressão de P-gp, assim como nas suas VEs; ii) compreender os mecanismos envolvidos na libertação de VEs por células RMF com sobre-expressão de P-gp e sua captação pelas células sensíveis a fármacos; iii) investigar o mecanismo de ação, particularmente a nível da autofagia, de uma pequena molécula previamente conhecida como tendo dupla atividade anti-tumoral e anti-P-gp. Para isso, na maioria dos estudos aqui apresentados, dois pares de linhas celulares de dois modelos diferentes de tumores [leucemia mieloide crónica (LMC) e cancro de pulmão de

células não pequenas (CPCNP)] foram utilizados, consistindo numa linha celular sensível a fármacos e numa linha celular homóloga RMF (com sobre-expressão de P-gp).

Em primeiro lugar, foi realizada uma análise de sequenciação pormenorizada do conteúdo em RNA dessas linhas celulares e das suas VEs. Os nossos resultados mostraram a presença de transcritos distintos nas células RMF e suas VEs, em comparação com as homólogas sensíveis a fármacos. De facto, os resultados da comparação do RNA entre as células RMF e as células sensíves a fármacos permitiram a identificação de 6 transcritos com expressão alterada de forma idêntica nas células tumorais RMF dos modelos CPCNP e LMC. Para além disso, verificou-se que dois pseudogenes (um novo pseudogene e o pseudogene 2 do RNA ribossomal 5.8 S) se encontravam aumentados nas VEs libertadas pelas células RMF de ambos os modelos tumorais. Os nossos resultados mostraram ainda que as células RMF do CPCNP e as suas EVs apresentam transcritos distintos das homólogas sensíveis a fármacos. De facto, encontrámos uma assinatura constituída por 6 miRs (miR-204-5p, miR-139-5p, miR-29c-5p, miR-551b-3p, miR-29b-2-5p, miR-204-3p) com níveis aumentados nas células CPCNP RMF e nas suas VEs.

Para além disso, os mecanismos envolvidos na libertação e captação de VEs por células RMF (com sobre-expressão de P-gp) e pelas homólogas sensíveis a fármacos também foram investigados. Verificou-se que as células RMF libertavam mais VEs do que as células sensíveis a fármacos e que estas captavam mais VEs do que as células RMF. Descobrimos ainda que a regulação da via endocítica é diferente nas células sensíveis a fármacos e nas células RMF, podendo influenciar a sua capacidade distinta para libertar e capturar VEs. Além disso, a manipulação da via “da reciclagem” influenciou a resposta das células sensíveis a fármacos ao tratamento com doxorrubicina.

Finalmente, investigou-se a modulação da autofagia por uma pequena molécula que previamente demonstrou possuir atividade anti-tumoral e anti-Pgp. Os nossos resultados demostraram que o tratamento de células de melanoma com a concentração correspondente ao GI_{50} desta molécula levou à acumulação de estruturas autofágicas. Para além disso, um aumento nos níveis de LC3-II também foi observado; verificou-se que este efeito foi revertido por um inibidor inicial da autofagia e que foi acentuado por um inibidor tardio da autofagia. É importante ressaltar que o inibidor inicial da autofagia reverteu também o efeito desta molécula na viabilidade celular, demonstrando o envolvimento da modulação da autofagia no seu mecanismo de ação.

Em suma, os resultados obtidos neste trabalho reforçam o importante papel das VEs na RMF associada à sobre-expressão da P-gp. Os nossos resultados mais relevantes mostraram que as células RMF e as suas VEs têm transcritos distintos, particularmente

RNAs não-codificantes, quando comparadas com as homólogas sensíveis a fármacos. Estes RNAs podem ser estudados (em trabalhos futuros) como potenciais biomarcadores de RMF. Além disso, descobrimos que as células RMF com sobre-expressão de P-gp e as células homólogas sensíveis a fármacos têm diferentes capacidades para libertar e capturar VEs.. É importante ressaltar ainda que demonstramos que a regulação da via endocítica está envolvida nesses mecanismos. O crescente conhecimento sobre os mediadores envolvidos na libertação e captura de VEs, por células RMF e as homólogas sensíveis a fármacos, pode contribuir para identificar alvos para impedir a transferência horizontal de MDR. Finalmente, os resultados obtidos no presente trabalho também acrescentaram conhecimento ao estudo de inibidores da P-gp e permitiram perceber melhor o papel controverso da autofagia no cancro. A molécula estudada pode servir como composto líder para o desenvolvimento de moduladores de autofagia com atividade antitumoral.

Palavras-chave: Resistência tumoral a múltiplos fármacos; Glicoproteína- P; Vesículas Extracellulares, Autofagia

TABLE OF CONTENTS

AUTHORS DECLARATION.....iv
AGRADECIMENTOS/ACKNOWLEDGMENTS.....viii
ABSTRACT x
RESUMO xii
TABLE OF CONTENTS xv
INDEX OF FIGURES xvii
INDEX OF TABLES xvii
INDEX OF ANNEXES xviii
ABBREVIATIONS xix

CHAPTER I- INTRODUCTION.....1
Part I- State of the Art.....3
1. Overview of Multidrug Resistance in Cancer.....5
1.1 Challenges for understanding multidrug resistance.....6
1.2 Altered cellular mechanisms in MDR.....7
1.2.1 Reduced drug-influx.....8
1.2.2 Increased drug-efflux.....9
1.2.3 Increased DNA damage repair.....9
1.2.4 Alterations in cell cycle.....10
1.2.5 Inhibition of cell death pathways.....11
1.2.6 Epigenetic and microRNAs alterations.....13
1.2.7 Other mechanisms involved in MDR.....14
1.3 Relevant molecular players
1.3.1 P-glycoprotein: a major cause of MDR.....15
1.3.1.1 Molecular characterization and intracellular localization of P-gp.....16
1.3.1.2 Regulation and modulation of P-gp levels.....17
1.3.2 MicroRNAs as regulators of MDR 18
1.3.2.1 MiRs biogenesis and mechanisms of action.....19
1.3.2.2 The effect of miRs regulation in pathways associated to MDR.....20
1.3.2.3 Circulating miRs 24
1.4.3 Other non-coding RNAs in MDR 25
2. Extracellular Vesicles 28
2.1 Cargo of EVs.....30
2.1.1 Proteins.....30
2.1.2 RNA 31

2.1.3 DNA 31
2.1.4 Lipids.....32
2.2 EVs biogenesis: membrane-trafficking processes.....32
2.3 EVs secretion 34
2.3.1 Secretion of EVs from endocytic origin.....35
2.3.2 Secretion of EVs originated from budding of plasma membrane.....35
2.4 Interaction of EVs with recipient cell.....36
2.5 EVs in cancer.....37
2.6 **REVIEW ARTICLE:** "Intercellular transfer of drug resistance traits by extracellular vesicles".....39
3. Interdependency of intracellular pathways in EVs production.....56
3.1 Central role of endocytic pathway: endosome as a dynamic organelle.....56
3.2 Routes for cargo degradation: role of lysosome and autophagosome.....57
3.3 Recycling endosome.....58

Part II- Objectives.....61

CHAPTER II- RESULTS AND DISCUSSION.....65

1. **RESEARCH ARTICLE:** "Deep sequencing analysis reveals distinctive non-coding RNAs when comparing tumour multidrug resistant cells and extracellular vesicles with drug-sensitive counterparts".....67
2. **RESEARCH ARTICLE:** "Multidrug Resistant cells have different ability to release and capture EVs than their sensitive counterparts: impact of endocytic pathway alterations".....96
3. **RESEARCH ARTICLE:** "Modulation of Autophagy by a Thioxanthone Decreases the Viability of Melanoma Cells".....133

CHAPTER III – GENERAL DISCUSSION AND FUTURE PERSPECTIVES.....153

REFERENCES.....163

ANNEXES.....187

INDEX OF FIGURES

Figure 1: Main challenges for understanding cancer MDR (represented in blue) and the four cardinals of MDR (represented in yellow)……..…7
Figure 2: Autophagy pathway…… ……..…13
Figure 3: Schematic representation of P-glycoprotein structure in the cell membrane… .17
Figure 4: Mechanisms involved in the canonical pathway of microRNAs biogenesis…….20
Figure 5: Membrane-trafficking processes involved in EVs production by inward and outward membrane budding……34
Figure 6: Interdependency of the intracellular pathways in EVs production…….59

INDEX OF TABLES

Table 1: Main cellular alterations involved in MDR phenotype and relevant players……..8
Table 2: Some of the most important non-coding RNAs associated to MDR…….21

INDEX OF ANNEXES

Supplementary files from research paper 1 "Deep sequencing analysis reveals distinctive non-coding RNAs when comparing tumour multidrug resistant cells and extracellular vesicles with drug-sensitive counterparts":

Annex 1: Table S2- Log Fold Change of RNA species expression between drug-sensitive (NCI-H460) cells and their MDR (NCI-H460/R) counterparts……190

Annex 2: Table S3- Log Fold Change of RNA species expression between drug-sensitive (K562) cells and their MDR (K562Dox) counterparts…….....196

Annex 3: Table S4- Log Fold Change of RNA species expression between EVs released by drug-sensitive (NCI-H460) cells and the EVs released by their MDR (NCI-H460/R) counterparts……..…217

Annex 4: Table S5- Log Fold Change of levels of RNA species between EVs released by drug-sensitive (K562) cells and EVs released by their MDR (K562Dox) counterparts….194

Annex 5: Table S6- Log Fold Change of levels of miRs between drug-sensitive (NCI-H460) cells and their MDR (NCI-H460/R) counterparts……..218

Annex 6: Table S7- Log Fold Change of miRs expression between drug-sensitive (K562) cells and their MDR (K562Dox) counterparts……222

Annex 7: Table S8- Log Fold Change of levels of miRs between EVs released by drug-sensitive (NCI-H460) cells and EVs released by their MDR (NCI-H460/R) counterparts..227

Annex 8: Table S9- Log Fold Change of miRs expression between drug-sensitive (K562) cells and EVs derived from their MDR (K562Dox) counterparts……...229

ABBREVIATIONS

ABC: ATP-binding cassette

ABCB1: ATP-binding cassette subfamily B member 1

ABCC1: ATP Binding Cassette Subfamily C Member 1

ABCG2: ATP Binding Cassette Subfamily G Member 2

Ago2: Argonaute 2

ARF1: ADP-ribosylation factor 1

ARF6: ADP-ribosylation factor 6

ATG: Autophagy-related gene

ATM: Ataxia telangiectasia mutated protein kinase

ATP: Adenosine triphosphate

ATP7A: ATPase copper transporting alpha

ATR: ATM and Rad3-related protein kinase

BCL2: B-cell lymphoma 2

BCR-ABL: Reciprocal translocation, t(9;22)(q34;q11) of BCR (breakpoint region protein) gene and ABL (Abelson leukemia) gene

BRCA1: Breast Cancer gene 1

BRCA2: Breast Cancer gene 2

BRCP: Breast cancer resistance protein

CML: Chronic myeloid leukaemia

CSCs: Cancer stem cells

CTR1: copper uptake protein 1

CYP: cytochrome P450

DNA: Deoxyribonucleic acid

ECM: Extracellular matrix

EEA1: Early Endosome Antigen 1

EGFR: Epidermal growth factor receptor

ER: Estrogen Receptor

ESCRT: Endosomal Sorting Complex Required for Transport

EV: Extracellular vesicle

gDNA: genomic DNA

GST: glutathione-S-transferase

hENT1: human equilibrate nucleoside transporter

IAP: inhibitors of apoptosis proteins

IFN: interferon

ILV: Intra luminal vesicle

ISEV: International Society of Extracellular Vesicles

LAMP-1: Lysosomal-associated membrane protein 1

LC3: Microtubule-associated protein light chain 3

LincROR: Long Intergenic Non-Protein Coding RNA

LncRNA NEAT1: Long non-coding RNA Nuclear paraspeckle Assembly Transcript 1

MAPK: Mitogen- activated protein kinase

MDR: Multidrug resistance

MDR1: Multidrug resistance protein 1

MGMT: O6-methylguanine-DNAmethyltransferase

miR: microRNA

MMR: Mismatch repair

MRP1 Multidrug resistance-associated protein 1

MRUL: MDR-related and upregulated lncRNA

mtDNA: Mitochondrial DNA

MVB: Multivesicular body

NBD: Nucleotide binding domain

ncRNA: non-coding RNA

NF-κB: factor nuclear kappa B

NGS: Next-generation sequencing

NSCLC: Non-small cell lung cancer

Nt: nucleotide

OCT4: Octamer-binding transcription factor 4

OCTN1/SLC22A4: carnitine/organic cation transporter/ Solute carrier family 22, member 4

PARP- *Poly (ADP-ribose) polymerase*

PGE2- Prostaglandina natural E

P-gp: P-glycoprotein

PKA: Protein kinase A

PKC: Protein kinase C

PLD2: Phospholipase D2

pre-miRs: Precursor miRs

pri-miRs: Primary microRNAs

Rac-GAP: *Rac*-GTPase-activating protein

RALBP1: RALA binding protein1

RanGTP- RAs-related nuclear protein

RFC/SLC19A1: Reduced folate carrier/Solute carrier family 19

RHEB: Ras homolog enriched in brain

RISC: RNA-induced silencing complex

RNA: Deoxyribonucleic acid

ROCK: RHO-associated protein kinase

rRNA: ribosomal RNA

SAHA: Suberoylanilide hydroxamic acid

SNARE: Soluble N-ethylmaleimide-sensitive component attachment protein receptor

SNP:Single nucleotide polymorphism

snRNA:small nuclear RNA

STAM-1: Signal transducing adapter molecule 1

STAT: Signal transducer and activator of transcription

TfR: Transferrin Receptor

TMD: Transmembrane domain

TNF: Tumour necrosis factor

TRAIL: TNF-related apoptosis-inducing ligand

tRNA:transference RNA

Trps1: Trichorhinophalangeal syndrome, type I factor

TSG10: Tumour susceptibility gene 101

UGT: uridine diphospho-glucuronosyltransferas

UTR: Untranslated region

VAMP7: Vesicle-associated membrane protein 7

Vps: Vacuolar protein sorting

XPO5: Exportin

CHAPTER I

INTRODUCTION

PART I- STATE OF THE ART

1. Overview of Multidrug Resistance in Cancer

Statistics indicate that drug resistance may be responsible for treatment failure in over 90% of patients with metastatic cancer [1]. Therefore, drug resistance is one of the major challenges for chemotherapy efficacy in cancer. Due to the high complexity of mechanisms involved, a broad perspective of this problem is necessary, taking into account the network of different processes altered in cancer.

Cancer drug resistance is classically categorized in: i) intrinsic (or innate) drug resistance and ii) acquired drug resistance. Intrinsic drug resistance occurs before patient receives chemotherapy and, in general, is related to mechanisms associated to the genetic landscape of the host. Acquired drug resistance is developed during drug treatment when a tumour, which initially responded to a certain drug, becomes unresponsive to that drug. The mechanisms responsible for acquired drug resistance are often associated to mutations or epigenetic phenomena (or other causes as explained below) that develop in tumour cells due to the drug treatment [2, 3].

Importantly, resistance may be limited to a drug used to treat patients (single agent resistance), or reflect failure to respond to different drugs structurally unrelated and with different mechanism of action - multidrug resistance (MDR) [3]. The original concept of MDR was introduced in 1970 [4], and since then many studies were carried out, which added knowledge to this complex problem.

The development of molecular targeted drugs, such as the ones targeting specific driver mutations in tumour cells, was initially viewed as a solution to treat tumour patients and avoid drug resistance [5]. Indeed, targeted therapies to BCR-ABL in chronic myeloid leukaemia, to BRAF mutations in melanoma or to EGFR mutations in non-small cell lung cancers are some examples of successful therapies [3]. However, patients treated with these targeted therapies developed drug resistance sometime after initiation of treatment. Further studies demonstrated that the classical MDR-associated mechanisms are also involved in causing resistance to targeted therapies [6]. Accordingly, it is currently accepted that mechanisms associated to MDR affect both classical chemotherapy and targeted therapy efficacy [6]. The complexity of factors involved in the development of MDR also influence MDR diagnosis and prognosis. Indeed, even though it is a very serious health problem, no available biomarkers of MDR have reached the clinic.

1.1 Challenges for understanding multidrug resistance

The mechanistic studies of drug resistance are predominantly carried out in cultured tumour cells that survived after successive drug treatment (named as “drug-resistant cell lines”) or in cells which were directly taken from drug-resistant tumours and cultivated for short intervals *ex vivo* [3]. In the last few years, an effort to improve this methodology was made in order to achieve outputs more applicable to the clinical setting.

Currently, the main challenges for understanding MDR are associated with three main problems, related not only to intrinsic tumours features but also to logistic problems associated to patients samples Regarding the intrinsic tumour features, the first major challenge is that drug resistance, and MDR in particular, is multifactorial in nature [5]. Indeed, although some drug resistance mechanisms result from a single alteration in well-known players, in many other cases the resistance effectors and the associated dysregulated pathways are considerably diverse. The second challenge is that, since tumours are heterogeneous, drug resistance is also heterogeneous both in space (within a single tumour and/or among metastasis) and in time. This may be mostly due to selective drug pressure (during which the sensitive cells dye but the resistant ones are selected for). For example, in some cases multiple metastasis respond differently to targeted therapy, while in other cases different tumour foci acquire similar resistance mechanisms [7, 8]. The third and final challenge to understanding cancer drug resistance is the lack of samples, or “under-sampling” for translational studies. Indeed, the availability of clinical samples from drug-sensitive (pre-treatment) and drug-resistant (mostly post-treatment) conditions is still very limited, and this difficulty is highly influenced by the two challenges described above. In summary, a triangle with (a) multifactorial nature of tumours (b) heterogeneity of tumours and (c) under-sampling from patients in each vertex (Figure 1), illustrates the main challenges for MDR comprehension [5].

Taking the referred challenges into account, a meticulous frame of the huge information (literally tens of thousands of publications) on the most important features of drug resistance is essential. An approach has been made by Gottesman *et al.* who elegantly reviewed this theme describing 4 main factors as the “main cardinal features of cancer drug resistance”: i) target or bypass mutations, ii) altered cellular pharmacology, iii) changes in differentiation pathways and homeostatic responses, iv) alterations in local physiology and substratum [3]. These “four cardinals of drug resistance” are also attributed to MDR (Figure 1). Importantly, all these modifications are facilitated by key processes such as cancer cell heterogeneity, robust and redundant cell survival pathways, dynamic variations in time and space and increased rate of genetic or epigenetic alterations [3].

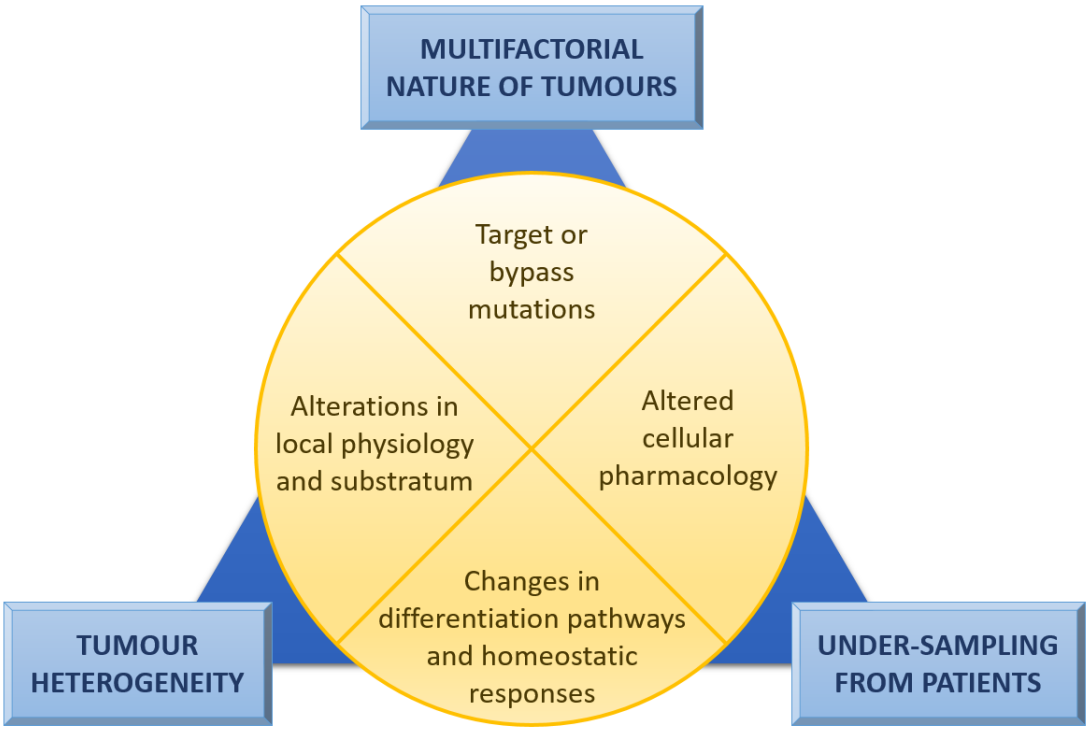


Figure 1: Main challenges for understanding cancer MDR (represented in blue) and the four cardinals of MDR (represented in yellow). Adapted from the description by Gottesman *et al* and Konieczkowski *et al* [3, 5].

1.2 Altered cellular mechanisms in MDR

Essentially, the features described above are the consequence of alterations in host factors (*i.e.* pharmacokinetic) or tumour factors (*i.e.* cellular alterations). The pharmacokinetic factors are related to drug solubility, systemic distribution, metabolism and elimination [2]. These host factors will not be further discussed since they were not the focus of this thesis. Regarding the cellular alterations in tumour cells, the most relevant ones associated to MDR are: decreased drug-influx, increased drug-efflux (by overexpression of drug-efflux pumps), increased DNA damage repair, alterations in cell cycle, decreased cell death, epigenetic and microRNAs alterations. A thorough study of these mechanisms and the identification of the most important players is essential, to gain new insights into the causes of MDR. Table 1 summarizes some of the most important mechanisms/players of MDR that will be briefly described hereafter.

Table 1: Main cellular alterations involved in MDR phenotype and relevant players.

MDR MECHANISM	SOME IMPORTANT PLAYERS	REFERENCES
Reduced drug-influx	RFC/SLC19A1, CTR1, OCTN1/SLC22A4 hENT1	[9-13]
Increased drug-efflux	P-gp, ABCG2 and MRP1	[14-17]
Increased DNA damage repair	ATM, ATR, p53,PARP, BRCA1/2,MGMT,Trps1	[18-21]
Alterations in cell cycle	P53, Bub1, BubR1	[22, 23]
Inhibition of cell death pathways	Bcl-2, IAPs, ATG protein families	[24-26]
Epigenetic and microRNAs alterations	MRUL, H19, miR 21, miR-9, miR-451,miR-27a,miR-298	[20, 27-31]

1.2.1 Reduced drug-influx

Cytotoxic drugs enter into tumour cells by passive diffusion, endocytosis or by the action of influx transporters [32]. In drug-resistant cells, alterations on the transporters involved in drug-influx were found, leading to intracellular sub-lethal concentrations of the substrate drugs. For example, downregulation of the folate carrier RFC/SLC19A1 was associated to methotrexate resistance [9]. Furthermore, the human equilibrate nucleoside transporter (hENT1) was shown to be involved in the uptake of gemcitabine by tumour cells. Dowregultaion of hENT1 was found in different gemcitabine induced-resistant human cholangiocarcinoma cell lines, being associated with multidrug resistance and enhanced invasiveness [33]. Patients with high levels of this transporter showed longer disease-free survival when treated with gemcitabine [13].

Although the transport of cisplatin by copper transporters is still under debate, it is known that the methionine-rich motif of the CTR1 influx transporter (where copper binds), also binds cisplatin [10], with the loss of ligands presumably leading to inactivation of the drug. In addition, low expression of CTR1 was associated with poor clinical outcome following platinum-based therapy in NSCLC patients [11]. Clinical trials using the copper scavenger “trientine” (which increases CTR1 expression and therefore cisplatin uptake) in combination with cisplatin, have been initiated [34].

1.2.2 Increased drug-efflux

Other cell membrane transporters have been associated to drug resistance, by promoting drug-efflux to the outside of tumour cells. In normal conditions, these proteins transport a variety of substrates including bile salts, sugars, lipids, endogenous metabolites and toxins, aiming to protect healthy cells [35]. However, in MDR cancer cells, those proteins are often over-expressed, causing the efflux of cytotoxic drugs and resulting in intracellular sub-lethal concentrations of the substrate drugs (as mentioned above for reduced drug uptake) [36].

The most studied family of proteins responsible for this effect is the ATP-binding cassette (ABC) transporters. ABC transporters are composed by two halves, each with two intracellular cytoplasmic domains that bind to ATP, known as nucleotide binding domains, and six transmembrane domains. Although this is a very large family of 49 members, only three play a major role in cancer MDR: P-glycoprotein (P-gp; also known as MDR1 or ABCB1), MDR-associated protein 1 (MRP1; also known as ABCC1) and breast cancer resistance protein (BCRP; also known as ABCG2). All of these three drug-efflux pumps show overlapping substrate specificity and are able to transport several hydrophobic compounds, including major chemotherapeutics such as taxanes, topoisomerase inhibitors, antimetabolites, kinase inhibitors or anthracyclines. The specificities of P-gp will be further discussed later on - section 1.3.1.

Moreover, increasing activity of other drug-efflux non-ABC proteins such as ATP7A/B transporters mays also contribute to drug resistance [6].

1.2.3 Increased DNA damage repair

DNA is the main target of many classical cytotoxic drugs, either directly (e.g. platinum based drugs) or indirectly (e.g. topoisomerase inhibitors). Thus, the increased capacity of tumour cells for DNA repair contributes to drug resistance. Tumour cells may present dysfunction of, at least, one DNA damage repair pathway [2]. The main repair mechanisms involved in drug resistance include: reversion repair, base excision repair, nucleotide excision repair, mismatch repair and double strand break repair [6].

MGMT (O6-methylguanine-DNAmethyltransferase) is often responsible for resistance of tumour cells to methylation agents. This enzyme was recently associated to MDR in particular, by regulation via Trichorhinophalangeal syndrome, type I factor (Trps1). In a drug-resistant lung cancer cell line, the expression of both Trps1 and MGMT was found. Trps1 was shown to bind MGMT promoter inducing its expression. Importantly, silencing of

Trps1 (and consequent decrease in MGMT expression) reduced the drug resistance of that cell line [18].

In addition to alterations in the effectors of DNA repair, the DNA repair pathways also have important regulators which can be altered and associated with drug resistance. The ATM, ATR, p53, PARP, BRCA1/2 are important examples [6]. For example, the BRCA1/2 association to PARP-1 is responsible for the interesting concept of synthetic lethality. Basically, tumours harbouring BRAC1 or BRAC2 mutation become dependent on another DNA repair component for replication and progression, PARP-1. Indeed, inhibitors of PARP-1 showed high potential to efficiently treat breast and ovarian tumours with mutations in BRAC1 or 2 genes [37]. However, later resistance to these inhibitors was also shown [19, 38].

1.2.4 Alterations in cell cycle

Generally, upon DNA damage cell cycle arrest occurs, providing cells the necessary time to repair the damage. A variety of sensor proteins detect and signal the damage to downstream effectors which, in turn, arrest cell cycle and induce DNA repair. These proteins belong to cell cycle checkpoints and act at the G1-phase, S-phase and G2/M transition [39].

Several checkpoint effectors are found altered in cancer. Some of these alterations occur in oncogenes and in tumour suppressor genes, driving to gain-of-function of oncogenes and loss-of-function of tumour suppressor genes, thus contributing to malignancy of tumour cells [2].

One of the most studied tumour suppressor genes is p53, considered the guardian of the genome, which regulates different phases of the cellular checkpoints. Mutations in this protein are frequently associated with drug resistance [40]. Recently, p53 overexpression was shown to increase the drug sensitivity of multidrug resistant osteosarcoma cell lines [41]. Moreover, p53-negative tumour cells show increased proliferation, in part due to slippage of the mitotic spindle assembly checkpoint [39]. Indeed, in addition to overexpression of drug-efflux pumps, the mitotic slippage is believed to be a crucial mechanism for the development of resistance to anti-microtubule cancer drugs [42, 43]. Interestingly, depending on the cellular microenvironment, the drug used and the nature of the p53 mutation, p53 may act on the promotor of the *MDR1* gene, which codes for P-gp. [22].

1.2.5 Inhibition of cell death pathways

When DNA damage cannot be repaired, the destiny of normal cells should be cell death or permanent cell growth arrest (senescence) [39]. Cell death pathways induced by anti-tumour drugs are apoptosis, autophagy, mitotic catastrophe or necrosis. However, in drug-resistant cells all these cell death pathways may be altered, particularly apoptosis and autophagy [6] allowing cells to resist cell death induced by antitumour drugs.

APOPTOSIS

Apoptosis is triggered by intrinsic or extrinsic pathways, both causing the activation of caspases. However, caspase-independent has also been described to occur [44]. Apoptosis is highly regulated by an enormous number of players, such as the pro-apoptotic or anti-apoptotic proteins (e.g. the Bcl-2 family and the IAP family). Mutations, amplifications, chromosomal translocations and overexpression of genes coding for these proteins have been associated to drug resistance in various tumours [2].

The impact of the Bcl-2 family (constituted by pro- and anti-apoptotic proteins) in drug resistance has been largely studied. Nevertheless, so far the prognostic value of Bcl-2 in the response to chemotherapy could not be confirmed in all tumour types. Indeed, a correlation between Bcl-2 expression and response to therapy was found in patients with breast cancer, but the same evidence was not showed in NSCLC patients [24, 45, 46].

The impact of apoptosis in MDR is undeniable and known to be highly complex and influenced by different mechanisms. For example, ABC transporters could influence the activation of apoptosis. Tumour cells expressing P-glycoprotein are more resistant to caspase-dependent apoptosis, but not to caspase-independent apoptosis. Interestingly, this effect seems to be dependent on the overexpression of Bcl-X_L [47]. This anti-apoptotic role was also suggested for other ABC transporters like ABCG2 and MRP1 [48, 49].

AUTOPHAGY

Regarding autophagy, this is a programmed continuous cellular process which culminates with the degradation of cellular organelles and proteins. In the beginning of this process, an autophagosome is initially formed (through elongation of a phagophore) within a highly regulated network of proteins (e.g. Beclin, ATG and Vps family). Upon activation of the autophagic pathway, the cytosolic form of LC3 (microtubule-associated protein 1 light chain 3, LC3-I) is lipidated to form LC3–phosphatidylethanolamine (LC3-II), which is specifically recruited to the autophagosome [50]. The autophagosome is then fused with a lysosome (originating an autophagolysosome), where the cargo is degraded by lysosomal hydrolases under acidic pH (Figure 2).

Being a dynamic mehcanism, the study of the autophagic flux [*i.e*. whether an increase in autophagosomes presence is due to autophagy induction or to its blockage (after the formation of autphagosomes)] is complex. Thus, to evaluate autophagic flux, the levels of LC3-II (autophagosome associated) are compared following treatment with modulators of the different phases of autophagolysosome formation (e.g. bafylomicin A, wortmannin, 3-MA, metformin, LY294002, pepstatin) [51, 52].

The role of autophagy in cancer is paradoxical. Initially described as a pro-survival mechanim (cytoprotective), different studies have shown that it may result in other outcomes, namely in cell death [53]. In MDR, the paradoxical role of autophagy has been also described [54, 55].

In tumour samples from colorectal cancer patients, the expression of P-gp was positively correlated with LC3, Beclin1 and Rictor, suggesting that autophagy is associated with MDR development [48]. Also, upregulation of ATG-5 (a key regulator of autophagy) was associated with drug resistance in human gastric cancer [26]. In addition, a synergistic role of autophagy induction, P-gp expression and NF-κB pathways was shown in the development of epirubicin resistance, in triple negative breast cancer cells [56]. By contrast, decreased autophagy was associated to 5-FU resistance in a drug-resistant colon cancer cell line [57] and autophagy suppression by Rab5a (a key regulator of vesiculation) was shown to promote drug resistance in gastric cancer cells [58].

Due to this paradoxical role of autophagy, reports on the mechanism of action of several anticancer drugs have shown either a pro-survival or a pro-death role of autophagy. In some cases, when the cytotoxic drugs induce autophagy as a cell death mechanism, autophagy is inhibited in the MDR cells, thus impairing the drug efficiency [54].

Some studies demonstrated that some autophagy inducers mediated drug sensitization. For example, suberoylanilide hydroxamic acid induced autophagic cell death and significantly suppressed the growth of breast cancer cells resistant to tamoxifen [59]. Cryptotanshinone and dihydrotanshinone, also inhibited the growth of apoptosis-resistant colon cancer cells, by inducing autophagic cell death and *p53*-independent cytotoxicity [60]. In addition, a study carried out in drug-sensitive leukaemia cells and MDR counterparts, showed that combination of metformin (an autophagy inducer) with 2-deoxyglucose strongly increased autophagy, promoted significant cytotoxicity and increased apoptosis, in both cell lines. Interestingly, metformin is not a P-gp substrate but, treatment of MDR cells with metformin decreased the levels of P-gp in those cells [61].

However, in other cases, autophagy may be used by MDR cells as a process to obtain energy and escape from cytotoxic induced cell death. Indeed, various studies

indicate that autophagy induced by different chemotherapeutics, such as paclitaxel, tamoxifen, epirubicin and trastuzumab, may facilitate drug-resistant phenotype [62-65]. Taken together, all these findings show that the role of autophagy in MDR needs further clarification.

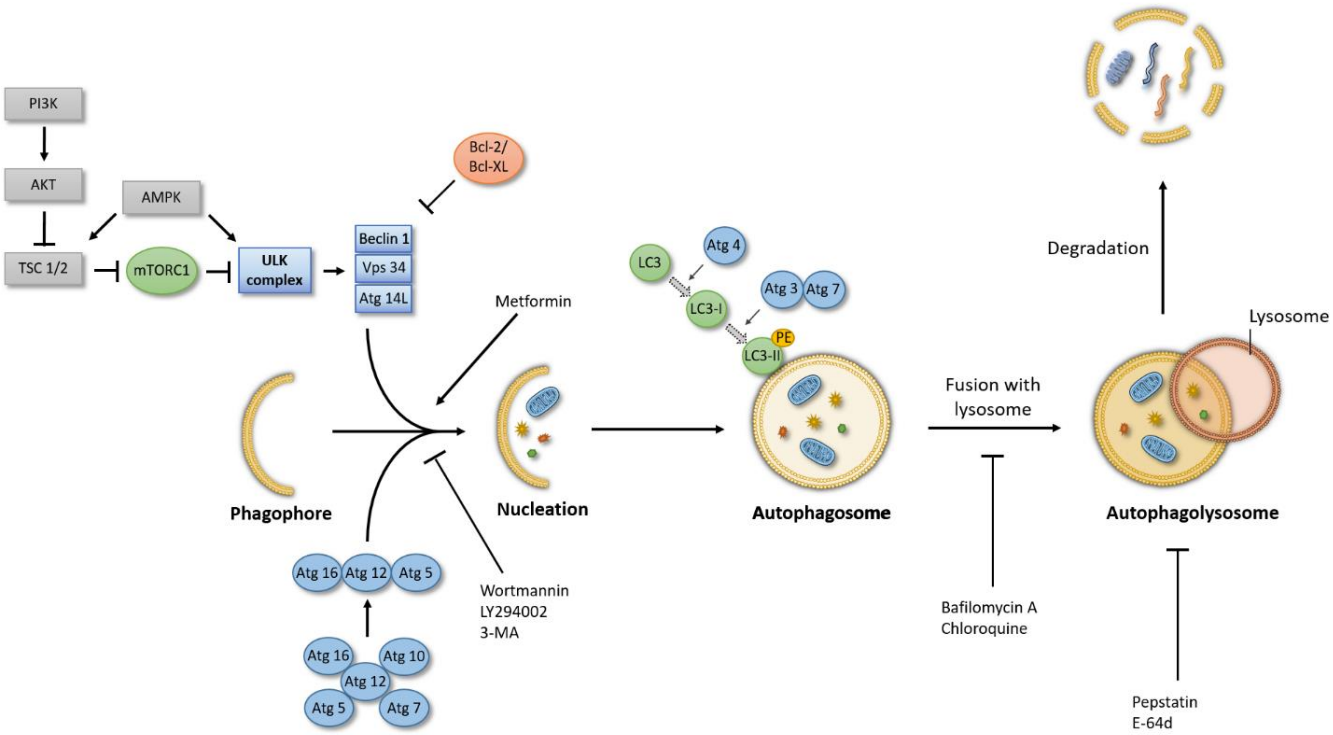


Figure 2: Autophagy pathway. Autophagy is a highly regulated process, focused on the lysosomal degradation of cellular components (such as proteins and organelles) and/or recycling of cytosolic compounds. See main text for details. Adapted from [66].

1.2.6 Epigenetic and microRNAs alterations

The main epigenetic events with impact in drug resistance are DNA methylation, histone acetylation and expression of non-coding RNAs, in particular microRNAs. Indeed, different cancers show up- or down- regulation of different types of cellular receptors, which is widely associated to epigenetic alterations. For example, aberrant methylation of CpG islands of the Estrogen Receptor promoter and histone deacetylation were described as predictors of poor outcome and tamoxifen resistance in breast cancer patients [1]

Regarding microRNAs, around 2600 human species were already described and many have been associated to regulation of proteins with tumour suppressor or tumour promotion properties. The impact of these non-coding RNAs in MDR will be further discussed - section 1.3.2.

1.2.7 Other mechanisms involved in MDR

In addition to the cellular alterations refered above, others such as: the tumour microenvironment, alterations in drug metabolism, the epithelial-mesenchymal transition (EMT) and the presence of cancer stem cells (CSCs) in the tumour mass, have also been associated to MDR.

The role of the tumour microenvironment in protecting tumour cells from cytotoxic drugs has been extensively studied. In non-haematological tumours, the tumour-associated fibroblasts, immune cells, inflammatory cells and blood vessels may contribute to MDR [67, 68]. In haematological tumours, the bone marrow stromal and endothelial cells, osteoclasts, osteoblasts, macrophages, T cells, among others may also contribute to MDR [69, 70]. At the molecular level, it is believed that integrins, cytokines and growth factors are key players in such process [2].

Alterations in drug metabolism, namely drug inactivation and detoxification, have also been associated to MDR. Indeed, a variety of chemotherapeutics undergo metabolic activation to acquire clinical efficacy. In drug-resistant cells, this activation is decreased and detoxification processes increased [71]. Different effectors such as the cytochrome P450 (CYP) system, the glutathione-S-transferase (GST) superfamily and the uridine diphospho-glucuronosyltransferase (UGT) superfamily were found altered in drug-resistant cells [72]. Clinical relevance was already described for these alterations in drug metabolism. For example, patients with multiple myeloma and unfavourable outcome showed downregulation of genes encoding for detoxification proteins [73].

Epithelial-mesenchymal transition (EMT) is characterized by the transition that epithelial cells may undergo towards a mesenchymal phenotype, losing their polarized organization and tight cell–cell junctions and leading to increased motility and invasive capacity [2]. The involvement of EMT in chemotherapy and targeted therapy resistance has been shown. For example, in a panel of NSCLC cell lines derived from treatment-naive patients, a gene signature constituted by some genes associated to EMT was considered an important predictive biomarker of resistance to the EGFR inhibitor erlotinib and to inhibitors of the PI3K–AKT–mTOR signaling [74].

Cancer stem cells may also contribute to tumour MDR. Even though the cancer stem cell model was published in 1960s [75], this area of research still faces many challenges, mostly because these cells possibly represent only around 1% of the tumour (variable depending on tumour type [76]). This model defends that primary tumours, prior to chemotherapy treatment, are constituted by conventional drug-sensitive cells and also by a subtype of cells – the CSCs or cancer cells with stem-cell-like properties - which are extremely resistant to drugs due to overexpression of ABC transporters, increased levels of

anti-apoptotic proteins or increased DNA damage repair [2]. Finding appropriate markers for these cells and studying the stability of the CSC phenotype is essential for a deeper understanding of the possible CSCs impact on patients tumour MDR.

In conclusion, in the cancer context, several of the mechanisms described above may be altered simultaneously, being responsible for the development, maintenance and evolution of a MDR phenotype in cancer patients. Therefore, several players such as P-gp, PARP, p53, Bcl-2 and different non-coding RNAs, have been molecularly targeted in order to overcome MDR at pre-clinical level. These efforts have shown interesting results, further highlighting the need to pursue this area of research.

1.3 Relevant molecular players

1.3.1 P-glycoprotein: a major cause of MDR

P-glycoprotein was the first ABC transporter identified [77]. P-gp acts as a drug-efflux pump being physiologically found in tissues with excretory and secretory function [78]. Tumours derived from those tissues, such as kidney, colon, adenocortical or hepatocellular carcinomas, may show intrinsic P-gp-mediated MDR. In addition, some malignant cells which did not present high levels of P-gp before drug treatment, may overexpress P-gp following exposure to drugs. Indeed, some haematological tumours illustrate this case of acquired MDR. For example, in a study of multiple myeloma patients, only 10-30% of those patients expressed *MDR1* gene at diagnosis while 50-80% of patients expressed this gene at relapse or resistant disease [79-81].

Several studies associated high levels of P-gp with drug resistance, particularly to MDR, in a variety of tumour types. The uptake of erlotinib was shown ineffective in glioblastoma patients during clinical trials, due to overexpression of P-gp and BCRP1 [82]. Furthermore, a meta-analysis indicated that patients with breast tumours expressing P-gp were three times more likely to fail response to chemotherapy [83]. In non-Hodgking's lymphoma, P-gp expression increased from 2-49% in untreated patients to 64% in post-treatment patients [84]. In non-small cell lung cancer patients, P-gp transcripts/protein were identified in 11-32% of surgical specimens; however, in tumours subjected to therapy the P-gp transcripts increased to 61% [85].

Importantly, as described above, P-gp (and other drug-efflux pumps) were already described as apoptosis inhibitors. However, the anti-apoptotic effect of P-gp is not associated with its drug-efflux activity. Various studies indicate the P-gp is associated to apoptosis by modulation of the assembly of pro-apoptotic membrane signalling complex, suppression of caspase activation, modulation of the activity of calcium channels and regulation of the expression of endogenous TNF-related apoptosis-inducing ligand (TRAIL) [86, 87].

1.3.1.1 Molecular characterization and intracellular localization of P-gp

Human P-gp is encoded by *ABCB1*/*MDR1* gene, located in the chromosome 7, which gives rise to a 170kDa protein, constituted by 1280 aminoacids [88-90]. The crystallographic structure of human P-gp has not been obtained yet. However, structures from bacterial and mouse P-gp deposited on the Protein Data Bank (PDB) have been helpful to gain insights into the mechanisms associated to the binding of ligands to P-gp [91, 92]. P-gp is organized in two halves. Each half contains six transmembrane domains (α-helices) (TMD) and a nucleotide binding domain (NBD) (Figure 3). Different mechanisms were described about the manner how P-gp binds ATP and allows drugs to cross the cellular membrane. Classically, it is accepted that P-gp can adopt two conformations: an “open” form able to interact with substrates and a “closed” form unable to bind molecules. The alternation between the “open” and the “closed” forms is dependent on energy from ATP hydrolysis [93].

P-gp interacts with a variety of substrates, including several antitumour drugs, such as etoposide, paclitaxel, docetaxel, doxorubicin, epirubicin or daunorubicin [94] among others. This large range of substrates strengthens the association of P-gp with a MDR phenotype.

Regarding P-gp cellular localization, although it was initially described mainly at the plasma membrane, further studies showed that in some cells it is also found in lysosomes, endosomes, endoplasmic reticulum, Golgi complex and nuclear envelope [95]. This broad intracellular distribution allows the transport of substrates from the cytoplasm to the lumen of organelles, by P-gp [96]. In chemotherapy-treated cells, this process results in sequestration of drugs, which may be later released from cells by exocytosis [93].

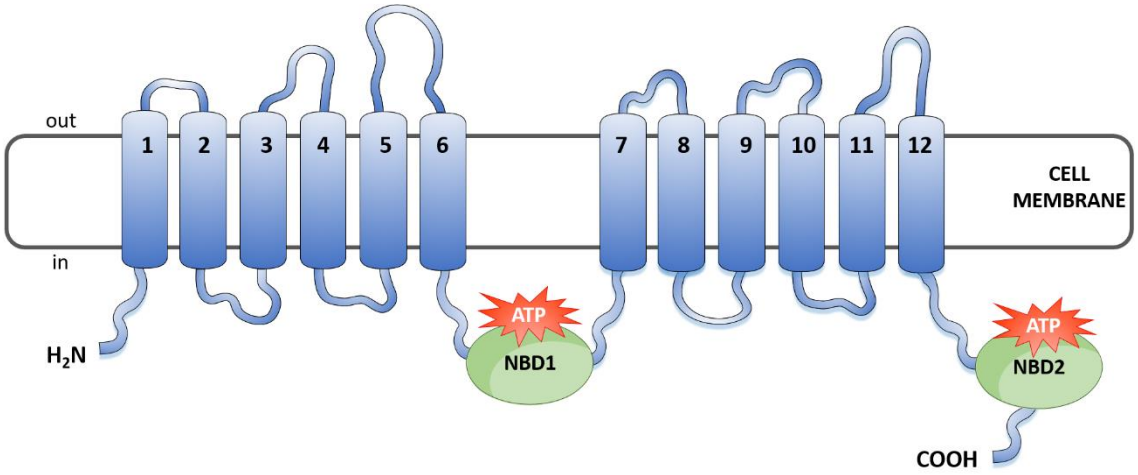


Figure 3: Schematic representation of P-glycoprotein structure in the cell membrane. Each half of contains six transmembrane domains (α-helices 1-6 and 7-12) and one NBD-nucleotide binding domain (NBD1 or NBD2), where ATP binds (adapted from [97]).

1.3.1.2 Regulation and modulation of P-gp levels

P-gp levels are regulated both transcriptionally and post-transcriptionally. Regulation of P-gp at transcriptional level involves: alternative promoter usage, alterations in gene transcription and gene amplification, alterations in mRNA stability, DNA methylation and histone acetylation [98]. In particular, the influence of non-coding RNAs in P-gp expression (mainly microRNAs and long non-coding RNAs) has been also described. The role of miRNAs (miRs) in P-gp expression is a result of direct and/or indirect regulation. MiR-451,-27a,-508-5p,-331-5p,-298,-145 are examples of miRs which are involved in direct regulation, while miR-137,-200c-122,-138,-19a/b,-130a are examples of miRs involved in indirect regulation [98]. Regarding long non-coding RNAs, the lncRNA NEAT1 was shown to be an important modulator of drug resistance in gastric cancer, by promoting the expression of P-gp and other associated proteins [99]. In addition, depletion of another ncRNA, the MRUL (MDR-related and upregulated lncRNA), located 400 kb downstream of ABCB1, was shown to reduce ABCB1 mRNA levels in a dose - and time - dependent manner. MRUL knockdown in resistant gastric cancer cells increased apoptosis and furthermore increased accumulation of drug and reduced doxorubicin release by the cell [27].

The main mechanisms associated to the post-transcriptional regulation of P-gp are: protein trafficking and recycling, P-gp stability, glycosylation regulated by Pim-1 Kinase, ubiquitin-proteasomal degradation, mitogen- activated protein kinase (MAPK) signalling pathway and phosphorylation by protein kinase C (PKC) and protein kinase A (PKA) [100].

P-gp is a very interesting molecular target involved in MDR due to: i) its diverse family of substrates, ii) alterations reported in various different tumours, iii) ability to promote drug sequestration within cells and iv) capacity to cause the efflux of drugs from cells.

Thus, different strategies emerged in order to decrease the levels of P-gp or inhibit its function, in an attempt to overcome MDR. Regarding approaches to decreased P-gp expression, companies such as Isis Pharmaceuticals and Hybridon have patented methods to downregulate P-gp expression with antisense oligonucleotides presenting improved stability and cellular permeability [101]. Indeed, downregulation of P-gp increased drug sensitivity of a resistant chronic myelogenous leukaemia cell line overexpressing P-gp [102]. Likewise, in ovarian tumour cells, P-gp silencing with short hairpin RNAs, sensitized resistant cells to paclitaxel [103]. Moreover, in colon tumour cells, stable transfection with siRNAs for P-gp reversed the MDR phenotype associated to P-gp [104].

Another approach for P-gp modulation is the development of inhibitors of synthesis and/or function of P-gp. To date, four generations of inhibitors of P-gp were developed. Importantly, some P-gp inhibitors reached clinical trials. For example, zosuquidar and tariquidar were very promising due to their high potency and specificity. However, disappointing results were obtained during clinical trials due to toxicity of those molecules or limited activity. Moreover, poor patient selection criteria is possibly also responsible for the ineffective translation of P-gp inhibitors to the clinical setting [105]. The limited achievements of these clinical trials are probably also associated to the complexity of factors involved in development of MDR. Importantly, Gottesman *et al.* in an elegant comment about the role of MDR efflux pumps in cancer, argued that a conclusive trial using appropriated doses of P-gp inhibitors in patients, known to overexpress P-gp in their tumours, has never been done properly and it would be very important [106].

1.3.2 MicroRNAs as regulators of MDR

MicroRNAs (miRs) are the most extensively studied non-coding RNAs. MiRs were firstly described in 1993 by Ambros *et al.*, in *C. elegans* [107, 108]. Since then, a huge body of evidence has been found, addressing miRs biogenesis, their cellular role and their impact in pathophysiology.

MiRs are an evolutionary conserved class of small non-coding RNAs, ranging 20-22 nucleotides. Around 2600 unique mature human miRs were already identified (miRBase version 20) [109]. MiRs regulate gene expression post-transcriptionally by binding to the target mRNAs, mostly to the 3'untranlated region (UTR) region. Nevertheless, miRs binding

sites have also been found in the 5'UTR [110] or the coding region [111]. Importantly, miRs can bind to several mRNAs, therefore each miR may target different mRNAs. And the same mRNA could be targeted by different miRs [112]. MiRs can be intragenic but also intergenic, being transcribed independently of a host gene and regulated by their own promoter [113, 114]. Some miRs are transcribed as a long transcript called "cluster" [115].

1.3.2.1 MiRs biogenesis and mechanisms of action

The biogenesis of miRs occurs by a canonical and a non-canonical pathway. In the predominant canonical pathway, miRs are transcribed from DNA sequences into primary miRNAs (pri-miRs) by RNA polymerase II in the nucleus, and further processed into precursor miRs (pre-miRs) by the microprocessor complex, consisting of an RNA binding protein DiGeorge Syndrome Critical Region 8 (DGCR8) and a ribonuclease III enzyme, Drosha (Figure 4). Pri-miR and Pre-miR are stem-loop structures. Pre-miR is then exported to cytoplasm by the action of the exportin 5(XPO5)/RanGTP complex, where the Dicer, an RNase II endonuclease, removes the terminal loop, producing a mature miR duplex. The miR duplex is then processed by helicase, being the two strands separated. One strand, the "mature" one, is loaded into the Argonaute/RNA-induced silencing complex (RISC). The unloaded strand is called the "passenger" and is degraded. Importantly, the direction of the miR strand will determine the name of the mature miR. Indeed, the name 5p or 3p is originated by the 5' or 3' end of pre-miR, respectively. Regarding the non-canonical biogenesis, in general is a result of different combinations of core proteins such as Drosha, Dicer, exportin 5 and Argonaute 2 (Ago2). Two main pathways for non-canonical biogenesis were described: the Drosha/DGCR8- independent and the Dicer-independent.

No matter which pathway is activated (canonical or non-canonical), any mature miR strand usually is associated to RISC complex, being then guided to the target-site *i.e.* a particular sequence of mRNA, where it acts to silence gene expression. Here, if a perfect or nearly perfect annealing occurs (between miR and mRNA), a degradation of the target mRNA occurs. On other hand, if the annealing is imperfect or only partial, the ribosomes cannot access the mRNA and translation cannot occur.

Of note, although the great majority of studies associate miRs to repression of gene expression, under specific conditions miRs may be involved in causing gene-upregulation. The induction of gene expression by miRs was found in quiescent cells [116, 117] or in conditions of aminoacid starvation [118].

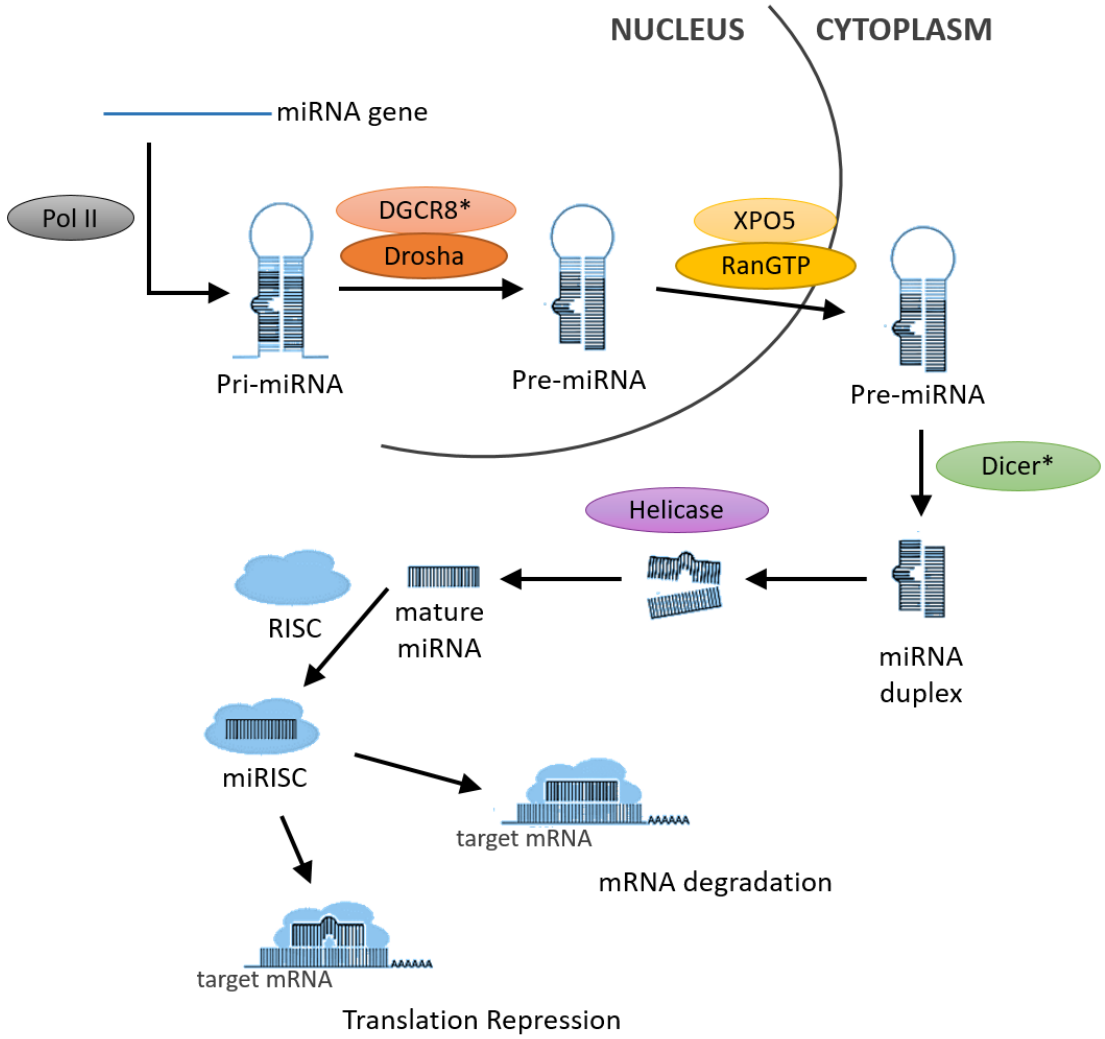


Figure 4: Mechanisms involved in the canonical pathway of microRNAs biogenesis. * indicates proteins/complexes which may not be involved in the non-canonical pathway of microRNAs biogenesis. Adapted from [119].

1.3.2.2 The effect of microRNAs regulation in pathways associated to MDR

Due to their diverse targets, miRs are linked to all hallmarks of cancer [120]. Importantly, alterations in miRs expression profile has been reported between drug-

sensitive and drug-resistant cellular counterparts [121]. Deep sequencing tools have been used to increase this knowledge. For example, next generation sequencing identified the relevance of miR-508-5p in MDR phenotype. Indeed, following the NGS analysis, in this study the authors showed that the overexpression of miR-508-5p was able to reverse resistance to multiple drugs *in vitro* and to sensitize tumours to chemotherapy *in vivo* [122]. Interestingly, after this work, miR-508-5p was shown to have a synergistic effect with miR-27b, forming the miR-27b/CCNG1/p53/miR-508-5p axis, which plays an important role in gastric cancer-associated MDR [123].

MiRs regulate MDR by targeting a specific gene and a single cellular signalling pathway or by targeting several genes and diverse cellular signalling pathways [124]. Indeed, miRs modulate different mechanisms described above as altered in MDR phenotype (section 1.2). In Table 2, some miRs involved in cellular pathways altered in MDR and their respective targets are shown. In addition, the most relevant studies addressing these miRs will be further described below.

Table 2: Some of the most important non-coding RNAs associated to MDR. *not fully understood.

Type of non-coding RNA	Non-coding RNA	Possible target	MDR mechanism altered	References
Long non-coding RNA	**MRUL**	P-gp	Drug-efflux	[27]
	H19	MDR1/P95	Drug-efflux	[125, 126]
	ROR	P53	DNA damage repair, cell cycle	[127]
	HOX antisense intergenic RNA (HOTAIR)	P21	Cell cycle	[128]
	CUDR	Caspase-3	Cell death pathways	[129]
microRNAs	**miR-451,-27a,-138,-298,-381,-495**	P-gp	Drug-efflux	[31, 130-133]

	miR-328,-519	ABCG2	Drug-efflux	[134, 135]
	miR-125b,-140,-122	P53	Cell death pathways and cell cycle	[136-138]
	miR-27b	CYP1B1	Drug metabolism	[139]
	miR-892a	CYP1A1	Drug metabolism	[140]
	miR-133b	GST	Drug metabolism	[141]
	miR-513a-3p	GSTP1	Drug metabolism	[142]
	miR-182	BRCA1	DNA damage repair	[143]
	miR-9	BRCA1	DNA damage repair	[20]
	miR-21	MMR	DNA damage repair	[144]
	miR-497, -15b,-16	Bcl-2	Cell death pathways	[145, 146]
	miR-574-3p	Bcl-XL	Cell death pathways	[147]
	miR-30a	Beclin and ATG5	Cell death pathways	[148, 149]
	miR-200b	ATG12	Cell death pathways	[150]
	miR-200b,c/429 cluster	XIAP	Cell death pathways	[151]
Pseudogenes	**CYP4Z2P**	*	*	[152]
	OCT4-pg1	*	*	[153]

Effect on Drug-efflux

A variety of miRs were associated to P-gp levels. Indeed, some miRs were found to participate in MDR modulation through regulation of P-gp expression (Table 2). In MDR leukaemia cells, upregulation of miR-138 decreased P-gp expression and reversed resistance to adriamycin [132]. Two other miRs, miR-381 and miR-495, were also associated to regulation of P-gp levels and consequently modulation of MDR [133]. Interestingly, two independent groups showed that miR-451 and miR-27a were upregulated in MDR tumour cell lines and increased P-gp levels in those cells [30, 154]. However, other studies reported the negative role of miR-451 on P-gp expression and drug resistance in leukaemia, breast and hepatocellular tumour cell lines [130, 155, 156]. These contradictory results confirm that, as described above, the role of miRs is highly complex. MiRs have multiple targets and may influence diverse cellular pathways, further suggesting that their role is influenced by the tumour cell model studied.

Also, miRs can regulate several MDR-associated proteins simultaneously. For example, in human glioma cells, downregulation of miR-106a reversed MDR phenotype by reducing the levels of P-gp and MRP1 as well as others proteins involved in apoptosis and survival [157].

Effect on Drug Metabolism

The miR binding sites described for most of the drug-metabolizing enzymes are poorly conserved, suggesting that other forms of regulation are more relevant for drug metabolism [158]. Indeed, few studies were conducted addressing the role of miRs in drug metabolism and their impact in drug resistance. Despite this, miR-27b was shown to possibly have a role in sensitization of malignant cells to a variety of anti-tumour drugs, both *in vivo* and *in vitro*, by reducing CYP1B1-dependent drug detoxification and activating p53-dependent apoptosis [159]. Furthermore, overexpression of miR-513a-3p was shown to decrease GSTP1 levels, sensitizing lung tumour cells to cisplatin [142]. In addition, miR-133b decreased the GST-Pi expression and reversed drug resistance [141].

Effect on DNA damage repair

The concept of synthetic lethality with the involvement of BRAC1 and PARP1 was described above (section 1.2.3). High expression of miR-182 in multiple breast tumour cell lines was shown to influence BRCA1 levels and sensitivity to PARP1 inhibitors [143]. In addition, in ovarian cancer, miR-9 was shown to downregulate BRAC1, decreasing DNA damage repair and consequently increasing the sensitivity of tumour cells to cisplatin and PARP inhibitors [20]. In colorectal tumour cells, overexpression of miR-21 decreased the expression of mismatch repair (MMR) proteins (hMSH2 and hMSH6) and reduced the

therapeutic efficacy of 5-FU [144]. Other MMR proteins, such as MSH2, MSH6, MLH1 and PMS2, were also reported to be negatively regulated by miR-155 [160].

Effect on cell cycle

Several miRs were already associated to regulation of p53 levels. In particular, miR-25, -30d and -504 have been shown to directly target p53 [161]. Their upregulation decreases p53 levels, impairing p53 functions such as cell cycle arrest, apoptosis and p53-mediated transcriptional activation. Also, their upregulation promotes resistance to etoposide-induced cell death [162, 163]. In Ewing sarcoma/primitive neuro-ectodermal tumour (EWS) cells, upregulation of miR-125b suppressed p53-dependent apoptosis and induced drug resistance to doxorubicin, vincristine, etoposide and mafosfamide [136].

Effect on cell death pathways

In MDR gastric tumour cells, downregulation of miR-15b and miR-16 correlated with upregulation of the anti-apoptotic protein Bcl-2. By contrast, upregulation of miR-15b or miR-16 dramatically reduced Bcl-2 protein levels and sensitized cells to antitumour drugs [146].

One member of the inhibitor of apoptosis family, XIAP, is targeted by the miR-200bc/429 cluster, which may be involved in reduced resistance of gastric and lung tumour cells to cisplatin, doxorubicin, vincristine and etoposide [151].

Interestingly, it is possible that a single miR regulates more than one mechanism of cell death, e.g. both apoptosis and autophagy. Indeed, a cross-talk between apoptosis and autophagy, mediated by miRs, has been described by different authors. MiR-204 modulates anti-apoptotic effects and inhibits autophagy [164, 165]. Alterations in miR-204 expression modulates the crosstalk of apoptosis and autophagy, influencing the response of tumour cells to drugs [124]. Likewise, overexpression of miR-16 and miR-17 decreased Beclin1 and Bcl-2 levels, inhibiting autophagy and inducing apoptosis. Upregulation of those miRs sensitized resistant lung cancer cells to paclitaxel treatment [166].

1.3.2.3 Circulating miRs

MiRs may be released into the extracellular environment as a result of apoptotic or necrotic cell death (as complexes associated to Ago2 protein) or encapsulated into vesicles named extracellular vesicles. The association of miRs to extracellular vesicles will be further discussed in section 2 of this thesis.

The potential of circulating miRs in the cancer field as possible biomarkers has been explored, since they have been found in serum, plasma, urine, saliva and breast milk [167]. Importantly, miRs show increased stability in those biological fluids and can be measured by different molecular biology techniques [120]. Tumour-specific miRs were identified for the first time in the serum of patients with diffuse large B-cell lymphoma. In this study, high levels of miR-21 were correlated with improved relapse-free survival [168]. Afterwards, several circulating miRs have been associated to other types of cancer, such as miR-141 in prostate cancer [169], miR-486, miR-30d, miR-1, and miR-499 in NSCLC [170], miR-17-3p and miR-92 in colorectal cancer [171], miR-195 and let7-a in breast cancer [172], and miR-500 in liver cancer [173]. Several studies using clinical samples have been published in the recent years, in order to unravel to potential of circulating miRs as prognostic, diagnostic and therapy response biomarkers in cancer[174].

1.4.3 Other non-coding RNAs in MDR

Interestingly, 98% of genome does not code for proteins, indicating that cells assemble an unimaginable amount of information that in the past was completely ignored [175]. Transcripts that are not translated into proteins are called non-coding RNAs (ncRNAs). In the last years, the advances in high-throughput technologies allowed the identification of a huge amount of ncRNAs. Their biological significance has been addressed by different authors, however little is known about the role of ncRNAs in MDR.

The ncRNAs may be classified based on their function and/or size. Generally, ncRNAs may be divided into: i) translation-related RNAs (e.g. rRNA and tRNA), ii) short ncRNAs (with 19-31 nt; e.g. miRNAs and PIWI-interacting RNAs) iii) midsize ncRNAs (20-200 nt; e.g. small nucleolar RNAs) and iv) long ncRNAs (>200 nucleotides; e.g. pseudogenes, circular RNAs, antisense transcripts) [175, 176]. Importantly, the mode of action of each ncRNA depends on its nature. Due to their high heterogeneity, it is not yet possible to understand how these species act in order to regulate different processes; instead, each ncRNA subtype should be evaluated independently.

The biological functions described for the different ncRNA species include telomere maintenance, epigenetic changes, structural organization, imprinting, transcriptional interference, post-transcriptional and translational control, cell differentiation and development [177]. A number of ncRNAs were found altered in cancer, being associated to tumour initiation, progression, metastization and response to therapy. According to Santoch

et al., the diagnostic use of ncRNAs is advantageous over protein-coding RNAs because RNA itself is the effector molecule and its expression levels may be a better indicator of tumour features [175].

A bioinformatic based study of the published literature identified 388 ncRNAs-drugs interactions [178]. Importantly, this literature analysis indicated that microRNAs and long ncRNAs have more impact in drug resistance than other types of RNAs. Indeed, a network of interactions between those ncRNAs and the mechanisms described above as being altered in MDR (section 1.2) has been demonstrated in several studies. Table 2 summarizes some of the most important ncRNAs and the altered mechanisms associated to MDR.

Long non-coding RNAs regulate gene expression by interacting with DNA, RNA or proteins at different levels. They can serve as molecular scaffolds for recruitment of chromatin-modifying complexes [179, 180], interact with chromatin remodeling proteins [181] or bind specific gene clusters to prevent the binding of transcriptional activators [182].

The long ncRNA Urothelial Cancer-Associated 1 (UCA1) is a competitive endogenous RNA (ceRNA) of MDR1, causing increased resistance to imatinib in chronic lymphocytic leukaemia cells, by sequestering miR-16 [183]. Furthermore, UCA1 overexpression increased MDR1 levels, resulting in imatinib resistance, whereas its silencing had the opposite effect [184]. Indeed, in breast cancer, UCA1 knockdown reverted a resistant phenotype and increased tamoxifen sensitivity through inhibition of the Wnt/b-Catenin pathway [185]. In bladder cancer, UCA1 induced resistance to cisplatin/gemcitabine through modulation of miR-195a [186]. Importantly, UCA1 was found present in extracellular vesicles released by tamoxifen-resistant breast tumour cells, being responsible for increased drug resistance in Estrogen Receptor-positive cells [187]. Another lncRNA associated to drug resistance is LINC-ROR. This lncRNA was shown to inhibit EMT and enhance tamoxifen sensitivity by increasing miR-205 [188]. Moreover, in breast cancer patients, LINC-ROR inhibition reversed resistance to tamoxifen by inducing autophagy [189]. Interestingly, in hepatocellular carcinoma cells, the mediation of sorafenib sensitivity by LINC-ROR was shown to be associated to the release of extracellular vesicles [127]. In addition, other lncRNAs were associated with drug resistance such as: CUDR, HOTAIR, PANDA, AK126698, H19, ARA and SnaR, among others [190].

Regarding pseudogenes, they were initially described as evolutionary remnants with no biological significance. However, different works revealed their role in gene regulation, mainly of their primary genes. Indeed, different types of tumours showed dynamic expression pattern of pseudogenes [176]. The mechanisms by which pseudogenes regulate gene expression are not fully understood. Some authors suggested that pseudogenes compete with parental genes for RNA-binding proteins or for the translational

machinery, possibly by generating endogenous small interfering RNAs which will compete with parental genes [191-193]. Other authors defend the competing endogenous RNA (ceRNA) hypothesis, in which pseudogenes act as “molecular sponges” to sequester miRNAs that repress the corresponding genes [194, 195].

Concerning drug resistance, CYP4Z1 and CYP4Z2P pseudogene were found increased in MCF-7 cells resistant to tamoxifen, when compared with the parental MCF-7 cells. Interestingly, upregulation of CYP4Z1- or CYP4Z2P-3'UTR level increased resistance to tamoxifen. The authors defend that the competitive endogenous RNAs network between CYP4Z1 and pseudogene CYP4Z2P promote CDK3 expression, in Estrogen Receptor-positive breast cancer [152]. Another example is the OCT4 gene, which has multiple pseudogenes. One of them, the OCT4-pg1 (also known as POU5F1P1 or POU5F1B) is a polymorphic pseudogene that presents an A or a G nucleotide at the rs10505477 SNP. Patients with gastric cancer treated with cisplatin and that carry the GA/AA genotype had a poor overall survival, when compared to those who had undergone the same treatment but instead carry the GG genotype [153]. In addition, another study indicated that OCT4-pg1 overexpression induced upregulation of various growth factors in gastric cancer cells, induced angiogenesis and decreased apoptosis in gastric tumour xenografts [196].

2. Extracellular Vesicles

Extracellular vesicles (EVs) are cell-derived small particles enclosed by a lipid bilayer. The release of vesicles by plasma membrane budding was firstly described in the beginning of the 1980s in platelets or tumour cells [197, 198]. At that time, the physiological and pathological function of EVs was completely unknown. Some years later, two independent research groups demonstrated that during reticulocyte maturation, inward budding of endosome led to the production of intracellular vesicles which were then released from the cell [199].

In 1987, the word ‘exosome’ was first proposed for vesicles from endosomal origin [200]. Since then, different types of vesicles were discovered and their nomenclature has been widely discussed, because different labs were naming these vesicles inappropriately. EVs had traditionally been classified based on their size and/or biogenesis. The two main classes described are exosomes and microvesicles [201]. Typically, exosomes are produced along the endocytic pathway [through multivesicular body (MVB) maturation] and are smaller (30-150 nm). On the other hand, microvesicles result from the budding of plasma membrane, ranging in size between 50-1000 nm. Nevertheless, it became increasingly evident that many scientists were inappropriately using this classification since: i) the vesicle biogenesis through the endocytic pathway or by the budding of plasma membrane share some regulators (this will be discussed later, section 2.2 of this thesis); and ii) there is a size overlap between these two classes of vesicles, especially for the smaller particle range (30–150 nm) [202, 203]. In addition to the initial nomenclature of “exosomes” and “microvesicles”, a variety of names have been attributed to different populations of EVs, according to their size, origin and morphology. These include: prostasomes, tolerosomes, dexosomes, nanovesicles, exosome-like vesicles, microparticles, blebbing vesicles, shedding vesicles, oncosomes, migrasomes, neurospheres or apoptotic bodies [201]. The International Society of Extracellular Vesicles (ISEV) had a fundamental role on standardizing the nomenclature, suggesting the use of the term “EVs” for all types of lipid bilayer-enclosed extracellular structures which do not replicate. ISEV also advices a detailed description of EVs’ isolation methods and characterization [204]. Accordingly, in this thesis the term “EVs” will be generally used. In particular cases, EVs originated through the endocytic pathway will be distinguished from EVs originated by the plasma membrane outward budding.

EVs can be isolated by diverse methods such as differential centrifugation, filtration, size-exclusion or affinity chromatography, density gradient centrifugation, among others

[205]. The most appropriate isolation method depends on the nature of the sample. Importantly, each method isolates different populations of EVs. It is very challenging to isolate some types of EVs from other types, such as the traditionally called “exosomes” from the traditionally called “microvesicles”. A deeper understanding of the nature of the EV´s populations is expected within the next few years, by using improved EVs isolation and characterization techniques. One elegant study which aimed at the specification of EVs populations based on their deep characterization was carried out by J. Kowal *et al* [203]. In this study, exosomes enriched in late endosome components were defined as a small EV subtype bearing the tetraspanins CD63 (a protein accumulating in MVBs) and CD9/CD81 (which are mainly at the plasma membrane). Moreover, these authors define a set of protein categories displaying different relative abundance in distinct EV populations. For example, GP96 and other ER-associated proteins are mainly present in large EVs; actinin-4, mitofilin and possibly other mitochondrial proteins are present in both large and medium-sized EVs but absent in the small EVs; syntenin-1, TSG101, ADAM10, and EHD4 are only present in the small EVs; extracellular matrix (ECM) components, complement, and serum-derived factors (prothrombin, serum albumin) represent small EV-bound components of variable presence [203].

The release of EVs is an evolutionary conserved mechanism, suggesting their physiological relevance. All eukaryotes and also prokaryotic cells may shed EVs. Indeed, in addition to mammalian cells, EVs are also secreted by plant cells and pathogens such as bacteria, mycobacteria, archea and fungi [206, 207]. In humans, EVs were already found in a vast diversity of biological fluids such as blood, urine, saliva, breast milk, amniotic fluid, ascites, cerebrospinal fluid, bile and semen [206], which raised the possibility of using EVs as a source of biomarkers for several diseases since they carry cargo from their donor cells.

EVs may be responsible for intercellular communication, with either physiological or pathological relevance, by transferring their cargo from donor to recipient cells. In normal physiology, EVs are involved in an enormous number of processes such as blood coagulation, autophagy, reproductive biology, immunomodulation, tissue regeneration and angiogenesis [208-213]. EVs’ role in pathophysiology has been associated mainly with neurodegenerative disorders, autoimmune diseases and cancer [214-216]. In cancer in particular, EVs are involved in many mechanisms associated to the “hallmarks of cancer” [207].

2.1 Cargo of EVs

A proteomic study showed that exosomes contained a specific subset of proteins from endosomes, plasma membrane and cytosol and very few proteins from Golgi, mitochondria or nucleus [217]. Since then, many studies have shown different molecular compositions for various EVs populations, concluding that EVs' cargo is highly heterogeneous [218]. Indeed, nucleic acids, proteins, lipids and metabolites were already found in EVs cargo. While some of these are present only at the vesicle surface (such as MHC molecules, lipids, transmembrane proteins or adhesion molecules), others are exclusive from the vesicle lumen (such as transcriptional factors or splicing molecules). However, some components are located both at the surface and at the lumen of EVs, including oncoproteins (e.g. EGFR, pyruvate kinase, β-catenin), RNA-binding proteins, mRNAs, long non-coding RNAs or microRNAs [207]. Given the enormous amount of available data on EVs' content, three different databases with public access were created, in order to collect the datasets from the many EVs studies, named Exocarta, Vesiclopedia and EVpedia [219, 220].

2.1.1 Proteins

Regarding the protein content of EVs, some discrepancies are found in the literature, possibly due to the source and heterogeneity of the isolated EVs' populations in the various studies carried out. However, since this field is rapidly growing, new insights into the protein composition of EVs are expected within the next few years.

Proteins commonly found in EVs are usually those involved in EVs' biogenesis and release, including proteins associated to the endosomal pathway or components of the ESCRT machinery. Some examples include: Rab27a, Rab11B, ALIX, TSG101, ARF6 and tetraspanins like CD63, CD81 and CD9 [218]. The detection of some of those proteins is important for the characterization of isolated EVs populations [221]. In addition, transcription factors (e.g. as Notch or Wnt), proteins involved in signal transduction (e.g. EGFR), antigen presentation (e.g. MHC I and MHC II) and other transmembrane proteins (e.g. LAMP1, TfR) were also found in EVs [222].

In the cancer context, EVs were shown to carry mediators of tumorigenesis such as oncoproteins, growth factors or immunomodulatory molecules [223-225]. Regarding cancer MDR in particular, important MDR players such as drug-efflux pumps or inhibitors of apoptosis, were already found within EVs. This issue will be further discussed in section 2.6 of this thesis.

2.1.2 RNA

Horizontal transfer of RNA between donor and recipient cells has been proposed by Ratajczak *et al.* in 2006 [226]. Subsequently, Valadi and Skog have independently demonstrated that the intercellular transfer of mRNAs and microRNAs by EVs was a novel mechanism of genetic exchange between cells [227, 228]. Afterwards, several RNA species were found in the EVs cargo, such as mRNAs, miRNAs, rRNAs, long and short non-coding RNAs, tRNA fragments, piwi-interacting RNAs, vault RNAs, and Y-RNAs [229-233]. Interestingly, circular RNAs are also enriched and stable in EVs [218].

Most of the RNA species found in EVs have around 200 kb [218] suggesting a possible function in gene regulation [233-235].

The first study describing the functional transfer of small RNAs via EVs showed that viral miRNAs, endogenously produced in Epstein-Barr virus-infected B cells, were secreted via EVs and regulated gene expression in recipient dendritic cells [236]. Importantly, in 2014 Melo *et al*. proposed that EVs from breast tumour cells harbour the protein machinery to process pre-miRNAs into mature miRNAs. Mature miRNAs generated within these EVs influenced the transcriptome of non-malignant target cells, promoting their transformation. This awaits independent confirmation [237].

Several mechanisms are involved in the sorting of miRs/mRNAs into EVs, such as the 3' non-template terminal nucleotide additions, 3' sequence motifs/protein guides, ceramide biosynthesis, RISC-associated proteins and cellular miRs/ target mRNA levels [238]. In addition, several RNA binding proteins were associated to regulation of RNA sorting into EVs but this issue needs further clarification [239].

Among the different RNAs found present in EVs' cargo, miRs have been the most studied species due to their potential as biomarkers, namely in the cancer drug resistance field. Indeed, using plasma, serum or cell culture supernatant as source for EVs, several studies described the role of EVs-associated miRs in drug resistance. MiR-21 and miR-106a in gastric cancer, let-7g and let-181b in colorectal cancer, miR-221 and 122 in hepatocellular carcinoma, mir-130a in ovarian cancer, miR-34a in prostate cancer are some examples of miRs known to be associated with drug resistance and that have been found in the cargo of EVs [174]. The functional impact of the intercellular transfer of miRs from drug-resistant cells to drug-sensitive counterparts will be further described in section 2.6 of this thesis.

2.1.3 DNA

Although RNA is the most abundant nucleic acid found in EVs cargo, fragmented genomic DNA (gDNA), as well as mitochondrial DNA (mtDNA) or even parasitic DNA have

also been found in EVs isolated from cell culture supernatant and plasma samples [240-242]. The regulation of the DNA packaging into EVs is still unknown, but some authors defend that it is a random process [243, 244]. Importantly, in the cancer context, it was hypothesized that EVs could contribute to the efficient removal of damaged DNA [245].

2.1.4 Lipids

The lipid composition of EVs shares many features of the donor cells. However, some lipids are found enriched in EVs, such as sphingomyelin, cholesterol, ganglioside GM3, disaturated lipids, phosphatidylserine and ceramide [246]. By contrast, the percentage of some lipids, such as phosphatidylcholine and diacyl-glycerol, is reduced when compared with the donor cells [247]. The presence and proportion of specific lipid structures may reflect the biogenesis of the different types of EVs, originated either from the MVBs or from the budding of the plasma membrane [218].

2.2 EVs biogenesis: membrane-trafficking processes

Electron and immuno-electron microscopy provided important information about the biogenesis of secreted vesicles [248-250]. Independently of the EVs class, the biogenesis of all EVs involves membrane-trafficking processes, either by inward budding of the multivesicular body (MVB) or by outward budding of the plasma membrane [250]. Indeed, several similar intracellular mechanisms and sorting machinery are involved in both the biogenesis of EVs of endocytic origin and the biogenesis of EVs resulting from the budding of cytoplasmic membrane (Figure 5).

The EVs' biogenesis through the endocytic pathway is initiated with the intraluminal vesicles (ILVs) production in the MVB. Details of the endocytic pathway will be further described in section 3 of this thesis. The ILV formation requires two distinct processes: i) re-organization of the endosomal membrane, with an enrichment in tetraspanins like CD9 and CD63 [251], and ii) recruitment of the Endosomal Sorting Complex Required for Transport (ESCRT) to the site of the ILV formation [252, 253]. The discovery of the involvement of the ESCRT machinery in membrane shaping and scission was the first breakthrough in the investigation of the intracellular mechanisms associated to ILVs and MVB formation [254]. Interestingly, further studies showed that some ESCRT complexes are important regulators of the budding at the plasma membrane [255, 256], as indicated in Figure 5. Therefore, it is now clear that dependence on ESCRT complexes does not necessarily demonstrate a MVB origin for EVs [257].

Different authors have been investigating the specific cellular role of each of the ESCRT complexes. Briefly, it is now accepted that ESCRT-0 and ESCRT-I subunits are responsible for cargo clustering into the membrane microdomain, by an ubiquitin-dependent manner. Then, ESCRT-III subunits are recruited via ESCRT-II, for the budding and fission of this membrane microdomain [201, 257].The ESCRT-accessory proteins, such as VPS4 and ALIX, are responsible for the dissociation and the recycling of the ESCRT machinery [218]. Importantly, a variety of studies demonstrated that reducing the expression of ESCRT components, such as HRSS and STAM1 (ESCRT-0), TSG-101 (ESCRT-I) or CHMP4 (ESCRT-III), resulted in a decrease in EVs secretion [257]. Nevertheless, those studies should be carefully interpreted since some of these proteins are also involved in processes such as cytokinesis [258, 259] and membrane repair [260], thus their modulation affects other cellular mechanisms beyond EVs' biogenesis [257].

Further investigation showed that ESCRT-independent mechanisms are also involved in EVs' biogenesis. The first ESCRT-independent mechanism described is regulated by ceramide [261]. Indeed, EVs were normally secreted by oligodendroglial cells after the inhibition of the ESCRT pathway. Moreover, when ceramide biogenesis was impaired, the secretion of EVs decreased. Ceramide was proposed to induce inward curvature of the limiting membrane. Another study attributed a similar role on membrane curvature to phosphatidic acid [262]. In addition, tetraspanins (such as CD63, CD81, CD82 and CD9), syntenin/syndecan and ARF6/PLD2 also regulate ESCRT-independent endosomal sorting [263-266].

The literature describes that the activation of ESCRT-dependent or ESCRT-independent mechanisms is dependent on the donor cell type, as well as on the cargo. Membrane lipid composition seems to influence which pathways are activated [267]. Interestingly, the same cell may show subpopulations of MVBs which are distinguishable by different lipid/protein compositions and morphology [265, 268]. One important aspect related to MVB formation that still needs clarification is whether in a single MVB both ESCRT-dependent and independent mechanisms may be activated at the same time and if MVBs matured by both mechanisms may co-exist in the same cell [201].

An important triggering factor for membrane budding is alteration in lipid/protein composition, associated with changes in Ca^{2+} levels. In plasma membrane budding in particular, aminophospholipid translocases, scramblases and calpain induce rearrangements in the asymmetry of membrane phospholipids (exposition of phosphatidylserine to the cell surface), causing membrane physical bending and re-structure of the cytoskeleton [201, 269, 270]. In addition, two other families of proteins, the RHO family of small GTPases and the RHO-associated protein kinase (ROCK), have been

associated to the biogenesis of EVs produced by plasma membrane-budding particularly in tumour cells, due to regulation of actin dynamics [271].

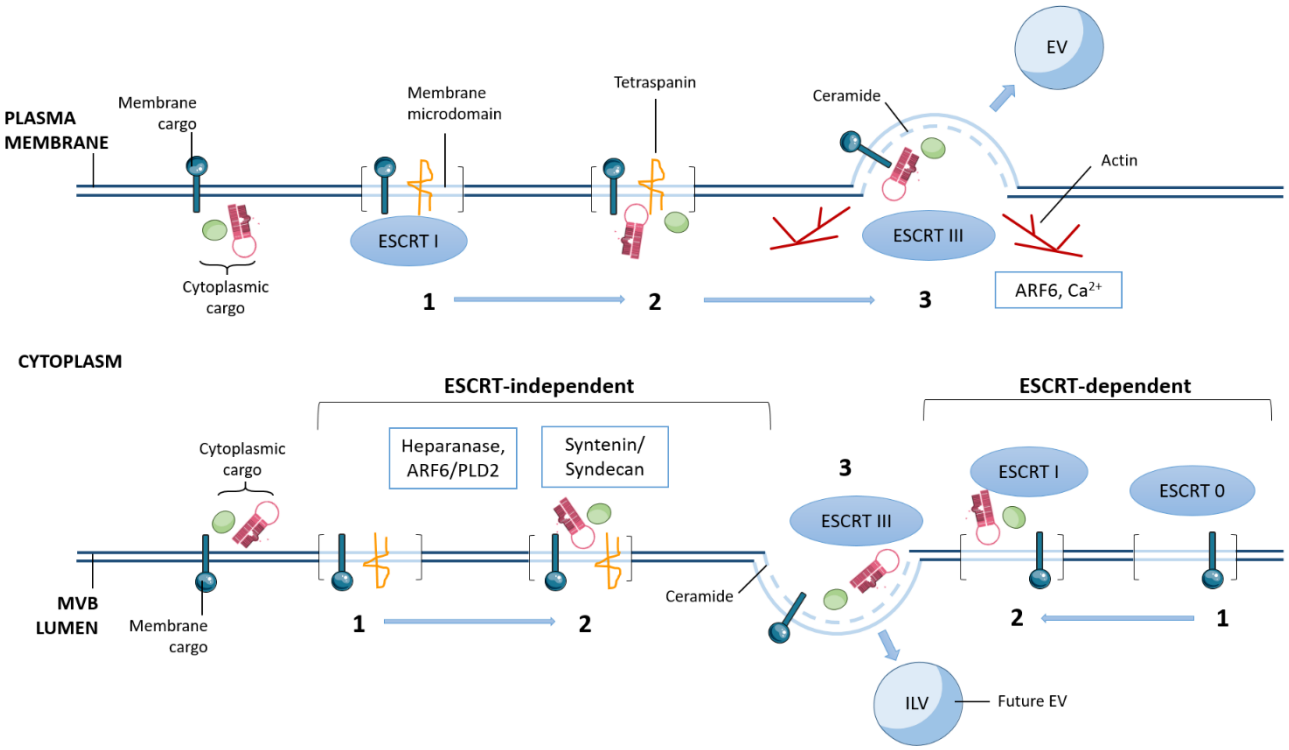


Figure 5: Membrane-trafficking processes involved in EVs production by inward and outward membrane budding. In ordered sequence: 1- Lipids and membrane-associated proteins are clustered in membrane microdomains of the plasma membrane or the limiting membrane of the multivesicular body (MVB). 2: Recruitment of soluble components, such as cytosolic proteins and RNA species, fated for sorting in extracellular vesicles. 3: Membrane budding followed by a fission process either at the plasma membrane or at the limiting membrane of the MVB. All these steps are tightly regulated by different components. Many regulators (e.g. ARF6, tetraspanins, ESCRT machinery and ceramide) are involved in biogenesis of EVs from both endocytic origin and budding of plasma membrane. Adapted from [201].

2.3 EVs secretion

The release of EVs generated by budding of the plasma membrane is faster than the release of EVs produced by the endocytic pathway [201]. In the first process, the cargo only needs to remain at the plasma membrane in order to be targeted into EVs. Then, its release naturally occurs following generation and fission of the plasma membrane. By contrast, release of EVs originated by the endocytic pathway requires additional steps to sort cargo into MVBs and ILVs; in addition, it requires further regulation to target MVBs to

the plasma membrane and subsequent secretion [201]. These differences may have an impact on the function of each of the types of EV.

2.3.1 Secretion of EVs from endocytic origin

MVBs which are destined for exocytosis are transported to the plasma membrane, along the microtubules, by the molecular motor kinesin [239]. A major class of proteins involved in the transport of MVBs to the plasma membrane is the RabGTPase family. The most described Rabs associated to MVB transport are: RAB11, RAB35, or RAB27A/27B. Different studies showed that silencing these proteins individually results in a reduction of the release of EVs originated by the endocytic pathway [272]. Nevertheless, as described for the ESCRT machinery, Rab proteins are involved in other cellular mechanisms [257], therefore these studies should be carefully interpreted.

Following transport and docking to the plasma membrane, secretory MVBs couple to the SNARE (soluble N-ethylmaleimide-sensitive component attachment protein receptor) membrane fusion machinery. The SNAREs proteins, namely SNAP23, Syntaxin-4 and VAMP7 have been associated to EVs release by tumour cells [273-275]. SNAREs activity is partly controlled by their phosphorylation profile, which influences their localization and their interaction with other SNARE partners [276]. Importantly, Ca^{2+} may also have a role in the activation of the SNARE complexes [277-279]. Following the fusion of MVBs with the plasma membrane (regulated by SNAREs), ILVs are released as EVs.

2.3.2 Secretion of EVs originated from budding of the plasma membrane

The release of EVs originated from budding of the plasma membrane requires a fission process, which is dependent on the interaction of actin and myosin with a subsequent ATP-dependent contraction [280, 281]. The regulation of this mechanism by small GTP binding proteins, such as ARF6 and ARF1, was described in tumour cells [282-284]. Importantly, ARF6 was also associated to secretion of EVs originated by the endocytic pathway, through activation of phospholipase D2 [262]. Interestingly, TSG101 and VPS4, both associated to the ESCRT machinery, also participate in the scission and release of EVs originated from budding of the plasma membrane [284]. In addition, trimeric ATP-gated cation channels, named $P2X_7$ receptors, are involved in this process by translocating the acidic sphingomyelinase to the plasma membrane, where it generates ceramide, promoting membrane bending and EVs release [285-287]

2.4 Interaction of EVs with recipient cell

Once released, EVs may interact with recipient cells by different mechanisms. Following docking at the plasma membrane, it is accepted that EVs: i) activate surface receptors in recipient cells, and/or ii) fuse with recipient cells, and/or iii) are captured by recipient cells. All these processes are complex and may depend on the origin/composition of EVs, as well as on the presence of specific structures at the membrane of recipient cells [201]. Nevertheless, to date little is known about the fate of different subtypes of EVs once they reach recipient cells [272].

Regarding the activation of surface receptors in recipient cells, the main mediators described include: tetraspanins, integrins, lipids, lectins, heparin sulfate, proteoglycans and ECM components. Importantly, the interaction of integrins (in recipient cells) with the ECM has an important role in EVs' binding (either from plasma membrane budding or from endocytic origin) [288-290].

After binding recipient cells, EVs remain at the plasma membrane or are captured by different processes [265, 291]. When EVs remain at the cell plasma, the EV membrane surface can trigger signalling in the recipient cell through interaction with receptors/ligands on the cell surface without EV entry as, for example with EGFRvIII, Notch and RHEB and IFN-c/STAT[218]

Regarding the EVs' fusion with the plasma membrane of recipient cells, it is describe to occur at low pH conditions (such as the ones found in tumours) [292, 293]. Basically, the two outer-leaflets (from EVs and plasma membranes of recipient cells) come into direct contact, driving a hemi-fusion stalk with fused outer-leaflets. After this, a fusion pore opens and the two hydrophobic cores mix, resulting in one consistent structure [294-297]. Different proteins are involved in these mechanism such as SNAREs, Rabs, and Sec1/Munc-18 related proteins [297].

Concerning EVs' capture by recipient cell, the main mechanisms involved are clathrin-mediated or clathrin-independent endocytosis (micropinocytosis or phagocytosis [298-300]) and endocytosis via caveolae [301-303]. Importantly, the lipid composition of the plasma membrane of recipient cells, such as the presence of lipid rafts, also regulates EVs' endocytosis, since disruption of lipid rafts by cholesterol depletion decreases uptake of extracellular vesicles [304]. Lipid rafts are microdomains within the plasma membrane with altered phospholipid compositions, rich in protein receptors and sphingolipids. These rafts are found in the invaginations formed by caveolin-1 or in planar regions of the plasma membrane marked by flotillins [305]. Flotillins associated with lipid rafts, seems to mediate endocytosis in a clathrin and caveolin independent-manner [306, 307].

Depending on the EVs capture route, different players could be involved, such as heparan sulphate proteoglycans, galectin-5, fibronectin, actin, dynamin, flotillin, cholesterol or glycoshingolipids [308]. This research field needs more clarification since several players associated to EVs' capture are also involved in processes associated with membrane budding, which also influence the biogenesis of EVs.

Following capture, EVs enter into the endocytic pathway and reach MVBs. The most frequent fate of EVs is lysosomes, triggering degradation of proteins and lipids, providing an important source of building blocks to the recipient cells [309]. Nevertheless, EVs may also release their cargo into the cytoplasm of recipient cells [259], thus being an important process for nucleic acid intercellular transfer [201]. Importantly, there is no evidence to exclude recycling to the plasma membrane of endocytosed EVs. Further studies are needed to clarify this point.

2.5 EVs role in cancer

A large body of evidence has been demonstrating a great impact of EVs in tumour initiation, progression and relapse [225, 227]. Importantly, several authors suggested that tumour cells release increased number of EVs than non-malignant cells [239]. Indeed, various tumours showed upregulation of ESCRT constituents, syntenin and heparanase. It is now accepted that EVs are involved in a wide range of processes such as angiogenesis, lymphogenesis, cell migration, cell proliferation, immune suppression, inflammation, invasion, epithelial- to-mesenchymal transition, and metastasis [207].

In cancer, EVs may participate in intercellular communication by three different ways: i) from tumour cells to stroma cells, ii) from stroma cells to tumour cells, and iii) from tumour cells to other tumour cells. Briefly, EVs released by tumour cells may induce alterations in different types of stroma cells, "educating" them to have a proangiogenic, a prometastatic and an immune suppressive phenotype [310, 311]. Moreover, EVs from tumour cells may regulate the pre-metastatic niche formation, by altering the behavior of bone marrow-derived progenitors [225, 312]. In addition, EVs released by stromal cells may promote tumour cell growth, increase invasiveness and increase drug resistance [240, 313]. Finally, EVs from a tumour cell subpopulation (within a heterogeneous tumour) are able to transfer cargo to other subpopulations [239]. In a cancer drug-resistant context in particular, it is known that tumour drug-resistant cells (donor cells) may transfer different drug-resistant players to drug-sensitive cells (recipient cells), resulting in the acquisition of MDR traits by the recipient cells. This will be addressed in the following section of this thesis (section 2.6).

2.6 REVIEW ARTICLE:

Intercellular transfer of cancer drug resistance traits by extracellular vesicles

Diana Sousa, Raquel T. Lima and M. Helena Vasconcelos

Published in Trends Mol Med., 21 (10): 595-608 (2015)

Trends in Molecular Medicine

CellPress

Review

Intercellular Transfer of Cancer Drug Resistance Traits by Extracellular Vesicles

Diana Sousa,[1,2,3] Raquel T. Lima,[1,2,4] and M. Helena Vasconcelos[1,2,3,*]

Extracellular vesicles (EVs) are nanosized particles (100–1000 nm) enclosed by a phospholipid bilayer that have been described as important mediators of intercellular communication. The role of EVs in oncobiology has been extensively studied, including their contribution to the horizontal transfer of drug resistance from drug-resistant to drug-sensitive cancer cells. This review focuses on the EVs cargo responsible for this intercellular transfer of drug resistance; namely, drug-efflux pumps, miRNAs, long noncoding RNAs (lncRNAs), and other mediators. Additionally, the known molecular mechanisms and features of this transfer are discussed. This is an emerging area of research and we highlight topics that need to be further studied to fully understand and counteract the intercellular transfer of drug resistance mediated by EVs.

Trends

EVs shed by drug-resistant (donor) cells contribute to the dissemination of CDR by transferring their cargo to drug-sensitive (recipient) cells.

The cargo of the drug-resistant EVs may be selectively packaged and may include drug-efflux pumps, miRNAs, or lncRNAs.

The drug-efflux pumps transferred by EVs to drug-sensitive cells are functional in the recipient cells.

Drug-efflux pumps carried by EVs may be responsible for the sequestration of drugs in those EVs.

EVs may protect miRNAs from the action of RNase.

Evidence for the Transfer of a Cancer Drug Resistance Phenotype by EVs

Intercellular communication represents a highly complex network that influences the malignant potential of cancer cells [1]. Classically, this network has been described as involving direct secretion of molecules from cells or direct cell–cell interaction. Nevertheless, in the past 25 years another fundamental mechanism has emerged that is based on the shedding of EVs (Box 1) by some cells (the donor cells) and their incorporation by others (the recipient cells) [2].

The biogenesis, function, and cargo selection of EVs in normal physiology, as well as under pathological conditions, has received much attention over the past few years. Despite their recognized importance in autoimmune malignancies, neurodegeneration and, infection, so far the best understood role of EVs in disease is in the field of tumor biology, namely in tumor progression and aggressiveness [3]. Various studies have already described the signaling pathways involved in the role of EVs in: 'educating' the prometastatic behavior of progenitor bone marrow cells [4]; cancer cell protrusive activity, motility, and metastasis [5]; angiogenesis-modulating stimuli [6]; and cancer immune escape and progression [7].

Importantly, EVs have also been described as a noteworthy vehicle of dissemination of cancer drug resistance (CDR). The role of EVs in sustaining CDR networking has been associated with mechanisms such as promotion of immune escape, angiogenesis and metastasis, epithelial-to-mesenchymal transition, and fibroblast-like cell formation [8]. EVs may be shed from drug-resistant (donor) cells, transferring mediators of drug resistance to the drug-sensitive (recipient) cells, which then may acquire the CDR phenotype (Figure 1). In the past few years, several players associated with drug resistance in cancer cells have been identified as being transferred by EVs and, moreover, to be mediators of the dissemination of this phenotype (Table 1). These mediators include drug-efflux pumps, **miRNAs** (see Glossary), and **lncRNAs** (Table 1). In

[1]i3S-Instituto de Investigação e Inovação em Saúde, Universidade do Porto, Porto, Portugal
[2]Cancer Drug Resistance Group, Institute of Molecular Pathology and Immunology of the University of Porto, IPATIMUP, 4200-135 Porto, Portugal
[3]Department of Biological Sciences, Faculty of Pharmacy, University of Porto, 4050-313 Porto, Portugal
[4]Department of Pathology and Oncology, Faculty of Medicine of the University of Porto, 4200-319 Porto, Portugal

*Correspondence:
hvasconcelos@ipatimup.pt
(M.H. Vasconcelos).

© 2015 Elsevier Ltd. All rights reserved.

Box 1. EVs: Exosomes and Microvesicles

The term EVs collectively refers to several types of vesicle, such as microvesicles, exosomes, and apoptotic bodies, with different sizes, origin, and molecular cargo (which may be used as markers). The classification of the different types of vesicles remains a debatable issue, but currently there is a set of characteristics that is almost consensual. Exosomes seem to be smaller (30–100 nm) and to have an endocytic biogenesis. Microvesicles represent a larger and more heterogeneous population (100–1000 nm) and originate from cellular membrane budding (Figure 1) [76]. Currently available methods do not allow pure isolation of exosomes from microvesicles, therefore hindering the proper characterization of each type of vesicle individually. As a result, in the past few years the scientific community has been stressing the need that all published results in this field include a detailed description of the isolation protocols used and that authors refer to 'EVs' as a whole [37,77].

addition to the studies of their transfer to drug-sensitive cells, other reports have described the enrichment of some of these mediators (namely lncRNAs) in EVs, as well as an increase of their expression in the cells of origin, following treatment with chemotherapeutic agents [9,10]. Moreover, the involvement of EVs in the sequestration of drugs due to the presence of drug-efflux pumps in those EVs has also been described [11,12]. Additionally, tumor acidity was shown to increase the release of EVs by tumor cells [13] and drugs may be trapped within the highly acidic EVs released by tumor cells [14–16]. This sequestration of drugs in tumor-derived EVs decreases

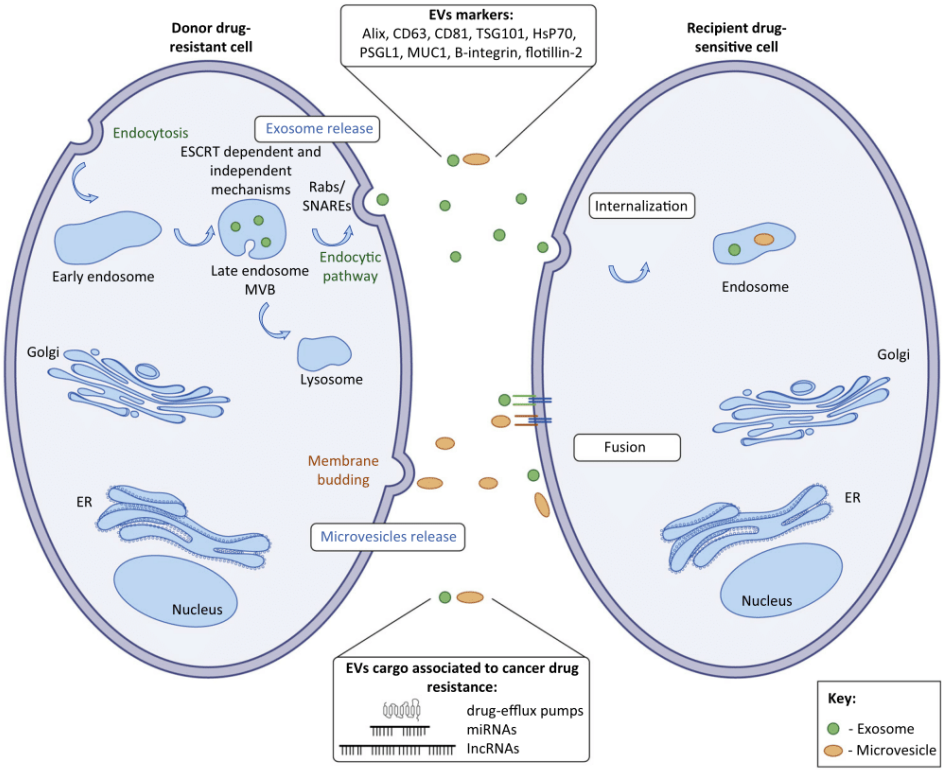


Figure 1. Mechanisms Involved in Intercellular Transfer of Drug Resistance Mediated by Extracellular Vesicles (EVs). Drug-resistant (donor) cells may communicate with drug-sensitive (recipient) cells by the intercellular transfer of various types of EVs, namely, exosomes and microvesicles. Exosomes, of endocytic origin, are formed by inward budding of the multivesicular body membrane. The initial steps of this process are usually controlled by the endosomal sorting complex required for transport (ESCRT). The mechanisms involved in the release of exosomes are also regulated by other protein families, such as Rab GTPases and SNARES. By contrast, microvesicles emerge from outward blebbing of the cellular plasma membrane. Once EVs reach the recipient cell, they may fuse with the plasma membrane or be internalized by the endocytic pathway. EVs may transfer miRNAs, long noncoding RNAs (lncRNAs), proteins (such as drug-efflux pumps), and other key players responsible for drug resistance, which allows the dissemination of cancer drug resistance traits to the recipient cells.

Glossary

Long noncoding RNAs (lncRNAs): a group of noncoding RNAs, more than 200 nucleotides long, that act as important transcriptional and post-transcriptional regulators.

miRNAs: small noncoding RNAs (18–24 nucleotides) that regulate gene expression. Alterations in miRNA profile have been associated with several malignancies such as cancer.

Multidrug resistance (MDR): a phenomenon whereby cancer cells develop cross-resistance to various drugs following exposure to one drug that is structurally and functionally very dissimilar. Overexpression of ABC transporters is one of the major causes of the MDR phenotype observed in cancer cells. The main function of ABC transporters is the efflux of several amphipathic substrates, thereby protecting normal cells from toxic xenobiotics. In a drug resistance context, high levels of these efflux pumps, such as P-gp, ABCG2/breast cancer resistance protein (BRCP), or MRP1/ABCC1, results in the efflux of chemotherapeutic drugs from cancer cells culminating in intracellular sublethal concentrations of these compounds.

Table 1. EVs from Donor Drug-Resistant Cells May Transfer Drug Resistance Phenotype to Recipient Drug-Sensitive Cells through Mechanisms Involving Various Modulators

Modulators of CDR Phenotype Transferred by EVs		Featured Findings	Most Significant Performed Assays	Refs
Drug-efflux pumps	P-gp	Intercellular transfer of functional P-gp occurred between various tumor cell types and resulted in increased drug resistance of recipient cells both *in vitro* and *in vivo*. The acquired resistance allowed the recipient tumor cells to survive potentially toxic drug concentrations long enough to develop intrinsic P-gp-mediated resistance.	Flow cytometry, fluorescence microscopy	[26,28]
	ABCG2	High levels of ABCG2 in EVs shed by mitoxantrone-resistant breast cancer cells mediate their resistant phenotype. The PI3K–Akt signaling pathway is a key regulator of subcellular localization of ABCG2, EV biogenesis, and their MDR function. Pharmacological inhibition of Akt signaling results in gradual relocalization of ABCG2 from the EV membrane to the cytoplasm.	Trypan blue exclusion assay, confocal microscopy	[18,21,34]
	MRP1	In a leukemia model, drug-resistant derived EVs transfer functional MRP1 to drug-sensitive cells. The recipient cells were shown to acquire a drug-resistant phenotype.	SEM, calcein-AM functional accumulation assay, qRT-PCR	[33]
	ABCA3	ABCA3 positively modulated EV release from B-cell lymphoma cells. This modulation was critical for the resistance of lymphoma cells to anti-CD20 antibody (used in immunotherapy of malignant B-cell lymphoma), since these EVs carried CD20, which bound the antibodies, consumed complement, and protected target cells from antibody attack.	Acetylcholinesterase activity, transfection with siRNAs	[39]
miRNAs	miR-100, miR-222, miR-30a	miR-100, miR-222, and miR-30a were transferred to drug-sensitive breast cancer cell lines after co-culture with EVs from various drug-resistant cell lines. miR-222-rich EVs altered target gene expression in drug-sensitive cells.	Microarray analysis, target gene prediction by bioinformatics, pathway analysis, transfection with mir-222 mimics	[58]
	miR-34a, miR-145	In response to 5-FU treatment, human colon cancer cells preferentially secreted, via EVs, tumor-suppressor miRNAs such as miR-34a and miR-145, resulting in a decrease in the intracellular levels of these miRNAs.	NTA, qRT- PCR, 5-ethynyl uridine assay	[60]
	miR-485-3p	Fludarabine treatment enhanced the release of prostate cancer secretory miRNA by EVs. Nevertheless, the surviving cells harbored a specific miR, miR-485-3p, suggesting its relevance for the cellular response to fludarabine.	qRT-PCR, co-immunoprecipitation, transfection with antagomir	[61]
	miR-1228, miR-1246, miR-1308, miR-149, miR-455-3p, miR-638, miR-923	EVs carried transcripts of the membrane vesiculation machinery and enzymes essential for miR biogenesis. Moreover, EVs were found to re-template the deleterious traits of donor drug-resistant cells in drug-sensitive cells. This effect is likely to be due to the selective packaging of specific miRNAs in EVs shed by drug-resistant cells (miR-1228, -1246, -1308, -149, -455-3p, -638, -923).	Microarray analysis, qRT-PCR, hierarchical clustering and target pathway analysis	[63]
	miR-1246, miR-23a, miR-1469, miR-638, miR-1915, miR-2861,	In a breast cancer model, 20 miRNAs were identified as the most abundant in EVs shed by drug-resistant cells. Of the significant	Target gene prediction and	[57]

Table 1. (continued)

Modulators of CDR Phenotype Transferred by EVs		Featured Findings	Most Significant Performed Assays	Refs
	miR-24, miR-149*, miR-3178, miR-3196, miR-16, miR-23b, miR-762, miR-663, miR-26a, miR-27a, miR-1,908, let-7a, let-7b, let-7c	pathways for these miRNAs, several were implicated in therapy failure. Moreover, it was reported that miRNAs present in these EVS caused an increase in resistance to docetaxel following EV incubation with drug-sensitive cells.	pathway analysis, qRT-PCR	
	miR-598,miR-34a, miR-148a, miR-146a	A direct correlation between the miRNAs expressed in donor prostate cancer cells and their derived EVs was found. Among the studied miRNAs, four were identified as potential biomarker signature. Particularly, miR-34a seems to have clinical relevance.	TEM, global miRNA profiling, qRT-PCR	[52]
	miR-22-3p, miR-185-5p, miR-503-5p, miR-652-3p, miR-1280	Five miRNAs were identified as potentially associated with the acquisition of a MDR phenotype mediated by EVs. miR-503-5p (inversely associated with metastasis) was shown to be downregulated in recipient breast cancer cells after incubation with drug-resistant derived EVs. It was suggested that EVs could provide a link between drug resistance and metastasis.	Global miRNA profiling, miR-503 antagomir transfection	[62]
lncRNAs	linc-ROR	Sorafenib treatment increased linc-ROR expression in HepG2 tumor cells as well as its levels in their released EVs. Moreover, EVs shed by HepG2 cells silenced for linc-ROR, when compared with EVs shed by cells transfected with control siRNAs, reduced the viability of HCC recipient cells following treatment with sorafenib; this suggested a correlation between the transfer of linc-ROR by EVs and drug response.	NTA, MTS, qRT-PCR, transfection with siRNA	[9]
	linc-VLDR	Co-culture of HCC cells with HCC-derived EVs reduced chemotherapy-induced cell death and increased linc-VLDR expression in recipient cells.	qRT-PCR-based assays, transfection with siRNA, cell viability, and cell growth assays	[78]
Other modulators	TrpC5	EVs from tumor cells transferred TrpC5 to human microvessel endothelial cells, inducing the expression of P-gp by activation of the transcription factor NFATc3. TrpC5-containing circulating EVs derived from breast cancer cells may transfer drug resistance properties to drug-sensitive recipient cells.	Adriamycin accumulation assay, confocal microscopy	[70,71]

NTA, nanoparticle tracking analysis; qRT-PCR, quantitative real-time PCR; SEM, scanning electron microscopy; TEM, transmission electron microscopy.

the available intracellular drug concentration in the tumor cells that release EVs and may therefore be considered a drug resistance mechanism in EVs-donor cells (but not EVs-recipient cells). Nevertheless, this review focuses only on the intercellular transfer of drug resistance mediated by EVs.

Several studies have been trying to unravel the molecular mechanisms underlying the dissemination of CDR traits by EVs [17–20]. This is reviewed in the following section.

Transfer of Drug Resistance Traits by EVs: Drug-Efflux Pumps

The presence of drug-efflux pumps in EVs is highly relevant in the context of drug resistance, not only because both P-glycoprotein (P-gp) and ATP-binding cassette (ABC) transporter G2 (ABCG2) present in EVs may mediate the active sequestration of drugs in those vesicles (leading

Box 2. Role of EVs in Drug Removal from Cells

It is known that cells may remove therapeutic drugs by secreting the drugs inside EVs [9], contributing to drug resistance in those cells. For example, doxorubicin and various small molecules have been found accumulated in EVs shed by tumor cells following treatment [10]. It has been proposed that the hydrophobic character of these drugs may promote their interaction with lipids from the EV membrane, resulting in the final elimination of the drug complexed with the lipids of the shed vesicles [10]. Interestingly, it was found that EVs from human ovarian cancer cells that were resistant to cisplatin contained 2.6 times more drug than EVs released from their sensitive counterpart cancer cells. Moreover, the observed increase in EVs-mediated drug export was accompanied by increased levels of the putative cisplatin export transporters MRP2, ATP7A, and ATP7B in these EVs [11].

to sublethal concentrations of these compounds in the donor cells; Box 2) but also because recipient cells may 'gain' the drug-efflux pumps that are shed from donor cells [11,21,22]. Various studies have recently emerged describing the transfer of these drug-efflux pumps by EVs from drug-resistant to drug-sensitive cells and their role in the acquisition of a **multidrug resistance (MDR)** phenotype by the drug-sensitive (recipient) cells [23,24].

P-gp

P-gp transfer from drug-resistant to drug-sensitive cells, independently of genetic mechanisms, has been described in several different models [25–28]. This 'non-genetic acquisition' of P-gp in the context of MDR was shown for the first time in a neuroblastoma model, in which a drug-sensitive cell line acquired functional P-gp following co-culture with a drug-resistant (P-gp expressing) counterpart cell line [26]. This phenotype persisted both under selective pressure with colchicine and in the presence of the donor (P-gp expressing) cells. Furthermore, as a consequence of P-gp transfer, the acquired resistant phenotype persisted for 4 months, suggesting that a stable resistant cell line had been selected. It was also proposed that P-gp transfer could result from the exchange of relatively large vesicles (800 nm maximum) [26]. Taking this into account, Bebawy and coworkers investigated the potential involvement of EVs averaging a typical size of 500 nm in P-gp transfer. Drug-sensitive leukemia cells were co-cultured with EVs isolated from their drug-resistant counterparts and, following incubation for 2 and 4 h, the recipient cells displayed expression of functional P-gp. The short time necessary for this effect suggested that the transfer of exogenous P-gp from donor cells had occurred, rather than induction of transcription and subsequent translation of the *MDR1* gene in recipient cells [28]. Another study using two docetaxel-resistant prostate cancer cell lines allowed the conclusion that EVs were important mediators of the acquisition of docetaxel resistance by recipient cells, partly due to P-gp transfer [29].

Since then, other studies have shown the EV-associated transfer of P-gp to be a mediator of the acquisition of CDR traits. A drug-sensitive breast cancer cell line was shown to acquire a drug-resistant phenotype following co-culture with EVs extracted from its docetaxel-resistant counterpart, which was not observed following incubation with their own EVs. Interestingly, this study also showed that the observed increase in P-gp levels of the recipient cells was proportional to the amount of the co-cultured EVs from drug-resistant cells [30]. A recent report showed that a drug-resistant prostate cancer cell line released up to three times more EVs than its drug-sensitive counterpart. P-gp was enriched in EVs shed by drug-resistant cells but not in EVs shed by drug-sensitive cells [19].

Moreover, the 'spread' of drug resistance by EVs isolated from a paclitaxel-resistant ovarian cancer cell line has been described. In this study, the transfer of functional P-gp to the drug-sensitive recipient cells was also observed [31].

In vivo studies have also been performed to investigate the EV-mediated transfer of P-gp in a drug resistance context. Lechvenko and colleagues, using neuroblastoma xenograft mouse models of drug-sensitive cells, drug-resistant cells, and a mixture of these cell populations,

confirmed the *in vivo* transfer of P-gp. They found that the levels of P-gp in recipient cells were dramatically increased compared with the *in vitro* experiments performed with the same cell lines, indicating higher efficiency of this transfer in a more physiological environment [26]. Likewise, using a breast tumor xenograft model, expression of P-gp following a single administration of EVs shed by drug-resistant cells was observed at two different time points (24 h and 2 weeks following administration of EVs), suggesting the capacity of EVs to promote prolonged retention of P-gp by the recipient cells, even without selective drug pressure [17]. The mechanisms behind this long-term P-gp expression are not understood and cannot be explained by the transfer of P-gp alone, since the half-life of P-gp is much shorter than 24 h (being approximately 14–17 h). This is an area of research that needs further investigation. It is possible that, together with P-gp, miRNA or even DNA is transferred, and this could be responsible for the long-term P-gp expression in recipient cells.

The characteristics and pathways by which drug-sensitive cells acquire resistance from EVs containing P-gp have been further investigated. Although some work has reported that EVs from drug-resistant cells carried P-gp inserted in the membrane with an orientation identical to the one observed in donor cells [28], one study has suggested that P-gp may also be inserted in EVs with an inverted orientation (with respect to its catalytic domains) [11]. This orientation seems to promote the influx of drugs to the interior of EVs, rather than the typical efflux function. These authors also claimed that although passive sequestration of chemotherapeutic drugs (in particular of the anthracycline class) occurred in EVs derived both from drug-sensitive and drug-resistant cells, only the EVs from drug-resistant cells were able to promote active sequestration of drugs. This further promotes drug resistance in the donor cells, by decreasing the intracellular concentration of the drug. The ability of EVs to sequester drugs was also dependent on their size [11]. Another unresolved issue is what happens to P-gp once the EV is incorporated into the recipient cells: is it inverted (with ATP-binding domains oriented to the outside of the membrane) or in the same position as in the donor cells? The answer to this question is crucial to understanding the role of P-gp in the intercellular transfer of drug resistance.

Interestingly, one report describes the transfer of cancer traits (namely, increased P-gp levels) from drug-resistant cells to drug-sensitive cells as a process dependent on the type of donor cell. EVs derived from drug-resistant breast cancer cells were shown to transfer P-gp to malignant recipient cells only, while EVs shed by leukemia cells transferred P-gp [and multidrug resistance-associated protein 1 (MRP1)] to both malignant and non-malignant cells [17]. These findings demonstrated for the first time that P-gp transfer by EVs may be 'tissue selective' and seems to be associated with the cellular origin of the EV itself rather than to a specific feature of the recipient cell membrane [17]. Another recent report explored the selectivity of the transfer of P-gp. EVs derived from drug-resistant leukemia cells were found to transfer P-gp to drug-sensitive breast and lung cancer cells, displaying no cell-type selectivity [32]. Taken together, these studies indicate that the selectivity of the EV cargo is a debatable issue and needs further investigation.

MRP1

The transfer of MRP1 by EVs has also been reported to be associated with CDR. A study by Lu and coworkers, in acute lymphoblastic leukemia cells, showed that drug-resistant cells spontaneously shed EVs that transferred functional MRP1 to drug-sensitive counterpart cells [33]. EVs were shown to alter traits and the transcriptional environment of recipient cells [33]. Interestingly, the MRP1-mediated drug-resistant phenotype was observed in the recipient cells up to 12 h following the transfer of EVs, which is longer than what had been described for P-gp in cell-culture experiments [28]. The authors suggested that this discrepancy may be due to either the different protocols used in the studies or the complexity of the MDR mediated by the efflux pumps carried by EVs.

ABCG2

As described above for P-gp, the involvement of ABCG2 in resistance to mitoxantrone was shown to be associated with the sequestration of the chemotherapeutic agent by ABCG2-rich EVs [21]. In addition, ABCG2-rich EVs were also shown to sequester riboflavin, topotecan, imidazoacridinones, and methotrexate [34]. This ability of ABCG2-rich EVs to sequester chemotherapeutic drugs could be a cellular mechanism used to overcome MDR. Interestingly, further work showed that if the accumulated drugs were photosensitive, the photoexcitation of these EVs led to their rapid lysis, which culminated in the death of the EVs' donor cells through the activation of a reactive oxygen species (ROS)-dependent lysosomal mechanism; the authors suggested this as a strategy to selectively target MDR cells [35].

ABCG2 is also relevant for EV production. A report aiming to understand the molecular mechanisms underlying ABCG2 localization and MDR showed a decrease in resistance to mitoxantrone and topotecan upon the inhibition of Akt signaling, which resulted in cytoplasmic relocalization of ABCG2. In addition, the retention of ABCG2 in the intracellular environment caused a decrease in the size and number of EVs, culminating in gradual EV elimination and in the overcoming of the MDR phenotype by the donor drug-resistant cells [18]. This study suggests that the membrane localization of ABCG2 (and possibly other drug-efflux pumps) may be relevant for the release of EVs from the cell (in terms of the number and size of EVs).

Ceramide, a sphingolipid associated with secretion of EVs, was shown to regulate the cellular localization of ABCG2. In a breast cancer cell model, an increase in ceramide reduced ABCG2 cellular levels by inducing its association and secretion by EVs. This resulted in the sensitization of cells to doxorubicin, suggesting the relevance of this mechanism to the MDR phenotype [36].

Further studies regarding the transfer of ABCG2 between drug-resistant EVs and drug-sensitive cells are needed. Most of the reports described above for the role of ABCG2 in the mediation of CDR are supported by cell-based studies, rather than using EVs isolated from drug-resistant cells, and these types of experiment remain controversial [37].

ABCA3

The lysosome-related, organelle-associated drug-efflux pump ABCA3, which is related to drug resistance [38], was shown to modulate EV release from B-cell lymphoma cells. This modulation was described as a determinant of the susceptibility of tumor cells to antibody therapy [39]. Silencing of ABCA3 resulted in a decrease in EVs released by various B-cell lymphoma cell lines. Accordingly, overexpression of this efflux pump promoted an increase in EVs shed by some of those cells, associated with an increased resistance to rituximab.

Transfer of Drug Resistance Traits by EVs: miRNAs

miRNAs are commonly deregulated during tumorigenesis and metastization and can affect drug responses [40–46]. Due to their stable detection in serum and plasma, miRNA signature profiles have become useful tools for cancer diagnosis and prognosis. Interestingly, miRNAs packaged into EVs are protected from the action of RNases compared with naked miRNAs [47]. In addition, reports about the transport of miRNAs by EVs introduced reliable evidence to justify not only the study of novel strategies for targeting miRNAs but also the use of miRNAs carried by EVs as prognostic markers of drug response and/or drug resistance [48,49]. Several studies have discussed the use of circulatory miRNAs carried by EVs as potential biomarkers of cancers with poor survival and with chemo- and radioresistance [48–51]. Additionally, global miRNA profiling of docetaxel-resistant cell lines and their EVs allowed the identification of a panel of four miRNAs (miR-598, -34-a, -148a, and -146a) with possible clinical relevance as biomarker signature for prostate cancer progression [52]. Importantly, this study also showed that

exosomal miRNA profiles reflected their cells of origin, which is in agreement with what had been described in other studies using different models [49,53,54].

In the past few years, cell-based studies have shown the influence of miRNAs carried by EVs in the intercellular transfer of CDR traits [55]. For example, Jaiswal and colleagues showed that EVs shed by MDR cells may: (i) incorporate and transfer miRNAs from drug-resistant to drug-sensitive cells; and (ii) modulate transcripts in recipient cells. This re-templating of the transcriptional landscape of recipient cells, mediated by MDR EVs, illustrates the implications of this pathway in the dissemination and acquisition of deleterious traits in clinical oncology [56]. Comparison of the miRNA profiles of recipient (drug sensitive) cells following co-culture with drug-resistant EVs demonstrated the re-templating of cancer donor traits in the recipient cells in both hematological and non-hematological models. This work also revealed, for the first time, the interesting idea that miRNAs are 'selectively packaged' and transferred by donor drug-resistant EVs [56].

The selective packaging of specific miRNAs carried by drug-resistant EVs has been demonstrated by further studies. For example, a study based on an miRNA expression profile using docetaxel-resistant breast cancer cells and their derived EVs demonstrated a pattern of miRNAs shared by both [57]. In addition, a group of miRNAs were found only in the EVs from drug-resistant cells and not in the cells themselves, which supports the idea of selective packaging into EVs. The most abundant miRNAs in EVs derived from drug-resistant cells were: miR-1246, -23a, -1469, -638, -1915, -2861, -24, -149star, -3178, -3196, -16, -23b, -762, -663, -26a, -27a, and -1,908 and let-7a, -7b, and -7c. In addition, from the significant pathways regulated by those miRNAs, five were related to therapy failure, indicating that their transfer is possibly associated with the acquisition of a CDR phenotype. Co-culture of these drug-resistant EVs with drug-sensitive cells showed the transmission of drug resistance as well as the downregulation of reporter genes (including Sprouty2, a known target of miR-23a) [57]. The selective packaging of miRNAs into EVs has also been described in another report, which identified a miRNAs cluster that was enriched in breast cancer drug-resistant EVs when compared with their drug-sensitive counterparts [58]. The expression of these miRNAs was increased in drug-sensitive cells following incubation with drug-resistant EVs. Moreover, a clear reduction in apoptosis was found in drug-sensitive cells following incubation with drug-resistant EVs. Interestingly, these effects were markedly impaired by pretreatment of drug-resistant EVs with RNase, suggesting that the biological function of these EVs was mediated by shuttling of RNAs. In addition, one of the miRNAs identified in EVs, miR-222, was shown to alter target gene expression in the drug-sensitive recipient cells, as demonstrated with miR-mimic experiments [58].

Other reports have attempted to correlate the levels of specific miRNAs carried by EVs with the acquisition of donor drug-resistant traits. For example, expression of miR-221/222 was upregulated in breast cancer drug-resistant cells and enriched in their EVs, and its transfer to drug-sensitive cells was confirmed [59]. This transfer led to the transmission of tamoxifen resistance to drug-sensitive cells, which was reverted by antimiR-221/222 transfection. Moreover, the decrease in the levels of miR-221/222 targets (p27 and estrogen receptor α) in the recipient cells also explained the acquisition of drug-resistant traits by these cells [59].

Another suggestion of a possible correlation between the levels of specific miRNAs carried by EVs and drug resistance in the donor cells is a study in which a positive secretion via EVs of tumor suppressor miRNAs (miR-145 and miR-34a) was found in drug-resistant human colon cancer cell lines [60]. The authors proposed that the increase in the secretion of miR-145 and miR-34a via EVs (and their consequent low intracellular levels in donor cells) contributes to 5-fluorouracil (5-FU) resistance in the donor cells.

Another study has shown that the increase in the survival of drug-resistant cells could occur through an alternative effect: the reduced export of oncomiRNAs by EVs. In a prostate cancer cell line, treatment with fludarabine promoted the selection of cells expressing miR-485-3p (which targets prosurvival mRNAs) and reduced the association of miR-485-3p with the EVs shed by those cells, therefore reducing the release of this particular miRNA to the extracellular environment. Cells harvested at several days following treatment with this chemotherapeutic agent showed overexpression of miR-485-3p. Furthermore, nuclear transcription factor Y beta (NF-YB), which is regulated by this miRNA, was found to be downregulated in cells surviving the treatment. This protein is a repressor of the Top2α, MDR1, and CCNB2 genes; thus, as expected, their expression was found to be increased in these cells [61].

Excitingly, the mediation of CDR by the miRNAs carried in EVs has now been shown to be related to other additional factors, and not to the miRNA cargo alone. In a recent work, five regulatory miRNAs (miR-22-3p, -185-5p, -503-5p, -652-3p, and -1280) associated with the dissemination of MDR were identified in recipient cells (originally drug sensitive) following co-culture with EVs isolated from drug-resistant counterpart cells; this was shown in two models, breast adenocarcinoma and human acute lymphoblastic leukemia. The recipient cells were also shown to have increased levels of proline-rich tyrosine kinase 2, which is associated with migration and invasion. Surprisingly, this protein (and the corresponding mRNA) was not found in the drug-resistant EVs, suggesting that the acquisition of the MDR phenotype by recipient cells may have resulted from the transfer of other molecules that regulate the induction of downstream mediators. Therefore, these authors proposed that the spread of drug-resistant traits by EVs could be achieved in an indirect manner [62]. Importantly, EVs were also shown to harbor mRNAs encoding proteins involved in the membrane vesiculation machinery, as well as mRNAs encoding enzymes essential for the biogenesis of miRNAs, suggesting their importance in the regulation of both processes in recipient cells and the self-sufficiency of these vesicles in miRNA production [63,64]. Another study has further demonstrated the significance of the EV cargo, not only in the transfer of important regulators or oncomiRNAs but also in stabilizing the carried miRNAs. The presence of Argonaute 2 complexes in EVs has been shown to play a pivotal role in selectively protecting exosomal miRNAs from degradation by RNase A [65].

Transfer of Drug Resistance Traits by EVs: lncRNAs

Similarly to what has been described above for miRNAs, a recent study concluded that lncRNAs have differential abundance in EVs, which may indicate selective loading of these molecules into EVs [66]. The contribution of lncRNAs carried by EVs to the regulation of CDR phenotype remains poorly understood. However, some studies have been aiming to investigate this association. Recent work conducted in hepatocellular carcinoma (HCC) cells has shown that the intracellular signaling induced by TGF-β (which has been associated with drug resistance in several cancers [67]) may involve the mediation of lincRNA-ROR (linc-ROR), the most significantly upregulated lncRNA in malignant hepatocytes. Treatment with sorafenib increased the expression of linc-ROR in HCC cells as well as its levels in their derived EVs. EVs derived from linc-ROR-silenced HCC donor cells increased levels of apoptosis, as well as the cytotoxicity induced by chemotherapy in HCC recipient cells [9]. Moreover, TGF-β selectively enriched linc-ROR within HCC EVs, further supporting the potential role of this lncRNA in intercellular signalling in response to TGF-β [9].

Another study of HCC cells following treatment with various chemotherapeutic agents described the enrichment of lincRNA-VLDR (linc-VLDR) in treated cells and their derived EVs [10]. Furthermore, upregulation of linc-VLDR was observed in recipient cells after their co-culture with HCC-derived EVs. Incubation with these EVs also resulted in a reduction of cell death induced by chemotherapy. Interestingly, RNAi-mediated silencing of linc-VLDR in recipient cells (before incubation with EVs) resulted in decreased cellular viability as well as in reduced

expression of ABCG2, suggesting a role for linc-VLDR in promotion of drug resistance [10]. Together, these studies exemplified the ability of lncRNAs to mediate drug resistance.

Transfer of Drug Resistance Traits by EVs: Other Modulators

In addition to the drug-efflux pumps, miRNAs, and lncRNAs already known to act as mediators of CDR, other molecules that are transported in EVs (released by drug-resistant cells) may also have a role in the dissemination of the CDR phenotype, by inducing the production of EVs or by regulating other mediators (such as drug-efflux pumps) (Figure 2, Key Figure).

Key Figure

The Involvement of Various Mediators in the Intercellular Transfer of Drug Resistance by Extracellular Vesicles (EVs)

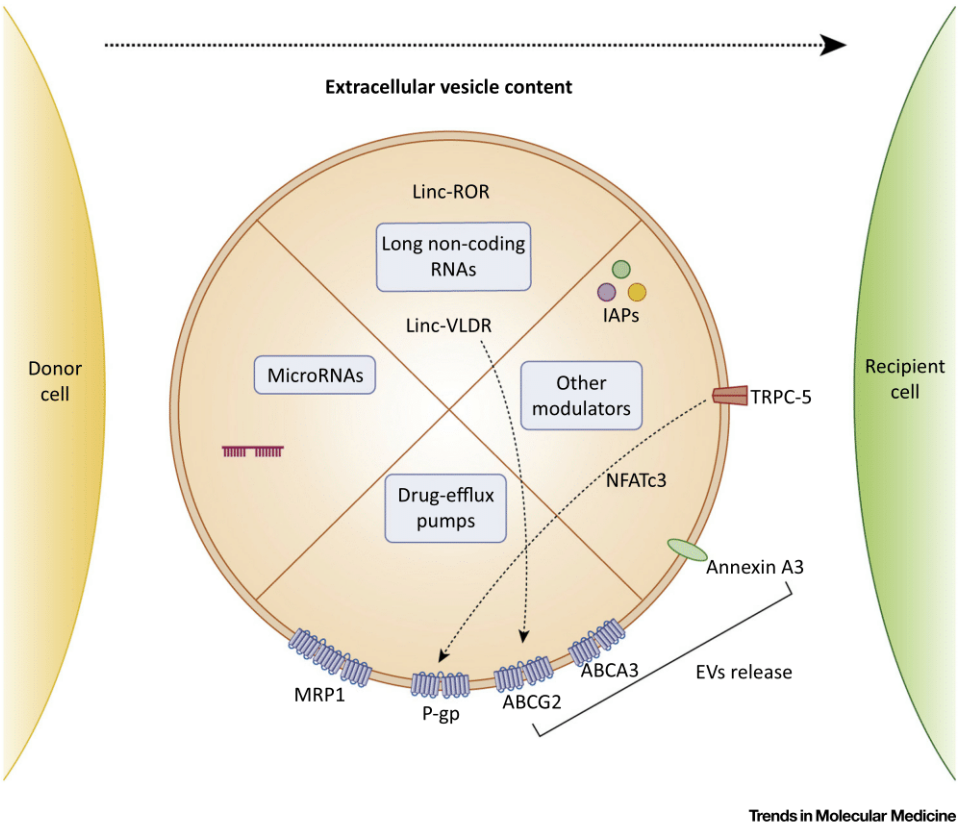


Figure 2. The best described mediators transported by EVs known to be implicated in the acquisition of deleterious drug resistance traits are: drug-efflux pumps, microRNAs (miRNAs), and long noncoding RNAs. One of the most important features of miRNA transfer is the selective packaging of specific miRNAs associated with drug resistance mechanisms, thus allowing the regulation of the expression of their 'targets' in recipient cells. Regarding the drug-efflux pumps, P-glycoprotein (P-gp), ATP-binding cassette (ABC) transporter G2 (ABCG2), multidrug resistance-associated protein 1 (MRP1), and lysosome-related organelle-associated ATP-binding cassete transporter A3 (ABCA3) have been shown to be transferred by EVs to recipient (drug sensitive) cells. The presence of these pumps in EVs may contribute to the sequestration of various drugs leading to sublethal concentrations of these drugs in the donor cells. The acquisition of a drug-resistant phenotype by recipient cells is a complex process where various modulators may interact with each other [e.g., the possible regulation of ABCG2 by lincRNA-VLDR (linc-VLDR), the regulation of P-gp by transient receptor potential channel 5 (TrpC5)]. Interestingly, some mediators of drug resistance (e.g., annexin A3, ABCG2, ABCA3) have also been shown to be involved in EV production.

Increased expression of annexin A3, a calcium-dependent phospholipid-binding protein, is a mechanism of platinum resistance in ovarian cancer cells [68]. Serum levels of annexin A3 were found to be significantly higher in platinum-resistant patients than in platinum-sensitive patients [69]. Interestingly, annexin A3 was shown to be secreted into the culture medium by an ovarian cancer cell line and there is some evidence that this was mediated by EVs. Annexin A3 could be detected in EVs derived from cisplatin-resistant ovarian cancer cells. Furthermore, ovarian cancer cells overexpressing annexin A3 were found to release an increased number of EVs, suggesting its possible involvement in the production of EVs [69].

Furthermore, EVs have been shown to transfer another calcium-related molecule, transient receptor potential channel 5 (TrpC5) from tumor cells to human microvessel endothelial cells [70]. This transfer caused the induction of P-gp expression by activation of the transcription factor nuclear factor of activated T cells isoform c3 (NFATc3). Other studies have also demonstrated TrpC5 transfer by EVs in a breast cancer cell model. Incubation with EVs from drug-resistant cells resulted in the acquisition of a drug-resistant phenotype by their counterpart cells [71]. Interestingly, TrpC5-containing EVs were found in breast cancer patients who underwent chemotherapy but were absent in patients who were not exposed to therapeutic drugs. This suggests the transfer of drug-resistant traits by the circulating TrpC5-derived EVs [71].

In malignant lymphoma, EVs were shown to play a role in resistance to the anti-CD20 chimeric antibody rituximab [72]. EVs derived from B-cell lymphoma cells shielded the target cells from the antibody, as the released EVs displayed CD20 that bound to anti-CD20 antibodies [39].

Finally, a recent study described the induction of a multifactorial phenotype by EVs. The presence of mRNA encoding inhibitors of apoptosis proteins (IAPs) in EVs derived from chronic myeloid leukemia cells was found. The incubation of drug-sensitive cells with drug-resistant derived EVs led to the accumulation of P-gp, IAPs, and miRNAs in the recipient cells. The authors suggested that the resistance displayed by the recipient cells was the result of the transfer of all of these mediators [32].

Transfer of functional mRNAs mediated by EVs from donor to recipient cells was also described [48]. The contribution of EV-delivered mRNAs to the activation of nuclear factor kappa B (NF-κB), which is known to be involved in the induction of drug resistance [73], was described. Although it remains unclear which RNAs are responsible for this observation, it was demonstrated that EV-RNA alone could trigger cell signaling and induce an NF-κB response in recipient cells [74]. The predictive value of specific mRNAs carried by EVs was recently reported. Using a microfluidics chip, the RNA levels of O^6-methylguanine DNA methyltransferase and alkylpurine-DNA-N-glycosylase (enzymes inversely related to treatment efficacy) were analyzed in EVs isolated from the blood of glioblastoma patients. It was found that during drug treatment the EV content of mRNAs from these enzymes was considerably altered. The authors proposed that if the same results were observed in a larger cohort, these changes in mRNA levels could be used as predictor variables for treatment outcome in glioblastoma patients [75].

Concluding Remarks

CDR is a major factor contributing to therapy failure. The ability of EVs shed by tumor drug-resistant (donor) cells to horizontally transfer a drug-resistant phenotype to drug-sensitive (recipient) cells has been recently described as an important mechanism of 'dissemination' of drug resistance. The known mediators of this horizontal transfer of drug resistance include drug-efflux pumps (such as P-gp, MRP1, ABCG2, and ABCA3), miRNAs (such as miR-34a and miR-145), lncRNAs (such as linc-ROR and linc-VLDR), and other molecules (such as TrpC-5 and IAPs). These mediators transferred to recipient cells (by the EVs shed from donor cells) are

Outstanding Questions

Does the cargo of EVs display selectivity regarding the recipient (or the donor) tumor cells?

How relevant for the cellular drug resistance phenotype is the sequestration of drugs by EVs?

Are all drugs sequestered in EVs?

Is the transmembrane orientation of the drug-efflux pumps in the EVs the same as in the drug-resistant cells? Or is it inverted?

Are drug-efflux pumps involved in the biogenesis of EVs?

How can the various mediators of intercellular transfer of drug resistance by EVs influence each other? How does the networking between the different types of mediator occur?

How relevant is the transfer of drug resistance mediated by EVs in patients?

Can the knowledge of the molecules involved in the intercellular transfer of drug resistance mediated by EVs contribute to the development of new biomarkers of drug resistance?

Will it be possible to therapeutically counteract the mechanisms of intercellular transfer of drug resistance mediated by EVs? Which would be the best drug targets for this purpose?

functional in those cells. It is interesting to note some discoveries regarding the packaging of EVs suggesting: (i) the selective packaging of some miRNAs and lncRNAs in EVs shed by drug-resistant cells; (ii) the possible involvement of some mediators of drug resistance in the production of EVs by donor cells; (iii) and the sequestration of drugs by EVs as a mechanism of drug elimination by donor cells.

In summary, the transfer of drug resistance facilitated by EVs is emerging as a pivotal area of research to counteract and predict drug resistance. Nevertheless, it will be necessary to keep in mind that the mediators of this drug resistance dissemination might be working together, as a network, and that there might be feedback loops of regulation.

Importantly, the recent discovery of this mechanism of drug resistance dissemination has presented a new opportunity not only to find approaches to counteract this phenomenon but also to identify biomarkers of drug resistance. In the years to come, clinical data will clarify the questions emerging from this field of research (see Outstanding Questions) and illuminate the scientific community regarding the real contribution of this horizontal transfer to drug resistance to patient response and clinical outcome.

Acknowledgments

IPATIMUP integrates the i3S Research Unit, which is partially supported by FCT, the Portuguese Foundation for Science and Technology. The work of the authors' laboratory is funded by FEDER funds through the Operational Programme for Competitiveness Factors–COMPETE and national funds through the FCT under the project 'PEst-C/SAU/LA0003/2013'. The authors also thank the FCT for grants to D.S. and R.T.L. (SFRH/BD/98054/2013 and SFRH/BPD/68787/2010, respectively) and the COST Action BM1202 European Network on Microvesicles and Exosomes in Health and Disease (ME-Had).

References

1. Rak, J. (2013) Extracellular vesicles – biomarkers and effectors of the cellular interactome in cancer. *Front. Pharmacol.* 4, 21
2. Raposo, G. and Stoorvogel, W. (2013) Extracellular vesicles: exosomes, microvesicles, and friends. *J. Cell Biol.* 200, 373–383
3. El Andaloussi, S. *et al.* (2013) Extracellular vesicles: biology and emerging therapeutic opportunities. *Nat. Rev. Drug Discov.* 12, 347–357
4. Peinado, H. *et al.* (2012) Melanoma exosomes educate bone marrow progenitor cells toward a pro-metastatic phenotype through MET. *Nat. Med.* 18, 883–891
5. Luga, V. *et al.* (2012) Exosomes mediate stromal mobilization of autocrine Wnt–PCP signaling in breast cancer cell migration. *Cell* 151, 1542–1556
6. Al-Nedawi, K. *et al.* (2009) Endothelial expression of autocrine VEGF upon the uptake of tumor-derived microvesicles containing oncogenic EGFR. *Proc. Natl. Acad. Sci. U.S.A.* 106, 3794–3799
7. Ashiru, O. *et al.* (2010) Natural killer cell cytotoxicity is suppressed by exposure to the human NKG2D ligand MICA*008 that is shed by tumor cells in exosomes. *Cancer Res.* 70, 481–489
8. Azmi, A.S. *et al.* (2013) Exosomes in cancer development, metastasis, and drug resistance: a comprehensive review. *Cancer Metastasis Rev.* 32, 623–642
9. Takahashi, K. *et al.* (2014) Extracellular vesicle-mediated transfer of long non-coding RNA ROR modulates chemosensitivity in human hepatocellular cancer. *FEBS Open Bio.* 4, 458–467
10. Takahashi, K. *et al.* (2014) Involvement of extracellular vesicle long noncoding RNA (linc-VLDLR) in tumor cell responses to chemotherapy. *Mol. Cancer Res.* 12, 1377–1387
11. Gong, J. *et al.* (2013) Microparticle drug sequestration provides a parallel pathway in the acquisition of cancer drug resistance. *Eur. J. Pharmacol.* 721, 116–125
12. Ifergan, I. *et al.* (2009) Riboflavin concentration within ABCG2-rich extracellular vesicles is a novel marker for multidrug resistance in malignant cells. *Biochem. Biophys. Res. Commun.* 380, 5–10
13. Parolini, I. *et al.* (2009) Microenvironmental pH is a key factor for exosome traffic in tumor cells. *J. Biol. Chem.* 284, 34211–34222
14. De Milito, A. and Fais, S. (2005) Tumor acidity, chemoresistance and proton pump inhibitors. *Future Oncol.* 1, 779–786
15. Fais, S. (2010) Proton pump inhibitor-induced tumour cell death by inhibition of a detoxification mechanism. *J. Intern. Med.* 267, 515–525
16. Spugnini, E.P. *et al.* (2014) Proton channels and exchangers in cancer. *Biochim. Biophys. Acta.* Published online October 20, 2014. http://dx.doi.org/10.1016/j.bbamem.2014.10.015
17. Jaiswal, R. *et al.* (2013) Breast cancer-derived microparticles display tissue selectivity in the transfer of resistance proteins to cells. *PLoS ONE* 8, e61515
18. Goler-Baron, V. *et al.* (2012) Inhibition of the PI3K–Akt signaling pathway disrupts ABCG2-rich extracellular vesicles and overcomes multidrug resistance in breast cancer cells. *Biochem. Pharmacol.* 83, 1340–1348
19. Kharaziha, P. *et al.* (2015) Molecular profiling of prostate cancer derived exosomes may reveal a predictive signature for response to docetaxel. *Oncotarget* (in press)
20. Beloribi-Djefaflia, S. *et al.* (2015) Exosomal lipids induce human pancreatic tumoral MiaPaCa-2 cells resistance through the CXCR4–SDF-1α signaling axis. *Oncoscience* 2, 15–30
21. Ifergan, I. *et al.* (2005) Novel extracellular vesicles mediate an ABCG2-dependent anticancer drug sequestration and resistance. *Cancer Res.* 65, 10952–10958
22. Zhao, L. *et al.* (2015) The role of exosomes and "exosomal shuttle microRNA" in tumorigenesis and drug resistance. *Cancer Lett.* 356, 339–346
23. Jaiswal, R. *et al.* (2014) Cellular communication via microparticles: role in transfer of multidrug resistance in cancer. *Future Oncol.* 10, 655–669
24. Lopes-Rodrigues, V. *et al.* (2014) The network of P-glycoprotein and microRNAs interactions. *Int. J. Cancer* 135, 253–263

25. Pasquier, J. *et al.* (2011) Consequences of cell-to-cell P-glycoprotein transfer on acquired multidrug resistance in breast cancer: a cell population dynamics model. *Biol. Direct* 6, 5
26. Levchenko, A. *et al.* (2005) Intercellular transfer of P-glycoprotein mediates acquired multidrug resistance in tumor cells. *Proc. Natl. Acad. Sci. U.S.A.* 102, 1933–1938
27. Rafii, A. *et al.* (2008) Oncologic trogocytosis of an original stromal cells induces chemoresistance of ovarian tumours. *PLoS ONE* 3, e3894
28. Bebawy, M. *et al.* (2009) Membrane microparticles mediate transfer of P-glycoprotein to drug sensitive cancer cells. *Leukemia* 23, 1643–1649
29. Corcoran, C. *et al.* (2012) Docetaxel-resistance in prostate cancer: evaluating associated phenotypic changes and potential for resistance transfer via exosomes. *PLoS ONE* 7, e50999
30. Lv, M.M. *et al.* (2014) Exosomes mediate drug resistance transfer in MCF-7 breast cancer cells and a probable mechanism is delivery of P-glycoprotein. *Tumour Biol.* 35, 10773–10779
31. Zhang, F.F. *et al.* (2014) Microvesicles mediate transfer of P-glycoprotein to paclitaxel-sensitive A2780 human ovarian cancer cells, conferring paclitaxel-resistance. *Eur. J. Pharmacol.* 738, 83–90
32. de Souza, P.S. *et al.* (2015) Microparticles induce multifactorial resistance through oncogenic pathways independently of cancer cell type. *Cancer Sci.* 106, 60–68
33. Lu, J.F. *et al.* (2013) Microparticles mediate MRP1 intercellular transfer and the re-templating of intrinsic resistance pathways. *Pharmacol. Res.* 76, 77–83
34. Goler-Baron, V. and Assaraf, Y.G. (2011) Structure and function of ABCG2-rich extracellular vesicles mediating multidrug resistance. *PLoS ONE* 6, e16007
35. Goler-Baron, V. and Assaraf, Y.G. (2012) Overcoming multidrug resistance via photodestruction of ABCG2-rich extracellular vesicles sequestering photosensitive chemotherapeutics. *PLoS ONE* 7, e35487
36. Kong, J.N. *et al.* (2015) Guggulsterone and bexarotene induce secretion of exosome-associated breast cancer resistance protein and reduce doxorubicin resistance in MDA-MB-231 cells. *Int. J. Cancer* 137, 1610–1620
37. Colombo, M. *et al.* (2014) Biogenesis, secretion, and intercellular interactions of exosomes and other extracellular vesicles. *Annu. Rev. Cell Dev. Biol.* 30, 255–289
38. Chapuy, B. *et al.* (2008) Intracellular ABC transporter A3 confers multidrug resistance in leukemia cells by lysosomal drug sequestration. *Leukemia* 22, 1576–1586
39. Aung, T. *et al.* (2011) Exosomal evasion of humoral immunotherapy in aggressive B-cell lymphoma modulated by ATP-binding cassette transporter A3. *Proc. Natl. Acad. Sci. U.S.A.* 108, 15336–15341
40. To, K.K. (2013) MicroRNA: a prognostic biomarker and a possible druggable target for circumventing multidrug resistance in cancer chemotherapy. *J. Biomed. Sci.* 20, 99
41. Yan, F. *et al.* (2014) Restoration of miR-101 suppresses lung tumorigenesis through inhibition of DNMT3a-dependent DNA methylation. *Cell Death Dis.* 5, e1413
42. Gao, W. *et al.* (2012) MiRNA-21: a biomarker predictive for platinum-based adjuvant chemotherapy response in patients with non-small cell lung cancer. *Cancer Biol. Ther.* 13, 330–340
43. Pignot, G. *et al.* (2013) MicroRNA expression profile in a large series of bladder tumors: identification of a 3-miRNA signature associated with aggressiveness of muscle-invasive bladder cancer. *Int. J. Cancer* 132, 2479–2491
44. Lima, R.T. *et al.* (2011) MicroRNA regulation of core apoptosis pathways in cancer. *Eur. J. Cancer* 47, 163–174
45. Seca, H. *et al.* (2010) miR signatures and the role of miRs in acute myeloid leukaemia. *Eur. J. Cancer* 46, 1520–1527
46. Seca, H. *et al.* (2013) Targeting miR-21 induces autophagy and chemosensitivity of leukemia cells. *Curr. Drug Targets* 14, 1135–1143
47. Koga, Y. *et al.* (2011) Exosome can prevent RNase from degrading microRNA in feces. *J. Gastrointest. Oncol.* 2, 215–222
48. Skog, J. *et al.* (2008) Glioblastoma microvesicles transport RNA and proteins that promote tumour growth and provide diagnostic biomarkers. *Nat. Cell Biol.* 10, 1470–1476
49. Taylor, D.D. and Gercel-Taylor, C. (2008) MicroRNA signatures of tumor-derived exosomes as diagnostic biomarkers of ovarian cancer. *Gynecol. Oncol.* 110, 13–21
50. Aushev, V.N. *et al.* (2013) Comparisons of microRNA patterns in plasma before and after tumor removal reveal new biomarkers of lung squamous cell carcinoma. *PLoS ONE* 8, e78649
51. Corcoran, C. *et al.* (2011) Intracellular and extracellular microRNAs in breast cancer. *Clin. Chem.* 57, 18–32
52. Corcoran, C. *et al.* (2014) miR-34a is an intracellular and exosomal predictive biomarker for response to docetaxel with clinical relevance to prostate cancer progression. *Prostate* 74, 1320–1334
53. Rabinowits, G. *et al.* (2009) Exosomal microRNA: a diagnostic marker for lung cancer. *Clin. Lung Cancer* 10, 42–46
54. Xiao, D. *et al.* (2012) Identifying mRNA, microRNA and protein profiles of melanoma exosomes. *PLoS ONE* 7, e46874
55. Xiao, X. *et al.* (2014) Exosomes: decreased sensitivity of lung cancer A549 cells to cisplatin. *PLoS ONE* 9, e89534
56. Jaiswal, R. *et al.* (2012) Microparticle-associated nucleic acids mediate trait dominance in cancer. *FASEB J.* 26, 420–429
57. Chen, W.X. *et al.* (2014) Exosomes from docetaxel-resistant breast cancer cells alter chemosensitivity by delivering microRNAs. *Tumour Biol.* 35, 9649–9659
58. Chen, W.X. *et al.* (2014) Exosomes from drug-resistant breast cancer cells transmit chemoresistance by a horizontal transfer of microRNAs. *PLoS ONE* 9, e95240
59. Wei, Y. *et al.* (2014) Exosomal miR-221/222 enhances tamoxifen resistance in recipient ER-positive breast cancer cells. *Breast Cancer Res. Treat.* 147, 423–431
60. Akao, Y. *et al.* (2014) Extracellular disposal of tumor-suppressor miRs-145 and -34a via microvesicles and 5-FU resistance of human colon cancer cells. *Int. J. Mol. Sci.* 15, 1392–1401
61. Lucotti, S. *et al.* (2013) Fludarabine treatment favors the retention of miR-485-3p by prostate cancer cells: implications for survival. *Mol. Cancer* 12, 52
62. Gong, J. *et al.* (2014) Microparticles mediate the intercellular regulation of microRNA-503 and proline-rich tyrosine kinase 2 to alter the migration and invasion capacity of breast cancer cells. *Front. Oncol.* 4, 220
63. Jaiswal, R. *et al.* (2012) Microparticle conferred microRNA profiles – implications in the transfer and dominance of cancer traits. *Mol. Cancer* 11, 37
64. Melo, S.A. *et al.* (2014) Cancer exosomes perform cell-independent microRNA biogenesis and promote tumorigenesis. *Cancer Cell* 26, 707–721
65. Li, L. *et al.* (2012) Argonaute 2 complexes selectively protect the circulating microRNAs in cell-secreted microvesicles. *PLoS ONE* 7, e46957
66. Gezer, U. *et al.* (2014) Long non-coding RNAs with low expression levels in cells are enriched in secreted exosomes. *Cell Biol. Int.* 38, 1076–1079
67. Biswas, S. *et al.* (2007) Inhibition of TGF-β with neutralizing antibodies prevents radiation-induced acceleration of metastatic cancer progression. *J. Clin. Invest.* 117, 1305–1313
68. Yan, X. *et al.* (2010) Increased expression of annexin A3 is a mechanism of platinum resistance in ovarian cancer. *Cancer Res.* 70, 1616–1624
69. Yin, J. *et al.* (2012) Secretion of annexin A3 from ovarian cancer cells and its association with platinum resistance in ovarian cancer patients. *J. Cell. Mol. Med.* 16, 337–348
70. Dong, Y. *et al.* (2014) Tumor endothelial expression of P-glycoprotein upon microvesicular transfer of TrpC5 derived from adriamycin-resistant breast cancer cells. *Biochem. Biophys. Res. Commun.* 446, 85–90
71. Ma, X. *et al.* (2014) Essential role for TrpC5-containing extracellular vesicles in breast cancer with chemotherapeutic resistance. *Proc. Natl. Acad. Sci. U.S.A.* 111, 6389–6394
72. Maloney, D.G. *et al.* (1994) Phase I clinical trial using escalating single-dose infusion of chimeric anti-CD20 monoclonal antibody

(IDEC-C2B8) in patients with recurrent B-cell lymphoma. *Blood* 84, 2457–2466

73. Bentires-Alj, M. *et al.* (2003) NF-κB transcription factor induces drug resistance through MDR1 expression in cancer cells. *Oncogene* 22, 90–97
74. Lai, C.P. *et al.* (2015) Visualization and tracking of tumour extracellular vesicle delivery and RNA translation using multiplexed reporters. *Nat. Commun.* 6, 7029
75. Shao, H. *et al.* (2015) Chip-based analysis of exosomal mRNA mediating drug resistance in glioblastoma. *Nat. Commun.* 6, 6999
76. Gyorgy, B. *et al.* (2011) Membrane vesicles, current state-of-the-art: emerging role of extracellular vesicles. *Cell. Mol. Life Sci.* 68, 2667–2688
77. Gould, S.J. and Raposo, G. (2013) As we wait: coping with an imperfect nomenclature for extracellular vesicles. *J. Extracell. Vesicles* Published online February 15, 2013. http://dx.doi.org/10.3402/jev.v2i0.20389
78. Takahashi, K. *et al.* (2014) Involvement of extracellular vesicle long non-coding RNA (linc-VLDLR) in tumor cell responses to chemotherapy. *Mol. Cancer Res.* 12, 1377–1387

3. Interdependency of intracellular pathways in EVs production

3.1 Central role of the endocytic pathway: endosome as a dynamic organelle

Allen *et al.* described for the first time back in the 1980s, by using electron microscopy, the existence of intracellular compartments that could be loaded with the endocytic marker horseradish peroxidase (HRP). These structures were named endosomes [314]. It is currently accepted that cells harbour distinct types of endosomes which are distinguishable based on kinetic, molecular, and morphological criteria [315].

An early endosome is located at the periphery of cells and receives almost instantly the cargo from endocytosis or from membrane fusion. Following the incorporation into an early endosome, the cargo is sorted into different pathways. Indeed, the early endosome is named by some authors as the “sorting” endosome. An accepted feature of an early endosome is a cytoplasmic clathrin coat that covers parts of its membrane [316].

Early endosomes undergo homotypic fusion (*i.e*. a fusion between compartments which are biochemically identical) being matured into late endosomes [315]. The key protein involved in this process is Rab5 [317]. The cargo sorted into the late endosomes is further mixed with cargo from other intracellular organelles, then followed by inward budding of the limiting membrane creating intraluminal vesicles that, ultimately, generate a multivesicular body. The nomenclature for late endosomes and MVBs is not consensual. Some authors distinguish the late endosome from a MVB, defending that the MVB is an organelle between early endosome and late endosome. However, the majority of studies indicates MVBs and late endosomes as being the same structure [318]. The unifying factor between these different points of view is that the increasing number of ILVs reflects the temporal progression of endosomes along the endocytic pathway [315].

Importantly, the crucial role of cytosol by providing peripheral proteins to all the membrane compartments has been described, since these proteins may be responsible for functions such as molecular sorting, membrane fusion and fission, compartment identity, and organelle motility [319]. The influence of post-translational modifications of cargo proteins on the MVB fate was recently suggested [320]. In addition, it seems that the destiny of the MVB may change due to alterations in cellular conditions. For example, starvation

induces MVB degradation by fusion with autophagosomes (autophagy), resulting in a decrease in the number of EVs released [321].

Following maturation, the late endosome/MVB may fuse with the plasma membrane to secrete EVs or be destined for cargo degradation. The regulation of the balance between secretory and degradative capacity of a MVB remains largely unexplored. The previous section 2 of this thesis was already dedicated to the transport of a MVB enriched in ILVs to the cell surface, where it releases the ILVs as EVs. Therefore, the focus of the next sections will be the degradation and recycling of the cargo. Interestingly, an interdependency of different intracellular pathways is observed in the sorting, degradation, recycling and secretion of the EVs' cargo, being the endosome the common organelle in all of these pathways (Figure 6).

3.2 Routes for cargo degradation: role of lysosome and autophagosome

One of the possible fates of late endosomes/MVBs is fusion with lysosomes. Lysosomes are spherical organelles, ranging between 200 nm to 1 µm [322]. Usually they are electron-dense (depending on the quantity of the cargo supplied). A late endosome/MVB may undergo transient ('kiss-and-run') fusions or full fusions with lysosomes [323]. Most of the (previous endosome/MVB) cargo is then degraded by the lysosome, originating products that are then transferred to the cytoplasm for metabolic reuse [324]. Importantly, a few components such as mannose-6-phosphate receptors, tetraspanins and SNAREs may escape degradation after fusion of late endosomes/MVBs with lysosomes [319].

Another possible fate of late endosomes/MVBs is fusion with the autophagosome. The initial studies trying to unravel the processes involved in the formation of autophagosomes showed no labelling of endosomal proteins in early autophagosomes [325]. However, recent data suggested that the endocytic pathway may contribute to phagophore formation and expansion [326]. One of the mechanisms proposed suggests that endosomes undergo homotypic fusion mediated by a VAMP7-containing SNARE complex [327], forming autophagosome precursor membranes that become LC3 positive [*i.e*. phosphatidylethanolamine (PE)-conjugated LC3 (LC3-II)]. Rab 7 and 11 are apparently other players of the autophagosome formation through endocytic vesicles [326, 328]. Either the recycling endosomes or the later endosomes/MVBs may fuse with autophagosomes, becoming an amphisome, which upon further fusion with lysosomes becomes an autophagolysosome [326]. Importantly, as previously referred, autophagy is highly

regulated by a network of signalling pathways, being the LC3, the Atg and Vps families key players of the autophagic flux [54] (Figure 2).

As desribed above, the mechanisms involved in the decision of the cargo fate (*i.e.* whether the sorted cargo is to be secreted or to be degraded) are not fully understood. However, in the recent years, some studies added new insights into this issue. It was suggested that regulation by syndecan–syntenin–ALIX may be restricted to EVs secretion [329], while the ESCRT machinery may be associated to degradative MVBs [267]. In addition, MHC class II apparently is involved in the sorting to lysosomal degradation through ubiquitination (probably recruiting the ESCRT machinery). By contrast, ubiquitin-independent mechanisms target MHC class II to MVBs destined for secretion [265, 330]. Also, TSG101 and Tetraspanin 6 may be involved in the regulation of MVB sorting for degradation [320, 331]. Regarding regulation of fate to the autophagosomes, it was shown that the prion protein (PrP) promotes EVs secretion by inhibiting autophagosome formation, through interaction with caveolin [332].

3.3 Recycling endosome

In parallel with the progressive maturation of early endosomes into late endosomes, the generation of tubules that emanate from the uncoated areas of the early endosome occurs [315]. These structures are responsible for the recycling of the cargo to the plasma membrane, by the so-called “recycling pathway” [315]. Usually the recycling endosomes are distributed in the cell periphery. Nevertheless, in some cells (e.g. in the Chinese hamster ovary cell line), the tubules of recycling endosomes localize with the peri-Golgi, forming a structure called the “endocytic recycling compartment” (ERC) [333]. Based on the above mentioned, it is accepted that the recycling of the cargo to the plasma membrane through the endocytic pathway may occur with either fast or slow kinetics [334, 335]. When a recycling endosome is distributed by the cell periphery, the faster pathway is increased; nevertheless, when a recycling endosome localizes with the peri-Golgi, the slower pathway is increased. Interestingly, a crosstalk between the recycling pathway and the biogenesis of vesicles from budding of the plasma membrane through a small GTPase, known as RAS-related protein RAB22A, was shown. Indeed, in hypoxic breast cancer cells, RAB22A co-localized with budding EVs and mediated packaging and loading of cargo proteins [336]. In addition, the interaction of recycling endosomes with autophagosomes was also described [326].

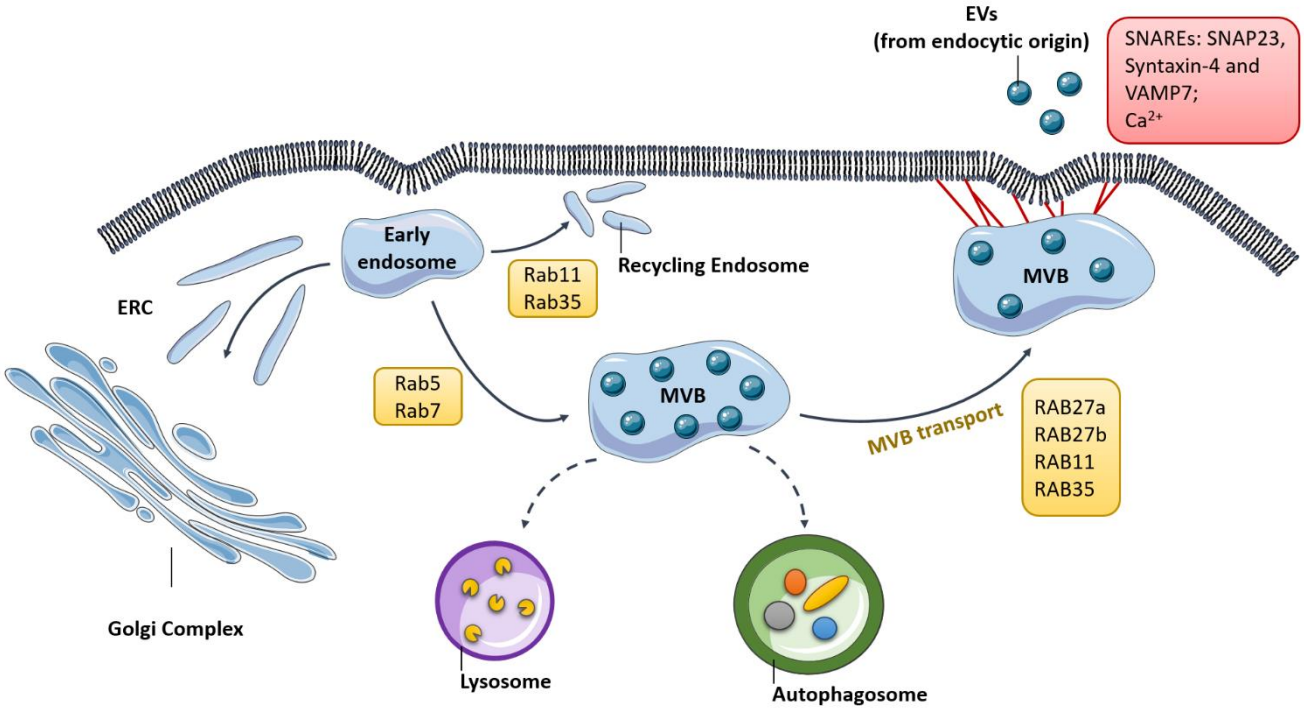


Figure 6: Interdependency of the intracellular pathways in EVs production. Adapted from [201] and [315].

In conclusion, the endocytic pathway seems to be the scaffold for other intracellular pathways, such as the recycling, lysosomal and the autophagic pathway, with the endosome being the main responsible for the interplay between these pathways. The interdependency of these pathways and their tight regulation allows a fine-tune balance between cargo's degradation or secretion (by EVs). Importantly, this equilibrium influences a series of cellular processes and consequently its dysregulation may cause different pathologies, including cancer [337].

PART II- OBJECTIVES

As already referred in the “State of the Art”, MDR is a major challenge of cancer treatment and results from a network of altered cellular mechanisms. Overexpression of P-gp in tumour cells is one of the most important factors responsible for MDR. In addition, interesting findings show that alterations in autophagy may be associated with tumour MDR, however this is still a debatable issue. Furthermore, discovery of EVs release by MDR cells and their interaction with drug-sensitive cells was a major breakthrough in the cancer research field, since this intercellular communication allows the dissemination of a MDR phenotype.

In the cargo of EVs released by MDR cells some players of MDR were previously found, including P-gp. Nevertheless, EVs may harbour other type of molecules, such as nucleic acids. Importantly, EVs are found in biological fluids. Even though studies characterizing the cargo of EVs released by MDR cells have been previously performed, this needs to be further understood, given the possible application of EVs as biomarkers of therapy response.

In addition, given the role of these EVs in the horizontal transfer of MDR, the regulation of the mechanisms involved in the release of EVs by MDR (donor) cells and in their interaction with (recipient) drug-sensitive counterpart cells requires further understanding. This may lead to new ways to counteract this type of MDR dissemination.

Also, given the controversial role of autophagy in MDR, it is important to clarify if molecules designed as P-gp inhibitors may modulate autophagy. This may contribute to the future identification of novel autophagy modulators and different therapeutic strategies.

Therefore, the overall aim of this thesis is to study the role of EVs (regarding their cargo and processes involved in their release and capture) in MDR associated with P-gp overexpression and also to evaluate the effect of a P-gp inhibitor on cellular autophagy. The knowledge gathered with this study will add value for the development of new tools to predict and overcome MDR.

For this, the following specific aims were pursued:

1. **Identify putative biomarkers of MDR in P-gp-overexpressing tumour cells and their EVs.**

To address this objective, deep sequencing analysis of RNA content was carried out in two pairs of MDR (P-gp overexpressing) cells and their drug-sensitive counterparts. The same

approach was carried out on the EVs released by those cells. The tumour cell models studied were non-small cell lung cancer (NSCLC) and chronic myeloid leukaemia (CML).

2. **Understand the mechanisms involved in the release of EVs by P-gp overexpressing MDR cells and their uptake by drug-sensitive counterparts.**

To accomplish this, the ability of drug-sensitive and their MDR counterpart cells to release and capture EVs was studied and compared. Moreover, the fate of EVs regarding the endocytic pathway was investigated, in both drug-sensitive and MDR counterpart cells. Finally, the role of the endocytic pathway in drug response was studied.

3. **Investigate the mechanism of action, particularly on autophagy, of a small molecule with dual anti-tumour and anti-P-gp activity**

For this, the effect of a P-gp inhibitor (previously described by our research group and collaborators) was investigated in a melanoma cell line, regarding the presence of autophagic structures and the autophagic flux. In addition, its effect in the cell cycle profile and apoptosis was also evaluated.

CHAPTER II

Results and Discussion

1. RESEARCH ARTICLE:

Deep sequencing analysis reveals distinctive non-coding RNAs when comparing tumour multidrug resistant cells and extracellular vesicles with drug-sensitive counterparts

Diana Sousa, Rune Matthiesen, Raquel T. Lima and M. Helena Vasconcelos

Submitted for publication (in Cancers)

Cancers **2019**, *11*, x FOR PEER REVIEW

Article

Deep sequencing analysis reveals distinctive non-coding RNAs when comparing tumour multidrug resistant cells and extracellular vesicles with drug-sensitive counterparts

Diana Sousa[1,2,3], Rune Matthiesen[4*], Raquel T.Lima[1,5,6], M. Helena Vasconcelos[1,2,3*]

[1]i3S- Instituto de Investigação e Inovação em Saúde, Universidade do Porto, 4200-135, Porto, Portugal [dsousa@ipatimup.pt (D.S.); rlima@ipatimup.pt (R.T.L.); hvasconcelos@ipatimup.pt (M.H.V)]
[2]Cancer Drug Resistance Group, IPATIMUP - Institute of Molecular Pathology and Immunology of the University of Porto, 4200-135 Porto, Portugal;
[3]Department of Biological Sciences, FFUP - Faculty of Pharmacy of the University of Porto, 4050-313 Porto, Portugal;
[4]Computational and Experimental Biology Group, CEDOC, Chronic Diseases Research Centre, NOVA Medical School, Faculdade de Ciências Médicas, Universidade NOVA de Lisboa, Campo dos Mártires da Pátria, 130, 1169-056 Lisboa, Portugal [rune.matthiesen@nms.unl.pt (R.M.)]
[5]Department of Pathology, FMUP - Faculty of Medicine of the University of Porto, 4200-319 Porto, Portugal;
[6]Cancer Signalling & Metabolism Group, IPATIMUP- Institute of Molecular Pathology and Immunology of the University of Porto, 4200-135 Porto, Portugal;

*corresponding authors: M. Helena Vasconcelos and Rune Matthiesen
Tel.: +351-**225 570 772**
E-mail: hvasconcelos@ipatimup.pt; rune.matthiesen@nms.unl.pt

Received: date; Accepted: date; Published: date

Abstract (200): Multidrug resistance (MDR) is one of the main limitations of cancer treatment. Overexpression of drug-efflux pumps, such as P-glycoprotein (P-gp), is a major cause of MDR. Importantly, different studies have shown that extracellular vesicles (EVs) participate in the communication between MDR cells and drug-sensitive counterparts, promoting the dissemination of the MDR phenotype. In the present work, we aimed to identify RNA species present in MDR cells and in EVs released by those cells, which may be associated to the MDR phenotype. The RNA content from two pairs (leukaemia and lung cancer) of MDR (P-gp overexpressing) cells and their drug-sensitive counterparts, as well as from their EVs, was analyzed by deep sequencing. Our results showed distinctive transcripts on MDR cells and their EVs, when compared with drug-sensitive counterparts. Remarkably, two pseudogenes (a novel pseudogene and RNA 5.8S ribosomal pseudogene 2) were found increased in EVs released by MDR cells, on both leukaemia and lung cancer models. Moreover, 6 miRs (miR-204-5p, miR-139-5p, miR-29c-5p, miR-551b-3p, miR-29b-2-5p, miR-204-3p) had increased levels in lung cancer MDR cells and in their EVs. This study provides insights into the contribution of EVs to MDR.

Keywords: Cancer; multidrug resistance; extracellular vesicles; next generation sequencing; small RNAs; microRNAs; pseudogenes

1. Introduction

Cancer multidrug resistance (MDR) is a particular case of drug resistance, in which tumour cells fail to respond to more than one drug with different molecular structures and mechanisms of action [1,2]. MDR is the result of a network of altered cellular mechanisms, being one of the major challenges of cancer treatment. The main cellular alterations responsible for the MDR phenotype are overexpression of drug-efflux pumps, decrease of drug uptake, changes in cell cycle and cell death pathways, increase in DNA damage repair and the more recently described release of extracellular vesicles by MDR cells [3].

Extracellular vesicles (EVs) are small particles enclosed by a lipid bilayer, found in different biological fluids such as urine, blood or saliva. EVs can be easily isolated from biological fluids or cell culture supernatants using different methodologies such as ultracentrifugation, size exclusion chromatography or affinity chromatography [4]. EVs are released and taken up by different types of cells, allowing horizontal communication between neighbour or distant cells [5]. EVs' size ranges from 30 to 1000 nm and their cargo is constituted by fragments of DNA, RNAs, lipids, proteins, sugars and metabolites [6]. Importantly, their rich heterogeneous cargo is protected from degradation caused by factors such as the ubiquitous extracellular RNases [7]. Remarkably, there is evidence that cancer cells release more EVs than normal cells [8], particularly after chemotherapy [9]. Therefore, EVs may represent an important source of biomarkers to be used in early diagnosis, prognosis or evaluation of therapy response in cancer [10,11].

The description of horizontal transfer of RNAs, particularly of microRNAs (miRs), as a mechanism of genetic exchange between cells mediated by EVs, was a breakthrough in the field [12]. Since then, many studies were conducted in the cancer MDR context in particular. Individual small RNAs or panels of small RNAs (particularly miRs) and long non-coding RNAs were found in EVs and described to be responsible, at least in part, for the MDR phenotype in recipient cells [5]. They have been described to have a role in senescence suppression [13], promotion of cell invasion [14] and migration [15]. However, the cellular and molecular mechanisms underlying MDR dissemination triggered by non-coding RNAs associated to EVs (i.e. present in their cargo) has not been fully understood yet [16].

In the present work, we aimed to: i) confirm if horizontal transfer of drug-resistant phenotype mediated by EVs is possible from MDR non-small cell lung cancer (NSCLC) cells to their drug-sensitive counterparts; ii) identify RNA species putatively associated to the MDR phenotype, in a NSCLC and a chronic myeloid leukaemia (CML) tumour cell model; and iii) verify if those RNAs are packaged into EVs shed by the NSCLC and CML MDR cells. To accomplish this, we performed analysis of drug response on sensitive cells following co-culture with EVs released by MDR cells and analysed the RNAs profile, by next generation sequencing, of drug-sensitive cells and their MDR counterparts, as well as of EVs released by those cells. To assess if those RNAs are specific of tumour type, two different tumour models were studied: NSCLC and CML.

2. Results

2.1 Extracellular Vesicles released by MDR cells transfer drug-resistance to recipient drug-sensitive cells

In the present work, to confirm that EVs released by MDR cells are able to transfer a drug-resistant phenotype to drug-sensitive cells, as previously described by others [17-19], NCI-H460 (drug-sensitive) cells were co-cultured with EVs isolated from the NCI-H460/R (MDR) cells and then treated with doxorubicin. Results (Figure 1) show that drug-sensitive cells, when previously incubated with EVs from MDR cells, became less sensitive to doxorubicin.

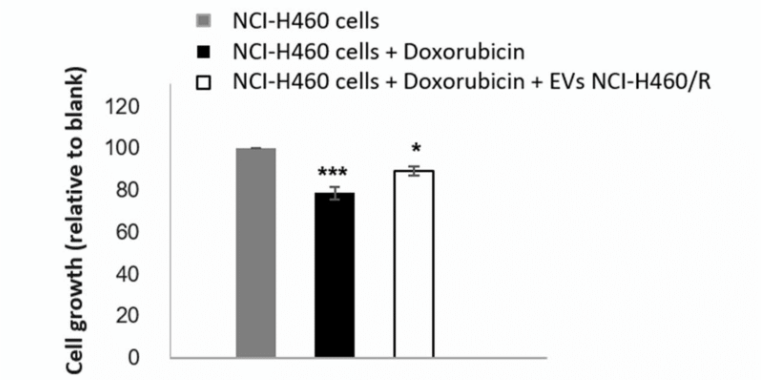


Figure 1: Effect of EVs released by MDR cells from NSCLC on response to doxorubicin treatment. Cell growth was determined on drug-sensitive cells (grey bar), drug-sensitive cells co-cultured without (black bar) or with (white bar) EVs released by MDR cells using SRB assay. Results are the mean ± S.E. of 3 independent experiments. *p<0.05; ***p <0.001 (NCI-H460 cells without drug treatment *vs* with doxorubicin treatment).

2.2 Differences were observed between the profile of small RNAs from cells and EVs

In order to identify non-coding RNAs associated to MDR, small RNA profile was analysed in two pairs of MDR and drug-sensitive counterparts, one pair from NSCLC and the other pair from CML. In addition, to investigate if those non-coding RNAs were packaged into the cargo of the EVs released by those cells, small RNA profile was performed in the two corresponding pairs of EVs.

The cellular small RNAs were more heterogeneous regarding size range, with the tRNA peak observed in all cell samples (˜66 nt) (Figure 2). By contrast, in EVs this peak was not evident. Interestingly, the small RNAs profile between the EVs from the two tumour models (NSCLC and CML) was different. Indeed, it was verified that EVs released from the NSCLC cells had greater amounts of small RNA species within the range of 20-40 nt than the EVs released from the CML cells. In both tumour models, a peak around 150 nt was present, possibly corresponding to ribosomal RNA 5.8S or small nuclear RNA [20,21].

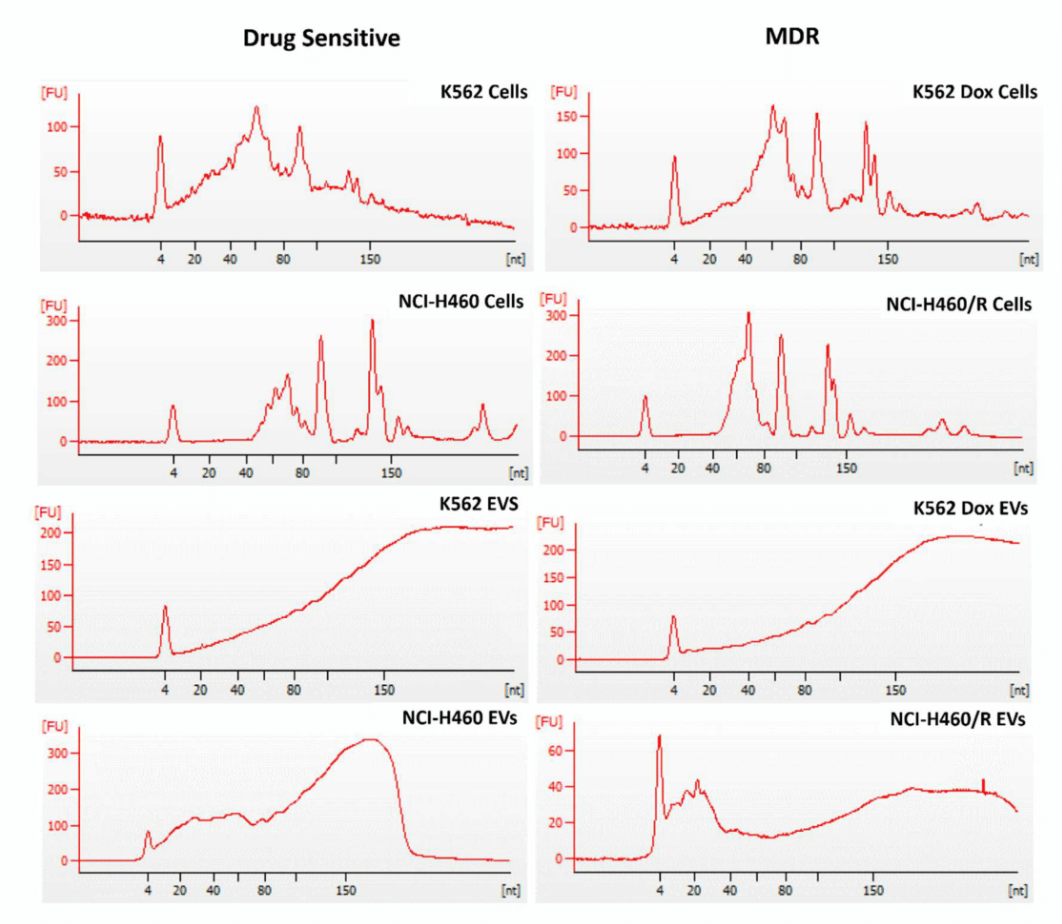


Figure 2: Profile of small RNAs from drug-sensitive and MDR counterpart cells and from the EVs released by those cells. Cells were from two models: NSCLC (NCI-H460 and NCI-H460/R) and CML (K562 and K562Dox). RNA was analysed using the Small RNA chip of the Bioanalyzer 2100 Agilent. Images are representative of three independent biological replicates.

2.3 RNA deep sequencing showed several classes of transcripts in cells and in EVs released by those cells

To further determine the identity of the small RNA molecules, next generation sequencing (NGS) was performed. Deep sequencing results were checked using FastQC and all 24 samples passed. Following this, alignment with human genome was performed. Between 70 to 95 % of successful alignment between RNA reads and HG19 was observed (Supplementary Table 1), even though only moderate coverage was obtained in the case of EVs.

Pie chart of the mapped reads distribution showed similar composition between RNA from cells and from EVs released by those cells (Figure 3). High levels of pseudogenes were found in all conditions. Moreover, in agreement with the Bioanalyzer profile, EVs released by NSCLC cells showed higher levels of miRs, when compared with EVs released by CML cells. By contrast, the levels of transcripts annotated as novel were higher in EVs shed by CML cells when compared with EVs shed by NSCLC cells. Importantly, multiple dimensional scaling analysis showed a cluster between the independent replicates in all conditions, indicating proper reproducibility. Furthermore, the two independent clusters observed for drug-sensitive *vs* MDR conditions, in

cells and EVs from both tumour models, suggest that results have biological relevance (Figure 4a and 4b).

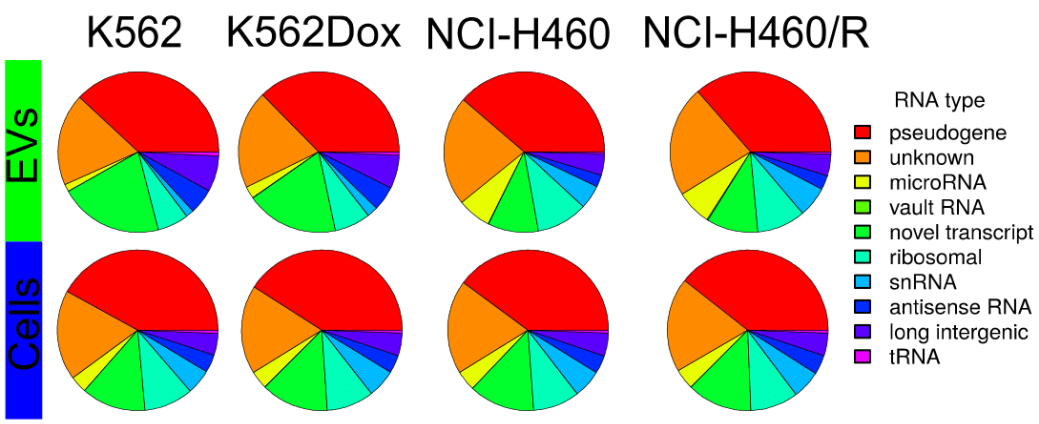
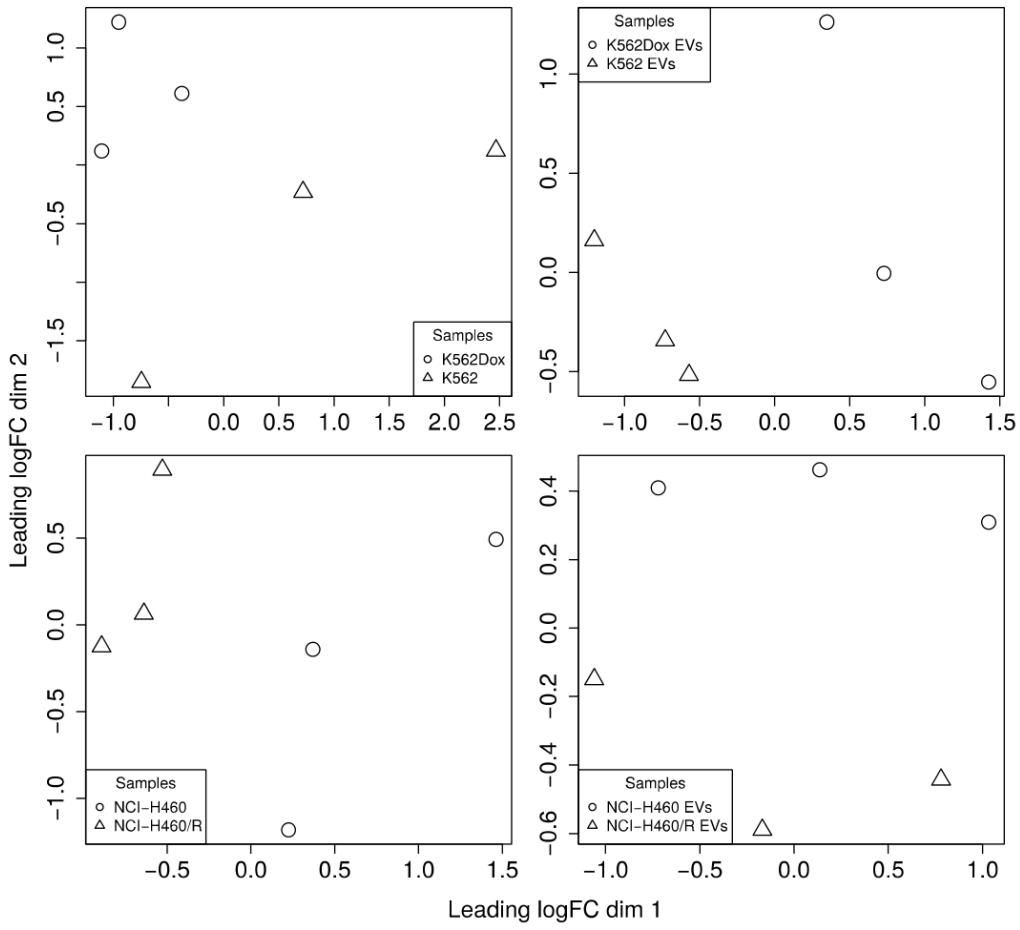


Figure 3: Composition of RNAs mapped reads in cells and EVs. Results were obtained by using ENSEMBL transcript annotation.

a)



b)

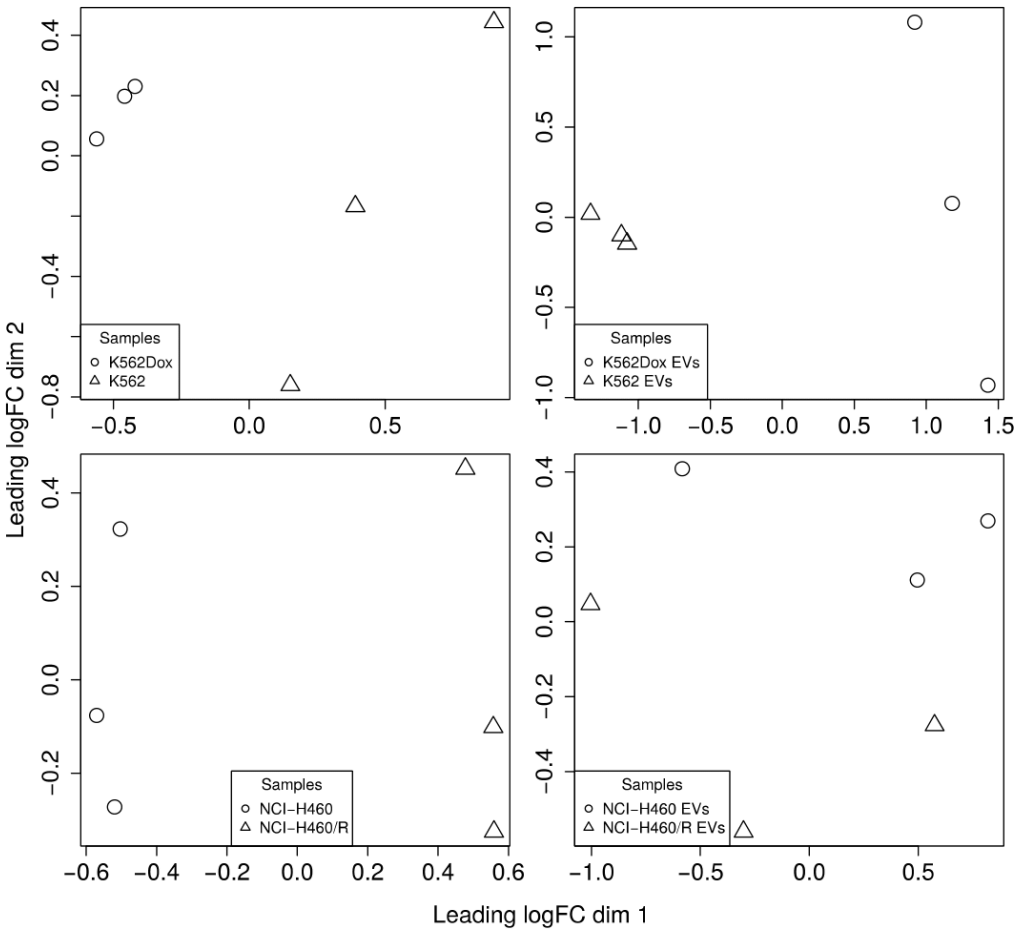
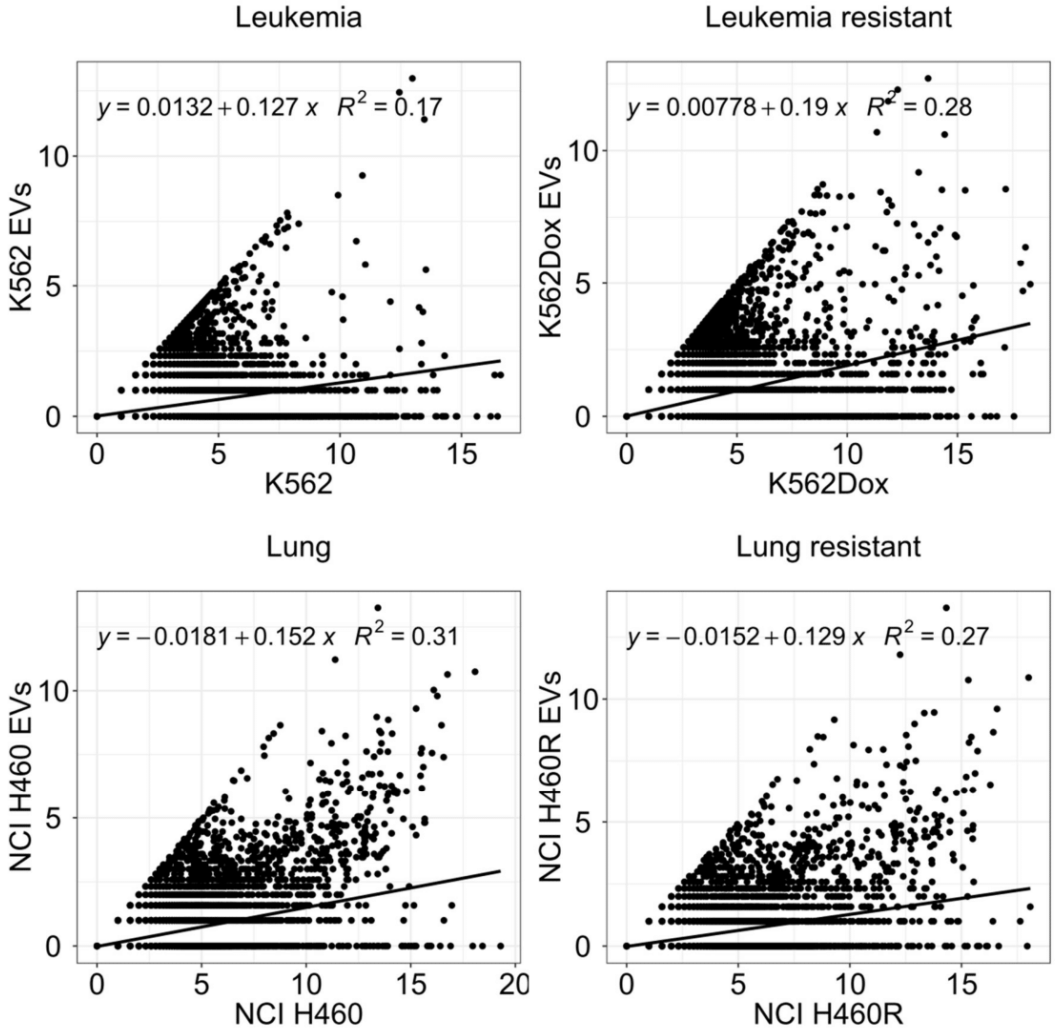


Figure 4. Multiple dimensional scaling using read counts of all mapped RNA transcripts (a) and all mapped miRs (b) as input.

2.4 Selective package of RNAs into the cargo of EVs released by MDR cells

To analyse if RNAs present in EVs reflect the intracellular RNAs, linear regression plots (log2 reads) were performed between the sequenced reads in EVs and cells (for each condition). As shown in Figure 5a, all RNA species present in EVs are also present in cells (as expected), on both tumour models. By contrast, EVs do not harbour all RNA species present in cells. The same observation was found regarding particularly the miRs content (Figure 5b).

a)



b)

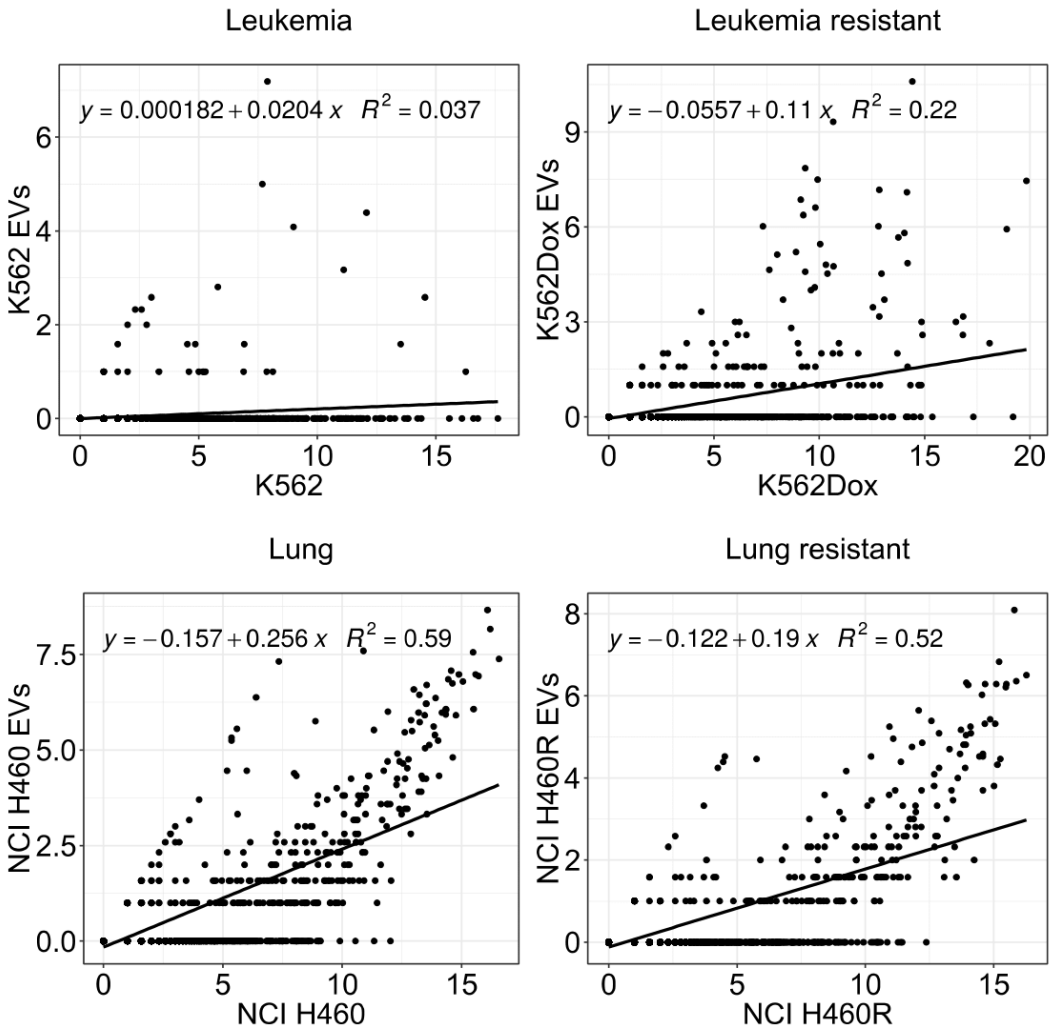


Figure 5. RNAs species (a) and miRs (b) abundance in the Extracellular Vesicles *versus* their donor cells. Values are presented in log2 scale and summarize the results from 3 independent biological replicates.

2.5 Significant regulated RNA species in MDR cells and/or EVs

Next, the differences between the data sequenced for drug-sensitive and MDR cells and from the EVs release by those cells were assessed. First, using ENSEMBL annotation for several RNA species with FeatureCounts software, aligned reads corresponding to ribosomal RNA, tRNA, snRNA, or pseudogenes were identified. These results were further analysed by the R package EdgeR which allowed pairwise comparison of drug-sensitive *versus* MDR for each of the

cell models, cells and EVs. RNA species presenting p-values<0.05 in each comparison, were considered differently expressed. The relative expression of each entity in each comparison is shown in Supplementary Tables 2-9.

Moreover, Venn diagrams were generated based on differences between drug-sensitive and MDR cells and also on differences between the EVs released by those cells. A total of 1927 differently expressed RNA species were found ($p < 0.05$) (Figure 6a).

Regarding the analysis of cells, 31 RNA species were found altered between drug-sensitive cells and their MDR counterparts, in both tumour models. From these, three transcripts (miR-383, miR4660 and chromosome 16 open reading frame 45) were identically found overexpressed in MDR cells of both tumour models (NSCLC and CML). In addition, two other transcripts (serglycin and FOXF1 adjacent non-coding developmental regulatory RNA) were identically found downregulated in MDR cells of both tumour models (NSCLC and CML, Table 1).

Regarding the analysis of EVs, three pseudogenes were found to have altered levels between drug-sensitive and MDR EVs, in both tumour models. From these, two have higher levels in the MDR EVs which are annotated as: a novel pseudogene and RNA 5.8S ribosomal pseudogene 2 (Table 1). To validate the alignment of reads of these three pseudogenes, the regions from the alignment were extracted using samtools [22] and manually visualized.

When comparing results from cells and EVs in the CML model, fifty species were found with different levels both in cells and EVs, between MDR and drug-sensitive counterparts. In the NSCLC model, three RNA species were found with different levels both in cells and EVs, between MDR and drug-sensitive counterparts. No RNA species was found differently expressed in both tumour models between MDR cells and their drug-sensitive counterparts and simultaneously on their EVs.

A parallel analysis using an annotation for miRs with FeatureCounts software was also performed. As described for RNA species analysis, the results from EdgeR software were overlapped in a Venn diagram. A total of 176 differentially expressed miRs were found (Figure 6b). Interestingly, 4 miRs (miR-383-5p, miR-335-5p, miR-504-5p and miR-933) were found to be differently expressed between drug-sensitive and MDR cells, in both CML and NSCLC models. From these, the ones found similarly increased or decreased in NSCLC and in CML MDR cells are shown in Table 1.

Moreover, 6 miRs (miR-204-5p, miR-139-5p, miR-29c-5p, miR-551b-3p, miR-29b-2-5p, miR-204-3p) have simultaneously altered levels in both cells and EVs from NSCLC.

To validate some of the results obtained, two miRs found altered and highly abundant were selected to be analysed by quantitative real-time PCR (qRT-PCR). Results (Figure 7) confirmed the previous ones obtained with NGS and bioinformatics analysis.

Table1: Transcripts found altered in MDR cells or in EVs shed by MDR cells, with identical regulation in NSCLC and CML tumour models.

	TRANCRIPT NAME	ENSEMBL_TRANSCRIPT_ID	ALTERATION OBSERVED IN MDR CONDITION
Cells	**miR-383**	ENST00000362257	increased
	miR-4660	ENST00000583549	increased
	chromosome 16 open reading frame 45	ENST00000565913	increased
	serglycin	ENST00000242465	decreased
	FOXF1 adjacent non-coding developmental regulatory RNA	ENST00000599749	decreased
	miR-504-5p	ENST00000385065	decreased
EVs	**novel pseudogene**	ENST00000311910	increased
	RNA, 5.8S ribosomal pseudogene 2	ENST00000363564	increased

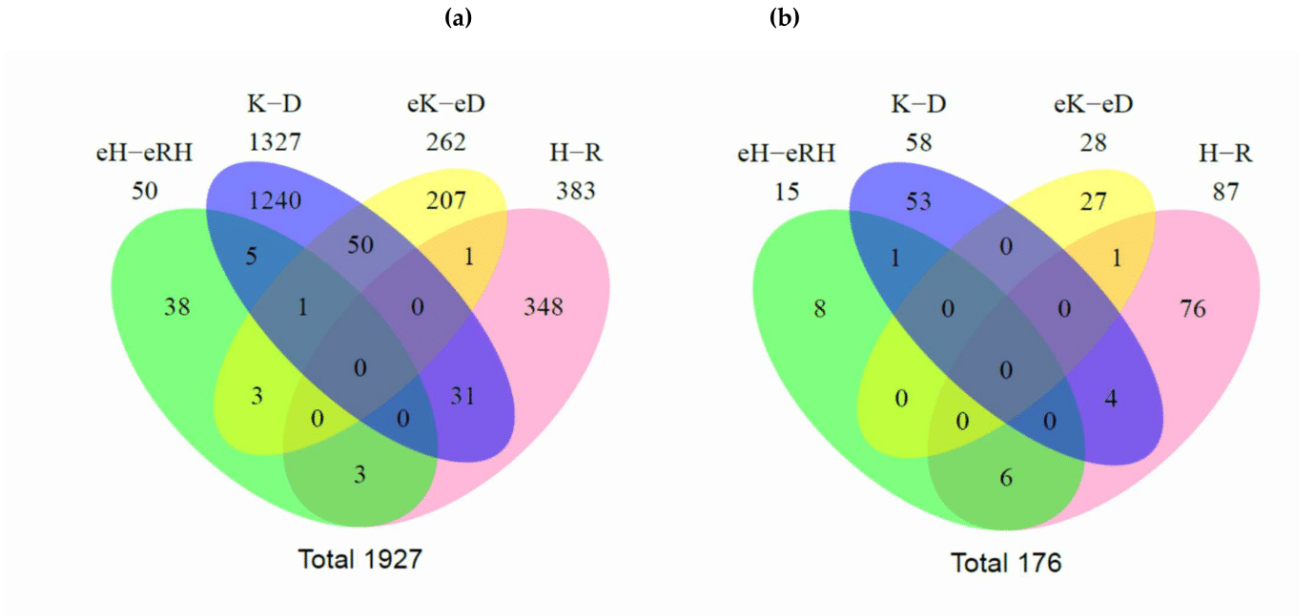


Figure 6: Venn diagram of significantly differentially regulated RNA species (A) and miRs (B). eH: NCI-H460 EVs; eRH: NCI-H460/R EVs; eK: K562 EVs; eD: K562Dox EVs; H: NCI-H460 cells; R:NCI-H460/R cells; K-K562 cells; D: K562Dox cells.

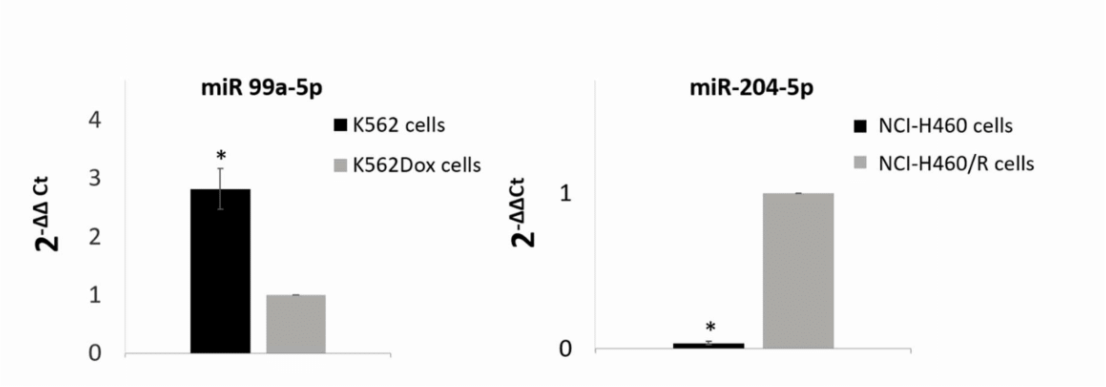


Figure 7: Validation of deep sequencing analysis of two of the miRs found altered, by qRT-PCR. The y-axis represents fold-change of selected genes by real-time PCR (ΔΔCt method) relative to MDR cells. Results are expressed as mean ± SEM**.**

2.6 Functional analysis of the targeted genes

To infer the biological relevance of the previous findings, two approaches were used. Firstly, a hierarchical clustering of all significantly regulated miRs was performed. In both models, drug-sensitive cells and MDR counterparts were clustered together, as expected (Figure S1a). Similar results were observed for the EVs (Figure S1b). Importantly, differential expression of some miRs was observed between drug-sensitive and MDR conditions in both tumour models, in agreement with the results from the Venn diagram.

Moreover, a functional analysis of the possible targeted mRNAs of the miRs found altered in the present study was performed, using the DAVID bioinformatics tools. Results indicated, as expected, that the dysregulated pathways between drug-sensitive and MDR conditions (cells and EVs, in both tumour models) are greatly associated with cancer (Figure S2). The molecular function analysis indicated that the targeted mRNAs are involved in regulation of transcriptome and proteome (Figure 8).

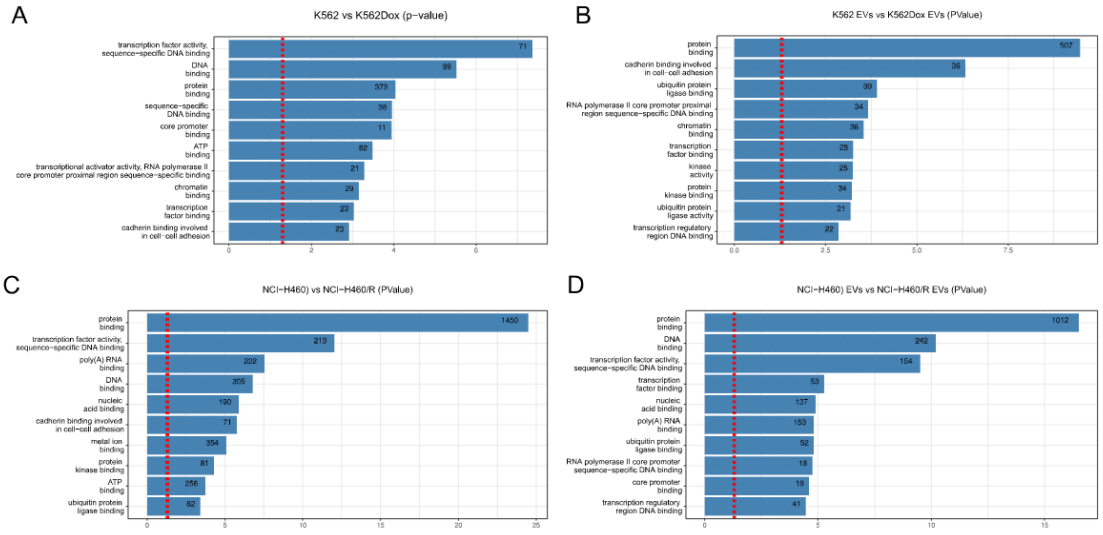


Figure 8: Molecular function of the possible target mRNAs of the significant regulated miRs. Functional analysis performed by DAVID analysis.

3. Discussion

MDR is one of the main limitations of cancer treatment efficacy. MDR results from a complex network of altered pathways that allows malignant cells to proliferate without responding to chemotherapy [1]. In order to overcome MDR in patients, it is essential to understand the multifactorial and complex nature of MDR, including the triggers and mechanisms involved in the development and dissemination of this phenotype. In recent years, the possibility that EVs released by MDR cells may contribute to drug resistance in recipient drug-sensitive cells has been described [5]. In addition, it was found that drug-efflux pumps (such as P-gp) as well as non-coding RNAs (namely microRNAs and long non-coding RNAs) are present in the cargo of EVs released by drug resistant cells [23], possibly contributing to the horizontal transfer of drug resistance to recipient cells [5]. Nonetheless, the majority of these studies were carried out with probe-based methodology [24]. Thus, using high throughput technology, which allows the analysis of a great amount of data (including previously undescribed species), in this work we aimed to analyse the RNA species from pairs of MDR and drug-sensitive cells and from the EVs released by those cells. We studied two different tumour models: CML and NSCLC. For each model, a pair of cell lines was used, consisting of a drug-sensitive cell line and its MDR (P-gp overexpressing) counterpart.

To the best of our knowledge, this is the first study assembling data obtained by deep sequencing from pairs of drug-sensitive and MDR counterpart cells as well as from their EVs. In our previous studies, EVs from drug-sensitive and MDR cells have been isolated using the same methodology as described in the present study and thoroughly characterized [25-27], presenting a size range from 50 to 150 nm and classical EVs markers (Hsp70, Syntenin, CD63 and TSG101). Some of those features were further confirmed in the EVs isolated in this study (Figure S3).

In the present work, we confirmed the evidence obtained by other authors [17-19], on the ability of EVs released by MDR cells to transfer a drug-resistant phenotype to drug-sensitive recipient cells. Furthermore, in order to identify important players of this MDR phenotype, we analysed the RNA content of both cells and EVs.

Our results showed that MDR cells and their drug-sensitive counterparts have a different content of RNA species. Moreover, the EVs released by MDR cells also have different RNA entities from the EVs released by their drug-sensitive counterparts. Importantly, following the

EVs isolation, treatment with proteinase K and RNase was performed before RNA extraction, strengthening the association of extracellular RNA results to EVs and not to protein-RNA precipitates.

First, we observed that the Bioanalyzer profile of small RNA molecules is different between cells and EVs, as previously shown by other authors [28]. Usually the ncRNAs are named according to their size: small RNAs (which include short ncRNAs with 17bp-32bp [miRNAs, piRNAs and tiRNAs], mid-size ncRNAs with 60bp-200bp [snoRNAs, PASRs, TSSs-RNAs and PROMPTs]) and long ncRNAs with more than 200 bp (lincRNAs, T-UCRs and other long ncRNAs)) [29]. In our models, the type of RNA species was, in general, similar between cells and EVs. Importantly, pseudogenes were the most abundant RNA species present in all samples, with around 40% abundance, with miRs representing only approximately 4-7% of the total small RNAs. This value seems lower than expected but another study showed that miRs may be a minor form of RNAs in the EVs cargo, whereas tRNA fragments and Y-RNAs were described to be specifically secreted into EVs (by the donor cells) [30]. By contrast, another study showed that even though EVs contain proportionally less small RNAs than cells, their small RNA fraction was enriched in miRs [31]. Therefore, the relative abundance of miRs in the EVs cargo is still under debate and it might be influenced by pathophysiological changes [32]. In the present study, a relative higher abundance of miRs (compared to total RNA species) was found in EVs released by NSCLC cells than in those cells. Nevertheless, this finding was not confirmed in the CML model, indicating that the relative abundance of miRs could also be dependent of the tumour type.

Deep sequencing tools have revealed that the small RNA species found in cells go far beyond the classical small interfering, piwi-associated and miR families. Non-protein-coding functional RNAs such as rRNA, tRNA, snRNA and snoRNA have also a role, or at least a predictive role, in pathways regulation [30]. Our results showed differential levels of some RNA species between drug-sensitive and MDR conditions (cells and EVs). To better comprehend the data, a Venn diagram allowed the interception of the four groups (drug-sensitive cells *vs* MDR cells; drug-sensitive EVs *vs* MDR EVs, from both NSCLC and CML models). A total of 1927 RNA species were found altered between drug-sensitive and MDR conditions. Importantly, three species were found altered in the EVs from both models. Interestingly, these three species were all pseudogenes. This result is in agreement with the pie chart results showing the distribution of mapped reads, where the higher percentage was of pseudogenes. Two of these pseudogenes were increased in EVs released by MDR cells from both tumour models: a novel pseudogene and the RNA5.8S ribosomal pseudogene 2. Pseudogenes are genes that lost their ability to synthesize proteins due to events such as premature stop codons, splicing errors and frameshift- causing deletions or insertions [33]. The diagnostic and prognostic value of pseudogenes in cancer has been described. Some studies have associated alterations in pseudogenes with overall survival or disease free survival [34]. Three important examples are *PTENP1*, *E2F3P1* and *OCT4-pg1* in renal cell carcinoma [35], hepatocellular carcinoma [36] and gastric cancer [37], respectively. Interestingly, the presence of pseudogenes in EVs was previously found. Indeed, pseudogenes associated to ribosomal proteins or heat-shock proteins, among others, were previously detected in other studies, as confirmed in the Vesiclepedia (a database of EVs content [38]). However, in the majority of those studies, the presence of pseudogenes was not discussed. Thus, the role of pseudogenes in cells and in EVs needs further clarification. We argue that the two pseudogenes here found to be increased in EVs released by MDR cells (from NSCLC and CML) may be further studied regarding their possible application as MDR-related biomarkers in blood plasma. Importantly, five transcripts were also found similarly altered (increased or decreased) in MDR cells from both models: miR-383, miR-4660, chromosome 16 open reading frame 45, FOXF1 adjacent non-coding developmental regulatory RNA and serglycin. These transcripts may be also further investigated as putative MDR-biomarkers. Interestingly, four of these transcripts were

previously associated with regulation of tumour cell proliferation [39], epithelial-mesenchymal transition [40], stemness [40], metastization [40-42], poor prognosis [41] and poor survival [43].

There are different triggering factors for MDR traits, some of them being tumour-specific mechanisms (e.g. genetic alterations). Notably, as mentioned above, in the present work an haematological (CML) and a non-haematological (NSCLC) tumour model were studied. The cellular features of both models are very different, but both the MDR cell lines have in common the overexpression of P-gp as the main mechanism responsible for their MDR phenotype. Thus, the study of these two different tumour MDR models may allow the identification of alterations associated with a MDR phenotype caused by (or responsible for) P-gp overexpression. Importantly, in the hierarchical clustering of miRs, each pair of cell lines (drug sensitive and MDR) clustered together, suggesting that the drug resistant phenotype has a smaller effect on miRs regulation than the source of the cell line. The same result was observed for EVs.

The specific differential expression of miRs between drug-sensitive and MDR (cells and EVs) was also analysed by a Venn diagram. The obtained results showed a panel of 6 miRs with different levels between drug-sensitive and MDR cells and EVs in the NSCLC model: miR-204-5p, miR-139-5p, miR-29c-5p, miR-551b-3p, miR-29b-2-5p, miR-204-3p. Thus, we suggest that these miRs should be further studied as potential MDR biomarkers of NSCLC. Indeed, all these miRs were previously associated to tumour cell proliferation or cancer progression [44-48]. Importantly, the differential expression of miR-204-5p was further validated by qRT-PCR. Further analysis of the Venn diagram allowed the identification of 2 miRs with altered levels between drug-sensitive and MDR cells, in both tumour models: miR-383-5p and miR-504-5p. Thus, we suggest that they may have a putative role in P-gp-associated MDR. Importantly, both miRs were previously associated with regulation of tumour cell proliferation and cancer drug resistance [39,49,50]. It is well known that one single miR has different cellular targets and therefore, depending on the cellular context, the same miR may have tumour suppressor or tumour promotion properties. Thus, miR relative levels described above should be interpreted taking into account the alterations observed (decrease or increase in MDR condition, for each model). For example, published studies by two independent groups had shown that miR-451 and miR-27a were upregulated in MDR tumour cell lines and caused an increase in P-gp levels [51,52]. However, other studies have described the opposite effect for these two miRs, regarding effect on P-gp expression and drug resistance [53,54]. These apparently contradictory results may be explained by the different cellular context in the different studies.

The mechanisms postulated for sorting of small RNAs (particularly miRs) into EVs were elegantly reviewed by R. Boheme *et al.*[55]. Briefly, miRs sorting is regulated by i) RISC-associated proteins, ii) cellular miRs/ target mRNA levels, iii) 3' non-template terminal nucleotide additions, iv) 3' sequence motifs/protein guides and v) ceramide biosynthesis. Nonetheless, the selection of the EVs' cargo by the donor cells is still under extensive study and not fully understood. Some authors describe that the sorting of RNA species into EVs is selective, while other authors defend a non-selective packaging of this cargo [30,56]. In our models, we observed that all species present in EVs were also present in the respective cells (as expected). However, some species present in cells were not found in EVs. This evidence indicates a selective sorting/packaging of some RNA species into EVs. Indeed, from the Venn diagram analysis of either the RNA species or of the miRs in particular, some RNA entities were found differentially present, between MDR and drug-sensitive models, only in the EVs and not in the cells, in both tumour models. Moreover, the pie chart analysis (of the NSCLC model) showed higher percentage of miRs in EVs, when compared with cells. Taken together, these results suggest that some RNA species probably are selectively packaged into EVs.

4. Materials and Methods

Cell culture

Two pairs of cell lines from two different human tumour models were used, consisting of a drug-sensitive cell line (DS) and its MDR (P-gp overexpressing) counterpart: i) NCI-H460 (DS) and NCI-H460/R (MDR) non-small cell lung cancer cells (NSCLC), a kind gift of Dr. M. Pešić, Belgrade, Serbia [57,58]) and ii) K562 (DS) and K562Dox (MDR), chronic myeloid leukaemia cells (CML) a kind gift of Dr. J.P. Marie, Paris, France [59,60]). To maintain the MDR phenotype, 100 nM doxorubicin was added to the NCI-H460/R cells every month and 1 μM doxorubicin was added to the K562Dox cells every 2 weeks. All cell lines were genotyped and routinely monitored for possible mycoplasma contamination by PCR (Cell Culture and Genotyping Service, i3S). Cells were cultured in RPMI-1640 medium with Ultraglutamine I and 25mM HEPES (Biowest) supplemented with 10% fetal bovine serum (FBS, Biowest) at 37°C in a humidified incubator with 5% CO_2 in air. Experiments were performed with cells in exponential growth and over 90% viability.

EVs Isolation

Cells were grown in conditioned media consisting of RPMI with 10% EVs-depleted FBS (previously ultracentrifuged at 4°C for at least 16h). Cell culture medium was collected and differentially centrifuged as described by Thery *et al* [61]. Briefly, the sequence of centrifugations was the following: 300 g for 10 min; 2000 g for 10 min; 10 000g for 30 min; 100 000g for 1h15. The final pellet was washed in PBS. For RNA downstream analysis, pellet was re-suspended in PBS and stored at -80°C For co-culture studies, the pellet was re-suspended in FBS-depleted medium and immediately used.

Co-culture of EVs with cells

NCI-H460 cells were seeded in 96-well plates (5000 cells/well). After 24h, the EVs isolated from NCI-H460/R cells were added to the cells and 24h later, doxorubicin-HCl (Sigma-Aldrich®) treatment was performed (50 nM). Following 24h, the SRB (sulphorhodamine B) assay was carried out as previously described [62]. Briefly, cells were fixed with 10% (w/v) ice cold trichloroacetic acid (TCA), washed with distilled water and incubated with 0.4% (w/v) SRB for 30 minutes. After washing with 1% acetic acid, Tris base 10 mM was used to solubilize the SRB. Absorbance was measured at 510 nm using a multiplate reader (Synergy Mx, Biotek Instruments Inc.), as previously described [62].

RNA extraction

The isolated EVs were treated with proteinase K (0.05μg/μl) and RNase (0.5μg/μl) [63]. RNA was then extracted using the miRCURY™ RNA Isolation Kit – Cell & Plant (Exiqon), following the manufacturer instructions. RNA quality was evaluated using Bioanalyzer (Agilent 2100). Samples (from three independent biological replicates) were stored at -80°C until library preparation.

Library preparation and next generation sequencing

Libraries were constructed according to the Ion Total RNA-Seq Kit v2 protocol (Life Technologies) and pooled. Each sample was ligated to a unique barcode (BC) for sample identification and tracking. Due to the presence of adapter dimers in some of the samples, an adapted protocol was developed consisting in the running of the final libraries into an agarose gel and band excision, thus avoiding the adapter dimer bands. The pooled libraries were further processed on Ion Chef™ System (Life Technologies) and the resulting 550™ chips were sequenced on Ion S5™XL System [64].

Bioinformatics and statistical Analysis

A total of 24 FASTQ files from Ion Torrent sequencer were analysed. Files were trimmed using CutAdapt with the parameters: minimum fragment length was set to 10 and minimum quality to 20 [65]. Quality of the trimmed reads were assessed by FASTQC [Andrews S. Fast QC, A Quality Control tool for High Throughput Sequence Data, 2014;[66]. Reads were then aligned by Bowtie1 to human genome assembly (hg19) allowing one mismatch. Read count was calculated using FeatureCounts [67] software implemented in miARma-Seq [68] using minimum quality of 10. The genome annotation files miRBase_Annotation_20_for_hsa_mature_miRNA.gtf and /Homo_sapiens.GRCh37.75.gtf for miRNAs and all RNAs, respectively. Significant differential expression was calculated using EdgeR [69] minimum count per million cut-off of 2. biomaRt [70] were used to retrieve transcript annotation. MDS plots were made with the R package Limma using minimum count per million cut-off of 2 [71]. Target mRNAs was determined by extracting significant regulated miRNA after correction of multiple testing (p value < 0.05) and mapping targets using miRTarBase. GO and KEGG functional analysis were performed by DAVID [72] using FDR corrected p values.

NGS validation by qRT-PCR

For both tumour models, one miR was selected for further validation of NGS results, by quantitative Real time PCR (qRT-PCR). Total RNA (2 ng) was reverse transcribed using the miScript II Reverse Transcription Kit (Qiagen), according to the manufacturer's instructions. The miRNA expression levels were then measured using miSCRIPT Primer Assay and the Quantitect SYBR Green PCR Kit (Qiagen), according to the manufacturer's instructions. Dissociation curves were generated. The relative expression ratio of each miR was normalized to another miR found to be abundantly expressed and also whose expression levels did not differ in drug-sensitive and MDR conditions. Data was analysed with the $2^{-\Delta\Delta Ct}$ method [73].

5. Conclusions

In the present work, using high throughput technology, we were able to compare the RNA species present in drug-sensitive and MDR counterpart cells and in the EVs released by those cells. Importantly, two pseudogenes (a novel pseudogene and RNA 5.8S ribosomal pseudogene 2) were found upregulated in EVs released by MDR cells, on both tumour models studied (NSCLC and CML). In addition, a panel constituted by miR-204-5p, miR-139-5p, miR-29c-5p, miR-551b-3p, miR-29b-2-5p, miR-204-3p was also found upregulated in EVs released by MDR cells and in their donor MDR NCSLC cells. Thus, these pseudogenes and miRs should be further studied as potential biomarkers of MDR in cancer and further studies need to be carried out to confirm their role in MDR.

Supplementary Materials:

Supplementary Methods

Electron microscopy

EVs re-suspended in PBS were adsorbed onto Formvar-carbon coated electron microscopy grids at room temperature for 2 min. Following this, EVs were stained with 5% uranyl acetate and visualized in a JEM 1400 transmission electron microscope at an accelerating voltage of 80 kV (Jeol).

Dynamic light scattering

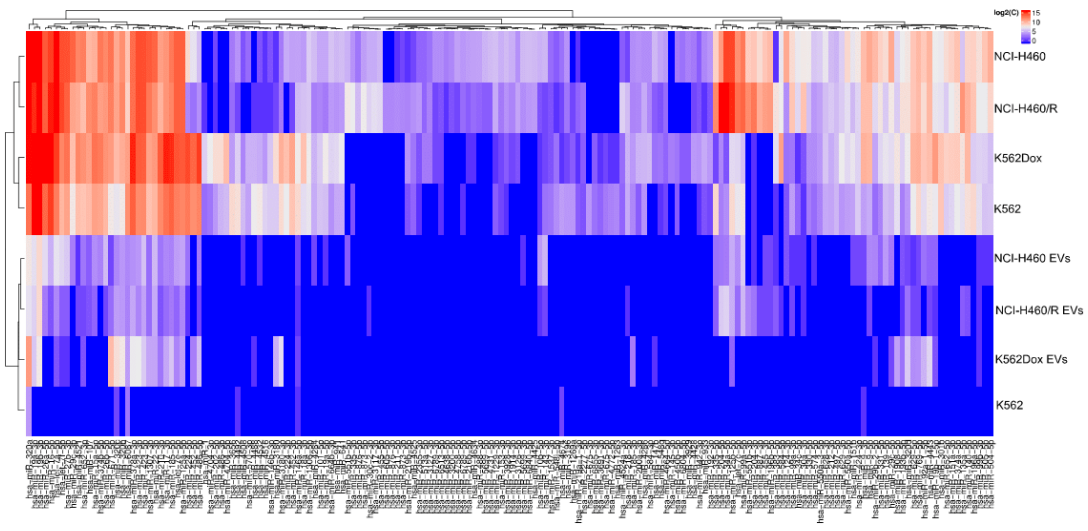
The EV size/diameter was measured by dynamic light scattering (DLS), using a Nano series Malvern Zetasizer Instrument (Prager Instruments). Measurements were carried out at 20 °C, at 633 nm and recording the back scattered light at an angle of 173°. The mean hydrodynamic diameter of exosomes was calculated by fitting a Gaussian function to the measured size distribution. Three measurements per sample were performed.

Western-blotting

EVs were lysed in Winman's buffer (1% NP-40, 0.1 M Tris–HCl pH 8.0, 0.15 M NaCl, and 5 mM EDTA) with EDTA-free protease inhibitor cocktail (Roche), and quantified using a modified Lowry assay (Bio-Rad). After quantification, proteins, 5 µg were separated on a 12% Bis–Tris SDS-PAGE gel and transferred into a nitrocellulose membrane (GE Healthcare). Membranes were then incubated with the anti-syntenin and anti-cytochrome c primary antibody. Signal was detected using the ECL Western blot Detection.

Supplementary Figures

a



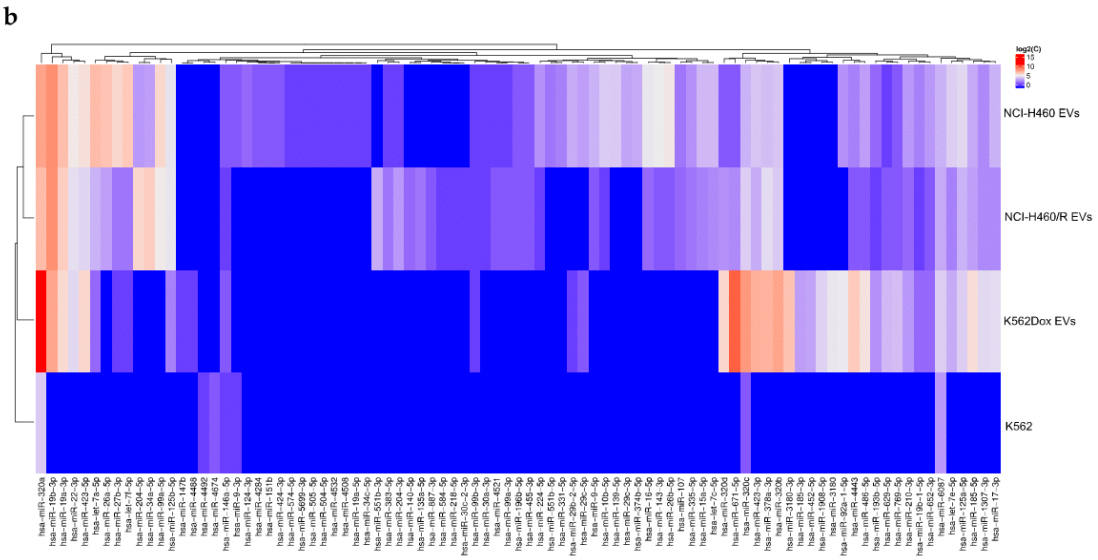


Figure S1. Hierarchical clustering of significant regulated miRs in drug-sensitive and MDR counterparts cells (a) and their respective EVs (b).

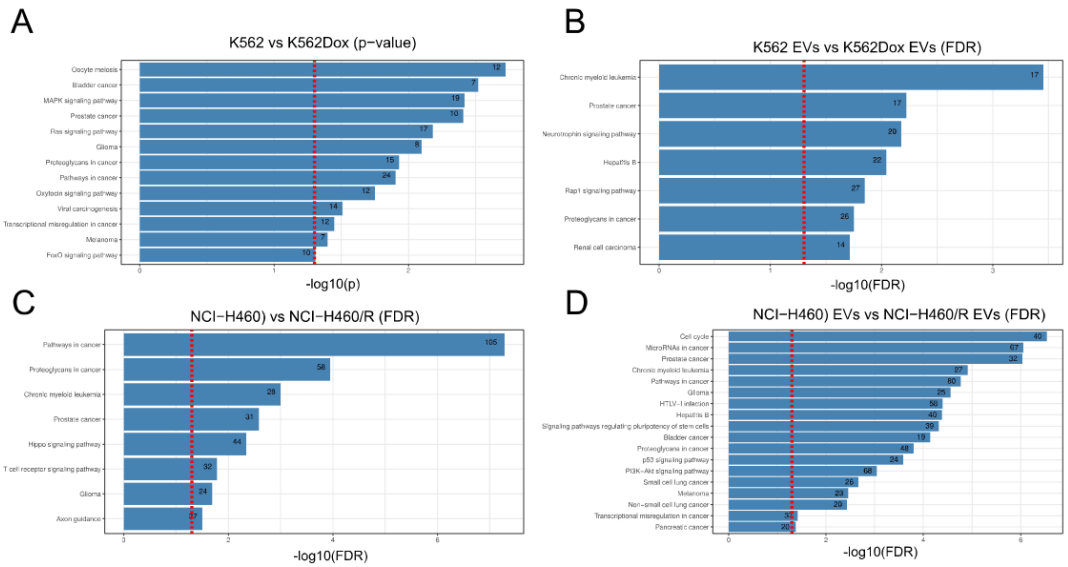


Figure S2: Functional analysis of the possible target mRNAs of the miRs found significantly altered. The functional analyse were performed by DAVID.

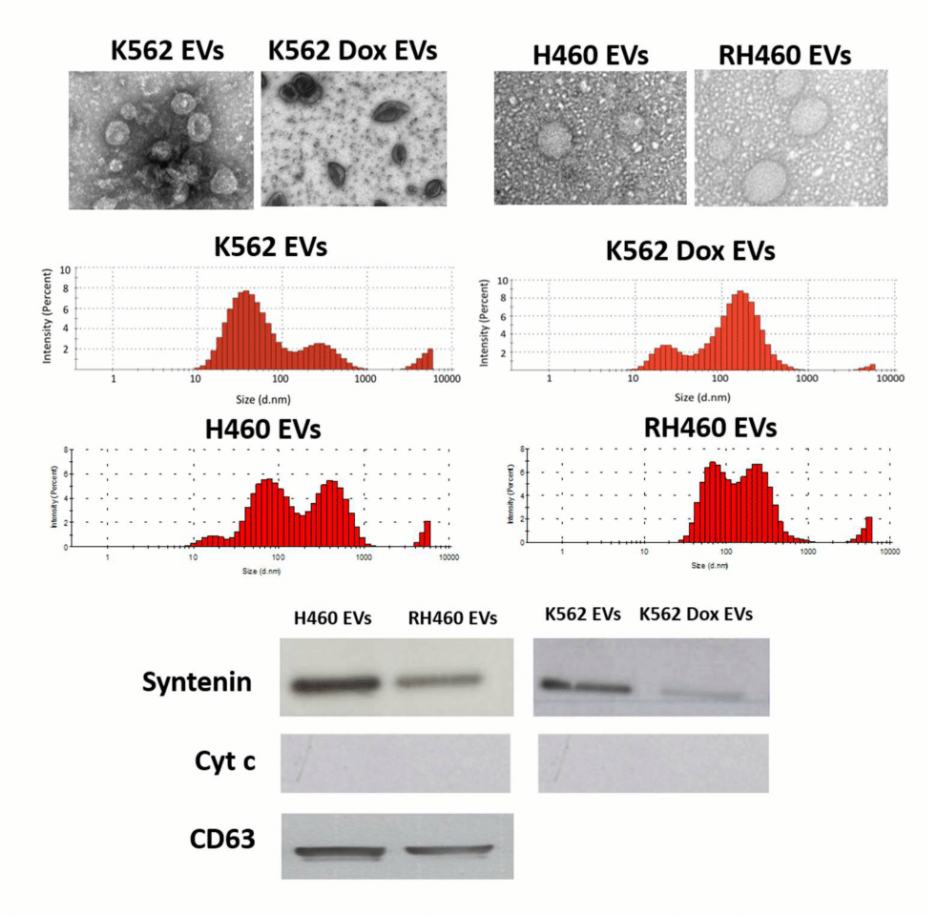


Figure S3: Characterization of EVs isolated from pairs of drug-sensitive and MDR cells, from NSCLC and CML cell lines (NCI-H460/ NCI-H460/R pair and K562/K562Dox pair, respectively). a) Morphology of EVs, analysed by TEM. **b)** EVs' size distribution, analysed by DLS. **c)** Levels of syntenin, cytochrome c (and CD63 in the case of lung cancer) in cells and EVs, analysed by Western blot.

Supplementary Tables:

Table S1: Total number of sequenced reads, number of processed reads after FASTQ quality control, number of alignments mapped to human genome (HG19) and reads obtained in FeatureCounts **(RNA species) for each biological replicate of drug-sensitive and MDR cells, as well as respective EVs, in both CML (K562,K562Dox) and NSCLC (NCI-H460,NCI-H460/R) cell models.**

	Total raw reads	Processed reads	Aligned reads to HG19	Percentage of aligned reads	FeatureCounts reads
K562 Cells_1	1303598	1213245	1023829	84.39	250165
K562 Cells_1	3319788	3140842	2697865	85.90	657641
K562 Cells_1	3908697	3589748	3034739	84.54	621579
K562 Dox Cells_1	6084950	5797019	4806333	82.91	1353561
K562 Dox Cells_2	3906430	3712734	3184057	85.76	786221
K562 Dox Cells_3	14336331	13652775	11127816	81.51	2892744
NCI-H460 Cells_1	9167846	8656379	6701715	77.42	1713464
NCI-H460 Cells_2	12264338	11651693	9014105	77.36	2287726
NCI-H460 Cells_3	6505867	5858996	4823313	82.32	1191529
NCI-H460/R Cells_1	8853281	8296848	6062231	73.07	1569477
NCI-H460/R Cells_2	8678351	8104700	5934614	73.22	1583488
NCI-H460/R Cells_3	5432190	5045464	3660955	72.56	913450
K562 EVs_1	355649	312999	295370	94.37	16959
K562 EVs_2	344606	287909	257278	89.36	11966
K562 EVs_3	192891	173521	152627	87.96	7366
K562 Dox EVs_1	610966	514262	428994	83.42	24944
K562 Dox EVs_2	219798	186092	160607	86.31	10232
K562 Dox EVs_3	453339	373974	346129	92.55	19071
NCI-H460 EVs_1	216024	186935	145052	77.59	20758
NCI-H460 EVs_2	135428	122800	90991	74.10	7294
NCI-H460 EVs_3	161862	144634	103519	71.57	11393
NCI-H460/R EVs_1	114887	105198	71957	68.40	8818
NCI-H460/R EVs_2	117803	104749	75390	71.97	6335
NCI-H460/R EVs_3	265850	233415	170923	73.23	23900

Tables S2 to S9: attached excel Files

Supplementary Tables legends:
Table S2: Log Fold Change of RNA species expression between drug-sensitive (NCI-H460) cells and their MDR (NCI-H460/R) counterparts. Log FC above > 1 and P value < 0.05 indicate up regulation in MDR condition.

Table S3: Log Fold Change of RNA species expression between drug-sensitive (K562) cells and their MDR (K562Dox) counterparts. Log FC above > 1 and P value < 0.05 indicate up regulation in MDR condition.

Table S4 Log Fold Change of RNA species expression between EVs released by drug-sensitive (NCI-H460) cells and the EVs released by their MDR (NCI-H460/R) counterparts. Log FC above > 1 and P value < 0.05 indicate up regulation in MDR condition.

Table S5: Log Fold Change of levels of RNA species between EVs released by drug-sensitive (K562) cells and EVs released by their MDR (K562Dox) counterparts. Log FC above > 1 and P value < 0.05 indicate up regulation in MDR condition.

Table S6: Log Fold Change of levels of miRs between drug-sensitive (NCI-H460) cells and their MDR (NCI-H460/R) counterparts. Log FC above > 1 and P value < 0.05 indicate up regulation in MDR condition.

Table S7: Log Fold Change of miRs expression between drug-sensitive (K562) cells and their MDR (K562Dox) counterparts. Log FC above > 1 and P value < 0.05 indicate up regulation in MDR condition.

Table S8: Log Fold Change of levels of miRs between EVs released by drug-sensitive (NCI-H460) cells and EVs released by their MDR (NCI-H460/R) counterparts. Log FC above > 1 and P value < 0.05 indicate up regulation in MDR condition.

Table S9: Log Fold Change of miRs expression between drug-sensitive (K562) cells and EVs derived from their MDR (K562Dox) counterparts. Log FC above > 1 and P value < 0.05 indicate up regulation in MDR condition.

Author Contributions: Conceptualization, M. Helena Vasconcelos; Funding acquisition, M. Helena Vasconcelos; Methodology, Diana Sousa; Project administration, M. Helena Vasconcelos; Software, Rune Matthiesen; Supervision, Raquel T. Lima and M. Helena Vasconcelos; Validation, Diana Sousa and Rune Matthiesen; Writing – original draft, Diana Sousa and M. Helena Vasconcelos; Writing – review & editing, Diana Sousa, Rune Matthiesen, Raquel T. Lima and M. Helena Vasconcelos

Funding: This article is a result of the project NORTE-01-0145-FEDER-000029, supported by Norte Portugal Regional Programme (NORTE 2020), under the PORTUGAL 2020 Partnership Agreement, through the European Regional Development Fund (ERDF). This work was partially financed by FEDER - Fundo Europeu de Desenvolvimento Regional funds through the COMPETE 2020 - Operacional Programme for Competitiveness and Internationalisation (POCI), Portugal 2020, and by Portuguese funds through FCT - Fundação para a Ciência e a Tecnologia/Ministério da Ciência, Tecnologia e Ensino Superior in the framework of the project "Institute for Research and Innovation in Health Sciences" (POCI-01-0145-FEDER-007274). This work is also a result of the GenomePT project (POCI-01-0145-FEDER-022184), supported by COMPETE 2020 - Operational Programme for Competitiveness and Internationalisation (POCI), Lisboa Portugal Regional Operational Programme (Lisboa2020), Algarve Portugal Regional Operational

Programme (CRESC Algarve2020), under the PORTUGAL 2020 Partnership Agreement, through the European Regional Development Fund (ERDF), and by Fundação para a Ciência e a Tecnologia (FCT). The authors thank the Portuguese Foundation for Science and Technology (FCT) for the PhD grant of DS (SFRH/BD/98054/2013).

Acknowledgments: The next generation sequencing was performed at the GenCore i3S Scientific Platform with the assistance of Mafalda Rocha.

Conflicts of Interest: The authors declare no conflict of interest.

References

1. Gottesman, M.M.; Lavi, O.; Hall, M.D.; Gillet, J.P. Toward a Better Understanding of the Complexity of Cancer Drug Resistance. *Annu Rev Pharmacol Toxicol* **2016**, *56*, 85-102, doi:10.1146/annurev-pharmtox-010715-103111.
2. Lage, H. An overview of cancer multidrug resistance: a still unsolved problem. *Cell Mol Life Sci* **2008**, *65*, 3145-3167, doi:10.1007/s00018-008-8111-5.
3. Holohan, C.; Van Schaeybroeck, S.; Longley, D.B.; Johnston, P.G. Cancer drug resistance: an evolving paradigm. *Nat Rev Cancer* **2013**, *13*, 714-726, doi:10.1038/nrc3599.
4. Konoshenko, M.Y.; Lekchnov, E.A.; Vlassov, A.V.; Laktionov, P.P. Isolation of Extracellular Vesicles: General Methodologies and Latest Trends. *Biomed Res Int* **2018**, *2018*, 8545347, doi:10.1155/2018/8545347.
5. Sousa, D.; Lima, R.T.; Vasconcelos, M.H. Intercellular Transfer of Cancer Drug Resistance Traits by Extracellular Vesicles. *Trends Mol Med* **2015**, *21*, 595-608, doi:10.1016/j.molmed.2015.08.002.
6. Colombo, M.; Raposo, G.; Thery, C. Biogenesis, secretion, and intercellular interactions of exosomes and other extracellular vesicles. *Annu Rev Cell Dev Biol* **2014**, *30*, 255-289, doi:10.1146/annurev-cellbio-101512-122326.
7. Cheng, L.; Sharples, R.A.; Scicluna, B.J.; Hill, A.F. Exosomes provide a protective and enriched source of miRNA for biomarker profiling compared to intracellular and cell-free blood. *J Extracell Vesicles* **2014**, *3*, doi:10.3402/jev.v3.23743.
8. Whiteside, T.L. Tumor-Derived Exosomes and Their Role in Cancer Progression. *Adv Clin Chem* **2016**, *74*, 103-141, doi:10.1016/bs.acc.2015.12.005.
9. Aubertin, K.; Silva, A.K.; Luciani, N.; Espinosa, A.; Djemat, A.; Charue, D.; Gallet, F.; Blanc-Brude, O.; Wilhelm, C. Massive release of extracellular vesicles from cancer cells after photodynamic treatment or chemotherapy. *Sci Rep* **2016**, *6*, 35376, doi:10.1038/srep35376.
10. Xu, R.; Rai, A.; Chen, M.; Suwakulsiri, W.; Greening, D.W.; Simpson, R.J. Extracellular vesicles in cancer - implications for future improvements in cancer care. *Nat Rev Clin Oncol* **2018**, *15*, 617-638, doi:10.1038/s41571-018-0036-9.
11. Fais, S.; O'Driscoll, L.; Borras, F.E.; Buzas, E.; Camussi, G.; Cappello, F.; Carvalho, J.; Cordeiro da Silva, A.; Del Portillo, H.; El Andaloussi, S., et al. Evidence-Based Clinical Use of Nanoscale Extracellular Vesicles in Nanomedicine. *ACS Nano* **2016**, *10*, 3886-3899, doi:10.1021/acsnano.5b08015.
12. Valadi, H.; Ekstrom, K.; Bossios, A.; Sjostrand, M.; Lee, J.J.; Lotvall, J.O. Exosome-mediated transfer of mRNAs and microRNAs is a novel mechanism of genetic exchange between cells. *Nat Cell Biol* **2007**, *9*, 654-659, doi:10.1038/ncb1596.
13. van Balkom, B.W.; de Jong, O.G.; Smits, M.; Brummelman, J.; den Ouden, K.; de Bree, P.M.; van Eijndhoven, M.A.; Pegtel, D.M.; Stoorvogel, W.; Wurdinger, T., et al. Endothelial cells require miR-214 to secrete exosomes that suppress senescence and induce angiogenesis in human and mouse endothelial cells. *Blood* **2013**, *121*, 3997-4006, S3991-3915, doi:10.1182/blood-2013-02-478925.
14. Yang, M.; Chen, J.; Su, F.; Yu, B.; Su, F.; Lin, L.; Liu, Y.; Huang, J.D.; Song, E. Microvesicles secreted by macrophages shuttle invasion-potentiating microRNAs into breast cancer cells. *Mol Cancer* **2011**, *10*, 117, doi:10.1186/1476-4598-10-117.

15. Kanlikilicer, P.; Rashed, M.H.; Bayraktar, R.; Mitra, R.; Ivan, C.; Aslan, B.; Zhang, X.; Filant, J.; Silva, A.M.; Rodriguez-Aguayo, C., et al. Ubiquitous Release of Exosomal Tumor Suppressor miR-6126 from Ovarian Cancer Cells. *Cancer Res* **2016**, *76*, 7194-7207, doi:10.1158/0008-5472.CAN-16-0714.
16. Bach, D.H.; Hong, J.Y.; Park, H.J.; Lee, S.K. The role of exosomes and miRNAs in drug-resistance of cancer cells. *Int J Cancer* **2017**, *141*, 220-230, doi:10.1002/ijc.30669.
17. Chen, W.X.; Liu, X.M.; Lv, M.M.; Chen, L.; Zhao, J.H.; Zhong, S.L.; Ji, M.H.; Hu, Q.; Luo, Z.; Wu, J.Z., et al. Exosomes from drug-resistant breast cancer cells transmit chemoresistance by a horizontal transfer of microRNAs. *PLoS One* **2014**, *9*, e95240, doi:10.1371/journal.pone.0095240.
18. Choi, D.Y.; You, S.; Jung, J.H.; Lee, J.C.; Rho, J.K.; Lee, K.Y.; Freeman, M.R.; Kim, K.P.; Kim, J. Extracellular vesicles shed from gefitinib-resistant nonsmall cell lung cancer regulate the tumor microenvironment. *Proteomics* **2014**, *14*, 1845-1856, doi:10.1002/pmic.201400008.
19. Zhang, F.F.; Zhu, Y.F.; Zhao, Q.N.; Yang, D.T.; Dong, Y.P.; Jiang, L.; Xing, W.X.; Li, X.Y.; Xing, H.; Shi, M., et al. Microvesicles mediate transfer of P-glycoprotein to paclitaxel-sensitive A2780 human ovarian cancer cells, conferring paclitaxel-resistance. *Eur J Pharmacol* **2014**, *738*, 83-90, doi:10.1016/j.ejphar.2014.05.026.
20. N.V.Bhagavan, C.-E.H. Chapter 23 - RNA and Protein Synthesis. *Essentials of Medical Biochemistry* **2011**, 301-320.
21. Shao, H.; Im, H.; Castro, C.M.; Breakefield, X.; Weissleder, R.; Lee, H. New Technologies for Analysis of Extracellular Vesicles. *Chem Rev* **2018**, *118*, 1917-1950, doi:10.1021/acs.chemrev.7b00534.
22. Li, H.; Handsaker, B.; Wysoker, A.; Fennell, T.; Ruan, J.; Homer, N.; Marth, G.; Abecasis, G.; Durbin, R.; Genome Project Data Processing, S. The Sequence Alignment/Map format and SAMtools. *Bioinformatics* **2009**, *25*, 2078-2079, doi:10.1093/bioinformatics/btp352.
23. Samuel, P.; Fabbri, M.; Carter, D.R.F. Mechanisms of Drug Resistance in Cancer: The Role of Extracellular Vesicles. *Proteomics* **2017**, *17*, doi:10.1002/pmic.201600375.
24. Jaiswal, R.; Luk, F.; Gong, J.; Mathys, J.M.; Grau, G.E.; Bebawy, M. Microparticle conferred microRNA profiles--implications in the transfer and dominance of cancer traits. *Mol Cancer* **2012**, *11*, 37, doi:10.1186/1476-4598-11-37.
25. Lopes-Rodrigues, V.; Di Luca, A.; Sousa, D.; Seca, H.; Meleady, P.; Henry, M.; Lima, R.T.; O'Connor, R.; Vasconcelos, M.H. Multidrug resistant tumour cells shed more microvesicle-like EVs and less exosomes than their drug-sensitive counterpart cells. *Biochim Biophys Acta* **2016**, *1860*, 618-627, doi:10.1016/j.bbagen.2015.12.011.
26. Lopes-Rodrigues, V.; Di Luca, A.; Sousa, D.; Seca, H.; Meleady, P.; Henry, M.; Lima, R.T.; O'Connor, R.; Vasconcelos, M.H. Data supporting the shedding of larger extracellular vesicles by multidrug resistant tumour cells. *Data Brief* **2016**, *6*, 1023-1027, doi:10.1016/j.dib.2016.02.004.
27. Lopes-Rodrigues, V.; Di Luca, A.; Mleczko, J.; Meleady, P.; Henry, M.; Pesic, M.; Cabrera, D.; van Liempd, S.; Lima, R.T.; O'Connor, R., et al. Identification of the metabolic alterations associated with the multidrug resistant phenotype in cancer and their intercellular transfer mediated by extracellular vesicles. *Sci Rep* **2017**, *7*, 44541, doi:10.1038/srep44541.
28. Lunavat, T.R.; Cheng, L.; Kim, D.K.; Bhadury, J.; Jang, S.C.; Lasser, C.; Sharples, R.A.; Lopez, M.D.; Nilsson, J.; Gho, Y.S., et al. Small RNA deep sequencing discriminates subsets of extracellular vesicles released by melanoma cells--Evidence of unique microRNA cargos. *RNA Biol* **2015**, *12*, 810-823, doi:10.1080/15476286.2015.1056975.
29. Silva, M.; Melo, S.A. Non-coding RNAs in Exosomes: New Players in Cancer Biology. *Curr Genomics* **2015**, *16*, 295-303, doi:10.2174/1389202916666150707154719.
30. Tosar, J.P.; Gambaro, F.; Sanguinetti, J.; Bonilla, B.; Witwer, K.W.; Cayota, A. Assessment of small RNA sorting into different extracellular fractions revealed by high-throughput sequencing of breast cell lines. *Nucleic Acids Res* **2015**, *43*, 5601-5616, doi:10.1093/nar/gkv432.
31. Goldie, B.J.; Dun, M.D.; Lin, M.; Smith, N.D.; Verrills, N.M.; Dayas, C.V.; Cairns, M.J. Activity-associated miRNA are packaged in Map1b-enriched exosomes released from depolarized neurons. *Nucleic Acids Res* **2014**, *42*, 9195-9208, doi:10.1093/nar/gku594.
32. Skog, J.; Wurdinger, T.; van Rijn, S.; Meijer, D.H.; Gainche, L.; Sena-Esteves, M.; Curry, W.T., Jr.; Carter, B.S.; Krichevsky, A.M.; Breakefield, X.O. Glioblastoma microvesicles transport RNA and proteins that promote tumour growth and provide diagnostic biomarkers. *Nat Cell Biol* **2008**, *10*, 1470-1476, doi:10.1038/ncb1800.
33. Hu, X.; Yang, L.; Mo, Y.Y. Role of Pseudogenes in Tumorigenesis. *Cancers (Basel)* **2018**, *10*, doi:10.3390/cancers10080256.

34. Poliseno, L.; Marranci, A.; Pandolfi, P.P. Pseudogenes in Human Cancer. *Front Med (Lausanne)* **2015**, *2*, 68, doi:10.3389/fmed.2015.00068.
35. Yu, G.; Yao, W.; Gumireddy, K.; Li, A.; Wang, J.; Xiao, W.; Chen, K.; Xiao, H.; Li, H.; Tang, K., et al. Pseudogene PTENP1 functions as a competing endogenous RNA to suppress clear-cell renal cell carcinoma progression. *Mol Cancer Ther* **2014**, *13*, 3086-3097, doi:10.1158/1535-7163.MCT-14-0245.
36. Pan, Y.; Sun, C.; Huang, M.; Liu, Y.; Qi, F.; Liu, L.; Wen, J.; Liu, J.; Xie, K.; Ma, H., et al. A genetic variant in pseudogene E2F3P1 contributes to prognosis of hepatocellular carcinoma. *J Biomed Res* **2014**, *28*, 194-200, doi:10.7555/JBR.28.20140052.
37. Shen, L.; Du, M.; Wang, C.; Gu, D.; Wang, M.; Zhang, Q.; Zhao, T.; Zhang, X.; Tan, Y.; Huo, X., et al. Clinical significance of POU5F1P1 rs10505477 polymorphism in Chinese gastric cancer patients receving cisplatin-based chemotherapy after surgical resection. *Int J Mol Sci* **2014**, *15*, 12764-12777, doi:10.3390/ijms150712764.
38. Pathan, M.; Fonseka, P.; Chitti, S.V.; Kang, T.; Sanwlani, R.; Van Deun, J.; Hendrix, A.; Mathivanan, S. Vesiclepedia 2019: a compendium of RNA, proteins, lipids and metabolites in extracellular vesicles. *Nucleic Acids Res* **2019**, *47*, D516-D519, doi:10.1093/nar/gky1029.
39. Jiang, J.; Xie, C.; Liu, Y.; Shi, Q.; Chen, Y. Up-regulation of miR-383-5p suppresses proliferation and enhances chemosensitivity in ovarian cancer cells by targeting TRIM27. *Biomed Pharmacother* **2019**, *109*, 595-601, doi:10.1016/j.biopha.2018.10.148.
40. Miao, L.; Huang, Z.; Zengli, Z.; Li, H.; Chen, Q.; Yao, C.; Cai, H.; Xiao, Y.; Xia, H.; Wang, Y. Loss of long noncoding RNA FOXF1-AS1 regulates epithelial-mesenchymal transition, stemness and metastasis of non-small cell lung cancer cells. *Oncotarget* **2016**, *7*, 68339-68349, doi:10.18632/oncotarget.11630.
41. Xu, T.P.; Huang, M.D.; Xia, R.; Liu, X.X.; Sun, M.; Yin, L.; Chen, W.M.; Han, L.; Zhang, E.B.; Kong, R., et al. Decreased expression of the long non-coding RNA FENDRR is associated with poor prognosis in gastric cancer and FENDRR regulates gastric cancer cell metastasis by affecting fibronectin1 expression. *J Hematol Oncol* **2014**, *7*, 63, doi:10.1186/s13045-014-0063-7.
42. Li, X.J.; Qian, C.N. Serglycin in human cancers. *Chin J Cancer* **2011**, *30*, 585-589, doi:10.5732/cjc.011.10314.
43. Slattery, M.L.; Herrick, J.S.; Pellatt, D.F.; Mullany, L.E.; Stevens, J.R.; Wolff, E.; Hoffman, M.D.; Wolff, R.K.; Samowitz, W. Site-specific associations between miRNA expression and survival in colorectal cancer cases. *Oncotarget* **2016**, *7*, 60193-60205, doi:10.18632/oncotarget.11173.
44. Chaluvally-Raghavan, P.; Jeong, K.J.; Pradeep, S.; Silva, A.M.; Yu, S.; Liu, W.; Moss, T.; Rodriguez-Aguayo, C.; Zhang, D.; Ram, P., et al. Direct Upregulation of STAT3 by MicroRNA-551b-3p Deregulates Growth and Metastasis of Ovarian Cancer. *Cell Rep* **2016**, *15*, 1493-1504, doi:10.1016/j.celrep.2016.04.034.
45. Shu, Y.J.; Bao, R.F.; Jiang, L.; Wang, Z.; Wang, X.A.; Zhang, F.; Liang, H.B.; Li, H.F.; Ye, Y.Y.; Xiang, S.S., et al. MicroRNA-29c-5p suppresses gallbladder carcinoma progression by directly targeting CPEB4 and inhibiting the MAPK pathway. *Cell Death Differ* **2017**, *24*, 445-457, doi:10.1038/cdd.2016.146.
46. Li, C.; Dong, Q.; Che, X.; Xu, L.; Li, Z.; Fan, Y.; Hou, K.; Wang, S.; Qu, J.; Xu, L., et al. MicroRNA-29b-2-5p inhibits cell proliferation by directly targeting Cbl-b in pancreatic ductal adenocarcinoma. *BMC Cancer* **2018**, *18*, 681, doi:10.1186/s12885-018-4526-z.
47. Huang, L.L.; Huang, L.W.; Wang, L.; Tong, B.D.; Wei, Q.; Ding, X.S. Potential role of miR-139-5p in cancer diagnosis, prognosis and therapy. *Oncol Lett* **2017**, *14*, 1215-1222, doi:10.3892/ol.2017.6351.
48. Diaz-Martinez, M.; Benito-Jardon, L.; Alonso, L.; Koetz-Ploch, L.; Hernando, E.; Teixido, J. miR-204-5p and miR-211-5p Contribute to BRAF Inhibitor Resistance in Melanoma. *Cancer Res* **2018**, *78*, 1017-1030, doi:10.1158/0008-5472.CAN-17-1318.
49. Ye, M.F.; Zhang, J.G.; Guo, T.X.; Pan, X.J. MiR-504 inhibits cell proliferation and invasion by targeting LOXL2 in non small cell lung cancer. *Biomed Pharmacother* **2018**, *97*, 1289-1295, doi:10.1016/j.biopha.2017.11.005.
50. Yuanyuan Bai, L.X., Pengbo Hu, Bo Zhou. miR-504 regulates chemosensitivity in triple negative breast cancer (TNBC) cells via targeting ABCB8. *Int J Clin Exp Pathol* **2017**, *10*, 1372-1379.
51. Zhu, H.; Wu, H.; Liu, X.; Evans, B.R.; Medina, D.J.; Liu, C.G.; Yang, J.M. Role of MicroRNA miR-27a and miR-451 in the regulation of MDR1/P-glycoprotein expression in human cancer cells. *Biochem Pharmacol* **2008**, *76*, 582-588, doi:10.1016/j.bcp.2008.06.007.

52. Li, Z.; Hu, S.; Wang, J.; Cai, J.; Xiao, L.; Yu, L.; Wang, Z. MiR-27a modulates MDR1/P-glycoprotein expression by targeting HIPK2 in human ovarian cancer cells. *Gynecol Oncol* **2010**, *119*, 125-130, doi:10.1016/j.ygyno.2010.06.004.
53. Kovalchuk, O.; Filkowski, J.; Meservy, J.; Ilnytskyy, Y.; Tryndyak, V.P.; Chekhun, V.F.; Pogribny, I.P. Involvement of microRNA-451 in resistance of the MCF-7 breast cancer cells to chemotherapeutic drug doxorubicin. *Mol Cancer Ther* **2008**, *7*, 2152-2159, doi:10.1158/1535-7163.MCT-08-0021.
54. Feng, D.D.; Zhang, H.; Zhang, P.; Zheng, Y.S.; Zhang, X.J.; Han, B.W.; Luo, X.Q.; Xu, L.; Zhou, H.; Qu, L.H., et al. Down-regulated miR-331-5p and miR-27a are associated with chemotherapy resistance and relapse in leukaemia. *J Cell Mol Med* **2011**, *15*, 2164-2175, doi:10.1111/j.1582-4934.2010.01213.x.
55. Bhome, R.; Del Vecchio, F.; Lee, G.H.; Bullock, M.D.; Primrose, J.N.; Sayan, A.E.; Mirnezami, A.H. Exosomal microRNAs (exomiRs): Small molecules with a big role in cancer. *Cancer Lett* **2018**, *420*, 228-235, doi:10.1016/j.canlet.2018.02.002.
56. Abels, E.R.; Breakefield, X.O. Introduction to Extracellular Vesicles: Biogenesis, RNA Cargo Selection, Content, Release, and Uptake. *Cell Mol Neurobiol* **2016**, *36*, 301-312, doi:10.1007/s10571-016-0366-z.
57. Pesic, M.; Markovic, J.Z.; Jankovic, D.; Kanazir, S.; Markovic, I.D.; Rakic, L.; Ruzdijic, S. Induced resistance in the human non small cell lung carcinoma (NCI-H460) cell line in vitro by anticancer drugs. *J Chemother* **2006**, *18*, 66-73, doi:10.1179/joc.2006.18.1.66.
58. Podolski-Renic, A.; Jadranin, M.; Stankovic, T.; Bankovic, J.; Stojkovic, S.; Chiourea, M.; Aljancic, I.; Vajs, V.; Tesevic, V.; Ruzdijic, S., et al. Molecular and cytogenetic changes in multi-drug resistant cancer cells and their influence on new compounds testing. *Cancer Chemother Pharmacol* **2013**, *72*, 683-697, doi:10.1007/s00280-013-2247-1.
59. Marie, J.P.; Faussat-Suberville, A.M.; Zhou, D.; Zittoun, R. Daunorubicin uptake by leukemic cells: correlations with treatment outcome and mdr1 expression. *Leukemia* **1993**, *7*, 825-831.
60. Seca, H.; Lima, R.T.; Guimaraes, J.E.; Helena Vasconcelos, M. Simultaneous targeting of P-gp and XIAP with siRNAs increases sensitivity of P-gp overexpressing CML cells to imatinib. *Hematology* **2011**, *16*, 100-108, doi:10.1179/102453311X12940641877803.
61. Thery, C.; Amigorena, S.; Raposo, G.; Clayton, A. Isolation and characterization of exosomes from cell culture supernatants and biological fluids. *Curr Protoc Cell Biol* **2006**, *Chapter 3*, Unit 3 22, doi:10.1002/0471143030.cb0322s30.
62. Azevedo, C.M.; Afonso, C.M.; Soares, J.X.; Reis, S.; Sousa, D.; Lima, R.T.; Vasconcelos, M.H.; Pedro, M.; Barbosa, J.; Gales, L., et al. Pyranoxanthones: Synthesis, growth inhibitory activity on human tumor cell lines and determination of their lipophilicity in two membrane models. *Eur J Med Chem* **2013**, *69*, 798-816, doi:10.1016/j.ejmech.2013.09.012.
63. Shelke, G.V.; Lasser, C.; Gho, Y.S.; Lotvall, J. Importance of exosome depletion protocols to eliminate functional and RNA-containing extracellular vesicles from fetal bovine serum. *J Extracell Vesicles* **2014**, *3*, doi:10.3402/jev.v3.24783.
64. Cheng, L.; Hill, A.F. Small RNA Library Construction for Exosomal RNA from Biological Samples for the Ion Torrent PGM and Ion S5 System. *Methods Mol Biol* **2017**, *1545*, 71-90, doi:10.1007/978-1-4939-6728-5_6.
65. Schmieder, R.; Edwards, R. Quality control and preprocessing of metagenomic datasets. *Bioinformatics* **2011**, *27*, 863-864, doi:10.1093/bioinformatics/btr026.
66. http://www.bioinformatics.babraham.ac.uk/projects/fastqc.
67. Liao, Y.; Smyth, G.K.; Shi, W. featureCounts: an efficient general purpose program for assigning sequence reads to genomic features. *Bioinformatics* **2014**, *30*, 923-930, doi:10.1093/bioinformatics/btt656.
68. Andres-Leon, E.; Rojas, A.M. miARma-Seq, a comprehensive pipeline for the simultaneous study and integration of miRNA and mRNA expression data. *Methods* **2019**, *152*, 31-40, doi:10.1016/j.ymeth.2018.09.002.
69. Robinson, M.D.; McCarthy, D.J.; Smyth, G.K. edgeR: a Bioconductor package for differential expression analysis of digital gene expression data. *Bioinformatics* **2010**, *26*, 139-140, doi:10.1093/bioinformatics/btp616.
70. Durinck, S.; Spellman, P.T.; Birney, E.; Huber, W. Mapping identifiers for the integration of genomic datasets with the R/Bioconductor package biomaRt. *Nat Protoc* **2009**, *4*, 1184-1191, doi:10.1038/nprot.2009.97.

71. Soneson, C.; Love, M.I.; Robinson, M.D. Differential analyses for RNA-seq: transcript-level estimates improve gene-level inferences. *F1000Res* **2015**, *4*, 1521, doi:10.12688/f1000research.7563.2.
72. Huang da, W.; Sherman, B.T.; Lempicki, R.A. Systematic and integrative analysis of large gene lists using DAVID bioinformatics resources. *Nat Protoc* **2009**, *4*, 44-57, doi:10.1038/nprot.2008.211.
73. Zhou, X.; Jiao, Z.; Ji, J.; Li, S.; Huang, X.; Lu, X.; Zhao, H.; Peng, J.; Chen, X.; Ji, Q., et al. Characterization of mouse serum exosomal small RNA content: The origins and their roles in modulating inflammatory response. *Oncotarget* **2017**, *8*, 42712-42727, doi:10.18632/oncotarget.17448.



© 2019 by the authors. Submitted for possible open access publication under the terms and conditions of the Creative Commons Attribution (CC BY) license (http://creativecommons.org/licenses/by/4.0/).

2. RESEARCH ARTICLE:

Multidrug Resistant cells have different ability to release and capture EVs than their sensitive counterparts: impact of endocytic pathway alterations

Diana Sousa, Raquel T. Lima, Vanessa Lopes-Rodrigues, Esperanza Gonzalez, Félix Royo, J. M. Falcón-Pérez, M. Helena Vasconcelos

Under revision (in Journal of Extracellular Vesicles)

Multidrug Resistant cells have different ability to release and capture EVs than their sensitive counterparts: impact of endocytic pathway alterations

D.Sousa[1,2,3], R.T. Lima[1,2,4,5], V. Lopes-Rodrigues[1,2,6], Esperanza Gonzalez[7], Félix Royo[7], Juan Manuel Falcón-Pérez[7,8], M.H. Vasconcelos[1,2,3*]

[1]i3S- Instituto de Investigação e Inovação em Saúde, Universidade do Porto, 4200-135, Porto, Portugal
[2]Cancer Drug Resistance Group, IPATIMUP - Institute of Molecular Pathology and Immunology of the University of Porto, 4200-135 Porto, Portugal;
[3]Department of Biological Sciences, FFUP - Faculty of Pharmacy of the University of Porto, 4050-313 Porto, Portugal;
[4]Department of Pathology, FMUP - Faculty of Medicine of the University of Porto, 4200-319 Porto, Portugal;
[5]Cancer Signaling & Metabolism Group, IPATIMUP- Institute of Molecular Pathology and Immunology of the University of Porto, 4200-135 Porto, Portugal;
[6]ICBAS-UP – Institute of Biomedical Sciences Abel Salazar of the University of Porto, 4099-003 Porto, Portugal
[7]Exosomes Lab. & Metabolomics Platform, CIC bioGUNE, CIBERehd, Derio 28160, Bizkaia Spain;
[8]IKERBASQUE Basque Foundation for Science, Bilbao, 48013 Bizkaia, Spain.

*corresponding author: M. Helena Vasconcelos
Tel.: +351-**225 570 772**
E-mail: hvasconcelos@ipatimup.pt

Keywords: cancer multidrug resistance, extracellular vesicles, endocytic pathway, recycling pathway

Abstract

Cancer multidrug resistance (MDR) is one of the main challenges for cancer treatment efficacy. MDR is a phenomenon by which tumor cells become resistant to several unrelated drugs. Some studies have previously described the important role of extracellular vesicles (EVs) in the dissemination of a MDR phenotype. EVs' cargo may include different players of MDR, such as microRNAS and drug-efflux pumps, which may be transferred from donor MDR cells to recipient drug sensitive counterparts. The present work aimed to: i) compare the ability of drug sensitive and their MDR counterpart cells to release and capture EVs, ii) study and relate those differences with a distinct fate of the endocytic pathway in these counterpart cells and iii) verify if manipulation of this pathway affects drug response.

Our results showed that MDR cells released more EVs than their drug sensitive counterparts and also that the drug sensitive cells captured more EVs than their MDR counterparts. This difference in the release and capture of EVs was associated to differences in the endocytic pathway between drug sensitive and MDR cells. Importantly, manipulation of the recycling pathway influenced the response of drug sensitive cells to doxorubicin treatment. In conclusion, the present study shows that the endocytic pathway has an important impact in the MDR phenotype of cancer cells through mechanisms associated to EVs' release and uptake.

Introduction

Drug resistance is a major impediment for cancer treatment success[1]. Multidrug resistance (MDR) occurs in cells which become resistant to a variety of structurally and mechanistically unrelated drugs in addition to the drug initially administered[2]. Several mechanisms, such as increase of drug efflux, inhibition of apoptosis, alterations in cell cycle profile, or decrease in drug influx, may be responsible for MDR phenotype[3]. Different studies have addressed not only the mechanisms involved in MDR but also how MDR may be disseminated to drug-sensitive cells, since impairment of the acquisition of the MDR phenotype is an important strategy to overcome this problem.

The documented intercellular transfer of the drug-efflux pump P-glycoprotein (P-gp), mediated by extracellular vesicles (EVs) released by MDR cells and the subsequent acquisition of a MDR phenotype by the recipient sensitive tumour cells, was an important finding in this field of research[4]. Since then, several studies showing the intercellular transfer mediated by EVs of different players involved in MDR have emerged[5-9]. In some of those works, the EVs isolated from MDR cells, when in contact with drug-sensitive cells, induced the MDR phenotype in the recipient drug-sensitive cells [10-12].

Extracellular vesicles are membrane vesicles enclosed by a lipid bilayer which contain cytosol from the donor (releasing) cells[13]. Their properties such as size, density, cargo or origin have been extensively studied in order to better understand their role under normal and pathological conditions [14]. Nevertheless, the heterogeneity among the EVs populations fetch high complexity to this comprehension. Concerning the EVs origin, the two main accepted processes are: i) the outward budding and fission of the plasmatic membrane and

ii) the multivesicular body (MVB) formation along the endocytic pathway [13]. Several proteins were described as markers of these two processes, however further studies showed that some of these regulators were not exclusive of either pathway[15]. Thus, the differentiation between the two pathways of EVs' biogenesis is still very challenging. In the endocytic pathway, the early endosome is the repository of the material internalized from the plasma membrane, and is an organelle involved in the endocytic cargo' s sorting that generate other organelles such as: i) the late endosome, or the ii) recycling endosomes. The content of this latter compartment returns to the plasma membrane. However, the cargo sorted into the late endosomes is further mixed with other cargo from other intracellular organelles, a process that involves inward budding of the limiting membrane creating intraluminal vesicles (ILVs) that, ultimately, generate a multivesicular body (MVB). The fate of the MVBs could be the fusion with lysosomes for degradation, or fusion with plasma membrane, releasing exosomes to the extracellular space [16, 17]. The maturation of the early endosome is tightly regulated and has been a matter of extensive study [18].

In the present work, we show that the ability of drug sensitive and their MDR counterpart cells to release and capture EVs is different. This difference is caused by a distinct fate of the endocytic pathway in the two types of cells. Importantly, manipulating this pathway may be an important strategy to overcome MDR.

Material and Methods

Cell Culture

The following pairs of drug sensitive and MDR counterpart cell lines were used: the NCI-H460 non-small cell lung cancer (NSCLC) cell line and the NCI-H460/R counterpart which is MDR due to overexpression of P-gp (a kind gift of Dr. M. Pešić, Belgrade, Serbia)[19, 20]; the K562 cell line derived from a chronic myeloid leukaemia (CML) patient (ECACC) and the K562Dox counterpart which is MDR also due to P-gp overexpression (a kind gift of Dr. J.P. Marie, Paris, France)[21, 22]. To preserve the MDR phenotype, 1 µM doxorubicin was added to the K562Dox cells every 2 weeks and 100 nM doxorubicin was added every month to the NCI-H460/R cells. Cell lines were genotyped and routinely monitored by PCR for possible mycoplasma contamination (Cell Culture and Genotyping Service, i3S). Cells were grown in

RPMI-1640 medium with Ultraglutamine I and 25mM HEPES (Lonza or Biowest) supplemented with 10% fetal bovine serum (FBS, Biowest) at 37°C in a humidified incubator with 5% CO_2 in air. Experiments were performed with cells in exponential growth and over 90 % viability.

Extracellular Vesicles Isolation

EVs-depleted FBS was obtained by ultracentrifugation of FBS overnight (at least 16 h). Cells were cultured in medium supplemented with 10% EVs-depleted FBS during 72 h. Following that period, the supernatant was collected and EVs were isolated by differential ultracentrifugation as previously described[23]. Cellular viability was assessed by trypan blue exclusion assay prior the EVs isolation. EVs pellet was resuspended in PBS and processed according to different protocols as follows. EVs characterization regarding size, morphology, and presence of classical markers was previously published[23].

Nanoparticle Tracking Analysis

Protein was quantified using the Bio-Rad DC protein assay, according to the manufacturer's instructions. EVs were diluted in 500 µl PBS and analyzed in a NanoSight LM10 system (Malvern). Results for each sample were the average of at least 2 independent dilutions. Each dilution was analyzed twice. The post-acquisition settings were the same for all samples.

PKH67 EVs labelling

Isolated EVs were labelled with PKH67 (Sigma), according to manufacturer instructions. Medium with no contact with cells was also subjected to EVs isolation, as negative control. In order to eliminate dye aggregates, the previously PKH67-labelled EVs were applied in a 30 % sucrose cushion as described by Thery *et al*[24]. Those EVs were then incubated with recipient cells for 24 h. The same quantity of EVs was used for all incubations (inferred by protein quantification). The recipient cells were collected, washed in PBS, fixed with formaldehyde 2% and analysed by flow cytometry using FACS Canto II (BD Biosciences), plotting at least 10 000 events per sample, after debris exclusion. Data analysis was performed using the FlowJo 7.6.5 software (Tree Star, Inc.).

DiI staining

Donor cells were labelled with the fluorescent dye DiI (Molecular Probes) during 12 h at 37ºC. Recipient cells (50 000 cells/well) were seeded into a 12-well plate and the Trans-well Permeable Support, 0.4 µm poliester membrane (Costar) placed above. Donor-labelled cells (500 000 cells/well) were placed on the top of trans-well. With this system, no direct contact between the drug sensitive and MDR cells occurred. Following an incubation period of 48 h at 37ºC, cells were collected, washed in PBS, fixed with formaldehyde 2% and analysed by flow cytometry using FACS Canto II (BD Biosciences), plotting at least 10 000 events per sample, after debris exclusion?. Data analysis was performed using the FlowJo 7.6.5 software (Tree Star, Inc.)

Fluid-phase endocytosis assay

Cells were incubated with 0.1 mg/mL anionic fixable dextran, 10 000 MW (ThermoFisher) at 37ºC during 30 minutes. As negative control, dextran's incubation was also performed at 4º C. Cells were then washed in PBS and analysed by flow cytometry using the BD Accuri™ C6 Flow cytometer, plotting at least 15 000 events per sample, after cell debris exclusion. Data analysis was performed and using the FlowJo 7.6.5 software (Tree Star, Inc.).

Protein Expression Analysis

Cells were lysed in Winman's buffer (1% NP-40, 0.1 M Tris-HCl pH 8.0, 0.15 M NaCl, and 5 mM EDTA) supplemented with EDTA-free protease inhibitor cocktail (Roche). Protein lysates were quantified with DC™ Protein Assay kit (Bio-Rad) and 30 µg of protein loaded on 12% sodium dodecyl sulfate polyacrylamide gel electrophoresis (SDS-PAGE) gel. After electrophoretic transfer into nitrocellulose membranes (GE Healthcare), the following primary antibodies were used: Rab5 (BD Biosciences), Rab11 (BD Biosciences), Rab27 (R&D Systems), AP-1 (BD Biosciences), AP-2 (BD Biosciences), Dynamin (ThermoFisher), Flotillin (Santa Cruz), Annexin II (Abcam) and Annexin V (Abcam). Then, the corresponding secondary antibodies were used: ECL Mouse IgG HRP-Linked whole Ab (Enzymatic), ECL Rabbit IgG HRP-Linked whole Ab (Enzymatic), anti-mouse IgG-HRP (Santa Cruz), anti-rabbit IgG-HRP (Santa Cruz) or anti-goat IgG-HRP (Santa Cruz) . Signal was detected using

Amersham™ ECL Western blotting detection reagents (GE Healthcare), Amersham Hyperfilm ECL (GE Healthcare) and Kodak GBX developer and fixer (Sigma-Aldrich). Data analysis was performed using the image software Quantity One – 1D Analysis (Bio-Rad)[25].

Transmission electron microscopy

In brief, samples were fixed overnight with 2.5% glutaraldehyde/ 2% paraformaldehyde in cacodylate buffer 0.1 M (pH 7.4). Samples were washed in 0.1 M sodium cacodylate buffer and fixed in 2% osmium tetroxide in the 0.1 M sodium cacodylate buffer overnight, followed by new fixation in 1% uranyl acetate overnight.

Dehydration was performed in gradient series of ethanol solutions and propylene oxide and included in Epon resin by immersion of samples in increasing series of propylene oxide to EPON (till 0:1 ratio) for 60 min each. Sample inclusion in EPON resin was performed in a silicon mold.

Sections with 60 nm thickness were prepared on a RMC Ultramicrotome (PowerTome, USA) using a diamond knife and recovered to 200 mesh Formvar Ni-grids, followed by 2% uranyl acetate and saturated lead citrate solution. Visualization was performed at 80 kV in a (JEOL JEM 1400 microscope (Japan)) and digital images were acquired using a CCD digital camera Orious 1100 W (Tokyo, Japan), at the HEMS core facility at i3S, University of Porto, Portugal.

Bodipy staining

Cells were incubated with bodipy (molecular probes) for 30 minutes and washed in PBS. Images were taken with In Cell Analyzer 2000 microscope and processed with the ilastik and Cell Profiler™ software, as described below.

Immunofluorescence

NCI-H460 cells were seeded on coverslips and grown to at least 80% confluence. Fixation was performed with 4% formaldeyde in PBS for 20 min, followed by washing and blocking in 0.1% BSA and 0.1% saponin in PBS for 30 min at room temperature. Cells were incubated with the following primary antibodies for 1 h at room temperature: Transferin Receptor (Hybridoma Bank), EEA-1 (BD Biosciences), LAMP-1 (Hybridoma Bank). The, cells were further incubated with an Alexa Fluor 488 secondary antibody for 1 h. After washing, the

coverslips were mounted and images were acquired on In Cell Analyzer 2000 microscope and processed with the ilastik and Cell Profiler™ software, as described below.

Fluorescence quantification

For fluorescence analysis, we used two software: ilastik and Cell profiler™ (Supplementary Figure 2). For EEA-1 analysis, Cell Profiler™ was used for nuclear segmentation followed by expansion; FITC intensity was then quantified. For LAMP-1 analysis, ilastik was used for cell segmentation. Then, nuclear segmentation, expansion and puncta identification were performed, using Cell Profiler™. LAMP-1 staining area and FITC intensity were quantified in the overlay outlines. For Transferrin Receptor analysis, first ilastik was used for cell segmentation. After, to delineate cells, nuclear segmentation and FITC propagation were performed using Cell Profiler™. Cell intensity edge and FITC intensity were then quantified in the overlay outlines.

For all analysis, a merge between overlays and original images was performed by Fiji/ImageJ, as quality control of the results. At least 3000 cells were analyzed for each replicate.

N-acetyl-D-glucosaminidase (NAG) activity

The same number of cells was lysed in lysis buffer (Tris-HCl 50 mM, pH 8.0, 0.5% Triton X-100). NAG activity was assessed using the β-N-Acetylglucosaminidase Assay Kit (Sigma) performed according to manufacturer instructions. The results were normalized for total protein content (determined with the DC protein assay (Biorad).

Sulforhodamine B assay

The Sulforhodamine B (SRB) assay was performed to evaluate the effect of ONO-RS-82 and doxorubicin treatment in the growth of NCI-H460 cells. Cells were seeded in 96-well plates (2500 cells/well), pre-treated with ONO-RS-82 (2.5 mM) for 16 h and then treated in duplicate with doxorubicin (4.7 nM). NCI-H460 cells treated with ONO-RS-82 only, and vehicle solvent as control Following 48 h, cells were fixed in 10% (w/v) ice cold trichloroacetic acid (TCA), washed with distilled water and proteins were stained with 0.4% (w/v) SRB. After, cells were washed with 1% (v/v) acetic acid and the bound SRB was

solubilized with 10 mM Tris base. Absorbance was measured at 510 nm in a multiplate reader (Synergy Mx, Biotek Instruments Inc.)[26]. The ratio between treated cells and the control cells was calculated.

Statistical analysis.

Data was statistically analysed with the two-tailed Student's t-test. Results were considered statistically significant when p≤0.05. NS-non significant.

Results

MDR cells released more EVs than their drug-sensitive counterparts

Cancer drug sensitive and their MDR counterpart cells [from both non-small cell lung cancer (NSCLC; NCI-H460 and NCI-H460/R) and leukaemia (K562 and K562DOX) models] were cultured in EVs-depleted medium. Their culture medium was then collected and EVs were isolated. The characterization of the EVs isolated from these cell lines and with this procedure was previously published by our group, regarding their size, morphology and classical EV markers [23]. However, further data regarding their characterization is shown in Supplementary Figure 1). To quantify the number of particles released by drug sensitive and their MDR counterpart cells, from both NSCLC and leukaemia models, nanoparticle tracking analysis (NTA) was performed in triplicate. In both models, the number of particles quantified by NTA was higher in the MDR cells than in their sensitive cell counterparts. This difference was statistically significant (p≤0.05) in both models studied (Figure 1).

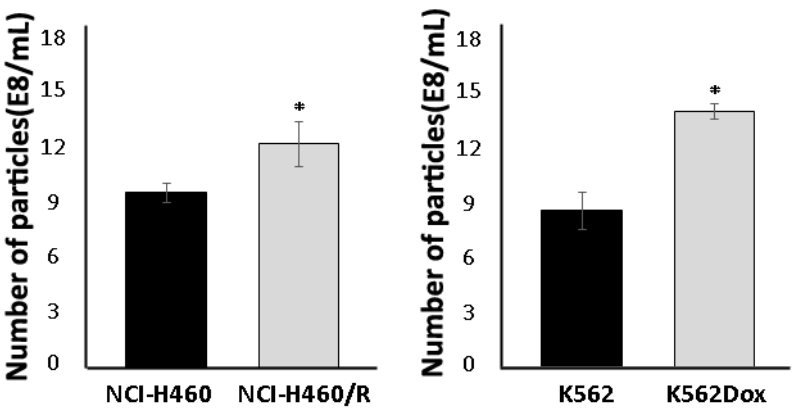
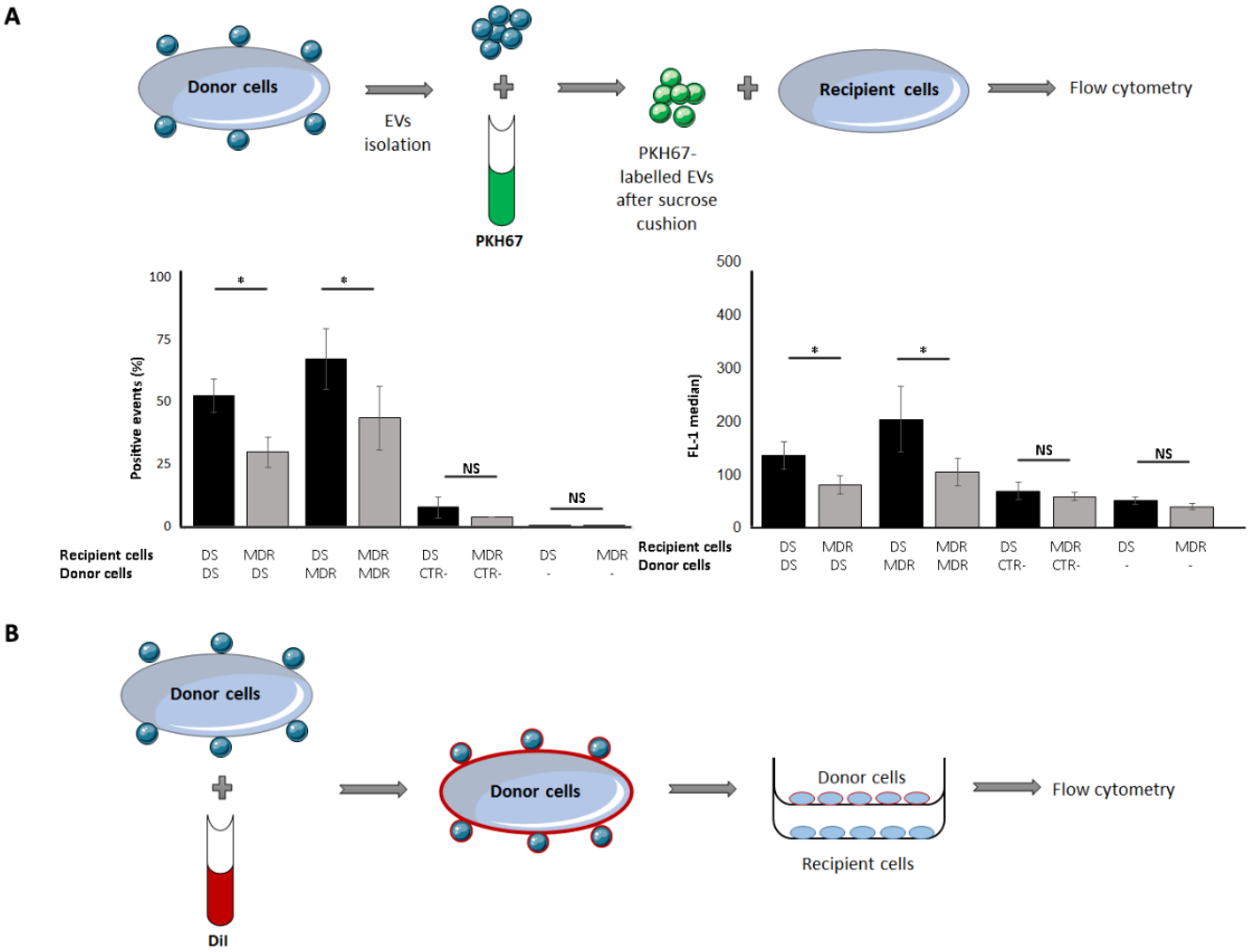


Figure 1. Comparison of the number of EVs released by drug sensitive (NCI-H460 and K562) and MDR (NCI-H460/R and K562Dox) counterpart cells, estimated by NTA measurements of EVs preparations. Results represent the mean ± SEM from at least three independent experiments. *p≤0.05

Drug sensitive cells captured more EVs than their MDR counterparts

To evaluate the ability of cells to capture EVs, two different approaches were used. In the first, EVs isolated from drug sensitive and MDR counterpart cells (K562 and K562Dox, respectively) were labelled with the fluorescent membrane dye PKH67[27]. Following a 30% sucrose cushion to eliminate dye aggregates, the labelled EVs were incubated with recipient cells and the amount of captured EVs determined by flow cytometry. Results showed that independently of the phenotype of the donor cells (drug sensitive or MDR), the EVs' capture was increased ($p \leq 0.05$, n=3) when the recipient cells were drug sensitive (Figure 2A). The EVs' uptake was also slightly increased when the donor cells were MDR. In the second approach, a porous trans-well system was used to evaluate the ability of recipient cells to capture EVs. The donor cells (K562 or K562Dox) were labelled with the long-term fluorescent dye DiI. DiI is weakly fluorescent until incorporation into membranes; therefore, all EVs released by donor cells were DiI-labelled. The labelled donor cells were placed in the upper part of a trans-well, and the recipient cells (NCI-H40 or NCI-H460/R) were placed in the bottom part of the trans-well (Figure 2B). Consistent with results obtained in first approach, the EVs' uptake by drug sensitive cells was higher than that by MDR cells, independently of the type of (drug sensitive or MDR) donor cell (Figure 2B).



Recipient cells	Donor cells	Relative percentage of positive events	Relative PE-A median
DS	DS	4.0 ± 0.4*	1.3 ± 0.2
MDR	DS	1.0 ± 0.0	1.0 ± 0.0
DS	MDR	3.2 ± 0.3*	1.2 ± 0.02
MDR	MDR	1.0 ± 0.0	1.0 ± 0.0

Figure 2: Comparison of EVs capture by drug sensitive and MDR cells, using two approaches: PKH67 labelling of EVs (A) and DiI labelling of donor cells (B). A) EVs isolated from K562 and K562Dox cells were labelled with PKH67 and incubated with recipient cells (K562 or K562Dox). Upper panel) Experiment layout. Lower panel) Percentage of positive events and FL-1 median values. Results are presented as mean± SEM from three independent experiments. **B)** Donor cells (K562 or K562Dox) were labelled with DiI and incubated with recipient cells (H460 or H460/R) using a trans-well system (0.4 µm). Upper panel) Experiment layout. Lower panel) Percentage of positive events and PE-A median (relative to MDR cells as recipient). Results are presented as mean ± SEM from three independent experiments. *p≤0.05, NS-non significant

Fluid-phase endocytosis was higher in drug sensitive cells

In order to confirm the previous observations regarding the increased ability of drug sensitive cells to capture EVs, we explored if there was any difference between MDR and sensitive cells in the endocytosis process. The fluid-phase endocytosis of drug sensitive and MDR cells, from both leukaemia and NSCLC models, was studied using the anionic fixable dextran (10,000 MW)[28,29]. After a period of incubation of the cells with same concentration of dextran, the abundance of incorporated dextran was quantified by flow cytometry (Figure 3). The results indicated a significant increase in the endocytosis rate of drug sensitive cells (NCI-H460 and K562) when compared with the MDR counterpart cells (NCI-H460/R and K562Dox) (Figure 3).

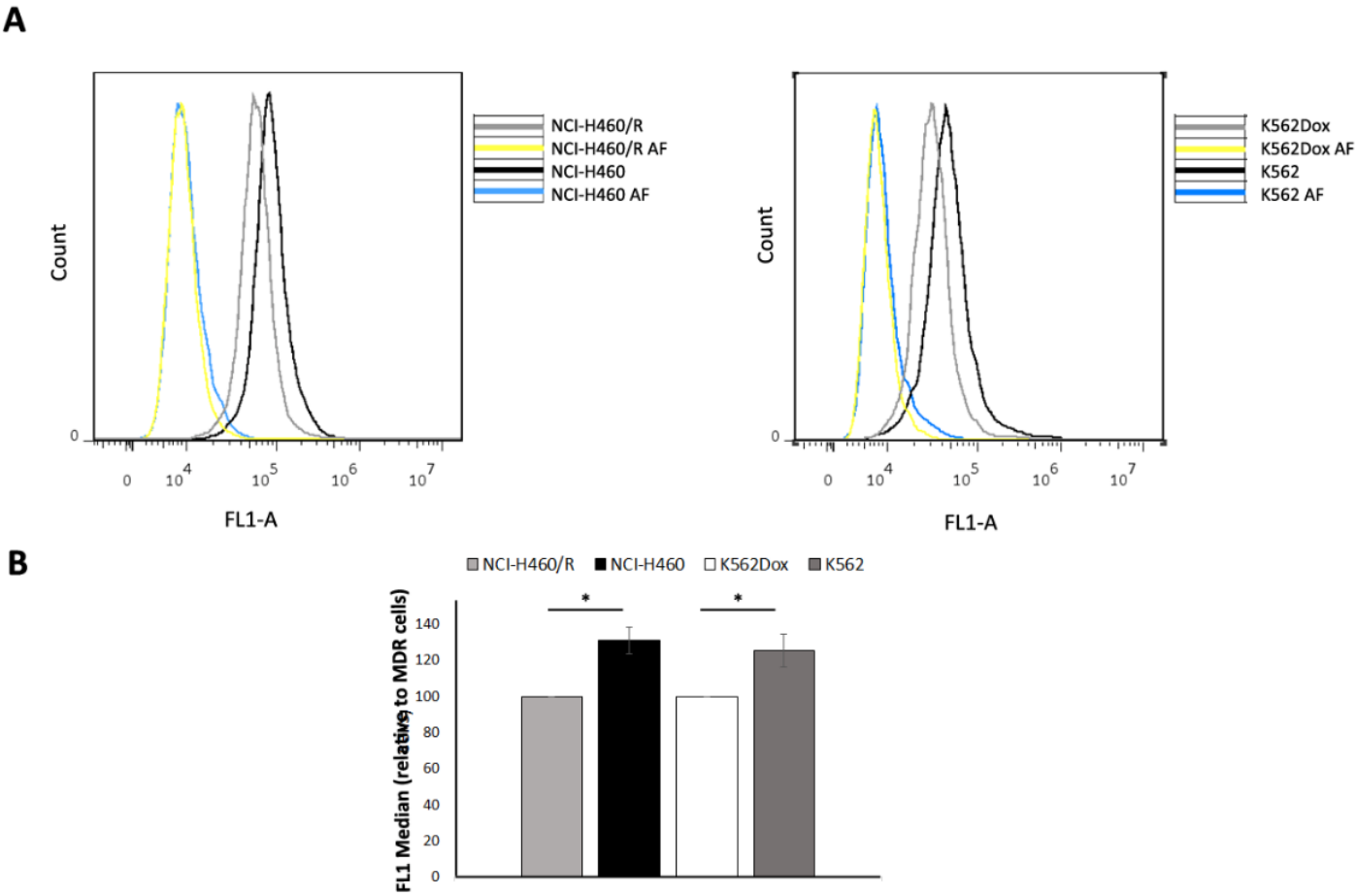


Figure 3. Comparison of the levels of fluid-phase endocytosis of dextran between drug sensitive (NCI-H460, K562) and MDR (NCI-H460/R, K562Dox) counterpart cells, analysed by flow cytometry. A) Histograms representative of three independent experiments. **B)** Relative FL1 median of NCI-H460/R *vs* NCI-H460 cells and of K562Dox *vs* K562 cells. Data represents the mean ± SEM from three independent experiments. *p≤0.05. Incubation of cells at 4ºC was performed as a negative control (Ratio of FL1 median between DS *vs* MDR cells: 97% and 106% for the NSCLC cells (NCI-H460/NCI-H460/R pair) and CML cells (K562/K562Dox pair), respectively). AF-autofluorescence.

The expression levels of proteins involved in the process of EVs' shedding or capture were altered in MDR and drug sensitive counterpart cells

Since we observed alterations between drug sensitive and their counterpart MDR cells regarding their ability to shed and capture EVs, the expression of regulators of each of these mechanisms (or of both) was analysed by Western blot and quantified by Quantity One. Rab5, -11 and -27 were found increased in MDR cells in both models (lung and leukemia); in contrast, Flotillin was increased in drug sensitive cells (Figure 4). Additionally, the levels of Dynamin, AP1/2 as well as of Annexin II and -V were similar in drug sensitive and MDR counterpart cells (Figure 4).

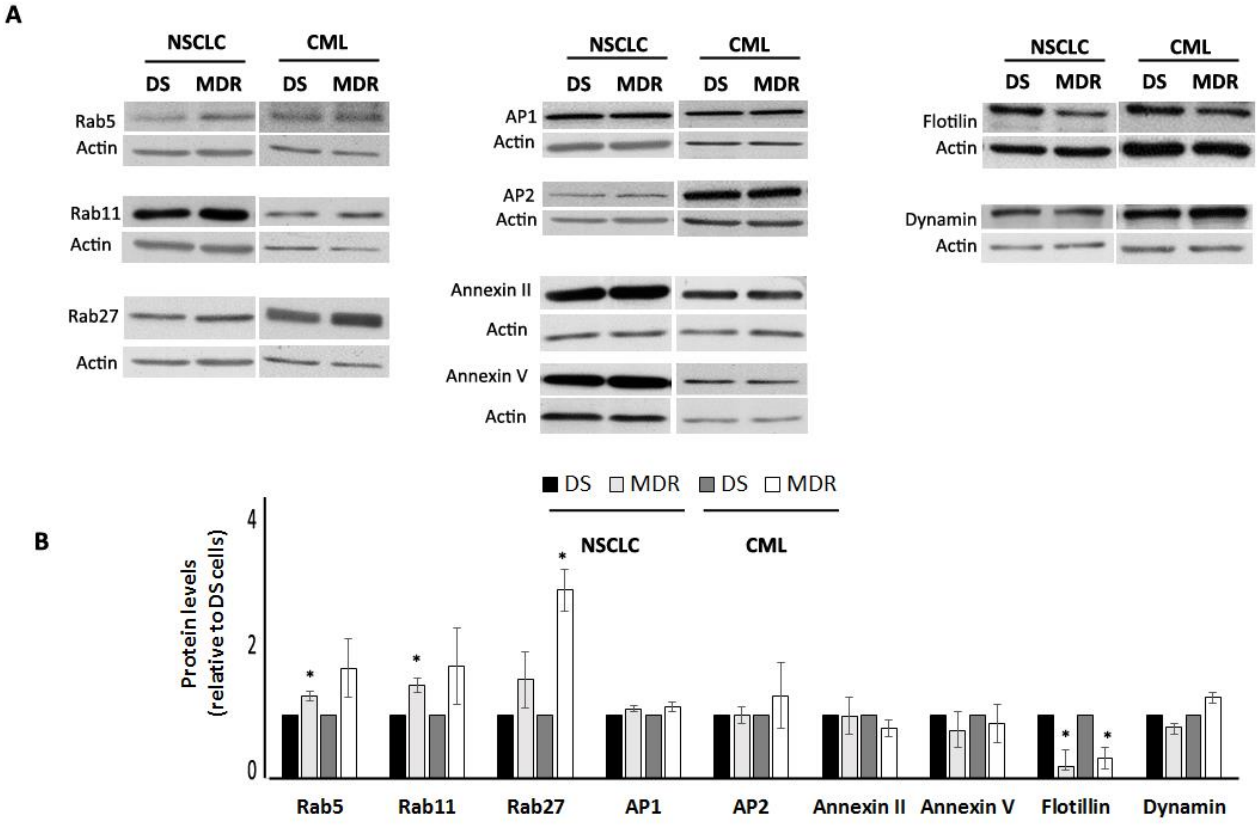


Figure 4. Comparison of the levels of proteins associated to the release or capture of EVs between drug sensitive (DS, NCI-H460) and MDR (NCI-H460/R) counterpart cells, analysed by Western blot. A) Representative images of blots from at least 3 independent experiments. **B)** Densitometry analysis expressed after normalization of the values obtained for each protein with the values obtained for actin [and further expressed in relation to drug sensitive (DS) cells]. Results represent the mean ± SEM from at least three independent experiments. *p≤0.05.

Drug sensitive cells showed increased lipid rafts (Bodipy staining)

Since we found higher levels of Flotillin, a marker of lipid rafts, in drug sensitive cells, we further assessed the abundance of these structures in drug sensitive (NCI-H460) and MDR (NCI-H460/R) counterpart cells by incubating the cells with Bodipy, as a probe to detect lipid rafts[30]. The fluorescence intensity was analysed using ilastik and Cell Profiler™ software. As observed in Figure 5, Bodipy fluorescence signal was increased in drug-sensitive cells indicating the presence of more lipid raft, in agreement with the previously observed Flotillin increase in these cells.

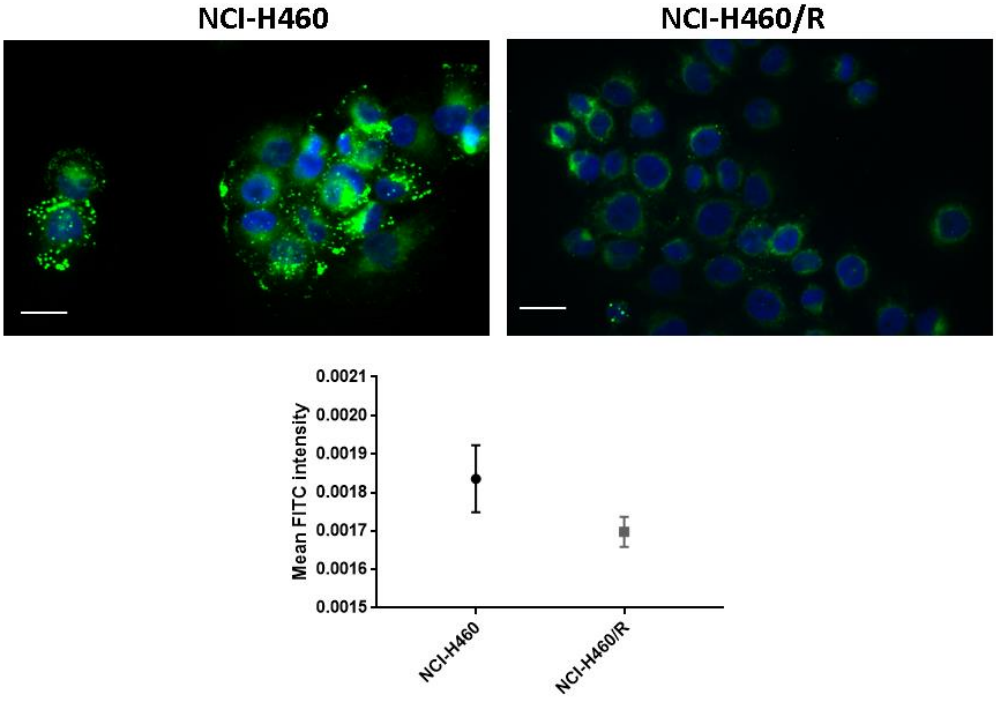


Figure 5. Comparison of the lipid raft content between drug sensitive (DS, NCI-H460) and MDR (NCI-H460/R) counterpart cells, assessed by bodipy staining. A) Representative images of three independent experiments. **B)** Quantification of mean FITC intensity. Results are presented as mean + SEM (n=3) obtained by image analysis using ilastik and Cell Profiler™ software. Bar corresponds to 20 µm.

Drug sensitive and their MDR counterparts presented different fate of endocytic pathway

To evaluate the maturation from early (or sorting) endosome to late endosome, immunofluorescence for two proteins present in these structures (EEA-1 and LAMP-1, respectively[17]) was performed in the pair of sensitive and counterpart MDR NSCLC cell lines. Drug sensitive (NCI-H460) cells showed an increase in EEA-1 cellular expression. In contrast, no alterations in LAMP-1 expression were observed between drug sensitive (NCI-H460) and MDR (NCI-H460/R) cells. Nevertheless, the intracellular distribution of LAMP-1 was different between the two cell lines (Figure 6). Indeed, using cell image analysis software (ilastik and Cell Profiler™), the area of the LAMP-1 staining was quantified. In drug sensitive cells, the patches of LAMP-1 staining were bigger; in the MDR counterpart cells LAMP-1 was distributed as puncta (Figure 7 A). In addition, a marker of the recycling pathway, transferrin receptor[31], was also analyzed by immunofluorescence and quantified with the previously referred cell image analysis software. Drug sensitive and MDR cells did not show differences in transferrin receptors' expression (Figure 6). Nevertheless, the machine learning tools indicated an increase in TfR cell surface expression in the MDR cells (Figure 7 B).

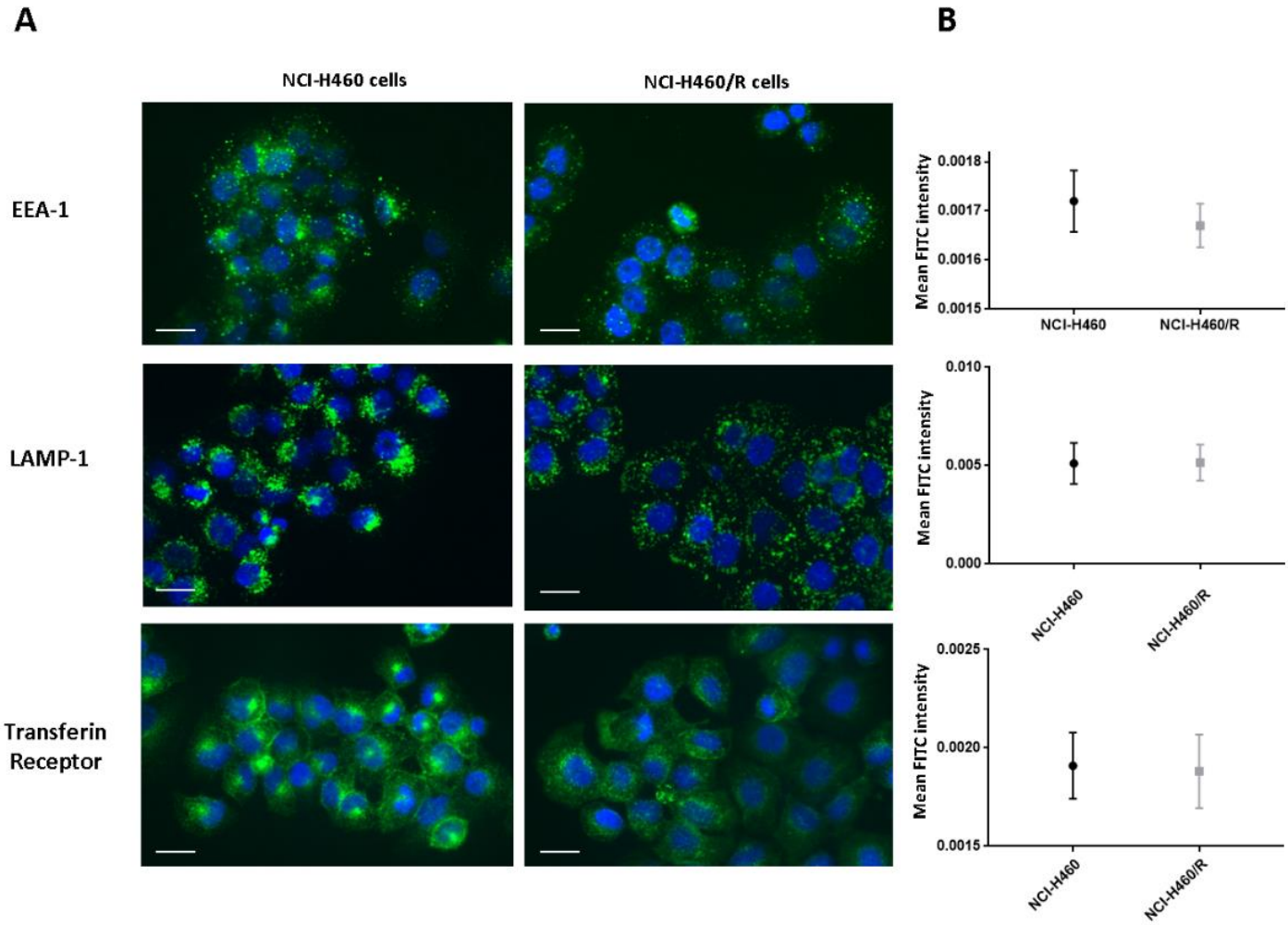


Figure 6. Comparison of the levels of expression of the endocytic markers EEA-1, LAMP-1 and transferrin receptor, between drug sensitive (DS, NCI-H460) and MDR (NCI-H460/R) counterpart cells by immunofluorescence A) Fluorescence microscopy of three independent experiments. Bar corresponds to 20 µm **B)** Mean FITC intensity obtained for each protein following image analysis using ilastik and Cell Profiler™ and Ilastik. Results represent mean ± SEM (n=3).

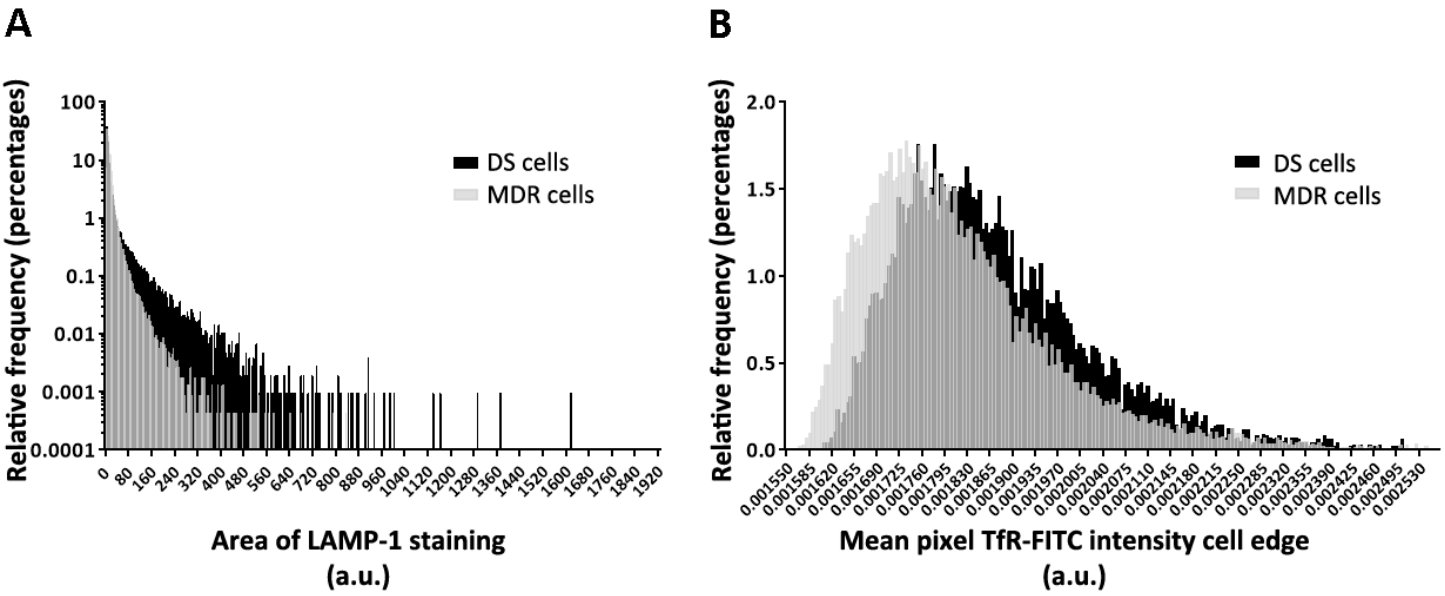


Figure 7. Comparison of LAMP-1 intracellular distribution (A) and cell surface presence of transferin receptor (TfR) (B) between drug sensitive (DS, NCI-H460) and MDR (NCI-H460/R) counterpart cells. Results obtained by immunofluorescence were quantified using the ilastik and Cell Profile™ software to assess the cellular distribution of both proteins. Data corresponds to the analysis of three independent experiments.

Early endosomes were more frequent in drug sensitive cells (NCI-H460) and late endosomes were more frequent in the counterpart MDR cells (NCI-H460/R)

The analysis of the endo-lysosomal system by light microscopy has some limitations related to some features of the markers used[16]. Therefore, to evaluate specific morphological characteristics of drug sensitive (NCI-H460) and MDR (NCI-H460/R) cells, their ultrastructure was observed by transmission electron microscopy (TEM). The early endosome is mainly electron lucent, with sporadic intraluminal vesicles (ILVs). ILVs are generated in the maturation of early endosome to late endosome, by the invagination of the endosomal membrane. Therefore, late endosomes typically show higher amount of ILVs[17]. Therefore, based on the morphological aspect of endosomes [including the presence of intraluminal vesicles (ILVs)], we found that early endosomes were more frequent in drug sensitive cells (NCI-H460) and that late endosomes were more frequent in the counterpart MDR cells (NCI-H460/R) (Figure 8).

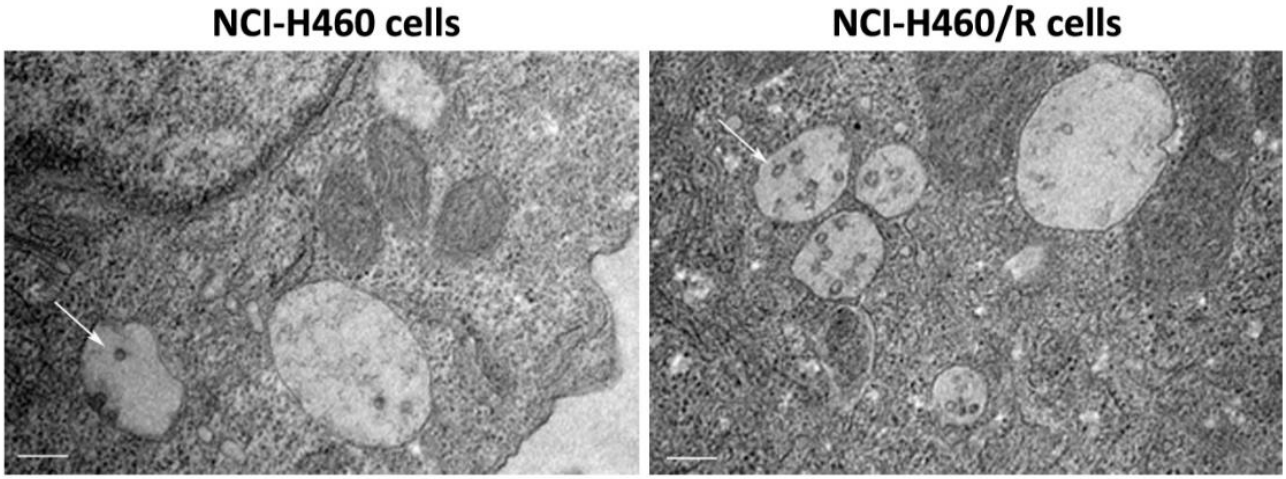


Figure 8. Comparison of endosomes ultrastructure between drug sensitive (DS, NCI-H460) and MDR (NCI-H460/R) counterpart cells, analysed by TEM. Arrows correspond to intraluminal vesicles (ILVs). Bar corresponds to 0.2µm. Images are representative from two independent experiments.

N-acetyl-D-glucosaminidase (NAG) activity was increased in drug sensitive cells (NCI-H460)

NAG is a lysosomal enzyme responsible for degradation of glycolipids and glycoproteins[32]. In order to assess NAG activity, a specific enzymatic assay was performed. Drug sensitive cells (NCI-H460) showed higher activity of NAG enzyme when compared with MDR cells (NCI-H460/R) (Figure 9). Results were normalized for protein content.

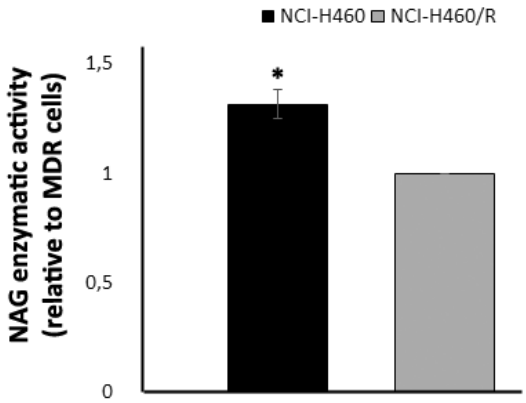


Figure 9: N-acetyl-D-glucosaminidase (NAG) enzymatic activity analyzed in drug sensitive cells (NCI-H460) and MDR counterparts (NCI-H460/R). Data was normalized for total protein content and further analyzed in relation to MDR cells. Results are expressed as the mean ± SEM from three independent experiments. *p≤0.05.

The recycling pathway inhibitor, ONO-RS-082, increased the resistance of drug sensitive cells to doxorubicin.

To evaluate the contribution of the recycling pathways to drug response, the NCI-H460 cells were pre-treated with ONO-RS-082 for 16 h and then treated with doxorubicin (4.7 nM) for further 48 h. ONO-RS-82 was previously described as an inhibitor of the recycling pathway, by inhibiting the phospholipase A2 activity[33]. After assessing the toxicity of ONO-RS-082 treatment alone using SRB assay (which caused a 10% decrease in cell growth), its effect in the cells' sensitivity to doxorubicin was determined. Results showed that the drug sensitive cells pre-treated with the recycling pathway inhibitor (ONO-RS-082) were more resistant to doxorubicin than the drug sensitive cells without such pre-treatment (Figure 10).

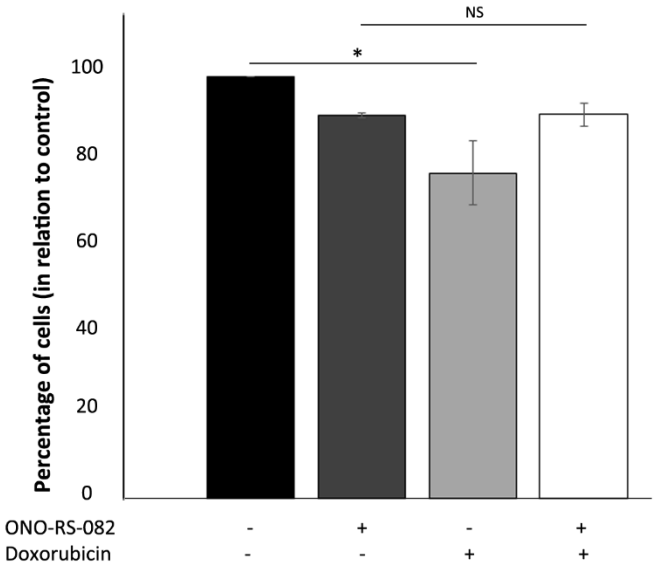


Figure 10. Analysis of the effect of a recycling pathway inhibitor (ONO-RS-082) in the response of NCI-H460 cells to doxorubicin, by SRB. Cells were pre-treated for 16 h with ONO-RS-082 (2.5 mM) and further treated for 48 h with doxorubicin (4.7 nM). Results were analyzed in relation to control cells and are presented as the mean ± SEM from three independent experiments. *p≤0.05, NS-non significant

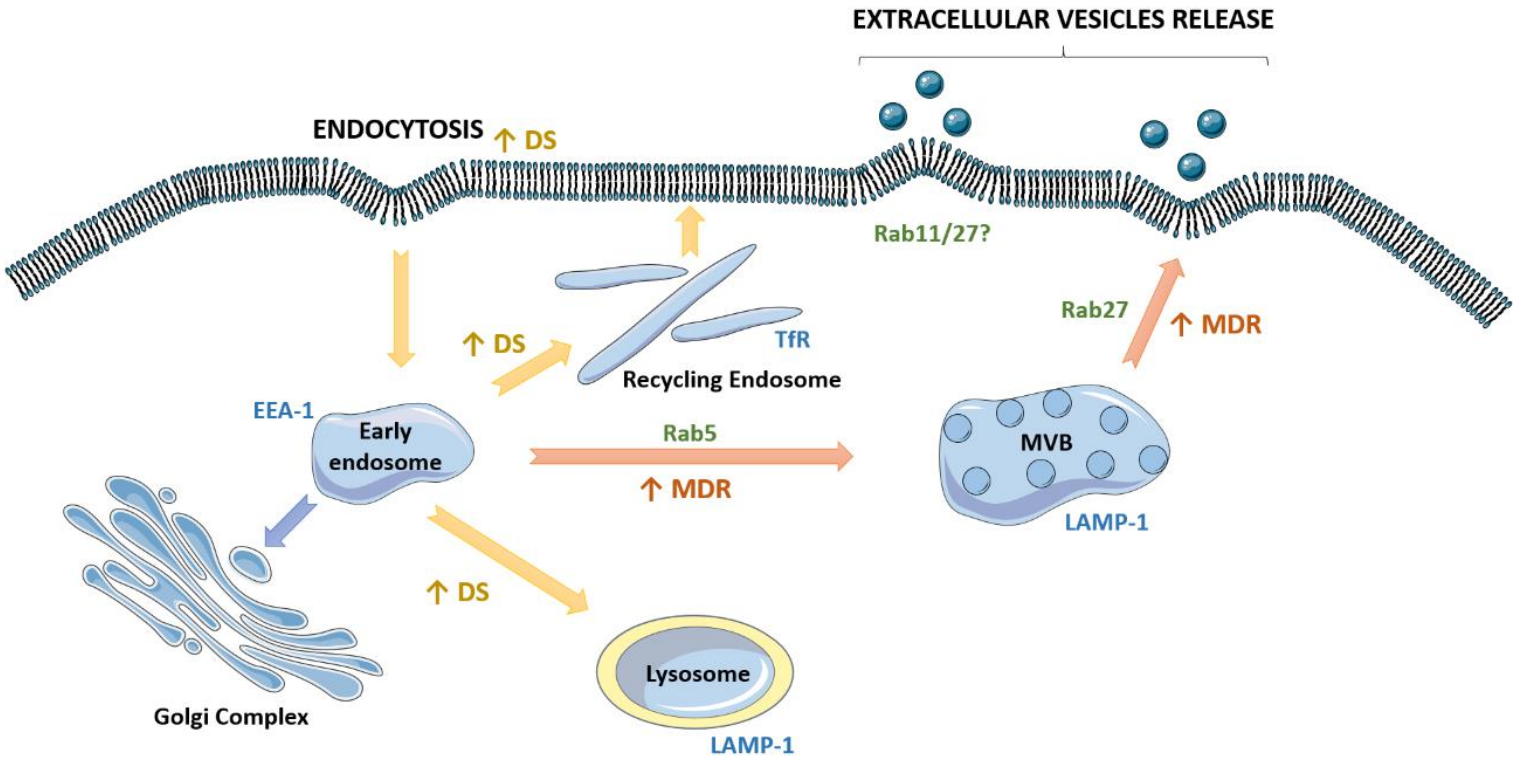


Figure 11: Schematic representation of the different fate of the endocytic pathway (EP) between drug sensitive and MDR tumor cells. MVB- multivesicular body (late endosome). Blue font: classic markers of organelles; Green font: Rab proteins family contribution to EVs release by endocytic and budding processes; Yellow arrows: EP fate of drug sensitive (DS) tumor cells; Orange arrows: EP fate of MDR tumor cells.

Discussion

Chemotherapy efficacy is strongly impaired by MDR. Understanding how drug sensitive cells acquire this phenotype is essential to overcome MDR. The horizontal transfer of MDR players between cancer cells has been described by several authors[34]. This is mediated by EVs released by donor MDR cells, which may be captured by recipient drug sensitive cells. In the current study, we aimed to verify if drug sensitive and their counterpart MDR cells were differentially prone to capture and release higher amount of EVs. Furthermore, we aimed to confirm if any differences found could be related to a different fate of the endocytic pathway between those cells.

The increase in EVs' release under stress/pathological conditions was already described in a variety of studies [35-37]. Our previous work indicated that there is an increase in EVs'

shedding by MDR cells[38]; however, this observation needed to be further confirmed. Here, using NTA analysis, which allows the quantification of number of particles, we confirmed that MDR cells (NCI-H460/R and K562Dox) shed higher amount of EVs than their drug sensitive counterpart cells (NCI-H460 and K562 cells).

A complex network of proteins have been described to regulate the release of EVs, thus we decided to study the expression of proteins from three different families involved in this process. First, we studied the levels of some Rab family GTPases, one of the most studied families regarding the release of EVs. Rab5 was described as an essential modulator of early endosome maturation[17]. Rab11, the first Rab associated to exosome secretion, is an important player for tethering, docking and fusion of MVB, regulating exosome release as well as microvesicle budding in *C. elegans* and *Drosophila*[39]. Rab27 is mostly localized in the late-endosome/lysosome-related organelles[13] and its knocking-down resulted in decrease of exosomes' release. In addition, some data also indicated the association of Rab27 to microvesicle budding[39]. Secondly, we also studied the expression of some members of the Annexin family (Ca^{2+}-binding proteins) which have been also described as important players in the budding process, regulating membrane dynamics. Annexin A2 was shown to induce membrane deformations, participating in the budding of viruses and in the formation of vesicles shed from cells[40]. Finally, we studied the levels of clathrin adaptor proteins (APs), usually associated to endocytosis due to cargo selection in clathrin coated- vesicles, but which may be also related to EVs' release since they participate in the budding of viruses [41, 42]. Our findings revealed that MDR cells have higher levels of Rab5, Rab11 and Rab27 proteins, indicating that the increased ability of MDR cells to produce and release EVs involves the Rab family. However, no involvement of AP1/2 or Annexin II/V was found.

The study of the interaction of EVs with recipient cells is still very challenging due to the: i) high heterogeneity of isolated EVs (which may interact in a different manner with the recipient cells), and the ii) variety of mechanisms involved in this process (e.g. membrane fusion or different types of endocytosis). The use of lipophilic dyes is frequent in such studies; however, interpretation of results should be cautious, since these dyes may form precipitates or may interact with wash buffers producing aggregates. Alternatively, some studies described the genetic manipulation of donor cells in order to produce fluorescently tagged EVs-associated proteins (e.g. tetraspanins) which are sorted in EVs shed by these

cells. However, the target protein must be carefully chosen if more than one condition is being studied, and its expression must not be altered between the different conditions under study. More complex techniques have also been developed such as the use of multiplexed reporters[43]. Nevertheless, they are time-consuming and require the use of more technological advanced facilities. In the present study, in order to analyze the uptake of EVs by recipient cells, we used two fluorescent-based technologies: in the first approach, we labelled the isolated EVs; in the second, we labelled the donor cells. Taking into consideration the pitfalls described above, we performed a 30% sucrose cushion of the fluorescent labeled-EVs before their incubation with recipient cells, to eliminate artefacts. These strategies was efficient since the negative control (medium without cell contact, subjected to the same labelling procedure) showed lower signal when compared with conditioned medium. With both methods, we verified that drug sensitive cells captured higher amount of EVs than their MDR counterparts. Cell-specific EV uptake has been previously reported in other contexts. For example, Rana *et al* described that Tetraspanin 8 positive-EVs shed by lymph node stromal cells were more internalized by endothelial and pancreatic cells than by parental cells[44]. Another work, carried out with EVs derived from rat pancreatic adenocarcinoma, concluded that subpopulations of leucocytes varied regarding exosome uptake; EVs were more captured by peritoneal exudate cells and less by granulocytes[45]. To our knowledge, this work presents the first evidence that drug sensitive cells are more capable of capturing EVs than their MDR counterpart cells.

In addition, we also observed an increase in EVs' uptake when the donor cell was MDR. We would like to suggest that these two observations (increased EVs' uptake by drug sensitive recipient cells, particularly when with MDR donor cells), in association with the previously mentioned evidence that there is increased release of EVs by MDR cells, may have an important impact in the dissemination of MDR in cancer. Indeed, it is known that different players of MDR, such as drug-efflux pumps or non-coding RNAs, are present in EVs' cargo. When EVs' release of MDR cells and uptake by DS cells processes are faster, the dissemination of a MDR phenotype may be more effective.

EVs capture is triggered by different pathways, namely membrane fusion clathrin-mediated endocytois, caveolin-mediated endocytosis, phagocytosis, micropinocytosis and lipid raft-mediated endocytosis[46]. Endocytosis is the most reported process for EVs' uptake[46]. Using

a 10 000 MW dextran, we confirmed the higher ability of drug sensitive cells to fluid-phase endocytosis. Also, the upregulation of EEA-1 (localized in a very early stage of early endosome[17]) observed in drug sensitive cells, suggested an increase of endocytosis, since endocytic vesicles merge with the early endosome [47]. Importantly, flotillin is one of the constituents of lipid-rafts[48]. Flotillin-mediated endocytosis has been demonstrated to be either dependent or independent of dynamin [49]. We observed an increase in flotillin levels in drug sensitive cells (from both the NSCLC and leukemia cell models) but no alterations in dynamin levels, suggesting that in our studied models, the endocytosis of EVs is mediated by flotillin-associated lipid rafts, independently of dynamin. In addition, the performed bodipy staining corroborated the increased presence of lipid rafts in drug sensitive cells. The analysis of caveolin levels showed no alterations between K562 cells and K562Dox cells and an increase in NCI-H460/R levels (justified by the effect of caveolin in drug-resistance[50]) (data not shown). Importantly, it was described that lipid-rafts which participate in EVs endocytosis may be independent of caveolin[46]. In addition, no alterations were observed in AP1/2 levels between drug sensitive and MDR counterpart cells, also indicating that the endocytosis of these EVs was independent of clathrin. Nevertheless, we are not excluding the presence of other processes aforementioned. Different EVs' capture pathways could occur at the same time in the same cell In addition, it is important to note that we studied a highly heterogeneous EVs populations since we isolated them by differential ultracentrifugation, without any concentration method. Moreover, some of the previous reported proteins are associated to more than one pathway.

The endocyted content merges with early endosomes and is sorted for degradation, recycling or segregation. Previous reports showed that the majority of cargo internalized by ongoing endocytosis in mammalian cells, is recycled back to membrane[51]. In drug sensitive cells, transferrin receptor expression was increased at the cell surface, indicating that these cells have an upregulation of the recycling pathway. In those cells, LAMP-1 localization indicated an increase in the lysosomal system, suggesting that the content not recycled to the membrane was degraded by lysosomes. Indeed, drug sensitive cells showed higher activity of NAG enzyme (associated to lysosome). In contrast, in MDR cells, the analysis of LAMP-1 distribution revealed the maturation of early endosomes to late endosomes. We suggest that the increase in the EVs' released by MDR cells, previously

quantified by NTA, is a consequence of this activation. Late endosomes maturation is followed by EVs' release. In the current work, only features related to the early, late and recycling endosomes were studied. The endosomal recycling compartment associated to the Golgi complex was not the focus of this study.

The difference observed in the fate of the endocytic pathway between drug sensitive and MDR cells had an impact in drug response. Our results revealed that drug sensitive cells treated with ONO-RS-082, a phospholipase 2 inhibitor which impairs the recycling pathway[33], decreased cellular response to doxorubicin. The decrease on the recycling pathway in MDR cells possibly results in a decrease of drug carriers and transporters at the cell surface, therefore decreasing the uptake of drugs. Indeed, a previous work described the importance of the endocytic pathway for a drug resistant phenotype. Liang *et al.* reported that the endocytic recycling compartment (ERC) was disperse in drug resistant cells when compared with their parental counterpart cells. This alteration in the ERC of drug resistant cells influenced their response to drugs [52, 53].

Conclusions

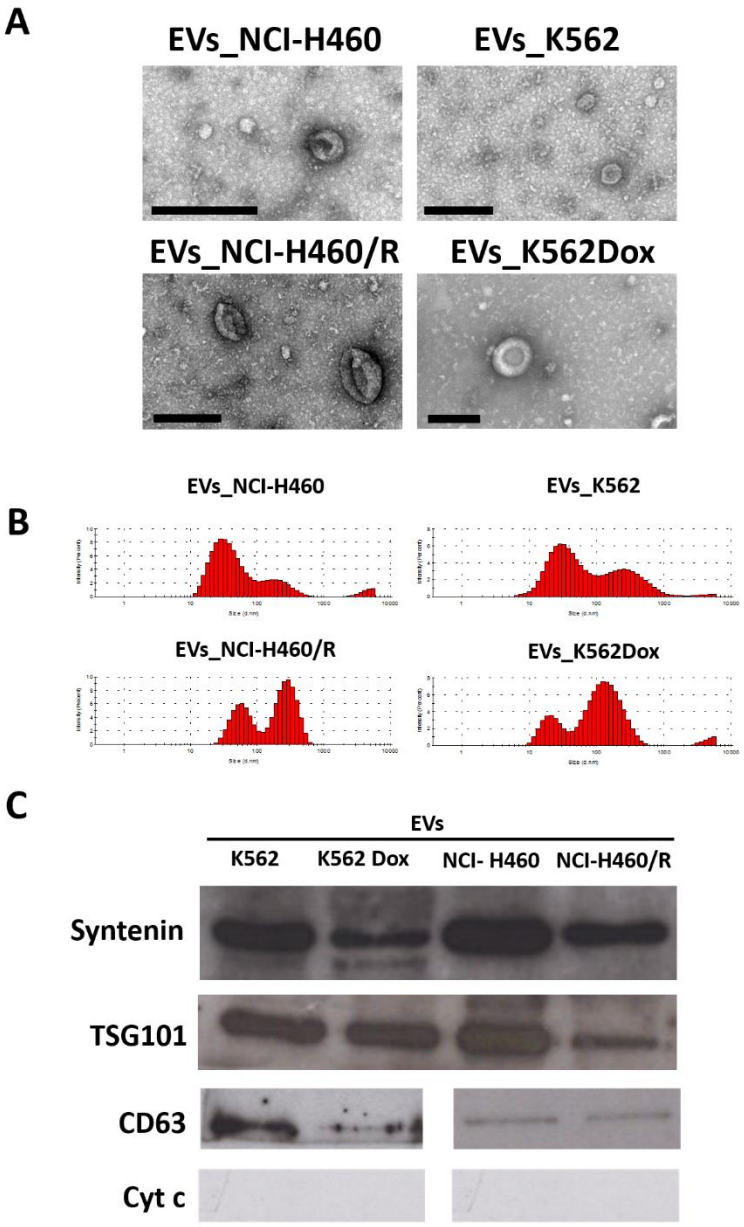
The rate of processes such as protein's recycling to the cell surface or the release of EVs to the extracellular environment has an important impact in cellular homeostasis. Alterations in those processes can lead to aberrant protein localization and altered intercellular communication, which results in pathological conditions. Here, we found a natural ability of i) MDR cells to release higher amount of EVs than their DS counterpart cells and ii) drug sensitive cells to capture more EVs than their MDR counterpart cells. We believe that this might have an impact on the MDR phenotype acquisition (by horizontal transfer) by drug sensitive cells. A variety of previous studies described that MDR-derived EVs promote the acquisition of MDR phenotype by sensitive cells, by transferring different players of this phenotype to drug sensitive cells.

Based on the results here obtained, we argue that the different status of the endocytic pathway between MDR and drug sensitive cells explains, at least in part, our initial findings regarding differences in EVs release and capture by such cells. Importantly, inhibition of the recycling pathway, decreased the drug response of cells.

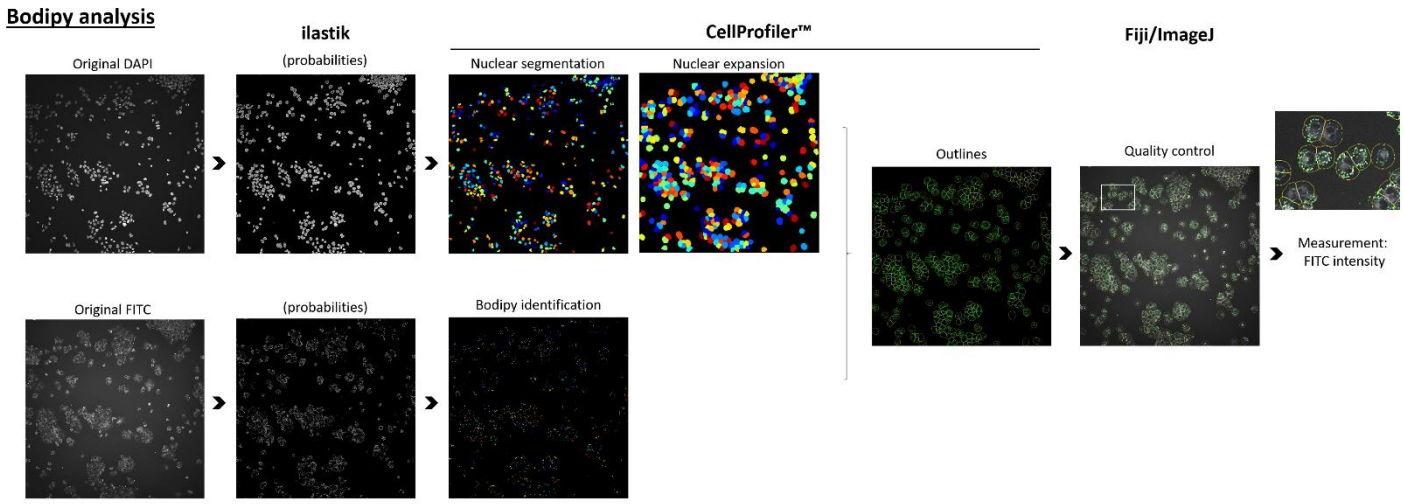
Alterations on the recycling ability of drug resistant cells was previously explored with cisplatin resistant cells showing a defect in formation of endocytic recycling compartments, possibly due to alterations in amount and distribution of microtubules[52]. Nonetheless, to the best of our knowledge, this is the first study associating alterations on the endocytic pathway between cancer DS and MDR cells to their capacity to release and capture of EVs (Figure 11). Increasing knowledge about the players involved may contribute to identifying targets to overcome the horizontal transfer of MDR.

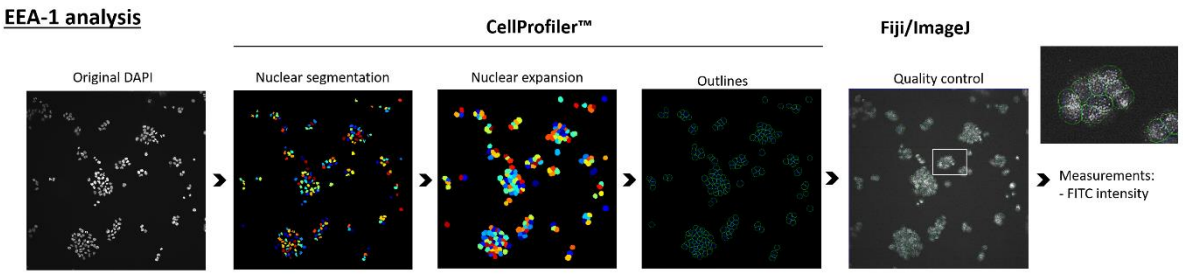
Supplementary material

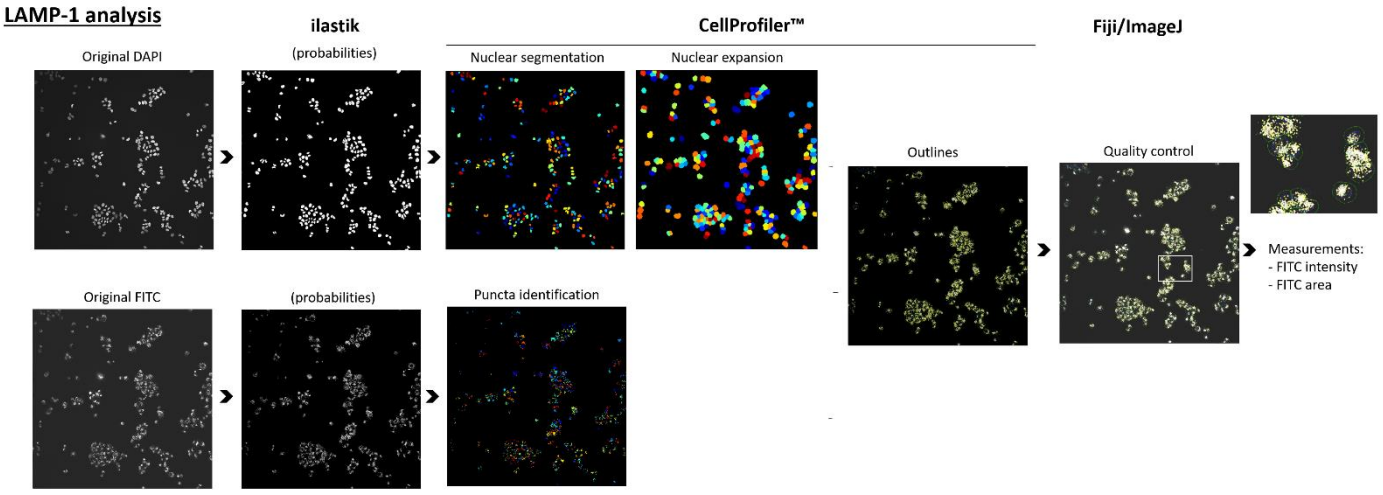
Supplementary figures

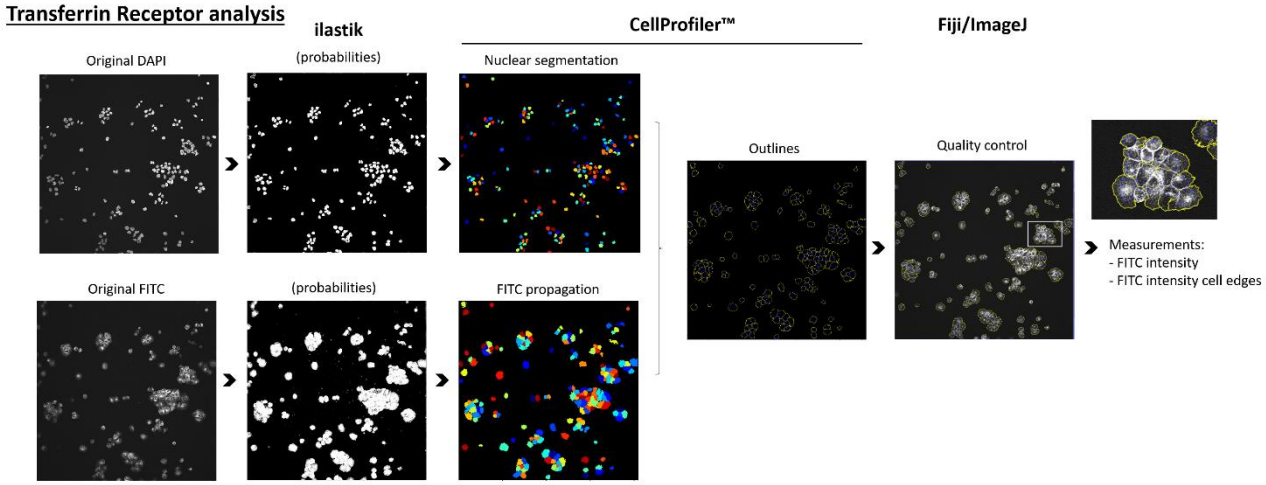


Supplementary Figure 1: Characterization of EVs isolated from drug sensitive and MDR cells from both NSCLC and CML models (NCI-H460/ NCI-H460/R pair and K562/K562Dox pair, respectively). A) Morphology of EVs, analysed by TEM. **B)** EVs' size distribution, analysed by DLS. **C)** Levels of Syntenin, TSG101 CD63 and cytochrome c in EVs, analysed by Western blot.


Bodipy analysis
ilastik
CellProfiler™
Fiji/ImageJ
Original DAPI
(probabilities)
Nuclear segmentation
Nuclear expansion
Outlines
Quality control
Measurement:
FITC intensity
Original FITC
(probabilities)
Bodipy identification


EEA-1 analysis
CellProfiler™
Fiji/ImageJ
Original DAPI
Nuclear segmentation
Nuclear expansion
Outlines
Quality control
Measurements:
- FITC intensity


LAMP-1 analysis
ilastik
CellProfiler™
Fiji/ImageJ
Original DAPI
(probabilities)
Nuclear segmentation
Nuclear expansion
Outlines
Quality control
Measurements:
- FITC intensity
- FITC area
Original FITC
(probabilities)
Puncta identification


Transferrin Receptor analysis
ilastik
CellProfiler™
Fiji/ImageJ
Original DAPI
(probabilities)
Nuclear segmentation
Outlines
Quality control
Measurements:
- FITC intensity
- FITC intensity cell edges
Original FITC
(probabilities)
FITC propagation

Supplementary Figure 2: Layout of the image analysis using ilastik and Cell Profiler™ software which allowed image cell segmentation and signal quantification.

Supplementary Methods

Transmission Electron Microscopy

EVs re-suspended in PBS, were adsorbed onto Formvar-carbon coated electron microscopy grids. EVs were then stained with 5% uranyl acetate and visualized in a JEM 1400 transmission electron microscope at an accelerating voltage of 80 kV (Jeol). Digital images were obtained using Orius 1100 W (Gatan).

Dynamic light scattering (DLS)

EVs re-suspended in PBS were placed in cuvette with a 10 mm path length and analyzed using a Nano series Malvern Zetasizer Instrument (Prager Instruments). DLS measurements were conducted at 20 °C, operating at 633 nm and recording the back scattered light at an angle of 173°. The sample temperature was allowed to equilibrate for 7 min before each measurement.

Figure Captions

Figure 1. Comparison of the number of EVs released by drug sensitive (NCI-H460 and K562) and MDR (NCI-H460/R and K562Dox) counterpart cells, estimated by NTA measurements of EVs preparations. Results represent the mean ± SEM from at least three independent experiments. *p≤0.05

Figure 2: Comparison of EVs capture by drug sensitive and MDR cells, using two approaches: PKH67 labelling of EVs (A) and DiI labelling of donor cells (B). A) EVs isolated from K562 and K562Dox cells were labelled with PKH67 and incubated with recipient cells (K562 or K562Dox). Upper panel) Experiment layout. Lower panel) Percentage of positive events and FL-1 median values. Results are presented as mean± SEM from three independent experiments. **B)** Donor cells (K562 or K562Dox) were labelled with DiI and incubated with recipient cells (H460 or H460/R) using a trans-well system (0.4 µm). Upper panel) Experiment layout. Lower panel) Percentage of positive events and PE-A median (relative to MDR cells as recipient). Results are presented as mean ± SEM from three independent experiments. *p≤0.05, NS-non significant

Figure 3. Comparison of the levels of fluid-phase endocytosis of dextran between drug sensitive (NCI-H460, K562) and MDR (NCI-H460/R, K562Dox) counterpart cells, analysed by flow cytometry. A) Histograms representative of three independent experiments. **B)** Relative FL1 median of NCI-H460/R *vs* NCI-H460 cells and of K562Dox *vs* K562 cells. Data represents the mean ± SEM from three independent experiments. *p≤0.05. Incubation of cells at 4^{o}C was performed as a negative control (Ratio of FL1 median between DS *vs* MDR cells: 97% and 106% for the NSCLC cells (NCI-H460/NCI-H460/R pair) and CML cells (K562/K562Dox pair), respectively). AF-autofluorescence.

Figure 4. Comparison of the levels of proteins associated to the release or capture of EVs between drug sensitive (DS, NCI-H460) and MDR (NCI-H460/R) counterpart cells, analysed by Western blot. A) Representative images of blots from at least 3 independent experiments. **B)** Densitometry analysis expressed after normalization of the values obtained for each protein with the values obtained for actin [and further expressed in relation to drug sensitive (DS) cells]. Results represent the mean ± SEM from at least three independent experiments. *p≤0.05.

Figure 5. Comparison of the lipid raft content between drug sensitive (DS, NCI-H460) and MDR (NCI-H460/R) counterpart cells, assessed by bodipy staining. A) Representative images of three independent experiments. **B)** Quantification of mean FITC intensity. Results are presented as mean + SEM (n=3) obtained by image analysis using ilastik and Cell Profiler™ software. Bar corresponds to 20 µm.

Figure 6. Comparison of the levels of expression of the endocytic markers EEA-1, LAMP-1 and transferrin receptor, between drug sensitive (DS, NCI-H460) and MDR (NCI-H460/R) counterpart cells by immunofluorescence A) Fluorescence microscopy of three independent experiments. Bar corresponds to 20 µm **B)** Mean FITC intensity obtained for each protein following image analysis using ilastik and Cell Profiler™ and Ilastik. Results represent mean ± SEM (n=3).

Figure 7. Comparison of LAMP-1 intracellular distribution (A) and cell surface presence of transferin receptor (TfR) (B) between drug sensitive (DS, NCI-H460) and MDR (NCI-H460/R) counterpart cells. Results obtained by immunofluorescence were quantified using the ilastik and Cell Profile™ software to assess the cellular distribution of both proteins. Data corresponds to the analysis of three independent experiments.

Figure 8. Comparison of endosomes ultrastructure between drug sensitive (DS, NCI-H460) and MDR (NCI-H460/R) counterpart cells, analysed by TEM. Arrows correspond to intraluminal vesicles (ILVs). Bar corresponds to 0.2µm. Images are representative from two independent experiments.

Figure 9: N-acetyl-D-glucosaminidase (NAG) enzymatic activity analyzed in drug sensitive cells (NCI-H460) and MDR counterparts (NCI-H460/R). Data was normalized for total protein content and further analyzed in relation to MDR cells. Results are expressed as the mean ± SEM from three independent experiments. *p≤0.05.

Figure 10. Analysis of the effect of a recycling pathway inhibitor (ONO-RS-082) in the response of NCI-H460 cells to doxorubicin, by SRB. Cells were pre-treated for 16 h with ONO-RS-082 (2.5 mM) and further treated for 48 h with doxorubicin (4.7 nM). Results were analyzed in relation to control cells and are presented as the mean ± SEM from three independent experiments. *p≤0.05, NS-non significant

Figure 11: Schematic representation of the different fate of the endocytic pathway (EP) between drug sensitive and MDR tumor cells. MVB- multivesicular body (late endosome). Blue font: classic markers of organelles; Green font: Rab proteins family contribution to EVs release by endocytic and budding processes; Yellow arrows: EP fate of drug sensitive (DS) tumor cells; Orange arrows: EP fate of MDR tumor cells.

Acknowledgments

This article is a result of the project NORTE-01-0145-FEDER-000029, supported by Norte Portugal Regional Programme (NORTE 2020), under the PORTUGAL 2020 Partnership Agreement, through the European Regional Development Fund (ERDF). This work was partially financed by FEDER - Fundo Europeu de Desenvolvimento Regional funds through the COMPETE 2020 - Operacional Programme for Competitiveness and Internationalisation (POCI), Portugal 2020, and by Portuguese funds through FCT - Fundação para a Ciência e a Tecnologia/Ministério da Ciência, Tecnologia e Inovação in the framework of the project "Institute for Research and Innovation in Health Sciences" (POCI-01-0145-FEDER-007274). The authors acknowledge the support of the BioSciences Screening i3S Scientific Platform, member of the national infrastructure PPBI - Portuguese Platform of Bioimaging (PPBI-POCI-01-0145-FEDER-022122). The authors thank the Portuguese Foundation for Science and Technology (FCT) for the PhD grant of DS (SFRH/BD/98054/2013). The authors also acknowledge the European COST Action- European Network on Microvesicles and Exosomes in Health and Disease (ME-HaD, BM1202) for short-term mission fellowship (ECOST-STSM-BM1202-150317-083396) and Grupo Español de investigacion en Vesiculas Extracelulares for GEIVEX mobility fellowship which allowed the work of DS in CICbioGUNE. We thank Spanish MINECO (SAF2015-66312 to JMF) and for the REDIEX (Spanish Excellence Network in Exosomes) and the Severo Ochoa Excellence Accreditation (SEV-2016-0644).

Conflict of interest

Authors declare no conflict of interest.

References

1. Xavier, C.P., Pesic, M. & Vasconcelos, M.H. Understanding Cancer Drug Resistance by Developing and Studying Resistant Cell Line Models. *Curr Cancer Drug Targets* **16**, 226-237 (2016).
2. Gillet, J.P. & Gottesman, M.M. Mechanisms of multidrug resistance in cancer. *Methods Mol Biol* **596**, 47-76 (2010).
3. Aberuyi, N., Rahgozar, S. & Moafi, A. The role of ATP-binding cassette transporter A2 in childhood acute lymphoblastic leukemia multidrug resistance. *Iran J Ped Hematol Oncol* **4**, 118-126 (2014).

4. Levchenko, A. *et al.* Intercellular transfer of P-glycoprotein mediates acquired multidrug resistance in tumor cells. *Proc Natl Acad Sci U S A* **102**, 1933-1938 (2005).
5. Corcoran, C., Rani, S. & O'Driscoll, L. miR-34a is an intracellular and exosomal predictive biomarker for response to docetaxel with clinical relevance to prostate cancer progression. *Prostate* **74**, 1320-1334 (2014).
6. Chen, W.X. *et al.* Exosomes from drug-resistant breast cancer cells transmit chemoresistance by a horizontal transfer of microRNAs. *PLoS One* **9**, e95240 (2014).
7. Takahashi, K., Yan, I.K., Wood, J., Haga, H. & Patel, T. Involvement of extracellular vesicle long noncoding RNA (linc-VLDLR) in tumor cell responses to chemotherapy. *Mol Cancer Res* **12**, 1377-1387 (2014).
8. Dong, Y. *et al.* Tumor endothelial expression of P-glycoprotein upon microvesicular transfer of TrpC5 derived from adriamycin-resistant breast cancer cells. *Biochem Biophys Res Commun* **446**, 85-90 (2014).
9. Lopes-Rodrigues, V. *et al.* Identification of the metabolic alterations associated with the multidrug resistant phenotype in cancer and their intercellular transfer mediated by extracellular vesicles. *Sci Rep* **7**, 44541 (2017).
10. Lu, J.F. *et al.* Microparticles mediate MRP1 intercellular transfer and the re-templating of intrinsic resistance pathways. *Pharmacol Res* **76**, 77-83 (2013).
11. Lv, M.M. *et al.* Exosomes mediate drug resistance transfer in MCF-7 breast cancer cells and a probable mechanism is delivery of P-glycoprotein. *Tumour Biol* **35**, 10773-10779 (2014).
12. Zhang, F.F. *et al.* Microvesicles mediate transfer of P-glycoprotein to paclitaxel-sensitive A2780 human ovarian cancer cells, conferring paclitaxel-resistance. *Eur J Pharmacol* **738**, 83-90 (2014).
13. Colombo, M., Raposo, G. & Thery, C. Biogenesis, secretion, and intercellular interactions of exosomes and other extracellular vesicles. *Annu Rev Cell Dev Biol* **30**, 255-289 (2014).
14. Yanez-Mo, M. *et al.* Biological properties of extracellular vesicles and their physiological functions. *J Extracell Vesicles* **4**, 27066 (2015).
15. Ghossoub, R. *et al.* Syntenin-ALIX exosome biogenesis and budding into multivesicular bodies are controlled by ARF6 and PLD2. *Nat Commun* **5**, 3477 (2014).
16. Naslavsky, N. & Caplan, S. The enigmatic endosome - sorting the ins and outs of endocytic trafficking. *J Cell Sci* **131** (2018).
17. Klumperman, J. & Raposo, G. The complex ultrastructure of the endolysosomal system. *Cold Spring Harb Perspect Biol* **6**, a016857 (2014).
18. Scott, C.C., Vacca, F. & Gruenberg, J. Endosome maturation, transport and functions. *Semin Cell Dev Biol* **31**, 2-10 (2014).
19. Pesic, M. *et al.* Induced resistance in the human non small cell lung carcinoma (NCI-H460) cell line in vitro by anticancer drugs. *J Chemother* **18**, 66-73 (2006).
20. Podolski-Renic, A. *et al.* Molecular and cytogenetic changes in multi-drug resistant cancer cells and their influence on new compounds testing. *Cancer Chemother Pharmacol* **72**, 683-697 (2013).
21. Marie, J.P., Faussat-Suberville, A.M., Zhou, D. & Zittoun, R. Daunorubicin uptake by leukemic cells: correlations with treatment outcome and mdr1 expression. *Leukemia* **7**, 825-831 (1993).
22. Seca, H., Lima, R.T., Guimaraes, J.E. & Helena Vasconcelos, M. Simultaneous targeting of P-gp and XIAP with siRNAs increases sensitivity of P-gp overexpressing CML cells to imatinib. *Hematology* **16**, 100-108 (2011).
23. Lopes-Rodrigues, V. *et al.* Multidrug resistant tumour cells shed more microvesicle-like EVs and less exosomes than their drug-sensitive counterpart cells. *Biochim Biophys Acta* **1860**, 618-627 (2016).

24. Thery, C., Amigorena, S., Raposo, G. & Clayton, A. Isolation and characterization of exosomes from cell culture supernatants and biological fluids. *Curr Protoc Cell Biol* **Chapter 3**, Unit 3 22 (2006).
25. Lima M. João, S.D., Lima RT, Carvalho Ana Maria, Ferreira I.C.F.R., Vasconcelos M H Flower extracts of Filipendula ulmaria (L.) Maxim inhibit the proliferation of the NCI-H460 tumour cell line. *Industrial Crops and Products* **59**, 149-153 (2014).
26. Barbosa, J. *et al.* Screening a Small Library of Xanthones for Antitumor Activity and Identification of a Hit Compound which Induces Apoptosis. *Molecules* **21**, 81 (2016).
27. Chiba, M., Kimura, M. & Asari, S. Exosomes secreted from human colorectal cancer cell lines contain mRNAs, microRNAs and natural antisense RNAs, that can transfer into the human hepatoma HepG2 and lung cancer A549 cell lines. *Oncol Rep* **28**, 1551-1558 (2012).
28. Plank, C., Oberhauser, B., Mechtler, K., Koch, C. & Wagner, E. The influence of endosome-disruptive peptides on gene transfer using synthetic virus-like gene transfer systems. *J Biol Chem* **269**, 12918-12924 (1994).
29. Falcon-Perez, J.M., Nazarian, R., Sabatti, C. & Dell'Angelica, E.C. Distribution and dynamics of Lamp1-containing endocytic organelles in fibroblasts deficient in BLOC-3. *J Cell Sci* **118**, 5243-5255 (2005).
30. Mikhalyov, I. & Samsonov, A. Lipid raft detecting in membranes of live erythrocytes. *Biochim Biophys Acta* **1808**, 1930-1939 (2011).
31. Maxfield, F.R. & McGraw, T.E. Endocytic recycling. *Nat Rev Mol Cell Biol* **5**, 121-132 (2004).
32. Legler, G., Lullau, E., Kappes, E. & Kastenholz, F. Bovine N-acetyl-beta-D-glucosaminidase: affinity purification and characterization of its active site with nitrogen containing analogs of N-acetylglucosamine. *Biochim Biophys Acta* **1080**, 89-95 (1991).
33. Doody, A.M., Antosh, A.L. & Brown, W.J. Cytoplasmic phospholipase A2 antagonists inhibit multiple endocytic membrane trafficking pathways. *Biochem Biophys Res Commun* **388**, 695-699 (2009).
34. Sousa, D., Lima, R.T. & Vasconcelos, M.H. Intercellular Transfer of Cancer Drug Resistance Traits by Extracellular Vesicles. *Trends Mol Med* **21**, 595-608 (2015).
35. Xiao, X. *et al.* Exosomes: decreased sensitivity of lung cancer A549 cells to cisplatin. *PLoS One* **9**, e89534 (2014).
36. King, H.W., Michael, M.Z. & Gleadle, J.M. Hypoxic enhancement of exosome release by breast cancer cells. *BMC Cancer* **12**, 421 (2012).
37. Kanemoto, S. *et al.* Multivesicular body formation enhancement and exosome release during endoplasmic reticulum stress. *Biochem Biophys Res Commun* **480**, 166-172 (2016).
38. Lopes-Rodrigues, V. *et al.* Data supporting the shedding of larger extracellular vesicles by multidrug resistant tumour cells. *Data Brief* **6**, 1023-1027 (2016).
39. Beer, K.B. & Wehman, A.M. Mechanisms and functions of extracellular vesicle release in vivo-What we can learn from flies and worms. *Cell Adh Migr* **11**, 135-150 (2017).
40. Drucker, P., Pejic, M., Galla, H.J. & Gerke, V. Lipid segregation and membrane budding induced by the peripheral membrane binding protein annexin A2. *J Biol Chem* **288**, 24764-24776 (2013).
41. Camus, G. *et al.* The clathrin adaptor complex AP-1 binds HIV-1 and MLV Gag and facilitates their budding. *Mol Biol Cell* **18**, 3193-3203 (2007).
42. Mori, Y. *et al.* Human herpesvirus-6 induces MVB formation, and virus egress occurs by an exosomal release pathway. *Traffic* **9**, 1728-1742 (2008).
43. Lai, C.P. *et al.* Visualization and tracking of tumour extracellular vesicle delivery and RNA translation using multiplexed reporters. *Nat Commun* **6**, 7029 (2015).
44. Rana, S., Yue, S., Stadel, D. & Zoller, M. Toward tailored exosomes: the exosomal tetraspanin web contributes to target cell selection. *Int J Biochem Cell Biol* **44**, 1574-1584 (2012).

45. Zech, D., Rana, S., Buchler, M.W. & Zoller, M. Tumor-exosomes and leukocyte activation: an ambivalent crosstalk. *Cell Commun Signal* **10**, 37 (2012).
46. Mulcahy, L.A., Pink, R.C. & Carter, D.R. Routes and mechanisms of extracellular vesicle uptake. *J Extracell Vesicles* **3** (2014).
47. Abels, E.R. & Breakefield, X.O. Introduction to Extracellular Vesicles: Biogenesis, RNA Cargo Selection, Content, Release, and Uptake. *Cell Mol Neurobiol* **36**, 301-312 (2016).
48. Meister, M. & Tikkanen, R. Endocytic trafficking of membrane-bound cargo: a flotillin point of view. *Membranes (Basel)* **4**, 356-371 (2014).
49. Otto, G.P. & Nichols, B.J. The roles of flotillin microdomains--endocytosis and beyond. *J Cell Sci* **124**, 3933-3940 (2011).
50. Lavie, Y., Fiucci, G. & Liscovitch, M. Upregulation of caveolin in multidrug resistant cancer cells: functional implications. *Adv Drug Deliv Rev* **49**, 317-323 (2001).
51. Huotari, J. & Helenius, A. Endosome maturation. *EMBO J* **30**, 3481-3500 (2011).
52. Liang, X.J., Mukherjee, S., Shen, D.W., Maxfield, F.R. & Gottesman, M.M. Endocytic recycling compartments altered in cisplatin-resistant cancer cells. *Cancer Res* **66**, 2346-2353 (2006).
53. Liang, X.J., Shen, D.W., Garfield, S. & Gottesman, M.M. Mislocalization of membrane proteins associated with multidrug resistance in cisplatin-resistant cancer cell lines. *Cancer Res* **63**, 5909-5916 (2003).

3. RESEARCH ARTICLE:

Modulation of Autophagy by a Thioxanthone Decreases the Viability of Melanoma Cells

Raquel T. Lima*, **Diana Sousa*,** Ana M. Paiva, Andreia Palmeira, João Barbosa, Madalena Pedro, Madalena M. Pinto, Emília Sousa, and M. Helena Vasconcelos

Molecules 21, 1343 (2016)

***** These authors have equally contributed to the work

molecules

MDPI

Article

Modulation of Autophagy by a Thioxanthone Decreases the Viability of Melanoma Cells

Raquel T. Lima [1,2,3,†], Diana Sousa [1,2,4,†], Ana M. Paiva [5], Andreia Palmeira [5], João Barbosa [6], Madalena Pedro [6], Madalena M. Pinto [5,7], Emília Sousa [5,7] and M. Helena Vasconcelos [1,2,4,*]

1 i3S-Instituto de Investigação e Inovação em Saúde, Universidade do Porto, Rua Alfredo Allen 208, 4200-135 Porto, Portugal; rlima@ipatimup.pt (R.T.L.); dsousa@ipatimup.pt (D.S.)
2 Cancer Drug Resistance Group, IPATIMUP—Institute of Molecular Pathology and Immunology of the University of Porto, Rua Júlio Amaral de Carvalho, 45, 4200-135 Porto, Portugal
3 Department of Pathology, FMUP—Faculty of Medicine of the University of Porto, Alameda Prof. Hernâni Monteiro, 4200-319 Porto, Portugal
4 Laboratory of Microbiology, Department of Biological Sciences, FFUP—Faculty of Pharmacy, University of Porto, Rua de Jorge Viterbo Ferreira 228, 4050-313 Porto, Portugal
5 Laboratory of Organic and Pharmaceutical Chemistry, Department of Chemical Sciences, FFUP—Faculty of Pharmacy, University of Porto, Rua de Jorge Viterbo Ferreira 228, 4050-313 Porto, Portugal; gpaivamafalda@gmail.com (A.M.P.); andreiapalmeira@gmail.com (A.P.); madalena@ff.up.pt (M.M.P.); esousa@ff.up.pt (E.S.)
6 CESPU, Instituto de Investigação e Formação Avançada em Ciências e Tecnologias da Saúde, IUCS—Instituto Universitário de Ciências da Saúde, Rua Central de Gandra 1317, 4585-116 Gandra, Portugal; j.filipebarbosa@hotmail.com (J.B.); madalena.oliveira.pedro@gmail.com (M.P.)
7 CIIMAR/CIMAR—Centro Interdisciplinar de Investigação Marinha e Ambiental, Universidade do Porto, Terminal de Cruzeiros do Porto de Leixões, Avenida General Norton de Matos, S/N, 4450-208 Matosinhos, Portugal
* Correspondence: hvasconcelos@ipatimup.pt; Tel.: +351-225-570-700; Fax: +351-225-570-799
† These authors equally contributed to this work.

Academic Editor: Jean Jacques Vanden Eynde
Received: 9 August 2016; Accepted: 1 October 2016; Published: 10 October 2016

Abstract: (1) Background: Our previous studies unveiled the hit thioxanthone TXA1 as an inhibitor of P-glycoprotein (drug efflux pump) and of human tumor cells growth, namely of melanoma cells. Since TXA1 is structurally similar to lucanthone (an autophagy inhibitor and apoptosis inducer) and to N^{10}-substituted phenoxazines (isosteres of thioxanthones, and autophagy inducers), this study aimed at further assessing its cytotoxic mechanism and evaluating its potential as an autophagy modulator in A375-C5 melanoma cells; (2) Methods: Flow cytometry with propidium iodide (PI) for cell cycle profile analysis; Terminal deoxynucleotidyl transferase dUTP nick end labeling (TUNEL) assay, flow cytometry with Annexin V/PI labeling and Western blot for apoptosis analysis were conducted. A pharmacophore approach was used for mapping TXA1 onto pharmacophores for autophagy induction. Autophagy analyses included transmission electron microscopy for visualization of autophagic structures, fluorescence microscopy for observation of monodansylcadaverine (MDC) staining, pattern of LC3 expression in the cells and acridine orange staining, and Western blot for autophagic proteins expression; (3) Results: TXA1 induced autophagy of melanoma cells at the GI_{50} concentration (3.6 μM) and apoptosis at twice that concentration. Following treatment with TXA1, autophagic structures were observed, together with the accumulation of autophagosomes and the formation of autophagolysosomes. An increase in LC3-II levels was also observed, which was reverted by 3-methyladenine (3-MA) (an early stage autophagy-inhibitor) but further increased by E-64d/pepstatin (late-stage autophagy inhibitors). Finally, 3-MA also reverted the effect of TXA1 in cellular viability; (4) Conclusion: TXA1 decreases the viability of melanoma cells by modulation of autophagy and may, therefore, serve as a lead compound for the development of autophagy modulators with antitumor activity.

Keywords: thioxanthones; melanoma; autophagy; cell death; apoptosis

1. Introduction

Autophagy is a catabolic process which targets cellular organelles and cytoplasmic constituents to the lysosomes for degradation, allowing the cell to maintain homeostasis and being particularly relevant during nutrient deprivation and other stresses [1]. Alterations in autophagy are frequently found in diseases, such as cancer [2], and might be relevant for cancer response to therapy. Although autophagy has been traditionally regarded as a pro-survival mechanism, it has also been related to cell death [2,3]. In fact, a cross-talk between autophagy and apoptosis has been documented, with these pathways sharing various mediators [4–6].

The effect of autophagy in cancer therapy is still under debate and may depend on several factors, such as the cellular context, as well as on the levels and duration of cellular autophagy [7,8]. Indeed, targeting autophagy may provide new opportunities for cancer drug discovery. Several small molecules which modulate autophagy have been already described [8–10]. Interestingly, promotion of cell death for cancer therapy has been observed not only with autophagy inducers, but also with autophagy inhibitors [11].

The use of autophagy inhibitors, such as chloroquine, hydroxychloroquine, and lucanthone, in association with chemotherapeutic agents, has already reached clinical trials [7]. On the other hand, the use of small molecules that promote autophagy has also been shown to induce cell death in cancer cells [8]. Indeed, resveratrol was shown to induce cell death in several human tumor cell lines by triggering both autophagy and apoptosis [12–14]. In addition, imatinib (Gleevec), a known inducer of apoptosis, was shown to activate the cellular autophagy machinery in mammalian cell lines, including chronic myelogenous leukemia cells [15]. Furthermore, tetrahydrocannabinol was reported as an inducer of cell death by activating autophagy in glioma cells [16]. Likewise, curcumin [17], as well as some of its derivatives [18–20], were shown to activate autophagy in human cancer cell lines. Additionally, a novel small molecule (STF-62247) was shown to promote autophagic cell death in Von Hippel Lindau (*VHL*)-deficient renal cell carcinoma cells [21]. Finally, phenethyl isothiocyanate suppressed the Akt/mTOR pathway in human prostate cancer cell lines, leading to several autophagic features [22].

In previous studies from our group, the thioxanthone TXA1 has emerged as a hit compound, modulating P-glycoprotein activity in chronic myeloid leukemia cells [23], inhibiting human tumor cell growth and inducing apoptosis [23,24]. This compound has been shown to be particularly potent in melanoma cells [24].

Since the mechanism of action of this hit molecule is still not fully understood and since TXA1 was structurally similar to molecules known to modulate autophagy (lucanthone and to N^{10}-substituted phenoxazines) [25,26], this study aimed at further assessing the cytotoxic mechanism of TXA1 in A375-C5 melanoma cells, particularly at further evaluating its potential as an autophagy modulator.

2. Results

2.1. Treatment of A375-C5 Melanoma Cells with Twice the GI_{50} Concentration of TXA1 Alters the Cell Cycle Profile and Induces Apoptosis Although No Effect Is Found with the GI_{50} Concentration

The effect of TXA1 on the A375-C5 cell cycle profile was analyzed, testing two concentrations of this molecule: the previously-determined GI_{50} concentration (3.6 μM) [24] and twice this concentration ($2 \times GI_{50}$). Results showed that treatment with 3.6 μM of TXA1 did not cause any major alterations in the cell cycle profile (Figure 1) but pronounced alterations in the cell cycle profile were observed with the highest concentration tested (7.2 μM). In particular, a strong increase in the sub-G1 population

was observed when cells were treated with this concentration, which suggested that TXA1 induces apoptosis at this higher concentration, but not at the GI_{50} concentration.

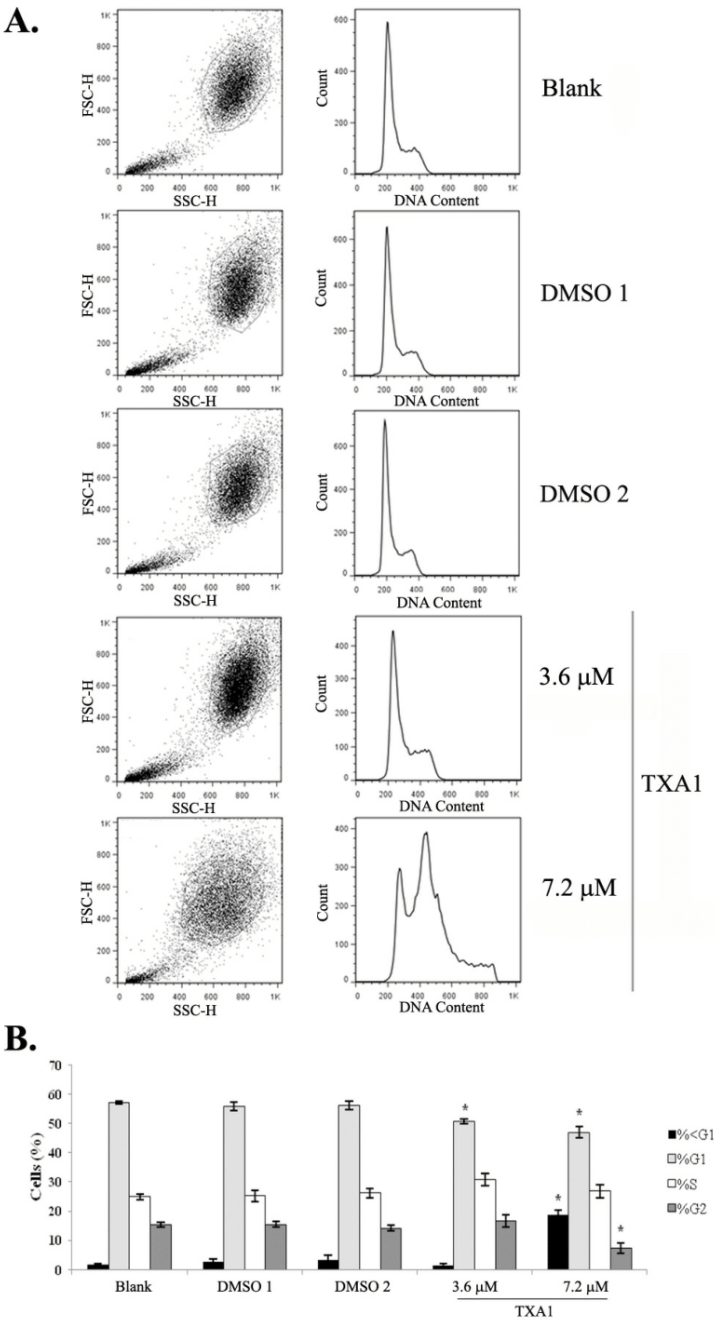


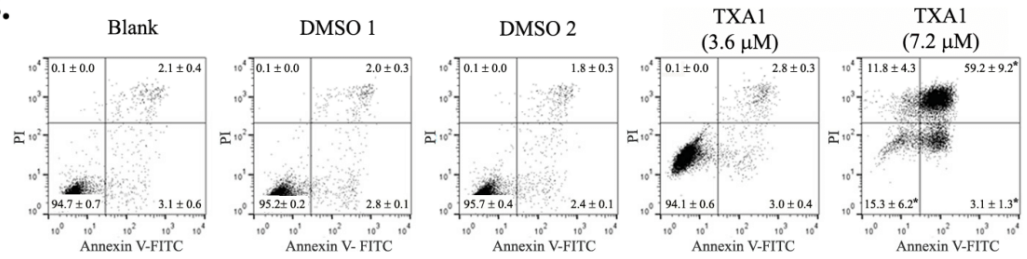
Figure 1. The effect of TXA1 on the cell cycle profile of A373-C5 cells. Cells were treated for 48 h with medium (blank), with TXA1 (3.6 μM and 7.2 μM), or with the corresponding DMSO concentrations (DMSO 1 and DMSO 2, respectively). (**A**) Representative images of flow cytometry analyzed following DNA staining with propidium iodide (PI). Left panels correspond to dot plots of forward vs. side scatter (FSC vs. SSC) and show the gated population. Right panels correspond to the histograms with cell cycle profile of the gated population, following the exclusion of cellular aggregates and debris (data not shown); (**B**) The percentage of cells in the different cell cycle phases. Results are the mean ± SEM of four independent experiments. * $p < 0.05$ blank vs. treatment. Etoposide (2 μM) was used as positive control: G0/G1: 6.3% ± 2.0%; S: 10.4% ± 2.3%; G2/M: 78.3% ± 0.7%.

Induction of apoptotic cell death following treatment with 7.2 μM of TXA1 (but not with 3.6 μM) was further confirmed with the Terminal deoxynucleotidyl transferase dUTP nick end labeling (TUNEL) assay (Figure 2A) and by flow cytometry analysis following Annexin V/FITC and PI staining (Figure 2B). Results from both of these assays clearly showed that treatment with 7.2 μM of TXA1 strongly induced cell death by apoptosis, although no alterations were observed following treatment with 3.6 μM TXA1 (GI_{50} concentration). These results were further corroborated by the analysis of PARP cleavage in these cells, by Western blot (Figure 2C). Indeed, a very strong increase in PARP cleavage was detected only following treatment with the highest TXA1 concentration tested (7.2 μM).

A.

		Programmed cell death (%)
Blank		1.0 ± 0.1
DMSO 1		1.0 ± 0.0
DMSO 2		0.7 ± 0.1
Compound 1	**3.6 μM**	1.1 ± 0.3
	7.2 μM	39.9 ± 5.2*

B.



C.

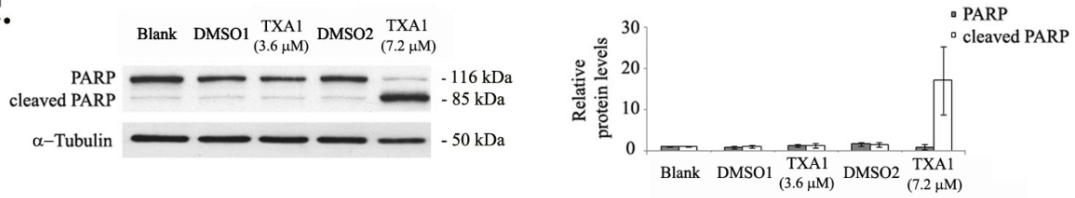


Figure 2. The effect of TXA1 on cell death by apoptosis of A373-C5 cells. Cells were treated for 48 h with medium (blank), TXA1 (3.6 μM and 7.2 μM), or with the corresponding DMSO concentrations (DMSO 1 and DMSO 2, respectively). (**A**) Levels of programmed cell death were analyzed with the TUNEL assay. Etoposide (1 μM) was used as a positive control (4% ± 0.1% of programmed cell death). * $p < 0.05$ Blank vs. treatment (**B**) Flow cytometry analysis of apoptotic cell death following Annexin V-FITC/PI staining. Images are representative of three independent experiments (values correspond to the mean ± SEM). Etoposide (1 μM) was used as positive control (18% ± 1.4% apoptosis); (**C**) PARP levels were analyzed by Western blot. Image is representative of 4 independent experiments (left panel). Densitometry analysis of the Western blots is expressed after normalization of the values obtained for each protein with the values obtained for tubulin (in relation to blank cells) and represent the mean ± SEM from four independent experiments (right panel).

2.2. *TXA1 Maps onto a Pharmacophore for Autophagy Induction*

Given the similarity of TXA1 with N^{10}-substituted phenoxazines (isosteres of thioxanthones which were described as autophagy inducers [26]) and since a pharmacophore had been previously developed for autophagy induction using these compounds [26], the possibility of the involvement of autophagy in the mechanism of action of TXA1 was considered using a pharmacophore approach. This was carried out using the referred pharmacophore and verifying its ability to identify autophagy

Molecules **2016**, *21*, 1343

inducers with different scaffolds from those it had been created from. TXA1 was mapped to the tree-feature pharmacophore (Figure 3) with results showing that TXA1 fits the pharmacophore for autophagy induction in 125 possible conformations. In all of the conformations, the nitrogen from the tertiary amine fits the positive ionizable group (red sphere on Figure 3). In 90% of the mapped conformations, one aromatic ring from the thioxanthonic scaffold fits one of the hydrophobic features, whereas the propoxyl carbonated chain fits the remaining hydrophobic feature (blue spheres on Figure 3).

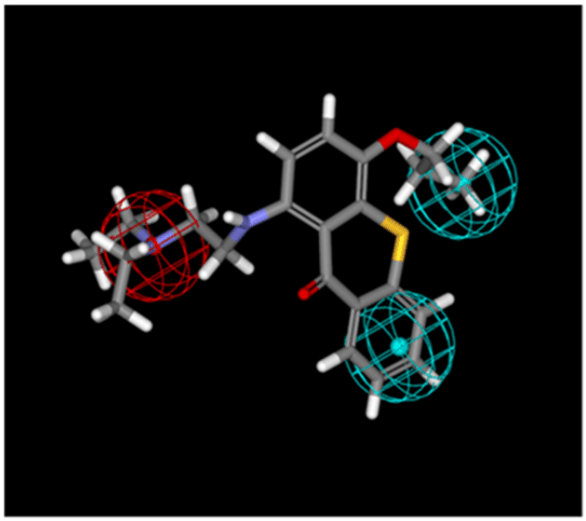


Figure 3. TXA1 mapped to the pharmacophore for autophagy induction. The red sphere represents the positive ionizable group and the blue sphere represents the hydrophobic region.

2.3. The GI_{50} Concentration of TXA1 Induces A375-C5 Cellular Autophagy

The possible involvement of autophagy in the TXA1 mechanism of action was evaluated in vitro, in the A375-C5 cells. The GI_{50} concentration of TXA1 (3.6 μM) was selected to carry out these studies, in order to avoid alterations in apoptosis or in the cell cycle profile (observed above when using the 7.2 μM treatment but not the 3.6 μM treatment).

The ultrastructural analysis (by transmission electron microscopy) of A375-C5 cells treated with 3.6 μM TXA1 showed the presence of autophagic structures (whereas the presence of such structures was very seldom seen in control cells) (Figure 4A). In agreement with this, MDC staining of A375-C5 cells following treatment with 3.6 μM TXA1 showed a clear punctate accumulation of MDC, indicating the presence of autophagosomes (Figure 4B). Other assays further confirmed the involvement of autophagy in the mechanism of action of TXA1. Indeed, transfection of A375-C5 cells with a mCherry-LC3 (microtubule-associated protein 1 light chain 3) expression vector allowed further visualization of the presence of LC3-II in autophagosomes, with a punctuated LC3 expression pattern being evident in transfected cells following TXA1 treatment (Figure 4B). Moreover, the formation of autophagolysosomes following TXA1 treatment was confirmed by fluorescence microscopy following staining with acridine orange. Indeed, results showed that untreated control cells presented predominantly green fluorescence with very minimal red fluorescence, whereas cells treated with TXA1 displayed considerable red fluorescence, typical of acidic vacuolar organelles (Figure 4B).

Molecules **2016**, *21*, 1343

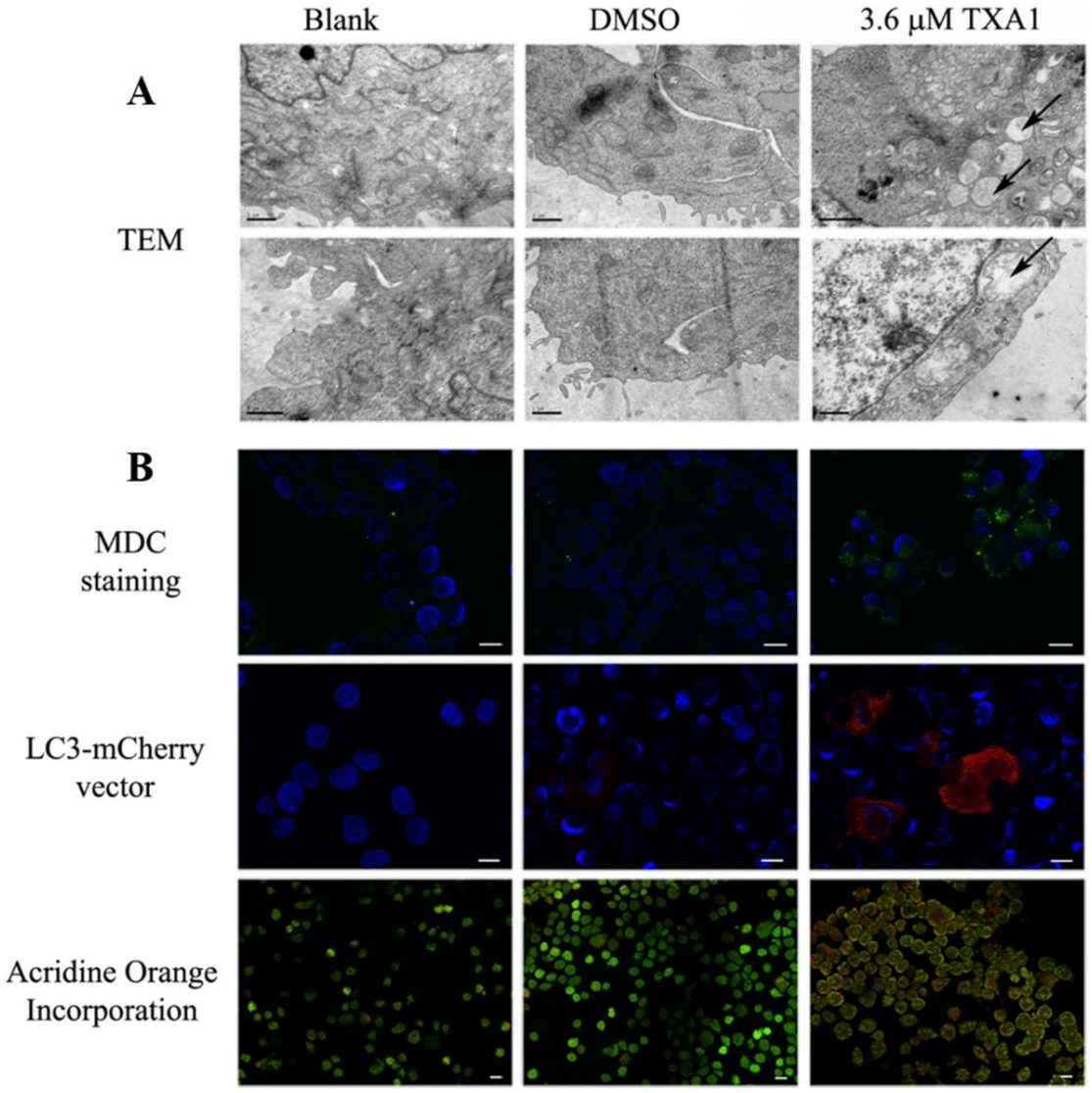


Figure 4. The effect of TXA1 on A375-C5 cellular autophagy. Cells were treated for 48 h with medium (blank), TXA1 (3.6 μM) or with the corresponding concentration of DMSO. (**A**) Transmission electron microscopy (TEM). Images are representative of two independent experiments. Arrows indicate autophagic structures. Bar corresponds to 1 μm; (**B**) Fluorescence microscopy analysis after (top panel) MDC staining (green); (middle panel) transfection with LC3-mCherry vector (red); and (lower panel) acridine orange incorporation (orange-red). Cell nuclei are stained with DAPI (blue). Bar = 20 μm. Images are representative of two experiments (except for MDC assay which is representative of three experiments).

Moreover, LC3-II levels were also analyzed by Western blot (Figure 5A). Results showed an increase in LC3-II levels following treatment with 3.6 μM TXA1, further indicating that TXA1 modulates autophagy in A375-C5 cells.

To further understand if TXA1 was an inducer or an inhibitor of autophagy, treatment with this compound was carried out in the presence of 3-methyl adenine (3-MA, a selective inhibitor of the early stages of autophagy [27]) or with E-64d/pepstatin (lysossomal protease inhibitors which inhibits autophagy at the later stage), to assess the autophagic flux [28–30]. Results showed that 3-MA treatment clearly reduced the levels of LC3-II induced by TXA1 (Figure 5B), supporting the idea that TXA1 was an inducer of autophagy. Furthermore, an additive increase in the levels of LC3-II was

observed after co-treatment with E-64d/pepstatin, when compared to TXA1 treatment alone, showing that the autophagic flux was occurring in TXA1-treated cells. Thus, it may be concluded that TXA1 is an inducer of autophagy.

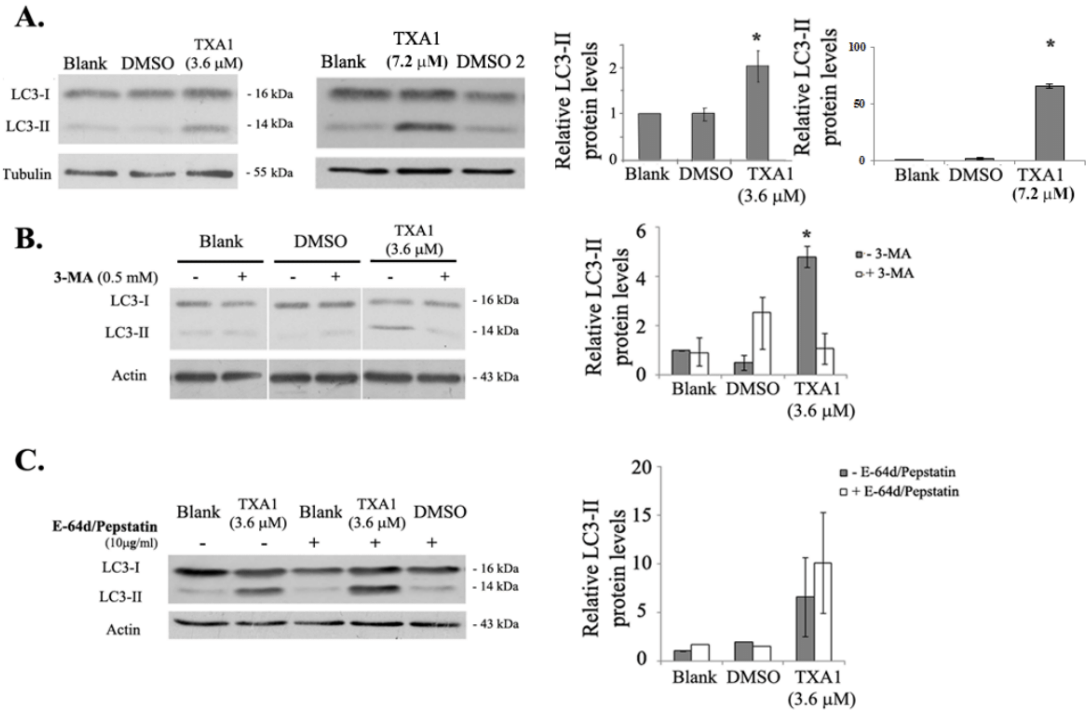


Figure 5. Effect of TXA1 on the expression levels of LC3-II in A375-C5 cells. Cells were treated for 48 h with medium (blank), TXA1 (3.6 μM or 7.2 μM), or with the corresponding DMSO concentrations (DMSO or DMSO2, respectively) LC3-II protein levels were analyzed by Western blot. (**A**) Following treatment with TXA1 alone; (**B**) following co-treatment with 3-MA; and (**C**) following co-treatment with E-64d/pepstatin. Images are representative of, at least, three independent experiments (except for the case of blank and DMSO treatments in the presence of E-64d/pepstatin, which result from two experiments only). Results of the densitometry analysis are expressed after normalization of the values obtained for each protein with the values obtained for tubulin or actin (and further expressed in relation to blank cells) and represent the mean ± SEM from, at least, three independent experiments (except for the case of blank and DMSO treatments in the presence of E-64d/pepstatin, which result from two experiments only). * $p \leq 0.05$ Blank vs. treatment.

A similar autophagic effect was observed for TXA1 hydrochloride (TXA1.HCl) on a breast adenocarcinoma cell line, with increases in the autophagic structures and LC3-II levels (Supplementary Figure S2).

Finally, the effect of cellular co-treatment with TXA1 and 3-MA was verified on viable cell numbers, in order to confirm whether the induction of autophagy by TXA1 was responsible for the cytotoxic effect of this molecule. As expected, treatment with 3-MA alone had no effect on A375-C5 viable cell numbers (Figure 6). However, the presence of 3-MA reverted the cytotoxic effect of TXA1, proving that the cytotoxic effect of TXA1 is dependent on autophagy induction.

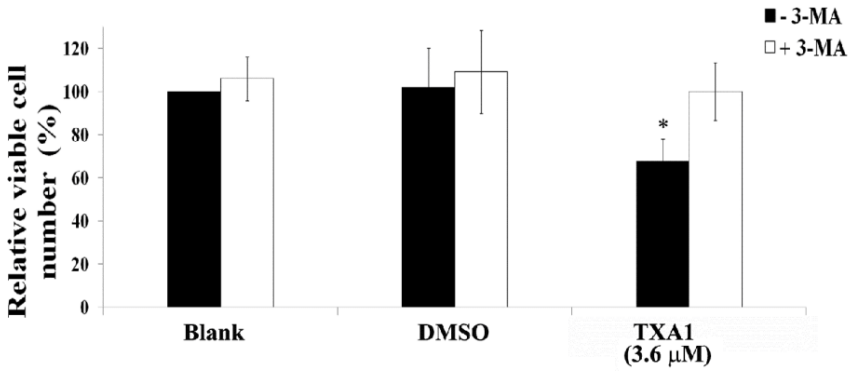


Figure 6. Effect of co-treating A375-C5 cells with TXA1 and 3-MA, on viable cell number. Cells were treated for 48 h with medium (blank), TXA1 (3.6 μM), or with the corresponding concentration of DMSO, in the absence or presence of 3-MA. Viable cell numbers were analyzed with a trypan blue exclusion assay. Results are presented as the percentage of viable cells in relation to blank cells and are the mean ± SE of three independent experiments. * $p \leq 0.05$ Blank vs. treatment.

3. Discussion

Although autophagy is mainly considered a survival mechanism, there is increasing evidence that it plays dual roles in cancer, acting also as a tumor suppressor mechanism, or even as a cell death mechanism. This may depend not only on the cellular context, but also on the levels and duration of cellular autophagy [7,8,31]. Excessive or sustained autophagy has the potential to induce tumor cell death and this may explain the antitumor effect of autophagy inducers [7,8]. Indeed, several antineoplastic agents have been described to induce autophagy, leading to cell death [32]. These agents include conventional cytotoxic drugs, as well as molecularly-targeted anticancer drugs, such as imatinib [15,31], cetuximab [33], and histone deacetylase (HDAC) inhibitors [34]. Thus, there is increasing interest in the development of compounds which modulate autophagy for anticancer therapy.

We have been studying thioxanthonic molecules and derivatives, since their heterocyclic scaffold has been associated with several biological properties, including anti-parasitic, anti-oxidative, and antitumor activities [35]. In our previous studies, TXA1 has emerged as a hit thioxanthone presenting tumor cell growth inhibitory activity towards several human tumor cell lines. In addition, it has also been verified that TXA1 did not affect the growth of non-tumor MRC5 cells [23,24]. This compound presented a 2-(diethylamino)ethylamine side chain located at position 1 which was identical to the amine in the same position of lucanthone, the first thioxanthone described as a potential antitumor agent (originally used as an anti-schistosomal drug) which reached clinical trials [35,36], being currently in Phase II clinical trials for glioblastoma multiforme [37]. Moreover, TXA1 was also structurally similar to N^{10}-substituted phenoxazines (isosteres of thioxanthones). Interestingly, autophagy modulation had been previously described for both lucanthone (described as a chemo- and radio-sensitizer associated with autophagy inhibition [25]) and for N^{10}-substituted phenoxazines (described as inducers of autophagy [26]). Considering the structural similarity of TXA1 with the referred compounds, the present study explored the mechanism of action of TXA1 in melanoma cells, particularly regarding the modulation of autophagy.

A promising association of TXA1 to the autophagic process resulted from the fact that TXA1 fitted a pharmacophore for autophagy induction in 125 possible conformations (Figure 3). When analyzing the effect of this compound in vitro, in A375-C5 cells, while not inducing apoptosis (or affecting cell cycle profile) at the GI_{50} concentrations, this treatment caused a clear accumulation of autophagic structures. This was observed not only by TEM (Figure 4A), which is described as a gold standard method for autophagy detection [30], but also by the increase in MDC staining and LC3 punctate pattern (Figure 4B). Autophagy modulation by TXA1 was further confirmed by the

conversion of the LC3 from the cytosolic form (LC3-I) into the autophagosome-associated form (LC3-II), which is considered a marker for autophagy (observed by Western blot, Figure 5) [38,39]. Moreover, this increase in LC3-II levels following TXA1 treatment was reverted in the presence of the early-stage autophagy inhibitor 3-MA (Figure 5B).

Nonetheless, the observation of an increase in the LC3-II levels could be due to an induction of autophagy or to an inhibition of the autophagic flux. One common strategy to evaluate this is by analyzing LC3-II levels, by Western blot, in the presence and absence of lysosomal degradation inhibitors [29,30]. The fact that the presence of these inhibitors (E-64d/pepstatin) further increased LC3-II levels when compared to treatment with TXA1 alone (Figure 5C), showed that TXA1 promoted an increase in the autophagic flux. Moreover, acridine orange staining further corroborated these results by showing the presence of acidic structures, such as autophagolysosomes, in TXA1-treated cells (Figure 4B).

Finally, the cytotoxicity of TXA1 (3.6 μM) in A375-C5 cells was reverted by the inhibition of autophagy with 3-MA (Figure 6). Indeed, this compound is a widely accepted inhibitor of autophagosome formation, acting through the inhibition of class III phosphatidylinositol 3 (PI3)-kinase [8]. Several other studies have also described the use of 3-MA to investigate the involvement of autophagy in the cytotoxic effect of different molecules/natural extracts [40–43]. In the present study, in addition to the reversion of the increase in LC3 II levels induced by TXA1, pretreatment with 3-MA also rescued A375-C5 cellular viability, further supporting the role of autophagy in the cytotoxic effect of TXA1 in these cells.

4. Materials and Methods

4.1. Compound

TXA1, 1-{[2-(diethylamino)ethyl]amino}-4-propoxy-9*H*-thioxanthen-9-one, has been previously synthesized by our group as described [23]. Its purity was determined by High-Performance Liquid Chromatography with Diode-Array Detection (HPLC-DAD) analysis using an isocratic elution of MeOH/H_2O basified with triethylamine (TEA) (1%) at a constant flow rate of 1.0 mL/min [23]. A 60 mM stock solution was prepared in DMSO and stored at −20 °C.

4.2. Mapping of TXA1 onto Pharmacophores for Autophagy Induction

A common feature pharmacophore model was created using HipHop module of Catalyst (Accelrys 2.1, San Diego, CA, USA) in order to reproduce a pharmacophore for autophagy induction, as previously described by Tsvetkov et al. [26]. This pharmacophore is composed of one positive ionizable group and two hydrophobic groups. TXA1 was subjected to energy minimization using HyperChem version 8.0 (Gainesville, FL, USA). The semi-empirical AM1 (Austin Model 1) [44] method with the Polak-Ribière algorithm was employed for molecular minimization [45]. The mapping of TXA1 onto the three-feature previously-described pharmacophore for autophagy induction was performed using the "Best Fit" method in Catalyst. During the flexible fitting process, conformations on TXA1 were calculated within the 20 kcal/mol energy threshold. Maximum omitted features were set to zero.

4.3. Cell Culture

The A375-C5 melanoma cell line (ECACC, Salisbury, UK) was genotyped at IPATIMUP´s Parentage and Genetic Identification Services Unit, using a PowerPlex® 16 HS System (Promega, Fitchburg, MA, USA) according to International Society for Forensic Genetics (ISFG) guidelines. Cells were routinely cultured in RPMI-1640 with UltraGlutamine I and 25 mM 4-(2-hydroxyethyl)-1-piperazineethanesulfonic acid (HEPES) buffer (Lonza, Basel, Switzerland) supplemented with 10% FBS (Fetal Bovine Serum, PAA, Cölbe, Germany), and maintained in a humidified incubator at 37 °C with 5% CO_2. Cell number and viability were determined with trypan blue exclusion assay.

4.4. Cell Treatment with TXA1

Cells were plated in six-well plates (1×10^5 cells/well) and allowed to adhere for 24 h. Cells were then treated with the previously-determined GI_{50} concentration (3.6 μM) [24] and with twice that concentration ($2 \times GI_{50}$, 7.2 μM) of TXA1. Control treatments were included, such as: untreated cells (blank); cells treated with DMSO as a negative control (corresponding to the volume used for the GI_{50} (DMSO 1) or for the $2 \times GI_{50}$ (DMSO 2) concentrations); cells treated with etoposide (Sigma-Aldrich, St. Louis, MO, USA) as a positive control for cell death and cell cycle analysis; and, finally, cells under serum starvation (i.e., without FBS), as a positive control for autophagy induction. Following the indicated time points (see Figure legends), cell number and viability were determined with the trypan blue exclusion assay and cells were further processed according to the following procedures.

4.5. Cell Cycle Profile

Cells were fixed in 70% ice-cold ethanol and subsequently resuspended in 0.1 mg/mL RNase A and 5 μg/mL propidium iodide in PBS for 1 h. Cellular DNA content was measured by flow cytometry using a FACSCalibur flow cytometer (BD Biosciences, Erembodegem, Belgium). The percentage of cells in the different phases of the cell cycle and in the sub-G1 peak were determined using FlowJo 7.6.5 software (Tree Star, Inc., Ashland, OR, USA) after cell debris and aggregate exclusion [23,46] and plotting at least 10,000 events per sample.

4.6. Programmed Cell Death

TUNEL assay was carried out using the "In situ cell death detection kit—fluorescein" (Roche, Boulogne-Billancourt Cedex, France) as previously described [47,48]. Briefly, cells were fixed in 4% paraformaldehyde (PFA) and cytospins were prepared. Cells were then permeabilized in ice-cold 0.1% Triton X-100 in 0.1% sodium citrate and incubated with TUNEL reaction mixture (enzyme dilution 1:20). Slides were mounted in Vectashield Mounting Media with DAPI (Vector Laboratories Inc., Burlingame, CA, USA), observed in a DM2000 fluorescence microscope (Leica, Wetzlar, Germany) and a semi-quantitative evaluation was performed by counting a minimum of 500 cells per slide. In addition, a specific assay for apoptosis was carried out using the "Human Annexin-V-FITC/PI apoptosis" kit (Bender MedSystems, Vienna, Austria) as previously described [49]. All flow cytometry analyses were performed using the FACSCalibur flow cytometer (BD Biosciences), plotting at least 10,000 events per sample and using the FlowJo 7.6.5 software (Tree Star, Inc.).

4.7. Expression of Apoptotic and Autophagic Proteins

Cells were lysed in Winman's buffer (1% NP-40, 0.1 M Tris-HCl pH 8.0, 0.15 M NaCl, and 5 mM EDTA) supplemented with a protease inhibitor cocktail (Roche). Protein lysates were quantified using a DC™ Protein Assay kit (Bio-Rad, Hercules, CA, USA), according to the manufacturer's instructions and 20 μg of protein loaded on 12% sodium dodecyl sulfate polyacrylamide gel electrophoresis (SDS-PAGE) gel [50,51]. After electrophoretic transfer into nitrocellulose membranes (Amersham, Cleveland, OH, USA), membranes were incubated with the following primary antibodies: rabbit anti-poly (ADP-ribose) polymerase PARP (H-250), (1:2000, Santa Cruz Biotechnology, Heidelberg, Germany), rabbit anti-light chain 3 B, LC3 (1:1000, Cell Signaling, Leiden, Netherlands), goat anti-actin antibody (1:2000, Santa Cruz Biotechnology), or mouse anti-tubulin antibody (1:10,000, Sigma-Aldrich), and with the corresponding secondary antibodies: goat anti-rabbit IgG-HRP (1:2000, Santa Cruz Biotechnology), donkey anti-goat IgG-HRP (1:2000, Santa Cruz Biotechnology), or goat anti-mouse IgG-HRP (1:2000, Santa Cruz Biotechnology). Signals were detected using Amersham™ ECL Western blotting detection reagents (GE Healthcare, Cleveland, OH, USA), Amersham Hyperfilm ECL (GE Healthcare) and Kodak GBX developer and fixer (Sigma-Aldrich).

4.8. Monodansylcadaverine (MDC) and Acridine Orange Staining

For MDC staining, studies were carried out following 48 h incubation with 3.6 μM of TXA1 (or controls). Cells were incubated for 1 h with freshly prepared MDC (50 μM) and fixed as described above. For acridine orange staining, cells were incubated with acridine orange (1 μM) for 15 min. In both cases, cytospins were prepared and mounted in Vectashield Mounting Media with DAPI (Vector Laboratories Inc., Burlingame, CA, USA). Cells were observed using a fluorescence microscope (Axio Imager.Z1 coupled with ApoTome Imaging System microscope, Zeiss, (Oberkochen, Germany).

4.9. Transfection with LC3-mCherry Expression Vector

Cells were plated in culture slides (Falcon; 2×10^4 cells/well) and allowed to adhere for 24 h. Transfection with LC3-mCherry vector (a kind gift from T. Johansen [52]) was then carried out using lipofectamine (Invitrogen, Carlsbad, CA, USA) according to the manufacturer's instructions. During the initial 4 h transfection, cells were incubated with medium with 5% FBS, then replaced by medium with 10% FBS [53]. Following 24 h transfection, cells were treated for 48 h with 3.6 μM of TXA1 or with controls (blank and DMSO). Cells were then fixed in 4% PFA in PBS and analyzed in a fluorescence microscope (Axio Imager.Z1 coupled with ApoTome Imaging System microscope, Zeiss).

4.10. Transmission Electron Microscopy

Following 48 h incubation with 3.6 μM TXA1 (or controls), cells were fixed with 2% glutaraldehyde and 2% PFA in 0.1 M phosphate buffer (PB), washed with 0.1% Millipore-filtered PB tannic acid, post-fixed with 1% PB osmium tetroxide for 1 h, and stained with 1% Millipore-filtered uranyl acetate. Samples were dehydrated in increasing concentrations of ethanol and, finally, in propylene oxide for 30 min. Samples were then infiltrated and embedded directly in Epon resin and polymerized in a 70 °C oven for two days. Cuts were performed on ultrathin (50–100 nm) sections with a Leica (Wetzlar, Germany) Ultracut microtome and each section was stained with 5% uranyl acetate solution and with Reynold's lead citrate solution. Images were examined in a Jeol JEM 1400 transmission electron microscope (Tokyo, Japan) at an accelerating voltage of 80 kV. Digital images were obtained using a Gatan SC 1000 ORIUS CCD camera (Warrendale, PA, USA).

4.11. Treatment with Autophagy Inhibitors

Cells were plated in six-well plates (1×10^5 cells/well) and allowed to adhere for 24 h. Cells were then treated for 1 h with 0.5 mM 3-methyladenine (3-MA, Sigma) or with 10 μg/mL E-64d (AppliChem, Darmstadt, Germany) and Pepstatin A (Cayman Chemical, Ann Arbor, MI, USA) and then co-incubated with 3.6 μM of TXA1, or with control treatments (blank, DMSO) for 48 h. Viable cell numbers were then assessed by trypan blue assay and protein expression analyzed by Western blot, as described above.

4.12. Statistical Analysis

Results are expressed as mean ± standard error. Values for each treatment (or solvent) were compared by Student's *t*-test, and the differences were considered statistically significant if $p \leq 0.05$.

5. Conclusions

This work reinforces the anticancer potential of the hit thioxanthonic small molecule TXA1. In particular, it shows that this compound decreases the viability of human tumor cell lines by inducing autophagy. Therefore, TXA1 may serve as lead compound for the development of new autophagy modulators with antitumor activity. Future work will allow to further elucidate the intracellular signaling cascades associated with the effect of TXA1 in autophagy, such as the phosphatidylinositol 3-kinase/mammalian target of rapamycin (PI3K/mTOR) or the AMP-activated protein kinase (AMPK) signaling pathways [11]. Furthermore, future studies with human tumor xenograft models in

nude mice will allow confirmation of the in vivo lack of toxicity and antitumor potential of this hit compound.

Supplementary Materials: Supplementary materials can be accessed at: http://www.mdpi.com/1420-3049/21/10/1343/s1.

Acknowledgments: This work was financed by FEDER—Fundo Europeu de Desenvolvimento Regional funds through the COMPETE 2020—Operacional Programme for Competitiveness and Internationalisation (POCI), Portugal 2020, and by Portuguese funds through FCT—Fundação para a Ciência e a Tecnologia/ Ministério da Ciência, Tecnologia e Inovação in the framework of the project "Institute for Research and Innovation in Health Sciences (POCI-01-0145-FEDER-007274)". The work was also funded by ERDF, COMPETE, and FCT under the projects PTDC/SAU-OSM/101437/2008, PTDC/MAR-BIO/4694/2014, and INNOVMAR—reference NORTE-01-0145-FEDER-000035, Research Line NOVELMAR. The authors also thank: FCT for D. Sousa and R.T. Lima grants (PTDC/SAU-FCT/100930/2008 and SFRH/BPD/68787/2010, respectively), QREN for D. Sousa grant (NORTE-07-0124-FEDER-000023).

Author Contributions: E.S. and M.H.V. conceived the study. M.H.V. and R.T.L. designed experiments. D.S., R.T.L., J.B. and A.M.P. carried out experiments. M.H.V. supervised the experiments. A.P. carried out the pharmacophore study, supervised by E.S., R.T.L. and D.S. organized data and carried out statistical analysis. R.T.L. and M.H.V. wrote the manuscript. M.M.P., E.S. and M.P. critically revised the manuscript. All authors read and approved the final version of the manuscript.

Conflicts of Interest: The authors declare no conflict of interest.

References

1. Maycotte, P.; Thorburn, A. Autophagy and cancer therapy. *Cancer Boil. Ther.* **2011**, *11*, 127–137. [CrossRef]
2. Rosenfeldt, M.T.; Ryan, K.M. The multiple roles of autophagy in cancer. *Carcinogenesis* **2011**, *32*, 955–963. [CrossRef] [PubMed]
3. Yang, S.; Kimmelman, A.C. A critical role for autophagy in pancreatic cancer. *Autophagy* **2011**, *7*, 912–913. [CrossRef] [PubMed]
4. Maiuri, M.C.; Zalckvar, E.; Kimchi, A.; Kroemer, G. Self-eating and self-killing: Crosstalk between autophagy and apoptosis. *Nat. Rev. Mol. Cell Biol.* **2007**, *8*, 741–752. [CrossRef] [PubMed]
5. Eisenberg, T.; Knauer, H.; Schauer, A.; Buttner, S.; Ruckenstuhl, C.; Carmona-Gutierrez, D.; Ring, J.; Schroeder, S.; Magnes, C.; Antonacci, L.; et al. Induction of autophagy by spermidine promotes longevity. *Nat. Cell Biol.* **2009**, *11*, 1305–1314. [CrossRef] [PubMed]
6. Rubinstein, A.D.; Kimchi, A. Life in the balance—A mechanistic view of the crosstalk between autophagy and apoptosis. *J. Cell Sci.* **2012**, *125*, 5259–5268. [CrossRef] [PubMed]
7. Yang, Z.J.; Chee, C.E.; Huang, S.; Sinicrope, F.A. The role of autophagy in cancer: Therapeutic implications. *Mol. Cancer Ther.* **2011**, *10*, 1533–1541. [CrossRef] [PubMed]
8. Baek, K.H.; Park, J.; Shin, I. Autophagy-regulating small molecules and their therapeutic applications. *Chem. Soc. Rev.* **2012**, *41*, 3245–3263. [CrossRef] [PubMed]
9. Fleming, A.; Noda, T.; Yoshimori, T.; Rubinsztein, D.C. Chemical modulators of autophagy as biological probes and potential therapeutics. *Nat. Chem. Boil.* **2011**, *7*, 9–17. [CrossRef] [PubMed]
10. Cho, Y.S.; Kwon, H.J. Control of autophagy with small molecules. *Arch. Pharm. Res.* **2010**, *33*, 1881–1889. [CrossRef] [PubMed]
11. Sui, X.; Chen, R.; Wang, Z.; Huang, Z.; Kong, N.; Zhang, M.; Han, W.; Lou, F.; Yang, J.; Zhang, Q.; et al. Autophagy and chemotherapy resistance: A promising therapeutic target for cancer treatment. *Cell Death Dis.* **2013**, *4*, e838. [CrossRef] [PubMed]
12. Opipari, A.W., Jr.; Tan, L.; Boitano, A.E.; Sorenson, D.R.; Aurora, A.; Liu, J.R. Resveratrol-induced autophagocytosis in ovarian cancer cells. *Cancer Res.* **2004**, *64*, 696–703. [CrossRef] [PubMed]
13. Scarlatti, F.; Maffei, R.; Beau, I.; Codogno, P.; Ghidoni, R. Role of non-canonical Beclin 1-independent autophagy in cell death induced by resveratrol in human breast cancer cells. *Cell. Death Differ.* **2008**, *15*, 1318–1329. [CrossRef] [PubMed]
14. Lang, F.; Qin, Z.; Li, F.; Zhang, H.; Fang, Z.; Hao, E. Apoptotic Cell Death Induced by Resveratrol Is Partially Mediated by the Autophagy Pathway in Human Ovarian Cancer Cells. *PLoS ONE* **2015**, *10*, e0129196. [CrossRef] [PubMed]

15. Ertmer, A.; Huber, V.; Gilch, S.; Yoshimori, T.; Erfle, V.; Duyster, J.; Elsasser, H.P.; Schatzl, H.M. The anticancer drug imatinib induces cellular autophagy. *Leuk. Off. J. Leuk. Soc. Am. Leuk. Res. Fund UK* **2007**, *21*, 936–942. [CrossRef] [PubMed]
16. Salazar, M.; Carracedo, A.; Salanueva, I.J.; Hernandez-Tiedra, S.; Lorente, M.; Egia, A.; Vazquez, P.; Blazquez, C.; Torres, S.; Garcia, S.; et al. Cannabinoid action induces autophagy-mediated cell death through stimulation of ER stress in human glioma cells. *J. Clin. Investing.* **2009**, *119*, 1359–1372. [CrossRef]
17. Gupta, S.C.; Kismali, G.; Aggarwal, B.B. Curcumin, a component of turmeric: From farm to pharmacy. *BioFactors* **2013**, *39*, 2–13. [CrossRef] [PubMed]
18. Zhou, G.Z.; Xu, S.L.; Sun, G.C.; Chen, X.B. Novel curcumin analogue IHCH exhibits potent antiproliferative effects by inducing autophagy in A549 lung cancer cells. *Mol. Med. Rep.* **2014**, *10*, 441–446. [PubMed]
19. Qu, W.; Xiao, J.; Zhang, H.; Chen, Q.; Wang, Z.; Shi, H.; Gong, L.; Chen, J.; Liu, Y.; Cao, R.; et al. B19, a novel monocarbonyl analogue of curcumin, induces human ovarian cancer cell apoptosis via activation of endoplasmic reticulum stress and the autophagy signaling pathway. *Int. J. Biol. Sci.* **2013**, *9*, 766–777. [CrossRef] [PubMed]
20. Zhou, G.Z.; Zhang, S.N.; Zhang, L.; Sun, G.C.; Chen, X.B. A synthetic curcumin derivative hydrazinobenzoylcurcumin induces autophagy in A549 lung cancer cells. *Pharm. Boil.* **2014**, *52*, 111–116. [CrossRef] [PubMed]
21. Turcotte, S.; Chan, D.A.; Sutphin, P.D.; Hay, M.P.; Denny, W.A.; Giaccia, A.J. A molecule targeting *VHL*-deficient renal cell carcinoma that induces autophagy. *Cancer Cell* **2008**, *14*, 90–102. [CrossRef] [PubMed]
22. Bommareddy, A.; Hahm, E.R.; Xiao, D.; Powolny, A.A.; Fisher, A.L.; Jiang, Y.; Singh, S.V. Atg5 regulates phenethyl isothiocyanate-induced autophagic and apoptotic cell death in human prostate cancer cells. *Cancer Res.* **2009**, *69*, 3704–3712. [CrossRef] [PubMed]
23. Palmeira, A.; Vasconcelos, M.H.; Paiva, A.; Fernandes, M.X.; Pinto, M.; Sousa, E. Dual inhibitors of P-glycoprotein and tumor cell growth: (Re)discovering thioxanthones. *Biochem. Pharm.* **2012**, *83*, 57–68. [CrossRef] [PubMed]
24. Barbosa, J.; Lima, R.T.; Sousa, D.; Gomes, A.S.; Palmeira, A.; Seca, H.; Choosang, K.; Pakkong, P.; Bousbaa, H.; Pinto, M.M.; et al. Screening a Small Library of Xanthones for Antitumor Activity and Identification of a Hit Compound which Induces Apoptosis. *Molecules* **2016**, *21*. [CrossRef] [PubMed]
25. Carew, J.S.; Espitia, C.M.; Esquivel, J.A.; Mahalingam, D.; Kelly, K.R.; Reddy, G.; Giles, F.J.; Nawrocki, S.T. Lucanthone is a novel inhibitor of autophagy that induces cathepsin D-mediated apoptosis. *J. Biol. Chem.* **2011**, *286*, 6602–6613. [CrossRef] [PubMed]
26. Tsvetkov, A.S.; Miller, J.; Arrasate, M.; Wong, J.S.; Pleiss, M.A.; Finkbeiner, S. A small-molecule scaffold induces autophagy in primary neurons and protects against toxicity in a Huntington disease model. *Proc. Natl. Acad. Sci. USA* **2010**, *107*, 16982–16987. [CrossRef] [PubMed]
27. Seglen, P.O.; Gordon, P.B. 3-Methyladenine: Specific inhibitor of autophagic/lysosomal protein degradation in isolated rat hepatocytes. *Proc. Natl. Acad. Sci. USA* **1982**, *79*, 1889–1892. [CrossRef] [PubMed]
28. Mizushima, N.; Yoshimori, T. How to interpret LC3 immunoblotting. *Autophagy* **2007**, *3*, 542–545. [CrossRef] [PubMed]
29. Zhang, X.J.; Chen, S.; Huang, K.X.; Le, W.D. Why should autophagic flux be assessed? *Acta. Pharmacol. Sin.* **2013**, *34*, 595–599. [CrossRef] [PubMed]
30. Klionsky, D.J.; Abdelmohsen, K.; Abe, A.; Abedin, M.J.; Abeliovich, H.; Acevedo Arozena, A.; Adachi, H.; Adams, C.M.; Adams, P.D.; Adeli, K.; et al. Guidelines for the use and interpretation of assays for monitoring autophagy (3rd edition). *Autophagy* **2016**, *12*, 1–222. [CrossRef] [PubMed]
31. Shingu, T.; Fujiwara, K.; Bogler, O.; Akiyama, Y.; Moritake, K.; Shinojima, N.; Tamada, Y.; Yokoyama, T.; Kondo, S. Inhibition of autophagy at a late stage enhances imatinib-induced cytotoxicity in human malignant glioma cells. *Int. J. Cancer* **2009**, *124*, 1060–1071. [CrossRef] [PubMed]
32. Eberhart, K.; Oral, O.; Gozuacik, D. Chapter 13—Induction of Autophagic Cell Death by Anticancer Agents. In *Autophagy: Cancer, Other Pathologies, Inflammation, Immunity, Infection, and Aging*; Hayat, M.A., Ed.; Academic Press: Amsterdam, The Netherlands, 2014; pp. 179–202.
33. Li, X.; Fan, Z. The epidermal growth factor receptor antibody cetuximab induces autophagy in cancer cells by downregulating HIF-1α and Bcl-2 and activating the beclin 1/hVps34 complex. *Cancer Res.* **2010**, *70*, 5942–5952. [CrossRef] [PubMed]

34. Liu, Y.L.; Yang, P.M.; Shun, C.T.; Wu, M.S.; Weng, J.R.; Chen, C.C. Autophagy potentiates the anti-cancer effects of the histone deacetylase inhibitors in hepatocellular carcinoma. *Autophagy* **2010**, *6*, 1057–1065. [CrossRef] [PubMed]
35. Paiva, A.M.; Pinto, M.M.; Sousa, E. A century of thioxanthones: Through synthesis and biological applications. *Curr. Med. Chem.* **2013**, *20*, 2438–2457. [CrossRef] [PubMed]
36. Naidu, M.D.; Agarwal, R.; Pena, L.A.; Cunha, L.; Mezei, M.; Shen, M.; Wilson, D.M.; Liu, Y.; Sanchez, Z.; Chaudhary, P.; et al. Lucanthone and its derivative hycanthone inhibit apurinic endonuclease-1 (APE1) by direct protein binding. *PLoS ONE* **2011**, *6*, e23679. [CrossRef] [PubMed]
37. Safety and Efficacy Study of Lucanthone When Used in Combination With Temozolomide(TMZ) and Radiation to Treat Glioblastoma Multiforme(GBM). Available online: https://clinicaltrials.gov/ct2/show/NCT01587144 (accessed on 7 October 2016).
38. Tanida, I.; Ueno, T.; Kominami, E. LC3 and Autophagy. *Methods Mol. Biol.* **2008**, *445*, 77–88. [PubMed]
39. Yang, C.; Kaushal, V.; Shah, S.V.; Kaushal, G.P. Autophagy is associated with apoptosis in cisplatin injury to renal tubular epithelial cells. *Am. J. Physiol. Renal Physiol.* **2008**, *294*, F777–F787. [CrossRef] [PubMed]
40. Li, J.; Yang, D.; Wang, W.; Piao, S.; Zhou, J.; Saiyin, W.; Zheng, C.; Sun, H.; Li, Y. Inhibition of autophagy by 3-MA enhances IL-24-induced apoptosis in human oral squamous cell carcinoma. *J. Exp. Clin. Cancer Res.* **2015**, *34*, 97. [CrossRef] [PubMed]
41. Seca, H.; Lima, R.T.; Lopes-Rodrigues, V.; Guimarães, J.E.; Almeida, G.M.; Vasconcelos, M.H. Targeting miR-21 induces autophagy and chemosensitivity of leukemia cells. *Curr. Drug Targets* **2013**, *14*, 1135–1143. [CrossRef] [PubMed]
42. Jiang, Y.Y.; Yang, R.; Wang, H.J.; Huang, H.; Wu, D.; Tashiro, S.; Onodera, S.; Ikejima, T. Mechanism of autophagy induction and role of autophagy in antagonizing mitomycin C-induced cell apoptosis in silibinin treated human melanoma A375-S2 cells. *Eur. J. Pharmacol.* **2011**, *659*, 7–14. [CrossRef] [PubMed]
43. Liu, B.; Cheng, Y.; Zhang, B.; Bian, H.J.; Bao, J.K. Polygonatum cyrtonema lectin induces apoptosis and autophagy in human melanoma A375 cells through a mitochondria-mediated ROS-p38-p53 pathway. *Cancer Lett.* **2009**, *275*, 54–60. [CrossRef] [PubMed]
44. Froimowitz, M. HyperChem: A software package for computational chemistry and molecular modeling. *BioTechniques* **1993**, *14*, 1010–1013. [PubMed]
45. Zhang, L. A descent modified Polak-Ribière-Polyak conjugate gradient method and its global convergence. *IMA J. Numer. Anal.* **2006**, *26*, 11. [CrossRef]
46. Abreu, R.M.V.; Ferreira, I.C.F.R.; Calhelha, R.C.; Lima, R.T.; Vasconcelos, M.H.; Adega, F.; Chaves, R.; Queiroz, M.J.R.P. Anti-hepatocellular carcinoma activity using human HepG2 cells and hepatotoxicity of 6-substituted methyl 3-aminothieno[3,2-*b*pyridine-2-carboxylate derivatives: In vitro evaluation, cell cycle analysis and QSAR studies. *Eur. J. Med. Chem.* **2011**, *46*, 5800–5806. [PubMed]
47. Lima, R.T.; Martins, L.M.; Guimaraes, J.E.; Sambade, C.; Vasconcelos, M.H. Specific downregulation of bcl-2 and xIAP by RNAi enhances the effects of chemotherapeutic agents in MCF-7 human breast cancer cells. *Cancer Gene Ther.* **2004**, *11*, 309–316. [CrossRef] [PubMed]
48. Queiroz, M.J.; Calhelha, R.C.; Vale-Silva, L.A.; Pinto, E.; Lima, R.T.; Vasconcelos, M.H. Efficient synthesis of 6-(hetero)arylthieno[3,2-*b*]pyridines by Suzuki-Miyaura coupling. Evaluation of growth inhibition on human tumor cell lines, SARs and effects on the cell cycle. *Eur. J. Med. Chem.* **2010**, *45*, 5628–5634. [CrossRef] [PubMed]
49. Queiroz, M.J.; Calhelha, R.C.; Vale-Silva, L.A.; Pinto, E.; Almeida, G.M.; Vasconcelos, M.H. Synthesis and evaluation of tumor cell growth inhibition of methyl 3-amino-6-[(hetero)arylethynyl]thieno[3,2-*b*]pyridine-2-carboxylates. Structure-activity relationships, effects on the cell cycle and apoptosis. *Eur. J. Med. Chem.* **2011**, *46*, 236–240. [CrossRef] [PubMed]
50. Lima, R.T.; Barron, G.A.; Grabowska, J.A.; Bermano, G.; Kaur, S.; Roy, N.; Vasconcelos, M.H.; Lin, P.K. Cytotoxicity and cell death mechanisms induced by a novel bisnaphthalimidopropyl derivative against the NCI-H460 non-small lung cancer cell line. *Anti-Cancer Agents Med. Chem.* **2013**, *13*, 414–421.
51. Preto, A.; Goncalves, J.; Rebocho, A.P.; Figueiredo, J.; Meireles, A.M.; Rocha, A.S.; Vasconcelos, H.M.; Seca, H.; Seruca, R.; Soares, P.; et al. Proliferation and survival molecules implicated in the inhibition of BRAF pathway in thyroid cancer cells harbouring different genetic mutations. *BMC Cancer* **2009**, *9*, 387. [CrossRef] [PubMed]

52. Pankiv, S.; Clausen, T.H.; Lamark, T.; Brech, A.; Bruun, J.A.; Outzen, H.; Overvatn, A.; Bjorkoy, G.; Johansen, T. p62/SQSTM1 binds directly to Atg8/LC3 to facilitate degradation of ubiquitinated protein aggregates by autophagy. *J. Biol. Chem.* **2007**, *282*, 24131–24145. [CrossRef] [PubMed]
53. Birame, B.M.; Jigui, W.; Fuxian, Y.; Shuang, W.; Li, Y.D.; Jiazeng, S.; Zhili, L.; Bao, Y.; Weiquan, L. Co-expression of apoptin (VP3) and antibacterial peptide cecropin B mutant (ABPS1) genes induce higher rate of apoptosis in HepG2 and A375 cell lines. *Afr. J. Biotechnol.* **2012**, *11*, 8. [CrossRef]

Sample Availability: Samples of the compound TXA1 are available from the authors.



© 2016 by the authors; licensee MDPI, Basel, Switzerland. This article is an open access article distributed under the terms and conditions of the Creative Commons Attribution (CC-BY) license (http://creativecommons.org/licenses/by/4.0/).

Molecules **2016**, *21*, 1343; doi:10.3390/molecules21101343

Supplementary Materials: Modulation of Autophagy by a Thioxanthone Decreases the Viability of Melanoma Cells

Raquel T. Lima, Diana Sousa, Ana M. Paiva, Andreia Palmeira, João Barbosa, Madalena Pedro, Madalena M. Pinto, Emília Sousa and M. Helena Vasconcelos

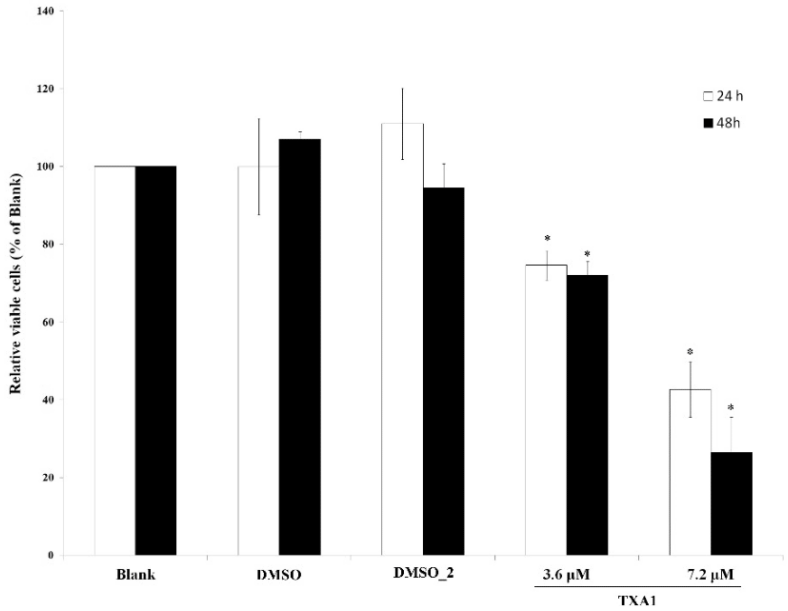


Figure S1. Treatment of A375-C5 cells with TXA1 reduced the viable cell number. Cells were treated for 48 h with medium (Blank), TXA1 (3.6 μM and 7.2 μM), or with the corresponding DMSO concentrations (DMSO and DMSO 2, respectively). Results are presented as the percentage of viable cells in relation to Blank cells (treated with medium only) and are the mean ± SE of four independent experiments (except for results from the 48 h treatment with the lowest DMSO control treatment, which are the mean of three experiments only). * $p < 0.05$ Blank vs. treatment.

Molecules **2016**, *21*, 1343

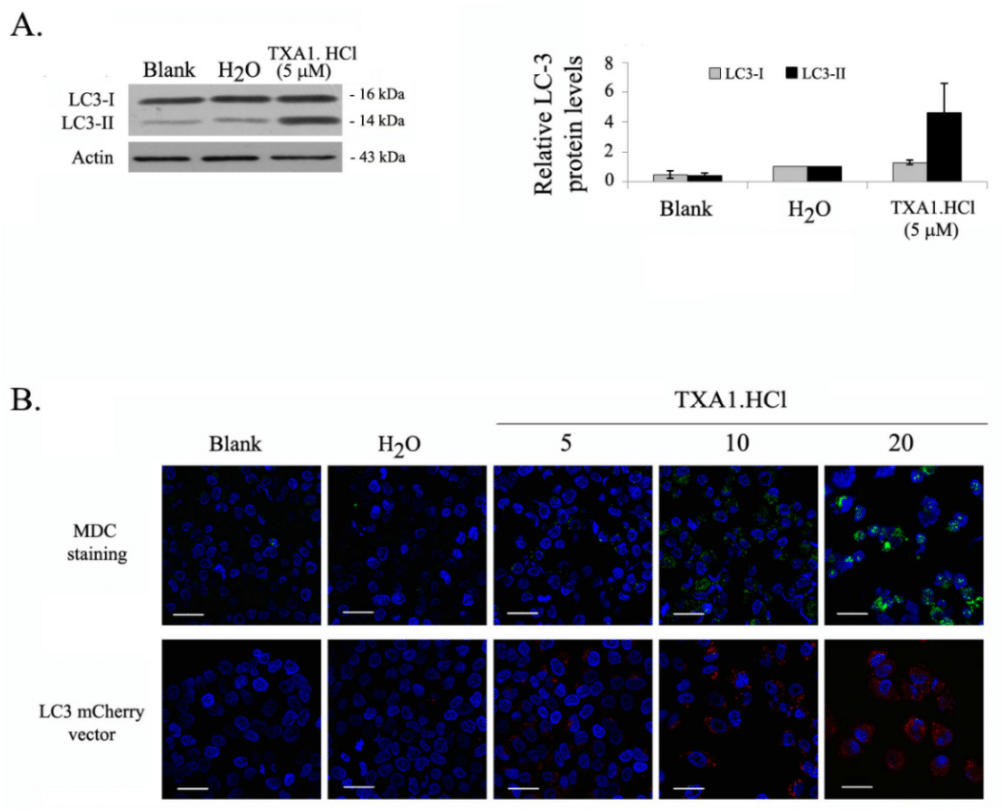


Figure S2. TXA1.HCl induces autophagy in breast adenocarcinoma MCF7 cells. (**A**) Representative Western blot showing increased LC3-II levels in cells treated for 48 h with medium (Blank), TXA1.HCl (the hydrosoluble salt of TXA1 [24]), or the corresponding solvent (H_2O). Results of the densitometry analysis are expressed after normalization of the values obtained for each protein with the values obtained for actin (and further expressed in relation to solvent treatment) and represent the mean ± SEM from three independent experiments; (**B**) MDC staining of cells treated with medium (Blank), H_2O (control), or with 5, 10, or 20 μM of TXA1.HCl, showing the presence of autophagic structures analyzed by fluorescence microscopy. Upper panel: MDC staining (green); lower panel: transfection with LC3-mCherry vector (red). Cell nuclei are stained with DAPI (blue). Bar = 20 μm. Images are representative of three experiments (except for MDC assay which is representative of two experiments).

CHAPTER III

GENERAL DISCUSSION AND FUTURE PERSPECTIVES

Cancer incidence and mortality continue to be high due to: i) aging of the population, ii) growth of the world population and iii) failure of cancer treatment caused by intrinsic or acquired resistance mechanisms. Indeed, drug resistance may be responsible for treatment failure in over 90% of patients with metastatic cancer [1, 338]. The aggressiveness of this condition is related to the heterogeneity of the processes involved. In the particular case of MDR (characterized by resistance of tumour cells to several drugs with different structures), the network of mechanisms underlying this problem is even more complex. MDR may develop from a variety of dysregulated processes (described in chapter I- section 1.2). Nonetheless, the most frequently altered cellular mechanism in tumour MDR is the overexpression of drug-efflux proteins, in particular P-glycoprotein (P-gp). Alterations in autophagy have been also related with MDR. However, this issue requires further clarification, namely on the role of MDR inhibitors, on this process. In addition, in recent years, the contribution of EVs released by MDR cells to the dissemination of MDR traits was reported, further increasing the complexity of the MDR phenotype. Deeper understanding of the network of intercellular communication mediated by EVs, in MDR P-gp overexpressing tumour cells, is required to identify mechanisms which may be modulated in order to overcome this problem.

Thus, to add knowledge to the role of EVs in tumour MDR associated with P-gp overexpression and to the effect of a P-gp inhibitor on cellular autophagy we aimed to: i) identify RNA species associated with MDR of P-gp overexpressing tumour cells and their EVs; ii) understand the mechanisms involved in the release of EVs by MDR (P-gp overexpressing) cells and their uptake by drug-sensitive counterparts; iii) study the mechanism of action of a P-gp inhibitor with anti-tumour activity.

To accomplish this, we studied two pairs of drug-sensitive and MDR counterpart cell lines, from two different human tumour models that had been previously established by other groups, from non-small cell lung cancer (NSCLC) and chronic myeloid leukaemia (CML). Importantly, in both models, the MDR cells present P-gp overexpression. Of note, the EVs studied along the present study, were isolated by differential ultra-centrifugation, one of the most used protocols for EVs' isolation. A deep characterization of the isolated EVs regarding their size, morphology and presence of EVs markers was previously published by our group [339-341] and further confirmed during the studies presented in this thesis.

In the present work, we confirmed that EVs released by MDR cells were able to transfer a drug-resistant phenotype to drug-sensitive recipient cells. This

observation is in agreement with other previously published reports. Indeed, in the last decade, the participation of EVs in the horizontal transfer of MDR traits was described in several tumour models such as leukaemia, breast, lung, prostate [342-344]. The ability of EVs to induce this phenotype change has been associated to the cargo transferred from donor cells to recipient cells [345].

Next, in order to identify important players of the MDR phenotype associated with P-gp overexpression, we analysed the RNA content of both (pairs of MDR and drug-sensitive) cells and EVs. **The results presented in this thesis clearly showed that MDR cells express distinct RNA species from their drug-sensitive counterparts. Moreover, the EVs released by MDR cells also harbour distinct RNA entities from the EVs released by their drug-sensitive counterparts.** Next generation sequencing was selected to perform this analysis since this methodology, through the high number of reads obtained, allows the discovery, characterization and quantification of a large amount of known and also unknown RNAs. Indeed, in the EVs' field, deep sequencing has made significant contributions to our understanding of EVs' RNA content [231, 346]. Our results showed a total of 1927 RNA species altered between drug-sensitive and MDR conditions (cells and EVs). The comparison of the EVs content identified three RNA species, remarkably all pseudogenes, with differential levels when comparing MDR and drug-sensitive conditions. Two of these pseudogenes (a novel pseudogene and the RNA 5.8S ribosomal pseudogene 2) were found increased in EVs released by MDR cells from both tumour models. In addition, five transcripts were also found similarly altered (increased or decreased) in CML snd NDCLC MDR cells: miR-383, miR-4660, chromosome 16 open reading frame 45, FOXF1 adjacent non-coding developmental regulatory RNA and serglycin. Interestingly, the pseudogenes found altered in EVs released by MDR cells were not previously associated to cancer. However, four of the five transcripts altered in MDR cells were previously associated with tumour cell proliferation [37], epithelial-mesenchymal transition [38], stemness [38], metastization [38-40], poor prognosis [39] and poor survival [41].

Following the analysis of the different RNA species, a particular study of the miRs content was performed and **a panel of 6 miRs altered simultaneously in MDR EVs and cells of the NSCLC model was found.** This "NSCLC panel" was constituted by miR-204-5p, miR-139-5p, miR-29c-5p, miR-551b-3p, miR-29b-2-5p, miR-204-3p. **Moreover, 2 miRs (**miR-383-5p and miR-504-5p**) were shown differently expressed in both MDR tumour cell models.** Importantly, all these miRs were previously associated with regulation of tumour cell proliferation, cancer progression or cancer drug resistance [347-353].

Therefore, in the present work **we identified RNA species that could be used as specific MDR biomarkers of NSCLC**, as well as species that may have an impact in the P-gp-mediated MDR. **Importantly, further studies will be required to validate these species as MDR biomarkers**. Indeed, the investigation of reliable biomarkers for early diagnosis, prognosis and therapy response of cancer is the 'holy grail' in cancer research field [207]. Despite a progressively increasing number of possible biomarker reports, to date few FDA approved biomarkers have reached the clinic [354, 355]. Importantly, the National Institute of Health (NIH) is developing a reference database for extracellular RNAs as biomarkers, to enable unbiased cross-platform comparison and to reduce inconsistencies associated to protocol differences [346].

In the present work, NGS analysis also allowed the characterization of the RNA content of the EVs from the studied tumour models. **Many non-coding RNA types were identified in the EVs' cargo and also in their donor cells.** In general, similar types of RNA were found in cells and EVs: pseudogenes, microRNAs, rRNA, tRNA, snRNA or novel transcripts. Studies from other authors also showed that EVs are rich in different types of RNAs [229, 231, 356]. Interestingly, in our results the most abundant RNA species were pseudogenes (approximately 40% of total RNA species, in both cells and EVs). Although the role of pseudogenes has been previously associated with cancer overall survival and also with cancer drug resistance [152, 153, 357-359], their mechanism of action needs to be further understood. Of note, the presence of pseudogenes in EVs cargo has not been previously highlighted and thoroughly studied. However, by carefully searching the Vesiclepedia (a database of EVs content, [360]), it was possible to verify that pseudogenes were previously found in EVs cargo, in different studies, although their presence was not discussed in the respective publications. Thus, further investigation of the function of pseudogenes in EVs is required.

The present study also demonstrates that the RNA content of EVs reflects the RNA content of their donor cells, however with a selective packaging of particular entities into EVs. Indeed, in both NSCLC and CML models, as expected all RNA species present in EVs were also present in the respective donor cells. Nevertheless, some species were present in cells but not in EVs, indicating a selective packaging of some RNA species into EVs. Other studies are in agreement with these results, showing that EVs contain a substantial proportion of the mRNA pool from their donor cells [356, 361]. Nevertheless, the sorting of RNAs into EVs is still a controversial issue. While some authors describe the selective packaging of RNA species into EVs, particularly of miRs [362], other authors suggest a non-selective sorting into EVs [363, 364]. An interesting recent study described different patterns of secretion for various small RNA families and their sorting into different

extracellular compartments [365]. Most probably both non-selective and selective secretion may occur. We hypothesized that the pathophysiological status, as well as the cell type, may influence the occurrence (possibly even an alternation) of these mechanisms.

In addition to EVs cargo analysis, **results presented in this thesis showed that MDR cells released more EVs than their drug-sensitive counterparts.** Indeed, the quantification of the number of particles was higher in EV´s isolated from MDR cells. Our findings revealed that these cells showed upregulation of some proteins of the Rab family: Rab5, Rab11 and Rab27. As previously described (chapter I- section 2), those proteins are known to be involved in the biogenesis of EVs, suggesting that the increased ability of MDR cells to produce and release EVs may involve the Rab family. Other proteins associated to EVs biogenesis were also studied, such as AP1/2 and Annexin II/V; however their expression was not altered between drug-sensitive and MDR conditions, indicating no involvement of those proteins in the biogenesis of EVs from the tumour cellular models studied in this work. In agreement with these results, the effect of pathological conditions in the secretion of EVs was previously described. For example, there is evidence that cancer cells release more EVs than normal cells [8], particularly after chemotherapy [9]. Moreover, the association of drug resistance with EVs release was also described by others authors. It was previously hypothesized that this observation (association of EVs release to drug resistance) may be related to the calcium signalling as well as to the presence of ABC transporters [366-369]. In the tumour MDR cellular models (from NSCLC and CML) studied in this thesis, since they overexpress P-gp, it is possible that P-gp may also be associated to the higher release of EVs by the MDR cells (in addition to the Rab family). Indeed, biophysically, the increased presence of P-gp (or other transmembrane proteins) creates a physical tension in the curvature of the cell surface, thus may promote increased EVs release.

The present work also showed that the drug-sensitive cells captured more EVs than their MDR counterparts. As described above (chapter I- section 2.4), several mechanisms are associated with EVs capture. Our findings revealed that the EVs from MDR cells which interact with recipient drug-sensitive cells are endocytosed. Endocytosis has, in fact, been described as the most frequent mechanism for EVs' uptake [308]. Moreover, our results suggest an increase in the presence of lipid rafts in drug-sensitive cells. Interestingly, flotillin, a component of the lipid rafts, was found increased in both NSCLC and leukaemia drug-sensitive cells. Of note, no alterations in dynamin (involved in some cases of flotillin-mediated endocytosis [307]) levels were observed. These findings suggest that in the studied tumour cell line models, the increased EVs' capture by drug-sensitive cells is associated to EVs endocytosis mediated by flotillin-associated lipid rafts, independent of

dynamin. Other studies also described specificity for EVs' uptake by recipient cells. Tetraspanin 8 positive-EVs shed by lymph node stromal cells were more internalized by endothelial and pancreatic cells than by parental cells [370], and EVs derived from rat pancreatic adenocarcinoma were more captured by peritoneal exudate cells and less by granulocytes [371].

Importantly, two relevant features should be taken into account when interpreting the results that indicate increased EVs released by MDR cells and increased EVs capture by drug-sensitive counterparts. Firstly, the EVs population studied in this thesis is heterogeneous since it is obtained by differential ultracentrifugation, a method that allows isolation of EVs with different sizes and origins. Secondly, as described in chapter I- section 2, various proteins such as ESCRT components, ARF protein family or tetraspanins, regulate the membrane budding processes involved in both release and capture of EVs. Therefore, to mechanistically distinguish these two processes (EVs capture and release) is a very challenging task. Based on these features, we argue that the major routes involved are: i) the upregulation of the Rab family for the increased EVs release by MDR cells, and ii) the endocytosis mediated by flotillin-associated lipid rafts for the increased EVs capture by drug-sensitive counterparts. However, we cannot exclude the association of other processes in other less abundant EVs subpopulations.

Moreover, regarding EVs capture, as previously described in chapter I- section 2.4, EVs may interact with the recipient cell by three main mechanisms: activation of receptors at the cell surface, membrane fusion or capture. In the present study we only investigated the more common route: capture by endocytosis. Nevertheless, we cannot exclude the possible involvement of other routes. Mathieu *et al.* defended in an elegant review that the capture route might be more dependent on the recipient cell type than on the EVs themselves [272]. Here, we argue that both donor and recipient cells influence the capture of EVs, since we also observed an increase in EVs' uptake when the donor cells were MDR (than when the donor cells were drug-sensitive cells). **Importantly, this study raises the possibility that increased EVs' uptake by drug-sensitive recipient cells, together with the previously mentioned increased EVs' release by MDR cells, may have an important impact on the dissemination of cancer MDR.**

The results presented in this thesis also showed differences in the endocytic pathway between drug-sensitive and MDR cells. More specifically, the fate of early endosomes cargo was found to be different for drug-sensitive or MDR cells. **In drug-sensitive cells, an increase in recycling and in lysosomal degradation was found. By contrast, in MDR cells the fate to secretion was increased,** explaining the previous

findings of higher numbers of EVs released by MDR cells. Interestingly, the different fate of the endocytic pathway (between drug-sensitive and MDR cells) seems to have an impact in drug response. Indeed, the impairment of the recycling pathway in drug-sensitive cells caused a decrease in their sensitivity to doxorubicin. Other studies are in agreement with our results, namely suggesting the involvement of the endocytic pathway in tumour resistance to cisplatin [372]. A very recent work focusing on the study of the influence of Rab7A in tumour cisplatin resistance, described that Rab7A regulates cisplatin resistance by determining alterations in late endocytic trafficking and subsequent drug-efflux through EVs [372]. In addition, Liang *et al.* reported that the endocytic recycling compartment (ERC) was altered in cisplatin resistant cells, influencing their response to drugs [373, 374]. We argue that, in our work**, the reduction of the recycling pathway in MDR cells may result in the decrease of drug carriers and transporters at the cell surface decreasing also the uptake of drugs**. In addition, the **different fate of the endocytic intracellular pathway may be responsible (or be a consequence), at least in part, for the observed differences in release and capture of EVs between MDR and drug-sensitive cells.**

Interestingly, in this work we also showed that alterations in intracellular pathways, namely in autophagy, were associated with the mechanism of action of a P-gp inhibitor. In a previous work from our group, a thioxanthone (TXA1) emerged as a hit compound since it: i) modulated the P-glycoprotein activity and ii) inhibited the cell growth of several human tumour cell lines, including a CML and a NSCLC cell line [375, 376]. However, the mechanism of action of this hit molecule had not been fully understood. Here, we showed that **this P-gp inhibitor (TXA1), when used at the GI_{50} concentration, caused a clear accumulation of autophagic structures. Moreover, we proved that this was associated with an increase in the autophagic flux (and not with an autophagy block).** Interestingly, cellular treatment with this concentration (GI_{50}) did not induce apoptosis or affects the cell cycle profile. It would be interesting to extend this mechanistic study to the MDR cells used in the present thesis. Meanwhile, other study by our group has shown that this molecule also affects tumour cellular growth *in vivo* as well as alter the expression of proteins involved in steroid trafficking and affects the cholesterol trafficking [377].

The role of autophagy in MDR requires clarification. As Li *et al.* reviewed recently, autophagy can be a double-edged sword for MDR tumours: it participates in the development of MDR, protecting cancer cells from chemotherapeutics, but can also induce cell death of MDR cells [54]. In our study, as MDR cells from both tumour cell models tested showed an increase in EVs secretion, it is possible that TXA1 may act in MDR cells at three different levels: i) by inducing cell death via autophagy, ii) by inhibiting P-gp activity, iii) by

decreasing EVs' release which indirectly may affect dissemination of MDR traits to neighbouring tumour cells. Given the balance between secretion and degradation (by lysosomes or autofagosomes) of the endocytic cargo previously described in chapter I section 3, in future work it would be relevant to evaluate whether autophagy induction by TXA1 may cause a decrease in EVs secretion by MDR cells.

In conclusion, the work presented in this thesis allowed to gain new insights into P-gp associated tumour MDR. A number of transcripts with potential as putative MDR biomarkers were found, particularly in the cargo of EVs released by MDR cells. Furthermore, EVs were shown to be relevant for MDR dissemination. Importantly, alterations in the endocytic pathway between drug-sensitive and MDR (P-gp-overexpressing) cells were found. In addition, they may have an impact in the drug-resistant phenotype and in the mechanisms associated with the production and capture of EVs. Interestingly, the mechanism of action of a small molecule previously described to have dual activity (as anti-tumour and P-gp inhibitor), was associated with autophagy. Future work will focus on assessing the relevance of these observations to the clinical setting.

REFERENCES

[1] J. Rueff, A.S. Rodrigues, Cancer Drug Resistance: A Brief Overview from a Genetic Viewpoint, Methods Mol Biol, 1395 (2016) 1-18.
[2] C. Holohan, S. Van Schaeybroeck, D.B. Longley, P.G. Johnston, Cancer drug resistance: an evolving paradigm, Nat Rev Cancer, 13 (2013) 714-726.
[3] M.M. Gottesman, O. Lavi, M.D. Hall, J.P. Gillet, Toward a Better Understanding of the Complexity of Cancer Drug Resistance, Annu Rev Pharmacol Toxicol, 56 (2016) 85-102.
[4] J.L. Biedler, H. Riehm, Cellular resistance to actinomycin D in Chinese hamster cells in vitro: cross-resistance, radioautographic, and cytogenetic studies, Cancer Res, 30 (1970) 1174-1184.
[5] D.J. Konieczkowski, C.M. Johannessen, L.A. Garraway, A Convergence-Based Framework for Cancer Drug Resistance, Cancer Cell, 33 (2018) 801-815.
[6] H. Lage, An overview of cancer multidrug resistance: a still unsolved problem, Cell Mol Life Sci, 65 (2008) 3145-3167.
[7] G. Gundem, P. Van Loo, B. Kremeyer, L.B. Alexandrov, J.M.C. Tubio, E. Papaemmanuil, D.S. Brewer, H.M.L. Kallio, G. Hognas, M. Annala, K. Kivinummi, V. Goody, C. Latimer, S. O'Meara, K.J. Dawson, W. Isaacs, M.R. Emmert-Buck, M. Nykter, C. Foster, Z. Kote-Jarai, D. Easton, H.C. Whitaker, I.P. Group, D.E. Neal, C.S. Cooper, R.A. Eeles, T. Visakorpi, P.J. Campbell, U. McDermott, D.C. Wedge, G.S. Bova, The evolutionary history of lethal metastatic prostate cancer, Nature, 520 (2015) 353-357.
[8] D. Juric, P. Castel, M. Griffith, O.L. Griffith, H.H. Won, H. Ellis, S.H. Ebbesen, B.J. Ainscough, A. Ramu, G. Iyer, R.H. Shah, T. Huynh, M. Mino-Kenudson, D. Sgroi, S. Isakoff, A. Thabet, L. Elamine, D.B. Solit, S.W. Lowe, C. Quadt, M. Peters, A. Derti, R. Schegel, A. Huang, E.R. Mardis, M.F. Berger, J. Baselga, M. Scaltriti, Convergent loss of PTEN leads to clinical resistance to a PI(3)Kalpha inhibitor, Nature, 518 (2015) 240-244.
[9] Y.G. Assaraf, Molecular basis of antifolate resistance, Cancer Metastasis Rev, 26 (2007) 153-181.
[10] S.E. Crider, R.J. Holbrook, K.J. Franz, Coordination of platinum therapeutic agents to met-rich motifs of human copper transport protein1, Metallomics, 2 (2010) 74-83.
[11] E.S. Kim, X. Tang, D.R. Peterson, D. Kilari, C.W. Chow, J. Fujimoto, N. Kalhor, S.G. Swisher, D.J. Stewart, Wistuba, II, Z.H. Siddik, Copper transporter CTR1 expression and tissue platinum concentration in non-small cell lung cancer, Lung Cancer, 85 (2014) 88-93.
[12] Z.D. Liang, Y. Long, W.B. Tsai, S. Fu, R. Kurzrock, M. Gagea-Iurascu, F. Zhang, H.H. Chen, B.T. Hennessy, G.B. Mills, N. Savaraj, M.T. Kuo, Mechanistic basis for overcoming platinum resistance using copper chelating agents, Mol Cancer Ther, 11 (2012) 2483-2494.
[13] J.J. Farrell, H. Elsaleh, M. Garcia, R. Lai, A. Ammar, W.F. Regine, R. Abrams, A.B. Benson, J. Macdonald, C.E. Cass, A.P. Dicker, J.R. Mackey, Human equilibrative nucleoside transporter 1 levels predict response to gemcitabine in patients with pancreatic cancer, Gastroenterology, 136 (2009) 187-195.
[14] M.M. Gottesman, T. Fojo, S.E. Bates, Multidrug resistance in cancer: role of ATP-dependent transporters, Nat Rev Cancer, 2 (2002) 48-58.
[15] K. Nooter, G. Brutel de la Riviere, M.P. Look, K.E. van Wingerden, S.C. Henzen-Logmans, R.J. Scheper, M.J. Flens, J.G. Klijn, G. Stoter, J.A. Foekens, The prognostic significance of expression of the multidrug resistance-associated protein (MRP) in primary breast cancer, Br J Cancer, 76 (1997) 486-493.
[16] R.W. Robey, S. Shukla, K. Steadman, T. Obrzut, E.M. Finley, S.V. Ambudkar, S.E. Bates, Inhibition of ABCG2-mediated transport by protein kinase inhibitors with a bisindolylmaleimide or indolocarbazole structure, Mol Cancer Ther, 6 (2007) 1877-1885.
[17] H. Thomas, H.M. Coley, Overcoming multidrug resistance in cancer: an update on the clinical strategy of inhibiting p-glycoprotein, Cancer Control, 10 (2003) 159-165.
[18] H. Liu, Y. Liao, M. Tang, T. Wu, D. Tan, S. Zhang, H. Wang, Trps1 is associated with the multidrug resistance of lung cancer cell by regulating MGMT gene expression, Cancer Med, 7 (2018) 1921-1932.

[19] S.L. Edwards, R. Brough, C.J. Lord, R. Natrajan, R. Vatcheva, D.A. Levine, J. Boyd, J.S. Reis-Filho, A. Ashworth, Resistance to therapy caused by intragenic deletion in BRCA2, Nature, 451 (2008) 1111-1115.
[20] C. Sun, N. Li, Z. Yang, B. Zhou, Y. He, D. Weng, Y. Fang, P. Wu, P. Chen, X. Yang, D. Ma, J. Zhou, G. Chen, miR-9 regulation of BRCA1 and ovarian cancer sensitivity to cisplatin and PARP inhibition, J Natl Cancer Inst, 105 (2013) 1750-1758.
[21] M. Eich, W.P. Roos, T. Nikolova, B. Kaina, Contribution of ATM and ATR to the resistance of glioblastoma and malignant melanoma cells to the methylating anticancer drug temozolomide, Mol Cancer Ther, 12 (2013) 2529-2540.
[22] J.A. Bush, G. Li, Cancer chemoresistance: the relationship between p53 and multidrug transporters, Int J Cancer, 98 (2002) 323-330.
[23] T. Chong, A. Sarac, C.Q. Yao, L. Liao, N. Lyttle, P.C. Boutros, J.M.S. Bartlett, M. Spears, Deregulation of the spindle assembly checkpoint is associated with paclitaxel resistance in ovarian cancer, J Ovarian Res, 11 (2018) 27.
[24] A. Bonetti, M. Zaninelli, R. Leone, G.L. Cetto, G. Pelosi, S. Biolo, A. Menghi, E. Manfrin, F. Bonetti, Q. Piubello, bcl-2 but not p53 expression is associated with resistance to chemotherapy in advanced breast cancer, Clin Cancer Res, 4 (1998) 2331-2336.
[25] M. Notarbartolo, M. Cervello, P. Poma, L. Dusonchet, M. Meli, N. D'Alessandro, Expression of the IAPs in multidrug resistant tumor cells, Oncol Rep, 11 (2004) 133-136.
[26] J. Ge, Z. Chen, J. Huang, J. Chen, W. Yuan, Z. Deng, Z. Chen, Upregulation of autophagy-related gene-5 (ATG-5) is associated with chemoresistance in human gastric cancer, PLoS One, 9 (2014) e110293.
[27] Y. Wang, D. Zhang, K. Wu, Q. Zhao, Y. Nie, D. Fan, Long noncoding RNA MRUL promotes ABCB1 expression in multidrug-resistant gastric cancer cell sublines, Mol Cell Biol, 34 (2014) 3182-3193.
[28] P. Jiang, P. Wang, X. Sun, Z. Yuan, R. Zhan, X. Ma, W. Li, Knockdown of long noncoding RNA H19 sensitizes human glioma cells to temozolomide therapy, Onco Targets Ther, 9 (2016) 3501-3509.
[29] M. Manikandan, A.K. Deva Magendhra Rao, K.S. Rajkumar, R. Rajaraman, A.K. Munirajan, Altered levels of miR-21, miR-125b-2*, miR-138, miR-155, miR-184, and miR-205 in oral squamous cell carcinoma and association with clinicopathological characteristics, J Oral Pathol Med, 44 (2015) 792-800.
[30] H. Zhu, H. Wu, X. Liu, B.R. Evans, D.J. Medina, C.G. Liu, J.M. Yang, Role of MicroRNA miR-27a and miR-451 in the regulation of MDR1/P-glycoprotein expression in human cancer cells, Biochem Pharmacol, 76 (2008) 582-588.
[31] L. Bao, S. Hazari, S. Mehra, D. Kaushal, K. Moroz, S. Dash, Increased expression of P-glycoprotein and doxorubicin chemoresistance of metastatic breast cancer is regulated by miR-298, Am J Pathol, 180 (2012) 2490-2503.
[32] P.D. Dobson, D.B. Kell, Carrier-mediated cellular uptake of pharmaceutical drugs: an exception or the rule?, Nat Rev Drug Discov, 7 (2008) 205-220.
[33] W. Wattanawongdon, C. Hahnvajanawong, N. Namwat, S. Kanchanawat, T. Boonmars, P. Jearanaikoon, C. Leelayuwat, A. Techasen, W. Seubwai, Establishment and characterization of gemcitabine-resistant human cholangiocarcinoma cell lines with multidrug resistance and enhanced invasiveness, Int J Oncol, 47 (2015) 398-410.
[34] S. Fu, A. Naing, C. Fu, M.T. Kuo, R. Kurzrock, Overcoming platinum resistance through the use of a copper-lowering agent, Mol Cancer Ther, 11 (2012) 1221-1225.
[35] I.A. Cree, P. Charlton, Molecular chess? Hallmarks of anti-cancer drug resistance, BMC Cancer, 17 (2017) 10.
[36] U.A. Germann, I. Pastan, M.M. Gottesman, P-glycoproteins: mediators of multidrug resistance, Semin Cell Biol, 4 (1993) 63-76.

[37] H. Farmer, N. McCabe, C.J. Lord, A.N. Tutt, D.A. Johnson, T.B. Richardson, M. Santarosa, K.J. Dillon, I. Hickson, C. Knights, N.M. Martin, S.P. Jackson, G.C. Smith, A. Ashworth, Targeting the DNA repair defect in BRCA mutant cells as a therapeutic strategy, Nature, 434 (2005) 917-921.
[38] W. Sakai, E.M. Swisher, B.Y. Karlan, M.K. Agarwal, J. Higgins, C. Friedman, E. Villegas, C. Jacquemont, D.J. Farrugia, F.J. Couch, N. Urban, T. Taniguchi, Secondary mutations as a mechanism of cisplatin resistance in BRCA2-mutated cancers, Nature, 451 (2008) 1116-1120.
[39] R. Visconti, R. Della Monica, D. Grieco, Cell cycle checkpoint in cancer: a therapeutically targetable double-edged sword, J Exp Clin Cancer Res, 35 (2016) 153.
[40] S. Fan, W.S. el-Deiry, I. Bae, J. Freeman, D. Jondle, K. Bhatia, A.J. Fornace, Jr., I. Magrath, K.W. Kohn, P.M. O'Connor, p53 gene mutations are associated with decreased sensitivity of human lymphoma cells to DNA damaging agents, Cancer Res, 54 (1994) 5824-5830.
[41] S. Ye, J. Shen, E. Choy, C. Yang, H. Mankin, F. Hornicek, Z. Duan, p53 overexpression increases chemosensitivity in multidrug-resistant osteosarcoma cell lines, Cancer Chemother Pharmacol, 77 (2016) 349-356.
[42] S.B. Horwitz, D. Cohen, S. Rao, I. Ringel, H.J. Shen, C.P. Yang, Taxol: mechanisms of action and resistance, J Natl Cancer Inst Monogr, (1993) 55-61.
[43] C.H. Topham, S.S. Taylor, Mitosis and apoptosis: how is the balance set?, Curr Opin Cell Biol, 25 (2013) 780-785.
[44] C. Cande, N. Vahsen, C. Garrido, G. Kroemer, Apoptosis-inducing factor (AIF): caspase-independent after all, Cell Death Differ, 11 (2004) 591-595.
[45] T.A. Buchholz, D.W. Davis, D.J. McConkey, W.F. Symmans, V. Valero, A. Jhingran, S.L. Tucker, L. Pusztai, M. Cristofanilli, F.J. Esteva, G.N. Hortobagyi, A.A. Sahin, Chemotherapy-induced apoptosis and Bcl-2 levels correlate with breast cancer response to chemotherapy, Cancer J, 9 (2003) 33-41.
[46] L.M. Krug, V.A. Miller, D.A. Filippa, E. Venkatraman, K.K. Ng, M.G. Kris, Bcl-2 and bax expression in advanced non-small cell lung cancer: lack of correlation with chemotherapy response or survival in patients treated with docetaxel plus vinorelbine, Lung Cancer, 39 (2003) 139-143.
[47] R.W. Johnstone, E. Cretney, M.J. Smyth, P-glycoprotein protects leukemia cells against caspase-dependent, but not caspase-independent, cell death, Blood, 93 (1999) 1075-1085.
[48] D.A. Evseenko, P. Murthi, J.W. Paxton, G. Reid, B.S. Emerald, K.M. Mohankumar, P.E. Lobie, S.P. Brennecke, B. Kalionis, J.A. Keelan, The ABC transporter BCRP/ABCG2 is a placental survival factor, and its expression is reduced in idiopathic human fetal growth restriction, FASEB J, 21 (2007) 3592-3605.
[49] D.J. de Groot, M. van der Deen, T.K. Le, A. Regeling, S. de Jong, E.G. de Vries, Indomethacin induces apoptosis via a MRP1-dependent mechanism in doxorubicin-resistant small-cell lung cancer cells overexpressing MRP1, Br J Cancer, 97 (2007) 1077-1083.
[50] X. Yang, D.D. Yu, F. Yan, Y.Y. Jing, Z.P. Han, K. Sun, L. Liang, J. Hou, L.X. Wei, The role of autophagy induced by tumor microenvironment in different cells and stages of cancer, Cell Biosci, 5 (2015) 14.
[51] Z.J. Yang, C.E. Chee, S. Huang, F.A. Sinicrope, The role of autophagy in cancer: therapeutic implications, Mol Cancer Ther, 10 (2011) 1533-1541.
[52] A. du Toit, J.S. Hofmeyr, T.J. Gniadek, B. Loos, Measuring autophagosome flux, Autophagy, 14 (2018) 1060-1071.
[53] M.T. Rosenfeldt, K.M. Ryan, The multiple roles of autophagy in cancer, Carcinogenesis, 32 (2011) 955-963.
[54] Y.J. Li, Y.H. Lei, N. Yao, C.R. Wang, N. Hu, W.C. Ye, D.M. Zhang, Z.S. Chen, Autophagy and multidrug resistance in cancer, Chin J Cancer, 36 (2017) 52.
[55] J. Thorburn, L. Staskiewicz, M.L. Goodall, L. Dimberg, A.E. Frankel, H.L. Ford, A. Thorburn, Non-cell-autonomous Effects of Autophagy Inhibition in Tumor Cells Promote Growth of Drug-resistant Cells, Mol Pharmacol, 91 (2017) 58-64.

[56] L.H. Zhang, A.J. Yang, M. Wang, W. Liu, C.Y. Wang, X.F. Xie, X. Chen, J.F. Dong, M. Li, Enhanced autophagy reveals vulnerability of P-gp mediated epirubicin resistance in triple negative breast cancer cells, Apoptosis, 21 (2016) 473-488.
[57] C.W. Yao, K.A. Kang, M.J. Piao, Y.S. Ryu, P. Fernando, M.C. Oh, J.E. Park, K. Shilnikova, S.Y. Na, S.U. Jeong, S.J. Boo, J.W. Hyun, Reduced Autophagy in 5-Fluorouracil Resistant Colon Cancer Cells, Biomol Ther (Seoul), 25 (2017) 315-320.
[58] W. Xu, Q. Shi, X. Qian, B. Zhou, J. Xu, L. Zhu, L. Feng, H. Jin, X. Wang, Rab5a suppresses autophagy to promote drug resistance in cancer cells, Am J Transl Res, 10 (2018) 1229-1236.
[59] Y.J. Lee, A.J. Won, J. Lee, J.H. Jung, S. Yoon, B.M. Lee, H.S. Kim, Molecular mechanism of SAHA on regulation of autophagic cell death in tamoxifen-resistant MCF-7 breast cancer cells, Int J Med Sci, 9 (2012) 881-893.
[60] T. Hu, L. Wang, L. Zhang, L. Lu, J. Shen, R.L. Chan, M. Li, W.K. Wu, K.K. To, C.H. Cho, Sensitivity of apoptosis-resistant colon cancer cells to tanshinones is mediated by autophagic cell death and p53-independent cytotoxicity, Phytomedicine, 22 (2015) 536-544.
[61] C. Xue, C. Wang, Q. Liu, Q. Meng, H. Sun, X. Huo, X. Ma, Z. Liu, X. Ma, J. Peng, K. Liu, Targeting P-glycoprotein expression and cancer cell energy metabolism: combination of metformin and 2-deoxyglucose reverses the multidrug resistance of K562/Dox cells to doxorubicin, Tumour Biol, 37 (2016) 8587-8597.
[62] G.M. Ajabnoor, T. Crook, H.M. Coley, Paclitaxel resistance is associated with switch from apoptotic to autophagic cell death in MCF-7 breast cancer cells, Cell Death Dis, 3 (2012) e260.
[63] M.A. Qadir, B. Kwok, W.H. Dragowska, K.H. To, D. Le, M.B. Bally, S.M. Gorski, Macroautophagy inhibition sensitizes tamoxifen-resistant breast cancer cells and enhances mitochondrial depolarization, Breast Cancer Res Treat, 112 (2008) 389-403.
[64] W.L. Sun, J. Chen, Y.P. Wang, H. Zheng, Autophagy protects breast cancer cells from epirubicin-induced apoptosis and facilitates epirubicin-resistance development, Autophagy, 7 (2011) 1035-1044.
[65] A. Vazquez-Martin, C. Oliveras-Ferraros, J.A. Menendez, Autophagy facilitates the development of breast cancer resistance to the anti-HER2 monoclonal antibody trastuzumab, PLoS One, 4 (2009) e6251.
[66] P.M. Filipa S. Reis, Isabel C.F.R. Ferreira, M. Helena Vasconcelos, Mushrooms as a Source of Compounds that Induce Programmed Cell Death in Tumour Cells, Recent Progress in Medicinal Plants, 43 (2016).
[67] N.A. Bhowmick, E.G. Neilson, H.L. Moses, Stromal fibroblasts in cancer initiation and progression, Nature, 432 (2004) 332-337.
[68] S.L. Shiao, A.P. Ganesan, H.S. Rugo, L.M. Coussens, Immune microenvironments in solid tumors: new targets for therapy, Genes Dev, 25 (2011) 2559-2572.
[69] F. Caligaris-Cappio, L. Bergui, M.G. Gregoretti, G. Gaidano, M. Gaboli, M. Schena, A.Z. Zallone, P.C. Marchisio, 'Role of bone marrow stromal cells in the growth of human multiple myeloma, Blood, 77 (1991) 2688-2693.
[70] R. Bhatia, P.B. McGlave, G.W. Dewald, B.R. Blazar, C.M. Verfaillie, Abnormal function of the bone marrow microenvironment in chronic myelogenous leukemia: role of malignant stromal macrophages, Blood, 85 (1995) 3636-3645.
[71] G. Housman, S. Byler, S. Heerboth, K. Lapinska, M. Longacre, N. Snyder, S. Sarkar, Drug resistance in cancer: an overview, Cancers (Basel), 6 (2014) 1769-1792.
[72] M. Michael, M.M. Doherty, Tumoral drug metabolism: overview and its implications for cancer therapy, J Clin Oncol, 23 (2005) 205-229.
[73] W. Hassen, A. Kassambara, T. Reme, S. Sahota, A. Seckinger, L. Vincent, G. Cartron, J. Moreaux, D. Hose, B. Klein, Drug metabolism and clearance system in tumor cells of patients with multiple myeloma, Oncotarget, 6 (2015) 6431-6447.
[74] L.A. Byers, L. Diao, J. Wang, P. Saintigny, L. Girard, M. Peyton, L. Shen, Y. Fan, U. Giri, P.K. Tumula, M.B. Nilsson, J. Gudikote, H. Tran, R.J. Cardnell, D.J. Bearss, S.L. Warner, J.M. Foulks, S.B.

Kanner, V. Gandhi, N. Krett, S.T. Rosen, E.S. Kim, R.S. Herbst, G.R. Blumenschein, J.J. Lee, S.M. Lippman, K.K. Ang, G.B. Mills, W.K. Hong, J.N. Weinstein, Wistuba, II, K.R. Coombes, J.D. Minna, J.V. Heymach, An epithelial-mesenchymal transition gene signature predicts resistance to EGFR and PI3K inhibitors and identifies Axl as a therapeutic target for overcoming EGFR inhibitor resistance, Clin Cancer Res, 19 (2013) 279-290.
[75] S. Fiala, The cancer cell as a stem cell unable to differentiate. A theory of carcinogenesis, Neoplasma, 15 (1968) 607-622.
[76] C. Hirschmann-Jax, A.E. Foster, G.G. Wulf, J.G. Nuchtern, T.W. Jax, U. Gobel, M.A. Goodell, M.K. Brenner, A distinct "side population" of cells with high drug efflux capacity in human tumor cells, Proc Natl Acad Sci U S A, 101 (2004) 14228-14233.
[77] R.L. Juliano, V. Ling, A surface glycoprotein modulating drug permeability in Chinese hamster ovary cell mutants, Biochim Biophys Acta, 455 (1976) 152-162.
[78] S.V. Ambudkar, S. Dey, C.A. Hrycyna, M. Ramachandra, I. Pastan, M.M. Gottesman, Biochemical, cellular, and pharmacological aspects of the multidrug transporter, Annu Rev Pharmacol Toxicol, 39 (1999) 361-398.
[79] M. Tucci, C. Quatraro, F. Dammacco, F. Silvestris, Role of active drug transporters in refractory multiple myeloma, Curr Top Med Chem, 9 (2009) 218-224.
[80] W.S. Dalton, Mechanisms of drug resistance in hematologic malignancies, Semin Hematol, 34 (1997) 3-8.
[81] L.M. Pilarski, M.J. Mant, A.R. Belch, Drug resistance in multiple myeloma: novel therapeutic targets within the malignant clone, Leuk Lymphoma, 32 (1999) 199-210.
[82] N.A. de Vries, T. Buckle, J. Zhao, J.H. Beijnen, J.H. Schellens, O. van Tellingen, Restricted brain penetration of the tyrosine kinase inhibitor erlotinib due to the drug transporters P-gp and BCRP, Invest New Drugs, 30 (2012) 443-449.
[83] B.J. Trock, F. Leonessa, R. Clarke, Multidrug resistance in breast cancer: a meta-analysis of MDR1/gp170 expression and its possible functional significance, J Natl Cancer Inst, 89 (1997) 917-931.
[84] P. Sonneveld, Multidrug resistance in haematological malignancies, J Intern Med, 247 (2000) 521-534.
[85] D.J. Stewart, Tumor and host factors that may limit efficacy of chemotherapy in non-small cell and small cell lung cancer, Crit Rev Oncol Hematol, 75 (2010) 173-234.
[86] P.S. Souza, J.P. Madigan, J.P. Gillet, K. Kapoor, S.V. Ambudkar, R.C. Maia, M.M. Gottesman, K.L. Fung, Expression of the multidrug transporter P-glycoprotein is inversely related to that of apoptosis-associated endogenous TRAIL, Exp Cell Res, 336 (2015) 318-328.
[87] Correction: Ubiquitous Release of Exosomal Tumor Suppressor miR-6126 from Ovarian Cancer Cells, Cancer Res, 78 (2018) 3402.
[88] D.F. Callen, E. Baker, R.N. Simmers, R. Seshadri, I.B. Roninson, Localization of the human multiple drug resistance gene, MDR1, to 7q21.1, Hum Genet, 77 (1987) 142-144.
[89] J.E. Chin, R. Soffir, K.E. Noonan, K. Choi, I.B. Roninson, Structure and expression of the human MDR (P-glycoprotein) gene family, Mol Cell Biol, 9 (1989) 3808-3820.
[90] M. Hennessy, J.P. Spiers, A primer on the mechanics of P-glycoprotein the multidrug transporter, Pharmacol Res, 55 (2007) 1-15.
[91] H. Min, M. Niu, W. Zhang, J. Yan, J. Li, X. Tan, B. Li, M. Su, B. Di, F. Yan, Emodin reverses leukemia multidrug resistance by competitive inhibition and downregulation of P-glycoprotein, PLoS One, 12 (2017) e0187971.
[92] K. Condic-Jurkic, N. Subramanian, A.E. Mark, M.L. O'Mara, The reliability of molecular dynamics simulations of the multidrug transporter P-glycoprotein in a membrane environment, PLoS One, 13 (2018) e0191882.
[93] B.C. Baguley, Classical and Targeted Anticancer Drugs: An Appraisal of Mechanisms of Multidrug Resistance, Methods Mol Biol, 1395 (2016) 19-37.

[94] J.A. Endicott, V. Ling, The biochemistry of P-glycoprotein-mediated multidrug resistance, Annu Rev Biochem, 58 (1989) 137-171.
[95] A. Molinari, A. Calcabrini, S. Meschini, A. Stringaro, P. Crateri, L. Toccacieli, M. Marra, M. Colone, M. Cianfriglia, G. Arancia, Subcellular detection and localization of the drug transporter P-glycoprotein in cultured tumor cells, Curr Protein Pept Sci, 3 (2002) 653-670.
[96] T. Yamagishi, S. Sahni, D.M. Sharp, A. Arvind, P.J. Jansson, D.R. Richardson, P-glycoprotein mediates drug resistance via a novel mechanism involving lysosomal sequestration, J Biol Chem, 288 (2013) 31761-31771.
[97] E. Srinivas, J.N. Murthy, A.R. Rao, G.N. Sastry, Recent advances in molecular modeling and medicinal chemistry aspects of phospho-glycoprotein, Curr Drug Metab, 7 (2006) 205-217.
[98] V. Lopes-Rodrigues, H. Seca, D. Sousa, E. Sousa, R.T. Lima, M.H. Vasconcelos, The network of P-glycoprotein and microRNAs interactions, Int J Cancer, 135 (2014) 253-263.
[99] Y. Ma, L. Liu, F. Yan, W. Wei, J. Deng, J. Sun, Enhanced expression of long non-coding RNA NEAT1 is associated with the progression of gastric adenocarcinomas, World J Surg Oncol, 14 (2016) 41.
[100] K.N. Kazuhiro Katayama, and Yoshikazu Sugimoto, Regulations of P-Glycoprotein/ABCB1/MDR1 in Human Cancer Cells, New Journal of Science, (2014).
[101] M. Liscovitch, Y. Lavie, Cancer multidrug resistance: a review of recent drug discovery research, IDrugs, 5 (2002) 349-355.
[102] H. Seca, R.T. Lima, J.E. Guimaraes, M. Helena Vasconcelos, Simultaneous targeting of P-gp and XIAP with siRNAs increases sensitivity of P-gp overexpressing CML cells to imatinib, Hematology, 16 (2011) 100-108.
[103] H. Xu, F.Z. Hong, S. Li, P. Zhang, L. Zhu, Short hairpin RNA-mediated MDR1 gene silencing increases apoptosis of human ovarian cancer cell line A2780/Taxol, Chin J Cancer Res, 24 (2012) 138-142.
[104] Z. Xia, L. Zhang, Q. Chen, C. Royal, Z. Yu, Z. Liu, B.L. Adam, Stable reversal of multidrug resistance in colon cancer cells by RNA interference targeting the MDR1 gene, Mol Med Rep, 2 (2009) 579-584.
[105] M.M. Gottesman, I. Pastan, Biochemistry of multidrug resistance mediated by the multidrug transporter, Annu Rev Biochem, 62 (1993) 385-427.
[106] M.M. Gottesman, I.H. Pastan, The Role of Multidrug Resistance Efflux Pumps in Cancer: Revisiting a JNCI Publication Exploring Expression of the MDR1 (P-glycoprotein) Gene, J Natl Cancer Inst, 107 (2015).
[107] R.C. Lee, R.L. Feinbaum, V. Ambros, The C. elegans heterochronic gene lin-4 encodes small RNAs with antisense complementarity to lin-14, Cell, 75 (1993) 843-854.
[108] B. Wightman, I. Ha, G. Ruvkun, Posttranscriptional regulation of the heterochronic gene lin-14 by lin-4 mediates temporal pattern formation in C. elegans, Cell, 75 (1993) 855-862.
[109] A. Kozomara, S. Griffiths-Jones, miRBase: integrating microRNA annotation and deep-sequencing data, Nucleic Acids Res, 39 (2011) D152-157.
[110] Y. Tay, J. Zhang, A.M. Thomson, B. Lim, I. Rigoutsos, MicroRNAs to Nanog, Oct4 and Sox2 coding regions modulate embryonic stem cell differentiation, Nature, 455 (2008) 1124-1128.
[111] A. Brummer, J. Hausser, MicroRNA binding sites in the coding region of mRNAs: extending the repertoire of post-transcriptional gene regulation, Bioessays, 36 (2014) 617-626.
[112] J. Shu, Z. Xia, L. Li, E.T. Liang, N. Slipek, D. Shen, J. Foo, S. Subramanian, C.J. Steer, Dose-dependent differential mRNA target selection and regulation by let-7a-7f and miR-17-92 cluster microRNAs, RNA Biol, 9 (2012) 1275-1287.
[113] D. de Rie, I. Abugessaisa, T. Alam, E. Arner, P. Arner, H. Ashoor, G. Astrom, M. Babina, N. Bertin, A.M. Burroughs, A.J. Carlisle, C.O. Daub, M. Detmar, R. Deviatiiarov, A. Fort, C. Gebhard, D. Goldowitz, S. Guhl, T.J. Ha, J. Harshbarger, A. Hasegawa, K. Hashimoto, M. Herlyn, P. Heutink, K.J. Hitchens, C.C. Hon, E. Huang, Y. Ishizu, C. Kai, T. Kasukawa, P. Klinken, T. Lassmann, C.H. Lecellier, W. Lee, M. Lizio, V. Makeev, A. Mathelier, Y.A. Medvedeva, N. Mejhert, C.J. Mungall, S. Noma, M.

Ohshima, M. Okada-Hatakeyama, H. Persson, P. Rizzu, F. Roudnicky, P. Saetrom, H. Sato, J. Severin, J.W. Shin, R.K. Swoboda, H. Tarui, H. Toyoda, K. Vitting-Seerup, L. Winteringham, Y. Yamaguchi, K. Yasuzawa, M. Yoneda, N. Yumoto, S. Zabierowski, P.G. Zhang, C.A. Wells, K.M. Summers, H. Kawaji, A. Sandelin, M. Rehli, F. Consortium, Y. Hayashizaki, P. Carninci, A.R.R. Forrest, M.J.L. de Hoon, An integrated expression atlas of miRNAs and their promoters in human and mouse, Nat Biotechnol, 35 (2017) 872-878.
[114] Y.K. Kim, V.N. Kim, Processing of intronic microRNAs, EMBO J, 26 (2007) 775-783.
[115] A. Tanzer, P.F. Stadler, Molecular evolution of a microRNA cluster, J Mol Biol, 339 (2004) 327-335.
[116] S.S. Truesdell, R.D. Mortensen, M. Seo, J.C. Schroeder, J.H. Lee, O. LeTonqueze, S. Vasudevan, MicroRNA-mediated mRNA translation activation in quiescent cells and oocytes involves recruitment of a nuclear microRNP, Sci Rep, 2 (2012) 842.
[117] S.I.A. Bukhari, S.S. Truesdell, S. Lee, S. Kollu, A. Classon, M. Boukhali, E. Jain, R.D. Mortensen, A. Yanagiya, R.I. Sadreyev, W. Haas, S. Vasudevan, A Specialized Mechanism of Translation Mediated by FXR1a-Associated MicroRNP in Cellular Quiescence, Mol Cell, 61 (2016) 760-773.
[118] U.A. Orom, F.C. Nielsen, A.H. Lund, MicroRNA-10a binds the 5'UTR of ribosomal protein mRNAs and enhances their translation, Mol Cell, 30 (2008) 460-471.
[119] R.T. Lima, S. Busacca, G.M. Almeida, G. Gaudino, D.A. Fennell, M.H. Vasconcelos, MicroRNA regulation of core apoptosis pathways in cancer, Eur J Cancer, 47 (2011) 163-174.
[120] S. Anfossi, X. Fu, R. Nagvekar, G.A. Calin, MicroRNAs, Regulatory Messengers Inside and Outside Cancer Cells, Adv Exp Med Biol, 1056 (2018) 87-108.
[121] T. Fojo, Multiple paths to a drug resistance phenotype: mutations, translocations, deletions and amplification of coding genes or promoter regions, epigenetic changes and microRNAs, Drug Resist Updat, 10 (2007) 59-67.
[122] Y. Shang, Z. Zhang, Z. Liu, B. Feng, G. Ren, K. Li, L. Zhou, Y. Sun, M. Li, J. Zhou, Y. An, K. Wu, Y. Nie, D. Fan, miR-508-5p regulates multidrug resistance of gastric cancer by targeting ABCB1 and ZNRD1, Oncogene, 33 (2014) 3267-3276.
[123] Y. Shang, B. Feng, L. Zhou, G. Ren, Z. Zhang, X. Fan, Y. Sun, G. Luo, J. Liang, K. Wu, Y. Nie, D. Fan, The miR27b-CCNG1-P53-miR-508-5p axis regulates multidrug resistance of gastric cancer, Oncotarget, 7 (2016) 538-549.
[124] X. An, C. Sarmiento, T. Tan, H. Zhu, Regulation of multidrug resistance by microRNAs in anti-cancer therapy, Acta Pharm Sin B, 7 (2017) 38-51.
[125] L.A. Doyle, W. Yang, A.K. Rishi, Y. Gao, D.D. Ross, H19 gene overexpression in atypical multidrug-resistant cells associated with expression of a 95-kilodalton membrane glycoprotein, Cancer Res, 56 (1996) 2904-2907.
[126] W.P. Tsang, T.T. Kwok, Riboregulator H19 induction of MDR1-associated drug resistance in human hepatocellular carcinoma cells, Oncogene, 26 (2007) 4877-4881.
[127] K. Takahashi, I.K. Yan, T. Kogure, H. Haga, T. Patel, Extracellular vesicle-mediated transfer of long non-coding RNA ROR modulates chemosensitivity in human hepatocellular cancer, FEBS Open Bio, 4 (2014) 458-467.
[128] Z. Liu, M. Sun, K. Lu, J. Liu, M. Zhang, W. Wu, W. De, Z. Wang, R. Wang, The long noncoding RNA HOTAIR contributes to cisplatin resistance of human lung adenocarcinoma cells via downregualtion of p21(WAF1/CIP1) expression, PLoS One, 8 (2013) e77293.
[129] W.P. Tsang, T.W. Wong, A.H. Cheung, C.N. Co, T.T. Kwok, Induction of drug resistance and transformation in human cancer cells by the noncoding RNA CUDR, RNA, 13 (2007) 890-898.
[130] O. Kovalchuk, J. Filkowski, J. Meservy, Y. Ilnytskyy, V.P. Tryndyak, V.F. Chekhun, I.P. Pogribny, Involvement of microRNA-451 in resistance of the MCF-7 breast cancer cells to chemotherapeutic drug doxorubicin, Mol Cancer Ther, 7 (2008) 2152-2159.
[131] T. Hirota, Y. Date, Y. Nishibatake, H. Takane, Y. Fukuoka, Y. Taniguchi, N. Burioka, E. Shimizu, H. Nakamura, K. Otsubo, I. Ieiri, Dihydropyrimidine dehydrogenase (DPD) expression is negatively regulated by certain microRNAs in human lung tissues, Lung Cancer, 77 (2012) 16-23.

[132] X. Zhao, L. Yang, J. Hu, J. Ruan, miR-138 might reverse multidrug resistance of leukemia cells, Leuk Res, 34 (2010) 1078-1082.
[133] Y. Xu, S.J. Ohms, Z. Li, Q. Wang, G. Gong, Y. Hu, Z. Mao, M.F. Shannon, J.Y. Fan, Changes in the expression of miR-381 and miR-495 are inversely associated with the expression of the MDR1 gene and development of multi-drug resistance, PLoS One, 8 (2013) e82062.
[134] Y.Z. Pan, M.E. Morris, A.M. Yu, MicroRNA-328 negatively regulates the expression of breast cancer resistance protein (BCRP/ABCG2) in human cancer cells, Mol Pharmacol, 75 (2009) 1374-1379.
[135] X. Li, Y.Z. Pan, G.M. Seigel, Z.H. Hu, M. Huang, A.M. Yu, Breast cancer resistance protein BCRP/ABCG2 regulatory microRNAs (hsa-miR-328, -519c and -520h) and their differential expression in stem-like ABCG2+ cancer cells, Biochem Pharmacol, 81 (2011) 783-792.
[136] K. Iida, J. Fukushi, Y. Matsumoto, Y. Oda, Y. Takahashi, T. Fujiwara, Y. Fujiwara-Okada, M. Hatano, A. Nabashima, S. Kamura, Y. Iwamoto, miR-125b develops chemoresistance in Ewing sarcoma/primitive neuroectodermal tumor, Cancer Cell Int, 13 (2013) 21.
[137] S. Liang, X. Gong, G. Zhang, G. Huang, Y. Lu, Y. Li, MicroRNA-140 regulates cell growth and invasion in pancreatic duct adenocarcinoma by targeting iASPP, Acta Biochim Biophys Sin (Shanghai), 48 (2016) 174-181.
[138] F. Fornari, L. Gramantieri, C. Giovannini, A. Veronese, M. Ferracin, S. Sabbioni, G.A. Calin, G.L. Grazi, C.M. Croce, S. Tavolari, P. Chieco, M. Negrini, L. Bolondi, MiR-122/cyclin G1 interaction modulates p53 activity and affects doxorubicin sensitivity of human hepatocarcinoma cells, Cancer Res, 69 (2009) 5761-5767.
[139] Y. Tsuchiya, M. Nakajima, S. Takagi, T. Taniya, T. Yokoi, MicroRNA regulates the expression of human cytochrome P450 1B1, Cancer Res, 66 (2006) 9090-9098.
[140] Y.M. Choi, S. An, E.M. Lee, K. Kim, S.J. Choi, J.S. Kim, H.H. Jang, I.S. An, S. Bae, CYP1A1 is a target of miR-892a-mediated post-transcriptional repression, Int J Oncol, 41 (2012) 331-336.
[141] S. Chen, J.W. Jiao, K.X. Sun, Z.H. Zong, Y. Zhao, MicroRNA-133b targets glutathione S-transferase pi expression to increase ovarian cancer cell sensitivity to chemotherapy drugs, Drug Des Devel Ther, 9 (2015) 5225-5235.
[142] X. Zhang, J. Zhu, R. Xing, Y. Tie, H. Fu, X. Zheng, B. Yu, miR-513a-3p sensitizes human lung adenocarcinoma cells to chemotherapy by targeting GSTP1, Lung Cancer, 77 (2012) 488-494.
[143] P. Moskwa, F.M. Buffa, Y. Pan, R. Panchakshari, P. Gottipati, R.J. Muschel, J. Beech, R. Kulshrestha, K. Abdelmohsen, D.M. Weinstock, M. Gorospe, A.L. Harris, T. Helleday, D. Chowdhury, miR-182-mediated downregulation of BRCA1 impacts DNA repair and sensitivity to PARP inhibitors, Mol Cell, 41 (2011) 210-220.
[144] N. Valeri, P. Gasparini, C. Braconi, A. Paone, F. Lovat, M. Fabbri, K.M. Sumani, H. Alder, D. Amadori, T. Patel, G.J. Nuovo, R. Fishel, C.M. Croce, MicroRNA-21 induces resistance to 5-fluorouracil by down-regulating human DNA MutS homolog 2 (hMSH2), Proc Natl Acad Sci U S A, 107 (2010) 21098-21103.
[145] W. Zhu, D. Zhu, S. Lu, T. Wang, J. Wang, B. Jiang, Y. Shu, P. Liu, miR-497 modulates multidrug resistance of human cancer cell lines by targeting BCL2, Med Oncol, 29 (2012) 384-391.
[146] L. Xia, D. Zhang, R. Du, Y. Pan, L. Zhao, S. Sun, L. Hong, J. Liu, D. Fan, miR-15b and miR-16 modulate multidrug resistance by targeting BCL2 in human gastric cancer cells, Int J Cancer, 123 (2008) 372-379.
[147] T. Chiyomaru, S. Yamamura, S. Fukuhara, H. Hidaka, S. Majid, S. Saini, S. Arora, G. Deng, V. Shahryari, I. Chang, Y. Tanaka, Z.L. Tabatabai, H. Enokida, N. Seki, M. Nakagawa, R. Dahiya, Genistein up-regulates tumor suppressor microRNA-574-3p in prostate cancer, PLoS One, 8 (2013) e58929.
[148] H. Zhu, H. Wu, X. Liu, B. Li, Y. Chen, X. Ren, C.G. Liu, J.M. Yang, Regulation of autophagy by a beclin 1-targeted microRNA, miR-30a, in cancer cells, Autophagy, 5 (2009) 816-823.

[149] R. Xu, S. Liu, H. Chen, L. Lao, MicroRNA-30a downregulation contributes to chemoresistance of osteosarcoma cells through activating Beclin-1-mediated autophagy, Oncol Rep, 35 (2016) 1757-1763.
[150] B. Pan, B. Feng, Y. Chen, G. Huang, R. Wang, L. Chen, H. Song, MiR-200b regulates autophagy associated with chemoresistance in human lung adenocarcinoma, Oncotarget, 6 (2015) 32805-32820.
[151] W. Zhu, H. Xu, D. Zhu, H. Zhi, T. Wang, J. Wang, B. Jiang, Y. Shu, P. Liu, miR-200bc/429 cluster modulates multidrug resistance of human cancer cell lines by targeting BCL2 and XIAP, Cancer Chemother Pharmacol, 69 (2012) 723-731.
[152] L. Zheng, X. Li, X. Meng, J. Chou, J. Hu, F. Zhang, Z. Zhang, Y. Xing, Y. Liu, T. Xi, Competing endogenous RNA networks of CYP4Z1 and pseudogene CYP4Z2P confer tamoxifen resistance in breast cancer, Mol Cell Endocrinol, 427 (2016) 133-142.
[153] L. Shen, M. Du, C. Wang, D. Gu, M. Wang, Q. Zhang, T. Zhao, X. Zhang, Y. Tan, X. Huo, W. Gong, Z. Xu, J. Chen, Z. Zhang, Clinical significance of POU5F1P1 rs10505477 polymorphism in Chinese gastric cancer patients receving cisplatin-based chemotherapy after surgical resection, Int J Mol Sci, 15 (2014) 12764-12777.
[154] Z. Li, S. Hu, J. Wang, J. Cai, L. Xiao, L. Yu, Z. Wang, MiR-27a modulates MDR1/P-glycoprotein expression by targeting HIPK2 in human ovarian cancer cells, Gynecol Oncol, 119 (2010) 125-130.
[155] D.D. Feng, H. Zhang, P. Zhang, Y.S. Zheng, X.J. Zhang, B.W. Han, X.Q. Luo, L. Xu, H. Zhou, L.H. Qu, Y.Q. Chen, Down-regulated miR-331-5p and miR-27a are associated with chemotherapy resistance and relapse in leukaemia, J Cell Mol Med, 15 (2011) 2164-2175.
[156] Z. Chen, T. Ma, C. Huang, L. Zhang, X. Lv, T. Xu, T. Hu, J. Li, MiR-27a modulates the MDR1/P-glycoprotein expression by inhibiting FZD7/beta-catenin pathway in hepatocellular carcinoma cells, Cell Signal, 25 (2013) 2693-2701.
[157] Q. Wang, Z. Wang, L. Chu, X. Li, P. Kan, X. Xin, Y. Zhu, P. Yang, The Effects and Molecular Mechanisms of MiR-106a in Multidrug Resistance Reversal in Human Glioma U87/DDP and U251/G Cell Lines, PLoS One, 10 (2015) e0125473.
[158] B.C. Gomes, J. Rueff, A.S. Rodrigues, MicroRNAs and Cancer Drug Resistance, Methods Mol Biol, 1395 (2016) 137-162.
[159] W. Mu, C. Hu, H. Zhang, Z. Qu, J. Cen, Z. Qiu, C. Li, H. Ren, Y. Li, X. He, X. Shi, L. Hui, miR-27b synergizes with anticancer drugs via p53 activation and CYP1B1 suppression, Cell Res, 25 (2015) 477-495.
[160] N. Valeri, P. Gasparini, M. Fabbri, C. Braconi, A. Veronese, F. Lovat, B. Adair, I. Vannini, F. Fanini, A. Bottoni, S. Costinean, S.K. Sandhu, G.J. Nuovo, H. Alder, R. Gafa, F. Calore, M. Ferracin, G. Lanza, S. Volinia, M. Negrini, M.A. McIlhatton, D. Amadori, R. Fishel, C.M. Croce, Modulation of mismatch repair and genomic stability by miR-155, Proc Natl Acad Sci U S A, 107 (2010) 6982-6987.
[161] R.T.L. Hugo Seca , and M. Helena Vasconcelos, Chapter 11 MicroRNAs in Cancer Drug Resistance and Drug Sensitivity, MicroRNAs: Key Regulators of Oncogenesis, (2014).
[162] W. Hu, C.S. Chan, R. Wu, C. Zhang, Y. Sun, J.S. Song, L.H. Tang, A.J. Levine, Z. Feng, Negative regulation of tumor suppressor p53 by microRNA miR-504, Mol Cell, 38 (2010) 689-699.
[163] M. Kumar, Z. Lu, A.A. Takwi, W. Chen, N.S. Callander, K.S. Ramos, K.H. Young, Y. Li, Negative regulation of the tumor suppressor p53 gene by microRNAs, Oncogene, 30 (2011) 843-853.
[164] A.T. Sumbul, B. Gogebakan, S. Ergun, E. Yengil, C.Y. Batmaci, O. Tonyali, M. Yaldiz, miR-204-5p expression in colorectal cancer: an autophagy-associated gene, Tumour Biol, 35 (2014) 12713-12719.
[165] J. Xiao, X. Zhu, B. He, Y. Zhang, B. Kang, Z. Wang, X. Ni, MiR-204 regulates cardiomyocyte autophagy induced by ischemia-reperfusion through LC3-II, J Biomed Sci, 18 (2011) 35.
[166] A. Chatterjee, D. Chattopadhyay, G. Chakrabarti, MiR-16 targets Bcl-2 in paclitaxel-resistant lung cancer cells and overexpression of miR-16 along with miR-17 causes unprecedented sensitivity by simultaneously modulating autophagy and apoptosis, Cell Signal, 27 (2015) 189-203.

[167] J.A. Weber, D.H. Baxter, S. Zhang, D.Y. Huang, K.H. Huang, M.J. Lee, D.J. Galas, K. Wang, The microRNA spectrum in 12 body fluids, Clin Chem, 56 (2010) 1733-1741.
[168] C.H. Lawrie, S. Gal, H.M. Dunlop, B. Pushkaran, A.P. Liggins, K. Pulford, A.H. Banham, F. Pezzella, J. Boultwood, J.S. Wainscoat, C.S. Hatton, A.L. Harris, Detection of elevated levels of tumour-associated microRNAs in serum of patients with diffuse large B-cell lymphoma, Br J Haematol, 141 (2008) 672-675.
[169] P.S. Mitchell, R.K. Parkin, E.M. Kroh, B.R. Fritz, S.K. Wyman, E.L. Pogosova-Agadjanyan, A. Peterson, J. Noteboom, K.C. O'Briant, A. Allen, D.W. Lin, N. Urban, C.W. Drescher, B.S. Knudsen, D.L. Stirewalt, R. Gentleman, R.L. Vessella, P.S. Nelson, D.B. Martin, M. Tewari, Circulating microRNAs as stable blood-based markers for cancer detection, Proc Natl Acad Sci U S A, 105 (2008) 10513-10518.
[170] Z. Hu, X. Chen, Y. Zhao, T. Tian, G. Jin, Y. Shu, Y. Chen, L. Xu, K. Zen, C. Zhang, H. Shen, Serum microRNA signatures identified in a genome-wide serum microRNA expression profiling predict survival of non-small-cell lung cancer, J Clin Oncol, 28 (2010) 1721-1726.
[171] E.K. Ng, W.W. Chong, H. Jin, E.K. Lam, V.Y. Shin, J. Yu, T.C. Poon, S.S. Ng, J.J. Sung, Differential expression of microRNAs in plasma of patients with colorectal cancer: a potential marker for colorectal cancer screening, Gut, 58 (2009) 1375-1381.
[172] H.M. Heneghan, N. Miller, A.J. Lowery, K.J. Sweeney, J. Newell, M.J. Kerin, Circulating microRNAs as novel minimally invasive biomarkers for breast cancer, Ann Surg, 251 (2010) 499-505.
[173] Y. Yamamoto, N. Kosaka, M. Tanaka, F. Koizumi, Y. Kanai, T. Mizutani, Y. Murakami, M. Kuroda, A. Miyajima, T. Kato, T. Ochiya, MicroRNA-500 as a potential diagnostic marker for hepatocellular carcinoma, Biomarkers, 14 (2009) 529-538.
[174] D.H. Bach, J.Y. Hong, H.J. Park, S.K. Lee, The role of exosomes and miRNAs in drug-resistance of cancer cells, Int J Cancer, 141 (2017) 220-230.
[175] B. Santosh, A. Varshney, P.K. Yadava, Non-coding RNAs: biological functions and applications, Cell Biochem Funct, 33 (2015) 14-22.
[176] C.-P.L.a.L. He, Noncoding RNAs in Cancer Development, Annu. Rev. Cancer Biol. 2017. 1:8.1–8.22, 1 (2016).
[177] A. Fatica, I. Bozzoni, Long non-coding RNAs: new players in cell differentiation and development, Nat Rev Genet, 15 (2014) 7-21.
[178] F. Corra, C. Agnoletto, L. Minotti, F. Baldassari, S. Volinia, The Network of Non-coding RNAs in Cancer Drug Resistance, Front Oncol, 8 (2018) 327.
[179] H. Maamar, M.N. Cabili, J. Rinn, A. Raj, linc-HOXA1 is a noncoding RNA that represses Hoxa1 transcription in cis, Genes Dev, 27 (2013) 1260-1271.
[180] J.T. Lee, M.S. Bartolomei, X-inactivation, imprinting, and long noncoding RNAs in health and disease, Cell, 152 (2013) 1308-1323.
[181] A.M. Khalil, M. Guttman, M. Huarte, M. Garber, A. Raj, D. Rivea Morales, K. Thomas, A. Presser, B.E. Bernstein, A. van Oudenaarden, A. Regev, E.S. Lander, J.L. Rinn, Many human large intergenic noncoding RNAs associate with chromatin-modifying complexes and affect gene expression, Proc Natl Acad Sci U S A, 106 (2009) 11667-11672.
[182] C. Chu, K. Qu, F.L. Zhong, S.E. Artandi, H.Y. Chang, Genomic maps of long noncoding RNA occupancy reveal principles of RNA-chromatin interactions, Mol Cell, 44 (2011) 667-678.
[183] K.C. Wang, H.Y. Chang, Molecular mechanisms of long noncoding RNAs, Mol Cell, 43 (2011) 904-914.
[184] Y. Xiao, C. Jiao, Y. Lin, M. Chen, J. Zhang, J. Wang, Z. Zhang, lncRNA UCA1 Contributes to Imatinib Resistance by Acting as a ceRNA Against miR-16 in Chronic Myeloid Leukemia Cells, DNA Cell Biol, 36 (2017) 18-25.
[185] J. Li, Y.M. Wang, Y.L. Song, Knockdown of long noncoding RNA AB073614 inhibits glioma cell proliferation and migration via affecting epithelial-mesenchymal transition, Eur Rev Med Pharmacol Sci, 20 (2016) 3997-4002.

[186] J. Pan, X. Li, W. Wu, M. Xue, H. Hou, W. Zhai, W. Chen, Long non-coding RNA UCA1 promotes cisplatin/gemcitabine resistance through CREB modulating miR-196a-5p in bladder cancer cells, Cancer Lett, 382 (2016) 64-76.
[187] C.G. Xu, M.F. Yang, Y.Q. Ren, C.H. Wu, L.Q. Wang, Exosomes mediated transfer of lncRNA UCA1 results in increased tamoxifen resistance in breast cancer cells, Eur Rev Med Pharmacol Sci, 20 (2016) 4362-4368.
[188] H.Y. Zhang, F. Liang, J.W. Zhang, F. Wang, L. Wang, X.G. Kang, Effects of long noncoding RNA-ROR on tamoxifen resistance of breast cancer cells by regulating microRNA-205, Cancer Chemother Pharmacol, 79 (2017) 327-337.
[189] Y. Li, B. Jiang, H. Zhu, X. Qu, L. Zhao, Y. Tan, Y. Jiang, M. Liao, X. Wu, Inhibition of long non-coding RNA ROR reverses resistance to Tamoxifen by inducing autophagy in breast cancer, Tumour Biol, 39 (2017) 1010428317705790.
[190] J.J. Pan, X.J. Xie, X. Li, W. Chen, Long Non-coding RNAs and Drug Resistance, Asian Pac J Cancer Prev, 16 (2015) 8067-8073.
[191] E. Chiefari, S. Iiritano, F. Paonessa, I. Le Pera, B. Arcidiacono, M. Filocamo, D. Foti, S.A. Liebhaber, A. Brunetti, Pseudogene-mediated posttranscriptional silencing of HMGA1 can result in insulin resistance and type 2 diabetes, Nat Commun, 1 (2010) 40.
[192] O.H. Tam, A.A. Aravin, P. Stein, A. Girard, E.P. Murchison, S. Cheloufi, E. Hodges, M. Anger, R. Sachidanandam, R.M. Schultz, G.J. Hannon, Pseudogene-derived small interfering RNAs regulate gene expression in mouse oocytes, Nature, 453 (2008) 534-538.
[193] T. Watanabe, Y. Totoki, A. Toyoda, M. Kaneda, S. Kuramochi-Miyagawa, Y. Obata, H. Chiba, Y. Kohara, T. Kono, T. Nakano, M.A. Surani, Y. Sakaki, H. Sasaki, Endogenous siRNAs from naturally formed dsRNAs regulate transcripts in mouse oocytes, Nature, 453 (2008) 539-543.
[194] F.A. Karreth, M. Reschke, A. Ruocco, C. Ng, B. Chapuy, V. Leopold, M. Sjoberg, T.M. Keane, A. Verma, U. Ala, Y. Tay, D. Wu, N. Seitzer, C. Velasco-Herrera Mdel, A. Bothmer, J. Fung, F. Langellotto, S.J. Rodig, O. Elemento, M.A. Shipp, D.J. Adams, R. Chiarle, P.P. Pandolfi, The BRAF pseudogene functions as a competitive endogenous RNA and induces lymphoma in vivo, Cell, 161 (2015) 319-332.
[195] L. Poliseno, L. Salmena, J. Zhang, B. Carver, W.J. Haveman, P.P. Pandolfi, A coding-independent function of gene and pseudogene mRNAs regulates tumour biology, Nature, 465 (2010) 1033-1038.
[196] H. Hayashi, T. Arao, Y. Togashi, H. Kato, Y. Fujita, M.A. De Velasco, H. Kimura, K. Matsumoto, K. Tanaka, I. Okamoto, A. Ito, Y. Yamada, K. Nakagawa, K. Nishio, The OCT4 pseudogene POU5F1B is amplified and promotes an aggressive phenotype in gastric cancer, Oncogene, 34 (2015) 199-208.
[197] H.F. Dvorak, S.C. Quay, N.S. Orenstein, A.M. Dvorak, P. Hahn, A.M. Bitzer, A.C. Carvalho, Tumor shedding and coagulation, Science, 212 (1981) 923-924.
[198] J.N. George, L.L. Thoi, L.M. McManus, T.A. Reimann, Isolation of human platelet membrane microparticles from plasma and serum, Blood, 60 (1982) 834-840.
[199] M. Tkach, C. Thery, Communication by Extracellular Vesicles: Where We Are and Where We Need to Go, Cell, 164 (2016) 1226-1232.
[200] R.M. Johnstone, M. Adam, J.R. Hammond, L. Orr, C. Turbide, Vesicle formation during reticulocyte maturation. Association of plasma membrane activities with released vesicles (exosomes), J Biol Chem, 262 (1987) 9412-9420.
[201] G. van Niel, G. D'Angelo, G. Raposo, Shedding light on the cell biology of extracellular vesicles, Nat Rev Mol Cell Biol, 19 (2018) 213-228.
[202] R. Xu, D.W. Greening, A. Rai, H. Ji, R.J. Simpson, Highly-purified exosomes and shed microvesicles isolated from the human colon cancer cell line LIM1863 by sequential centrifugal ultrafiltration are biochemically and functionally distinct, Methods, 87 (2015) 11-25.
[203] J. Kowal, G. Arras, M. Colombo, M. Jouve, J.P. Morath, B. Primdal-Bengtson, F. Dingli, D. Loew, M. Tkach, C. Thery, Proteomic comparison defines novel markers to characterize

heterogeneous populations of extracellular vesicle subtypes, Proc Natl Acad Sci U S A, 113 (2016) E968-977.
[204] B. Gyorgy, T.G. Szabo, M. Pasztoi, Z. Pal, P. Misjak, B. Aradi, V. Laszlo, E. Pallinger, E. Pap, A. Kittel, G. Nagy, A. Falus, E.I. Buzas, Membrane vesicles, current state-of-the-art: emerging role of extracellular vesicles, Cell Mol Life Sci, 68 (2011) 2667-2688.
[205] M.Y. Konoshenko, E.A. Lekchnov, A.V. Vlassov, P.P. Laktionov, Isolation of Extracellular Vesicles: General Methodologies and Latest Trends, Biomed Res Int, 2018 (2018) 8545347.
[206] M. Colombo, G. Raposo, C. Thery, Biogenesis, secretion, and intercellular interactions of exosomes and other extracellular vesicles, Annu Rev Cell Dev Biol, 30 (2014) 255-289.
[207] R. Xu, A. Rai, M. Chen, W. Suwakulsiri, D.W. Greening, R.J. Simpson, Extracellular vesicles in cancer - implications for future improvements in cancer care, Nat Rev Clin Oncol, 15 (2018) 617-638.
[208] H.F. Heijnen, A.E. Schiel, R. Fijnheer, H.J. Geuze, J.J. Sixma, Activated platelets release two types of membrane vesicles: microvesicles by surface shedding and exosomes derived from exocytosis of multivesicular bodies and alpha-granules, Blood, 94 (1999) 3791-3799.
[209] D.W. Greening, S.K. Gopal, R. Xu, R.J. Simpson, W. Chen, Exosomes and their roles in immune regulation and cancer, Semin Cell Dev Biol, 40 (2015) 72-81.
[210] P.D. Robbins, A.E. Morelli, Regulation of immune responses by extracellular vesicles, Nat Rev Immunol, 14 (2014) 195-208.
[211] X. Teng, L. Chen, W. Chen, J. Yang, Z. Yang, Z. Shen, Mesenchymal Stem Cell-Derived Exosomes Improve the Microenvironment of Infarcted Myocardium Contributing to Angiogenesis and Anti-Inflammation, Cell Physiol Biochem, 37 (2015) 2415-2424.
[212] F. Baixauli, C. Lopez-Otin, M. Mittelbrunn, Exosomes and autophagy: coordinated mechanisms for the maintenance of cellular fitness, Front Immunol, 5 (2014) 403.
[213] C. Simon, D.W. Greening, D. Bolumar, N. Balaguer, L.A. Salamonsen, F. Vilella, Extracellular Vesicles in Human Reproduction in Health and Disease, Endocr Rev, 39 (2018) 292-332.
[214] V. Budnik, C. Ruiz-Canada, F. Wendler, Extracellular vesicles round off communication in the nervous system, Nat Rev Neurosci, 17 (2016) 160-172.
[215] H. Peinado, H. Zhang, I.R. Matei, B. Costa-Silva, A. Hoshino, G. Rodrigues, B. Psaila, R.N. Kaplan, J.F. Bromberg, Y. Kang, M.J. Bissell, T.R. Cox, A.J. Giaccia, J.T. Erler, S. Hiratsuka, C.M. Ghajar, D. Lyden, Pre-metastatic niches: organ-specific homes for metastases, Nat Rev Cancer, 17 (2017) 302-317.
[216] S.L.N. Maas, X.O. Breakefield, A.M. Weaver, Extracellular Vesicles: Unique Intercellular Delivery Vehicles, Trends Cell Biol, 27 (2017) 172-188.
[217] C. Thery, M. Boussac, P. Veron, P. Ricciardi-Castagnoli, G. Raposo, J. Garin, S. Amigorena, Proteomic analysis of dendritic cell-derived exosomes: a secreted subcellular compartment distinct from apoptotic vesicles, J Immunol, 166 (2001) 7309-7318.
[218] E.R. Abels, X.O. Breakefield, Introduction to Extracellular Vesicles: Biogenesis, RNA Cargo Selection, Content, Release, and Uptake, Cell Mol Neurobiol, 36 (2016) 301-312.
[219] S. Mathivanan, C.J. Fahner, G.E. Reid, R.J. Simpson, ExoCarta 2012: database of exosomal proteins, RNA and lipids, Nucleic Acids Res, 40 (2012) D1241-1244.
[220] D.K. Kim, B. Kang, O.Y. Kim, D.S. Choi, J. Lee, S.R. Kim, G. Go, Y.J. Yoon, J.H. Kim, S.C. Jang, K.S. Park, E.J. Choi, K.P. Kim, D.M. Desiderio, Y.K. Kim, J. Lotvall, D. Hwang, Y.S. Gho, EVpedia: an integrated database of high-throughput data for systemic analyses of extracellular vesicles, J Extracell Vesicles, 2 (2013).
[221] C. Thery, K.W. Witwer, E. Aikawa, M.J. Alcaraz, J.D. Anderson, R. Andriantsitohaina, A. Antoniou, T. Arab, F. Archer, G.K. Atkin-Smith, D.C. Ayre, J.M. Bach, D. Bachurski, H. Baharvand, L. Balaj, S. Baldacchino, N.N. Bauer, A.A. Baxter, M. Bebawy, C. Beckham, A. Bedina Zavec, A. Benmoussa, A.C. Berardi, P. Bergese, E. Bielska, C. Blenkiron, S. Bobis-Wozowicz, E. Boilard, W. Boireau, A. Bongiovanni, F.E. Borras, S. Bosch, C.M. Boulanger, X. Breakefield, A.M. Breglio, M.A. Brennan, D.R. Brigstock, A. Brisson, M.L. Broekman, J.F. Bromberg, P. Bryl-Gorecka, S. Buch, A.H.

Buck, D. Burger, S. Busatto, D. Buschmann, B. Bussolati, E.I. Buzas, J.B. Byrd, G. Camussi, D.R. Carter, S. Caruso, L.W. Chamley, Y.T. Chang, C. Chen, S. Chen, L. Cheng, A.R. Chin, A. Clayton, S.P. Clerici, A. Cocks, E. Cocucci, R.J. Coffey, A. Cordeiro-da-Silva, Y. Couch, F.A. Coumans, B. Coyle, R. Crescitelli, M.F. Criado, C. D'Souza-Schorey, S. Das, A. Datta Chaudhuri, P. de Candia, E.F. De Santana, O. De Wever, H.A. Del Portillo, T. Demaret, S. Deville, A. Devitt, B. Dhondt, D. Di Vizio, L.C. Dieterich, V. Dolo, A.P. Dominguez Rubio, M. Dominici, M.R. Dourado, T.A. Driedonks, F.V. Duarte, H.M. Duncan, R.M. Eichenberger, K. Ekstrom, S. El Andaloussi, C. Elie-Caille, U. Erdbrugger, J.M. Falcon-Perez, F. Fatima, J.E. Fish, M. Flores-Bellver, A. Forsonits, A. Frelet-Barrand, F. Fricke, G. Fuhrmann, S. Gabrielsson, A. Gamez-Valero, C. Gardiner, K. Gartner, R. Gaudin, Y.S. Gho, B. Giebel, C. Gilbert, M. Gimona, I. Giusti, D.C. Goberdhan, A. Gorgens, S.M. Gorski, D.W. Greening, J.C. Gross, A. Gualerzi, G.N. Gupta, D. Gustafson, A. Handberg, R.A. Haraszti, P. Harrison, H. Hegyesi, A. Hendrix, A.F. Hill, F.H. Hochberg, K.F. Hoffmann, B. Holder, H. Holthofer, B. Hosseinkhani, G. Hu, Y. Huang, V. Huber, S. Hunt, A.G. Ibrahim, T. Ikezu, J.M. Inal, M. Isin, A. Ivanova, H.K. Jackson, S. Jacobsen, S.M. Jay, M. Jayachandran, G. Jenster, L. Jiang, S.M. Johnson, J.C. Jones, A. Jong, T. Jovanovic-Talisman, S. Jung, R. Kalluri, S.I. Kano, S. Kaur, Y. Kawamura, E.T. Keller, D. Khamari, E. Khomyakova, A. Khvorova, P. Kierulf, K.P. Kim, T. Kislinger, M. Klingeborn, D.J. Klinke, 2nd, M. Kornek, M.M. Kosanovic, A.F. Kovacs, E.M. Kramer-Albers, S. Krasemann, M. Krause, I.V. Kurochkin, G.D. Kusuma, S. Kuypers, S. Laitinen, S.M. Langevin, L.R. Languino, J. Lannigan, C. Lasser, L.C. Laurent, G. Lavieu, E. Lazaro-Ibanez, S. Le Lay, M.S. Lee, Y.X.F. Lee, D.S. Lemos, M. Lenassi, A. Leszczynska, I.T. Li, K. Liao, S.F. Libregts, E. Ligeti, R. Lim, S.K. Lim, A. Line, K. Linnemannstons, A. Llorente, C.A. Lombard, M.J. Lorenowicz, A.M. Lorincz, J. Lotvall, J. Lovett, M.C. Lowry, X. Loyer, Q. Lu, B. Lukomska, T.R. Lunavat, S.L. Maas, H. Malhi, A. Marcilla, J. Mariani, J. Mariscal, E.S. Martens-Uzunova, L. Martin-Jaular, M.C. Martinez, V.R. Martins, M. Mathieu, S. Mathivanan, M. Maugeri, L.K. McGinnis, M.J. McVey, D.G. Meckes, Jr., K.L. Meehan, I. Mertens, V.R. Minciacchi, A. Moller, M. Moller Jorgensen, A. Morales-Kastresana, J. Morhayim, F. Mullier, M. Muraca, L. Musante, V. Mussack, D.C. Muth, K.H. Myburgh, T. Najrana, M. Nawaz, I. Nazarenko, P. Nejsum, C. Neri, T. Neri, R. Nieuwland, L. Nimrichter, J.P. Nolan, E.N. Nolte-'t Hoen, N. Noren Hooten, L. O'Driscoll, T. O'Grady, A. O'Loghlen, T. Ochiya, M. Olivier, A. Ortiz, L.A. Ortiz, X. Osteikoetxea, O. Ostergaard, M. Ostrowski, J. Park, D.M. Pegtel, H. Peinado, F. Perut, M.W. Pfaffl, D.G. Phinney, B.C. Pieters, R.C. Pink, D.S. Pisetsky, E. Pogge von Strandmann, I. Polakovicova, I.K. Poon, B.H. Powell, I. Prada, L. Pulliam, P. Quesenberry, A. Radeghieri, R.L. Raffai, S. Raimondo, J. Rak, M.I. Ramirez, G. Raposo, M.S. Rayyan, N. Regev-Rudzki, F.L. Ricklefs, P.D. Robbins, D.D. Roberts, S.C. Rodrigues, E. Rohde, S. Rome, K.M. Rouschop, A. Rughetti, A.E. Russell, P. Saa, S. Sahoo, E. Salas-Huenuleo, C. Sanchez, J.A. Saugstad, M.J. Saul, R.M. Schiffelers, R. Schneider, T.H. Schoyen, A. Scott, E. Shahaj, S. Sharma, O. Shatnyeva, F. Shekari, G.V. Shelke, A.K. Shetty, K. Shiba, P.R. Siljander, A.M. Silva, A. Skowronek, O.L. Snyder, 2nd, R.P. Soares, B.W. Sodar, C. Soekmadji, J. Sotillo, P.D. Stahl, W. Stoorvogel, S.L. Stott, E.F. Strasser, S. Swift, H. Tahara, M. Tewari, K. Timms, S. Tiwari, R. Tixeira, M. Tkach, W.S. Toh, R. Tomasini, A.C. Torrecilhas, J.P. Tosar, V. Toxavidis, L. Urbanelli, P. Vader, B.W. van Balkom, S.G. van der Grein, J. Van Deun, M.J. van Herwijnen, K. Van Keuren-Jensen, G. van Niel, M.E. van Royen, A.J. van Wijnen, M.H. Vasconcelos, I.J. Vechetti, Jr., T.D. Veit, L.J. Vella, E. Velot, F.J. Verweij, B. Vestad, J.L. Vinas, T. Visnovitz, K.V. Vukman, J. Wahlgren, D.C. Watson, M.H. Wauben, A. Weaver, J.P. Webber, V. Weber, A.M. Wehman, D.J. Weiss, J.A. Welsh, S. Wendt, A.M. Wheelock, Z. Wiener, L. Witte, J. Wolfram, A. Xagorari, P. Xander, J. Xu, X. Yan, M. Yanez-Mo, H. Yin, Y. Yuana, V. Zappulli, J. Zarubova, V. Zekas, J.Y. Zhang, Z. Zhao, L. Zheng, A.R. Zheutlin, A.M. Zickler, P. Zimmermann, A.M. Zivkovic, D. Zocco, E.K. Zuba-Surma, Minimal information for studies of extracellular vesicles 2018 (MISEV2018): a position statement of the International Society for Extracellular Vesicles and update of the MISEV2014 guidelines, J Extracell Vesicles, 7 (2018) 1535750.
[222] H. Kalra, G.P. Drummen, S. Mathivanan, Focus on Extracellular Vesicles: Introducing the Next Small Big Thing, Int J Mol Sci, 17 (2016) 170.

[223] F. Chalmin, S. Ladoire, G. Mignot, J. Vincent, M. Bruchard, J.P. Remy-Martin, W. Boireau, A. Rouleau, B. Simon, D. Lanneau, A. De Thonel, G. Multhoff, A. Hamman, F. Martin, B. Chauffert, E. Solary, L. Zitvogel, C. Garrido, B. Ryffel, C. Borg, L. Apetoh, C. Rebe, F. Ghiringhelli, Membrane-associated Hsp72 from tumor-derived exosomes mediates STAT3-dependent immunosuppressive function of mouse and human myeloid-derived suppressor cells, J Clin Invest, 120 (2010) 457-471.
[224] A. Clayton, J.P. Mitchell, J. Court, M.D. Mason, Z. Tabi, Human tumor-derived exosomes selectively impair lymphocyte responses to interleukin-2, Cancer Res, 67 (2007) 7458-7466.
[225] H. Peinado, M. Aleckovic, S. Lavotshkin, I. Matei, B. Costa-Silva, G. Moreno-Bueno, M. Hergueta-Redondo, C. Williams, G. Garcia-Santos, C. Ghajar, A. Nitadori-Hoshino, C. Hoffman, K. Badal, B.A. Garcia, M.K. Callahan, J. Yuan, V.R. Martins, J. Skog, R.N. Kaplan, M.S. Brady, J.D. Wolchok, P.B. Chapman, Y. Kang, J. Bromberg, D. Lyden, Melanoma exosomes educate bone marrow progenitor cells toward a pro-metastatic phenotype through MET, Nat Med, 18 (2012) 883-891.
[226] J. Ratajczak, K. Miekus, M. Kucia, J. Zhang, R. Reca, P. Dvorak, M.Z. Ratajczak, Embryonic stem cell-derived microvesicles reprogram hematopoietic progenitors: evidence for horizontal transfer of mRNA and protein delivery, Leukemia, 20 (2006) 847-856.
[227] J. Skog, T. Wurdinger, S. van Rijn, D.H. Meijer, L. Gainche, M. Sena-Esteves, W.T. Curry, Jr., B.S. Carter, A.M. Krichevsky, X.O. Breakefield, Glioblastoma microvesicles transport RNA and proteins that promote tumour growth and provide diagnostic biomarkers, Nat Cell Biol, 10 (2008) 1470-1476.
[228] H. Valadi, K. Ekstrom, A. Bossios, M. Sjostrand, J.J. Lee, J.O. Lotvall, Exosome-mediated transfer of mRNAs and microRNAs is a novel mechanism of genetic exchange between cells, Nat Cell Biol, 9 (2007) 654-659.
[229] R. Crescitelli, C. Lasser, T.G. Szabo, A. Kittel, M. Eldh, I. Dianzani, E.I. Buzas, J. Lotvall, Distinct RNA profiles in subpopulations of extracellular vesicles: apoptotic bodies, microvesicles and exosomes, J Extracell Vesicles, 2 (2013).
[230] L. Cheng, X. Sun, B.J. Scicluna, B.M. Coleman, A.F. Hill, Characterization and deep sequencing analysis of exosomal and non-exosomal miRNA in human urine, Kidney Int, 86 (2014) 433-444.
[231] X. Huang, T. Yuan, M. Tschannen, Z. Sun, H. Jacob, M. Du, M. Liang, R.L. Dittmar, Y. Liu, M. Liang, M. Kohli, S.N. Thibodeau, L. Boardman, L. Wang, Characterization of human plasma-derived exosomal RNAs by deep sequencing, BMC Genomics, 14 (2013) 319.
[232] Y. Ogawa, Y. Taketomi, M. Murakami, M. Tsujimoto, R. Yanoshita, Small RNA transcriptomes of two types of exosomes in human whole saliva determined by next generation sequencing, Biol Pharm Bull, 36 (2013) 66-75.
[233] E.N. Nolte-'t Hoen, H.P. Buermans, M. Waasdorp, W. Stoorvogel, M.H. Wauben, P.A. t Hoen, Deep sequencing of RNA from immune cell-derived vesicles uncovers the selective incorporation of small non-coding RNA biotypes with potential regulatory functions, Nucleic Acids Res, 40 (2012) 9272-9285.
[234] S.R. Baglio, T. Lagerweij, M. Perez-Lanzon, X.D. Ho, N. Leveille, S.A. Melo, A.M. Cleton-Jansen, E.S. Jordanova, L. Roncuzzi, M. Greco, M.A.J. van Eijndhoven, G. Grisendi, M. Dominici, R. Bonafede, S.M. Lougheed, T.D. de Gruijl, N. Zini, S. Cervo, A. Steffan, V. Canzonieri, A. Martson, K. Maasalu, S. Koks, T. Wurdinger, N. Baldini, D.M. Pegtel, Blocking Tumor-Educated MSC Paracrine Activity Halts Osteosarcoma Progression, Clin Cancer Res, 23 (2017) 3721-3733.
[235] D. Koppers-Lalic, M. Hackenberg, I.V. Bijnsdorp, M.A.J. van Eijndhoven, P. Sadek, D. Sie, N. Zini, J.M. Middeldorp, B. Ylstra, R.X. de Menezes, T. Wurdinger, G.A. Meijer, D.M. Pegtel, Nontemplated nucleotide additions distinguish the small RNA composition in cells from exosomes, Cell Rep, 8 (2014) 1649-1658.
[236] D.M. Pegtel, K. Cosmopoulos, D.A. Thorley-Lawson, M.A. van Eijndhoven, E.S. Hopmans, J.L. Lindenberg, T.D. de Gruijl, T. Wurdinger, J.M. Middeldorp, Functional delivery of viral miRNAs via exosomes, Proc Natl Acad Sci U S A, 107 (2010) 6328-6333.

[237] S.A. Melo, H. Sugimoto, J.T. O'Connell, N. Kato, A. Villanueva, A. Vidal, L. Qiu, E. Vitkin, L.T. Perelman, C.A. Melo, A. Lucci, C. Ivan, G.A. Calin, R. Kalluri, Cancer exosomes perform cell-independent microRNA biogenesis and promote tumorigenesis, Cancer Cell, 26 (2014) 707-721.
[238] R. Bhome, F. Del Vecchio, G.H. Lee, M.D. Bullock, J.N. Primrose, A.E. Sayan, A.H. Mirnezami, Exosomal microRNAs (exomiRs): Small molecules with a big role in cancer, Cancer Lett, 420 (2018) 228-235.
[239] M.P. Bebelman, M.J. Smit, D.M. Pegtel, S.R. Baglio, Biogenesis and function of extracellular vesicles in cancer, Pharmacol Ther, 188 (2018) 1-11.
[240] P. Sansone, C. Savini, I. Kurelac, Q. Chang, L.B. Amato, A. Strillacci, A. Stepanova, L. Iommarini, C. Mastroleo, L. Daly, A. Galkin, B.K. Thakur, N. Soplop, K. Uryu, A. Hoshino, L. Norton, M. Bonafe, M. Cricca, G. Gasparre, D. Lyden, J. Bromberg, Packaging and transfer of mitochondrial DNA via exosomes regulate escape from dormancy in hormonal therapy-resistant breast cancer, Proc Natl Acad Sci U S A, 114 (2017) E9066-E9075.
[241] X. Sisquella, Y. Ofir-Birin, M.A. Pimentel, L. Cheng, P. Abou Karam, N.G. Sampaio, J.S. Penington, D. Connolly, T. Giladi, B.J. Scicluna, R.A. Sharples, A. Waltmann, D. Avni, E. Schwartz, L. Schofield, Z. Porat, D.S. Hansen, A.T. Papenfuss, E.M. Eriksson, M. Gerlic, A.F. Hill, A.G. Bowie, N. Regev-Rudzki, Malaria parasite DNA-harbouring vesicles activate cytosolic immune sensors, Nat Commun, 8 (2017) 1985.
[242] L. Balaj, R. Lessard, L. Dai, Y.J. Cho, S.L. Pomeroy, X.O. Breakefield, J. Skog, Tumour microvesicles contain retrotransposon elements and amplified oncogene sequences, Nat Commun, 2 (2011) 180.
[243] C. Kahlert, S.A. Melo, A. Protopopov, J. Tang, S. Seth, M. Koch, J. Zhang, J. Weitz, L. Chin, A. Futreal, R. Kalluri, Identification of double-stranded genomic DNA spanning all chromosomes with mutated KRAS and p53 DNA in the serum exosomes of patients with pancreatic cancer, J Biol Chem, 289 (2014) 3869-3875.
[244] B.K. Thakur, H. Zhang, A. Becker, I. Matei, Y. Huang, B. Costa-Silva, Y. Zheng, A. Hoshino, H. Brazier, J. Xiang, C. Williams, R. Rodriguez-Barrueco, J.M. Silva, W. Zhang, S. Hearn, O. Elemento, N. Paknejad, K. Manova-Todorova, K. Welte, J. Bromberg, H. Peinado, D. Lyden, Double-stranded DNA in exosomes: a novel biomarker in cancer detection, Cell Res, 24 (2014) 766-769.
[245] A. Takahashi, R. Okada, K. Nagao, Y. Kawamata, A. Hanyu, S. Yoshimoto, M. Takasugi, S. Watanabe, M.T. Kanemaki, C. Obuse, E. Hara, Exosomes maintain cellular homeostasis by excreting harmful DNA from cells, Nat Commun, 8 (2017) 15287.
[246] A. Llorente, T. Skotland, T. Sylvanne, D. Kauhanen, T. Rog, A. Orlowski, I. Vattulainen, K. Ekroos, K. Sandvig, Molecular lipidomics of exosomes released by PC-3 prostate cancer cells, Biochim Biophys Acta, 1831 (2013) 1302-1309.
[247] K. Laulagnier, D. Grand, A. Dujardin, S. Hamdi, H. Vincent-Schneider, D. Lankar, J.P. Salles, C. Bonnerot, B. Perret, M. Record, PLD2 is enriched on exosomes and its activity is correlated to the release of exosomes, FEBS Lett, 572 (2004) 11-14.
[248] C. Harding, J. Heuser, P. Stahl, Receptor-mediated endocytosis of transferrin and recycling of the transferrin receptor in rat reticulocytes, J Cell Biol, 97 (1983) 329-339.
[249] C. Thery, S. Amigorena, G. Raposo, A. Clayton, Isolation and characterization of exosomes from cell culture supernatants and biological fluids, Curr Protoc Cell Biol, Chapter 3 (2006) Unit 3 22.
[250] G. Raposo, W. Stoorvogel, Extracellular vesicles: exosomes, microvesicles, and friends, J Cell Biol, 200 (2013) 373-383.
[251] M.S. Pols, J. Klumperman, Trafficking and function of the tetraspanin CD63, Exp Cell Res, 315 (2009) 1584-1592.
[252] T. Wollert, J.H. Hurley, Molecular mechanism of multivesicular body biogenesis by ESCRT complexes, Nature, 464 (2010) 864-869.

[253] M. Colombo, C. Moita, G. van Niel, J. Kowal, J. Vigneron, P. Benaroch, N. Manel, L.F. Moita, C. Thery, G. Raposo, Analysis of ESCRT functions in exosome biogenesis, composition and secretion highlights the heterogeneity of extracellular vesicles, J Cell Sci, 126 (2013) 5553-5565.
[254] J.H. Hurley, ESCRT complexes and the biogenesis of multivesicular bodies, Curr Opin Cell Biol, 20 (2008) 4-11.
[255] A.M. Booth, Y. Fang, J.K. Fallon, J.M. Yang, J.E. Hildreth, S.J. Gould, Exosomes and HIV Gag bud from endosome-like domains of the T cell plasma membrane, J Cell Biol, 172 (2006) 923-935.
[256] K. Choudhuri, J. Llodra, E.W. Roth, J. Tsai, S. Gordo, K.W. Wucherpfennig, L.C. Kam, D.L. Stokes, M.L. Dustin, Polarized release of T-cell-receptor-enriched microvesicles at the immunological synapse, Nature, 507 (2014) 118-123.
[257] J. Kowal, M. Tkach, C. Thery, Biogenesis and secretion of exosomes, Curr Opin Cell Biol, 29 (2014) 116-125.
[258] W.M. Henne, H. Stenmark, S.D. Emr, Molecular mechanisms of the membrane sculpting ESCRT pathway, Cold Spring Harb Perspect Biol, 5 (2013).
[259] C. Bissig, J. Gruenberg, ALIX and the multivesicular endosome: ALIX in Wonderland, Trends Cell Biol, 24 (2014) 19-25.
[260] A.J. Jimenez, P. Maiuri, J. Lafaurie-Janvore, S. Divoux, M. Piel, F. Perez, ESCRT machinery is required for plasma membrane repair, Science, 343 (2014) 1247136.
[261] K. Trajkovic, C. Hsu, S. Chiantia, L. Rajendran, D. Wenzel, F. Wieland, P. Schwille, B. Brugger, M. Simons, Ceramide triggers budding of exosome vesicles into multivesicular endosomes, Science, 319 (2008) 1244-1247.
[262] R. Ghossoub, F. Lembo, A. Rubio, C.B. Gaillard, J. Bouchet, N. Vitale, J. Slavik, M. Machala, P. Zimmermann, Syntenin-ALIX exosome biogenesis and budding into multivesicular bodies are controlled by ARF6 and PLD2, Nat Commun, 5 (2014) 3477.
[263] A.C. Theos, S.T. Truschel, D. Tenza, I. Hurbain, D.C. Harper, J.F. Berson, P.C. Thomas, G. Raposo, M.S. Marks, A lumenal domain-dependent pathway for sorting to intralumenal vesicles of multivesicular endosomes involved in organelle morphogenesis, Dev Cell, 10 (2006) 343-354.
[264] G. van Niel, S. Charrin, S. Simoes, M. Romao, L. Rochin, P. Saftig, M.S. Marks, E. Rubinstein, G. Raposo, The tetraspanin CD63 regulates ESCRT-independent and -dependent endosomal sorting during melanogenesis, Dev Cell, 21 (2011) 708-721.
[265] S.I. Buschow, E.N. Nolte-'t Hoen, G. van Niel, M.S. Pols, T. ten Broeke, M. Lauwen, F. Ossendorp, C.J. Melief, G. Raposo, R. Wubbolts, M.H. Wauben, W. Stoorvogel, MHC II in dendritic cells is targeted to lysosomes or T cell-induced exosomes via distinct multivesicular body pathways, Traffic, 10 (2009) 1528-1542.
[266] A. Chairoungdua, D.L. Smith, P. Pochard, M. Hull, M.J. Caplan, Exosome release of beta-catenin: a novel mechanism that antagonizes Wnt signaling, J Cell Biol, 190 (2010) 1079-1091.
[267] E. Willms, H.J. Johansson, I. Mager, Y. Lee, K.E. Blomberg, M. Sadik, A. Alaarg, C.I. Smith, J. Lehtio, S. El Andaloussi, M.J. Wood, P. Vader, Cells release subpopulations of exosomes with distinct molecular and biological properties, Sci Rep, 6 (2016) 22519.
[268] W. Mobius, Y. Ohno-Iwashita, E.G. van Donselaar, V.M. Oorschot, Y. Shimada, T. Fujimoto, H.F. Heijnen, H.J. Geuze, J.W. Slot, Immunoelectron microscopic localization of cholesterol using biotinylated and non-cytolytic perfringolysin O, J Histochem Cytochem, 50 (2002) 43-55.
[269] K. Al-Nedawi, B. Meehan, J. Micallef, V. Lhotak, L. May, A. Guha, J. Rak, Intercellular transfer of the oncogenic receptor EGFRvIII by microvesicles derived from tumour cells, Nat Cell Biol, 10 (2008) 619-624.
[270] J.J. Jimenez, W. Jy, L.M. Mauro, C. Soderland, L.L. Horstman, Y.S. Ahn, Endothelial cells release phenotypically and quantitatively distinct microparticles in activation and apoptosis, Thromb Res, 109 (2003) 175-180.
[271] B. Li, M.A. Antonyak, J. Zhang, R.A. Cerione, RhoA triggers a specific signaling pathway that generates transforming microvesicles in cancer cells, Oncogene, 31 (2012) 4740-4749.

[272] M. Mathieu, L. Martin-Jaular, G. Lavieu, C. Thery, Specificities of secretion and uptake of exosomes and other extracellular vesicles for cell-to-cell communication, Nat Cell Biol, 21 (2019) 9-17.
[273] F.J. Verweij, M.P. Bebelman, C.R. Jimenez, J.J. Garcia-Vallejo, H. Janssen, J. Neefjes, J.C. Knol, R. de Goeij-de Haas, S.R. Piersma, S.R. Baglio, M. Verhage, J.M. Middeldorp, A. Zomer, J. van Rheenen, M.G. Coppolino, I. Hurbain, G. Raposo, M.J. Smit, R.F.G. Toonen, G. van Niel, D.M. Pegtel, Quantifying exosome secretion from single cells reveals a modulatory role for GPCR signaling, J Cell Biol, 217 (2018) 1129-1142.
[274] Y. Wei, D. Wang, F. Jin, Z. Bian, L. Li, H. Liang, M. Li, L. Shi, C. Pan, D. Zhu, X. Chen, G. Hu, Y. Liu, C.Y. Zhang, K. Zen, Pyruvate kinase type M2 promotes tumour cell exosome release via phosphorylating synaptosome-associated protein 23, Nat Commun, 8 (2017) 14041.
[275] C.M. Fader, D.G. Sanchez, M.B. Mestre, M.I. Colombo, TI-VAMP/VAMP7 and VAMP3/cellubrevin: two v-SNARE proteins involved in specific steps of the autophagy/multivesicular body pathways, Biochim Biophys Acta, 1793 (2009) 1901-1916.
[276] D.A. Snyder, M.L. Kelly, D.J. Woodbury, SNARE complex regulation by phosphorylation, Cell Biochem Biophys, 45 (2006) 111-123.
[277] J. Faure, G. Lachenal, M. Court, J. Hirrlinger, C. Chatellard-Causse, B. Blot, J. Grange, G. Schoehn, Y. Goldberg, V. Boyer, F. Kirchhoff, G. Raposo, J. Garin, R. Sadoul, Exosomes are released by cultured cortical neurones, Mol Cell Neurosci, 31 (2006) 642-648.
[278] G. Raposo, D. Tenza, S. Mecheri, R. Peronet, C. Bonnerot, C. Desaymard, Accumulation of major histocompatibility complex class II molecules in mast cell secretory granules and their release upon degranulation, Mol Biol Cell, 8 (1997) 2631-2645.
[279] A. Savina, C.M. Fader, M.T. Damiani, M.I. Colombo, Rab11 promotes docking and fusion of multivesicular bodies in a calcium-dependent manner, Traffic, 6 (2005) 131-143.
[280] R.E. McConnell, J.N. Higginbotham, D.A. Shifrin, Jr., D.L. Tabb, R.J. Coffey, M.J. Tyska, The enterocyte microvillus is a vesicle-generating organelle, J Cell Biol, 185 (2009) 1285-1298.
[281] C. D'Souza-Schorey, J.W. Clancy, Tumor-derived microvesicles: shedding light on novel microenvironment modulators and prospective cancer biomarkers, Genes Dev, 26 (2012) 1287-1299.
[282] V. Muralidharan-Chari, J. Clancy, C. Plou, M. Romao, P. Chavrier, G. Raposo, C. D'Souza-Schorey, ARF6-regulated shedding of tumor cell-derived plasma membrane microvesicles, Curr Biol, 19 (2009) 1875-1885.
[283] A.E. Sedgwick, J.W. Clancy, M. Olivia Balmert, C. D'Souza-Schorey, Extracellular microvesicles and invadopodia mediate non-overlapping modes of tumor cell invasion, Sci Rep, 5 (2015) 14748.
[284] S. Schlienger, S. Campbell, A. Claing, ARF1 regulates the Rho/MLC pathway to control EGF-dependent breast cancer cell invasion, Mol Biol Cell, 25 (2014) 17-29.
[285] F. Bianco, E. Pravettoni, A. Colombo, U. Schenk, T. Moller, M. Matteoli, C. Verderio, Astrocyte-derived ATP induces vesicle shedding and IL-1 beta release from microglia, J Immunol, 174 (2005) 7268-7277.
[286] L.M. Thomas, R.D. Salter, Activation of macrophages by P2X7-induced microvesicles from myeloid cells is mediated by phospholipids and is partially dependent on TLR4, J Immunol, 185 (2010) 3740-3749.
[287] F. Bianco, C. Perrotta, L. Novellino, M. Francolini, L. Riganti, E. Menna, L. Saglietti, E.H. Schuchman, R. Furlan, E. Clementi, M. Matteoli, C. Verderio, Acid sphingomyelinase activity triggers microparticle release from glial cells, EMBO J, 28 (2009) 1043-1054.
[288] B.H. Sung, T. Ketova, D. Hoshino, A. Zijlstra, A.M. Weaver, Directional cell movement through tissues is controlled by exosome secretion, Nat Commun, 6 (2015) 7164.
[289] A. Purushothaman, S.K. Bandari, J. Liu, J.A. Mobley, E.E. Brown, R.D. Sanderson, Fibronectin on the Surface of Myeloma Cell-derived Exosomes Mediates Exosome-Cell Interactions, J Biol Chem, 291 (2016) 1652-1663.

[290] M. Leiss, K. Beckmann, A. Giros, M. Costell, R. Fassler, The role of integrin binding sites in fibronectin matrix assembly in vivo, Curr Opin Cell Biol, 20 (2008) 502-507.
[291] K. Denzer, M. van Eijk, M.J. Kleijmeer, E. Jakobson, C. de Groot, H.J. Geuze, Follicular dendritic cells carry MHC class II-expressing microvesicles at their surface, J Immunol, 165 (2000) 1259-1265.
[292] I. Parolini, C. Federici, C. Raggi, L. Lugini, S. Palleschi, A. De Milito, C. Coscia, E. Iessi, M. Logozzi, A. Molinari, M. Colone, M. Tatti, M. Sargiacomo, S. Fais, Microenvironmental pH is a key factor for exosome traffic in tumor cells, J Biol Chem, 284 (2009) 34211-34222.
[293] I. Nakase, S. Futaki, Combined treatment with a pH-sensitive fusogenic peptide and cationic lipids achieves enhanced cytosolic delivery of exosomes, Sci Rep, 5 (2015) 10112.
[294] R. Jahn, T. Lang, T.C. Sudhof, Membrane fusion, Cell, 112 (2003) 519-533.
[295] L.V. Chernomordik, G.B. Melikyan, Y.A. Chizmadzhev, Biomembrane fusion: a new concept derived from model studies using two interacting planar lipid bilayers, Biochim Biophys Acta, 906 (1987) 309-352.
[296] L.V. Chernomordik, M.M. Kozlov, Mechanics of membrane fusion, Nat Struct Mol Biol, 15 (2008) 675-683.
[297] R. Jahn, T.C. Sudhof, Membrane fusion and exocytosis, Annu Rev Biochem, 68 (1999) 863-911.
[298] D. Feng, W.L. Zhao, Y.Y. Ye, X.C. Bai, R.Q. Liu, L.F. Chang, Q. Zhou, S.F. Sui, Cellular internalization of exosomes occurs through phagocytosis, Traffic, 11 (2010) 675-687.
[299] I. Nakase, N.B. Kobayashi, T. Takatani-Nakase, T. Yoshida, Active macropinocytosis induction by stimulation of epidermal growth factor receptor and oncogenic Ras expression potentiates cellular uptake efficacy of exosomes, Sci Rep, 5 (2015) 10300.
[300] T. Tian, Y.L. Zhu, Y.Y. Zhou, G.F. Liang, Y.Y. Wang, F.H. Hu, Z.D. Xiao, Exosome uptake through clathrin-mediated endocytosis and macropinocytosis and mediating miR-21 delivery, J Biol Chem, 289 (2014) 22258-22267.
[301] K. Laulagnier, C. Javalet, F.J. Hemming, M. Chivet, G. Lachenal, B. Blot, C. Chatellard, R. Sadoul, Amyloid precursor protein products concentrate in a subset of exosomes specifically endocytosed by neurons, Cell Mol Life Sci, 75 (2018) 757-773.
[302] A. Vargas, S. Zhou, M. Ethier-Chiasson, D. Flipo, J. Lafond, C. Gilbert, B. Barbeau, Syncytin proteins incorporated in placenta exosomes are important for cell uptake and show variation in abundance in serum exosomes from patients with preeclampsia, FASEB J, 28 (2014) 3703-3719.
[303] S. Kamerkar, V.S. LeBleu, H. Sugimoto, S. Yang, C.F. Ruivo, S.A. Melo, J.J. Lee, R. Kalluri, Exosomes facilitate therapeutic targeting of oncogenic KRAS in pancreatic cancer, Nature, 546 (2017) 498-503.
[304] C. Escrevente, S. Keller, P. Altevogt, J. Costa, Interaction and uptake of exosomes by ovarian cancer cells, BMC Cancer, 11 (2011) 108.
[305] S.P. Palecek, C.E. Schmidt, D.A. Lauffenburger, A.F. Horwitz, Integrin dynamics on the tail region of migrating fibroblasts, J Cell Sci, 109 (Pt 5) (1996) 941-952.
[306] O.O. Glebov, N.A. Bright, B.J. Nichols, Flotillin-1 defines a clathrin-independent endocytic pathway in mammalian cells, Nat Cell Biol, 8 (2006) 46-54.
[307] G.P. Otto, B.J. Nichols, The roles of flotillin microdomains--endocytosis and beyond, J Cell Sci, 124 (2011) 3933-3940.
[308] L.A. Mulcahy, R.C. Pink, D.R. Carter, Routes and mechanisms of extracellular vesicle uptake, J Extracell Vesicles, 3 (2014).
[309] H. Zhao, L. Yang, J. Baddour, A. Achreja, V. Bernard, T. Moss, J.C. Marini, T. Tudawe, E.G. Seviour, F.A. San Lucas, H. Alvarez, S. Gupta, S.N. Maiti, L. Cooper, D. Peehl, P.T. Ram, A. Maitra, D. Nagrath, Tumor microenvironment derived exosomes pleiotropically modulate cancer cell metabolism, Elife, 5 (2016) e10250.
[310] F. Haderk, R. Schulz, M. Iskar, L.L. Cid, T. Worst, K.V. Willmund, A. Schulz, U. Warnken, J. Seiler, A. Benner, M. Nessling, T. Zenz, M. Gobel, J. Durig, S. Diederichs, J. Paggetti, E. Moussay, S.

Stilgenbauer, M. Zapatka, P. Lichter, M. Seiffert, Tumor-derived exosomes modulate PD-L1 expression in monocytes, Sci Immunol, 2 (2017).
[311] H. Shinohara, Y. Kuranaga, M. Kumazaki, N. Sugito, Y. Yoshikawa, T. Takai, K. Taniguchi, Y. Ito, Y. Akao, Regulated Polarization of Tumor-Associated Macrophages by miR-145 via Colorectal Cancer-Derived Extracellular Vesicles, J Immunol, 199 (2017) 1505-1515.
[312] B. Costa-Silva, N.M. Aiello, A.J. Ocean, S. Singh, H. Zhang, B.K. Thakur, A. Becker, A. Hoshino, M.T. Mark, H. Molina, J. Xiang, T. Zhang, T.M. Theilen, G. Garcia-Santos, C. Williams, Y. Ararso, Y. Huang, G. Rodrigues, T.L. Shen, K.J. Labori, I.M. Lothe, E.H. Kure, J. Hernandez, A. Doussot, S.H. Ebbesen, P.M. Grandgenett, M.A. Hollingsworth, M. Jain, K. Mallya, S.K. Batra, W.R. Jarnagin, R.E. Schwartz, I. Matei, H. Peinado, B.Z. Stanger, J. Bromberg, D. Lyden, Pancreatic cancer exosomes initiate pre-metastatic niche formation in the liver, Nat Cell Biol, 17 (2015) 816-826.
[313] B.Y. Nabet, Y. Qiu, J.E. Shabason, T.J. Wu, T. Yoon, B.C. Kim, J.L. Benci, A.M. DeMichele, J. Tchou, J. Marcotrigiano, A.J. Minn, Exosome RNA Unshielding Couples Stromal Activation to Pattern Recognition Receptor Signaling in Cancer, Cell, 170 (2017) 352-366 e313.
[314] R.D. Allen, A.K. Fok, Membrane recycling and endocytosis in Paramecium confirmed by horseradish peroxidase pulse-chase studies, J Cell Sci, 45 (1980) 131-145.
[315] J. Klumperman, G. Raposo, The complex ultrastructure of the endolysosomal system, Cold Spring Harb Perspect Biol, 6 (2014) a016857.
[316] C. Raiborg, K.G. Bache, A. Mehlum, E. Stang, H. Stenmark, Hrs recruits clathrin to early endosomes, EMBO J, 20 (2001) 5008-5021.
[317] A. Wandinger-Ness, M. Zerial, Rab proteins and the compartmentalization of the endosomal system, Cold Spring Harb Perspect Biol, 6 (2014) a022616.
[318] J. Gruenberg, H. Stenmark, The biogenesis of multivesicular endosomes, Nat Rev Mol Cell Biol, 5 (2004) 317-323.
[319] J. Huotari, A. Helenius, Endosome maturation, EMBO J, 30 (2011) 3481-3500.
[320] C. Villarroya-Beltri, F. Baixauli, M. Mittelbrunn, I. Fernandez-Delgado, D. Torralba, O. Moreno-Gonzalo, S. Baldanta, C. Enrich, S. Guerra, F. Sanchez-Madrid, ISGylation controls exosome secretion by promoting lysosomal degradation of MVB proteins, Nat Commun, 7 (2016) 13588.
[321] C.M. Fader, D. Sanchez, M. Furlan, M.I. Colombo, Induction of autophagy promotes fusion of multivesicular bodies with autophagic vacuoles in k562 cells, Traffic, 9 (2008) 230-250.
[322] D.F. Bainton, The discovery of lysosomes, J Cell Biol, 91 (1981) 66s-76s.
[323] J.P. Luzio, P.R. Pryor, N.A. Bright, Lysosomes: fusion and function, Nat Rev Mol Cell Biol, 8 (2007) 622-632.
[324] T. Kolter, K. Sandhoff, Lysosomal degradation of membrane lipids, FEBS Lett, 584 (2010) 1700-1712.
[325] W.A. Dunn, Jr., Studies on the mechanisms of autophagy: formation of the autophagic vacuole, J Cell Biol, 110 (1990) 1923-1933.
[326] S.A. Tooze, A. Abada, Z. Elazar, Endocytosis and autophagy: exploitation or cooperation?, Cold Spring Harb Perspect Biol, 6 (2014) a018358.
[327] K. Moreau, B. Ravikumar, M. Renna, C. Puri, D.C. Rubinsztein, Autophagosome precursor maturation requires homotypic fusion, Cell, 146 (2011) 303-317.
[328] M.G. Gutierrez, D.B. Munafo, W. Beron, M.I. Colombo, Rab7 is required for the normal progression of the autophagic pathway in mammalian cells, J Cell Sci, 117 (2004) 2687-2697.
[329] M.F. Baietti, Z. Zhang, E. Mortier, A. Melchior, G. Degeest, A. Geeraerts, Y. Ivarsson, F. Depoortere, C. Coomans, E. Vermeiren, P. Zimmermann, G. David, Syndecan-syntenin-ALIX regulates the biogenesis of exosomes, Nat Cell Biol, 14 (2012) 677-685.
[330] G. van Niel, R. Wubbolts, T. Ten Broeke, S.I. Buschow, F.A. Ossendorp, C.J. Melief, G. Raposo, B.W. van Balkom, W. Stoorvogel, Dendritic cells regulate exposure of MHC class II at their plasma membrane by oligoubiquitination, Immunity, 25 (2006) 885-894.

[331] F.X. Guix, R. Sannerud, F. Berditchevski, A.M. Arranz, K. Horre, A. Snellinx, A. Thathiah, T. Saido, T. Saito, S. Rajesh, M. Overduin, S. Kumar-Singh, E. Radaelli, N. Corthout, J. Colombelli, S. Tosi, S. Munck, I.H. Salas, W. Annaert, B. De Strooper, Tetraspanin 6: a pivotal protein of the multiple vesicular body determining exosome release and lysosomal degradation of amyloid precursor protein fragments, Mol Neurodegener, 12 (2017) 25.
[332] M.V. Dias, B.L. Teixeira, B.R. Rodrigues, R. Sinigaglia-Coimbra, I. Porto-Carreiro, M. Roffe, G.N. Hajj, V.R. Martins, PRNP/prion protein regulates the secretion of exosomes modulating CAV1/caveolin-1-suppressed autophagy, Autophagy, 12 (2016) 2113-2128.
[333] D.J. Yamashiro, B. Tycko, S.R. Fluss, F.R. Maxfield, Segregation of transferrin to a mildly acidic (pH 6.5) para-Golgi compartment in the recycling pathway, Cell, 37 (1984) 789-800.
[334] F.R. Maxfield, T.E. McGraw, Endocytic recycling, Nat Rev Mol Cell Biol, 5 (2004) 121-132.
[335] B.D. Grant, J.G. Donaldson, Pathways and mechanisms of endocytic recycling, Nat Rev Mol Cell Biol, 10 (2009) 597-608.
[336] T. Wang, D.M. Gilkes, N. Takano, L. Xiang, W. Luo, C.J. Bishop, P. Chaturvedi, J.J. Green, G.L. Semenza, Hypoxia-inducible factors and RAB22A mediate formation of microvesicles that stimulate breast cancer invasion and metastasis, Proc Natl Acad Sci U S A, 111 (2014) E3234-3242.
[337] T. Stasyk, L.A. Huber, Spatio-Temporal Parameters of Endosomal Signaling in Cancer: Implications for New Treatment Options, J Cell Biochem, 117 (2016) 836-843.
[338] A. Jemal, F. Bray, M.M. Center, J. Ferlay, E. Ward, D. Forman, Global cancer statistics, CA Cancer J Clin, 61 (2011) 69-90.
[339] V. Lopes-Rodrigues, A. Di Luca, D. Sousa, H. Seca, P. Meleady, M. Henry, R.T. Lima, R. O'Connor, M.H. Vasconcelos, Multidrug resistant tumour cells shed more microvesicle-like EVs and less exosomes than their drug-sensitive counterpart cells, Biochim Biophys Acta, 1860 (2016) 618-627.
[340] V. Lopes-Rodrigues, A. Di Luca, D. Sousa, H. Seca, P. Meleady, M. Henry, R.T. Lima, R. O'Connor, M.H. Vasconcelos, Data supporting the shedding of larger extracellular vesicles by multidrug resistant tumour cells, Data Brief, 6 (2016) 1023-1027.
[341] V. Lopes-Rodrigues, A. Di Luca, J. Mleczko, P. Meleady, M. Henry, M. Pesic, D. Cabrera, S. van Liempd, R.T. Lima, R. O'Connor, J.M. Falcon-Perez, M.H. Vasconcelos, Identification of the metabolic alterations associated with the multidrug resistant phenotype in cancer and their intercellular transfer mediated by extracellular vesicles, Sci Rep, 7 (2017) 44541.
[342] F.F. Zhang, Y.F. Zhu, Q.N. Zhao, D.T. Yang, Y.P. Dong, L. Jiang, W.X. Xing, X.Y. Li, H. Xing, M. Shi, Y. Chen, I.C. Bruce, J. Jin, X. Ma, Microvesicles mediate transfer of P-glycoprotein to paclitaxel-sensitive A2780 human ovarian cancer cells, conferring paclitaxel-resistance, Eur J Pharmacol, 738 (2014) 83-90.
[343] W.X. Chen, X.M. Liu, M.M. Lv, L. Chen, J.H. Zhao, S.L. Zhong, M.H. Ji, Q. Hu, Z. Luo, J.Z. Wu, J.H. Tang, Exosomes from drug-resistant breast cancer cells transmit chemoresistance by a horizontal transfer of microRNAs, PLoS One, 9 (2014) e95240.
[344] D.Y. Choi, S. You, J.H. Jung, J.C. Lee, J.K. Rho, K.Y. Lee, M.R. Freeman, K.P. Kim, J. Kim, Extracellular vesicles shed from gefitinib-resistant nonsmall cell lung cancer regulate the tumor microenvironment, Proteomics, 14 (2014) 1845-1856.
[345] D. Sousa, R.T. Lima, M.H. Vasconcelos, Intercellular Transfer of Cancer Drug Resistance Traits by Extracellular Vesicles, Trends Mol Med, 21 (2015) 595-608.
[346] H. Shao, H. Im, C.M. Castro, X. Breakefield, R. Weissleder, H. Lee, New Technologies for Analysis of Extracellular Vesicles, Chem Rev, 118 (2018) 1917-1950.
[347] P. Chaluvally-Raghavan, K.J. Jeong, S. Pradeep, A.M. Silva, S. Yu, W. Liu, T. Moss, C. Rodriguez-Aguayo, D. Zhang, P. Ram, J. Liu, Y. Lu, G. Lopez-Berestein, G.A. Calin, A.K. Sood, G.B. Mills, Direct Upregulation of STAT3 by MicroRNA-551b-3p Deregulates Growth and Metastasis of Ovarian Cancer, Cell Rep, 15 (2016) 1493-1504.
[348] Y.J. Shu, R.F. Bao, L. Jiang, Z. Wang, X.A. Wang, F. Zhang, H.B. Liang, H.F. Li, Y.Y. Ye, S.S. Xiang, H. Weng, X.S. Wu, M.L. Li, Y.P. Hu, W. Lu, Y.J. Zhang, J. Zhu, P. Dong, Y.B. Liu, MicroRNA-

29c-5p suppresses gallbladder carcinoma progression by directly targeting CPEB4 and inhibiting the MAPK pathway, Cell Death Differ, 24 (2017) 445-457.
[349] C. Li, Q. Dong, X. Che, L. Xu, Z. Li, Y. Fan, K. Hou, S. Wang, J. Qu, L. Xu, T. Wen, X. Yang, X. Qu, Y. Liu, MicroRNA-29b-2-5p inhibits cell proliferation by directly targeting Cbl-b in pancreatic ductal adenocarcinoma, BMC Cancer, 18 (2018) 681.
[350] L.L. Huang, L.W. Huang, L. Wang, B.D. Tong, Q. Wei, X.S. Ding, Potential role of miR-139-5p in cancer diagnosis, prognosis and therapy, Oncol Lett, 14 (2017) 1215-1222.
[351] M. Diaz-Martinez, L. Benito-Jardon, L. Alonso, L. Koetz-Ploch, E. Hernando, J. Teixido, miR-204-5p and miR-211-5p Contribute to BRAF Inhibitor Resistance in Melanoma, Cancer Res, 78 (2018) 1017-1030.
[352] J. Jiang, C. Xie, Y. Liu, Q. Shi, Y. Chen, Up-regulation of miR-383-5p suppresses proliferation and enhances chemosensitivity in ovarian cancer cells by targeting TRIM27, Biomed Pharmacother, 109 (2019) 595-601.
[353] M.F. Ye, J.G. Zhang, T.X. Guo, X.J. Pan, MiR-504 inhibits cell proliferation and invasion by targeting LOXL2 in non small cell lung cancer, Biomed Pharmacother, 97 (2018) 1289-1295.
[354] A.K. Fuzery, J. Levin, M.M. Chan, D.W. Chan, Translation of proteomic biomarkers into FDA approved cancer diagnostics: issues and challenges, Clin Proteomics, 10 (2013) 13.
[355] A.P. Drabovich, E. Martinez-Morillo, E.P. Diamandis, Toward an integrated pipeline for protein biomarker development, Biochim Biophys Acta, 1854 (2015) 677-686.
[356] Z. Wei, A.O. Batagov, S. Schinelli, J. Wang, Y. Wang, R. El Fatimy, R. Rabinovsky, L. Balaj, C.C. Chen, F. Hochberg, B. Carter, X.O. Breakefield, A.M. Krichevsky, Coding and noncoding landscape of extracellular RNA released by human glioma stem cells, Nat Commun, 8 (2017) 1145.
[357] L. Poliseno, A. Marranci, P.P. Pandolfi, Pseudogenes in Human Cancer, Front Med (Lausanne), 2 (2015) 68.
[358] G. Yu, W. Yao, K. Gumireddy, A. Li, J. Wang, W. Xiao, K. Chen, H. Xiao, H. Li, K. Tang, Z. Ye, Q. Huang, H. Xu, Pseudogene PTENP1 functions as a competing endogenous RNA to suppress clear-cell renal cell carcinoma progression, Mol Cancer Ther, 13 (2014) 3086-3097.
[359] Y. Pan, C. Sun, M. Huang, Y. Liu, F. Qi, L. Liu, J. Wen, J. Liu, K. Xie, H. Ma, Z. Hu, H. Shen, A genetic variant in pseudogene E2F3P1 contributes to prognosis of hepatocellular carcinoma, J Biomed Res, 28 (2014) 194-200.
[360] M. Pathan, P. Fonseka, S.V. Chitti, T. Kang, R. Sanwlani, J. Van Deun, A. Hendrix, S. Mathivanan, Vesiclepedia 2019: a compendium of RNA, proteins, lipids and metabolites in extracellular vesicles, Nucleic Acids Res, 47 (2019) D516-D519.
[361] A.O. Batagov, I.V. Kurochkin, Exosomes secreted by human cells transport largely mRNA fragments that are enriched in the 3'-untranslated regions, Biol Direct, 8 (2013) 12.
[362] R. Jaiswal, F. Luk, J. Gong, J.M. Mathys, G.E. Grau, M. Bebawy, Microparticle conferred microRNA profiles--implications in the transfer and dominance of cancer traits, Mol Cancer, 11 (2012) 37.
[363] A. Turchinovich, L. Weiz, A. Langheinz, B. Burwinkel, Characterization of extracellular circulating microRNA, Nucleic Acids Res, 39 (2011) 7223-7233.
[364] M.L. Squadrito, C. Baer, F. Burdet, C. Maderna, G.D. Gilfillan, R. Lyle, M. Ibberson, M. De Palma, Endogenous RNAs modulate microRNA sorting to exosomes and transfer to acceptor cells, Cell Rep, 8 (2014) 1432-1446.
[365] J.P. Tosar, F. Gambaro, J. Sanguinetti, B. Bonilla, K.W. Witwer, A. Cayota, Assessment of small RNA sorting into different extracellular fractions revealed by high-throughput sequencing of breast cell lines, Nucleic Acids Res, 43 (2015) 5601-5616.
[366] V. Goler-Baron, I. Sladkevich, Y.G. Assaraf, Inhibition of the PI3K-Akt signaling pathway disrupts ABCG2-rich extracellular vesicles and overcomes multidrug resistance in breast cancer cells, Biochem Pharmacol, 83 (2012) 1340-1348.

[367] J. Yin, X. Yan, X. Yao, Y. Zhang, Y. Shan, N. Mao, Y. Yang, L. Pan, Secretion of annexin A3 from ovarian cancer cells and its association with platinum resistance in ovarian cancer patients, J Cell Mol Med, 16 (2012) 337-348.
[368] T. Aung, B. Chapuy, D. Vogel, D. Wenzel, M. Oppermann, M. Lahmann, T. Weinhage, K. Menck, T. Hupfeld, R. Koch, L. Trumper, G.G. Wulf, Exosomal evasion of humoral immunotherapy in aggressive B-cell lymphoma modulated by ATP-binding cassette transporter A3, Proc Natl Acad Sci U S A, 108 (2011) 15336-15341.
[369] A. Roseblade, F. Luk, A. Ung, M. Bebawy, Targeting microparticle biogenesis: a novel approach to the circumvention of cancer multidrug resistance, Curr Cancer Drug Targets, 15 (2015) 205-214.
[370] S. Rana, S. Yue, D. Stadel, M. Zoller, Toward tailored exosomes: the exosomal tetraspanin web contributes to target cell selection, Int J Biochem Cell Biol, 44 (2012) 1574-1584.
[371] D. Zech, S. Rana, M.W. Buchler, M. Zoller, Tumor-exosomes and leukocyte activation: an ambivalent crosstalk, Cell Commun Signal, 10 (2012) 37.
[372] F. Guerra, A. Paiano, D. Migoni, G. Girolimetti, A.M. Perrone, P. De Iaco, F.P. Fanizzi, G. Gasparre, C. Bucci, Modulation of RAB7A Protein Expression Determines Resistance to Cisplatin through Late Endocytic Pathway Impairment and Extracellular Vesicular Secretion, Cancers (Basel), 11 (2019).
[373] X.J. Liang, S. Mukherjee, D.W. Shen, F.R. Maxfield, M.M. Gottesman, Endocytic recycling compartments altered in cisplatin-resistant cancer cells, Cancer Res, 66 (2006) 2346-2353.
[374] X.J. Liang, D.W. Shen, S. Garfield, M.M. Gottesman, Mislocalization of membrane proteins associated with multidrug resistance in cisplatin-resistant cancer cell lines, Cancer Res, 63 (2003) 5909-5916.
[375] A. Palmeira, M.H. Vasconcelos, A. Paiva, M.X. Fernandes, M. Pinto, E. Sousa, Dual inhibitors of P-glycoprotein and tumor cell growth: (re)discovering thioxanthones, Biochem Pharmacol, 83 (2012) 57-68.
[376] J. Barbosa, R.T. Lima, D. Sousa, A.S. Gomes, A. Palmeira, H. Seca, K. Choosang, P. Pakkong, H. Bousbaa, M.M. Pinto, E. Sousa, M.H. Vasconcelos, M. Pedro, Screening a Small Library of Xanthones for Antitumor Activity and Identification of a Hit Compound which Induces Apoptosis, Molecules, 21 (2016) 81.
[377] R.T. Lima, D. Sousa, A.S. Gomes, N. Mendes, R. Matthiesen, M. Pedro, F. Marques, M.M. Pinto, E. Sousa, M.H. Vasconcelos, The Antitumor Activity of a Lead Thioxanthone is Associated with Alterations in Cholesterol Localization, Molecules, 23 (2018).

ANNEXES

Supplementary Tables from research paper 1 "**Deep sequencing analysis reveals distinctive non-coding RNAs when comparing tumour multidrug resistant cells and extracellular vesicles with drug-sensitive counterparts**":

The complete Supplementary Tables were submitted to "Cancers" (for online publication). However, due to space constraints, only the results with $p<0.05$ or log fold change<1, depending on the samples, are included in this thesis.

Annex 1: Table S2- Log Fold Change of RNA species expression between drug-sensitive (NCI-H460) cells and their MDR (NCI-H460/R) counterparts.

ensembl_transcript_id	ensembl_gene_id	logFC	logCPM	PValue	description
ENST00000362257	ENSG00000199127	8,828522389	6,686568583	8,3398E-20	microRNA 383 [Source:HGNC Symbol;Acc:HGNC:31876]
ENST00000384866	ENSG00000207598	-6,23856134	7,010302474	5,19711E-17	microRNA 124-3 [Source:HGNC Symbol;Acc:HGNC:31504]
ENST00000385081	ENSG00000207816	-5,95837547	6,972597494	6,63024E-17	microRNA 124-2 [Source:HGNC Symbol;Acc:HGNC:31503]
ENST00000384854	ENSG00000207586	5,269338884	8,842112136	3,42365E-15	microRNA 135a-2 [Source:HGNC Symbol;Acc:HGNC:31521]
ENST00000315274	ENSG00000196611	5,200586574	5,672065889	4,93846E-10	matrix metallopeptidase 1 [Source:HGNC Symbol;Acc:HGNC:7155]
ENST00000581569	ENSG00000265331	4,238612651	5,447299984	3,35828E-08	microRNA 4524b [Source:HGNC Symbol;Acc:HGNC:43520]
ENST00000401120	ENSG00000215939	2,89972431	6,149495057	2,0086E-06	microRNA 873 [Source:HGNC Symbol;Acc:HGNC:33663]
ENST00000368738	ENSG00000163220	-4,157690517	4,643346617	3,80652E-06	S100 calcium binding protein A9 [Source:HGNC Symbol;Acc:HGNC:10499]
ENST00000325602	ENSG00000181631	-5,801667083	4,708285842	3,95644E-06	purinergic receptor P2Y13 [Source:HGNC Symbol;Acc:HGNC:4537]
ENST00000481190	ENSG00000100292	2,641973535	5,579523331	6,70145E-05	heme oxygenase 1 [Source:HGNC Symbol;Acc:HGNC:5013]
ENST00000266546	ENSG00000139182	3,705936238	4,731457786	7,05975E-05	calsyntenin 3 [Source:HGNC Symbol;Acc:HGNC:18371]
ENST00000411281		-3,307122921	4,99852988	0,000103122	
ENST00000440465	ENSG00000229644	-3,605239034	5,009666661	0,000140166	nicotinamide phosphoribosyltransferase pseudogene 1 [Source:HGNC Sym
ENST00000359297	ENSG00000196182	5,370012765	4,95150829	0,000330791	serine/threonine kinase 40 [Source:HGNC Symbol;Acc:HGNC:21373]
ENST00000580000	ENSG00000266107	2,670223613	5,629750367	0,000343206	microRNA 4525 [Source:HGNC Symbol;Acc:HGNC:41903]
ENST00000505555	ENSG00000073578	-5,744437039	4,644207158	0,000424798	succinate dehydrogenase complex flavoprotein subunit A [Source:HGNC S
ENST00000509176	ENSG00000184305	-4,676031775	5,44620271	0,000484845	coiled-coil serine rich protein 1 [Source:HGNC Symbol;Acc:HGNC:29349]
ENST00000385078	ENSG00000207813	5,246775298	4,490319469	0,00056581	microRNA 605 [Source:HGNC Symbol;Acc:HGNC:32861]
ENST00000363064	ENSG00000199934	-1,972010966	6,114224829	0,000621824	
ENST00000607298	ENSG00000271734	-2,053291478	5,886448493	0,000646606	novel transcript
ENST00000411948	ENSG00000203667	-2,005200008	5,963677038	0,000744384	cytochrome c oxidase assembly factor COX20 [Source:HGNC Symbol;Acc:H
ENST00000384999	ENSG00000207732	3,851240161	5,410704529	0,000773059	microRNA 218-1 [Source:HGNC Symbol;Acc:HGNC:31595]
ENST00000486535	ENSG00000107902	3,131589624	4,593298494	0,000845063	phospholysine phosphohistidine inorganic pyrophosphate phosphatase [S
ENST00000362639	ENSG00000199509	-2,735140645	5,000443515	0,000890841	RNA, 5S ribosomal pseudogene 477 [Source:HGNC Symbol;Acc:HGNC:4337
ENST00000307366	ENSG00000168569	2,601665056	5,504872963	0,000911077	transmembrane protein 223 [Source:HGNC Symbol;Acc:HGNC:28464]
ENST00000358460	ENSG00000182518	-3,773144102	5,075789459	0,000944487	family with sequence similarity 104 member B [Source:HGNC Symbol;Acc:
ENST00000580859	ENSG00000265110	-3,118445415	4,932704384	0,001037231	microRNA 4731 [Source:HGNC Symbol;Acc:HGNC:41597]
ENST00000216968	ENSG00000101000	-2,719057535	4,58996104	0,001040158	protein C receptor [Source:HGNC Symbol;Acc:HGNC:9452]
ENST00000242351	ENSG00000105939	-2,144473665	6,878830868	0,001377413	zinc finger CCCH-type containing, antiviral 1 [Source:HGNC Symbol;Acc:HG
ENST00000261187	ENSG00000118596	-4,049330744	4,622080826	0,001394136	solute carrier family 16 member 7 [Source:HGNC Symbol;Acc:HGNC:10928
ENST00000514506	ENSG00000249906	2,889916229	4,567738323	0,00139885	
ENST00000324460	ENSG00000044574	-2,718350018	7,464324415	0,001921754	heat shock protein family A (Hsp70) member 5 [Source:HGNC Symbol;Acc:
ENST00000580706	ENSG00000154059	-4,478184729	4,415681337	0,002037372	impact RWD domain protein [Source:HGNC Symbol;Acc:HGNC:20387]
ENST00000578924	ENSG00000265724	-2,226305296	5,642881256	0,002311658	microRNA 4284 [Source:HGNC Symbol;Acc:HGNC:38322]
ENST00000367558	ENSG00000143333	-2,588297678	4,727112263	0,002414872	regulator of G protein signaling 16 [Source:HGNC Symbol;Acc:HGNC:9997]
ENST00000307365	ENSG00000168209	-2,726722175	4,615259315	0,002504929	DNA damage inducible transcript 4 [Source:HGNC Symbol;Acc:HGNC:2494
ENST00000280706	ENSG00000166800	2,908709047	4,864435629	0,002844813	lactate dehydrogenase A like 6A [Source:HGNC Symbol;Acc:HGNC:28335]
ENST00000491153	ENSG00000117139	-5,052621113	4,45524212	0,002903129	lysine demethylase 5B [Source:HGNC Symbol;Acc:HGNC:18039]
ENST00000385065	ENSG00000207800	-1,426119082	8,429407837	0,002957409	microRNA 504 [Source:HGNC Symbol;Acc:HGNC:32139]
ENST00000385278	ENSG00000208013	-2,318889616	10,59077314	0,002969655	microRNA 652 [Source:HGNC Symbol;Acc:HGNC:32908]
ENST00000371419	ENSG00000101132	2,772880094	4,611840158	0,003097432	prefoldin subunit 4 [Source:HGNC Symbol;Acc:HGNC:8868]
ENST00000584034	ENSG00000264720	1,602048487	5,748306762	0,003532863	microRNA 3117 [Source:HGNC Symbol;Acc:HGNC:38385]
ENST00000223642	ENSG00000106804	2,896028409	4,906297854	0,003544172	complement C5 [Source:HGNC Symbol;Acc:HGNC:1331]
ENST00000563972	ENSG00000204991	3,479288651	4,860297581	0,003572941	spire type actin nucleation factor 2 [Source:HGNC Symbol;Acc:HGNC:3062
ENST00000454901	ENSG00000236686	-3,090766943	4,436092491	0,003600929	basic leucine zipper and W2 domains 1 pseudogene 1 [Source:HGNC Symb
ENST00000408510		-5,010625445	4,448443163	0,003733723	
ENST00000507522	ENSG00000073578	-5,694274422	4,682871961	0,003833241	succinate dehydrogenase complex flavoprotein subunit A [Source:HGNC S
ENST00000531326	ENSG00000179295	-3,063995901	5,222558736	0,003950957	protein tyrosine phosphatase, non-receptor type 11 [Source:HGNC Symbo
ENST00000357618	ENSG00000010704	-4,347493235	4,379547901	0,004040602	homeostatic iron regulator [Source:HGNC Symbol;Acc:HGNC:4886]
ENST00000401147	ENSG00000215966	2,59583437	5,183992276	0,004107476	microRNA 876 [Source:HGNC Symbol;Acc:HGNC:33653]
ENST00000569146	ENSG00000153815	2,89853953	4,524544794	0,004198122	c-Maf inducing protein [Source:HGNC Symbol;Acc:HGNC:24319]
ENST00000323646	ENSG00000176485	2,233505908	4,521302906	0,004452586	phospholipase A2 group XVI [Source:HGNC Symbol;Acc:HGNC:17825]
ENST00000408404	ENSG00000221331	-2,797034874	4,766881589	0,004525743	microRNA 548q [Source:HGNC Symbol;Acc:HGNC:37312]
ENST00000559111	ENSG00000259706	-4,146529379	6,025530515	0,004610015	heat shock protein 90 beta family member 2, pseudogene [Source:HGNC S
ENST00000365153	ENSG00000202023	-2,144842774	5,05415399	0,005080474	
ENST00000384914	ENSG00000207647	-2,44225711	4,774957299	0,00508926	microRNA 153-1 [Source:HGNC Symbol;Acc:HGNC:31539]
ENST00000417727	ENSG00000237662	-3,19465491	4,482088172	0,005195133	suppressor of cytokine signaling 2 pseudogene 1 [Source:HGNC Symbol;Ac
ENST00000577474	ENSG00000153339	2,25801488	4,663953798	0,005206641	trafficking protein particle complex 8 [Source:HGNC Symbol;Acc:HGNC:29
ENST00000581094	ENSG00000126858	-2,336257302	4,864282257	0,005277588	ras homolog family member T1 [Source:HGNC Symbol;Acc:HGNC:21168]
ENST00000222553	ENSG00000105835	-2,17625273	5,200913287	0,005587208	nicotinamide phosphoribosyltransferase [Source:HGNC Symbol;Acc:HGNC
ENST00000586927	ENSG00000186115	3,031076129	4,808397365	0,005761234	cytochrome P450 family 4 subfamily F member 2 [Source:HGNC Symbol;A
ENST00000408552	ENSG00000221479	4,64591888	4,365983176	0,005825286	microRNA 1251 [Source:HGNC Symbol;Acc:HGNC:35317]
ENST00000244020	ENSG00000124193	-2,707437157	4,664078388	0,006207906	serine and arginine rich splicing factor 6 [Source:HGNC Symbol;Acc:HGNC:
ENST00000385200	ENSG00000207935	3,861503273	12,70856783	0,006336951	microRNA 204 [Source:HGNC Symbol;Acc:HGNC:31582]
ENST00000395067	ENSG00000066697	-2,589693948	4,764055104	0,006362928	Myb/SANT DNA binding domain containing 3 [Source:HGNC Symbol;Acc:H
ENST00000508619	ENSG00000250632	4,410131348	4,385847104	0,006446133	long intergenic non-protein coding RNA 2171 [Source:HGNC Symbol;Acc:H

ENST00000512782	ENSG00000215158	4,41422341	4,352218022	0,006480836	Putative beta-glucuronidase-like protein FLJ75287 pseudogene
ENST00000426767	ENSG00000225264	-1,934831205	5,34978577	0,006482438	zinc and ring finger 2 pseudogene 2 [Source:HGNC Symbol;Acc:HGNC:4279
ENST00000375121	ENSG00000178828	2,287858205	4,397677684	0,006625272	ring finger protein 186 [Source:HGNC Symbol;Acc:HGNC:25978]
ENST00000261037	ENSG00000144810	-2,063817502	5,112186535	0,006859708	collagen type VIII alpha 1 chain [Source:HGNC Symbol;Acc:HGNC:2215]
ENST00000461727	ENSG00000187017	-5,3472185	4,585074488	0,007135969	espin [Source:HGNC Symbol;Acc:HGNC:13281]
ENST00000460443	ENSG00000134255	3,086850347	4,462958376	0,007141149	choline/ethanolamine phosphotransferase 1 [Source:HGNC Symbol;Acc:H
ENST00000295633	ENSG00000163430	2,540577946	4,621758041	0,007171537	follistatin like 1 [Source:HGNC Symbol;Acc:HGNC:3972]
ENST00000297625	ENSG00000164976	-4,253869622	4,60179789	0,007250737	myogenesis regulating glycosidase (putative) [Source:HGNC Symbol;Acc:H
ENST00000246024	ENSG00000125827	-2,611228269	4,868499897	0,007283782	thioredoxin related transmembrane protein 4 [Source:HGNC Symbol;Acc:H
ENST00000492418	ENSG00000165091	-2,437710711	4,803056206	0,007370814	transmembrane channel like 1 [Source:HGNC Symbol;Acc:HGNC:16513]
ENST00000362532	ENSG00000199402	-1,77989188	5,773111693	0,00752791	RNA, 5S ribosomal pseudogene 308 [Source:HGNC Symbol;Acc:HGNC:4320
ENST00000363664	ENSG00000200534	-1,600467704	7,923169294	0,007629241	small nucleolar RNA, H/ACA box 33 [Source:HGNC Symbol;Acc:HGNC:3262
ENST00000492851	ENSG00000142156	-2,164491688	4,513395061	0,007762442	collagen type VI alpha 1 chain [Source:HGNC Symbol;Acc:HGNC:2211]
ENST00000274457	ENSG00000145780	-2,198201783	5,092530271	0,007821998	fem-1 homolog C [Source:HGNC Symbol;Acc:HGNC:16933]
ENST00000416826	ENSG00000236404	2,401298434	4,56335693	0,007828694	VLDLR antisense RNA 1 [Source:HGNC Symbol;Acc:HGNC:49621]
ENST00000564305	ENSG00000261617	1,944792575	5,03887756	0,007917614	long intergenic non-protein coding RNA 2177 [Source:HGNC Symbol;Acc:H
ENST00000417156	ENSG00000224797	4,133839212	4,297170183	0,008020902	ribosomal protein L37 (RPL37) pseudogene
ENST00000332395	ENSG00000182810	2,385268787	4,696107722	0,008134571	DEAD-box helicase 28 [Source:HGNC Symbol;Acc:HGNC:17330]
ENST00000385006	ENSG00000207739	4,517813519	4,635139812	0,00827063	microRNA 218-2 [Source:HGNC Symbol;Acc:HGNC:31596]
ENST00000316594	ENSG00000126945	-3,519107124	4,911753126	0,008418728	heterogeneous nuclear ribonucleoprotein H2 [Source:HGNC Symbol;Acc:H
ENST00000365400	ENSG00000202270	-3,230183563	5,542437241	0,008781911	small nucleolar RNA, C/D box 114-12 [Source:HGNC Symbol;Acc:HGNC:330
ENST00000515805	ENSG00000249708	3,535708892	5,140322388	0,009315363	novel transcript
ENST00000577066	ENSG00000226137	2,662444898	4,595254909	0,0095489	BAIAP2 divergent transcript [Source:HGNC Symbol;Acc:HGNC:44342]
ENST00000596207	ENSG00000267857	-4,322596513	4,41361542	0,009590153	novel transcript
ENST00000551295	ENSG00000018236	2,312741875	4,559444965	0,009605057	contactin 1 [Source:HGNC Symbol;Acc:HGNC:2171]
ENST00000384027	ENSG00000206754	-1,424044516	9,240925588	0,009634532	small nucleolar RNA, C/D box 101 [Source:HGNC Symbol;Acc:HGNC:32764
ENST00000227756	ENSG00000110328	-2,544499109	4,623165384	0,009698003	polypeptide N-acetylgalactosaminyltransferase 18 [Source:HGNC Symbol;
ENST00000583907	ENSG00000265541	3,125928626	4,45700498	0,01009297	H3 histone, family 3B pseudogene 2 [Source:HGNC Symbol;Acc:HGNC:429
ENST00000325346	ENSG00000172345	-2,280272058	4,588183737	0,010431232	StAR related lipid transfer domain containing 5 [Source:HGNC Symbol;Acc
ENST00000363156	ENSG00000200026	-1,378706736	7,167806568	0,010729405	
ENST00000260630		-2,90508392	4,949785571	0,010760315	
ENST00000369528	ENSG00000052723	-4,208717089	4,623170124	0,010794884	suppressor of IKBKE 1 [Source:HGNC Symbol;Acc:HGNC:26119]
ENST00000469003	ENSG00000160050	-4,708440178	4,424712119	0,010848717	coiled-coil domain containing 28B [Source:HGNC Symbol;Acc:HGNC:28163
ENST00000363608	ENSG00000200478	2,692100187	4,925137714	0,011059584	small nucleolar RNA, C/D box 115-41 [Source:HGNC Symbol;Acc:HGNC:330
ENST00000432191	ENSG00000134283	4,396575911	4,36476668	0,011091796	periphilin 1 [Source:HGNC Symbol;Acc:HGNC:19369]
ENST00000584249	ENSG00000265154	-1,348764681	6,53331037	0,011182787	microRNA 151b [Source:HGNC Symbol;Acc:HGNC:41588]
ENST00000286574	ENSG00000156076	2,205296445	4,745901478	0,011275572	WNT inhibitory factor 1 [Source:HGNC Symbol;Acc:HGNC:18081]
ENST00000600737	ENSG00000032444	1,959456679	4,857935341	0,011632746	patatin like phospholipase domain containing 6 [Source:HGNC Symbol;Acc
ENST00000362997	ENSG00000199867	-2,050981514	7,23035142	0,011757597	
ENST00000401258	ENSG00000216077	1,943598082	8,187328259	0,011800707	microRNA 887 [Source:HGNC Symbol;Acc:HGNC:33661]
ENST00000248594	ENSG00000127947	-2,978075853	4,481643949	0,012128682	protein tyrosine phosphatase, non-receptor type 12 [Source:HGNC Symbo
ENST00000581519	ENSG00000177728	2,887608593	4,365229847	0,012128682	transmembrane protein 94 [Source:HGNC Symbol;Acc:HGNC:28983]
ENST00000453270	ENSG00000185551	-2,860735436	4,42626577	0,012128682	nuclear receptor subfamily 2 group F member 2 [Source:HGNC Symbol;Acc
ENST00000458403	ENSG00000224821	2,155553999	4,393312329	0,012128682	COL4A2 antisense 2 [Source:HGNC Symbol;Acc:HGNC:39849]
ENST00000329399	ENSG00000107438	2,155465446	4,413127385	0,012128682	PDZ and LIM domain 1 [Source:HGNC Symbol;Acc:HGNC:2067]
ENST00000577171	ENSG00000261227	-4,309616723	4,395980934	0,012273835	novel transcript
ENST00000491701	ENSG00000115295	-1,158727219	5,84419142	0,012476027	CAP-Gly domain containing linker protein family member 4 [Source:HGNC
ENST00000363368	ENSG00000200238	-1,340896126	7,442131577	0,012640502	RNA, 5S ribosomal pseudogene 133 [Source:HGNC Symbol;Acc:HGNC:4303
ENST00000565468	ENSG00000261115	2,225093012	5,578935943	0,012721149	transmembrane protein 178B [Source:HGNC Symbol;Acc:HGNC:44112]
ENST00000367203	ENSG00000143842	-1,695013596	5,067868115	0,012860011	SRY-box 13 [Source:HGNC Symbol;Acc:HGNC:11192]
ENST00000443317	ENSG00000214185	-4,858888168	4,616040666	0,012947171	exportin for tRNA pseudogene 1 [Source:HGNC Symbol;Acc:HGNC:16586]
ENST00000362681	ENSG00000199551	-2,346529494	4,526614242	0,013512789	RNA, U6 small nuclear 545, pseudogene [Source:HGNC Symbol;Acc:HGNC:
ENST00000302190	ENSG00000169439	-4,381769021	4,405165713	0,013567207	syndecan 2 [Source:HGNC Symbol;Acc:HGNC:10659]
ENST00000462515	ENSG00000032389	1,957499198	4,690160058	0,013696443	EARP complex and GARP complex interacting protein 1 [Source:HGNC Sym
ENST00000362262	ENSG00000199132	-2,423029451	5,572624788	0,013812909	microRNA 450a-1 [Source:HGNC Symbol;Acc:HGNC:28008]
ENST00000295228	ENSG00000163083	-0,839465599	7,869722949	0,013925253	inhibin subunit beta B [Source:HGNC Symbol;Acc:HGNC:6067]
ENST00000364642	ENSG00000201512	-2,231322157	4,977814103	0,014004577	small nucleolar RNA, H/ACA box 71C [Source:HGNC Symbol;Acc:HGNC:326
ENST00000571100	ENSG00000171246	-1,865341165	4,531662776	0,014376332	neuronal pentraxin 1 [Source:HGNC Symbol;Acc:HGNC:7952]
ENST00000545752	ENSG00000158023	-2,965577539	4,464266464	0,014721164	WD repeat domain 66 [Source:HGNC Symbol;Acc:HGNC:28506]
ENST00000326840	ENSG00000057019	-1,917534512	4,883805279	0,01500281	discoidin, CUB and LCCL domain containing 2 [Source:HGNC Symbol;Acc:H
ENST00000296849	ENSG00000145506	-3,127551414	5,400202072	0,015291502	naked cuticle homolog 2 [Source:HGNC Symbol;Acc:HGNC:17046]
ENST00000260197	ENSG00000137642	3,107496509	4,467169049	0,015792221	sortilin related receptor 1 [Source:HGNC Symbol;Acc:HGNC:11185]
ENST00000315927	ENSG00000180667	2,390150091	4,455719602	0,015852126	YOD1 deubiquitinase [Source:HGNC Symbol;Acc:HGNC:25035]
ENST00000239761		-4,201383357	4,408565898	0,015936868	
ENST00000489226	ENSG00000167094	-4,201136753	4,388492057	0,015936868	tetratricopeptide repeat domain 16 [Source:HGNC Symbol;Acc:HGNC:2653
ENST00000566788		4,131771756	4,538333449	0,015936868	
ENST00000427551	ENSG00000234230	4,13168285	4,284100661	0,015936868	ZFX antisense RNA 1 [Source:HGNC Symbol;Acc:HGNC:40617]

ENST00000467312	ENSG00000160446	4,130920481	4,346652274	0,015936868	zinc finger DHHC-type containing 12 [Source:HGNC Symbol;Acc:HGNC:191
ENST00000363209	ENSG00000200079	-4,043747425	4,336252783	0,015936868	RNA, 5S ribosomal pseudogene 326 [Source:HGNC Symbol;Acc:HGNC:4322
ENST00000413342	ENSG00000225509	-4,041365081	4,371145562	0,015936868	apoptosis inducing factor, mitochondria associated 1 pseudogene 1 [Sourc
ENST00000476065	ENSG00000134184	-4,041075439	4,276783601	0,015936868	glutathione S-transferase mu 1 [Source:HGNC Symbol;Acc:HGNC:4632]
ENST00000419164	ENSG00000112559	3,954807075	4,319066709	0,015936868	MyoD family inhibitor [Source:HGNC Symbol;Acc:HGNC:6967]
ENST00000442082	ENSG00000223467	-3,863639848	4,300072806	0,015936868	calmodulin 1 pseudogene 1 [Source:HGNC Symbol;Acc:HGNC:1443]
ENST00000444184	ENSG00000204054	-3,863391588	4,364495316	0,015936868	long intergenic non-protein coding RNA 963 [Source:HGNC Symbol;Acc:HG
ENST00000473735	ENSG00000148824	-3,863122086	4,300418784	0,015936868	mitochondrial ribosome associated GTPase 1 [Source:HGNC Symbol;Acc:H
ENST00000397622	ENSG00000146842	-3,863100804	4,382458315	0,015936868	transmembrane protein 209 [Source:HGNC Symbol;Acc:HGNC:21898]
ENST00000335628		-3,534426374	5,245507933	0,016439046	
ENST00000593752		2,679245852	6,05027255	0,016783384	
ENST00000531081	ENSG00000149328	2,317828533	13,51121779	0,016812929	galactosidase beta 1 like 2 [Source:HGNC Symbol;Acc:HGNC:25129]
ENST00000595059	ENSG00000269473	2,286966122	4,573030727	0,017129499	novel transcript
ENST00000416242	ENSG00000231808	-2,408252999	4,599195472	0,017142818	long intergenic non-protein coding RNA 1388 [Source:HGNC Symbol;Acc:H
ENST00000401075	ENSG00000215899	-1,862790145	4,496974677	0,017250021	eukaryotic translation elongation factor 1 alpha 1 (EEF1A1) pseudogene
ENST00000362562		2,109940416	5,459620344	0,017514149	
ENST00000516858	ENSG00000252667	-1,166875345	6,085201567	0,018417361	RNA, 5S ribosomal pseudogene 523 [Source:HGNC Symbol;Acc:HGNC:4342
ENST00000364216	ENSG00000201086	-1,386197367	6,518696181	0,018491985	RNA, 5S ribosomal pseudogene 394 [Source:HGNC Symbol;Acc:HGNC:4329
ENST00000488500	ENSG00000156508	-4,188670323	4,36355856	0,0186885	eukaryotic translation elongation factor 1 alpha 1 [Source:HGNC Symbol;A
ENST00000362535	ENSG00000199405	-1,860328129	5,918886524	0,01884971	small nucleolar RNA, H/ACA box 1B [Source:HGNC Symbol;Acc:HGNC:5219
ENST00000363098	ENSG00000199968	2,82169708	5,201064256	0,019077773	small nucleolar RNA, C/D box 115-19 [Source:HGNC Symbol;Acc:HGNC:330
ENST00000332687	ENSG00000131263	-2,047879682	4,759464689	0,019147386	ring finger protein, LIM domain interacting [Source:HGNC Symbol;Acc:HGN
ENST00000365658	ENSG00000202528	-4,183073257	4,596878348	0,019345002	RNA, U6 small nuclear 650, pseudogene [Source:HGNC Symbol;Acc:HGNC:
ENST00000518392	ENSG00000185015	-1,481657081	5,48356944	0,01961833	carbonic anhydrase 13 [Source:HGNC Symbol;Acc:HGNC:14914]
ENST00000531207	ENSG00000179240	-3,567839397	4,945671534	0,019796082	GVQW motif containing 3 [Source:HGNC Symbol;Acc:HGNC:51239]
ENST00000518418	ENSG00000253298	2,26025922	6,303405431	0,019879265	long intergenic non-protein coding RNA 1845 [Source:HGNC Symbol;Acc:H
ENST00000516506	ENSG00000252315	-1,031722174	7,380824299	0,020050574	RNA, 5S ribosomal pseudogene 520 [Source:HGNC Symbol;Acc:HGNC:4342
ENST00000296027	ENSG00000163735	-1,725281069	4,594469586	0,02005284	C-X-C motif chemokine ligand 5 [Source:HGNC Symbol;Acc:HGNC:10642]
ENST00000364273	ENSG00000201143	2,556539375	5,028012695	0,020523412	small nucleolar RNA, C/D box 115-42 [Source:HGNC Symbol;Acc:HGNC:330
ENST00000401154	ENSG00000215973	-2,75596829	4,999250453	0,02063941	microRNA 933 [Source:HGNC Symbol;Acc:HGNC:33676]
ENST00000467507	ENSG00000142875	-2,133534319	5,364199196	0,02121202	protein kinase cAMP-activated catalytic subunit beta [Source:HGNC Symb
ENST00000322723	ENSG00000115053	-1,720630035	4,653790178	0,021280221	nucleolin [Source:HGNC Symbol;Acc:HGNC:7667]
ENST00000492136	ENSG00000153560	4,717361237	4,477766582	0,021489223	upstream binding protein 1 [Source:HGNC Symbol;Acc:HGNC:12507]
ENST00000495856	ENSG00000172339	-4,172947338	4,441733507	0,021529732	ALG14, UDP-N-acetylglucosaminyltransferase subunit [Source:HGNC Symb
ENST00000606510	ENSG00000272460	2,81032244	5,120533961	0,022032899	small nucleolar RNA, C/D box 115-40 [Source:HGNC Symbol;Acc:HGNC:330
ENST00000358047	ENSG00000198173	2,885277878	4,429789292	0,022069669	family with sequence similarity 47 member C [Source:HGNC Symbol;Acc:H
ENST00000580969	ENSG00000265178	2,88464596	4,389360348	0,022069669	microRNA 4728 [Source:HGNC Symbol;Acc:HGNC:41632]
ENST00000583549	ENSG00000263407	2,883215972	4,451413291	0,022069669	microRNA 4660 [Source:HGNC Symbol;Acc:HGNC:41861]
ENST00000552501	ENSG00000258359	-2,858165031	4,510208575	0,022069669	PEST containing nuclear protein pseudogene 1 [Source:HGNC Symbol;Acc:
ENST00000300574	ENSG00000167193	-2,858032255	4,361930792	0,022069669	CRK proto-oncogene, adaptor protein [Source:HGNC Symbol;Acc:HGNC:23
ENST00000529500	ENSG00000165916	-2,729049496	4,378692541	0,022069669	proteasome 26S subunit, ATPase 3 [Source:HGNC Symbol;Acc:HGNC:9549]
ENST00000536619		-2,72900175	4,370675542	0,022069669	
ENST00000469191	ENSG00000134697	-2,586582101	4,35940395	0,022069669	G protein nucleolar 2 [Source:HGNC Symbol;Acc:HGNC:29925]
ENST00000528080	ENSG00000166471	2,153889324	4,376584136	0,022069669	transmembrane protein 41B [Source:HGNC Symbol;Acc:HGNC:28948]
ENST00000503759	ENSG00000113083	2,012070762	4,357990474	0,022069669	lysyl oxidase [Source:HGNC Symbol;Acc:HGNC:6664]
ENST00000351217	ENSG00000156642	2,011308425	4,459499241	0,022069669	neuroplastin [Source:HGNC Symbol;Acc:HGNC:17867]
ENST00000467908	ENSG00000160209	-2,055750588	4,514162229	0,022224942	pyridoxal kinase [Source:HGNC Symbol;Acc:HGNC:8819]
ENST00000467908	ENSG00000160209	-2,055750588	4,514162229	0,022224942	pyridoxal kinase [Source:HGNC Symbol;Acc:HGNC:8819]
ENST00000250448	ENSG00000129514	1,776667101	4,500558453	0,022224942	forkhead box A1 [Source:HGNC Symbol;Acc:HGNC:5021]
ENST00000606771	ENSG00000272269	1,522886001	5,198649156	0,022486783	
ENST00000526431	ENSG00000254739	4,333838564	4,32146622	0,022836277	novel transcript
ENST00000533277	ENSG00000173653	-2,728556688	4,344191047	0,022960877	Ras converting CAAX endopeptidase 1 [Source:HGNC Symbol;Acc:HGNC:13
ENST00000580173		1,923685039	4,425955057	0,02325916	
ENST00000516449	ENSG00000252258	-2,855876511	4,517703977	0,02330931	
ENST00000217131	ENSG00000101160	-2,236830933	5,022443376	0,023580364	cathepsin Z [Source:HGNC Symbol;Acc:HGNC:2547]
ENST00000452383	ENSG00000186635	2,294369986	6,261599444	0,023887067	ArfGAP with RhoGAP domain, ankyrin repeat and PH domain 1 [Source:HG
ENST00000384993	ENSG00000207726	1,518438733	8,828512019	0,02400093	microRNA 455 [Source:HGNC Symbol;Acc:HGNC:32344]
ENST00000608412	ENSG00000273319	-1,725367341	4,780566498	0,024682075	novel transcript
ENST00000496286	ENSG00000239888	-3,204677948	4,613764801	0,024770779	RNA, 7SL, cytoplasmic 792, pseudogene [Source:HGNC Symbol;Acc:HGNC:
ENST00000426528	ENSG00000239407	-1,811190674	4,72948295	0,024788925	novel transcript
ENST00000312521	ENSG00000174738	-2,028742638	4,534818495	0,024810317	nuclear receptor subfamily 1 group D member 2 [Source:HGNC Symbol;Ac
ENST00000548577	ENSG00000219200	1,966776746	4,650827277	0,025062268	ribonuclease K [Source:HGNC Symbol;Acc:HGNC:33911]
ENST00000381033	ENSG00000139515	2,080214586	4,989243638	0,025090607	pancreatic and duodenal homeobox 1 [Source:HGNC Symbol;Acc:HGNC:61
ENST00000365452	ENSG00000202322	-1,150315574	7,494047535	0,025228765	RNA, 5S ribosomal pseudogene 131 [Source:HGNC Symbol;Acc:HGNC:4303
ENST00000547872	ENSG00000094916	1,476164478	4,938747293	0,025251747	chromobox 5 [Source:HGNC Symbol;Acc:HGNC:1555]
ENST00000292513	ENSG00000160951	-1,800946887	4,689645672	0,025258726	prostaglandin E receptor 1 [Source:HGNC Symbol;Acc:HGNC:9593]
ENST00000435350	ENSG00000236333	1,36212317	4,598130287	0,025469995	TRHDE antisense RNA 1 [Source:HGNC Symbol;Acc:HGNC:27471]

ENST00000447706	ENSG00000118197	-1,748029206	4,417501902	0,025488973	DEAD-box helicase 59 [Source:HGNC Symbol;Acc:HGNC:25360]
ENST00000513771	ENSG00000248473	-1,085629139	6,63439677	0,025624676	long intergenic non-protein coding RNA 1962 [Source:HGNC Symbol;Acc:H
ENST00000609641	ENSG00000273362	2,453564117	4,713748565	0,025706131	novel transcript
ENST00000261401	ENSG00000110880	-3,148722127	5,035338107	0,025763142	coronin 1C [Source:HGNC Symbol;Acc:HGNC:2254]
ENST00000470729	ENSG00000163046	-1,220517429	5,621492642	0,025896789	ankyrin repeat domain 30B like [Source:HGNC Symbol;Acc:HGNC:35167]
ENST00000390735	ENSG00000212024	-0,952654843	7,164404362	0,026656542	microRNA 550a-3 [Source:HGNC Symbol;Acc:HGNC:41870]
ENST00000384841	ENSG00000207573	-1,071748415	8,14554227	0,026887473	microRNA 550a-2 [Source:HGNC Symbol;Acc:HGNC:32805]
ENST00000363293	ENSG00000200163	2,074409361	5,314480859	0,027072814	small nucleolar RNA, C/D box 115-18 [Source:HGNC Symbol;Acc:HGNC:330
ENST00000565913	ENSG00000166780	1,770695305	4,633864854	0,027150045	chromosome 16 open reading frame 45 [Source:HGNC Symbol;Acc:HGNC:1
ENST00000522124	ENSG00000147481	-3,707940195	4,558617997	0,027250498	syntrophin gamma 1 [Source:HGNC Symbol;Acc:HGNC:13740]
ENST00000260810	ENSG00000163781	1,994974449	4,744407215	0,027467374	DNA topoisomerase II binding protein 1 [Source:HGNC Symbol;Acc:HGNC:1
ENST00000420512	ENSG00000167123	1,701822593	4,883285132	0,027492902	cerebral endothelial cell adhesion molecule [Source:HGNC Symbol;Acc:HG
ENST00000222573	ENSG00000105855	2,988254578	4,37936818	0,027571226	integrin subunit beta 8 [Source:HGNC Symbol;Acc:HGNC:6163]
ENST00000603701	ENSG00000271049	-1,985710536	5,134697528	0,027701994	small nuclear ribonucleoprotein polypeptide E (SNRPE) pseudogene
ENST00000390482	ENSG00000211834	2,297879463	4,61893971	0,027734374	T cell receptor alpha joining 57 [Source:HGNC Symbol;Acc:HGNC:12089]
ENST00000559923	ENSG00000100664	-1,316733138	6,564883622	0,027883099	eukaryotic translation initiation factor 5 [Source:HGNC Symbol;Acc:HGNC:
ENST00000410250	ENSG00000222182	-2,093510527	4,605842202	0,028327075	RNA, 5S ribosomal pseudogene 156 [Source:HGNC Symbol;Acc:HGNC:4305
ENST00000405460	ENSG00000164199	-2,182619967	4,740482456	0,028437529	adhesion G protein-coupled receptor V1 [Source:HGNC Symbol;Acc:HGNC:
ENST00000363762	ENSG00000200632	-2,727991773	5,419189504	0,028705444	small nucleolar RNA, C/D box 113-7 [Source:HGNC Symbol;Acc:HGNC:3298
ENST00000450912	ENSG00000230276	-1,986133263	4,703471486	0,028723318	NHP2 non-histone chromosome protein 2-like 1 (S. cerevisiae) (NHP2L1) p
ENST00000373980	ENSG00000185532	2,026826251	4,527262439	0,029173515	protein kinase cGMP-dependent 1 [Source:HGNC Symbol;Acc:HGNC:9414]
ENST00000389805	ENSG00000161011	1,636432935	5,363778647	0,029174085	sequestosome 1 [Source:HGNC Symbol;Acc:HGNC:11280]
ENST00000335681	ENSG00000170485	2,321206026	5,021674331	0,029216735	neuronal PAS domain protein 2 [Source:HGNC Symbol;Acc:HGNC:7895]
ENST00000535723	ENSG00000168496	-2,181847446	4,810681269	0,029557176	flap structure-specific endonuclease 1 [Source:HGNC Symbol;Acc:HGNC:36
ENST00000242465	ENSG00000122862	-2,051732701	5,16072619	0,029654345	serglycin [Source:HGNC Symbol;Acc:HGNC:9361]
ENST00000446026	ENSG00000163866	4,106371527	4,353876469	0,02989898	small integral membrane protein 12 [Source:HGNC Symbol;Acc:HGNC:251
ENST00000416904	ENSG00000139651	1,68877761	4,688274876	0,029920385	zinc finger protein 740 [Source:HGNC Symbol;Acc:HGNC:27465]
ENST00000432472	ENSG00000225447	2,831877528	6,420909604	0,030197242	ribosomal protein S15a pseudogene 10 [Source:HGNC Symbol;Acc:HGNC:3
ENST00000494744	ENSG00000177138	-1,729129072	4,838855529	0,030382157	family with sequence similarity 9 member B [Source:HGNC Symbol;Acc:HG
ENST00000572218	ENSG00000120071	-1,51203152	4,586687865	0,030403432	KAT8 regulatory NSL complex subunit 1 [Source:HGNC Symbol;Acc:HGNC:2
ENST00000269383	ENSG00000141569	1,881395706	4,642258485	0,030428712	tripartite motif containing 65 [Source:HGNC Symbol;Acc:HGNC:27316]
ENST00000530911	ENSG00000177595	-3,067013158	4,466313787	0,030453745	p53-induced death domain protein 1 [Source:HGNC Symbol;Acc:HGNC:164
ENST00000485915	ENSG00000242928	-1,218708848	8,200756918	0,031019531	RNA, 7SL, cytoplasmic 868, pseudogene [Source:HGNC Symbol;Acc:HGNC:
ENST00000440403	ENSG00000225555	3,951969677	4,290183027	0,031694686	novel transcript
ENST00000320672	ENSG00000145687	3,950529841	4,428782977	0,031694686	single stranded DNA binding protein 2 [Source:HGNC Symbol;Acc:HGNC:15
ENST00000475060	ENSG00000171793	-3,861007091	4,280747356	0,031694686	CTP synthase 1 [Source:HGNC Symbol;Acc:HGNC:2519]
ENST00000547196		-3,860716774	4,287545296	0,031694686	
ENST00000421515	ENSG00000197885	-3,860695526	4,295771072	0,031694686	NFKB inhibitor interacting Ras like 1 [Source:HGNC Symbol;Acc:HGNC:178
ENST00000315392	ENSG00000161381	3,748293404	4,321321129	0,031694686	plexin domain containing 1 [Source:HGNC Symbol;Acc:HGNC:20945]
ENST00000216286	ENSG00000087303	3,74536178	4,290044102	0,031694686	nidogen 2 [Source:HGNC Symbol;Acc:HGNC:13389]
ENST00000593133	ENSG00000180479	-3,657854805	4,300289053	0,031694686	zinc finger protein 571 [Source:HGNC Symbol;Acc:HGNC:25000]
ENST00000369518	ENSG00000198765	-3,657812124	4,36829905	0,031694686	synaptonemal complex protein 1 [Source:HGNC Symbol;Acc:HGNC:11487]
ENST00000442572	ENSG00000226289	-3,657812124	4,276160971	0,031694686	cell division cycle associated 4 pseudogene 3 [Source:HGNC Symbol;Acc:H
ENST00000608236	ENSG00000272654	-3,657812124	4,351008026	0,031694686	novel transcript
ENST00000552790	ENSG00000008405	-3,657563226	4,277323029	0,031694686	cryptochrome circadian regulator 1 [Source:HGNC Symbol;Acc:HGNC:2384
ENST00000245312	ENSG00000125255	-3,65754189	4,268779841	0,031694686	solute carrier family 10 member 2 [Source:HGNC Symbol;Acc:HGNC:10906
ENST00000571755	ENSG00000262081	-3,657250372	4,304185579	0,031694686	interleukin 9 receptor pseudogene 4 [Source:HGNC Symbol;Acc:HGNC:603
ENST00000417027	ENSG00000231022	-3,65698024	4,250747465	0,031694686	ribosomal protein S3a pseudogene 9 [Source:HGNC Symbol;Acc:HGNC:361
ENST00000608165	ENSG00000105656	-3,656958911	4,250662474	0,031694686	elongation factor for RNA polymerase II [Source:HGNC Symbol;Acc:HGNC:
ENST00000246080	ENSG00000125878	2,18075336	4,946961378	0,031753531	transcription factor 15 [Source:HGNC Symbol;Acc:HGNC:11627]
ENST00000429272	ENSG00000226915	2,071262756	7,799189794	0,031902395	ribosomal protein L19 (RPL19) pseudogene
ENST00000378187	ENSG00000204978	-1,590349192	4,671687424	0,03203073	glutamate rich 4 [Source:HGNC Symbol;Acc:HGNC:34497]
ENST00000604516	ENSG00000270362	2,419818951	4,661037337	0,032262021	HMGN3 antisense RNA 1 [Source:HGNC Symbol;Acc:HGNC:48984]
ENST00000374975	ENSG00000198502	1,584547121	4,536426697	0,03228554	major histocompatibility complex, class II, DR beta 5 [Source:HGNC Symbo
ENST00000596634	ENSG00000105221	1,508674587	4,732832635	0,032319605	AKT serine/threonine kinase 2 [Source:HGNC Symbol;Acc:HGNC:392]
ENST00000217260	ENSG00000101282	4,272190612	4,660325048	0,032417248	R-spondin 4 [Source:HGNC Symbol;Acc:HGNC:16175]
ENST00000379565	ENSG00000177189	-2,007183408	5,239330432	0,032490371	ribosomal protein S6 kinase A3 [Source:HGNC Symbol;Acc:HGNC:10432]
ENST00000545128	ENSG00000099139	-2,162093669	5,235142079	0,032659351	proprotein convertase subtilisin/kexin type 5 [Source:HGNC Symbol;Acc:H
ENST00000284637	ENSG00000154447	-4,25012491	5,860418698	0,032722406	SH3 domain containing ring finger 1 [Source:HGNC Symbol;Acc:HGNC:176
ENST00000603722	ENSG00000074935	3,744720034	4,396376981	0,032739335	tubulin epsilon 1 [Source:HGNC Symbol;Acc:HGNC:20775]
ENST00000516327	ENSG00000252136	-1,319081853	6,005820332	0,032826053	
ENST00000371531	ENSG00000095596	-4,262173045	4,433552327	0,032832199	cytochrome P450 family 26 subfamily A member 1 [Source:HGNC Symbol;
ENST00000507056	ENSG00000249667	2,264104159	7,278576788	0,032846076	long intergenic non-protein coding RNA 1259 [Source:HGNC Symbol;Acc:H
ENST00000363282	ENSG00000200152	-1,946539609	4,579445052	0,033069651	RNA, U6 small nuclear 216, pseudogene [Source:HGNC Symbol;Acc:HGNC:
ENST00000384324	ENSG00000207052	-1,3409428	5,966757876	0,033428916	RNA, U6 small nuclear 378, pseudogene [Source:HGNC Symbol;Acc:HGNC:
ENST00000419506	ENSG00000112038	-2,08017507	4,5779896	0,033502587	opioid receptor mu 1 [Source:HGNC Symbol;Acc:HGNC:8156]
ENST00000608442	ENSG00000272620	-1,888334595	4,703327975	0,033564883	AFAP1 antisense RNA 1 [Source:HGNC Symbol;Acc:HGNC:28141]

ENST00000577688	ENSG00000284074	-1,970283888	5,137219575	0,033708936	microRNA 4758 [Source:HGNC Symbol;Acc:HGNC:41836]
ENST00000362127	ENSG00000198997	1,588502523	10,18649067	0,034015452	microRNA 107 [Source:HGNC Symbol;Acc:HGNC:31496]
ENST00000339235	ENSG00000171823	-4,122074596	4,623872744	0,034363638	F-box and leucine rich repeat protein 14 [Source:HGNC Symbol;Acc:HGNC:
ENST00000517199	ENSG00000253008	1,845829186	4,686504749	0,034390442	microRNA 2355 [Source:HGNC Symbol;Acc:HGNC:38328]
ENST00000599749	ENSG00000268388	-3,847532301	4,441407841	0,034554438	FOXF1 adjacent non-coding developmental regulatory RNA [Source:HGNC
ENST00000296755	ENSG00000131711	-2,871833941	5,91314392	0,034576034	microtubule associated protein 1B [Source:HGNC Symbol;Acc:HGNC:6836]
ENST00000420997	ENSG00000234349	-1,751293506	4,583714825	0,034907712	glutamate dehydrogenase 1 pseudogene 9 [Source:HGNC Symbol;Acc:HGN
ENST00000367590	ENSG00000143324	-3,203329733	4,556636172	0,035120576	xenotropic and polytropic retrovirus receptor 1 [Source:HGNC Symbol;Acc
ENST00000595245	ENSG00000099326	-1,80545709	5,63137806	0,035186067	myeloid zinc finger 1 [Source:HGNC Symbol;Acc:HGNC:13108]
ENST00000432137	ENSG00000213362	-3,21211754	4,794701508	0,035230352	ferritin heavy chain 1 pseudogene 12 [Source:HGNC Symbol;Acc:HGNC:39
ENST00000384668	ENSG00000207399	-1,563701554	5,008041661	0,035462965	RNA, U6 small nuclear 1011, pseudogene [Source:HGNC Symbol;Acc:HGNC
ENST00000466609	ENSG00000244153	3,926290171	4,390311629	0,035706755	WW domain containing E3 ubiquitin protein ligase 1 pseudogene 1 [Source
ENST00000555485	ENSG00000258563	-3,687609554	4,30571628	0,035759866	proteasome subunit alpha 3 pseudogene [Source:HGNC Symbol;Acc:HGNC
ENST00000495869	ENSG00000183773	2,138784481	4,666395268	0,036774144	apoptosis inducing factor, mitochondria associated 3 [Source:HGNC Symbo
ENST00000487077		-2,061603969	4,930174007	0,037000141	
ENST00000385229	ENSG00000283891	-1,163643352	6,303675795	0,037436528	microRNA 628 [Source:HGNC Symbol;Acc:HGNC:32884]
ENST00000384916	ENSG00000207649	-1,369939409	10,29265427	0,037497846	microRNA 138-2 [Source:HGNC Symbol;Acc:HGNC:31525]
ENST00000312428	ENSG00000118997	-2,065642665	4,704190939	0,037503571	dynein axonemal heavy chain 7 [Source:HGNC Symbol;Acc:HGNC:18661]
ENST00000463695	ENSG00000163617	2,531836059	5,702698127	0,037516462	coiled-coil domain containing 191 [Source:HGNC Symbol;Acc:HGNC:29272
ENST00000410216	ENSG00000222148	2,87890475	4,786630873	0,037798428	RNA, Ro-associated Y4 pseudogene 30 [Source:HGNC Symbol;Acc:HGNC:4
ENST00000362298	ENSG00000199168	-1,128218554	8,38311925	0,038120045	microRNA 374a [Source:HGNC Symbol;Acc:HGNC:31788]
ENST00000582078	ENSG00000266179	-1,802047385	6,564969433	0,038316896	LSU rRNA pseudogene
ENST00000517146	ENSG00000252955	-1,563368285	5,329103143	0,038427768	RNA, U4atac small nuclear 9, pseudogene [Source:HGNC Symbol;Acc:HGN
ENST00000401182	ENSG00000216001	-3,081835665	4,657435552	0,03849221	microRNA 450b [Source:HGNC Symbol;Acc:HGNC:33642]
ENST00000362580	ENSG00000199450	3,547165675	4,263062474	0,038549123	RNA, 5S ribosomal pseudogene 276 [Source:HGNC Symbol;Acc:HGNC:4317
ENST00000588451	ENSG00000130023	1,498025183	4,59741243	0,038857115	ER membrane associated RNA degradation [Source:HGNC Symbol;Acc:HGI
ENST00000367511	ENSG00000135842	-2,485329341	4,931131355	0,039215812	family with sequence similarity 129 member A [Source:HGNC Symbol;Acc:
ENST00000274031	ENSG00000145391	-1,438567984	5,154267971	0,039226042	SET domain containing lysine methyltransferase 7 [Source:HGNC Symbol;A
ENST00000444127	ENSG00000229133	-3,839219762	4,463537499	0,03956261	ribosomal protein S7 pseudogene 4 [Source:HGNC Symbol;Acc:HGNC:3600
ENST00000339446	ENSG00000254409	2,155082714	4,415646099	0,039645727	novel transcript, sense overlapping C11orf96
ENST00000395388	ENSG00000204287	2,154747663	4,412046866	0,039645727	major histocompatibility complex, class II, DR alpha [Source:HGNC Symbol
ENST00000443866	ENSG00000226321	2,154004567	4,52447748	0,039645727	ciliary rootlet coiled-coil, rootletin family member 2 [Source:HGNC Symbo
ENST00000364983		-2,118898026	4,483802055	0,039645727	
ENST00000517992	ENSG00000172164	1,672995698	4,390823177	0,039645727	syntrophin beta 1 [Source:HGNC Symbol;Acc:HGNC:11168]
ENST00000527880		-1,629440635	4,483125521	0,039645727	
ENST00000565044	ENSG00000261104	-3,839179519	4,361709948	0,039701309	novel transcript
ENST00000470541	ENSG00000116584	-2,727133307	4,33133826	0,039863303	Rho/Rac guanine nucleotide exchange factor 2 [Source:HGNC Symbol;Acc:
ENST00000416284	ENSG00000198673	-2,586003302	4,42486886	0,039863303	family with sequence similarity 19 member A2, C-C motif chemokine like [
ENST00000359546	ENSG00000145920	-2,585339718	4,398415961	0,039863303	complexin 2 [Source:HGNC Symbol;Acc:HGNC:2310]
ENST00000437546	ENSG00000237458	-2,584803492	4,343121756	0,039863303	tubulin beta 4B class IVb pseudogene 3 [Source:HGNC Symbol;Acc:HGNC:4
ENST00000418592	ENSG00000237296	2,582225496	4,370594156	0,039863303	SMG1 pseudogene 1 [Source:HGNC Symbol;Acc:HGNC:44186]
ENST00000302904	ENSG00000108312	2,580624581	4,453191802	0,039863303	upstream binding transcription factor [Source:HGNC Symbol;Acc:HGNC:12
ENST00000606866	ENSG00000271803	-2,427149469	4,341731051	0,039863303	novel transcript, antisense to NECAB3
ENST00000472943	ENSG00000240875	2,009112411	4,415331042	0,039863303	long intergenic non-protein coding RNA 886 [Source:HGNC Symbol;Acc:HG
ENST00000305899	ENSG00000171942	1,852820105	4,371228094	0,039863303	olfactory receptor family 10 subfamily H member 2 [Source:HGNC Symbol
ENST00000569895	ENSG00000078328	1,851696472	4,466638099	0,039863303	RNA binding fox-1 homolog 1 [Source:HGNC Symbol;Acc:HGNC:18222]
ENST00000440614	ENSG00000235813	1,851226385	4,492870234	0,039863303	novel transcript
ENST00000225823	ENSG00000108684	1,850953772	4,469016545	0,039863303	acid sensing ion channel subunit 2 [Source:HGNC Symbol;Acc:HGNC:99]
ENST00000478713	ENSG00000100344	1,850953772	4,423343302	0,039863303	patatin like phospholipase domain containing 3 [Source:HGNC Symbol;Acc
ENST00000465082	ENSG00000135926	-1,747888934	4,573753677	0,040410259	transmembrane BAX inhibitor motif containing 1 [Source:HGNC Symbol;A
ENST00000504966	ENSG00000250504	-5,324573454	4,622779572	0,040510506	keratin 18 pseudogene 51 [Source:HGNC Symbol;Acc:HGNC:33421]
ENST00000471193	ENSG00000115414	1,678553262	5,103615972	0,040595176	fibronectin 1 [Source:HGNC Symbol;Acc:HGNC:3778]
ENST00000536262	ENSG00000256870	2,020157055	4,795510854	0,0406809	solute carrier family 5 member 8 [Source:HGNC Symbol;Acc:HGNC:19119]
ENST00000323013	ENSG00000189306	1,927535172	4,643199977	0,040716561	ribosomal RNA processing 7 homolog A [Source:HGNC Symbol;Acc:HGNC:2
ENST00000459143		-3,677500295	4,406353068	0,040843627	
ENST00000260443	ENSG00000137876	-1,968083338	4,778823371	0,041018103	ribosomal L24 domain containing 1 [Source:HGNC Symbol;Acc:HGNC:1847
ENST00000362963	ENSG00000199833	2,099889802	4,628555323	0,041116719	small nucleolar RNA, C/D box 115-21 [Source:HGNC Symbol;Acc:HGNC:330
ENST00000305997	ENSG00000143797	2,587563942	4,49902226	0,041209721	membrane bound O-acyltransferase domain containing 2 [Source:HGNC S
ENST00000489529	ENSG00000241074	-3,825579163	4,317205267	0,041341032	RNA, 7SL, cytoplasmic 813, pseudogene [Source:HGNC Symbol;Acc:HGNC:
ENST00000439870	ENSG00000233230	3,937341446	4,527890687	0,041452847	novel transcript
ENST00000364748	ENSG00000201618	-1,980854203	4,511090885	0,041467443	RNA, 5S ribosomal pseudogene 505 [Source:HGNC Symbol;Acc:HGNC:4340
ENST00000379499	ENSG00000185915	1,550384687	4,990674888	0,041476534	kelch like family member 34 [Source:HGNC Symbol;Acc:HGNC:26634]
ENST00000505092	ENSG00000251685	-1,715986232	5,213055831	0,041576443	UDP glucuronosyltransferase family 2 member B27, pseudogene [Source:H
ENST00000296575	ENSG00000164161	2,736518055	4,554966356	0,041840568	hedgehog interacting protein [Source:HGNC Symbol;Acc:HGNC:14866]
ENST00000384917	ENSG00000207650	-3,678878709	5,318838046	0,042034436	microRNA 570 [Source:HGNC Symbol;Acc:HGNC:32826]
ENST00000364543	ENSG00000201413	-1,757181823	7,993646931	0,042056015	RNA, 5S ribosomal pseudogene 141 [Source:HGNC Symbol;Acc:HGNC:4304
ENST00000557389	ENSG00000100906	-1,519027308	4,698332228	0,042059048	NFKB inhibitor alpha [Source:HGNC Symbol;Acc:HGNC:7797]

ENST00000456101	ENSG00000135596	1,350013068	4,589332569	0,042261707	microtubule associated monooxygenase, calponin and LIM domain contai
ENST00000429829	ENSG00000229807	-1,703303828	5,155833573	0,042486663	X inactive specific transcript [Source:HGNC Symbol;Acc:HGNC:12810]
ENST00000365050	ENSG00000201920	-2,045503803	9,269755375	0,042690904	RNA, 5S ribosomal pseudogene 442 [Source:HGNC Symbol;Acc:HGNC:4334
ENST00000587688	ENSG00000267741	-3,863106644	4,54784042	0,042929778	ubiquitin conjugating enzyme E2 L4 (pseudogene) [Source:HGNC Symbol;A
ENST00000495441	ENSG00000198203	2,660236187	15,56664231	0,042939223	sulfotransferase family 1C member 2 [Source:HGNC Symbol;Acc:HGNC:114
ENST00000394752	ENSG00000163935	2,014559066	4,530466039	0,043032451	Scm like with four mbt domains 1 [Source:HGNC Symbol;Acc:HGNC:20255
ENST00000565115	ENSG00000260431	1,734538556	8,137458919	0,043109119	C11orf2 chromosome 11 open reading frame 2 pseudogene
ENST00000447087	ENSG00000236692	2,0069518	5,086880091	0,043476699	mitochondrially encoded cytochrome c oxidase I (MT-CO1) pseudogene
ENST00000609200	ENSG00000272692	1,712108163	4,482385813	0,043675404	
ENST00000384984	ENSG00000207717	2,557795716	9,409409891	0,043728874	microRNA 551b [Source:HGNC Symbol;Acc:HGNC:32807]
ENST00000217420	ENSG00000101438	1,570324295	4,804764948	0,044207788	solute carrier family 32 member 1 [Source:HGNC Symbol;Acc:HGNC:11018
ENST00000518014	ENSG00000249669	-2,44169918	4,452450652	0,044340203	cardiac mesoderm enhancer-associated non-coding RNA [Source:HGNC Sy
ENST00000362912	ENSG00000199782	1,800019415	5,113919309	0,044532372	small nucleolar RNA, C/D box 115-9 [Source:HGNC Symbol;Acc:HGNC:3302
ENST00000454783	ENSG00000226979	-2,801315653	4,654009558	0,044714474	lymphotoxin alpha [Source:HGNC Symbol;Acc:HGNC:6709]
ENST00000510568	ENSG00000159692	-2,182278928	4,920581643	0,044850417	C-terminal binding protein 1 [Source:HGNC Symbol;Acc:HGNC:2494]
ENST00000520656	ENSG00000254294	-3,105226178	4,644253174	0,044933687	inosine monophosphate dehydrogenase 1 pseudogene 6 [Source:HGNC Sy
ENST00000364653	ENSG00000201523	-1,467082426	6,439452698	0,045065737	RNA, 5S ribosomal pseudogene 205 [Source:HGNC Symbol;Acc:HGNC:4310
ENST00000584559	ENSG00000264292	-1,974601478	4,412164457	0,045160982	microRNA 2467 [Source:HGNC Symbol;Acc:HGNC:41881]
ENST00000418914	ENSG00000134222	-1,697406801	5,111031005	0,045172243	proline and serine rich coiled-coil 1 [Source:HGNC Symbol;Acc:HGNC:2447
ENST00000306422	ENSG00000171540	-1,436344077	5,857316163	0,045207254	orthopedia homeobox [Source:HGNC Symbol;Acc:HGNC:8518]
ENST00000309758	ENSG00000173110	1,22195158	5,430227376	0,04538898	heat shock protein family A (Hsp70) member 6 [Source:HGNC Symbol;Acc:
ENST00000454001	ENSG00000213621	3,056289029	4,925421819	0,045440918	ribosomal protein SA pseudogene 54 [Source:HGNC Symbol;Acc:HGNC:363
ENST00000578975	ENSG00000105221	-4,92034235	4,53251278	0,045500138	AKT serine/threonine kinase 2 [Source:HGNC Symbol;Acc:HGNC:392]
ENST00000233638	ENSG00000115297	-2,711160634	4,431801377	0,045954148	T cell leukemia homeobox 2 [Source:HGNC Symbol;Acc:HGNC:5057]
ENST00000363090	ENSG00000199960	2,212340014	4,662392555	0,046417305	small nucleolar RNA, C/D box 115-14 [Source:HGNC Symbol;Acc:HGNC:330
ENST00000365073	ENSG00000201943	2,278853527	5,653222177	0,046474007	small nucleolar RNA, C/D box 115-10 [Source:HGNC Symbol;Acc:HGNC:330
ENST00000369026	ENSG00000143384	-1,685617141	5,58394258	0,046569731	MCL1, BCL2 family apoptosis regulator [Source:HGNC Symbol;Acc:HGNC:6
ENST00000447112	ENSG00000235071	1,9337494	5,283605424	0,046717751	heat shock protein pseudogene
ENST00000320241	ENSG00000176678	1,165166432	6,583861068	0,046994707	forkhead box L1 [Source:HGNC Symbol;Acc:HGNC:3817]
ENST00000369500	ENSG00000173212	-3,687766284	4,419452046	0,047340304	mab-21 like 3 [Source:HGNC Symbol;Acc:HGNC:26787]
ENST00000281938	ENSG00000152137	-1,506432574	4,522053637	0,047549117	heat shock protein family B (small) member 8 [Source:HGNC Symbol;Acc:H
ENST00000457964	ENSG00000238010	-4,470019831	4,353358197	0,047553646	novel transcript, sense intronic to LMX1B
ENST00000460006	ENSG00000101290	2,00005952	10,22124127	0,047638221	CDP-diacylglycerol synthase 2 [Source:HGNC Symbol;Acc:HGNC:1801]
ENST00000578903	ENSG00000263511	-1,847089587	5,400220859	0,047766757	microRNA 5699 [Source:HGNC Symbol;Acc:HGNC:43456]
ENST00000333274	ENSG00000184349	-2,459587972	4,361193889	0,047859973	ephrin A5 [Source:HGNC Symbol;Acc:HGNC:3225]
ENST00000590376	ENSG00000267345	1,517442866	4,664188577	0,0480747	novel transcript, antisense to ZNF420
ENST00000248564	ENSG00000127920	-1,825987482	4,568234738	0,048298089	G protein subunit gamma 11 [Source:HGNC Symbol;Acc:HGNC:4403]
ENST00000584437	ENSG00000108375	0,96745979	5,687839609	0,048309838	ring finger protein 43 [Source:HGNC Symbol;Acc:HGNC:18505]
ENST00000391303	ENSG00000212605	-2,121733945	4,630301238	0,048398664	RNA, U1 small nuclear 56, pseudogene [Source:HGNC Symbol;Acc:HGNC:4
ENST00000390725	ENSG00000212014	-2,007071023	4,405300386	0,048625919	microRNA 509-3 [Source:HGNC Symbol;Acc:HGNC:33675]
ENST00000395761	ENSG00000163739	-1,987085507	4,451554149	0,048724998	C-X-C motif chemokine ligand 1 [Source:HGNC Symbol;Acc:HGNC:4602]
ENST00000456999	ENSG00000230690	1,624085101	4,682588145	0,049224053	novel transcript
ENST00000270288		1,878354868	4,514866875	0,049327607	
ENST00000519927	ENSG00000104313	3,565772598	4,925364542	0,049469683	EYA transcriptional coactivator and phosphatase 1 [Source:HGNC Symbol;A
ENST00000365411	ENSG00000202281	-1,135116098	6,857877986	0,049503283	RNA, 5S ribosomal pseudogene 235 [Source:HGNC Symbol;Acc:HGNC:4313
ENST00000256015	ENSG00000133639	-2,180118256	4,930809633	0,049507249	BTG anti-proliferation factor 1 [Source:HGNC Symbol;Acc:HGNC:1130]
ENST00000237853	ENSG00000118985	-2,010356857	4,613150995	0,049553955	elongation factor for RNA polymerase II 2 [Source:HGNC Symbol;Acc:HGN
ENST00000367405	ENSG00000177888	-1,842943529	5,183104645	0,049888137	zinc finger and BTB domain containing 41 [Source:HGNC Symbol;Acc:HGN
ENST00000362583	ENSG00000199453	1,619356445	5,306254343	0,04999519	small nucleolar RNA, C/D box 115-12 [Source:HGNC Symbol;Acc:HGNC:330
ENST00000398900	ENSG00000213174	1,994370257	4,394923543	0,049999055	ribosomal protein L28 (RPL28) pseudogene

Annex 2: Table S3- Log Fold Change of RNA species expression between drug-sensitive (K562) cells and their MDR (K562Dox) counterparts.

ensembl_transcript_id	ensembl_gene_id	logFC	logCPM	PValue	description
ENST00000384981	ENSG00000207714	11,81715862	8,550239324	1,70786E-45	microRNA 584 [Source:HGNC Symbol;Acc:HGNC:32840]
ENST00000555332	ENSG00000248441	8,726290566	5,790022963	5,87588E-12	long intergenic non-protein coding RNA 1197 [Source:HGNC Symb
ENST00000555332	ENSG00000248441	8,726290566	5,790022963	5,87588E-12	long intergenic non-protein coding RNA 1197 [Source:HGNC Symb
ENST00000362257	ENSG00000199127	5,459576561	6,686568583	1,32151E-10	microRNA 383 [Source:HGNC Symbol;Acc:HGNC:31876]
ENST00000385198	ENSG00000207933	4,040306737	7,746677149	6,09591E-10	microRNA 9-1 [Source:HGNC Symbol;Acc:HGNC:31641]
ENST00000375898	ENSG00000139826	5,980681388	6,687288271	4,56648E-09	abhydrolase domain containing 13 [Source:HGNC Symbol;Acc:HGI
ENST00000411797	ENSG00000225000	7,664432689	5,185023097	1,04847E-08	novel transcript
ENST00000569588	ENSG00000260305	9,226576992	6,154062322	5,9397E-08	NTRK3 antisense RNA 1 [Source:HGNC Symbol;Acc:HGNC:27532]
ENST00000568148	ENSG00000176953	9,012405703	6,014473089	8,65161E-08	nuclear factor of activated T cells 2 interacting protein [Source:HG
ENST00000287675	ENSG00000157036	6,945531949	4,873768774	3,2179E-07	exo/endonuclease G [Source:HGNC Symbol;Acc:HGNC:3347]
ENST00000568063	ENSG00000261402	5,608155108	5,215525917	3,93849E-07	novel transcript
ENST00000384471	ENSG00000207200	3,017055251	7,23494887	7,70379E-07	RNA, U6 small nuclear 45, pseudogene [Source:HGNC Symbol;Acc
ENST00000273320	ENSG00000196345	7,501397778	5,101591546	9,13363E-07	zinc finger with KRAB and SCAN domains 7 [Source:HGNC Symbol;
ENST00000532223	ENSG00000254709	6,761569578	4,805921289	1,10588E-06	immunoglobulin lambda like polypeptide 5 [Source:HGNC Symbol
ENST00000384355	ENSG00000207083	3,601869621	6,418068305	1,38501E-06	RNA, U6 small nuclear 22, pseudogene [Source:HGNC Symbol;Acc
ENST00000430298	ENSG00000214189	6,739249348	4,777182376	1,93896E-06	zinc finger family member 788, pseudogene [Source:HGNC Symbo
ENST00000545923	ENSG00000255652	6,653180325	6,447058052	2,01161E-06	novel transcript
ENST00000405755	ENSG00000113448	6,03236079	4,632050371	2,11758E-06	phosphodiesterase 4D [Source:HGNC Symbol;Acc:HGNC:8783]
ENST00000454043	ENSG00000236790	6,503850537	4,739925508	2,86637E-06	long intergenic non-protein coding RNA 299 [Source:HGNC Symbo
ENST00000455579	ENSG00000242540	5,217187266	4,991065499	3,34988E-06	novel transcript
ENST00000387974	ENSG00000210709	3,200646494	6,179800622	4,03089E-06	RNA, U6atac small nuclear 3, pseudogene [Source:HGNC Symbol;A
ENST00000519803	ENSG00000253270	6,205184842	4,662140131	4,67257E-06	novel transcript
ENST00000439118	ENSG00000198885	7,787757669	6,451953351	6,11624E-06	ITPRIP like 1 [Source:HGNC Symbol;Acc:HGNC:29371]
ENST00000581678	ENSG00000263561	3,53496021	7,650693362	6,3159E-06	microRNA 4704 [Source:HGNC Symbol;Acc:HGNC:41602]
ENST00000384048	ENSG00000206775	2,396085693	8,225246116	8,42926E-06	small nucleolar RNA, C/D box 37 [Source:HGNC Symbol;Acc:HGNC
ENST00000581063	ENSG00000266580	5,694708967	4,528093831	9,21665E-06	microRNA 4254 [Source:HGNC Symbol;Acc:HGNC:38193]
ENST00000362705	ENSG00000199575	6,714833155	4,881896824	1,30145E-05	small nucleolar RNA, C/D box 114-1 [Source:HGNC Symbol;Acc:HG
ENST00000337227	ENSG00000089050	6,540334961	4,811936955	1,3506E-05	RB binding protein 9, serine hydrolase [Source:HGNC Symbol;Acc:
ENST00000384527	ENSG00000207257	2,510503103	8,097318249	1,50992E-05	RNA, U6 small nuclear 18, pseudogene [Source:HGNC Symbol;Acc
ENST00000364232	ENSG00000201102	2,687855955	7,027775413	1,62434E-05	
ENST00000364802	ENSG00000201672	4,190076902	4,616756782	1,63232E-05	small nucleolar RNA, C/D box 113-4 [Source:HGNC Symbol;Acc:HG
ENST00000384248	ENSG00000206975	2,475493529	7,687371964	1,96327E-05	RNA, U6 small nuclear 13, pseudogene [Source:HGNC Symbol;Acc
ENST00000505156	ENSG00000249917	6,656362626	4,889215661	2,1722E-05	long intergenic non-protein coding RNA 536 [Source:HGNC Symbo
ENST00000446489	ENSG00000229512	5,755084695	4,552473615	2,25348E-05	novel transcript
ENST00000406452	ENSG00000176623	4,212360549	4,86807261	2,71517E-05	regulator of microtubule dynamics 1 [Source:HGNC Symbol;Acc:H
ENST00000327968	ENSG00000184735	5,541440501	4,501606717	3,54068E-05	DEAD-box helicase 53 [Source:HGNC Symbol;Acc:HGNC:20083]
ENST00000444082	ENSG00000227242	5,535799519	4,567899275	3,54068E-05	NBPF member 13, pseudogene [Source:HGNC Symbol;Acc:HGNC:3
ENST00000421733	ENSG00000243766	3,9225462	4,496667868	4,48645E-05	HOXA distal transcript antisense RNA [Source:HGNC Symbol;Acc:H
ENST00000588682	ENSG00000176170	8,878042966	7,111059319	4,55934E-05	sphingosine kinase 1 [Source:HGNC Symbol;Acc:HGNC:11240]
ENST00000438248	ENSG00000223820	-3,95349817	4,535987033	4,84142E-05	cofilin 1 pseudogene 1 [Source:HGNC Symbol;Acc:HGNC:28560]
ENST00000357727	ENSG00000146592	6,567921175	4,94343061	6,15059E-05	cAMP responsive element binding protein 5 [Source:HGNC Symbo
ENST00000333437	ENSG00000182459	6,605673941	4,837296446	6,15233E-05	testis expressed 19 [Source:HGNC Symbol;Acc:HGNC:33802]
ENST00000408945	ENSG00000221887	5,455065332	4,515259801	6,95216E-05	histocompatibility minor serpin domain containing [Source:HGNC
ENST00000481203	ENSG00000114354	5,455065332	4,529769525	6,95216E-05	TRK-fused gene [Source:HGNC Symbol;Acc:HGNC:11758]
ENST00000363543	ENSG00000200413	3,92175725	5,339176197	7,64893E-05	small nucleolar RNA, C/D box 114-26 [Source:HGNC Symbol;Acc:H
ENST00000486157	ENSG00000243160	3,783502657	4,938287785	8,93947E-05	ribosomal protein L7a (RPL7A) pseudogene
ENST00000264741	ENSG00000144668	5,228621229	5,059436268	9,2218E-05	integrin subunit alpha 9 [Source:HGNC Symbol;Acc:HGNC:6145]
ENST00000384968	ENSG00000207701	3,211893329	5,637520909	9,60788E-05	microRNA 597 [Source:HGNC Symbol;Acc:HGNC:32853]
ENST00000383874	ENSG00000206601	2,943142963	6,20243801	0,000102749	RNA, U6 small nuclear 431, pseudogene [Source:HGNC Symbol;Ac
ENST00000365120	ENSG00000201990	4,452531062	5,768042499	0,00010478	
ENST00000553658	ENSG00000258410	3,599023308	4,945932185	0,000109572	novel transcript
ENST00000384689	ENSG00000207420	4,123176179	4,919925388	0,000111294	
ENST00000233627	ENSG00000115286	4,013106216	6,631752732	0,000123475	NADH:ubiquinone oxidoreductase core subunit S7 [Source:HGNC
ENST00000385189	ENSG00000207924	-2,496984465	8,040335329	0,00013058	microRNA 196a-2 [Source:HGNC Symbol;Acc:HGNC:31568]
ENST00000384768	ENSG00000207499	4,360055396	5,384452462	0,000134865	
ENST00000514293	ENSG00000249847	5,359216532	4,431243354	0,000136669	novel transcript
ENST00000518826	ENSG00000169154	5,269499915	4,408610029	0,000136669	glutamic-oxaloacetic transaminase 1 like 1 [Source:HGNC Symbol;
ENST00000384105	ENSG00000206832	2,998198176	6,609906878	0,00014147	RNA, U6 small nuclear variant sequence with SNRPE pseudogene
ENST00000365542	ENSG00000202412	4,095344189	5,217210542	0,000150541	RNA, Ro-associated Y3 pseudogene 13 [Source:HGNC Symbol;Acc:
ENST00000384604	ENSG00000207334	2,479869928	7,779883357	0,00015333	RNA, U6 small nuclear 12, pseudogene [Source:HGNC Symbol;Acc
ENST00000367571	ENSG00000118495	3,598312217	5,026767599	0,000158401	PLAG1 like zinc finger 1 [Source:HGNC Symbol;Acc:HGNC:9046]
ENST00000295228	ENSG00000163083	1,572151519	7,869722949	0,000162638	inhibin subunit beta B [Source:HGNC Symbol;Acc:HGNC:6067]
ENST00000243913	ENSG00000124091	6,207553825	4,709956409	0,000166864	glucosaminyl (N-acetyl) transferase family member 7 [Source:HGN

ENST00000362147	ENSG00000199017	3,405803511	4,919113763	0,000181995	microRNA 1-1 [Source:HGNC Symbol;Acc:HGNC:31499]
ENST00000515941	ENSG00000251750	3,258266608	6,941790629	0,000189971	RNA, U5F small nuclear 8, pseudogene [Source:HGNC Symbol;Acc
ENST00000364758	ENSG00000201628	3,365608499	5,475975232	0,000191647	RNA, U4 small nuclear 7, pseudogene [Source:HGNC Symbol;Acc:H
ENST00000584884	ENSG00000266262	5,740417911	4,664193669	0,000191943	microRNA 4428 [Source:HGNC Symbol;Acc:HGNC:41667]
ENST00000363979	ENSG00000200849	2,868821006	6,010936444	0,000208805	
ENST00000383885	ENSG00000206612	3,351142805	6,931493649	0,000219544	small nucleolar RNA, H/ACA box 2A [Source:HGNC Symbol;Acc:HG
ENST00000384583	ENSG00000207313	3,475735952	7,613555084	0,000233125	small nucleolar RNA, H/ACA box 2B [Source:HGNC Symbol;Acc:HG
ENST00000420404	ENSG00000228876	3,228678129	4,581533328	0,00023316	novel transcript
ENST00000531479	ENSG00000254443	9,506922708	6,499688535	0,000246405	novel transcript
ENST00000400831	ENSG00000203688	4,846908143	4,88605773	0,000247438	long intergenic non-protein coding RNA 2487 [Source:HGNC Symb
ENST00000552266	ENSG00000170515	5,54720665	4,453496526	0,000257819	proliferation-associated 2G4 [Source:HGNC Symbol;Acc:HGNC:855
ENST00000516371		3,169514553	4,571403667	0,000262088	
ENST00000362723	ENSG00000199593	5,263356991	4,542022296	0,000268995	small nucleolar RNA, C/D box 114-14 [Source:HGNC Symbol;Acc:H
ENST00000423440	ENSG00000231460	5,263356991	4,390909868	0,000268995	novel transcript
ENST00000410508	ENSG00000222440	2,220719497	7,71044737	0,000271234	RNA, U2 small nuclear 26, pseudogene [Source:HGNC Symbol;Acc
ENST00000384028	ENSG00000206755	3,546961541	6,289522368	0,000293981	small nucleolar RNA, H/ACA box 30 [Source:HGNC Symbol;Acc:HG
ENST00000363549	ENSG00000200419	2,580182734	6,057228544	0,000297313	
ENST00000391231	ENSG00000212533	3,437290207	4,792603217	0,00030566	
ENST00000384762	ENSG00000207493	3,038941114	7,649111811	0,000315876	small nucleolar RNA, H/ACA box 46 [Source:HGNC Symbol;Acc:HG
ENST00000384121	ENSG00000206848	5,400943909	4,504432211	0,000325311	RNA, U6 small nuclear 890, pseudogene [Source:HGNC Symbol;Ac
ENST00000356215	ENSG00000197301	2,610488093	6,314179501	0,000329638	uncharacterized LOC100129940 [Source:NCBI gene;Acc:100129940
ENST00000365400	ENSG00000202270	3,966457208	5,542437241	0,000337667	small nucleolar RNA, C/D box 114-12 [Source:HGNC Symbol;Acc:H
ENST00000363767	ENSG00000200637	5,413790241	4,524220322	0,000339236	RNA, U5F small nuclear 3, pseudogene [Source:HGNC Symbol;Acc
ENST00000364383	ENSG00000201253	2,911961704	5,99475036	0,000363	RNA, U4 small nuclear 10, pseudogene [Source:HGNC Symbol;Acc
ENST00000450025	ENSG00000226857	5,532307767	4,533801466	0,000369165	deoxyuridine triphosphatase pseudogene 3 [Source:HGNC Symbo
ENST00000384304	ENSG00000207031	3,334449788	11,31700618	0,000403403	small nucleolar RNA, C/D box 59A [Source:HGNC Symbol;Acc:HGN
ENST00000411315	ENSG00000223247	2,205471471	8,623093451	0,000476303	RNA, U2 small nuclear 64, pseudogene [Source:HGNC Symbol;Acc
ENST00000385084	ENSG00000284329	4,412128204	9,390160183	0,000476667	microRNA 9-3 [Source:HGNC Symbol;Acc:HGNC:31646]
ENST00000390649	ENSG00000171487	5,863418235	4,880931399	0,000478176	NLR family pyrin domain containing 5 [Source:HGNC Symbol;Acc:H
ENST00000604271	ENSG00000270571	5,205853832	4,431349035	0,000478982	novel transcript, antisense to TACR1
ENST00000265340	ENSG00000069011	4,340567393	6,619039495	0,000487758	paired like homeodomain 1 [Source:HGNC Symbol;Acc:HGNC:900
ENST00000391141	ENSG00000212443	1,958125566	6,608969108	0,00049115	small nucleolar RNA, H/ACA box 53 [Source:HGNC Symbol;Acc:HG
ENST00000596009	ENSG00000268949	5,393431947	4,629453378	0,000493542	mitochondrial ribosomal protein S17 pseudogene 1 [Source:HGNC
ENST00000440351	ENSG00000235620	6,782489994	4,906163576	0,000516559	novel transcript
ENST00000522536	ENSG00000253828	3,279509012	5,229663704	0,000521132	MT-ND2 pseudogene 38 [Source:HGNC Symbol;Acc:HGNC:52069]
ENST00000371106	ENSG00000122121	6,238138864	4,766748237	0,000525135	X-prolyl aminopeptidase 2 [Source:HGNC Symbol;Acc:HGNC:1282
ENST00000525824	ENSG00000105397	5,160951831	4,378638944	0,00053008	tyrosine kinase 2 [Source:HGNC Symbol;Acc:HGNC:12440]
ENST00000364904	ENSG00000201774	2,28629702	5,461940943	0,00053405	
ENST00000411053	ENSG00000222985	2,402260246	7,142142419	0,000553696	RNA, U2 small nuclear 14, pseudogene [Source:HGNC Symbol;Acc
ENST00000384302	ENSG00000207029	2,798457311	5,576952238	0,000564518	RNA, U6 small nuclear 43, pseudogene [Source:HGNC Symbol;Acc
ENST00000415675	ENSG00000225670	5,388353329	4,407227007	0,000581431	CADM3 antisense RNA 1 [Source:HGNC Symbol;Acc:HGNC:40812]
ENST00000384042	ENSG00000206769	2,625355641	5,654039281	0,000581946	RNA, U6 small nuclear 116, pseudogene [Source:HGNC Symbol;Ac
ENST00000384029	ENSG00000206756	3,380354519	4,419984405	0,000622256	
ENST00000365658	ENSG00000202528	3,440301188	4,596878348	0,000638696	RNA, U6 small nuclear 650, pseudogene [Source:HGNC Symbol;Ac
ENST00000359827	ENSG00000221866	-3,188612751	5,488682683	0,000655836	plexin A4 [Source:HGNC Symbol;Acc:HGNC:9102]
ENST00000368847	ENSG00000173214	2,050989529	5,810908439	0,000673014	major facilitator superfamily domain containing 4B [Source:HGNC
ENST00000602872		3,534511793	4,935587616	0,000700952	
ENST00000363858	ENSG00000200728	2,481841327	7,683779083	0,000707859	RNA, U6 small nuclear 271, pseudogene [Source:HGNC Symbol;Ac
ENST00000265724	ENSG00000085563	5,934484407	4,55735876	0,00072995	ATP binding cassette subfamily B member 1 [Source:HGNC Symbo
ENST00000464924	ENSG00000178104	5,073438182	4,372277436	0,000732204	phosphodiesterase 4D interacting protein [Source:HGNC Symbol;A
ENST00000306560	ENSG00000103044	5,553381503	4,693655567	0,000802386	hyaluronan synthase 3 [Source:HGNC Symbol;Acc:HGNC:4820]
ENST00000362002	ENSG00000198881	6,978478207	5,011275667	0,000811654	ankyrin repeat and SOCS box containing 12 [Source:HGNC Symbol
ENST00000517288	ENSG00000253097	4,123008286	5,149032661	0,000840936	RNA, U2 small nuclear 19, pseudogene [Source:HGNC Symbol;Acc
ENST00000328504	ENSG00000185594	7,189915159	5,110349607	0,000858126	spermatogenesis associated 8 [Source:HGNC Symbol;Acc:HGNC:2
ENST00000383860	ENSG00000206587	2,255772689	7,117025805	0,00094954	RNA, U6 small nuclear 46, pseudogene [Source:HGNC Symbol;Acc
ENST00000384148	ENSG00000206875	2,777056611	5,444369343	0,000959635	RNA, U6 small nuclear 761, pseudogene [Source:HGNC Symbol;Ac
ENST00000383948	ENSG00000206675	2,593601335	6,414175361	0,000992992	RNA, U6 small nuclear 32, pseudogene [Source:HGNC Symbol;Acc
ENST00000459386	ENSG00000238886	3,113709819	13,52948999	0,000999594	small nucleolar RNA, C/D box 121A [Source:HGNC Symbol;Acc:HG
ENST00000544824	ENSG00000256892	2,122135347	5,889904739	0,001000261	MT-RNR2 like 7 [Source:HGNC Symbol;Acc:HGNC:37164]
ENST00000554976	ENSG00000042088	6,960470889	5,581107793	0,001030361	tyrosyl-DNA phosphodiesterase 1 [Source:HGNC Symbol;Acc:HGN
ENST00000412321	ENSG00000226308	-5,147515234	4,381191293	0,001045834	novel transcript
ENST00000599234	ENSG00000268412	-5,144004387	4,386653959	0,001045834	tRNA methyltransferase subunit 11-2 pseudogene 6 [Source:HGN
ENST00000500262	ENSG00000244945	5,049125188	4,501770737	0,001045834	
ENST00000461043	ENSG00000125991	-5,045140495	4,355262016	0,001045834	ERGIC and golgi 3 [Source:HGNC Symbol;Acc:HGNC:15927]

ENST00000496714	ENSG00000145743	5,044568744	4,39441956	0,001045834	F-box and leucine rich repeat protein 17 [Source:HGNC Symbol;Ac
ENST00000505115	ENSG00000249654	4,929194275	4,527503931	0,001045834	vomeronasal 1 receptor 104 pseudogene [Source:HGNC Symbol;A
ENST00000577370	ENSG00000263456	3,177095623	4,368555496	0,001045834	microRNA 5189 [Source:HGNC Symbol;Acc:HGNC:43515]
ENST00000459360	ENSG00000238797	3,174149042	4,392213483	0,001045834	
ENST00000363742	ENSG00000200612	3,818734086	5,300489076	0,001073825	small nucleolar RNA, C/D box 114-25 [Source:HGNC Symbol;Acc:H
ENST00000408175	ENSG00000221102	3,636890544	5,014801378	0,001085642	small nucleolar RNA, H/ACA box 11B [Source:HGNC Symbol;Acc:H
ENST00000363664	ENSG00000200534	2,289666278	7,923169294	0,001098169	small nucleolar RNA, H/ACA box 33 [Source:HGNC Symbol;Acc:HG
ENST00000384246	ENSG00000206973	3,773894701	4,643705578	0,001110204	RNA, U6 small nuclear 1145, pseudogene [Source:HGNC Symbol;A
ENST00000516768	ENSG00000252577	2,553891272	6,72452236	0,001138981	small Cajal body-specific RNA 20 [Source:HGNC Symbol;Acc:HGNC
ENST00000516993	ENSG00000252802	2,025137274	5,981131727	0,00118057	
ENST00000384600	ENSG00000207330	2,495693533	6,1340525	0,00120723	RNA, U6 small nuclear 73, pseudogene [Source:HGNC Symbol;Acc
ENST00000417123	ENSG00000232564	5,050900449	4,452175848	0,001218748	MRTFA antisense RNA 1 [Source:HGNC Symbol;Acc:HGNC:40681]
ENST00000529192	ENSG00000180423	7,672348552	5,793914934	0,001247032	harbinger transposase derived 1 [Source:HGNC Symbol;Acc:HGNC
ENST00000584239	ENSG00000265078	2,870301217	6,611131218	0,001254056	RNA, 7SL, cytoplasmic 664, pseudogene [Source:HGNC Symbol;Ac
ENST00000459249	ENSG00000238561	2,498136125	8,17167908	0,001264501	RNA, U6atac small nuclear 28, pseudogene [Source:HGNC Symbol
ENST00000364200	ENSG00000201070	2,861980437	5,712811684	0,001264902	RNA, U4 small nuclear 84, pseudogene [Source:HGNC Symbol;Acc
ENST00000384965	ENSG00000207698	1,933042304	9,099969096	0,001269664	microRNA 32 [Source:HGNC Symbol;Acc:HGNC:31631]
ENST00000429469	ENSG00000223881	6,239359324	4,747564831	0,001289639	novel transcript
ENST00000516659	ENSG00000252468	2,003644614	7,615062614	0,001293709	RNA, U2 small nuclear 57, pseudogene [Source:HGNC Symbol;Acc
ENST00000406739	ENSG00000226967	5,418725582	4,467790018	0,001337242	HAUS augmin like complex subunit 4 pseudogene 1 [Source:HGNC
ENST00000364110		3,338988926	4,413811884	0,001366071	
ENST00000455337	ENSG00000237309	3,664707361	5,911185548	0,001386114	MT-ND2 pseudogene 6 [Source:HGNC Symbol;Acc:HGNC:42107]
ENST00000384433	ENSG00000207162	3,684430846	4,596706213	0,00139413	RNA, U6 small nuclear 549, pseudogene [Source:HGNC Symbol;Ac
ENST00000411283	ENSG00000223215	3,207168547	5,334545835	0,001452242	RNA, U6 small nuclear 607, pseudogene [Source:HGNC Symbol;Ac
ENST00000606802	ENSG00000272078	3,793102153	5,267105184	0,001464362	novel transcript, antisense to CASZ1
ENST00000363215	ENSG00000200085	3,492413802	4,755430106	0,001469502	
ENST00000299413	ENSG00000166326	-4,191107245	5,027130608	0,001475664	tripartite motif containing 44 [Source:HGNC Symbol;Acc:HGNC:19
ENST00000391162	ENSG00000212464	3,474007976	5,729209715	0,001486591	small nucleolar RNA, H/ACA box 12 [Source:HGNC Symbol;Acc:HG
ENST00000365512	ENSG00000202382	2,054437088	7,714221302	0,001542179	
ENST00000300026	ENSG00000166794	-3,356879178	4,703420182	0,001582784	peptidylprolyl isomerase B [Source:HGNC Symbol;Acc:HGNC:9255
ENST00000600213	ENSG00000269028	1,983847313	9,641229146	0,001607306	MT-RNR2 like 12 [Source:HGNC Symbol;Acc:HGNC:37169]
ENST00000364752	ENSG00000201622	5,256882755	4,484793679	0,001653009	RNA, U6 small nuclear 621, pseudogene [Source:HGNC Symbol;Ac
ENST00000435212	ENSG00000229604	2,00925366	8,517407398	0,001655373	MT-ATP8 pseudogene 2 [Source:HGNC Symbol;Acc:HGNC:44572]
ENST00000527315	ENSG00000255346	2,679414256	5,985616606	0,001668375	NADPH oxidase 5 [Source:HGNC Symbol;Acc:HGNC:14874]
ENST00000384875	ENSG00000207607	3,109341662	5,207648967	0,001715448	microRNA 200a [Source:HGNC Symbol;Acc:HGNC:31578]
ENST00000549240	ENSG00000140104	5,036679729	4,468446021	0,001734192	clathrin binding box of aftiphilin containing 1 [Source:HGNC Symb
ENST00000384979	ENSG00000207712	2,247628515	6,157922097	0,001747244	microRNA 627 [Source:HGNC Symbol;Acc:HGNC:32883]
ENST00000384376	ENSG00000207104	2,671368402	5,643696257	0,001758802	RNA, U6 small nuclear 434, pseudogene [Source:HGNC Symbol;Ac
ENST00000391305	ENSG00000212607	2,689415452	8,020478425	0,001814855	small nucleolar RNA, H/ACA box 3B [Source:HGNC Symbol;Acc:HG
ENST00000463460		3,926669017	5,078390089	0,001904427	
ENST00000516826	ENSG00000252635	3,010856529	6,988698981	0,001911121	RNA, U2 small nuclear 56, pseudogene [Source:HGNC Symbol;Acc
ENST00000585693	ENSG00000168259	3,730315657	4,589903121	0,001937811	DnaJ heat shock protein family (Hsp40) member C7 [Source:HGNC
ENST00000384255	ENSG00000206982	3,772206056	4,837549868	0,001945682	
ENST00000582078	ENSG00000266179	3,309716676	6,564969433	0,001977839	LSU rRNA pseudogene
ENST00000516903	ENSG00000252712	2,87845686	6,134572733	0,002015103	small Cajal body-specific RNA 14 [Source:HGNC Symbol;Acc:HGNC
ENST00000384703	ENSG00000207434	2,293926214	5,517501621	0,002031287	RNA, U6 small nuclear 1072, pseudogene [Source:HGNC Symbol;A
ENST00000576936	ENSG00000162104	5,981917446	4,544065971	0,00205347	adenylate cyclase 9 [Source:HGNC Symbol;Acc:HGNC:240]
ENST00000517097	ENSG00000252906	2,502061749	7,619261948	0,002065665	small Cajal body-specific RNA 3 [Source:HGNC Symbol;Acc:HGNC:
ENST00000381708		-5,037011266	4,374133639	0,002065911	
ENST00000569450	ENSG00000175318	4,926681925	4,339485544	0,002065911	GRAM domain containing 2A [Source:HGNC Symbol;Acc:HGNC:27
ENST00000445105	ENSG00000114279	4,924620554	4,406137221	0,002065911	fibroblast growth factor 12 [Source:HGNC Symbol;Acc:HGNC:3668
ENST00000454224	ENSG00000236008	4,924173685	4,461159376	0,002065911	long intergenic non-protein coding RNA 1814 [Source:HGNC Symb
ENST00000504510	ENSG00000124406	4,921669542	4,323208629	0,002065911	ATPase phospholipid transporting 8A1 [Source:HGNC Symbol;Acc:
ENST00000485918	ENSG00000133794	4,796730507	4,328709113	0,002065911	aryl hydrocarbon receptor nuclear translocator like [Source:HGNC
ENST00000519280	ENSG00000253496	7,757728999	6,149181271	0,002143446	novel transcript
ENST00000364647	ENSG00000201517	2,06622442	6,481650172	0,002230293	RNA, U6 small nuclear 707, pseudogene [Source:HGNC Symbol;Ac
ENST00000363804	ENSG00000200674	2,329490274	7,975808271	0,002241988	RNA, 7SK small nuclear pseudogene 160 [Source:HGNC Symbol;Ac
ENST00000428234	ENSG00000233007	6,782773412	5,036725148	0,002242226	UBTF like 11 (pseudogene) [Source:HGNC Symbol;Acc:HGNC:5028
ENST00000363345	ENSG00000200215	3,318738199	4,813037555	0,002278961	small nucleolar RNA, C/D box 113-6 [Source:HGNC Symbol;Acc:HG
ENST00000383934	ENSG00000206661	4,799641345	4,540778321	0,002289343	
ENST00000427426	ENSG00000229344	2,287038101	11,35805039	0,002302996	MT-CO2 pseudogene 12 [Source:HGNC Symbol;Acc:HGNC:52028]
ENST00000455776	ENSG00000227382	2,286654462	5,07793515	0,002307226	eukaryotic translation initiation factor 4A2 pseudogene 2 [Source
ENST00000362865	ENSG00000199735	3,204682439	4,823142205	0,002347178	RNA, U6 small nuclear 227, pseudogene [Source:HGNC Symbol;Ac
ENST00000607168	ENSG00000272113	1,88964518	6,18970525	0,002350561	

ENST00000384637	ENSG00000207367	2,109240536	6,955410032	0,002351279	RNA, U6 small nuclear 29, pseudogene [Source:HGNC Symbol;Acc
ENST00000365423	ENSG00000202293	3,79888416	5,537880538	0,002371393	small nucleolar RNA, C/D box 114-22 [Source:HGNC Symbol;Acc:H
ENST00000534945	ENSG00000139364	3,052145196	4,518049582	0,002390181	transmembrane protein 132B [Source:HGNC Symbol;Acc:HGNC:2
ENST00000516057	ENSG00000251866	4,350988811	4,70116823	0,002398182	small Cajal body-specific RNA 21B [Source:HGNC Symbol;Acc:HGN
ENST00000471853	ENSG00000162441	-4,232381167	4,940544979	0,002463231	leucine zipper and CTNNBIP1 domain containing [Source:HGNC Sy
ENST00000459326	ENSG00000239149	3,097827582	4,948281551	0,002471004	small nucleolar RNA, H/ACA box 59A [Source:HGNC Symbol;Acc:H
ENST00000458770	ENSG00000238531	3,285294962	12,42810362	0,002551114	small nucleolar RNA, C/D box 105B [Source:HGNC Symbol;Acc:HG
ENST00000362921	ENSG00000199791	2,787262323	4,547023323	0,002592664	RNA, U6 small nuclear 451, pseudogene [Source:HGNC Symbol;Ac
ENST00000408789	ENSG00000221716	3,127531614	5,323023369	0,002600637	small nucleolar RNA, H/ACA box 11 [Source:HGNC Symbol;Acc:HG
ENST00000383904	ENSG00000206631	3,54947209	4,559596227	0,002652733	RNA, U6 small nuclear 657, pseudogene [Source:HGNC Symbol;Ac
ENST00000363387	ENSG00000200257	2,589809038	5,043841689	0,002692572	RNA, U6 small nuclear 97, pseudogene [Source:HGNC Symbol;Acc
ENST00000383903	ENSG00000206630	2,883729461	13,28163672	0,002718025	small nucleolar RNA, C/D box 60 [Source:HGNC Symbol;Acc:HGNC
ENST00000545326		3,477007976	4,742466995	0,0027227	
ENST00000362420	ENSG00000199290	1,850342559	6,426905717	0,002746517	
ENST00000384205	ENSG00000206932	2,829365236	10,77623839	0,002783521	RNA, U6 small nuclear 4, pseudogene [Source:HGNC Symbol;Acc:H
ENST00000383932	ENSG00000206659	2,52853789	5,676539411	0,002795907	
ENST00000607261	ENSG00000272474	2,649070135	4,647470167	0,002821127	small nucleolar RNA, C/D box 113-5 [Source:HGNC Symbol;Acc:HG
ENST00000364744		2,565204621	5,905786167	0,002844759	
ENST00000584249	ENSG00000265154	1,994875833	6,53331037	0,002848311	microRNA 151b [Source:HGNC Symbol;Acc:HGNC:41588]
ENST00000390930	ENSG00000212232	2,086327691	9,410023052	0,002881128	small nucleolar RNA, C/D box 17 [Source:HGNC Symbol;Acc:HGNC
ENST00000369167	ENSG00000203814	5,601245661	5,232724792	0,002897352	histone cluster 2 H2B family member f [Source:HGNC Symbol;Acc:
ENST00000363399	ENSG00000200269	2,587865133	5,43357426	0,002937571	RNA, U6 small nuclear 838, pseudogene [Source:HGNC Symbol;Ac
ENST00000583596	ENSG00000263436	2,908508371	5,310123889	0,002942025	microRNA 3158-1 [Source:HGNC Symbol;Acc:HGNC:38196]
ENST00000536684	ENSG00000255823	1,974959318	9,656152348	0,002958369	MT-RNR2 like 8 [Source:HGNC Symbol;Acc:HGNC:37165]
ENST00000275072	ENSG00000146281	-2,938283759	5,260562375	0,002959816	peptidase M20 domain containing 2 [Source:HGNC Symbol;Acc:HG
ENST00000515909	ENSG00000251718	4,113428093	5,454338823	0,002974877	RNA, U2 small nuclear 13, pseudogene [Source:HGNC Symbol;Acc
ENST00000384314	ENSG00000207041	2,874374904	9,393472357	0,002974954	RNA, U6 small nuclear 3, pseudogene [Source:HGNC Symbol;Acc:H
ENST00000516145	ENSG00000251954	5,10932268	4,559283685	0,003004813	RNA, U6 small nuclear 496, pseudogene [Source:HGNC Symbol;Ac
ENST00000582203	ENSG00000266104	2,460064325	6,302685802	0,003016867	microRNA 4326 [Source:HGNC Symbol;Acc:HGNC:38314]
ENST00000384165	ENSG00000206892	2,521130579	8,039525242	0,003032482	RNA, U6 small nuclear 42, pseudogene [Source:HGNC Symbol;Acc
ENST00000363524	ENSG00000200394	2,245086116	6,604167406	0,00308711	small nucleolar RNA, H/ACA box 38B [Source:HGNC Symbol;Acc:H
ENST00000516458	ENSG00000252267	5,182843937	4,990659566	0,003143408	RNA, 5S ribosomal pseudogene 495 [Source:HGNC Symbol;Acc:HG
ENST00000459577	ENSG00000238793	3,247193274	6,185074407	0,003162575	small nucleolar RNA, C/D box 124 [Source:HGNC Symbol;Acc:HGN
ENST00000568183	ENSG00000260796	5,055949513	4,358181932	0,003236575	novel transcript, antisense to ATXN2L
ENST00000553041	ENSG00000111144	3,613439249	4,643188311	0,003297571	leukotriene A4 hydrolase [Source:HGNC Symbol;Acc:HGNC:6710]
ENST00000384499	ENSG00000238825	1,594383604	7,135654905	0,003326037	RNA, U1 small nuclear 13, pseudogene [Source:HGNC Symbol;Acc
ENST00000516473	ENSG00000252282	5,080526593	4,549708025	0,003352495	RNA, U6 small nuclear 1089, pseudogene [Source:HGNC Symbol;A
ENST00000376775	ENSG00000204620	4,813612583	4,622650636	0,003383023	novel transcript, antisense to RBM3
ENST00000384027	ENSG00000206754	1,917919775	9,240925588	0,003392843	small nucleolar RNA, C/D box 101 [Source:HGNC Symbol;Acc:HGN
ENST00000423240	ENSG00000236060	-4,94944162	4,328278938	0,003402159	heat shock protein family B (small) member 1 pseudogene 1 [Sou
ENST00000507199	ENSG00000188388	-3,814776449	5,018194419	0,003425219	golgin A6 family-like 3 [Source:HGNC Symbol;Acc:HGNC:37441]
ENST00000384693	ENSG00000277846	2,153306042	9,209618445	0,003447084	small nucleolar RNA, C/D box 30 [Source:HGNC Symbol;Acc:HGNC
ENST00000362215	ENSG00000199085	2,137249291	10,6965115	0,003451428	microRNA 148a [Source:HGNC Symbol;Acc:HGNC:31535]
ENST00000242465	ENSG00000122862	-5,690785185	5,16072619	0,003461144	serglycin [Source:HGNC Symbol;Acc:HGNC:9361]
ENST00000458848		1,909167495	5,942537811	0,003530682	
ENST00000428285	ENSG00000233993	7,211713875	5,240376914	0,003535477	
ENST00000384662	ENSG00000207392	3,082475252	8,79342406	0,003545671	small nucleolar RNA, H/ACA box 20 [Source:HGNC Symbol;Acc:HG
ENST00000364370	ENSG00000201240	4,371752997	5,241168886	0,003560394	small nucleolar RNA, C/D box 114-9 [Source:HGNC Symbol;Acc:HG
ENST00000384388	ENSG00000207116	3,313912735	10,82823266	0,003583914	RNA, U6 small nuclear 31, pseudogene [Source:HGNC Symbol;Acc
ENST00000364558	ENSG00000201428	1,957507988	5,700297542	0,003595762	RNA, 7SK small nuclear pseudogene 71 [Source:HGNC Symbol;Acc
ENST00000434771	ENSG00000231931	4,061537379	4,593355649	0,003652684	pseudogene similiar to part of tumor protein, translationally-cont
ENST00000468439	ENSG00000240890	3,28642718	4,398084994	0,003663092	G2/M-phase specific E3 ubiquitin ligase (G2E3) pseudogene
ENST00000515982	ENSG00000251791	1,774295365	8,281375345	0,003773892	small Cajal body-specific RNA 6 [Source:HGNC Symbol;Acc:HGNC:
ENST00000364310	ENSG00000201180	2,67907146	4,930993396	0,00379369	RNA, U6 small nuclear 115, pseudogene [Source:HGNC Symbol;Ac
ENST00000386307	ENSG00000209042	2,957171745	14,72911453	0,003810275	small nucleolar RNA, C/D box 12C [Source:HGNC Symbol;Acc:HGN
ENST00000411041	ENSG00000222973	1,85030556	6,898532697	0,003816578	RNA, U2 small nuclear 25, pseudogene [Source:HGNC Symbol;Acc
ENST00000417816	ENSG00000078114	-2,660318128	4,600499531	0,00391833	nebulette [Source:HGNC Symbol;Acc:HGNC:16932]
ENST00000244051	ENSG00000124217	3,916468188	4,713412339	0,003929888	molybdenum cofactor synthesis 3 [Source:HGNC Symbol;Acc:HGN
ENST00000568567	ENSG00000261127	2,262932901	4,936912202	0,003930437	protein phosphatase 2, regulatory subunit B'', beta (PPP2R3B) pse
ENST00000388006	ENSG00000210741	-2,485495868	6,642177287	0,004008759	microRNA 196a-1 [Source:HGNC Symbol;Acc:HGNC:31567]
ENST00000451763	ENSG00000106686	3,022424792	7,579307122	0,004052914	spermatogenesis associated 6 like [Source:HGNC Symbol;Acc:HGN
ENST00000364693	ENSG00000201563	2,60011848	4,500425525	0,004074014	
ENST00000453647	ENSG00000224233	4,793038814	4,318401428	0,004085918	olfactory receptor family 2 subfamily J member 4 pseudogene [So
ENST00000477976	ENSG00000188976	4,793038814	4,439568824	0,004085918	NOC2 like nucleolar associated transcriptional repressor [Source:H

ENST00000511866	ENSG00000169762	4,793038814	4,318401428	0,004085918	transmembrane anterior posterior transformation 1 [Source:HGN
ENST00000606534	ENSG00000271923	4,792591056	4,524330645	0,004085918	RNA, U6 small nuclear 86, pseudogene [Source:HGNC Symbol;Acc
ENST00000362637	ENSG00000238560	4,792143434	4,388150081	0,004085918	
ENST00000420330	ENSG00000236255	4,792143434	4,332897085	0,004085918	novel transcript
ENST00000416689	ENSG00000227533	4,790078501	4,487575452	0,004085918	SLC2A1 antisense RNA 1 [Source:HGNC Symbol;Acc:HGNC:44187]
ENST00000482625	ENSG00000241367	4,790078501	4,336186287	0,004085918	ribosomal protein L7a pseudogene 23 [Source:HGNC Symbol;Acc:
ENST00000363031	ENSG00000199901	4,788462739	4,371893237	0,004085918	
ENST00000384670	ENSG00000207401	4,788016342	4,35719638	0,004085918	
ENST00000555725	ENSG00000259082	4,788016342	4,301938523	0,004085918	long intergenic non-protein coding RNA 2314 [Source:HGNC Symb
ENST00000604583	ENSG00000270591	4,788016342	4,426012041	0,004085918	protein phosphatase 2, regulatory subunit B', gamma (PPP2R5C)
ENST00000510463	ENSG00000155011	4,65215277	4,343743973	0,004085918	dickkopf WNT signaling pathway inhibitor 2 [Source:HGNC Symbo
ENST00000605573	ENSG00000270959	4,650522757	4,512642907	0,004085918	LPP antisense RNA 2 [Source:HGNC Symbol;Acc:HGNC:27952]
ENST00000604882	ENSG00000271043	1,662689376	10,31160386	0,004123635	MT-RNR2 like 2 [Source:HGNC Symbol;Acc:HGNC:37156]
ENST00000552200	ENSG00000139174	-3,521932178	5,503389612	0,004133878	prickle planar cell polarity protein 1 [Source:HGNC Symbol;Acc:HG
ENST00000251089	ENSG00000013523	-5,26981832	4,535353527	0,004140379	angel homolog 1 [Source:HGNC Symbol;Acc:HGNC:19961]
ENST00000606769	ENSG00000272533	2,565428945	8,229228679	0,004142607	small nucleolar RNA, H/ACA box 28 [Source:HGNC Symbol;Acc:HG
ENST00000516540	ENSG00000252349	2,18459911	6,987709311	0,004168134	
ENST00000384245	ENSG00000206972	1,986882066	6,656569301	0,004194448	RNA, U6 small nuclear 17, pseudogene [Source:HGNC Symbol;Acc
ENST00000364789	ENSG00000201659	2,376863112	5,373784785	0,004211986	RNA, U12 small nuclear 2, pseudogene [Source:HGNC Symbol;Acc
ENST00000384519	ENSG00000207248	2,808766921	5,957036002	0,004212117	RNA, U6 small nuclear 1005, pseudogene [Source:HGNC Symbol;A
ENST00000429829	ENSG00000229807	2,683509876	5,155833573	0,004294912	X inactive specific transcript [Source:HGNC Symbol;Acc:HGNC:128
ENST00000383873	ENSG00000206600	2,320077695	8,563743389	0,004303433	RNA, U6 small nuclear 25, pseudogene [Source:HGNC Symbol;Acc
ENST00000581495	ENSG00000264764	-3,271120611	4,426197243	0,004343597	microRNA 4772 [Source:HGNC Symbol;Acc:HGNC:41741]
ENST00000356661	ENSG00000198681	-5,482177979	4,581627269	0,004347108	MAGE family member A1 [Source:HGNC Symbol;Acc:HGNC:6796]
ENST00000554988	ENSG00000259001	5,237726726	4,411873307	0,004394463	ribonuclease P RNA component H1
ENST00000365080	ENSG00000201950	4,156838045	5,330804114	0,004409185	small nucleolar RNA, C/D box 113-9 [Source:HGNC Symbol;Acc:HG
ENST00000384136	ENSG00000206863	2,458190326	6,935213509	0,00444173	RNA, U5A small nuclear 6, pseudogene [Source:HGNC Symbol;Acc
ENST00000386967	ENSG00000209702	2,993927287	14,10475465	0,004492537	small nucleolar RNA, C/D box 41 [Source:HGNC Symbol;Acc:HGNC
ENST00000345617	ENSG00000068024	-2,244070928	6,036982166	0,004494488	histone deacetylase 4 [Source:HGNC Symbol;Acc:HGNC:14063]
ENST00000450912	ENSG00000230276	5,018810631	4,703471486	0,004537218	NHP2 non-histone chromosome protein 2-like 1 (S. cerevisiae) (NH
ENST00000384281	ENSG00000207008	2,637856571	7,419734127	0,004537882	small nucleolar RNA, H/ACA box 54 [Source:HGNC Symbol;Acc:HG
ENST00000364478	ENSG00000201348	2,177159527	5,612432386	0,004541493	RNA, U105B small nucleolar [Source:HGNC Symbol;Acc:HGNC:101
ENST00000363384	ENSG00000200254	2,700727148	4,584144364	0,00454522	RNA, U6 small nuclear 536, pseudogene [Source:HGNC Symbol;Ac
ENST00000542256	ENSG00000008394	3,402907536	4,779058421	0,004586287	microsomal glutathione S-transferase 1 [Source:HGNC Symbol;Ac
ENST00000552061	ENSG00000257298	6,874891045	6,96609624	0,004606912	novel transcript, sense intronic to LIMA1
ENST00000455228	ENSG00000227744	6,799809964	5,138385065	0,004647649	long intergenic non-protein coding RNA 1940 [Source:HGNC Symb
ENST00000496932	ENSG00000066322	2,916006558	4,513843993	0,004655633	ELOVL fatty acid elongase 1 [Source:HGNC Symbol;Acc:HGNC:144
ENST00000384776	ENSG00000207507	2,608909905	10,96474379	0,004739103	RNA, U6 small nuclear 9 [Source:HGNC Symbol;Acc:HGNC:34269]
ENST00000262460	ENSG00000101003	2,726715368	4,651805931	0,004749089	GINS complex subunit 1 [Source:HGNC Symbol;Acc:HGNC:28980]
ENST00000598907	ENSG00000160410	3,129022635	5,017719966	0,004769818	SH3KBP1 binding protein 1 [Source:HGNC Symbol;Acc:HGNC:1921
ENST00000528297	ENSG00000255189	5,271336503	4,79879477	0,00479782	glycine-N-acyltransferase like 1 pseudogene 1 [Source:HGNC Sym
ENST00000516336	ENSG00000252145	2,633220547	5,200986077	0,004823098	RNA, U6 small nuclear 1225, pseudogene [Source:HGNC Symbol;A
ENST00000384426	ENSG00000207155	2,170248447	6,251164521	0,004844119	RNA, Ro-associated Y1 pseudogene 14 [Source:HGNC Symbol;Acc:
ENST00000384172	ENSG00000206899	2,794247899	10,53279396	0,004854558	RNA, U6 small nuclear 36, pseudogene [Source:HGNC Symbol;Acc
ENST00000363839	ENSG00000200709	3,356247632	5,27862639	0,004904584	RNA, 5S ribosomal pseudogene 27 [Source:HGNC Symbol;Acc:HGN
ENST00000362535	ENSG00000199405	2,449315957	5,918886524	0,00490822	small nucleolar RNA, H/ACA box 1B [Source:HGNC Symbol;Acc:HG
ENST00000454092	ENSG00000198868	2,673034313	7,967920495	0,004946816	MT-ND4L pseudogene 30 [Source:HGNC Symbol;Acc:HGNC:42264
ENST00000384254	ENSG00000206981	2,66654659	6,062590332	0,004969805	RNA, U6 small nuclear 40, pseudogene [Source:HGNC Symbol;Acc
ENST00000331563	ENSG00000184363	-4,781408042	4,579073818	0,005043436	plakophilin 3 [Source:HGNC Symbol;Acc:HGNC:9025]
ENST00000365177	ENSG00000202047	4,838457946	4,681484521	0,005119893	RNA, 5S ribosomal pseudogene 324 [Source:HGNC Symbol;Acc:HG
ENST00000591006	ENSG00000013306	3,441075131	5,32347336	0,005133297	solute carrier family 25 member 39 [Source:HGNC Symbol;Acc:HG
ENST00000391112	ENSG00000212414	2,151395281	7,050719968	0,00517058	small nucleolar RNA, C/D box 77B [Source:HGNC Symbol;Acc:HGN
ENST00000410423	ENSG00000222355	2,081377223	5,720492578	0,005191053	RNA, U2 small nuclear 29, pseudogene [Source:HGNC Symbol;Acc
ENST00000364015	ENSG00000200885	2,275881787	10,34808016	0,005241518	RNA, U1 small nuclear 146, pseudogene [Source:HGNC Symbol;Ac
ENST00000410438	ENSG00000222370	1,7932253	7,523260805	0,005250775	small nucleolar RNA, H/ACA box 36B [Source:HGNC Symbol;Acc:H
ENST00000410457	ENSG00000222389	2,267808299	6,10085423	0,005280629	RNA, U2 small nuclear 28, pseudogene [Source:HGNC Symbol;Acc
ENST00000318008	ENSG00000002834	-2,944424817	4,668557204	0,005328383	LIM and SH3 protein 1 [Source:HGNC Symbol;Acc:HGNC:6513]
ENST00000390904	ENSG00000212206	2,990438337	5,076210793	0,005384202	
ENST00000591531	ENSG00000267260	2,444007414	4,44016518	0,005401311	uncharacterized LOC728485 [Source:NCBI gene;Acc:728485]
ENST00000517138	ENSG00000252947	2,203946201	7,620230922	0,005415233	small Cajal body-specific RNA 1 [Source:HGNC Symbol;Acc:HGNC:
ENST00000384017	ENSG00000206744	2,887719688	4,915242651	0,005490097	RNA, U6 small nuclear 620, pseudogene [Source:HGNC Symbol;Ac
ENST00000349139	ENSG00000065183	-4,100864467	4,70545456	0,005499733	WD repeat domain 3 [Source:HGNC Symbol;Acc:HGNC:12755]
ENST00000387943	ENSG00000210678	2,707106462	10,60862173	0,005520802	RNA, U6atac small nuclear 2, pseudogene [Source:HGNC Symbol;A
ENST00000384238	ENSG00000206965	2,708876582	9,065724382	0,005538239	RNA, U6 small nuclear 5, pseudogene [Source:HGNC Symbol;Acc:H

ENST00000383907	ENSG00000206634	2,047075475	8,362891182	0,005582795	small nucleolar RNA, H/ACA box 22 [Source:HGNC Symbol;Acc:HG
ENST00000607344	ENSG00000272469	3,38302762	4,890997783	0,00562251	RNA, 7SL, cytoplasmic 760, pseudogene [Source:HGNC Symbol;Ac
ENST00000264711	ENSG00000115137	3,354065847	5,429672739	0,00562671	DnaJ heat shock protein family (Hsp40) member C27 [Source:HGN
ENST00000410718	ENSG00000222650	1,885300809	8,263501132	0,005661387	RNA, U2 small nuclear 70, pseudogene [Source:HGNC Symbol;Acc
ENST00000364830	ENSG00000201700	3,211284359	5,095124359	0,00569563	small nucleolar RNA, C/D box 113-3 [Source:HGNC Symbol;Acc:HG
ENST00000391208	ENSG00000212510	3,323967344	4,824971184	0,005737505	RNA, U6 small nuclear 972, pseudogene [Source:HGNC Symbol;Ac
ENST00000384839	ENSG00000207571	1,966119959	7,474035517	0,00582411	microRNA 615 [Source:HGNC Symbol;Acc:HGNC:32871]
ENST00000522581	ENSG00000254172	2,740394908	6,162366728	0,005898474	RNA, U5A small nuclear 3, pseudogene [Source:HGNC Symbol;Acc
ENST00000396946	ENSG00000198286	-3,404911801	4,552592299	0,005905535	caspase recruitment domain family member 11 [Source:HGNC Syr
ENST00000453697	ENSG00000232727	-2,232507024	4,544816114	0,005911351	tyrosine 3-monooxygenase/tryptophan 5-monooxygenase activat
ENST00000384225	ENSG00000206952	2,74032414	6,71881899	0,005921188	small nucleolar RNA, H/ACA box 50A [Source:HGNC Symbol;Acc:H
ENST00000567736	ENSG00000167522	-3,455711955	4,599916651	0,006008577	ankyrin repeat domain 11 [Source:HGNC Symbol;Acc:HGNC:21316
ENST00000390833	ENSG00000212135	2,867654609	10,11186273	0,006022241	small nucleolar RNA, C/D box 67 [Source:HGNC Symbol;Acc:HGNC
ENST00000401154	ENSG00000215973	2,836629018	4,999250453	0,006098657	microRNA 933 [Source:HGNC Symbol;Acc:HGNC:33676]
ENST00000452761	ENSG00000225108	-4,963356072	4,439816135	0,006251344	zinc finger and BTB domain containing 45 pseudogene 1 [Source:H
ENST00000410433	ENSG00000222365	2,954336416	15,23457503	0,006342255	small nucleolar RNA, C/D box 12B [Source:HGNC Symbol;Acc:HGN
ENST00000455094	ENSG00000236603	-3,737074746	4,835577156	0,006344037	RAN, member RAS oncogene family pseudogene 1 [Source:HGNC
ENST00000384793	ENSG00000207524	2,752426359	9,200595909	0,006359183	RNA, U6 small nuclear 33, pseudogene [Source:HGNC Symbol;Acc
ENST00000384223	ENSG00000206950	1,938819896	6,227707775	0,006397235	
ENST00000384041	ENSG00000206768	4,68129218	4,491191074	0,006400149	
ENST00000364923	ENSG00000201793	2,725945696	5,10406818	0,006429654	RNA, 7SK small nuclear pseudogene 9 [Source:HGNC Symbol;Acc:H
ENST00000394329	ENSG00000196159	3,408511889	5,518779887	0,006459808	FAT atypical cadherin 4 [Source:HGNC Symbol;Acc:HGNC:23109]
ENST00000329203	ENSG00000182103	-2,488779726	6,652175407	0,006470385	family with sequence similarity 181 member B [Source:HGNC Sym
ENST00000362970	ENSG00000199840	2,517021482	4,851713225	0,006532068	
ENST00000372443	ENSG00000156113	7,16812384	5,336588964	0,006544053	potassium calcium-activated channel subfamily M alpha 1 [Source
ENST00000431486	ENSG00000231216	2,902474748	4,578609871	0,006557221	unknown transcript [Source:NCBI gene;Acc:100093698]
ENST00000365138	ENSG00000202008	2,259509551	5,372197722	0,00659854	
ENST00000363354	ENSG00000200224	2,780988762	4,77637868	0,006617697	RNA, U6 small nuclear 626, pseudogene [Source:HGNC Symbol;Ac
ENST00000363386	ENSG00000200256	3,172990524	4,423491097	0,006719134	
ENST00000384858	ENSG00000207590	3,172543933	4,41836622	0,006719134	microRNA 215 [Source:HGNC Symbol;Acc:HGNC:31592]
ENST00000580269	ENSG00000266038	3,170490668	4,385459444	0,006719134	microRNA 4659a [Source:HGNC Symbol;Acc:HGNC:41857]
ENST00000383895	ENSG00000206622	2,272310322	4,553797262	0,006719134	small nucleolar RNA, H/ACA box 69 [Source:HGNC Symbol;Acc:HG
ENST00000391145	ENSG00000212447	3,132161432	12,91869093	0,006736871	small nucleolar RNA, C/D box 90 [Source:HGNC Symbol;Acc:HGNC
ENST00000365031	ENSG00000201901	1,796509943	6,603846899	0,006753585	RNA, 7SK small nuclear pseudogene 48 [Source:HGNC Symbol;Acc
ENST00000400555	ENSG00000154845	-4,989655243	4,365525523	0,006797038	protein phosphatase 4 regulatory subunit 1 [Source:HGNC Symbo
ENST00000384078	ENSG00000206805	2,742035572	5,767220261	0,006877361	
ENST00000384106	ENSG00000206833	1,962506603	5,693040548	0,006887976	RNA, U6 small nuclear 20, pseudogene [Source:HGNC Symbol;Acc
ENST00000410413	ENSG00000222345	2,457429329	12,12594378	0,006898099	small nucleolar RNA, C/D box 19C [Source:HGNC Symbol;Acc:HGN
ENST00000347667	ENSG00000182240	5,41677329	4,782285059	0,00691156	beta-secretase 2 [Source:HGNC Symbol;Acc:HGNC:934]
ENST00000384344	ENSG00000207072	1,87870213	7,766348429	0,006968981	RNA, U6 small nuclear 39, pseudogene [Source:HGNC Symbol;Acc
ENST00000362807	ENSG00000199677	3,34465941	4,959178747	0,007043282	
ENST00000517697	ENSG00000253549	-3,524972272	4,671343199	0,007055941	CA3 antisense RNA 1 [Source:HGNC Symbol;Acc:HGNC:51657]
ENST00000548943	ENSG00000257611	6,020472261	4,903168823	0,007151428	thyroid hormone receptor interactor 11 (TRIP11) pseudogene
ENST00000411187		3,589637379	4,788721073	0,007178813	
ENST00000384500	ENSG00000207229	2,36236112	5,663670942	0,007183641	
ENST00000439870	ENSG00000233230	-3,537400969	4,527890687	0,007219241	novel transcript
ENST00000374791	ENSG00000182667	-3,092490949	4,589800325	0,007293414	neurotrimin [Source:HGNC Symbol;Acc:HGNC:17941]
ENST00000441788	ENSG00000105325	-5,239667668	4,634425726	0,007395525	fizzy and cell division cycle 20 related 1 [Source:HGNC Symbol;Acc
ENST00000312655	ENSG00000175155	3,260685889	4,605933861	0,007427578	yippee like 2 [Source:HGNC Symbol;Acc:HGNC:18326]
ENST00000365161	ENSG00000202031	1,983965032	8,152123289	0,007457557	small nucleolar RNA, C/D box 38A [Source:HGNC Symbol;Acc:HGN
ENST00000447645	ENSG00000178385	4,809032814	4,609052415	0,007532102	pleckstrin homology domain containing M3 [Source:HGNC Symbo
ENST00000244221	ENSG00000124374	3,27691888	5,067762659	0,00758358	poly(A) binding protein interacting protein 2B [Source:HGNC Syml
ENST00000384294	ENSG00000207021	1,788760311	7,487892925	0,007592766	
ENST00000384506	ENSG00000207235	2,326425379	4,623760744	0,007633626	
ENST00000474788	ENSG00000115956	4,773447217	4,421804942	0,007794888	pleckstrin [Source:HGNC Symbol;Acc:HGNC:9070]
ENST00000603719	ENSG00000271687	1,866870775	8,138403898	0,007861248	MT-ND5 pseudogene 10 [Source:HGNC Symbol;Acc:HGNC:42272]
ENST00000447430	ENSG00000233559	3,162612529	4,493108892	0,00786491	long intergenic non-protein coding RNA 513 [Source:HGNC Symbo
ENST00000363035	ENSG00000199905	2,504533564	4,490561762	0,007920425	RNA, U6 small nuclear 492, pseudogene [Source:HGNC Symbol;Ac
ENST00000593685	ENSG00000105204	4,21590252	6,00833188	0,007934617	dual specificity tyrosine phosphorylation regulated kinase 1B [Sou
ENST00000408479	ENSG00000221406	2,208290816	8,488314322	0,007973406	microRNA 320b-2 [Source:HGNC Symbol;Acc:HGNC:35256]
ENST00000384324	ENSG00000207052	1,524232256	5,966757876	0,00801246	RNA, U6 small nuclear 378, pseudogene [Source:HGNC Symbol;Ac
ENST00000384262	ENSG00000206989	2,562099308	16,85597197	0,008012871	small nucleolar RNA, C/D box 63 [Source:HGNC Symbol;Acc:HGNC
ENST00000591258	ENSG00000267541	3,479158339	5,225481972	0,008049882	MT-CO2 pseudogene 2 [Source:HGNC Symbol;Acc:HGNC:25354]
ENST00000595245	ENSG00000099326	3,659147909	5,63137806	0,008056649	myeloid zinc finger 1 [Source:HGNC Symbol;Acc:HGNC:13108]

ENST00000581275	ENSG00000263535	-4,778843597	4,321389146	0,008090933	adenylate kinase 4 pseudogene 1 [Source:HGNC Symbol;Acc:HGN
ENST00000589470	ENSG00000267142	-4,778843597	4,394399202	0,008090933	acyl-CoA thioesterase 2 (ACOT2) pseudogene
ENST00000322927	ENSG00000198026	-4,777796699	4,349933084	0,008090933	zinc finger protein 335 [Source:HGNC Symbol;Acc:HGNC:15807]
ENST00000371236	ENSG00000173406	4,647996754	4,396934638	0,008090933	DAB1, reelin adaptor protein [Source:HGNC Symbol;Acc:HGNC:26
ENST00000362530	ENSG00000199400	4,645922982	4,441287158	0,008090933	RNA, Ro-associated Y4 pseudogene 19 [Source:HGNC Symbol;Acc:
ENST00000517030	ENSG00000252839	4,64547495	4,516709515	0,008090933	RNA, U6 small nuclear 419, pseudogene [Source:HGNC Symbol;Ac
ENST00000384640	ENSG00000207370	4,643404611	4,288655492	0,008090933	
ENST00000526629	ENSG00000120458	4,642957332	4,341005396	0,008090933	Myb/SANT DNA binding domain containing 2 [Source:HGNC Symb
ENST00000467438	ENSG00000267272	-4,638847121	4,460486164	0,008090933	long intergenic non-protein coding RNA 1140 [Source:HGNC Symb
ENST00000229595	ENSG00000111875	-4,634236624	4,345467718	0,008090933	anti-silencing function 1A histone chaperone [Source:HGNC Symb
ENST00000311481	ENSG00000174903	-4,634236624	4,30457819	0,008090933	RAB1B, member RAS oncogene family [Source:HGNC Symbol;Acc:
ENST00000354461		-4,634236624	4,325777473	0,008090933	
ENST00000526774	ENSG00000052841	4,486450435	4,28782029	0,008090933	tetratricopeptide repeat domain 17 [Source:HGNC Symbol;Acc:HG
ENST00000602788	ENSG00000141279	4,486000882	4,322673158	0,008090933	aminopeptidase puromycin sensitive [Source:HGNC Symbol;Acc:H
ENST00000264144	ENSG00000058085	4,485551465	4,283690641	0,008090933	laminin subunit gamma 2 [Source:HGNC Symbol;Acc:HGNC:6493]
ENST00000364732	ENSG00000201602	4,485551465	4,283690641	0,008090933	
ENST00000433572	ENSG00000229245	4,485551465	4,324271155	0,008090933	novel transcript
ENST00000560237	ENSG00000259700	4,485551465	4,321516065	0,008090933	novel transcript, antisense to CEP152
ENST00000413312	ENSG00000144451	2,775055248	4,344965789	0,008090933	sperm associated antigen 16 [Source:HGNC Symbol;Acc:HGNC:232
ENST00000401766	ENSG00000108576	2,616030734	4,37941664	0,008090933	solute carrier family 6 member 4 [Source:HGNC Symbol;Acc:HGNC
ENST00000355849	ENSG00000131773	-3,941042497	4,842184273	0,00815237	KH RNA binding domain containing, signal transduction associated
ENST00000365012	ENSG00000201882	2,564014202	11,1002676	0,008163225	
ENST00000463678	ENSG00000162650	-5,295090988	4,654486798	0,008189301	ataxin 7 like 2 [Source:HGNC Symbol;Acc:HGNC:28713]
ENST00000418282	ENSG00000232416	5,130503781	4,523982495	0,00820039	blepharophimosis, epicanthus inversus and ptosis candidate 1 [So
ENST00000515997		2,32216449	13,61854586	0,00823019	
ENST00000508948	ENSG00000113369	-3,373372458	4,506253143	0,008277235	arrestin domain containing 3 [Source:HGNC Symbol;Acc:HGNC:29
ENST00000363138	ENSG00000200008	1,880596901	5,698773914	0,008323917	
ENST00000408100		2,415075027	6,61017829	0,008327944	
ENST00000555226	ENSG00000140022	3,018810003	4,976162208	0,008416359	stonin 2 [Source:HGNC Symbol;Acc:HGNC:30652]
ENST00000364264	ENSG00000201134	2,212996298	5,203517843	0,008463675	
ENST00000362680	ENSG00000199550	2,17526199	6,516076314	0,008480667	
ENST00000384417	ENSG00000207146	2,220902377	5,045661434	0,008480808	
ENST00000410792	ENSG00000222724	2,349207024	8,901306317	0,00850301	RNA, U2 small nuclear 63, pseudogene [Source:HGNC Symbol;Acc
ENST00000384737	ENSG00000207468	2,374379273	11,07160633	0,008544998	small nucleolar RNA, H/ACA box 19 [Source:HGNC Symbol;Acc:HG
ENST00000411381	ENSG00000223313	2,45296439	4,594987382	0,008546317	RNA, U6 small nuclear 516, pseudogene [Source:HGNC Symbol;Ac
ENST00000411146	ENSG00000223078	2,857375742	4,777716532	0,008552738	RNA, U2 small nuclear 55, pseudogene [Source:HGNC Symbol;Acc
ENST00000385047	ENSG00000207781	1,746818921	8,944331345	0,008632997	microRNA 625 [Source:HGNC Symbol;Acc:HGNC:32881]
ENST00000607707	ENSG00000271852	2,73661883	13,91519556	0,008637683	small nucleolar RNA, C/D box 11B [Source:HGNC Symbol;Acc:HGN
ENST00000564848	ENSG00000167173	-2,699891099	4,565559892	0,008651774	chromosome 15 open reading frame 39 [Source:HGNC Symbol;Ac
ENST00000408716	ENSG00000221643	1,619077209	6,415505487	0,008745161	small nucleolar RNA, H/ACA box 77 [Source:HGNC Symbol;Acc:HG
ENST00000384892	ENSG00000207624	1,727027595	6,622696376	0,008795028	microRNA 194-1 [Source:HGNC Symbol;Acc:HGNC:31564]
ENST00000364326	ENSG00000201196	3,015019386	4,70183219	0,008807052	
ENST00000260682	ENSG00000138109	4,491569375	4,451640177	0,008811316	cytochrome P450 family 2 subfamily C member 9 [Source:HGNC S
ENST00000408324	ENSG00000221251	-3,025671901	4,920024356	0,008871773	microRNA 1263 [Source:HGNC Symbol;Acc:HGNC:35329]
ENST00000384530	ENSG00000207260	2,048010304	6,685764894	0,008888768	RNA, U6 small nuclear 35, pseudogene [Source:HGNC Symbol;Acc
ENST00000391313	ENSG00000212615	3,677540204	5,607751943	0,008896767	
ENST00000308893	ENSG00000149930	-3,494305125	4,656729083	0,008907998	TAO kinase 2 [Source:HGNC Symbol;Acc:HGNC:16835]
ENST00000576677	ENSG00000141556	-5,027727056	4,633051209	0,008936995	tubulin folding cofactor D [Source:HGNC Symbol;Acc:HGNC:11581
ENST00000363301	ENSG00000200171	1,905055865	6,530954278	0,008953331	
ENST00000341460	ENSG00000097096	-2,131230172	5,408491159	0,008963973	synapse defective Rho GTPase homolog 2 [Source:HGNC Symbol;A
ENST00000262839	ENSG00000072315	2,777609718	4,513333967	0,008977481	transient receptor potential cation channel subfamily C member 5
ENST00000365444	ENSG00000202314	2,390625582	14,84654307	0,008996453	small nucleolar RNA, C/D box 6 [Source:HGNC Symbol;Acc:HGNC:
ENST00000410557	ENSG00000222489	3,000724197	7,826943845	0,009028802	small nucleolar RNA, H/ACA box 79B [Source:HGNC Symbol;Acc:H
ENST00000365487	ENSG00000202357	1,895344898	6,973016984	0,009047545	
ENST00000400405	ENSG00000215475	2,26742117	6,494176989	0,00906882	siah E3 ubiquitin protein ligase family member 3 [Source:HGNC Sy
ENST00000362449	ENSG00000199319	4,747215695	4,51412591	0,009099441	RNA, 7SK small nuclear pseudogene 25 [Source:HGNC Symbol;Acc
ENST00000391061	ENSG00000212363	3,214322773	4,815175431	0,009153973	
ENST00000407112	ENSG00000174945	-4,092823741	4,630206866	0,00922939	archaelysin family metallopeptidase 1 [Source:HGNC Symbol;Acc:
ENST00000516999		1,872712575	7,908324475	0,00923736	
ENST00000563942	ENSG00000248334	-2,502458712	5,23883746	0,009245186	WAS protein homolog associated with actin, golgi membranes and
ENST00000569858	ENSG00000260735	3,716126352	4,686023186	0,009267496	
ENST00000507884	ENSG00000251668	-5,196437049	5,376202372	0,009393577	pseudogene similar to part of microtubule associated serine/thre
ENST00000511037	ENSG00000248923	1,829923692	8,85099013	0,009428714	MT-ND5 pseudogene 11 [Source:HGNC Symbol;Acc:HGNC:42273]
ENST00000369783	ENSG00000183128	-5,045086072	5,298564466	0,009439772	calcium homeostasis modulator 3 [Source:HGNC Symbol;Acc:HGN

ENST00000384997	ENSG00000207730	3,028603163	4,974435877	0,009460812	microRNA 200b [Source:HGNC Symbol;Acc:HGNC:31579]
ENST00000546835	ENSG00000257883	2,771594626	4,388547521	0,009496746	novel transcript
ENST00000381722	ENSG00000224902	-4,737003596	4,368803074	0,00962644	G antigen 12H [Source:HGNC Symbol;Acc:HGNC:31908]
ENST00000382751	ENSG00000142207	-1,974947372	5,716908523	0,009643758	URB1 ribosome biogenesis homolog [Source:HGNC Symbol;Acc:H
ENST00000365528	ENSG00000202398	1,966030499	6,081299461	0,009693537	RNA, U6 small nuclear 61, pseudogene [Source:HGNC Symbol;Acc
ENST00000365652	ENSG00000202522	2,496809142	4,72471667	0,009713588	
ENST00000362881	ENSG00000199751	3,720830548	5,176282356	0,009757583	
ENST00000384668	ENSG00000207399	2,874616569	5,008041661	0,009802334	RNA, U6 small nuclear 1011, pseudogene [Source:HGNC Symbol;A
ENST00000383977	ENSG00000206704	2,055058285	5,445884908	0,009817451	
ENST00000445946	ENSG00000227268	1,891456979	5,704929853	0,009824735	killin, p53 regulated DNA replication inhibitor [Source:HGNC Symb
ENST00000459229	ENSG00000239183	2,443927628	7,640478672	0,009883935	small nucleolar RNA, H/ACA box 84 [Source:HGNC Symbol;Acc:HG
ENST00000362766	ENSG00000199636	2,549998259	4,514135557	0,009889995	
ENST00000410712	ENSG00000222644	5,259992908	4,921049294	0,009924818	RNA, U2 small nuclear 16, pseudogene [Source:HGNC Symbol;Acc
ENST00000394253	ENSG00000164663	2,272271385	4,865788637	0,009944423	ubiquitin specific peptidase 49 [Source:HGNC Symbol;Acc:HGNC:2
ENST00000423059	ENSG00000005108	2,709437644	4,867702889	0,009962992	thrombospondin type 1 domain containing 7A [Source:HGNC Sym
ENST00000526401	ENSG00000183020	2,464601535	5,990336725	0,010020396	adaptor related protein complex 2 subunit alpha 2 [Source:HGNC
ENST00000369558	ENSG00000163349	-3,590973502	4,462175544	0,010079262	homeodomain interacting protein kinase 1 [Source:HGNC Symbol
ENST00000363091	ENSG00000199961	2,426074505	12,61370876	0,0101457	small nucleolar RNA, C/D box 1B [Source:HGNC Symbol;Acc:HGNC
ENST00000464294	ENSG00000164050	3,932651522	4,619411326	0,010175182	plexin B1 [Source:HGNC Symbol;Acc:HGNC:9103]
ENST00000383866	ENSG00000206593	2,557582975	4,969266419	0,010222407	RNA, U6 small nuclear 47, pseudogene [Source:HGNC Symbol;Acc
ENST00000384714	ENSG00000207445	1,918158364	10,12513559	0,010231671	small nucleolar RNA, C/D box 15B [Source:HGNC Symbol;Acc:HGN
ENST00000516089	ENSG00000251898	1,825688304	7,118680759	0,010234537	small Cajal body-specific RNA 11 [Source:HGNC Symbol;Acc:HGNC
ENST00000331163	ENSG00000100311	-2,713571417	5,950522146	0,010299903	platelet derived growth factor subunit B [Source:HGNC Symbol;Ac
ENST00000529976	ENSG00000215440	4,654437791	4,660567929	0,010398312	aminopeptidase like 1 [Source:HGNC Symbol;Acc:HGNC:16244]
ENST00000516862	ENSG00000252671	2,288503601	6,15669235	0,010442354	
ENST00000506002	ENSG00000249119	2,075401998	6,833300105	0,010457542	MT-ND6 pseudogene 4 [Source:HGNC Symbol;Acc:HGNC:39467]
ENST00000517284	ENSG00000253093	4,890227987	4,773714925	0,010480516	RNA, 5S ribosomal pseudogene 179 [Source:HGNC Symbol;Acc:HG
ENST00000516080	ENSG00000251889	3,846938829	4,819776229	0,010481788	RNA, U4 small nuclear 49, pseudogene [Source:HGNC Symbol;Acc
ENST00000467115	ENSG00000240409	1,874942469	8,847167676	0,010608647	MT-ATP8 pseudogene 1 [Source:HGNC Symbol;Acc:HGNC:44571]
ENST00000398542	ENSG00000121753	-2,943115838	4,859989526	0,010622365	adhesion G protein-coupled receptor B2 [Source:HGNC Symbol;Ac
ENST00000577887	ENSG00000265706	2,817357288	12,37349762	0,010629883	small nucleolar RNA, C/D box 53B [Source:HGNC Symbol;Acc:HGN
ENST00000363868	ENSG00000200738	2,233456195	5,665819732	0,010666944	RNA, 5S ribosomal pseudogene 472 [Source:HGNC Symbol;Acc:HG
ENST00000362105	ENSG00000198975	1,536050236	11,68855224	0,010683784	microRNA let-7a-2 [Source:HGNC Symbol;Acc:HGNC:31477]
ENST00000408749	ENSG00000221676	2,553023401	10,67592336	0,010793987	RNA, U6atac small nuclear (U12-dependent splicing) [Source:HGN
ENST00000384227	ENSG00000206954	3,155283141	4,644173985	0,010806806	RNA, U6 small nuclear 1201, pseudogene [Source:HGNC Symbol;A
ENST00000364234	ENSG00000201104	2,560048254	8,448669317	0,010860757	RNA, U6 small nuclear 11, pseudogene [Source:HGNC Symbol;Acc
ENST00000384385	ENSG00000207113	2,240714054	7,423388024	0,010864271	RNA, U6 small nuclear 16, pseudogene [Source:HGNC Symbol;Acc
ENST00000384337	ENSG00000207065	2,374265396	5,301715266	0,010928365	RNA, U5A small nuclear 2, pseudogene [Source:HGNC Symbol;Acc
ENST00000343889	ENSG00000149527	-2,574876913	5,613417845	0,010956568	phospholipase C eta 2 [Source:HGNC Symbol;Acc:HGNC:29037]
ENST00000411292	ENSG00000223224	2,798496645	12,28935768	0,011012572	small nucleolar RNA, C/D box 71 [Source:HGNC Symbol;Acc:HGNC
ENST00000382352		-3,150129717	5,031205027	0,011033274	
ENST00000365271	ENSG00000202141	2,063844433	5,223028054	0,011052636	
ENST00000384168	ENSG00000206895	1,794009912	6,452428022	0,011132352	
ENST00000516422	ENSG00000252231	3,073219156	4,606555788	0,011141975	RNA, 5S ribosomal pseudogene 67 [Source:HGNC Symbol;Acc:HGN
ENST00000384577	ENSG00000207307	2,283418998	6,036807608	0,011169917	RNA, U6 small nuclear 145, pseudogene [Source:HGNC Symbol;Ac
ENST00000362396	ENSG00000199266	2,129531545	5,253740243	0,011277595	small nucleolar RNA, H/ACA box 60 [Source:HGNC Symbol;Acc:HG
ENST00000326005	ENSG00000180304	-2,993912086	4,676077467	0,011331978	ornithine decarboxylase antizyme 2 [Source:HGNC Symbol;Acc:HG
ENST00000373588	ENSG00000136931	-2,926716522	5,905843303	0,011414606	nuclear receptor subfamily 5 group A member 1 [Source:HGNC Sy
ENST00000373980	ENSG00000185532	-4,731275646	4,527262439	0,011610883	protein kinase cGMP-dependent 1 [Source:HGNC Symbol;Acc:HGN
ENST00000396789	ENSG00000213903	3,666078759	5,115602907	0,011695755	leukotriene B4 receptor [Source:HGNC Symbol;Acc:HGNC:6713]
ENST00000373673	ENSG00000179774	-2,905918856	4,742596526	0,011711639	atonal bHLH transcription factor 7 [Source:HGNC Symbol;Acc:HGN
ENST00000579470		1,848341305	8,366715741	0,011726502	
ENST00000410949	ENSG00000222881	2,129968259	8,154741744	0,011755594	
ENST00000370544	ENSG00000143013	-3,801531832	4,796726656	0,011769875	LIM domain only 4 [Source:HGNC Symbol;Acc:HGNC:6644]
ENST00000604619	ENSG00000271207	2,782760788	5,395354376	0,011787257	MT-CO1 pseudogene 22 [Source:HGNC Symbol;Acc:HGNC:52087]
ENST00000384158	ENSG00000206885	2,981390693	9,042454878	0,011788811	small nucleolar RNA, H/ACA box 75 [Source:HGNC Symbol;Acc:HG
ENST00000384161	ENSG00000206888	2,08738551	8,430950067	0,011799633	RNA, U6 small nuclear 48, pseudogene [Source:HGNC Symbol;Acc
ENST00000299092	ENSG00000166073	4,749172499	4,396397888	0,011807363	G protein-coupled receptor 176 [Source:HGNC Symbol;Acc:HGNC:
ENST00000383898	ENSG00000206625	2,610843205	9,045650376	0,011810895	RNA, U6 small nuclear 1 [Source:HGNC Symbol;Acc:HGNC:10227]
ENST00000473640	ENSG00000152092	4,199393149	4,805369163	0,01181264	astrotactin 1 [Source:HGNC Symbol;Acc:HGNC:773]
ENST00000583030	ENSG00000214719	4,7469866	4,724426886	0,011821156	
ENST00000526625	ENSG00000254454	-4,887243862	4,65975559	0,011882759	regulator of chromosome condensation 2 pseudogene 6 [Source:H
ENST00000384154	ENSG00000206881	2,415717835	5,685953363	0,011906296	RNA, U6 small nuclear 190, pseudogene [Source:HGNC Symbol;Ac
ENST00000515924	ENSG00000251733	2,087766103	7,263435092	0,011924954	small Cajal body-specific RNA 8 [Source:HGNC Symbol;Acc:HGNC:

ENST00000429327	ENSG00000228930	4,67709255	4,693990592	0,011986365	MT-CO1 pseudogene 3 [Source:HGNC Symbol;Acc:HGNC:39604]
ENST00000362585	ENSG00000199455	1,566352588	6,592470861	0,011995491	RNA, 5S ribosomal pseudogene 191 [Source:HGNC Symbol;Acc:HG
ENST00000362302	ENSG00000199172	1,554661544	9,389491409	0,012001098	microRNA 331 [Source:HGNC Symbol;Acc:HGNC:31772]
ENST00000364588	ENSG00000201458	2,250229418	5,41228618	0,012026956	RNA, U4 small nuclear 4, pseudogene [Source:HGNC Symbol;Acc:H
ENST00000274093	ENSG00000145451	3,388438977	4,689384637	0,012044104	glycine receptor alpha 3 [Source:HGNC Symbol;Acc:HGNC:4328]
ENST00000408636	ENSG00000221563	-2,216934692	4,589894512	0,012160228	microRNA 1269a [Source:HGNC Symbol;Acc:HGNC:35337]
ENST00000355594	ENSG00000198483	2,657117784	4,47069823	0,012183396	ankyrin repeat domain 35 [Source:HGNC Symbol;Acc:HGNC:26323
ENST00000484090	ENSG00000185658	-3,535628733	4,57406821	0,012214193	bromodomain and WD repeat domain containing 1 [Source:HGNC
ENST00000362607	ENSG00000199477	1,960793515	5,67676653	0,012217239	small nucleolar RNA, H/ACA box 31 [Source:HGNC Symbol;Acc:HG
ENST00000362797	ENSG00000199667	2,121903516	5,606037979	0,012231924	
ENST00000516603	ENSG00000252412	1,853460712	5,415494809	0,01225624	
ENST00000384752	ENSG00000207483	2,244925985	5,114234926	0,012261861	RNA, U6 small nuclear 1067, pseudogene [Source:HGNC Symbol;A
ENST00000411631		-3,157845343	4,480926978	0,012266682	
ENST00000597407	ENSG00000269386	3,049648874	4,351488894	0,012266682	RAB11B antisense RNA 1 [Source:HGNC Symbol;Acc:HGNC:44178]
ENST00000569762	ENSG00000156873	2,265231716	4,420863717	0,012266682	phosphorylase kinase catalytic subunit gamma 2 [Source:HGNC Sy
ENST00000526214	ENSG00000212789	-2,253763647	4,364662301	0,012266682	ST13, Hsp70 interacting protein pseudogene 5 [Source:HGNC Sym
ENST00000450525	ENSG00000126351	-2,434683127	4,827529241	0,01233898	thyroid hormone receptor alpha [Source:HGNC Symbol;Acc:HGNC
ENST00000365447	ENSG00000202317	2,366904382	4,614393662	0,012510201	RNA, U1 small nuclear 84, pseudogene [Source:HGNC Symbol;Acc
ENST00000516666	ENSG00000252475	4,715037707	4,519936707	0,012515374	RNA, U6 small nuclear 1332, pseudogene [Source:HGNC Symbol;A
ENST00000378119	ENSG00000112308	-2,129370936	5,881935034	0,012552435	chromosome 6 open reading frame 62 [Source:HGNC Symbol;Acc:
ENST00000518249	ENSG00000105339	4,578732192	4,513398078	0,012598089	DENN domain containing 3 [Source:HGNC Symbol;Acc:HGNC:2913
ENST00000385582		2,115423252	17,27360558	0,012670252	
ENST00000607315	ENSG00000271869	2,730443234	4,354100545	0,012690718	novel transcript
ENST00000408612	ENSG00000221539	2,458934938	14,70029872	0,012696384	small nucleolar RNA, C/D box 99 [Source:HGNC Symbol;Acc:HGNC
ENST00000459124	ENSG00000238317	2,265171809	13,83117752	0,012790035	small nucleolar RNA, C/D box 11 [Source:HGNC Symbol;Acc:HGNC
ENST00000441633	ENSG00000230916	3,593957671	5,424869533	0,012829962	MT-CO1 pseudogene 53 [Source:HGNC Symbol;Acc:HGNC:52118]
ENST00000564748	ENSG00000261758	2,626503618	4,64086169	0,012842446	novel transcript, antisense to STAG1
ENST00000384582	ENSG00000207312	2,137264554	5,419315614	0,012878925	RNA, U6 small nuclear 429, pseudogene [Source:HGNC Symbol;Ac
ENST00000586240	ENSG00000168259	4,646863288	4,602053539	0,012894458	DnaJ heat shock protein family (Hsp40) member C7 [Source:HGNC
ENST00000516861		1,694172429	6,253807417	0,012956984	
ENST00000378693	ENSG00000198944	-2,377494014	5,639212526	0,012963504	sosondowah ankyrin repeat domain family member A [Source:HG
ENST00000363592	ENSG00000200462	3,127036887	4,566468582	0,012999689	RNA, U6 small nuclear 727, pseudogene [Source:HGNC Symbol;Ac
ENST00000607441	ENSG00000283279	2,307160167	5,044123075	0,013028452	microRNA 376c [Source:HGNC Symbol;Acc:HGNC:31782]
ENST00000464490	ENSG00000178026	-4,047019166	4,668393653	0,013039057	leucine rich repeat containing 75B [Source:HGNC Symbol;Acc:HGN
ENST00000380087	ENSG00000102054	-5,054906054	4,436660503	0,013048906	RB binding protein 7, chromatin remodeling factor [Source:HGNC
ENST00000364488	ENSG00000201358	5,481217604	4,711019332	0,013050156	RNA, 7SK small nuclear pseudogene 193 [Source:HGNC Symbol;Ac
ENST00000384276	ENSG00000207003	2,192597814	5,569337073	0,013177793	RNA, U6 small nuclear 611, pseudogene [Source:HGNC Symbol;Ac
ENST00000516209	ENSG00000252018	2,153317289	6,126157945	0,013223569	RNA, U2 small nuclear 30, pseudogene [Source:HGNC Symbol;Acc
ENST00000592659	ENSG00000102575	3,481288126	5,220746536	0,013258873	acid phosphatase 5, tartrate resistant [Source:HGNC Symbol;Acc:H
ENST00000410506	ENSG00000222438	2,663133049	4,813316111	0,013279801	RNA, U6 small nuclear 1077, pseudogene [Source:HGNC Symbol;A
ENST00000447906	ENSG00000164164	-2,876141617	4,663494835	0,013350097	OTU deubiquitinase 4 [Source:HGNC Symbol;Acc:HGNC:24949]
ENST00000364793	ENSG00000201663	3,088043267	4,880852685	0,013420118	
ENST00000325980	ENSG00000151650	-2,253691732	4,550603023	0,013498413	VENT homeobox [Source:HGNC Symbol;Acc:HGNC:13639]
ENST00000516047	ENSG00000251856	2,841685759	4,752423577	0,013551518	microRNA 449c [Source:HGNC Symbol;Acc:HGNC:37302]
ENST00000492154	ENSG00000180251	1,613936013	7,606030837	0,013583039	solute carrier family 9 member A4 [Source:HGNC Symbol;Acc:HGN
ENST00000459475	ENSG00000238344	2,414177074	11,19406096	0,013598493	small nucleolar RNA, C/D box 126 [Source:HGNC Symbol;Acc:HGN
ENST00000363491	ENSG00000200361	2,471904409	4,928590951	0,013615425	
ENST00000363179	ENSG00000200049	2,675237482	4,807444078	0,013619161	
ENST00000235310	ENSG00000116670	-2,58150079	4,453177256	0,013706259	mitotic arrest deficient 2 like 2 [Source:HGNC Symbol;Acc:HGNC:6
ENST00000521431	ENSG00000143801	-2,083177555	4,533685374	0,013706259	presenilin 2 [Source:HGNC Symbol;Acc:HGNC:9509]
ENST00000481107	ENSG00000011295	1,992335465	4,576466026	0,013706259	tetratricopeptide repeat domain 19 [Source:HGNC Symbol;Acc:HG
ENST00000363765	ENSG00000200635	1,863230378	4,87289022	0,013767557	
ENST00000408376	ENSG00000221303	2,918936494	8,156276692	0,013867179	small nucleolar RNA, H/ACA box 79 [Source:HGNC Symbol;Acc:HG
ENST00000296464	ENSG00000164070	-2,946443078	4,584290602	0,014018179	heat shock protein family A (Hsp70) member 4 like [Source:HGNC
ENST00000585470	ENSG00000267675	4,829037275	4,52920774	0,014036799	novel transcript
ENST00000364765	ENSG00000201635	4,718590289	4,339769791	0,014146457	
ENST00000606404		1,843099519	6,291456414	0,014149291	
ENST00000335624	ENSG00000186806	-2,498623712	4,968315854	0,014150725	V-set and immunoglobulin domain containing 10 like [Source:HGN
ENST00000563949	ENSG00000261096	3,370647344	4,760238402	0,014246192	novel transcript
ENST00000384641	ENSG00000207371	3,805235342	4,579357459	0,014300094	
ENST00000594883	ENSG00000268379	1,562718769	7,307867174	0,014332982	pentatricopeptide repeat domain 3 pseudogene
ENST00000364977	ENSG00000201847	2,073021814	7,797503617	0,014417263	small nucleolar RNA, C/D box 31B [Source:HGNC Symbol;Acc:HGN
ENST00000517041	ENSG00000252850	1,92353554	7,028441318	0,014421324	RNA, U1 small nuclear 117, pseudogene [Source:HGNC Symbol;Ac
ENST00000568316	ENSG00000122257	-5,399564698	4,602665556	0,014447597	RB binding protein 6, ubiquitin ligase [Source:HGNC Symbol;Acc:H

ENST00000382369	ENSG00000196476	5,455497136	4,57965185	0,014450376	chromosome 20 open reading frame 96 [Source:HGNC Symbol;Ac
ENST00000391232	ENSG00000212534	2,289616079	13,60061461	0,01445227	small nucleolar RNA, C/D box 70 [Source:HGNC Symbol;Acc:HGNC
ENST00000459143		4,406276145	4,406353068	0,014503781	
ENST00000364969	ENSG00000201839	3,311356957	5,829181264	0,014566089	small nucleolar RNA, C/D box 114-3 [Source:HGNC Symbol;Acc:HG
ENST00000563701	ENSG00000261079	5,704341283	4,856971511	0,014636256	novel transcript
ENST00000364394	ENSG00000201264	2,6437298	6,449260234	0,014655488	small nucleolar RNA, C/D box U73B (pseudogene) [Source:HGNC S
ENST00000362378	ENSG00000199248	2,506826861	5,86937566	0,014660875	RNA, U6 small nuclear 28, pseudogene [Source:HGNC Symbol;Acc
ENST00000459126	ENSG00000238936	3,507800682	4,609534448	0,014677106	small nucleolar RNA, C/D box 65B [Source:HGNC Symbol;Acc:HGN
ENST00000516146	ENSG00000251955	2,079580086	6,637732463	0,014687577	RNA, U6 small nuclear 27, pseudogene [Source:HGNC Symbol;Acc
ENST00000411323		1,711082181	5,223810221	0,014765106	
ENST00000384841	ENSG00000207573	1,46307182	8,14554227	0,014810639	microRNA 550a-2 [Source:HGNC Symbol;Acc:HGNC:32805]
ENST00000384405	ENSG00000207134	3,038604915	4,460810523	0,014927599	RNA, U6 small nuclear 106, pseudogene [Source:HGNC Symbol;Ac
ENST00000298310	ENSG00000165525	2,46045277	4,556907531	0,014991201	nuclear export mediator factor [Source:HGNC Symbol;Acc:HGNC:1
ENST00000540040	ENSG00000256618	1,672700619	9,552880151	0,015177361	MT-RNR2 like 1 [Source:HGNC Symbol;Acc:HGNC:37155]
ENST00000384360	ENSG00000207088	1,897614676	7,071989183	0,015228204	small nucleolar RNA, H/ACA box 7B [Source:HGNC Symbol;Acc:HG
ENST00000365467	ENSG00000202337	2,428203052	8,763198102	0,0153024	RNA, U6 small nuclear 8 [Source:HGNC Symbol;Acc:HGNC:34285]
ENST00000311575	ENSG00000174721	-3,317981479	4,980156468	0,015313322	fibroblast growth factor binding protein 3 [Source:HGNC Symbol;A
ENST00000442751	ENSG00000231437	-2,655721012	5,225344178	0,015442062	long intergenic non-protein coding RNA 1750 [Source:HGNC Symb
ENST00000410991	ENSG00000222923	2,104223093	7,670998146	0,015568925	RNA, U2 small nuclear 41, pseudogene [Source:HGNC Symbol;Acc
ENST00000408573	ENSG00000221500	2,668046227	17,6670399	0,015676843	small nucleolar RNA, C/D box 100 [Source:HGNC Symbol;Acc:HGN
ENST00000364960	ENSG00000201830	2,356630516	4,989084386	0,015700483	
ENST00000264436	ENSG00000075340	-4,989017095	4,832995716	0,015718698	adducin 2 [Source:HGNC Symbol;Acc:HGNC:244]
ENST00000268864		-1,789199427	6,087498837	0,015732121	
ENST00000269399	ENSG00000173894	3,031702449	4,586215834	0,015902814	chromobox 2 [Source:HGNC Symbol;Acc:HGNC:1552]
ENST00000364328	ENSG00000201198	2,247885527	5,63839313	0,015918988	RNA, U6 small nuclear 879, pseudogene [Source:HGNC Symbol;Ac
ENST00000516672	ENSG00000252481	2,449800778	7,587014201	0,015952599	small Cajal body-specific RNA 13 [Source:HGNC Symbol;Acc:HGNC
ENST00000391625	ENSG00000212939	2,214181109	5,626149325	0,015978685	novel transcript
ENST00000409687	ENSG00000186193	-2,311994077	5,641530254	0,016019365	suppressor APC domain containing 2 [Source:HGNC Symbol;Acc:H
ENST00000490318	ENSG00000227709	-4,633188716	4,31610409	0,016041343	small nuclear ribonucleoprotein 40kDa (U5) (SNRNP40) pseudoge
ENST00000557800	ENSG00000259744	4,484368979	4,281509664	0,016041343	novel transcript, sense intronic to LARP6
ENST00000248248	ENSG00000103111	4,483920051	4,46358863	0,016041343	MON1 homolog B, secretory trafficking associated [Source:HGNC
ENST00000503106	ENSG00000249364	4,483920051	4,279441888	0,016041343	
ENST00000377957	ENSG00000204923	4,48347126	4,391989999	0,016041343	F-box protein 48 [Source:HGNC Symbol;Acc:HGNC:33857]
ENST00000516516	ENSG00000252325	4,48347126	4,35265562	0,016041343	RNA, U6 small nuclear 1038, pseudogene [Source:HGNC Symbol;A
ENST00000562158	ENSG00000261364	4,48347126	4,277373525	0,016041343	novel transcript
ENST00000490182	ENSG00000172845	4,481842072	4,310228707	0,016041343	Sp3 transcription factor [Source:HGNC Symbol;Acc:HGNC:11208]
ENST00000365308		4,480945873	4,345639904	0,016041343	
ENST00000383985	ENSG00000206712	4,47931939	4,320367273	0,016041343	RNA, U6 small nuclear 26, pseudogene [Source:HGNC Symbol;Acc
ENST00000400465		-4,476707917	4,33567717	0,016041343	
ENST00000412580	ENSG00000213239	-4,476707917	4,363198502	0,016041343	nucleophosmin 1 pseudogene 32 [Source:HGNC Symbol;Acc:HGN
ENST00000469484	ENSG00000244586	-4,475656457	4,356158968	0,016041343	WNT5A antisense RNA 1 [Source:HGNC Symbol;Acc:HGNC:40616]
ENST00000532289	ENSG00000184007	-4,473134153	4,257897993	0,016041343	protein tyrosine phosphatase type IVA, member 2 [Source:HGNC
ENST00000561653	ENSG00000260095	-4,473134153	4,295445025	0,016041343	novel transcript, antisense to CCNF
ENST00000520512	ENSG00000253438	4,303740374	4,472088322	0,016041343	prostate cancer associated transcript 1 [Source:HGNC Symbol;Acc
ENST00000363508	ENSG00000200378	4,302101619	4,322693769	0,016041343	RNA, U5B small nuclear 4, pseudogene [Source:HGNC Symbol;Acc
ENST00000364403	ENSG00000201273	4,30165179	4,28312654	0,016041343	RNA, U6 small nuclear 776, pseudogene [Source:HGNC Symbol;Ac
ENST00000384325	ENSG00000207053	4,30165179	4,322438682	0,016041343	RNA, U6 small nuclear 937, pseudogene [Source:HGNC Symbol;Ac
ENST00000384332	ENSG00000207060	4,30165179	4,355778316	0,016041343	RNA, U6 small nuclear 480, pseudogene [Source:HGNC Symbol;Ac
ENST00000506231	ENSG00000133706	4,30165179	4,283115702	0,016041343	leucyl-tRNA synthetase [Source:HGNC Symbol;Acc:HGNC:6512]
ENST00000362825	ENSG00000199695	2,613051559	4,347296816	0,016041343	RNA, U6 small nuclear 1128, pseudogene [Source:HGNC Symbol;A
ENST00000364419	ENSG00000201289	2,61142237	4,39484235	0,016041343	RNA, 7SK small nuclear pseudogene 76 [Source:HGNC Symbol;Acc
ENST00000429534	ENSG00000223899	2,431681918	4,350947806	0,016041343	SEC13 homolog, nuclear pore and COPII coat complex component
ENST00000371761	ENSG00000123080	2,431232089	4,277174973	0,016041343	cyclin dependent kinase inhibitor 2C [Source:HGNC Symbol;Acc:H
ENST00000364432	ENSG00000201302	2,784705812	10,06483488	0,016058209	small nucleolar RNA, H/ACA box 65 [Source:HGNC Symbol;Acc:HG
ENST00000376708	ENSG00000204612	-2,779557365	5,263714773	0,016104642	forkhead box B2 [Source:HGNC Symbol;Acc:HGNC:23315]
ENST00000370924	ENSG00000050628	1,746210088	4,64977674	0,016104917	prostaglandin E receptor 3 [Source:HGNC Symbol;Acc:HGNC:9595
ENST00000516438	ENSG00000252247	2,655281738	4,828035222	0,016108771	RNA, U6 small nuclear 70, pseudogene [Source:HGNC Symbol;Acc
ENST00000364902	ENSG00000201772	1,474392281	6,230065285	0,016171851	small nucleolar RNA, H/ACA box 5C [Source:HGNC Symbol;Acc:HG
ENST00000384627	ENSG00000207357	2,647568738	10,52289759	0,016255937	RNA, U6 small nuclear 2 [Source:HGNC Symbol;Acc:HGNC:34270]
ENST00000272645	ENSG00000144231	2,061945002	5,538471946	0,016260056	RNA polymerase II subunit D [Source:HGNC Symbol;Acc:HGNC:91
ENST00000384458	ENSG00000207187	2,092602714	4,840600995	0,016339224	small nucleolar RNA, H/ACA box 10B [Source:HGNC Symbol;Acc:H
ENST00000597920	ENSG00000239665	4,788569036	4,333199136	0,01637425	novel transcript
ENST00000516075	ENSG00000251884	1,404067534	7,351727906	0,016397062	RNA, 5S ribosomal pseudogene 288 [Source:HGNC Symbol;Acc:HG
ENST00000463756	ENSG00000163686	-2,43872524	4,609948423	0,016430958	abhydrolase domain containing 6 [Source:HGNC Symbol;Acc:HGN

ENST00000403133	ENSG00000219902	3,440146869	4,807533802	0,016451728	ribosomal protein L35 pseudogene 3 [Source:HGNC Symbol;Acc:H
ENST00000355703	ENSG00000197136	-2,55226178	5,054732005	0,01648001	pecanex 3 [Source:HGNC Symbol;Acc:HGNC:18760]
ENST00000392968		3,156753482	5,146362332	0,016549208	
ENST00000525043	ENSG00000255394	-2,166751965	6,309957377	0,016616983	chromosome 8 open reading frame 49 (putative) [Source:HGNC Sy
ENST00000362350	ENSG00000199220	1,845351744	5,109595627	0,016633245	
ENST00000363762	ENSG00000200632	3,756471269	5,419189504	0,01664358	small nucleolar RNA, C/D box 113-7 [Source:HGNC Symbol;Acc:HG
ENST00000369445		-2,036545815	4,87187581	0,01664451	
ENST00000516775		4,484532344	4,430687376	0,016647791	
ENST00000295266	ENSG00000163114	2,614362457	4,454834657	0,016664335	pyruvate dehydrogenase E1 alpha 2 subunit [Source:HGNC Symbo
ENST00000513574	ENSG00000164116	-4,622308541	4,400267884	0,016690085	guanylate cyclase 1 soluble subunit alpha 1 [Source:HGNC Symbol
ENST00000369206	ENSG00000148704	-2,403138906	5,904355323	0,016824813	ventral anterior homeobox 1 [Source:HGNC Symbol;Acc:HGNC:12
ENST00000589123	ENSG00000141905	-1,818835224	5,874776319	0,016837269	nuclear factor I C [Source:HGNC Symbol;Acc:HGNC:7786]
ENST00000391150	ENSG00000212452	2,310187444	15,79234474	0,016877576	small nucleolar RNA, C/D box 69 [Source:HGNC Symbol;Acc:HGNC
ENST00000315251	ENSG00000016391	-2,018443844	6,066365376	0,016907775	choline dehydrogenase [Source:HGNC Symbol;Acc:HGNC:24288]
ENST00000391278	ENSG00000212580	3,27336662	4,673507248	0,016967732	
ENST00000459002	ENSG00000239069	2,664270695	4,648850297	0,017035118	
ENST00000538692		3,179163006	4,594496069	0,017042471	
ENST00000383935	ENSG00000206662	2,453588133	5,479231343	0,017046809	
ENST00000398295	ENSG00000235847	-3,859172771	4,593391004	0,017061085	lactate dehydrogenase A pseudogene 7 [Source:HGNC Symbol;Ac
ENST00000384409	ENSG00000207138	2,130904667	5,091877683	0,017159641	RNA, U6 small nuclear 869, pseudogene [Source:HGNC Symbol;Ac
ENST00000433688	ENSG00000188070	-2,14519529	6,170320639	0,017324074	chromosome 11 open reading frame 95 [Source:HGNC Symbol;Ac
ENST00000261275	ENSG00000104059	-2,364852201	5,051498108	0,017325727	family with sequence similarity 189 member A1 [Source:HGNC Sy
ENST00000364619	ENSG00000201489	1,625562324	6,340265963	0,017336583	
ENST00000496264	ENSG00000138835	2,28007027	5,749128271	0,017436173	regulator of G protein signaling 3 [Source:HGNC Symbol;Acc:HGN
ENST00000384899	ENSG00000207631	1,705059658	6,299453821	0,017533557	microRNA 641 [Source:HGNC Symbol;Acc:HGNC:32897]
ENST00000516846	ENSG00000252655	2,245287994	5,324461655	0,017604708	
ENST00000595737	ENSG00000228065	4,596906764	4,444192513	0,017687228	long intergenic non-protein coding RNA 1515 [Source:HGNC Symb
ENST00000386037	ENSG00000208772	1,697255788	7,041576924	0,017787055	small nucleolar RNA, C/D box 94 [Source:HGNC Symbol;Acc:HGNC
ENST00000604952	ENSG00000270672	2,489047978	8,470566606	0,017863763	MT-RNR2 like 6 [Source:HGNC Symbol;Acc:HGNC:37163]
ENST00000385299	ENSG00000284538	2,116136911	12,66015315	0,017887135	microRNA 92a-2 [Source:HGNC Symbol;Acc:HGNC:31644]
ENST00000385104	ENSG00000207839	2,128559005	9,794638968	0,017933893	microRNA 33b [Source:HGNC Symbol;Acc:HGNC:32791]
ENST00000299290	ENSG00000166220	5,309352134	5,034296343	0,018005393	thymus, brain and testes associated [Source:HGNC Symbol;Acc:HG
ENST00000355300	ENSG00000169783	-2,372151387	5,367010867	0,018047177	leucine rich repeat and Ig domain containing 1 [Source:HGNC Sym
ENST00000393792	ENSG00000168246	-2,513758722	5,010451685	0,018080037	ubiquitin domain containing 2 [Source:HGNC Symbol;Acc:HGNC:2
ENST00000528284	ENSG00000131626	1,732592249	7,320979229	0,018196869	PTPRF interacting protein alpha 1 [Source:HGNC Symbol;Acc:HGN
ENST00000384744	ENSG00000207475	2,364687827	9,441419128	0,018238004	small nucleolar RNA, H/ACA box 80E [Source:HGNC Symbol;Acc:H
ENST00000408966	ENSG00000221990	3,491661347	5,308486367	0,018376222	EXOC3 antisense RNA 1 [Source:HGNC Symbol;Acc:HGNC:25175]
ENST00000256367	ENSG00000133985	-2,254058776	6,082939177	0,018401201	tetratricopeptide repeat domain 9 [Source:HGNC Symbol;Acc:HGN
ENST00000364210		3,242619935	4,91633898	0,018411543	
ENST00000493216	ENSG00000099917	2,479314255	4,555083868	0,018575231	mediator complex subunit 15 [Source:HGNC Symbol;Acc:HGNC:14
ENST00000563778	ENSG00000102879	4,612542634	4,302455821	0,018596156	coronin 1A [Source:HGNC Symbol;Acc:HGNC:2252]
ENST00000562685	ENSG00000260511	4,306200601	4,545057895	0,018657781	novel transcript, sense intronic to WWOX
ENST00000532431	ENSG00000255156	1,994754141	6,600075396	0,018735419	RNA, Ro-associated Y1 pseudogene 9 [Source:HGNC Symbol;Acc:H
ENST00000359315	ENSG00000141933	-2,368424383	4,957919731	0,018736152	tubulin polyglutamylase complex subunit 1 [Source:HGNC Symbol
ENST00000408314	ENSG00000221241	2,206762564	8,615234383	0,018790978	small nucleolar RNA, C/D box 88A [Source:HGNC Symbol;Acc:HGN
ENST00000364353	ENSG00000201223	2,42688105	5,134889883	0,018804688	RNA, U6 small nuclear 1305, pseudogene [Source:HGNC Symbol;A
ENST00000288699	ENSG00000157851	-1,997848352	4,64246837	0,018855272	dihydropyrimidinase like 5 [Source:HGNC Symbol;Acc:HGNC:2063
ENST00000578688	ENSG00000266407	2,198568188	4,971594892	0,019008977	microRNA 3157 [Source:HGNC Symbol;Acc:HGNC:38172]
ENST00000452643	ENSG00000225489	2,070674787	6,479819579	0,019039377	novel transcript
ENST00000410692	ENSG00000222624	1,67799432	6,646466081	0,019058498	RNA, U2 small nuclear 15, pseudogene [Source:HGNC Symbol;Acc
ENST00000487817	ENSG00000196187	2,100461888	6,145636348	0,019121843	transmembrane protein 63A [Source:HGNC Symbol;Acc:HGNC:29
ENST00000455537	ENSG00000155980	1,756417041	4,683580345	0,019248402	kinesin family member 5A [Source:HGNC Symbol;Acc:HGNC:6323]
ENST00000221770	ENSG00000105171	3,882000357	5,264248665	0,019262246	POP4 homolog, ribonuclease P/MRP subunit [Source:HGNC Symb
ENST00000384553	ENSG00000207283	2,751465111	5,031910458	0,019303426	
ENST00000452122		1,75907963	4,741131401	0,019303962	
ENST00000364161	ENSG00000201031	1,908738931	6,51567528	0,019304333	
ENST00000311630	ENSG00000174013	-5,33990286	4,622204091	0,019331346	F-box protein 45 [Source:HGNC Symbol;Acc:HGNC:29148]
ENST00000551626	ENSG00000246985	-3,664095844	4,547401075	0,019395352	SOCS2 antisense RNA 1 [Source:HGNC Symbol;Acc:HGNC:27054]
ENST00000442718	ENSG00000227430	2,124681485	6,87585033	0,019485112	H3 histone, family 3B (H3.3B) (H3F3B) pseudogene
ENST00000489872	ENSG00000275014	2,477970602	4,632570647	0,019597363	RNA, 7SL, cytoplasmic 166, pseudogene [Source:HGNC Symbol;Ac
ENST00000384526	ENSG00000207256	2,627318268	5,406968237	0,019598753	RNA, U6 small nuclear 880, pseudogene [Source:HGNC Symbol;Ac
ENST00000364337	ENSG00000201207	1,6333807	5,859435455	0,019676097	
ENST00000364784	ENSG00000201654	2,420709364	10,2184753	0,019677614	RNA, U6 small nuclear 7 [Source:HGNC Symbol;Acc:HGNC:34284]
ENST00000357320		-2,987213651	6,211375447	0,019703124	

ENST00000363610	ENSG00000200480	2,490466763	5,514825488	0,01970819	small nucleolar RNA, C/D box 114-28 [Source:HGNC Symbol;Acc:H
ENST00000365530	ENSG00000202400	2,271687321	15,57279939	0,01971729	small nucleolar RNA, C/D box 82 [Source:HGNC Symbol;Acc:HGNC
ENST00000506028	ENSG00000095587	5,64536529	5,384580569	0,019763324	tolloid like 2 [Source:HGNC Symbol;Acc:HGNC:11844]
ENST00000520300	ENSG00000254164	2,89914158	4,843516703	0,019863796	novel transcript
ENST00000363237	ENSG00000200107	2,119474467	5,165894074	0,020052677	RNA, U6 small nuclear 1249, pseudogene [Source:HGNC Symbol;A
ENST00000222381	ENSG00000005421	-4,731683258	4,382552556	0,020080577	paraoxonase 1 [Source:HGNC Symbol;Acc:HGNC:9204]
ENST00000458790	ENSG00000238363	1,818519952	6,752421603	0,020090647	small nucleolar RNA, H/ACA box 13 [Source:HGNC Symbol;Acc:HG
ENST00000528572	ENSG00000187479	-2,553459306	4,697846884	0,020099841	chromosome 11 open reading frame 96 [Source:HGNC Symbol;Ac
ENST00000365439	ENSG00000202309	2,601356517	4,759466908	0,020119803	
ENST00000474101	ENSG00000163235	-4,328813958	4,348443296	0,020208574	transforming growth factor alpha [Source:HGNC Symbol;Acc:HGN
ENST00000396651	ENSG00000142937	-2,468280902	4,557700293	0,020235431	ribosomal protein S8 [Source:HGNC Symbol;Acc:HGNC:10441]
ENST00000565936	ENSG00000260343	2,349292925	5,140749344	0,020308368	long intergenic non-protein coding RNA 1043 [Source:HGNC Symb
ENST00000516131	ENSG00000251940	2,217861877	5,58434965	0,020329919	
ENST00000339209	ENSG00000130024	-3,47962857	4,537104058	0,020335378	PHD finger protein 10 [Source:HGNC Symbol;Acc:HGNC:18250]
ENST00000384271	ENSG00000206998	4,447788082	4,338230677	0,020404625	
ENST00000577915	ENSG00000263793	2,183826967	4,669245667	0,020419015	microRNA 3115 [Source:HGNC Symbol;Acc:HGNC:38371]
ENST00000459538	ENSG00000239127	2,539796504	9,631212832	0,020556306	small nucleolar RNA, C/D box 125 [Source:HGNC Symbol;Acc:HGN
ENST00000365532	ENSG00000202402	1,911922078	5,181799589	0,020569262	
ENST00000338270	ENSG00000187682	4,686436292	4,546546222	0,020581395	ES cell expressed Ras [Source:HGNC Symbol;Acc:HGNC:5174]
ENST00000384592	ENSG00000207322	1,873816219	6,8782215	0,020617934	RNA, U1 small nuclear 89, pseudogene [Source:HGNC Symbol;Acc
ENST00000391002	ENSG00000212304	2,307152863	12,08502148	0,020618163	small nucleolar RNA, C/D box 12 [Source:HGNC Symbol;Acc:HGNC
ENST00000390947	ENSG00000212249	1,893007202	4,613755914	0,020718263	
ENST00000505219	ENSG00000249020	1,97441571	6,413423593	0,02080741	small nucleolar RNA, H/ACA box 58 [Source:HGNC Symbol;Acc:HG
ENST00000606623	ENSG00000272055	2,65248618	10,52224944	0,020879669	RNA, U6 small nuclear 6, pseudogene [Source:HGNC Symbol;Acc:H
ENST00000230588	ENSG00000112818	-1,765492247	4,897923905	0,020882589	meprin A subunit alpha [Source:HGNC Symbol;Acc:HGNC:7015]
ENST00000478085	ENSG00000100359	4,324675163	4,507340369	0,020883725	small G protein signaling modulator 3 [Source:HGNC Symbol;Acc:H
ENST00000408564	ENSG00000221491	3,163447	6,443535324	0,02119609	small nucleolar RNA, H/ACA box 2C [Source:HGNC Symbol;Acc:HG
ENST00000384780	ENSG00000207511	2,918101074	4,626616094	0,021196829	RNA, U6 small nuclear 771, pseudogene [Source:HGNC Symbol;Ac
ENST00000262238	ENSG00000100811	-1,976122113	6,33990577	0,021298532	YY1 transcription factor [Source:HGNC Symbol;Acc:HGNC:12856]
ENST00000515048	ENSG00000249506	3,240014558	5,038388368	0,021316435	zinc finger E-box binding homeobox 2 pseudogene 1 [Source:HGN
ENST00000362695	ENSG00000199565	2,135899711	5,019973722	0,021386208	
ENST00000458981	ENSG00000238723	2,060703432	5,45352199	0,021389964	
ENST00000263408	ENSG00000113600	4,16439971	4,350143296	0,021430247	complement C9 [Source:HGNC Symbol;Acc:HGNC:1358]
ENST00000472516	ENSG00000131504	4,438804355	4,377938382	0,021453324	diaphanous related formin 1 [Source:HGNC Symbol;Acc:HGNC:287
ENST00000391100	ENSG00000212402	2,279851006	7,792211254	0,021511531	small nucleolar RNA, H/ACA box 74B [Source:HGNC Symbol;Acc:H
ENST00000578231		1,688182936	8,17555314	0,021592576	
ENST00000516633		1,963382036	5,560411815	0,021744682	
ENST00000569473	ENSG00000261441	2,166535279	9,974631044	0,0219047	novel transcript, antisense to POLG
ENST00000362574	ENSG00000199444	3,429185986	4,51204672	0,021911497	
ENST00000584260		4,549577246	5,135535723	0,021933107	
ENST00000376919	ENSG00000126752	-5,05278792	4,351966935	0,022026823	SSX family member 1 [Source:HGNC Symbol;Acc:HGNC:11335]
ENST00000454610	ENSG00000180822	3,016530002	5,207592409	0,022034203	proteasome assembly chaperone 4 [Source:HGNC Symbol;Acc:HG
ENST00000361069	ENSG00000050555	-2,0741777	5,771454634	0,022049411	laminin subunit gamma 3 [Source:HGNC Symbol;Acc:HGNC:6494]
ENST00000397525	ENSG00000184708	-4,663021854	4,420071596	0,022145588	eukaryotic translation initiation factor 4E nuclear import factor 1
ENST00000363311		2,569112348	11,77921661	0,022201585	
ENST00000337970	ENSG00000169813	2,139865835	4,752723868	0,022229746	heterogeneous nuclear ribonucleoprotein F [Source:HGNC Symbo
ENST00000365176	ENSG00000202046	2,918960738	4,394290388	0,022265975	
ENST00000366181	ENSG00000203356	2,916447434	4,41440456	0,022265975	long intergenic non-protein coding RNA 1562 [Source:HGNC Symb
ENST00000519600	ENSG00000131773	2,914384663	4,415519554	0,022265975	KH RNA binding domain containing, signal transduction associate
ENST00000358771	ENSG00000198053	-2,904171439	4,444111858	0,022265975	signal regulatory protein alpha [Source:HGNC Symbol;Acc:HGNC:9
ENST00000366424	ENSG00000203635	2,778074694	4,47292786	0,022265975	novel transcript
ENST00000488133	ENSG00000213176	2,133194547	4,488533484	0,022265975	ribosomal protein L13 pseudogene 6 [Source:HGNC Symbol;Acc:H
ENST00000310954	ENSG00000173930	-2,11908509	4,38164665	0,022265975	solute carrier organic anion transporter family member 4C1 [Sour
ENST00000464696	ENSG00000213270	-1,981635992	4,42191668	0,022265975	ribosomal protein L6 pseudogene 25 [Source:HGNC Symbol;Acc:H
ENST00000377276	ENSG00000165059	-2,271502158	4,5697065	0,022275692	protein kinase cAMP-activated catalytic subunit gamma [Source:H
ENST00000309244	ENSG00000105379	-4,709195224	4,309365625	0,022318432	electron transfer flavoprotein subunit beta [Source:HGNC Symbol
ENST00000562272	ENSG00000166851	2,910282067	4,867806584	0,022323114	polo like kinase 1 [Source:HGNC Symbol;Acc:HGNC:9077]
ENST00000592416	ENSG00000176624	-2,18053211	4,945113965	0,02234262	mex-3 RNA binding family member C [Source:HGNC Symbol;Acc:H
ENST00000384534	ENSG00000207264	2,0861281	8,975925976	0,022426358	RNA, U6 small nuclear 15, pseudogene [Source:HGNC Symbol;Acc
ENST00000317063	ENSG00000127586	-2,527777828	4,716286042	0,022452478	chromosome transmission fidelity factor 18 [Source:HGNC Symbo
ENST00000384531	ENSG00000207261	2,236096226	4,844977881	0,02249867	RNA, U6 small nuclear 738, pseudogene [Source:HGNC Symbol;Ac
ENST00000384654	ENSG00000207384	2,136140524	4,76051194	0,022530678	
ENST00000460565	ENSG00000240306	2,098230146	4,509673246	0,022546311	RNA, 7SL, cytoplasmic 100, pseudogene [Source:HGNC Symbol;Ac
ENST00000515945	ENSG00000251754	2,780846292	4,987441953	0,022551213	RNA, U6 small nuclear 999, pseudogene [Source:HGNC Symbol;Ac

ENST00000408625	ENSG00000221552	4,420675822	4,536648484	0,022641014	microRNA 1303 [Source:HGNC Symbol;Acc:HGNC:35301]
ENST00000510890	ENSG00000181751	-2,870128874	4,5743317	0,022677472	chromosome 5 open reading frame 30 [Source:HGNC Symbol;Acc:
ENST00000390994	ENSG00000212296	2,474182208	14,97628741	0,022772885	small nucleolar RNA, C/D box 72 [Source:HGNC Symbol;Acc:HGNC
ENST00000365174	ENSG00000202044	1,915820816	5,605300594	0,022783876	RNA, 5S ribosomal pseudogene 223 [Source:HGNC Symbol;Acc:HG
ENST00000545059	ENSG00000185344	3,837303188	6,347637501	0,022841546	ATPase H+ transporting V0 subunit a2 [Source:HGNC Symbol;Acc:
ENST00000572615	ENSG00000197879	4,317943364	4,711727608	0,022880716	myosin IC [Source:HGNC Symbol;Acc:HGNC:7597]
ENST00000358438	ENSG00000228049	4,449346155	4,5691466	0,022945252	RNA polymerase II subunit J2 [Source:HGNC Symbol;Acc:HGNC:23
ENST00000517242	ENSG00000253051	2,226616677	7,981833499	0,022983199	
ENST00000384561	ENSG00000207291	2,640660677	5,152737218	0,022989719	RNA, U6 small nuclear 30, pseudogene [Source:HGNC Symbol;Acc
ENST00000364524	ENSG00000201394	1,852945686	5,210135098	0,023107917	RNA, 5S ribosomal pseudogene 140 [Source:HGNC Symbol;Acc:HG
ENST00000364997	ENSG00000201867	2,145940007	5,201924253	0,023145446	
ENST00000364915	ENSG00000201785	2,189350494	11,89295439	0,023152877	small nucleolar RNA, C/D box 117 [Source:HGNC Symbol;Acc:HGN
ENST00000384467	ENSG00000207196	2,438919685	4,838715624	0,023201883	
ENST00000365188	ENSG00000202058	2,028574354	5,110621041	0,023290984	RNA, 7SK small nuclear pseudogene 80 [Source:HGNC Symbol;Acc
ENST00000521726	ENSG00000156482	4,48009285	4,46615625	0,023321761	ribosomal protein L30 [Source:HGNC Symbol;Acc:HGNC:10333]
ENST00000427998	ENSG00000217801	3,408681533	4,864420842	0,023374519	
ENST00000261637	ENSG00000120800	-2,197225136	4,997346176	0,023491959	UTP20, small subunit processome component [Source:HGNC Syml
ENST00000421673	ENSG00000184956	2,250497018	5,104922958	0,023511969	mucin 6, oligomeric mucus/gel-forming [Source:HGNC Symbol;Acc
ENST00000457622	ENSG00000229349	-2,481644646	4,482352126	0,023527362	actin gamma 1 pseudogene 9 [Source:HGNC Symbol;Acc:HGNC:15
ENST00000507678	ENSG00000129128	-2,478585975	4,417541066	0,023527362	signal peptidase complex subunit 3 [Source:HGNC Symbol;Acc:HG
ENST00000360770	ENSG00000221864	-2,476468011	4,425423437	0,023527362	keratin associated protein 12-2 [Source:HGNC Symbol;Acc:HGNC:2
ENST00000393414	ENSG00000115590	2,383435273	4,455601269	0,023527362	interleukin 1 receptor type 2 [Source:HGNC Symbol;Acc:HGNC:59
ENST00000384402	ENSG00000207131	2,38038962	4,489144471	0,023527362	
ENST00000381811	ENSG00000205794	-2,37467349	4,429085988	0,023527362	
ENST00000363759	ENSG00000200629	2,091740765	5,407616357	0,023545851	RNA, Ro-associated Y1 pseudogene 11 [Source:HGNC Symbol;Acc:
ENST00000364900	ENSG00000201770	2,910125751	4,545028542	0,023591963	RNA, U6 small nuclear 384, pseudogene [Source:HGNC Symbol;Ac
ENST00000383949	ENSG00000206676	2,174604797	6,613312609	0,023629475	
ENST00000365430	ENSG00000202300	2,741348569	4,911308223	0,023708314	RNA, U6 small nuclear 487, pseudogene [Source:HGNC Symbol;Ac
ENST00000410878	ENSG00000222810	2,182856246	6,213424432	0,023710891	RNA, U2 small nuclear 68, pseudogene [Source:HGNC Symbol;Acc
ENST00000469562	ENSG00000205639	-2,42500626	4,592012079	0,023757655	major facilitator superfamily domain containing 2B [Source:HGNC
ENST00000556260	ENSG00000078304	4,792348054	4,459037198	0,023946518	protein phosphatase 2 regulatory subunit B'gamma [Source:HGNC
ENST00000384307	ENSG00000207034	4,991631846	4,348204701	0,023981519	
ENST00000384630	ENSG00000207360	2,191516204	6,375376391	0,024086996	RNA, U6 small nuclear 14, pseudogene [Source:HGNC Symbol;Acc
ENST00000384289	ENSG00000207016	2,558290043	5,285268653	0,024198393	small nucleolar RNA, H/ACA box 36C [Source:HGNC Symbol;Acc:H
ENST00000383960	ENSG00000206687	3,106616186	5,30640186	0,024215194	RNA, U1 small nuclear 109, pseudogene [Source:HGNC Symbol;Ac
ENST00000421351	ENSG00000112378	2,264365809	5,424220489	0,024252996	PERP, TP53 apoptosis effector [Source:HGNC Symbol;Acc:HGNC:1
ENST00000608316	ENSG00000273113	4,761332043	5,163091341	0,024333085	novel transcript
ENST00000384173	ENSG00000206900	1,544489897	6,252577944	0,024361649	RNA, U6 small nuclear 98, pseudogene [Source:HGNC Symbol;Acc
ENST00000391254	ENSG00000212556	2,741052068	8,046761382	0,024485236	
ENST00000359491	ENSG00000214770	-3,405635715	4,771804336	0,024491749	novel transcript
ENST00000464704	ENSG00000243918	2,150317739	4,586579846	0,02450206	eukaryotic translation initiation factor 4B pseudogene 8 [Source:H
ENST00000478175	ENSG00000169679	3,502242192	4,525481042	0,024534581	BUB1 mitotic checkpoint serine/threonine kinase [Source:HGNC S
ENST00000263409	ENSG00000113594	2,523894528	5,442620664	0,024568716	LIF receptor alpha [Source:HGNC Symbol;Acc:HGNC:6597]
ENST00000354960	ENSG00000138735	-4,664860098	4,297077982	0,024609555	phosphodiesterase 5A [Source:HGNC Symbol;Acc:HGNC:8784]
ENST00000364757	ENSG00000201627	4,423421461	4,26677139	0,02465784	
ENST00000516950	ENSG00000252759	1,502178655	6,125063846	0,024682187	
ENST00000411281		2,701728623	4,99852988	0,024837825	
ENST00000270800	ENSG00000142677	2,357274882	4,921527512	0,024853467	interleukin 22 receptor subunit alpha 1 [Source:HGNC Symbol;Acc
ENST00000384479	ENSG00000207208	2,717496224	5,288362968	0,024861293	RNA, U6 small nuclear 790, pseudogene [Source:HGNC Symbol;Ac
ENST00000508813	ENSG00000248115	3,014303917	4,662814738	0,02487251	novel transcript
ENST00000364052	ENSG00000200922	1,978085801	4,549843672	0,024883362	
ENST00000411193	ENSG00000223125	1,626187214	7,398445879	0,024947895	RNA, U2 small nuclear 32, pseudogene [Source:HGNC Symbol;Acc
ENST00000248996		-2,012722915	4,908354218	0,024969171	
ENST00000365537	ENSG00000202407	1,804102615	5,638844293	0,024986363	
ENST00000580913	ENSG00000263631	1,684663822	5,718522282	0,025015323	microRNA 378d-1 [Source:HGNC Symbol;Acc:HGNC:41550]
ENST00000411005	ENSG00000222937	2,446119342	11,30450608	0,025036122	small nucleolar RNA, C/D box 63B [Source:HGNC Symbol;Acc:HGN
ENST00000384440	ENSG00000207169	2,420008262	4,768016722	0,025084486	RNA, U6 small nuclear 24, pseudogene [Source:HGNC Symbol;Acc
ENST00000427159	ENSG00000108592	-2,565093577	4,464770189	0,025215211	FtsJ RNA methyltransferase homolog 3 [Source:HGNC Symbol;Acc
ENST00000365328	ENSG00000202198	2,192673863	12,21759897	0,025344079	
ENST00000365118	ENSG00000201988	1,878704949	5,188904318	0,025437427	
ENST00000363536	ENSG00000200406	3,524626475	5,06093741	0,025453338	small nucleolar RNA, C/D box 114-23 [Source:HGNC Symbol;Acc:H
ENST00000391130	ENSG00000212432	3,154608359	4,405121512	0,025531559	
ENST00000558754	ENSG00000255571	-4,656613233	4,676785791	0,025610808	MIR9-3 host gene [Source:HGNC Symbol;Acc:HGNC:27388]
ENST00000327449		4,314130379	4,572452868	0,02562815	

ENST00000384562	ENSG00000207292	1,698604316	6,692841491	0,025662471	
ENST00000384320	ENSG00000207047	1,927761746	11,67194337	0,02576844	small nucleolar RNA, C/D box 51 [Source:HGNC Symbol;Acc:HGNC
ENST00000364578	ENSG00000201448	4,65425703	5,299172334	0,025870108	small nucleolar RNA, H/ACA box 63C [Source:HGNC Symbol;Acc:H
ENST00000607016	ENSG00000272325	-2,501244005	4,919553851	0,025882121	nudix hydrolase 3 [Source:HGNC Symbol;Acc:HGNC:8050]
ENST00000364778	ENSG00000201648	2,526490535	5,467245488	0,025943836	RNA, U4 small nuclear 91, pseudogene [Source:HGNC Symbol;Acc
ENST00000384567	ENSG00000207297	2,440416522	9,432934533	0,025946548	small nucleolar RNA, C/D box 7 [Source:HGNC Symbol;Acc:HGNC:3
ENST00000363050	ENSG00000199920	2,254722362	7,89832517	0,026019886	RNA, U4 small nuclear 44, pseudogene [Source:HGNC Symbol;Acc
ENST00000320095	ENSG00000176845	-3,003145742	4,856681933	0,02610286	meteorin like, glial cell differentiation regulator [Source:HGNC Sy
ENST00000439622	ENSG00000226310	-2,849853258	6,520446278	0,02617553	novel transcript
ENST00000365128	ENSG00000201998	2,422890628	8,175618438	0,026185851	small nucleolar RNA, H/ACA box 23 [Source:HGNC Symbol;Acc:HG
ENST00000248071	ENSG00000127528	-2,804746792	5,920093361	0,026200717	Kruppel like factor 2 [Source:HGNC Symbol;Acc:HGNC:6347]
ENST00000364020	ENSG00000200890	3,244879837	4,798740632	0,02625868	RNA, 5S ribosomal pseudogene 99 [Source:HGNC Symbol;Acc:HGN
ENST00000408154	ENSG00000221081	2,176525671	6,697315489	0,026319651	microRNA 320d-2 [Source:HGNC Symbol;Acc:HGNC:35388]
ENST00000484567	ENSG00000103335	4,556801025	4,280318434	0,026364221	piezo type mechanosensitive ion channel component 1 [Source:H
ENST00000233840	ENSG00000115488	2,649493283	4,581953505	0,026419613	neuraminidase 2 [Source:HGNC Symbol;Acc:HGNC:7759]
ENST00000460298	ENSG00000283154	-2,401777755	4,523097829	0,026428872	IQCJ-SCHIP1 readthrough [Source:HGNC Symbol;Acc:HGNC:38842
ENST00000460298	ENSG00000283154	-2,401777755	4,523097829	0,026428872	IQCJ-SCHIP1 readthrough [Source:HGNC Symbol;Acc:HGNC:38842
ENST00000458893	ENSG00000238423	1,71572772	7,07984207	0,026441466	small nucleolar RNA, C/D box 42B [Source:HGNC Symbol;Acc:HGN
ENST00000364359	ENSG00000201229	2,089513143	5,44460564	0,026452482	small nucleolar RNA, H/ACA box 63D [Source:HGNC Symbol;Acc:H
ENST00000365522	ENSG00000202392	2,126347918	7,277557304	0,026486203	RNA, 7SK small nuclear pseudogene 292 [Source:HGNC Symbol;Ac
ENST00000469523		-3,308320642	4,458840044	0,026488705	
ENST00000416441	ENSG00000149930	2,180560825	5,97008869	0,026573925	TAO kinase 2 [Source:HGNC Symbol;Acc:HGNC:16835]
ENST00000362698	ENSG00000199568	2,758531107	14,96588967	0,026591433	RNA, U5A small nuclear 1 [Source:HGNC Symbol;Acc:HGNC:10211
ENST00000378279	ENSG00000205002	-2,074447183	4,626550971	0,026622668	alanine and arginine rich domain containing protein [Source:HGN
ENST00000272233	ENSG00000143878	-2,546587461	6,079269214	0,026725279	ras homolog family member B [Source:HGNC Symbol;Acc:HGNC:6
ENST00000421896	ENSG00000233503	-1,87445841	4,682003604	0,026775557	heterogeneous nuclear ribonucleoprotein L pseudogene 1 [Source
ENST00000364551	ENSG00000201421	2,132142588	5,31176371	0,026817159	
ENST00000397412	ENSG00000007545	-4,833853918	4,335802182	0,026885375	cramped chromatin regulator homolog 1 [Source:HGNC Symbol;A
ENST00000579969	ENSG00000265145	2,624010878	13,5215734	0,027001154	small nucleolar RNA, C/D box 53 [Source:HGNC Symbol;Acc:HGNC
ENST00000436520	ENSG00000226781	-2,048412009	4,495620125	0,027028115	tubulin folding cofactor A pseudogene 1 [Source:HGNC Symbol;Ac
ENST00000562034	ENSG00000103528	3,311078774	5,149702726	0,027040829	synaptotagmin 17 [Source:HGNC Symbol;Acc:HGNC:24119]
ENST00000332290	ENSG00000185127	-1,747859534	4,982743812	0,027053153	chromosome 6 open reading frame 120 [Source:HGNC Symbol;Ac
ENST00000534428	ENSG00000167257	-2,59692994	4,936724544	0,027118502	ring finger protein 214 [Source:HGNC Symbol;Acc:HGNC:25335]
ENST00000364358	ENSG00000201228	1,422106569	5,94946599	0,027145801	
ENST00000423021	ENSG00000236567	2,57883882	5,585891873	0,027205062	transcription factor 3 pseudogene 1 [Source:HGNC Symbol;Acc:HG
ENST00000267163	ENSG00000139687	1,714634691	4,589132263	0,027235387	RB transcriptional corepressor 1 [Source:HGNC Symbol;Acc:HGNC
ENST00000363043	ENSG00000199913	2,47403946	4,54069003	0,027242469	
ENST00000539391	ENSG00000256596	2,212677144	4,86925187	0,027280548	novel transcript
ENST00000419069	ENSG00000238265	1,779804137	5,105261791	0,027355933	long intergenic non-protein coding RNA 317 [Source:HGNC Symbo
ENST00000599749	ENSG00000268388	-3,01378865	4,441407841	0,027439308	FOXF1 adjacent non-coding developmental regulatory RNA [Sourc
ENST00000318445	ENSG00000176463	-3,20718763	6,208772296	0,027449642	solute carrier organic anion transporter family member 3A1 [Sour
ENST00000383913	ENSG00000206640	1,987600151	5,061378439	0,027505473	
ENST00000377142	ENSG00000125820	-2,487982677	5,338965753	0,027833459	NK2 homeobox 2 [Source:HGNC Symbol;Acc:HGNC:7835]
ENST00000335568	ENSG00000135226	4,371128277	4,487795124	0,027902731	UDP glucuronosyltransferase family 2 member B28 [Source:HGNC
ENST00000375943	ENSG00000162438	3,733023903	4,639905167	0,027973148	chymotrypsin C [Source:HGNC Symbol;Acc:HGNC:2523]
ENST00000364813	ENSG00000201683	1,874754838	4,720322607	0,028030584	
ENST00000394725	ENSG00000196470	-3,011565499	4,477794199	0,02807284	siah E3 ubiquitin protein ligase 1 [Source:HGNC Symbol;Acc:HGNC
ENST00000574371	ENSG00000262902	1,971798082	7,181266964	0,028177196	MT-CO1 pseudogene 40 [Source:HGNC Symbol;Acc:HGNC:52105]
ENST00000390136		2,101385962	7,906389468	0,028188381	
ENST00000410104	ENSG00000144036	2,677775523	5,375024102	0,028253054	exocyst complex component 6B [Source:HGNC Symbol;Acc:HGNC:
ENST00000438005	ENSG00000223549	1,546303665	7,376398823	0,028258832	MT-ND5 pseudogene 28 [Source:HGNC Symbol;Acc:HGNC:42290]
ENST00000384975	ENSG00000207708	1,978862343	6,617663644	0,028357917	microRNA 141 [Source:HGNC Symbol;Acc:HGNC:31528]
ENST00000450173	ENSG00000237955	2,501587925	5,893131862	0,028412651	mitochondrial ribosomal protein L40 (MRPL40) pseudogene
ENST00000384550	ENSG00000207280	2,367617496	13,55604992	0,028468377	small nucleolar RNA, C/D box 20 [Source:HGNC Symbol;Acc:HGNC
ENST00000481242	ENSG00000136895	3,179212463	4,873370144	0,028478771	GTPase activating Rap/RanGAP domain like 3 [Source:HGNC Symb
ENST00000384063	ENSG00000206790	2,195040971	7,272110963	0,028482508	
ENST00000416193	ENSG00000226419	-4,677073762	4,291554566	0,028527102	SLC16A1 antisense RNA 1 [Source:HGNC Symbol;Acc:HGNC:49445
ENST00000349529	ENSG00000194717	4,551919265	4,766574191	0,028583753	microRNA 494 [Source:HGNC Symbol;Acc:HGNC:32084]
ENST00000386157	ENSG00000208892	1,855581335	7,017139883	0,028927209	small nucleolar RNA, H/ACA box 49 [Source:HGNC Symbol;Acc:HG
ENST00000372638	ENSG00000179862	-2,182672637	5,323939461	0,029047459	Cbp/p300 interacting transactivator with Glu/Asp rich carboxy-te
ENST00000516392		2,300503931	5,297970651	0,0291203	
ENST00000411395	ENSG00000223327	2,094514014	5,807457989	0,029144264	RNA, U2 small nuclear 71, pseudogene [Source:HGNC Symbol;Acc
ENST00000463397	ENSG00000239899	1,715760647	8,211378063	0,029254269	RNA, 7SL, cytoplasmic 674, pseudogene [Source:HGNC Symbol;Ac
ENST00000542638	ENSG00000012660	-2,52378411	4,711942517	0,029374832	ELOVL fatty acid elongase 5 [Source:HGNC Symbol;Acc:HGNC:213

ENST00000387446	ENSG00000210181	2,796375012	5,020339644	0,029377889	RNA, U6atac small nuclear 4, pseudogene [Source:HGNC Symbol;A
ENST00000364951	ENSG00000201821	2,467138908	5,116484756	0,02940056	RNA, U4 small nuclear 9, pseudogene [Source:HGNC Symbol;Acc:H
ENST00000545517	ENSG00000204583	3,515961783	4,549588958	0,029404415	leucine rich colipase like 1 [Source:HGNC Symbol;Acc:HGNC:4416(
ENST00000384277	ENSG00000207004	4,846689605	4,366896582	0,029414455	RNA, U6 small nuclear 301, pseudogene [Source:HGNC Symbol;Ac
ENST00000384849	ENSG00000207581	2,163525005	6,257873556	0,02947991	microRNA 199b [Source:HGNC Symbol;Acc:HGNC:31573]
ENST00000609190	ENSG00000272990	4,422179034	4,334727685	0,029635048	novel transcript, antisense to KCNAB1
ENST00000362846	ENSG00000199716	1,60988507	5,420661328	0,029707943	
ENST00000384452	ENSG00000207181	1,370352401	7,61392759	0,02980466	small nucleolar RNA, H/ACA box 14B [Source:HGNC Symbol;Acc:H
ENST00000415292	ENSG00000229932	-3,230931313	4,79593971	0,029901627	tyrosine 3-monooxygenase/tryptophan 5-monooxygenase activat
ENST00000360256	ENSG00000185010	1,925795236	4,963319937	0,029914726	coagulation factor VIII [Source:HGNC Symbol;Acc:HGNC:3546]
ENST00000461988	ENSG00000127948	-4,770147529	4,323188689	0,030032626	cytochrome p450 oxidoreductase [Source:HGNC Symbol;Acc:HGN
ENST00000362438	ENSG00000199308	2,586739848	5,134177289	0,030057946	RNA, U6 small nuclear 222, pseudogene [Source:HGNC Symbol;Ac
ENST00000329962	ENSG00000182272	-1,670581101	5,397530266	0,030111629	beta-1,4-N-acetyl-galactosaminyltransferase 4 [Source:HGNC Sym
ENST00000444527	ENSG00000248522	2,528406792	6,632478505	0,030223805	SET binding factor 1 pseudogene 1 [Source:HGNC Symbol;Acc:HGN
ENST00000323944	ENSG00000168952	-3,242868872	4,439214861	0,030224139	syntaxin binding protein 6 [Source:HGNC Symbol;Acc:HGNC:1966(
ENST00000607298	ENSG00000271734	1,917124959	5,886448493	0,030280558	novel transcript
ENST00000384606	ENSG00000207336	2,304044217	4,952608022	0,030303282	RNA, U6 small nuclear 658, pseudogene [Source:HGNC Symbol;Ac
ENST00000489116	ENSG00000231162	-2,943706084	4,889387618	0,030357173	COX11, cytochrome c oxidase copper chaperone pseudogene 1 [S
ENST00000362841	ENSG00000199711	2,149494719	4,705884493	0,030360725	
ENST00000253233	ENSG00000130921	2,985941065	4,828941226	0,030524959	chromosome 12 open reading frame 65 [Source:HGNC Symbol;Ac
ENST00000363313	ENSG00000200183	2,546450412	4,718178569	0,030577904	RNA, U6 small nuclear 238, pseudogene [Source:HGNC Symbol;Ac
ENST00000459004	ENSG00000238835	2,406930186	8,658052467	0,030583193	small Cajal body-specific RNA 18 [Source:HGNC Symbol;Acc:HGNC
ENST00000543500	ENSG00000256222	1,631655968	6,433501397	0,030623415	MT-RNR2 like 3 [Source:HGNC Symbol;Acc:HGNC:37157]
ENST00000398645	ENSG00000173120	-2,071051858	5,34806715	0,030761506	lysine demethylase 2A [Source:HGNC Symbol;Acc:HGNC:13606]
ENST00000322157	ENSG00000141279	-4,367671272	4,438819999	0,03076612	aminopeptidase puromycin sensitive [Source:HGNC Symbol;Acc:H
ENST00000585078	ENSG00000264994	2,50452292	13,05508204	0,030827596	small nucleolar RNA, C/D box 92 [Source:HGNC Symbol;Acc:HGNC
ENST00000398631	ENSG00000251664	-1,608507852	5,242682123	0,031101458	protocadherin alpha 12 [Source:HGNC Symbol;Acc:HGNC:8666]
ENST00000385037	ENSG00000207771	1,390837652	8,158680238	0,031126383	microRNA 550a-1 [Source:HGNC Symbol;Acc:HGNC:32804]
ENST00000340099	ENSG00000125170	-1,94871777	4,502561755	0,031161527	docking protein 4 [Source:HGNC Symbol;Acc:HGNC:19868]
ENST00000331581	ENSG00000182985	-2,176614962	5,288163532	0,031224153	cell adhesion molecule 1 [Source:HGNC Symbol;Acc:HGNC:5951]
ENST00000374888	ENSG00000198455	-1,984495996	5,436091911	0,031263907	zinc finger X-linked duplicated B [Source:HGNC Symbol;Acc:HGNC
ENST00000408518	ENSG00000221445	2,151612402	9,63028791	0,031291809	microRNA 1301 [Source:HGNC Symbol;Acc:HGNC:35253]
ENST00000459135	ENSG00000238959	3,244889819	4,91005461	0,031353413	RNA, U7 small nuclear 19 pseudogene [Source:HGNC Symbol;Acc:
ENST00000508269	ENSG00000248890	-3,890227694	4,547645452	0,031373562	HHIP antisense RNA 1 [Source:HGNC Symbol;Acc:HGNC:44182]
ENST00000410535	ENSG00000222467	1,414853992	5,646194825	0,03137806	
ENST00000384305	ENSG00000207032	1,826091529	6,841235982	0,031394182	
ENST00000362452	ENSG00000199322	2,668933886	5,286847304	0,031417443	RNA, 5S ribosomal pseudogene 183 [Source:HGNC Symbol;Acc:HG
ENST00000467931	ENSG00000164692	2,030186387	6,058669302	0,031447626	collagen type I alpha 2 chain [Source:HGNC Symbol;Acc:HGNC:219
ENST00000599358	ENSG00000226674	4,625255497	5,661648378	0,03147344	testis expressed 41 [Source:HGNC Symbol;Acc:HGNC:48667]
ENST00000415752		-4,617756801	4,278398971	0,031494851	
ENST00000580243	ENSG00000179981	1,811356529	5,647187718	0,031595821	teashirt zinc finger homeobox 1 [Source:HGNC Symbol;Acc:HGNC:
ENST00000364007	ENSG00000200877	2,621862172	4,810353096	0,031611577	RNA, U6 small nuclear 560, pseudogene [Source:HGNC Symbol;Ac
ENST00000343242	ENSG00000198517	-2,179445568	4,926699885	0,031630909	MAF bZIP transcription factor K [Source:HGNC Symbol;Acc:HGNC:
ENST00000384036	ENSG00000206763	1,728515413	6,63561023	0,031645562	RNA, U6 small nuclear 10, pseudogene [Source:HGNC Symbol;Acc
ENST00000309383	ENSG00000160469	-2,846868391	5,067830439	0,03166602	BR serine/threonine kinase 1 [Source:HGNC Symbol;Acc:HGNC:18
ENST00000367696	ENSG00000135870	-4,779761993	4,500801346	0,031693664	ring finger and CCCH-type domains 1 [Source:HGNC Symbol;Acc:H
ENST00000416718	ENSG00000198744	1,877975698	11,04869713	0,031705406	MT-CO3 pseudogene 12 [Source:HGNC Symbol;Acc:HGNC:52042]
ENST00000531169	ENSG00000197580	2,951247192	4,584626067	0,031733012	beta-carotene oxygenase 2 [Source:HGNC Symbol;Acc:HGNC:1850
ENST00000402590		-4,763283147	4,32707261	0,031734064	
ENST00000230882	ENSG00000112964	-3,208775987	4,387948625	0,031765448	growth hormone receptor [Source:HGNC Symbol;Acc:HGNC:4263]
ENST00000365547	ENSG00000202417	2,157775411	5,131513843	0,031769486	
ENST00000585433	ENSG00000224699	4,643929665	4,360482835	0,031774102	LAMTOR5 antisense RNA 1 [Source:HGNC Symbol;Acc:HGNC:4082
ENST00000397068	ENSG00000167311	3,458427961	4,827115963	0,031817489	ADP-ribosyltransferase 5 [Source:HGNC Symbol;Acc:HGNC:24049]
ENST00000344951	ENSG00000036257	-4,472085232	4,354006946	0,031843285	cullin 3 [Source:HGNC Symbol;Acc:HGNC:2553]
ENST00000392088	ENSG00000127824	-4,472085232	4,444353005	0,031843285	tubulin alpha 4a [Source:HGNC Symbol;Acc:HGNC:12407]
ENST00000455997	ENSG00000211456	-4,472085232	4,330011008	0,031843285	SAC1 like phosphatidylinositide phosphatase [Source:HGNC Symb
ENST00000571796	ENSG00000141556	-4,472085232	4,299726663	0,031843285	tubulin folding cofactor D [Source:HGNC Symbol;Acc:HGNC:11581
ENST00000602529	ENSG00000269934	-4,472085232	4,342090703	0,031843285	novel transcript, antisense to OBSCN
ENST00000604036	ENSG00000188352	-4,472085232	4,439743235	0,031843285	focadhesin [Source:HGNC Symbol;Acc:HGNC:23377]
ENST00000383945	ENSG00000206672	4,301202098	4,261650972	0,031843285	
ENST00000569080	ENSG00000062038	4,301202098	4,261650972	0,031843285	cadherin 3 [Source:HGNC Symbol;Acc:HGNC:1762]
ENST00000428457	ENSG00000136205	4,300015294	4,50454077	0,031843285	tensin 3 [Source:HGNC Symbol;Acc:HGNC:21616]
ENST00000516485	ENSG00000252294	4,299566094	4,29596013	0,031843285	RNA, U6 small nuclear 589, pseudogene [Source:HGNC Symbol;Ac
ENST00000410122	ENSG00000222054	4,299117032	4,46953051	0,031843285	RNA, 5S ribosomal pseudogene 177 [Source:HGNC Symbol;Acc:HG

ENST00000520657	ENSG00000187840	4,297483281	4,250937416	0,031843285	eukaryotic translation initiation factor 4E binding protein 1 [Sourc
ENST00000516409	ENSG00000252218	4,297034847	4,395672766	0,031843285	
ENST00000600410	ENSG00000105373	4,29658655	4,37286636	0,031843285	NOP53 ribosome biogenesis factor [Source:HGNC Symbol;Acc:HGI
ENST00000354333	ENSG00000182912	-4,294918041	4,33833314	0,031843285	TSPEAR antisense RNA 2 [Source:HGNC Symbol;Acc:HGNC:16428]
ENST00000359003	ENSG00000198646	-4,294918041	4,490991025	0,031843285	nuclear receptor coactivator 6 [Source:HGNC Symbol;Acc:HGNC:1
ENST00000477214	ENSG00000185269	-4,294918041	4,311791652	0,031843285	notum, palmitoleoyl-protein carboxylesterase [Source:HGNC Sym
ENST00000334493	ENSG00000187260	-4,291329662	4,282251508	0,031843285	WD repeat domain 86 [Source:HGNC Symbol;Acc:HGNC:28020]
ENST00000484597	ENSG00000244381	-4,291329662	4,294302797	0,031843285	succinate dehydrogenase complex, subunit D, integral membrane
ENST00000515049	ENSG00000249176	-4,291329662	4,244251618	0,031843285	mRNA turnover 4 homolog (S. cerevisiae) (MRTO4) pseudogene
ENST00000596689	ENSG00000104888	-4,291329662	4,305351166	0,031843285	solute carrier family 17 member 7 [Source:HGNC Symbol;Acc:HGN
ENST00000369763	ENSG00000121931	-4,290279721	4,257254273	0,031843285	ligand dependent nuclear receptor interacting factor 1 [Source:HG
ENST00000397646	ENSG00000214147	-4,290279721	4,303620182	0,031843285	enabled homolog (Drosophila) (ENAH) pseudogene
ENST00000479752	ENSG00000241313	-4,290279721	4,303779215	0,031843285	WWTR1 antisense RNA 1 [Source:HGNC Symbol;Acc:HGNC:41035]
ENST00000508146	ENSG00000197894	-4,290279721	4,298812942	0,031843285	alcohol dehydrogenase 5 (class III), chi polypeptide [Source:HGNC
ENST00000509173	ENSG00000250441	-4,290279721	4,237879733	0,031843285	LSM2 homolog, U6 small nuclear RNA associated (S. cerevisiae) (L
ENST00000525699	ENSG00000168522	-4,290279721	4,257577517	0,031843285	farnesyltransferase, CAAX box, alpha [Source:HGNC Symbol;Acc:H
ENST00000485376	ENSG00000063601	-4,287749792	4,326078333	0,031843285	myotubularin related protein 1 [Source:HGNC Symbol;Acc:HGNC:7
ENST00000553886	ENSG00000258893	-4,287749792	4,292155777	0,031843285	SET pseudogene 2 [Source:HGNC Symbol;Acc:HGNC:20032]
ENST00000590310	ENSG00000136448	-4,287749792	4,253557822	0,031843285	N-myristoyltransferase 1 [Source:HGNC Symbol;Acc:HGNC:7857]
ENST00000426257	ENSG00000234436	4,094709743	4,254241987	0,031843285	leukocyte immunoglobulin-like receptor, subfamily A pseudogene
ENST00000448412	ENSG00000226640	4,093064066	4,249901284	0,031843285	novel transcript
ENST00000364749	ENSG00000201619	4,092613328	4,584565342	0,031843285	
ENST00000375412	ENSG00000188938	4,092613328	4,45222726	0,031843285	family with sequence similarity 120A opposite strand [Source:HGI
ENST00000385016	ENSG00000207749	4,092613328	4,247798309	0,031843285	microRNA 299 [Source:HGNC Symbol;Acc:HGNC:31618]
ENST00000391171	ENSG00000212473	4,092613328	4,286971461	0,031843285	RNA, U1 small nuclear 101, pseudogene [Source:HGNC Symbol;Ac
ENST00000463224	ENSG00000156384	4,092613328	4,247798309	0,031843285	SWI5 dependent homologous recombination repair protein 1 [Sou
ENST00000583549	ENSG00000263407	4,092613328	4,451413291	0,031843285	microRNA 4660 [Source:HGNC Symbol;Acc:HGNC:41861]
ENST00000364351	ENSG00000201221	4,092162728	4,265377224	0,031843285	RNA, U4 small nuclear 40, pseudogene [Source:HGNC Symbol;Acc
ENST00000562474	ENSG00000103197	4,092162728	4,245694751	0,031843285	TSC complex subunit 2 [Source:HGNC Symbol;Acc:HGNC:12363]
ENST00000577717	ENSG00000263909	4,092162728	4,322717616	0,031843285	microRNA 5000 [Source:HGNC Symbol;Acc:HGNC:43464]
ENST00000592662	ENSG00000179115	4,090969942	4,411408168	0,031843285	phenylalanyl-tRNA synthetase subunit alpha [Source:HGNC Symb
ENST00000362682	ENSG00000199552	4,090519841	4,354364486	0,031843285	
ENST00000363417	ENSG00000200287	4,090519841	4,389425354	0,031843285	
ENST00000364472	ENSG00000201342	4,090519841	4,392388071	0,031843285	RNA, U4 small nuclear 38, pseudogene [Source:HGNC Symbol;Acc
ENST00000380342	ENSG00000147003	4,090519841	4,334039774	0,031843285	collectrin, amino acid transport regulator [Source:HGNC Symbol;A
ENST00000516143	ENSG00000251952	4,090519841	4,318067605	0,031843285	RNA, U6 small nuclear 1219, pseudogene [Source:HGNC Symbol;A
ENST00000516289	ENSG00000252098	4,090519841	4,241339955	0,031843285	
ENST00000587834	ENSG00000166562	4,090519841	4,280153487	0,031843285	SEC11 homolog C, signal peptidase complex subunit [Source:HGN
ENST00000448031	ENSG00000233139	-4,089985338	4,250771116	0,031843285	ornithine aminotransferase (gyrate atrophy) (OAT) pseudogene
ENST00000372220	ENSG00000130714	-4,087427825	4,306741517	0,031843285	protein O-mannosyltransferase 1 [Source:HGNC Symbol;Acc:HGN
ENST00000508968	ENSG00000177822	-4,087427825	4,30000586	0,031843285	TENM3 antisense RNA 1 [Source:HGNC Symbol;Acc:HGNC:28076]
ENST00000227520	ENSG00000110104	-4,086373511	4,365897787	0,031843285	coiled-coil domain containing 86 [Source:HGNC Symbol;Acc:HGNC
ENST00000556779		-4,086373511	4,495333195	0,031843285	
ENST00000596046	ENSG00000083845	-4,086373511	4,371650418	0,031843285	ribosomal protein S5 [Source:HGNC Symbol;Acc:HGNC:10426]
ENST00000433465	ENSG00000223768	-3,846591512	4,285599048	0,031843285	long intergenic non-protein coding RNA 205 [Source:HGNC Symbo
ENST00000391220		2,430782397	4,385350944	0,031843285	
ENST00000450454	ENSG00000204219	2,429146393	4,451652932	0,031843285	transcription elongation factor A3 [Source:HGNC Symbol;Acc:HGN
ENST00000417166		2,428697331	4,347729234	0,031843285	
ENST00000609118	ENSG00000273010	2,428697331	4,330098873	0,031843285	novel transcript, antisense to LRIF1
ENST00000377453	ENSG00000102805	2,426166848	4,372131466	0,031843285	CLN5, intracellular trafficking protein [Source:HGNC Symbol;Acc:H
ENST00000456758		2,224290041	4,267827563	0,031843285	
ENST00000610159	ENSG00000273247	2,222193626	4,395613094	0,031843285	novel transcript, antisense to RAB33B
ENST00000365049	ENSG00000201919	2,220550241	4,316493653	0,031843285	RNA, U6 small nuclear 1022, pseudogene [Source:HGNC Symbol;A
ENST00000370763	ENSG00000162616	2,22010014	4,366035875	0,031843285	DnaJ heat shock protein family (Hsp40) member B4 [Source:HGNC
ENST00000381641	ENSG00000120210	2,22010014	4,366709037	0,031843285	insulin like 6 [Source:HGNC Symbol;Acc:HGNC:6089]
ENST00000392932		2,22010014	4,293064682	0,031843285	
ENST00000459384		2,22010014	4,486314892	0,031843285	
ENST00000523235	ENSG00000134824	2,22010014	4,354089062	0,031843285	fatty acid desaturase 2 [Source:HGNC Symbol;Acc:HGNC:3575]
ENST00000363284		2,103293147	8,480947654	0,031969674	
ENST00000365399	ENSG00000202269	1,775539233	4,573544025	0,031982458	
ENST00000506106	ENSG00000250961	4,46677928	4,742204874	0,032018819	novel transcript, antisense to ACTBL2
ENST00000411404	ENSG00000223336	2,517739308	9,90686183	0,032061312	RNA, U2 small nuclear 6, pseudogene [Source:HGNC Symbol;Acc:H
ENST00000422905	ENSG00000219930	-4,778911758	4,614087388	0,032102211	glyceraldehyde 3 phosphate dehydrogenase pseudogene 67 [Sou
ENST00000362072	ENSG00000149295	-4,459031665	4,280381437	0,032148008	dopamine receptor D2 [Source:HGNC Symbol;Acc:HGNC:3023]

ENST00000364982	ENSG00000201852	1,640349144	5,194268208	0,032213158	RNA, U6 small nuclear 702, pseudogene [Source:HGNC Symbol;Ac
ENST00000384923	ENSG00000207656	1,954512318	5,653318318	0,032320882	microRNA 489 [Source:HGNC Symbol;Acc:HGNC:32074]
ENST00000473136	ENSG00000175105	-1,797168834	4,560561593	0,032376689	zinc finger protein 654 [Source:HGNC Symbol;Acc:HGNC:25612]
ENST00000579846	ENSG00000264566	2,865073157	4,680855527	0,032389769	microRNA 23c [Source:HGNC Symbol;Acc:HGNC:38913]
ENST00000362692	ENSG00000199562	2,464621751	9,956805279	0,032431309	RNA, U6 small nuclear 37, pseudogene [Source:HGNC Symbol;Acc
ENST00000381725		-4,900091148	4,348183278	0,032471532	
ENST00000505813	ENSG00000248966	-2,096692559	4,786229642	0,032513182	BCL2 associated transcription factor 1 pseudogene 1 [Source:HGN
ENST00000410597	ENSG00000222529	1,452584702	6,365295288	0,032714856	
ENST00000385238	ENSG00000207973	1,277884164	8,548373517	0,032894481	microRNA 589 [Source:HGNC Symbol;Acc:HGNC:32845]
ENST00000363192	ENSG00000200062	2,089944793	6,104553678	0,032904179	RNA, U4 small nuclear 58, pseudogene [Source:HGNC Symbol;Acc
ENST00000580972	ENSG00000264229	2,278985872	9,896653885	0,032905216	RNA, U4atac small nuclear (U12-dependent splicing) [Source:HGN
ENST00000527644	ENSG00000214063	-2,104631769	5,262919934	0,032964538	tetraspanin 4 [Source:HGNC Symbol;Acc:HGNC:11859]
ENST00000364998	ENSG00000201868	2,363947801	4,543376382	0,03297423	
ENST00000413097	ENSG00000137817	4,090469251	4,450355523	0,032998999	poly(ADP-ribose) polymerase family member 6 [Source:HGNC Syn
ENST00000304984		4,430105626	4,328404209	0,033073048	
ENST00000563686	ENSG00000196628	1,979737978	6,014856225	0,033075284	transcription factor 4 [Source:HGNC Symbol;Acc:HGNC:11634]
ENST00000364112	ENSG00000200982	2,266561607	4,797322369	0,03308971	
ENST00000450764	ENSG00000105576	-2,929586664	4,623026462	0,033148094	transportin 2 [Source:HGNC Symbol;Acc:HGNC:19998]
ENST00000384122	ENSG00000206849	4,287367141	4,47876714	0,033243598	
ENST00000403109	ENSG00000218359	-2,07683425	4,464948262	0,033258142	SUMO2 pseudogene 13 [Source:HGNC Symbol;Acc:HGNC:49351]
ENST00000345060	ENSG00000188778	4,861366591	4,944667607	0,033377213	adrenoceptor beta 3 [Source:HGNC Symbol;Acc:HGNC:288]
ENST00000385039	ENSG00000207773	1,314544799	8,515783082	0,0333959	microRNA 642a [Source:HGNC Symbol;Acc:HGNC:32898]
ENST00000538126	ENSG00000040199	-3,130098367	4,404716773	0,033400962	PH domain and leucine rich repeat protein phosphatase 2 [Source
ENST00000504799	ENSG00000250706	2,575540233	4,964759375	0,033453845	novel transcript
ENST00000364571	ENSG00000201441	2,4227361	4,374330296	0,033714259	RNA, U6 small nuclear 646, pseudogene [Source:HGNC Symbol;Ac
ENST00000516611	ENSG00000252420	2,702266579	4,443269814	0,033781122	
ENST00000516978	ENSG00000252787	2,690395338	6,398726436	0,033815618	
ENST00000413990	ENSG00000227295	-4,438913315	4,357461862	0,033923741	elongation factor for RNA polymerase II 2 pseudogene 1 [Source:H
ENST00000323496	ENSG00000223551	-2,429139217	4,467641382	0,033931636	TMSB4X pseudogene 4 [Source:HGNC Symbol;Acc:HGNC:11886]
ENST00000364604	ENSG00000201474	2,036581789	6,920726341	0,033998226	RNA, U6 small nuclear 164, pseudogene [Source:HGNC Symbol;Ac
ENST00000582236	ENSG00000266761	1,675954274	6,074981971	0,034170677	microRNA 3194 [Source:HGNC Symbol;Acc:HGNC:38346]
ENST00000225174	ENSG00000108179	-4,274948499	4,331510678	0,034171023	peptidylprolyl isomerase F [Source:HGNC Symbol;Acc:HGNC:9259
ENST00000388402	ENSG00000211137	2,248554369	6,027648097	0,034275111	microRNA 190a [Source:HGNC Symbol;Acc:HGNC:31560]
ENST00000363059	ENSG00000199929	2,259741272	5,118179981	0,034317744	RNA, 5S ribosomal pseudogene 405 [Source:HGNC Symbol;Acc:HG
ENST00000364334		2,073756304	4,791268705	0,034438247	
ENST00000364562	ENSG00000201432	1,912899206	5,153883252	0,034442805	
ENST00000516564	ENSG00000252373	2,025484322	4,909972925	0,034451633	RNA, U6 small nuclear 358, pseudogene [Source:HGNC Symbol;Ac
ENST00000263238	ENSG00000115091	3,34161884	5,042465994	0,034468035	ARP3 actin related protein 3 homolog [Source:HGNC Symbol;Acc:I
ENST00000356818	ENSG00000196422	-3,126302262	4,814947105	0,034481002	protein phosphatase 1 regulatory subunit 26 [Source:HGNC Symb
ENST00000470093	ENSG00000107829	2,027169682	5,135847309	0,034528547	F-box and WD repeat domain containing 4 [Source:HGNC Symbol;
ENST00000364502	ENSG00000201372	1,984437861	5,435608733	0,034547857	RNA, U6 small nuclear 1251, pseudogene [Source:HGNC Symbol;A
ENST00000516492	ENSG00000252301	2,76664961	6,003319277	0,034585644	RNA, 5S ribosomal pseudogene 134 [Source:HGNC Symbol;Acc:HG
ENST00000410253	ENSG00000222185	4,572219231	4,395763196	0,034693895	
ENST00000378204	ENSG00000182197	-3,384565587	4,949805414	0,034695523	exostosin glycosyltransferase 1 [Source:HGNC Symbol;Acc:HGNC:3
ENST00000426867	ENSG00000231587	1,874709496	10,86842234	0,034740308	small nucleolar RNA, C/D box 62B [Source:HGNC Symbol;Acc:HGN
ENST00000589108	ENSG00000063241	4,236199454	4,260670939	0,034774319	isochorismatase domain containing 2 [Source:HGNC Symbol;Acc:H
ENST00000586803	ENSG00000179218	4,652050761	4,422932877	0,034827893	calreticulin [Source:HGNC Symbol;Acc:HGNC:1455]
ENST00000305031	ENSG00000198108	-4,445798392	4,574093101	0,034860781	chondroitin sulfate synthase 3 [Source:HGNC Symbol;Acc:HGNC:2
ENST00000460733	ENSG00000132376	-3,57217692	4,488173832	0,034863353	inositol polyphosphate-5-phosphatase K [Source:HGNC Symbol;Ac
ENST00000384614	ENSG00000207344	1,550025136	7,899505423	0,034865933	small nucleolar RNA, H/ACA box 22C [Source:HGNC Symbol;Acc:H
ENST00000375915	ENSG00000204442	-2,580736041	4,644287564	0,034955688	family with sequence similarity 155 member A [Source:HGNC Sym
ENST00000586394	ENSG00000267274	5,915759654	4,964815661	0,035001341	novel transcript, sense overlapping with ZNF700
ENST00000280481	ENSG00000150893	1,691585335	5,405623135	0,035059982	FRAS1 related extracellular matrix protein 2 [Source:HGNC Symbo
ENST00000299575	ENSG00000166454	-2,892831629	4,774390525	0,035363321	ATM interactor [Source:HGNC Symbol;Acc:HGNC:29034]
ENST00000423096	ENSG00000238150	-3,329739888	4,527590368	0,035417402	ribosomal protein, large, P1 (RPLP1) pseudogene
ENST00000317605	ENSG00000181541	-2,117341085	7,212739826	0,035469329	mab-21 like 2 [Source:HGNC Symbol;Acc:HGNC:6758]
ENST00000246229	ENSG00000126003	-2,838115675	4,811884604	0,035520113	PLAG1 like zinc finger 2 [Source:HGNC Symbol;Acc:HGNC:9047]
ENST00000256925	ENSG00000134508	-2,878774843	4,819866827	0,03552094	Cdk5 and Abl enzyme substrate 1 [Source:HGNC Symbol;Acc:HGN
ENST00000517239	ENSG00000253048	4,303187914	4,532611266	0,035523329	RNA, U4 small nuclear 60, pseudogene [Source:HGNC Symbol;Acc
ENST00000472035	ENSG00000108175	-5,197398904	4,391130104	0,03552415	zinc finger MIZ-type containing 1 [Source:HGNC Symbol;Acc:HGNC
ENST00000393567	ENSG00000157423	3,253800645	4,56293162	0,035555542	HYDIN, axonemal central pair apparatus protein [Source:HGNC Sy
ENST00000504931		1,725160412	5,787951128	0,035813742	
ENST00000408587	ENSG00000221514	2,310377288	13,46516821	0,035825129	small nucleolar RNA, C/D box 111B [Source:HGNC Symbol;Acc:HG
ENST00000252999	ENSG00000130702	-1,762312356	5,780165648	0,035969607	laminin subunit alpha 5 [Source:HGNC Symbol;Acc:HGNC:6485]

ENST00000363781	ENSG00000200651	1,63434105	6,17934455	0,036037494	
ENST00000426767	ENSG00000225264	1,897214461	5,34978577	0,036078507	zinc and ring finger 2 pseudogene 2 [Source:HGNC Symbol;Acc:HG
ENST00000411206	ENSG00000223138	1,837899447	5,417616912	0,036191011	RNA, 5S ribosomal pseudogene 450 [Source:HGNC Symbol;Acc:HG
ENST00000567788	ENSG00000214039	2,135461592	4,804729276	0,036204169	long intergenic non-protein coding RNA 2418 [Source:HGNC Symb
ENST00000532571	ENSG00000181135	-2,051379992	5,079796508	0,036283707	zinc finger protein 707 [Source:HGNC Symbol;Acc:HGNC:27815]
ENST00000532571	ENSG00000181135	-2,051379992	5,079796508	0,036283707	zinc finger protein 707 [Source:HGNC Symbol;Acc:HGNC:27815]
ENST00000363367	ENSG00000200237	2,116634909	6,265249732	0,036287428	
ENST00000468560	ENSG00000114098	2,408363244	4,751207154	0,036314078	armadillo repeat containing 8 [Source:HGNC Symbol;Acc:HGNC:24
ENST00000329146	ENSG00000182809	-2,268482347	5,865575605	0,036463683	cysteine rich protein 2 [Source:HGNC Symbol;Acc:HGNC:2361]
ENST00000364139	ENSG00000201009	1,530495531	9,432408489	0,036567757	
ENST00000437982	ENSG00000230756	4,395263288	4,538542256	0,036575738	ras homolog family member Q pseudogene 3 [Source:HGNC Symb
ENST00000579518	ENSG00000266320	1,444546663	6,405063397	0,036683605	microRNA 3909 [Source:HGNC Symbol;Acc:HGNC:38987]
ENST00000454171	ENSG00000224059	-1,708400392	4,51277054	0,036849597	heat shock protein family A (Hsp70) member 8 pseudogene 16 [Sc
ENST00000583997	ENSG00000266691	-2,902659966	5,562329812	0,036910038	fermitin family member 3 (FERMT3) pseudogene
ENST00000402326	ENSG00000217241	-4,403222102	4,298025769	0,036971978	chromobox 3 pseudogene 9 [Source:HGNC Symbol;Acc:HGNC:428
ENST00000363626	ENSG00000200496	1,384606357	8,010954475	0,037035925	
ENST00000354915	ENSG00000206178	-2,482660563	4,978930674	0,037064255	hemoglobin subunit zeta pseudogene 1 [Source:HGNC Symbol;Ac
ENST00000377777	ENSG00000158373	3,09103663	5,615970212	0,037227711	histone cluster 1 H2B family member d [Source:HGNC Symbol;Acc
ENST00000364025	ENSG00000200895	4,094645305	4,263163897	0,037306671	RNA, 7SK small nuclear pseudogene 245 [Source:HGNC Symbol;Ac
ENST00000363964	ENSG00000200834	2,197950736	9,892848709	0,03731013	
ENST00000404795	ENSG00000142700	2,997090748	4,893350845	0,037317069	DMRT like family A2 [Source:HGNC Symbol;Acc:HGNC:13908]
ENST00000397596	ENSG00000174775	-2,180727269	4,675075346	0,037322416	HRas proto-oncogene, GTPase [Source:HGNC Symbol;Acc:HGNC:5
ENST00000364792	ENSG00000201662	2,921286643	4,695000204	0,0373644	RNA, U6 small nuclear 60, pseudogene [Source:HGNC Symbol;Acc
ENST00000530405	ENSG00000165912	-4,589575641	4,310299792	0,037379512	protein kinase C and casein kinase substrate in neurons 3 [Source
ENST00000455793	ENSG00000236852	-3,399630895	4,446804195	0,037482416	Sjogren syndrome antigen B (autoantigen La) (SSB) pseudogene
ENST00000516041	ENSG00000251850	1,902215058	4,966122216	0,037554742	RNA, 5S ribosomal pseudogene 96 [Source:HGNC Symbol;Acc:HGN
ENST00000362883	ENSG00000199753	2,293170697	14,55161588	0,037572083	small nucleolar RNA, C/D box 104 [Source:HGNC Symbol;Acc:HGN
ENST00000505648	ENSG00000135317	4,104733648	4,34046541	0,037608709	sorting nexin 14 [Source:HGNC Symbol;Acc:HGNC:14977]
ENST00000429493		-4,317960393	4,389617861	0,037758697	
ENST00000505092	ENSG00000251685	2,420004262	5,213055831	0,037785214	UDP glucuronosyltransferase family 2 member B27, pseudogene [
ENST00000449934	ENSG00000204520	-4,404748658	4,270201506	0,037888319	MHC class I polypeptide-related sequence A [Source:HGNC Symbo
ENST00000369536	ENSG00000146282	-4,081176368	4,236834038	0,037947477	arginyl-tRNA synthetase 2, mitochondrial [Source:HGNC Symbol;A
ENST00000390533	ENSG00000211885	2,220808488	4,832632663	0,038018827	T cell receptor alpha joining 4 [Source:HGNC Symbol;Acc:HGNC:12
ENST00000365237		2,130158042	8,43149439	0,038039452	
ENST00000422113	ENSG00000151952	-2,109107145	4,953778895	0,038233084	transmembrane protein 132D [Source:HGNC Symbol;Acc:HGNC:25
ENST00000570843	ENSG00000261889	2,47356305	9,5223707	0,038321995	novel transcript
ENST00000363464	ENSG00000200334	2,026414437	4,637124825	0,038522386	
ENST00000536300	ENSG00000189120	-2,404299979	5,065975928	0,038584604	Sp6 transcription factor [Source:HGNC Symbol;Acc:HGNC:14530]
ENST00000370708	ENSG00000112200	2,166686734	5,043724607	0,03867935	zinc finger protein 451 [Source:HGNC Symbol;Acc:HGNC:21091]
ENST00000516795	ENSG00000252604	1,873717716	6,309535879	0,038892534	RNA, U2 small nuclear 44, pseudogene [Source:HGNC Symbol;Acc
ENST00000302909	ENSG00000171303	-2,009158128	7,934111659	0,038895224	potassium two pore domain channel subfamily K member 3 [Sour
ENST00000386910	ENSG00000209645	1,995871026	9,948321834	0,038940034	small nucleolar RNA, C/D box 105 [Source:HGNC Symbol;Acc:HGN
ENST00000384050	ENSG00000206777	2,314831056	4,89515213	0,039049003	RNA, U6 small nuclear 637, pseudogene [Source:HGNC Symbol;Ac
ENST00000607287	ENSG00000271945	4,288421044	4,69451351	0,039060825	novel transcript
ENST00000421383	ENSG00000143815	-2,309355113	5,92608826	0,03909687	lamin B receptor [Source:HGNC Symbol;Acc:HGNC:6518]
ENST00000361937	ENSG00000128908	-2,879438665	4,815556491	0,039168928	INO80 complex subunit [Source:HGNC Symbol;Acc:HGNC:26956]
ENST00000606738	ENSG00000269113	2,056003905	4,931714743	0,039179299	TraB domain containing 2B [Source:HGNC Symbol;Acc:HGNC:4420
ENST00000489171	ENSG00000107551	-3,030734502	4,410846993	0,039209642	Ras association domain family member 4 [Source:HGNC Symbol;A
ENST00000560079	ENSG00000166716	-2,344072116	4,423155541	0,039211362	zinc finger protein 592 [Source:HGNC Symbol;Acc:HGNC:28986]
ENST00000585045	ENSG00000168646	-2,028745708	6,325128731	0,039244594	axin 2 [Source:HGNC Symbol;Acc:HGNC:904]
ENST00000438469	ENSG00000230832	-2,456897551	4,402502443	0,039260991	Sjogren syndrome antigen B (autoantigen La) (SSB) pseudogene
ENST00000384995	ENSG00000207728	4,095900964	4,507262998	0,039295321	microRNA 449b [Source:HGNC Symbol;Acc:HGNC:32794]
ENST00000383876	ENSG00000206603	1,792378441	7,649727568	0,039304369	small nucleolar RNA, H/ACA box 22B [Source:HGNC Symbol;Acc:H
ENST00000261692	ENSG00000111328	-2,012561072	5,748458112	0,039461397	cyclin dependent kinase 2 associated protein 1 [Source:HGNC Sym
ENST00000308191	ENSG00000171408	2,360735525	5,046397944	0,039603242	phosphodiesterase 7B [Source:HGNC Symbol;Acc:HGNC:8792]
ENST00000431356	ENSG00000225355	-4,737083166	4,341394342	0,039689608	ADP ribosylation factor like GTPase 6 interacting protein 1 pseudo
ENST00000221249	ENSG00000032444	-2,255605105	6,92203257	0,039754492	patatin like phospholipase domain containing 6 [Source:HGNC Sy
ENST00000330949	ENSG00000182968	-1,983599957	6,106405628	0,039776817	SRY-box 1 [Source:HGNC Symbol;Acc:HGNC:11189]
ENST00000302472	ENSG00000171522	-2,215808594	5,519191836	0,039961397	prostaglandin E receptor 4 [Source:HGNC Symbol;Acc:HGNC:9596
ENST00000413558	ENSG00000230531	2,264093559	4,465580256	0,040004424	MT-ND5 pseudogene 7 [Source:HGNC Symbol;Acc:HGNC:42269]
ENST00000362620	ENSG00000199490	2,263199956	4,417941845	0,040004424	
ENST00000503217	ENSG00000163322	-2,252172009	4,443365531	0,040004424	abraxas 1, BRCA1 A complex subunit [Source:HGNC Symbol;Acc:H
ENST00000464731	ENSG00000239443	1,760069319	4,362786767	0,040004424	poly(A) binding protein cytoplasmic 1 pseudogene 10 [Source:HGI
ENST00000545904	ENSG00000256747	-1,752454059	4,476390574	0,040004424	novel transcript

ENST00000365336	ENSG00000202206	1,928587841	4,574250411	0,040009109	RNA, U6 small nuclear 169, pseudogene [Source:HGNC Symbol;Ac
ENST00000578238	ENSG00000188612	-4,244116175	4,314678052	0,040037352	small ubiquitin-like modifier 2 [Source:HGNC Symbol;Acc:HGNC:1
ENST00000363299	ENSG00000200169	1,863552167	10,34461189	0,040057354	RNA, U5D small nuclear 1 [Source:HGNC Symbol;Acc:HGNC:10214
ENST00000362097	ENSG00000189064	-4,584869164	4,435096071	0,040066547	G antigen 2A [Source:HGNC Symbol;Acc:HGNC:4099]
ENST00000362097	ENSG00000189064	-4,584869164	4,435096071	0,040066547	G antigen 2A [Source:HGNC Symbol;Acc:HGNC:4099]
ENST00000362097	ENSG00000189064	-4,584869164	4,435096071	0,040066547	G antigen 2A [Source:HGNC Symbol;Acc:HGNC:4099]
ENST00000365486	ENSG00000202356	4,252694561	4,431953746	0,040113546	RNA, 5S ribosomal pseudogene 277 [Source:HGNC Symbol;Acc:HG
ENST00000347364	ENSG00000125863	2,773470025	4,499555067	0,04013106	McKusick-Kaufman syndrome [Source:HGNC Symbol;Acc:HGNC:7
ENST00000408287	ENSG00000221214	2,773470025	4,552219572	0,04013106	microRNA 548e [Source:HGNC Symbol;Acc:HGNC:35275]
ENST00000545067	ENSG00000216937	2,771396874	4,461147754	0,04013106	coiled-coil domain containing 7 [Source:HGNC Symbol;Acc:HGNC:
ENST00000501271	ENSG00000130779	2,769326535	4,34818433	0,04013106	CAP-Gly domain containing linker protein 1 [Source:HGNC Symbol
ENST00000524582	ENSG00000134744	-2,76359948	4,31270761	0,04013106	terminal uridylyl transferase 4 [Source:HGNC Symbol;Acc:HGNC:2
ENST00000582240	ENSG00000154845	-2,759578769	4,342144506	0,04013106	protein phosphatase 4 regulatory subunit 1 [Source:HGNC Symbo
ENST00000257013	ENSG00000134590	-2,756472562	4,385891494	0,04013106	retrotransposon Gag like 8C [Source:HGNC Symbol;Acc:HGNC:256
ENST00000435214	ENSG00000215089	-2,756472562	4,418306005	0,04013106	keratin 18 pseudogene 11 [Source:HGNC Symbol;Acc:HGNC:6431]
ENST00000444995	ENSG00000100068	-2,756472562	4,381989668	0,04013106	LDL receptor related protein 5 like [Source:HGNC Symbol;Acc:HGN
ENST00000258455	ENSG00000135972	-2,115540089	4,336290978	0,04013106	mitochondrial ribosomal protein S9 [Source:HGNC Symbol;Acc:HG
ENST00000508760	ENSG00000113580	-1,975543613	4,44916966	0,04013106	nuclear receptor subfamily 3 group C member 1 [Source:HGNC Sy
ENST00000410441		1,124749761	6,169307617	0,040291374	
ENST00000417455	ENSG00000232004	-2,455364821	4,462988086	0,040495239	CAP1 pseudogene 2 [Source:HGNC Symbol;Acc:HGNC:31970]
ENST00000361488	ENSG00000169122	2,962517886	4,725385742	0,040611223	family with sequence similarity 110 member B [Source:HGNC Sym
ENST00000546283	ENSG00000115286	1,441892433	7,660933873	0,040640147	NADH:ubiquinone oxidoreductase core subunit S7 [Source:HGNC
ENST00000439976	ENSG00000091136	-2,59154665	4,911530774	0,040682116	laminin subunit beta 1 [Source:HGNC Symbol;Acc:HGNC:6486]
ENST00000484895	ENSG00000130592	-2,893892267	4,325942834	0,040762937	lymphocyte specific protein 1 [Source:HGNC Symbol;Acc:HGNC:67
ENST00000441453	ENSG00000106078	4,343215626	4,423468526	0,040813098	cordon-bleu WH2 repeat protein [Source:HGNC Symbol;Acc:HGNC
ENST00000219070	ENSG00000087245	-3,436995473	4,910794825	0,040842103	matrix metallopeptidase 2 [Source:HGNC Symbol;Acc:HGNC:7166
ENST00000479428	ENSG00000239224	1,563620324	4,97433907	0,040889682	RNA, 7SL, cytoplasmic 546, pseudogene [Source:HGNC Symbol;Ac
ENST00000384587	ENSG00000207317	1,833047687	4,677562833	0,040918644	
ENST00000414273	ENSG00000237973	2,17640238	11,02253595	0,040960034	MT-CO1 pseudogene 12 [Source:HGNC Symbol;Acc:HGNC:52014]
ENST00000297350	ENSG00000164761	-2,575828032	4,708156587	0,041034669	TNF receptor superfamily member 11b [Source:HGNC Symbol;Acc
ENST00000385573	ENSG00000208308	2,064411169	7,015753453	0,041120906	small nucleolar RNA, H/ACA box 40B [Source:HGNC Symbol;Acc:H
ENST00000496309	ENSG00000240606	1,705519884	5,483406715	0,041127577	RNA, 7SL, cytoplasmic 564, pseudogene [Source:HGNC Symbol;Ac
ENST00000481883	ENSG00000160305	1,784206152	7,242891626	0,041184084	disco interacting protein 2 homolog A [Source:HGNC Symbol;Acc:
ENST00000461535	ENSG00000141371	-1,864604342	5,101039904	0,041190869	chromosome 17 open reading frame 64 [Source:HGNC Symbol;Ac
ENST00000222345	ENSG00000105738	-1,774035457	8,180867149	0,041214316	signal induced proliferation associated 1 like 3 [Source:HGNC Sym
ENST00000315489	ENSG00000181781	2,539770699	4,633431827	0,041236741	outer dense fiber of sperm tails 3 like 2 [Source:HGNC Symbol;Acc
ENST00000384613	ENSG00000207343	3,001459951	4,720456425	0,041337977	RNA, U6 small nuclear 225, pseudogene [Source:HGNC Symbol;Ac
ENST00000364043	ENSG00000200913	2,201276422	12,75041786	0,041423708	small nucleolar RNA, C/D box 46 [Source:HGNC Symbol;Acc:HGNC
ENST00000602312	ENSG00000183921	-2,402705318	4,864286709	0,041552888	short chain dehydrogenase/reductase family 42E, member 2 [Sou
ENST00000604991	ENSG00000271696	4,323248106	4,900087321	0,041926882	abhydrolase domain containing 15 (ABHD15) pseudogene
ENST00000560412	ENSG00000090661	-1,348586489	5,785837359	0,041986496	ceramide synthase 4 [Source:HGNC Symbol;Acc:HGNC:23747]
ENST00000363376	ENSG00000200246	1,651557377	6,874796035	0,042009232	RNA, 5S ribosomal pseudogene 263 [Source:HGNC Symbol;Acc:HG
ENST00000529667	ENSG00000234899	-3,193796354	4,38307182	0,042057673	SOX9 antisense RNA 1 [Source:HGNC Symbol;Acc:HGNC:49321]
ENST00000529667	ENSG00000234899	-3,193796354	4,38307182	0,042057673	SOX9 antisense RNA 1 [Source:HGNC Symbol;Acc:HGNC:49321]
ENST00000432834	ENSG00000231015	2,786393557	4,952406593	0,042115423	novel transcript
ENST00000272224	ENSG00000143869	-1,389935686	6,333724963	0,042135701	growth differentiation factor 7 [Source:HGNC Symbol;Acc:HGNC:4
ENST00000385293	ENSG00000208028	1,51950994	5,779700427	0,042230226	microRNA 616 [Source:HGNC Symbol;Acc:HGNC:32872]
ENST00000495856	ENSG00000172339	4,090600754	4,441733507	0,042249514	ALG14, UDP-N-acetylglucosaminyltransferase subunit [Source:HG
ENST00000590960	ENSG00000266938	4,49138065	4,594855363	0,042282924	zinc finger protein pseudogene
ENST00000361217	ENSG00000198837	-2,694905798	5,472761356	0,042381401	DENN domain containing 4B [Source:HGNC Symbol;Acc:HGNC:290
ENST00000470546	ENSG00000241369	2,376462934	4,898105211	0,042406843	long intergenic non-protein coding RNA 1192 [Source:HGNC Symb
ENST00000564238	ENSG00000167523	4,277829885	4,423440317	0,042468363	spermatogenesis associated 33 [Source:HGNC Symbol;Acc:HGNC:
ENST00000477306	ENSG00000143321	-3,236289414	4,417666207	0,042468811	heparin binding growth factor [Source:HGNC Symbol;Acc:HGNC:4
ENST00000363101	ENSG00000199971	2,066528866	4,953496079	0,042518976	RNA, U6 small nuclear 797, pseudogene [Source:HGNC Symbol;Ac
ENST00000463134	ENSG00000240951	2,620459246	4,441836728	0,042571628	MT-CO2 pseudogene 6 [Source:HGNC Symbol;Acc:HGNC:52022]
ENST00000392477	ENSG00000111912	-4,652043297	4,390172455	0,04258425	nuclear receptor coactivator 7 [Source:HGNC Symbol;Acc:HGNC:2
ENST00000388106	ENSG00000210841	1,777319059	6,55354085	0,042666288	RNA, U6atac small nuclear 26, pseudogene [Source:HGNC Symbol
ENST00000301838	ENSG00000168040	-2,100166275	4,447237163	0,042730861	Fas associated via death domain [Source:HGNC Symbol;Acc:HGNC
ENST00000516851	ENSG00000252660	1,753238353	6,654411664	0,042730863	
ENST00000399413	ENSG00000214999	-4,881326425	4,56209925	0,042748924	
ENST00000334810	ENSG00000180264	2,249947158	6,020538581	0,042771461	adhesion G protein-coupled receptor D2 [Source:HGNC Symbol;Ac
ENST00000293255	ENSG00000105507	3,193107889	4,528929548	0,042936326	calcium binding protein 5 [Source:HGNC Symbol;Acc:HGNC:13714
ENST00000489044	ENSG00000163050	2,413562664	5,032698541	0,042962604	coenzyme Q8A [Source:HGNC Symbol;Acc:HGNC:16812]
ENST00000253329	ENSG00000131013	-2,452002738	4,45830011	0,04297156	peptidylprolyl isomerase like 4 [Source:HGNC Symbol;Acc:HGNC:1

ENST00000420503	ENSG00000218510	2,826145293	4,548880426	0,042999193	long intergenic non-protein coding RNA 339 [Source:HGNC Symbo
ENST00000364089	ENSG00000200959	1,445583583	9,662026921	0,043022624	small nucleolar RNA, H/ACA box 74A [Source:HGNC Symbol;Acc:H
ENST00000260970	ENSG00000138398	1,991956448	4,503702943	0,04305573	peptidylprolyl isomerase G [Source:HGNC Symbol;Acc:HGNC:1465
ENST00000365436	ENSG00000202306	2,022013873	6,011246999	0,043082327	
ENST00000461377	ENSG00000136280	-3,104801158	4,607784069	0,043110163	CCM2 scaffold protein [Source:HGNC Symbol;Acc:HGNC:21708]
ENST00000363107	ENSG00000199977	2,101223023	5,038236285	0,043243331	
ENST00000366756	ENSG00000198719	-2,17348505	5,464621027	0,043250692	delta like canonical Notch ligand 1 [Source:HGNC Symbol;Acc:HGN
ENST00000605277	ENSG00000261386	-4,347921767	4,489077394	0,043254085	novel transcript
ENST00000518808	ENSG00000130227	2,055848771	6,323605497	0,04327013	exportin 7 [Source:HGNC Symbol;Acc:HGNC:14108]
ENST00000364754	ENSG00000201624	2,669863772	9,492250148	0,043282472	
ENST00000373218	ENSG00000148730	-1,681856995	5,871943789	0,043358633	eukaryotic translation initiation factor 4E binding protein 2 [Sourc
ENST00000548873	ENSG00000257281	3,021967614	5,175430182	0,043498581	apolipoprotein B mRNA editing enzyme, catalytic polypeptide-like
ENST00000457590	ENSG00000104885	-1,883689026	5,131100366	0,043528741	DOT1 like histone lysine methyltransferase [Source:HGNC Symbol
ENST00000544932		1,560675487	8,416132179	0,043529499	
ENST00000526618	ENSG00000254579	2,458974448	5,498376008	0,043654364	zinc finger protein pseudogene
ENST00000319380	ENSG00000175931	-4,726644942	4,371959633	0,04366236	ubiquitin conjugating enzyme E2 O [Source:HGNC Symbol;Acc:HGI
ENST00000456880	ENSG00000230061	4,217753663	4,338313736	0,043666492	TRPM2 antisense RNA [Source:HGNC Symbol;Acc:HGNC:50758]
ENST00000517464	ENSG00000147364	4,58877163	4,348214092	0,043712726	F-box protein 25 [Source:HGNC Symbol;Acc:HGNC:13596]
ENST00000335613	ENSG00000167992	-4,604405849	4,408484688	0,043807891	von Willebrand factor C and EGF domains [Source:HGNC Symbol;A
ENST00000364115	ENSG00000200985	2,674501328	5,049494783	0,044118558	RNA, 5S ribosomal pseudogene 493 [Source:HGNC Symbol;Acc:HG
ENST00000364936	ENSG00000201806	2,322061977	6,154525257	0,044119719	RNA, U4 small nuclear 8, pseudogene [Source:HGNC Symbol;Acc:H
ENST00000513338	ENSG00000249215	-2,240682908	4,35898654	0,044260271	nuclear receptor coactivator 4 pseudogene 4 [Source:HGNC Symb
ENST00000390180	ENSG00000211514	1,26579637	9,271230488	0,044540238	microRNA 454 [Source:HGNC Symbol;Acc:HGNC:33137]
ENST00000362714	ENSG00000199584	1,917282513	4,845775773	0,044714085	
ENST00000384528	ENSG00000207258	2,313240528	4,971444762	0,044725944	
ENST00000384686	ENSG00000207417	1,601724641	6,988125355	0,044726399	
ENST00000580835	ENSG00000264916	1,453457473	6,07125113	0,044798974	RNA, 7SL, cytoplasmic 230, pseudogene [Source:HGNC Symbol;Ac
ENST00000363788		2,829421294	5,554581653	0,044814885	
ENST00000286808	ENSG00000156282	5,120649427	4,624690124	0,044821671	claudin 17 [Source:HGNC Symbol;Acc:HGNC:2038]
ENST00000364171	ENSG00000201041	1,218230445	7,350705512	0,044856589	RNA, 5S ribosomal pseudogene 242 [Source:HGNC Symbol;Acc:HG
ENST00000375077	ENSG00000106789	-2,271074244	4,525973926	0,044879251	coronin 2A [Source:HGNC Symbol;Acc:HGNC:2255]
ENST00000540480		-2,389543313	4,921921851	0,044905639	
ENST00000579667	ENSG00000266533	4,361568001	5,533081283	0,044988853	microRNA 3619 [Source:HGNC Symbol;Acc:HGNC:38998]
ENST00000523422	ENSG00000253477	2,620397503	4,533308521	0,044997612	
ENST00000245479	ENSG00000125398	-2,957371788	5,300541839	0,045180831	SRY-box 9 [Source:HGNC Symbol;Acc:HGNC:11204]
ENST00000384446	ENSG00000207175	2,035984686	8,938962455	0,045284347	RNA, U1 small nuclear 67, pseudogene [Source:HGNC Symbol;Acc
ENST00000529778	ENSG00000166313	-2,191360971	4,65576437	0,045327956	amyloid beta precursor protein binding family B member 1 [Sourc
ENST00000258873	ENSG00000103740	2,258534776	4,836594024	0,045337809	acyl-CoA synthetase bubblegum family member 1 [Source:HGNC S
ENST00000291442	ENSG00000160113	-2,401226413	5,504046368	0,045358409	nuclear receptor subfamily 2 group F member 6 [Source:HGNC Sy
ENST00000400454	ENSG00000171587	-1,955925278	4,98394837	0,045410368	DS cell adhesion molecule [Source:HGNC Symbol;Acc:HGNC:3039]
ENST00000565893	ENSG00000259905	4,210165678	4,545528105	0,045413227	Prader-Willi region non-protein coding RNA 1 [Source:HGNC Symb
ENST00000363217	ENSG00000200087	1,855118789	11,6973422	0,045487445	small nucleolar RNA, H/ACA box 73B [Source:HGNC Symbol;Acc:H
ENST00000565913	ENSG00000166780	2,768622927	4,633864854	0,045503817	chromosome 16 open reading frame 45 [Source:HGNC Symbol;Ac
ENST00000559923	ENSG00000100664	1,577945149	6,564883622	0,045557698	eukaryotic translation initiation factor 5 [Source:HGNC Symbol;Ac
ENST00000384460	ENSG00000207189	1,616962657	5,354139215	0,045821292	
ENST00000287042	ENSG00000156486	4,56907109	4,693084022	0,045833772	potassium voltage-gated channel modifier subfamily S member 2
ENST00000365529	ENSG00000202399	1,701339108	6,349060746	0,045869097	
ENST00000365645	ENSG00000202515	2,042337366	9,640322057	0,045890758	vault RNA 1-3 [Source:HGNC Symbol;Acc:HGNC:12656]
ENST00000443545	ENSG00000229357	-4,35073788	4,247853425	0,046050591	cytochrome c, somatic pseudogene 51 [Source:HGNC Symbol;Acc:
ENST00000554749	ENSG00000258634	-2,144505498	4,873049559	0,046090555	novel transcript, antisense to ALX3
ENST00000384907	ENSG00000207639	2,257951177	12,01219083	0,046123996	microRNA 193b [Source:HGNC Symbol;Acc:HGNC:32087]
ENST00000516186		1,930348879	5,38784851	0,046172706	
ENST00000391267	ENSG00000212569	2,007446337	8,318699377	0,046222963	
ENST00000363009	ENSG00000199879	1,193744521	6,133758297	0,046327424	RNA, U1 small nuclear 120, pseudogene [Source:HGNC Symbol;Ac
ENST00000365663	ENSG00000202533	1,143676479	5,858936739	0,046458878	
ENST00000201586	ENSG00000088002	1,983607688	8,070272867	0,046477916	sulfotransferase family 2B member 1 [Source:HGNC Symbol;Acc:H
ENST00000465858	ENSG00000137203	-3,232863956	4,478472833	0,046519385	transcription factor AP-2 alpha [Source:HGNC Symbol;Acc:HGNC:1
ENST00000378076	ENSG00000077943	4,135950575	4,751481016	0,046542484	integrin subunit alpha 8 [Source:HGNC Symbol;Acc:HGNC:6144]
ENST00000249075	ENSG00000128342	-2,69367601	5,010912135	0,046560345	LIF, interleukin 6 family cytokine [Source:HGNC Symbol;Acc:HGNC
ENST00000539009	ENSG00000256288	4,136130415	4,877311351	0,046630128	novel transcript
ENST00000366714	ENSG00000198835	-2,53117862	4,959039708	0,046695332	gap junction protein gamma 2 [Source:HGNC Symbol;Acc:HGNC:1
ENST00000401119	ENSG00000215938	2,010983568	4,643109399	0,046741363	microRNA 190b [Source:HGNC Symbol;Acc:HGNC:33656]
ENST00000356458	ENSG00000214595	-2,34259445	4,657735673	0,046766812	echinoderm microtubule associated protein like 6 [Source:HGNC S
ENST00000384792	ENSG00000207523	1,936727204	9,110379697	0,046789466	small nucleolar RNA, H/ACA box 66 [Source:HGNC Symbol;Acc:HG

ENST00000552175	ENSG00000257858	1,367840206	5,59069101	0,046803869	MT-ND1 pseudogene 24 [Source:HGNC Symbol;Acc:HGNC:42073]
ENST00000363286	ENSG00000200156	2,776115363	14,52473815	0,046886282	RNA, U5B small nuclear 1 [Source:HGNC Symbol;Acc:HGNC:10212
ENST00000529569	ENSG00000255350	2,613692489	4,990235896	0,046936361	MT-CO1 pseudogene 15 [Source:HGNC Symbol;Acc:HGNC:52017]
ENST00000555952	ENSG00000139926	4,100311454	4,243446209	0,047005324	FERM domain containing 6 [Source:HGNC Symbol;Acc:HGNC:1983
ENST00000267889	ENSG00000140323	-2,408017184	5,310078864	0,047026917	dispatched RND transporter family member 2 [Source:HGNC Syml
ENST00000561823	ENSG00000140941	1,9093955	6,217158823	0,047089893	microtubule associated protein 1 light chain 3 beta [Source:HGNC
ENST00000362606	ENSG00000199476	1,514874332	5,422570632	0,047143978	
ENST00000436865	ENSG00000163374	2,545636133	5,86459134	0,047175338	YY1 associated protein 1 [Source:HGNC Symbol;Acc:HGNC:30935]
ENST00000459455	ENSG00000238943	1,245126541	6,306360129	0,047185653	
ENST00000393350	ENSG00000178573	4,193900572	4,91367677	0,047237928	MAF bZIP transcription factor [Source:HGNC Symbol;Acc:HGNC:67
ENST00000384864	ENSG00000284155	1,285903121	7,107632013	0,047259889	microRNA 194-2 [Source:HGNC Symbol;Acc:HGNC:31565]
ENST00000535711		-1,838013713	4,576911823	0,047273332	
ENST00000604646	ENSG00000270188	1,524771563	6,290505826	0,047282213	MT-RNR2 like 11 [Source:HGNC Symbol;Acc:HGNC:37168]
ENST00000489253	ENSG00000228938	-2,101820884	4,318592152	0,047367857	small nuclear ribonucleoprotein D2 pseudogene 1 [Source:HGNC S
ENST00000516060	ENSG00000251869	1,912689983	6,761822969	0,047426151	small Cajal body-specific RNA 23 [Source:HGNC Symbol;Acc:HGNC
ENST00000363014	ENSG00000199884	1,733700833	6,570371533	0,047562428	
ENST00000375375	ENSG00000009709	-3,001444537	4,375419052	0,047692564	paired box 7 [Source:HGNC Symbol;Acc:HGNC:8621]
ENST00000363064	ENSG00000199934	1,722758011	6,114224829	0,04769525	
ENST00000467362	ENSG00000134255	2,247954537	4,476618316	0,04776209	choline/ethanolamine phosphotransferase 1 [Source:HGNC Symb
ENST00000364773	ENSG00000201643	1,842201302	5,706553521	0,047817791	small nucleolar RNA, H/ACA box 14A [Source:HGNC Symbol;Acc:H
ENST00000369150	ENSG00000178096	4,920051546	4,834959318	0,047818289	bolA family member 1 [Source:HGNC Symbol;Acc:HGNC:24263]
ENST00000299443	ENSG00000166351	4,156471089	4,290710322	0,047820858	POTE ankyrin domain family member D [Source:HGNC Symbol;Ac
ENST00000230895	ENSG00000112977	-1,936214852	5,974778586	0,047824936	death associated protein [Source:HGNC Symbol;Acc:HGNC:2672]
ENST00000348428	ENSG00000172175	-2,457051423	6,426188784	0,047832123	MALT1 paracaspase [Source:HGNC Symbol;Acc:HGNC:6819]
ENST00000385216	ENSG00000207951	1,734221933	5,345561485	0,047864886	microRNA 561 [Source:HGNC Symbol;Acc:HGNC:32817]
ENST00000384086	ENSG00000206813	4,296863675	4,296799675	0,047881631	
ENST00000543970	ENSG00000214650	4,225208018	4,970635341	0,048218982	novel transcript
ENST00000360947	ENSG00000165804	-1,843572295	5,739706313	0,048285693	zinc finger protein 219 [Source:HGNC Symbol;Acc:HGNC:13011]
ENST00000589152	ENSG00000118046	-1,906936644	4,701930125	0,04828835	serine/threonine kinase 11 [Source:HGNC Symbol;Acc:HGNC:1138
ENST00000604411	ENSG00000270641	1,970057192	5,034071118	0,048320203	TSIX transcript, XIST antisense RNA [Source:HGNC Symbol;Acc:HG
ENST00000386747	ENSG00000209482	2,249888006	11,91224086	0,048453905	small nucleolar RNA, C/D box 83A [Source:HGNC Symbol;Acc:HGN
ENST00000385130	ENSG00000284357	-3,293221879	13,32462663	0,048457391	microRNA 34a [Source:HGNC Symbol;Acc:HGNC:31635]
ENST00000458420	ENSG00000158258	2,278152519	4,811575628	0,048519567	calsyntenin 2 [Source:HGNC Symbol;Acc:HGNC:17448]
ENST00000215904	ENSG00000241360	-2,974759425	4,590672924	0,048543826	pyridoxal phosphatase [Source:HGNC Symbol;Acc:HGNC:30259]
ENST00000316249	ENSG00000178342	-1,7650949	5,327391472	0,048545379	potassium voltage-gated channel modifier subfamily G member 2
ENST00000329627	ENSG00000215193	-1,823885197	4,934360466	0,048627768	peroxisomal biogenesis factor 26 [Source:HGNC Symbol;Acc:HGNC
ENST00000384657	ENSG00000207387	2,590417617	4,960952111	0,048696425	
ENST00000592037		2,179106614	4,663785906	0,048696817	
ENST00000411370	ENSG00000223302	1,369044464	7,47507842	0,048850424	
ENST00000362443	ENSG00000199313	1,628018095	6,938019956	0,048859465	RNA, U4 small nuclear 82, pseudogene [Source:HGNC Symbol;Acc
ENST00000424002	ENSG00000232177	1,98389139	4,89313284	0,048955423	MT-ND4 pseudogene 24 [Source:HGNC Symbol;Acc:HGNC:42220]
ENST00000422488	ENSG00000234715	2,422705548	5,999431602	0,049115324	
ENST00000364639	ENSG00000277818	2,044442408	4,680819151	0,049256973	
ENST00000449721	ENSG00000224079	2,03461057	7,276609755	0,049300036	novel transcript
ENST00000441699	ENSG00000176826	1,836555834	4,763036353	0,049313494	FK506 binding protein 9 pseudogene 1 [Source:HGNC Symbol;Acc:
ENST00000329286	ENSG00000206418	-2,177814756	6,689212645	0,049367897	RAB12, member RAS oncogene family [Source:HGNC Symbol;Acc:
ENST00000306318	ENSG00000168505	-2,381243106	4,991922543	0,049413441	gastrulation brain homeobox 2 [Source:HGNC Symbol;Acc:HGNC:4
ENST00000517277	ENSG00000253086	2,221728291	5,172894532	0,049490488	RNA, U6 small nuclear 537, pseudogene [Source:HGNC Symbol;Ac
ENST00000384977	ENSG00000284043	2,011209883	6,787408958	0,049665677	microRNA 20b [Source:HGNC Symbol;Acc:HGNC:32024]
ENST00000500527	ENSG00000245614	2,445935432	4,904861519	0,049668218	DDX11 antisense RNA 1 [Source:HGNC Symbol;Acc:HGNC:44176]
ENST00000364153	ENSG00000201023	3,220231464	4,67021932	0,049751941	RNA, Ro-associated Y3 pseudogene 11 [Source:HGNC Symbol;Acc:
ENST00000302392	ENSG00000169964	-3,987366857	4,861350357	0,049770155	transmembrane protein 42 [Source:HGNC Symbol;Acc:HGNC:2844
ENST00000421059	ENSG00000127948	-1,953310904	4,839268793	0,049893856	cytochrome p450 oxidoreductase [Source:HGNC Symbol;Acc:HGN
ENST00000560493	ENSG00000068305	-3,090231483	4,764711999	0,049897206	myocyte enhancer factor 2A [Source:HGNC Symbol;Acc:HGNC:699

Annex 3: Table S4- Log Fold Change of RNA species expression between EVs released by drug-sensitive (NCI-H460) cells and the EVs released by their MDR (NCI-H460/R) counterparts.

ensembl_transcript_id	ensembl_gene_id	logFC	logCPM	PValue	description
ENST00000410794	ENSG00000222726	5,572717	7,324087	0,000411	RNA, U2 small nuclear 7, pseudogene [Source:HGNC Symbol;Acc:HGNC:42505]
ENST00000375980	ENSG00000142634	-5,134479	5,966055	0,000868	EF-hand domain family member D2 [Source:HGNC Symbol;Acc:HGNC:28670]
ENST00000606837	ENSG00000272036	-5,513845	7,198992	0,001834	microRNA 139 [Source:HGNC Symbol;Acc:HGNC:31526]
ENST00000270162	ENSG00000142178	-4,696272	6,57788	0,005271	salt inducible kinase 1 [Source:HGNC Symbol;Acc:HGNC:11142]
ENST00000463508		3,025931	7,860197	0,006189	
ENST00000390738	ENSG00000212027	-4,810985	11,15235	0,006195	microRNA 374b [Source:HGNC Symbol;Acc:HGNC:33665]
ENST00000385277	ENSG00000208012	-4,086074	10,68692	0,008125	microRNA let-7f-2 [Source:HGNC Symbol;Acc:HGNC:31484]
ENST00000303004	ENSG00000172216	-4,752165	6,511356	0,00866	CCAAT enhancer binding protein beta [Source:HGNC Symbol;Acc:HGNC:1834]
ENST00000362202	ENSG00000199072	-3,918067	12,18297	0,009245	microRNA let-7f-1 [Source:HGNC Symbol;Acc:HGNC:31483]
ENST00000362251	ENSG00000199121	-3,951045	10,77479	0,009694	microRNA 26b [Source:HGNC Symbol;Acc:HGNC:31612]
ENST00000531791	ENSG00000162241	2,524023	5,660719	0,010637	solute carrier family 25 member 45 [Source:HGNC Symbol;Acc:HGNC:27442]
ENST00000323534	ENSG00000181467	-4,511383	5,418591	0,010693	RAP2B, member of RAS oncogene family [Source:HGNC Symbol;Acc:HGNC:9862]
ENST00000530835	ENSG00000214391	-3,075564	6,733191	0,011005	tubulin alpha pseudogene 2 [Source:HGNC Symbol;Acc:HGNC:14531]
ENST00000365645	ENSG00000202515	-2,854449	9,640322	0,011249	vault RNA 1-3 [Source:HGNC Symbol;Acc:HGNC:12656]
ENST00000385129	ENSG00000207864	-3,512919	12,25328	0,012619	microRNA 27b [Source:HGNC Symbol;Acc:HGNC:31614]
ENST00000385130	ENSG00000284357	3,510157	13,32463	0,012842	microRNA 34a [Source:HGNC Symbol;Acc:HGNC:31635]
ENST00000340398	ENSG00000188375	4,384341	5,578992	0,012873	H3 histone family member 3C [Source:HGNC Symbol;Acc:HGNC:33164]
ENST00000405810	ENSG00000219451	-4,640028	5,459911	0,014173	ribosomal protein L23 pseudogene 8 [Source:HGNC Symbol;Acc:HGNC:36225]
ENST00000385200	ENSG00000207935	3,546401	12,70857	0,016854	microRNA 204 [Source:HGNC Symbol;Acc:HGNC:31582]
ENST00000280612	ENSG00000151012	-4,333759	6,086567	0,019044	solute carrier family 7 member 11 [Source:HGNC Symbol;Acc:HGNC:11059]
ENST00000569473	ENSG00000261441	1,954636	9,974631	0,020265	novel transcript, antisense to POLG
ENST00000362467	ENSG00000199337	2,127295	11,77768	0,020632	RNA, 5S ribosomal 3 [Source:HGNC Symbol;Acc:HGNC:34364]
ENST00000362467	ENSG00000199337	2,127295	11,77768	0,020632	RNA, 5S ribosomal 3 [Source:HGNC Symbol;Acc:HGNC:34364]
ENST00000426405	ENSG00000213695	-3,938841	4,79055	0,024175	ribosomal protein S7 pseudogene 14 [Source:HGNC Symbol;Acc:HGNC:36602]
ENST00000311910	ENSG00000215168	2,480026	6,766667	0,024566	novel pseudogene
ENST00000323686		-4,401473	5,690009	0,024858	
ENST00000369026	ENSG00000143384	-4,233857	5,583943	0,025032	MCL1, BCL2 family apoptosis regulator [Source:HGNC Symbol;Acc:HGNC:6943]
ENST00000362205	ENSG00000199075	-3,11047	12,80617	0,025336	microRNA 26a-1 [Source:HGNC Symbol;Acc:HGNC:31610]
ENST00000242351	ENSG00000105939	-2,474024	6,878831	0,025534	zinc finger CCCH-type containing, antiviral 1 [Source:HGNC Symbol;Acc:HGNC:23721]
ENST00000362552	ENSG00000199422	-2,718775	9,499851	0,026274	vault RNA 3-1, pseudogene [Source:HGNC Symbol;Acc:HGNC:23027]
ENST00000410344	ENSG00000222276	2,65535	8,968876	0,027015	RNA, U2 small nuclear 33, pseudogene [Source:HGNC Symbol;Acc:HGNC:48526]
ENST00000362263	ENSG00000199133	-2,68172	12,43308	0,027533	microRNA let-7d [Source:HGNC Symbol;Acc:HGNC:31481]
ENST00000363564	ENSG00000200434	1,806363	13,246	0,02914	RNA, 5.8S ribosomal pseudogene 2 [Source:HGNC Symbol;Acc:HGNC:41956]
ENST00000396477	ENSG00000213822	2,025623	6,15244	0,029761	carcinoembryonic antigen related cell adhesion molecule 18 [Source:HGNC Symbol;Acc:HGNC:31
ENST00000370355	ENSG00000099194	-4,287768	7,154262	0,030043	stearoyl-CoA desaturase [Source:HGNC Symbol;Acc:HGNC:10571]
ENST00000541682	ENSG00000179111	1,701716	9,222901	0,030709	hes family bHLH transcription factor 7 [Source:HGNC Symbol;Acc:HGNC:15977]
ENST00000602536	ENSG00000229547	3,262214	5,702377	0,031132	ubiquitin conjugating enzyme E2 D N-terminal like (pseudogene) [Source:HGNC Symbol;Acc:HGN
ENST00000292478	ENSG00000106246	-3,970286	4,652791	0,034109	pentatricopeptide repeat domain 1 [Source:HGNC Symbol;Acc:HGNC:22198]
ENST00000362117	ENSG00000198987	-3,158622	13,80348	0,034765	microRNA 16-2 [Source:HGNC Symbol;Acc:HGNC:31546]
ENST00000362295	ENSG00000199165	-1,709075	12,84374	0,035112	microRNA let-7a-1 [Source:HGNC Symbol;Acc:HGNC:31476]
ENST00000362227	ENSG00000284231	-3,945002	9,777068	0,036318	microRNA 424 [Source:HGNC Symbol;Acc:HGNC:31881]
ENST00000323492	ENSG00000064012	-3,018922	4,927478	0,036617	caspase 8 [Source:HGNC Symbol;Acc:HGNC:1509]
ENST00000370339	ENSG00000149658	2,365302	5,403216	0,037468	YTH N6-methyladenosine RNA binding protein 1 [Source:HGNC Symbol;Acc:HGNC:15867]
ENST00000263409	ENSG00000113594	-3,916677	5,442621	0,038296	LIF receptor alpha [Source:HGNC Symbol;Acc:HGNC:6597]
ENST00000385300	ENSG00000284182	-3,633879	5,653863	0,038343	microRNA 143 [Source:HGNC Symbol;Acc:HGNC:31530]
ENST00000377364		-2,75169	6,919135	0,039494	
ENST00000410694	ENSG00000222626	3,771899	7,296913	0,040135	RNA, U2 small nuclear 48, pseudogene [Source:HGNC Symbol;Acc:HGNC:48541]
ENST00000369783	ENSG00000183128	2,246186	5,298564	0,041111	calcium homeostasis modulator 3 [Source:HGNC Symbol;Acc:HGNC:23458]
ENST00000362302	ENSG00000199172	-3,825394	9,389491	0,045077	microRNA 331 [Source:HGNC Symbol;Acc:HGNC:31772]
ENST00000257604	ENSG00000135148	-3,62798	5,938576	0,045373	TRAF-type zinc finger domain containing 1 [Source:HGNC Symbol;Acc:HGNC:24808]
ENST00000382456	ENSG00000161203	3,427886	4,788693	0,048959	adaptor related protein complex 2 subunit mu 1 [Source:HGNC Symbol;Acc:HGNC:564]

Annex 4: Table S5- Log Fold Change of levels of RNA species between EVs released by drug-sensitive (K562) cells and EVs released by their MDR (K562Dox) counterparts.

	log FC	logCPM	PValue
hsa-miR-124-3p	-6.01319589402148	9.59591434897087	1.20091149062505E-15
hsa-miR-383-5p	8.90925633974598	8.39518355839927	9.4487841264683E-15
hsa-miR-135a-5p	5.25316355107853	10.5930374231035	8.66887221185837E-12
hsa-miR-4524a-3p	4.25293262536425	7.12501130614299	1.64934355389354E-09
hsa-miR-873-5p	2.96405794683731	7.67276580773612	3.90063472827267E-08
hsa-miR-29c-5p	-2.46896993577934	10.004657810989	1.33654116791548E-06
hsa-miR-224-3p	-5.96793827629981	9.24743491453635	3.16785428506108E-06
hsa-miR-224-5p	-4.10533383815784	13.1188761257331	0.0000112551807638879
hsa-miR-335-3p	2.94525214520332	7.47986752144944	0.0000269585762491608
hsa-miR-3117-3p	1.78285723820119	7.32269796920596	0.0000463257143650038
hsa-miR-204-3p	3.15263110204706	11.3778472139391	0.0000622059894360197
hsa-miR-147b	-3.10978173995149	6.65406146002437	0.0000663826103326156
hsa-miR-5699-5p	-2.89887943238126	6.42195871471413	0.00012436975617054
hsa-miR-335-5p	2.95585002401987	11.1034793922172	0.00014849068123317
hsa-miR-204-5p	4.0775375216032	13.7728586519982	0.00018349872786390 4
hsa-miR-29b-2-5p	-2.77685371141619	9.39781524913439	0.00018446023092250 9
hsa-miR-452-5p	-3.7479962064066	12.3536445577973	0.00019393807916300 1
hsa-miR-4731-5p	-3.08804572688754	6.52133604083279	0.00023459728122435 7
hsa-miR-218-5p	4.09806323238407	7.4667480906185	0.00032812142501578
hsa-miR-505-5p	-1.68796460896714	9.20209985721102	0.00036989165326659 4
hsa-miR-652-5p	-1.8090717702298	9.07486784842324	0.00042283350511511 9
hsa-miR-548q	-2.75843571627185	6.38866964585996	0.00052232518479870 9
hsa-miR-605-5p	4.8121626409086	6.03507276148064	0.00095672318457995 2
hsa-miR-876-3p	4.82104908730623	6.03930743181429	0.00096613281050787
hsa-miR-29c-3p	-2.19211256525384	12.0465557555841	0.00116561430023705
hsa-miR-452-3p	-3.30416542265031	10.2971875240949	0.00123906375058032
hsa-miR-652-3p	-2.31055181536258	11.8288563428096	0.00131131813995871
hsa-miR-4284	-2.2543204083184	7.53647233878283	0.00147887334893042
hsa-miR-550a-5p	-1.33332407770242	8.65314033200751	0.00152100297599287
hsa-miR-4758-5p	-3.10543610683416	6.20893706565821	0.00185965545081506
hsa-miR-330-5p	-1.4867132417661	7.83614342065372	0.00253273216774749
hsa-miR-30a-3p	1.70587809060032	9.23679937217119	0.0036800458657904
hsa-miR-4634	-1.81598072596873	6.30729883531355	0.00375890750656287
hsa-miR-504-5p	-1.38078740020915	9.86936233929104	0.0040531565030975
hsa-miR-4525	2.81362942154516	6.35732355726241	0.00432531147918981
hsa-miR-192-3p	-2.26548008492	6.48430336627496	0.00451948346495185
hsa-miR-887-3p	2.00488071650081	9.66719668631207	0.00498567397150925
hsa-miR-873-3p	2.58158375366192	6.08590511501896	0.00523187423108151
hsa-miR-876-5p	2.37040673994169	6.64589106356515	0.0054468121971027
hsa-miR-628-3p	-1.42185471588106	8.16041873000113	0.00551096722444092
hsa-miR-151b	-1.30415772465652	8.21282335029883	0.00615718587267601
hsa-miR-551b-3p	2.64062810921191	10.7677358723612	0.0061812290648841
hsa-miR-664b-3p	-1.2953686734625	7.51385750256183	0.00717116870942268
hsa-miR-6840-5p	-1.20604648286475	6.7694834089762	0.00758086893162786
hsa-miR-107	1.61935877471288	11.6316287563962	0.00813250125087013
hsa-miR-450b-5p	-4.74704937980179	6.28039034297018	0.00816670772488577

hsa-miR-455-5p	1.31182186346214	7.28812112912899	0.00863908038133188
hsa-miR-30c-2-3p	1.40968723880216	7.27335467143492	0.00990825460081198
hsa-miR-550a-3-5p	-1.25149321048396	7.31145729052664	0.0128556043727155
hsa-miR-2355-3p	2.00909505524821	6.28829515766835	0.0129198292990002
hsa-miR-551b-5p	2.16076634181417	7.95675347572863	0.0139209874023195
hsa-miR-488-3p	-2.04846154627687	6.33632283287643	0.0145730009920192
hsa-miR-151a-3p	-1.16082901022012	9.42619559504504	0.0148739404977672
hsa-miR-1914-3p	-1.33574530309374	6.51239480905953	0.0157770869932959
hsa-miR-933	-3.04656791247055	6.50892330903132	0.0163613753254516
hsa-miR-219b-5p	3.14152706130636	6.35168372118738	0.0164312409424983
hsa-miR-211-5p	3.29144404042002	6.04408203600902	0.0175905920559335
hsa-miR-139-5p	-1.79151129147099	9.1429001843526	0.0182777401448079
hsa-miR-3928-3p	-1.27099304275484	6.74522017784219	0.0195867616496693
hsa-miR-140-5p	1.40097962608635	10.453702064806	0.0198805049314309
hsa-miR-18a-3p	1.38131161350504	9.11255837095875	0.0208787047627378
hsa-miR-3200-5p	-1.86925137011305	6.0936668519728	0.021098676969867
hsa-miR-641	-1.16178709702105	7.86997436596717	0.0246746890851707
hsa-miR-153-3p	-1.67115534510652	6.5382545096325	0.0257640828398372
hsa-miR-3929	-4.3780639027149	6.01935684529307	0.0265027123338497
hsa-miR-196b-5p	1.36942774841276	10.5014789403789	0.0269830390373144
hsa-miR-574-5p	-1.35711810991347	7.13986370436037	0.0276751354207567
hsa-miR-15a-5p	1.80885665362383	12.4139706687703	0.0326880758718435
hsa-miR-6513-5p	-1.98910799754874	6.14270330462889	0.0335769821070907
hsa-miR-455-3p	1.53402560631522	10.2015458627204	0.0342585392238185
hsa-miR-3126-5p	0.950320259525043	6.57229578100554	0.0361016120449525
hsa-miR-374a-5p	-1.06181045186503	9.92050514563164	0.0362198660662788
hsa-miR-4286	1.16660342675879	7.1929491998823	0.0362604406644717
hsa-miR-374b-5p	-1.2489817432917	12.4765258721315	0.036807478194905
hsa-miR-570-3p	-3.65598319244043	6.96264668382132	0.0373596107193017
hsa-miR-19a-5p	-1.41862105959855	8.03993479577893	0.0387395471584931
hsa-miR-4664-5p	-1.5899612825439	6.38111438749487	0.0388979514006616
hsa-miR-2277-5p	3.94332353504313	6.07008896214493	0.0390959101167252
hsa-miR-6804-5p	-3.85799946571007	6.00953347302172	0.0391765092812849
hsa-miR-216b-5p	-2.1085789005263	6.30036339216676	0.0416892399602853
hsa-miR-6789-5p	-1.45148019831923	6.25227142118135	0.0427513242919777
hsa-miR-941	-1.08365585965006	7.63443746478541	0.0428053473747907
hsa-miR-4425	-0.919593603309289	6.69207879454841	0.0434996795674329
hsa-miR-6789-3p	-2.44199617288378	6.10646778396777	0.0435023968055799
hsa-miR-4638-5p	-2.68404964736585	5.97003023445696	0.0487704336999685
hsa-miR-5699-3p	-1.26362414177337	6.67607058383329	0.049075563974213
hsa-miR-4521	-1.65286539652345	12.0941045412182	0.0499130497472213

Annex 5: Table S6- Log Fold Change of levels of miRs between drug-sensitive (NCI-H460) cells and their MDR (NCI-H460/R) counterparts.

	logFC	logCPM	PValue
hsa-miR-584-5p	11.2287212029376	9.86771662563186	4.03022890780417E-20
hsa-miR-335-5p	-8.24893232910351	11.1034793922172	4.95129695415833E-11
hsa-miR-196a-5p	-3.46646059795181	9.99424557412796	1.13882423757059E-09
hsa-miR-9-3p	3.61849210126089	10.270357602399	8.77937772818369E-08
hsa-miR-675-3p	-6.59663765218649	6.35487999387866	9.99251330916043E-07
hsa-miR-202-5p	2.19999158730192	7.92208052136313	0.0000194047703838179
hsa-miR-4704-5p	2.39696973748467	8.9161523661559	0.0000389255386639477
hsa-miR-4704-3p	2.70689629557686	7.40181424373328	0.0000514473329823239
hsa-miR-383-5p	4.86048456348873	8.39518355839927	0.0000613779749648681
hsa-miR-584-3p	6.27342725060136	6.71700516638926	0.0000683345711817507
hsa-miR-1263	-4.62128513427855	6.24077684067952	0.000100515936983443
hsa-miR-1269a	-3.57872332504624	6.46691059665539	0.000115458518841669
hsa-miR-4772-5p	-4.3683726023801	6.17667402575273	0.000134723501164375
hsa-miR-146b-3p	-1.8083831880166	7.60980035473958	0.000310909815552051
hsa-miR-9-5p	3.18409779527762	10.6502500856428	0.000355594061651111
hsa-miR-3656	-5.49555206097072	9.23789818995092	0.0017659124160804
hsa-miR-548j-5p	-2.4707497156592	6.43759974977925	0.00207066392853546
hsa-miR-19b-1-5p	1.97829892892157	10.2289224375697	0.00219182882755446
hsa-miR-99a-5p	-3.49045491446878	12.8035377235306	0.00223090446242129
hsa-miR-1	2.14869278012796	6.90746330218762	0.00457216604865384
hsa-miR-629-3p	1.56632519969466	8.0484899682335	0.00529055380071006
hsa-miR-4488	-3.90808556899382	8.52522052612374	0.00532197176730743
hsa-miR-504-5p	-1.74314906923805	9.86936233929104	0.00540439293830136
hsa-miR-4516	-3.83804903829629	7.73276558217913	0.00649375478293425
hsa-miR-99a-3p	-2.77875378848196	9.19061898093821	0.00731328754166488
hsa-miR-486-3p	1.30497661529729	8.12429751544606	0.00954954616213872
hsa-miR-125b-5p	-2.96844169875416	13.9104296058799	0.00993530408041993
hsa-miR-146a-5p	-2.20502222567315	9.33392447829103	0.00993891970287092
hsa-miR-99b-3p	-1.92007317494709	9.01747270089735	0.0105331771586183
hsa-miR-34a-5p	-3.71899578352139	14.5115241980057	0.0105409748333152
hsa-miR-675-5p	-3.66020884320284	6.11761320665302	0.0105605658171782
hsa-miR-4492	-3.4479238707517	9.05681954620426	0.0115204522039844
hsa-miR-4428	5.15084658100659	6.24801413728353	0.012643378589541
hsa-miR-4532	-4.1329754576781	8.75383886209902	0.0143189819444449
hsa-miR-1537-3p	-2.73779020119594	6.24732239524233	0.0153445336023107
hsa-miR-301b	-1.33821251292716	10.0923487977179	0.0155158431437301
hsa-miR-4508	-3.60173402446403	7.22486524391009	0.0161451947124348
hsa-miR-3691-3p	-3.23955703489399	5.95306135694084	0.0166627171008659
hsa-miR-3196	-4.99915185567289	6.7830793220733	0.0172592328880049
hsa-miR-212-3p	-1.28223725155355	7.6127658260392	0.018161392185004
hsa-let-7c-5p	-1.9317303678254	12.0924112251579	0.022246443311884
hsa-miR-331-5p	1.51811998293921	8.98995605975425	0.0235830030362511
hsa-miR-933	1.80329070301869	6.50892330903132	0.0248147832653462
hsa-miR-1306-5p	-1.0650298202874	8.76859050421183	0.0260877226319777
hsa-miR-6855-3p	-2.3173988652484	6.08104615173212	0.0262558954935157
hsa-miR-200a-3p	1.7689486560205	6.81482820771122	0.0274520102453395
hsa-miR-4674	-5.40532012976594	6.71637378024098	0.0277455880905778
hsa-miR-34c-5p	-3.2291960523708	7.96567457451959	0.0307427313894522
hsa-miR-101-5p	-1.1398133403996	7.68239023629124	0.0321970378868233

hsa-miR-6087	-2.70321344827979	12.3450057543895	0.0347794452503769
hsa-miR-219a-1-3p	-2.91694250327365	6.05655872296335	0.0355495404905477
hsa-miR-942-3p	2.50214465406996	6.23464805894186	0.0375549874917424
hsa-miR-3127-3p	4.14559617676705	6.25012517621344	0.0387106074963014
hsa-miR-513a-5p	4.15385322204273	6.13401102409786	0.0394410778054229
hsa-miR-145-3p	4.27379928437246	5.95048654648693	0.0412280267185268
hsa-miR-497-5p	-1.11580279813864	7.7941928313518	0.042487943270457
hsa-miR-1229-3p	-2.98363091629835	6.95047233650406	0.0427211465108166
hsa-miR-424-3p	-1.14922358444416	8.73127858175613	0.0491906339605634

Annex 6: Table S7- Log Fold Change of miRs expression between drug-sensitive (K562) cells and their MDR (K562Dox) counterparts.

	logFC	logCPM	PValue
hsa-miR-204-5p	3.47181883726436	13.7728586519982	0.00185460230556585
hsa-let-7f-5p	-3.45835033398841	13.9136972446194	0.00280656831455875
hsa-miR-139-5p	-4.98643697522113	9.1429001843526	0.00371796111425252
hsa-miR-34a-5p	3.17848164973163	14.5115241980057	0.00438610874095439
hsa-miR-27b-3p	-3.01530108991401	13.548036145235	0.00775023461928557
hsa-miR-143-3p	-3.65799422534282	8.69453242448027	0.00990470683894555
hsa-miR-29c-5p	-4.25070717261593	10.004657810989	0.0145908440877052
hsa-miR-26b-5p	-3.31182004071978	12.2388115759423	0.0148887822116402
hsa-miR-26a-5p	-2.48563647981945	14.5208208731121	0.0224944534576407
hsa-miR-551b-3p	4.56841369554268	10.7677358723612	0.0273896210104777
hsa-miR-16-5p	-2.4773932155835	15.4485843652559	0.0304027837740629
hsa-let-7a-5p	-2.26510915797122	15.3136429687213	0.0331875725873694
hsa-miR-29b-2-5p	-4.29582263960949	9.39781524913439	0.036800088415543
hsa-miR-10b-5p	-3.34911155571464	7.51725061185573	0.0382334081009984
hsa-miR-204-3p	2.7454250702009	11.3778472139391	0.0395709076775726
hsa-miR-374b-5p	-4.11487354668969	12.4765258721315	0.051491415866453
hsa-miR-29c-3p	-4.05019174928688	12.0465557555841	0.0558837694439184
hsa-miR-15b-5p	-4.06621297222622	13.1948028598921	0.0588832461560646
hsa-miR-451a	-2.13571385802232	14.8039036738112	0.0714337882472269
hsa-miR-18a-5p	-1.7900392250775	16.8522733813782	0.0780528466415119
hsa-miR-20a-5p	-1.88603163427234	18.3806742483831	0.0969450194599634
hsa-miR-21-5p	-1.77774819031999	17.0144354005778	0.106225779731938
hsa-miR-92a-1-5p	-3.72183730142867	10.3480730568546	0.110595171401157
hsa-let-7g-5p	-1.57816828923369	13.8938023145324	0.117713952324724
hsa-let-7d-5p	-1.79852799724458	13.374129919213	0.119333250370142
hsa-miR-30c-5p	-1.48027120474074	14.1312978155508	0.122069960338201
hsa-miR-182-5p	-1.95259835696846	11.7407009567178	0.122536741844953
hsa-miR-92a-3p	-2.10576155601177	15.8468245763915	0.124829909040372
hsa-miR-29b-1-5p	-2.50423875937616	10.0808397909426	0.126091294707963
hsa-miR-9-5p	-1.87240390015432	10.6502500856428	0.129977447489053
hsa-miR-150-5p	-2.75024874784049	6.79397330069822	0.1316365725517
hsa-miR-331-5p	-3.33532464476927	8.98995605975425	0.140838362842561
hsa-miR-106b-5p	-1.52208652934485	14.7771440864595	0.141318998958288
hsa-miR-126-5p	-1.66074752504667	15.0833438534628	0.146204184175044
hsa-miR-503-5p	-3.47411816438886	10.8469211857572	0.152187561983503
hsa-miR-590-3p	-3.59997088192005	10.0843695668067	0.155818992553141
hsa-miR-27a-3p	-1.51823147637087	14.8108116654115	0.163033666337248
hsa-miR-27a-5p	-3.38534872260551	9.59659659172585	0.166144014701296
hsa-miR-671-5p	1.59719383597551	13.3544452207844	0.166409365165845
hsa-miR-1248	1.88780281157454	9.55450367420305	0.16813977069206
hsa-miR-126-3p	-1.55855989191463	16.8877132780926	0.178896021478087
hsa-miR-411-5p	-3.33310591801953	6.24437670807089	0.185286062994666
hsa-miR-22-5p	1.56053669994328	10.078974588484	0.191239391348217
hsa-miR-320d	1.74652212756532	10.1398539690163	0.199665080567731
hsa-miR-409-3p	3.34115005630982	6.08937619142041	0.205777505381414
hsa-miR-223-3p	-1.46523673277243	14.3603623770747	0.207547699121204
hsa-miR-128-3p	-1.46716936718003	12.1636821664501	0.248598335065004
hsa-let-7b-5p	-1.05924584507821	14.6331709183858	0.251708292464503
hsa-miR-19b-1-5p	-1.78534351583224	10.2289224375697	0.262128833801486

hsa-miR-383-5p	1.80249688636911	8.39518355839927	0.267985478901436
hsa-miR-191-5p	-1.11455258224826	14.9157957795776	0.268609633651504
hsa-miR-191-3p	-2.8108336752226	7.04889653768022	0.279551896978731
hsa-miR-195-5p	-3.12863239255606	9.52041202130798	0.281081907581071
hsa-miR-877-5p	-3.12854595151297	11.072768892232	0.281098539007809
hsa-miR-135a-5p	3.22211307081427	10.5930374231035	0.283517381376266
hsa-miR-181b-5p	1.01821391663072	14.0025664160002	0.283524448270065
hsa-miR-590-5p	1.59818240763563	11.2591960829192	0.284931451281221
hsa-miR-320c	0.960220670410203	12.2483529607493	0.28664158888887
hsa-miR-342-3p	-1.32867212417377	11.8491142799322	0.286863363949944
hsa-miR-935	-3.09802178647469	10.7781815742344	0.287319148419781
hsa-miR-221-3p	1.08287524739818	14.0415607213413	0.2878981862317
hsa-miR-3615	3.21608850506515	9.19457523085348	0.288153090103007
hsa-miR-1260b	-3.05938554172119	9.44989106231294	0.289834258330284
hsa-miR-98-5p	-3.08070922799671	9.06763197998563	0.291176401110403
hsa-miR-501-5p	2.61507718520838	8.71279727862906	0.292995743834013
hsa-miR-142-3p	-1.36291483978252	14.3118754183743	0.293096596680799
hsa-miR-7704	1.33291053264796	9.4634001433739	0.320251055621055
hsa-miR-486-5p	-1.46330239893943	13.2564367378955	0.362209366002288
hsa-miR-99b-5p	-1.69226780970915	12.7004559953976	0.374645633639254
hsa-miR-425-5p	0.760449227905118	13.3789619860543	0.377106771119556
hsa-miR-140-3p	0.86339966370748	13.867217189773	0.379051091956029
hsa-miR-652-3p	-1.4515789204421	11.8288563428096	0.379446500969136
hsa-miR-17-5p	-0.965479448667722	17.6797464338693	0.385320090950948
hsa-miR-24-3p	-0.869618387390948	15.149515926661	0.391520428898913
hsa-miR-93-5p	-0.96493804120806	15.278913477615	0.396141874871618
hsa-miR-375	0.791397578479367	12.7657876276761	0.423304173724466
hsa-miR-101-3p	-1.16328643595755	13.2094956216118	0.424827151962458
hsa-miR-33b-5p	-0.883250458680953	10.5013824022432	0.427942106964969
hsa-miR-30e-5p	-0.963316360494501	13.4991249466847	0.433330619866901
hsa-miR-4443	-1.06200328238986	11.0810234963945	0.435271825141219
hsa-miR-423-5p	-0.748070941190847	14.0686071314562	0.450358108167662
hsa-miR-3591-3p	-2.04115095690852	6.26551374158856	0.457000392603231
hsa-miR-378a-3p	0.805044807483744	14.3620762438099	0.462284443168174
hsa-miR-214-3p	-1.75216262359096	6.51366303280273	0.462711558571693
hsa-miR-151a-5p	-0.88572360242678	12.0729944831285	0.465401139109264
hsa-miR-23b-3p	-0.791048171448832	14.1745975933577	0.466785380326567
hsa-miR-17-3p	-0.85823272766003	13.8107423432952	0.479779124044064
hsa-miR-145-5p	-0.819207520328205	11.5071601533748	0.487952332063548
hsa-miR-31-5p	-0.699826056359926	14.7927068681897	0.497047779607407
hsa-let-7e-5p	-1.14777719273687	13.8404690044972	0.511071674715828
hsa-miR-25-5p	-2.68408556395192	7.49300665500736	0.511552193700601
hsa-miR-24-2-5p	-2.67936400268885	8.12883433074008	0.513100131905149
hsa-miR-181c-5p	-2.59598306230111	8.65941110446907	0.514632099181193
hsa-miR-340-5p	-2.92083015466966	9.78571928298067	0.514850429752022
hsa-miR-484	-1.55393270113774	13.2070800471402	0.515114228932098
hsa-miR-532-5p	1.00033209991204	9.29992724177179	0.516183653080232
hsa-miR-92b-5p	-2.27804421564618	9.46959109005717	0.51660604044428
hsa-miR-424-5p	-2.90635612462841	11.1995152383186	0.516632941208787
hsa-miR-502-3p	-2.57787023583119	9.18274036608603	0.517281862990211

hsa-miR-331-3p	-2.3436720538589	10.4955790019212	0.518199944204687
hsa-miR-124-3p	-2.66381039533604	9.59591434897087	0.518603002355161
hsa-miR-140-5p	2.87168276018186	10.453702064806	0.519074185846678
hsa-let-7d-3p	-2.56012655125032	11.2442249916764	0.520053048089045
hsa-miR-942-5p	2.86988205796451	8.26350149933706	0.520291129170694
hsa-miR-376c-3p	-2.36483015292052	6.72983986197342	0.521779679062315
hsa-miR-660-3p	0.937574255201939	8.41086806293808	0.522566906282856
hsa-miR-500a-5p	2.38324318695395	9.41006593312938	0.525200938853499
hsa-miR-887-3p	2.38261521247471	9.66719668631207	0.525822801325054
hsa-miR-99a-3p	0.946125756728503	9.19061898093821	0.527434818766991
hsa-miR-551b-5p	-2.81596703078987	7.95675347572863	0.530187420769712
hsa-miR-365a-5p	-2.50221605989642	7.86777677947559	0.530457093203266
hsa-miR-199a-3p	-1.27767003568467	7.9469372316105	0.531080750446279
hsa-miR-148a-5p	-2.42403333140255	6.79858195128131	0.535686843063023
hsa-miR-4521	0.959415120627557	12.0941045412182	0.53605106821817
hsa-miR-1291	2.37186941748558	6.66202681983995	0.536213352048986
hsa-miR-106a-5p	-2.78082742174629	14.2520698473432	0.536813251395874
hsa-miR-4497	1.30974681852392	6.68810364085751	0.537138429344513
hsa-miR-3687	-2.41891558496801	8.77322134361983	0.5376834639266
hsa-miR-338-3p	-2.41778459387907	6.62321858613006	0.541938388507127
hsa-miR-214-5p	-2.44560730260255	6.02597600179849	0.543010983119377
hsa-miR-4700-5p	2.35896445090186	5.99583315065765	0.548463612891271
hsa-miR-320a	-0.46301714350705	16.1913924050233	0.551962241158259
hsa-miR-3187-5p	-2.48299695661398	6.02720379888014	0.559853029204779
hsa-miR-138-5p	-1.01801768087518	12.8309482647707	0.571445704987514
hsa-miR-30b-5p	-0.777437586669466	13.6465355862108	0.575903385656287
hsa-miR-320b	0.49319316591697	12.5010909334645	0.590428645856608
hsa-miR-33a-5p	0.713632377836917	10.8039573470637	0.644891242815695
hsa-miR-423-3p	-0.568351022559912	14.0615575076359	0.645919629570622
hsa-miR-130b-5p	-1.66125756537628	9.58313511669898	0.651566136465361
hsa-miR-31-3p	-1.56597160243905	9.98973277059518	0.656848567879694
hsa-miR-23a-5p	-1.26244826935256	9.18920896957834	0.660475016625418
hsa-miR-15a-5p	-0.816581996498144	12.4139706687703	0.664125551292746
hsa-miR-125b-5p	0.456868636112704	13.9104296058799	0.677690727577774
hsa-miR-629-5p	1.1110571177524	10.4126093671627	0.681812496359501
hsa-miR-1307-5p	1.15194293123336	11.0138937530608	0.682943178040806
hsa-miR-125a-5p	-0.539312218788231	13.7281026120398	0.683278919803485
hsa-miR-186-5p	-0.530013720419083	11.7717247576307	0.710078734589691
hsa-miR-148b-3p	-1.04218937004064	10.904446400857	0.718842773060647
hsa-miR-96-5p	0.534216097781493	9.91270587719072	0.7189060847469
hsa-miR-148a-3p	-1.28687642029127	11.9966093089268	0.719526121432856
hsa-miR-22-3p	-0.366416966965482	12.9351473081114	0.721361480489805
hsa-miR-582-5p	0.357531099922734	10.9335709896042	0.728389946600665
hsa-miR-10a-5p	-1.24363489122335	12.8122468070208	0.729859892745286
hsa-miR-224-5p	-1.66876250132096	13.1188761257331	0.734048350990763
hsa-miR-199b-3p	-1.01724402361062	7.17997104180436	0.741723308018521
hsa-miR-210-3p	-0.839857203645212	12.8092104308389	0.749118379671007
hsa-miR-122-5p	-1.67354959787612	6.35032180944021	0.762237187323448
hsa-miR-99a-5p	-0.291857088837103	12.8035377235306	0.771603467644413
hsa-miR-130a-3p	-0.516038893372203	12.6490086095795	0.81445751216421

hsa-miR-1307-3p	0.290549217238708	12.7608935330049	0.822088236489562
hsa-miR-19b-3p	0.274119471573014	19.2261925480084	0.828794405820198
hsa-let-7c-5p	-0.577513263811675	12.0924112251579	0.842794045431374
hsa-miR-30a-5p	0.281960361953713	14.6907146890672	0.846551137204513
hsa-miR-29a-3p	0.242031174576084	14.9259219488034	0.847076135666258
hsa-miR-23a-3p	-0.222160394120015	15.8568205781655	0.847547851287947
hsa-miR-181a-5p	-0.191699913044976	14.9879635597885	0.88113746792778
hsa-miR-222-3p	0.165128718361812	12.7816264920462	0.905734311025808
hsa-miR-29b-3p	0.12560653683921	15.8053261786006	0.909030650336531
hsa-miR-345-5p	0.148985942187153	10.2523395311299	0.913528333907374
hsa-miR-3182	-0.0564324269152499	9.38860877707303	0.932371525728904
hsa-let-7i-5p	-0.0489812607733079	16.4466953102539	0.985501672250936
hsa-miR-4284	-2.24246636462726	7.53647233878283	0.99999999999999
hsa-miR-107	0.0748210294195495	11.6316287563962	0.99999999999999
hsa-miR-362-5p	1.64551902093211	8.64878082249902	0.999999999999991
hsa-miR-505-3p	0.451877230300165	10.452264355559	0.999999999999991
hsa-miR-25-3p	-0.359781733228961	11.4622940076873	0.999999999999992
hsa-miR-432-5p	1.63641727632075	5.82594483082756	0.999999999999992
hsa-miR-219a-5p	1.72835776796966	7.67161205287955	0.999999999999993
hsa-miR-550a-3p	0.184516439820552	10.5405698481163	0.999999999999994
hsa-miR-425-3p	-0.924759945089482	9.22556672129637	0.999999999999994
hsa-miR-3140-3p	-1.64945163106367	6.56492471819571	0.999999999999995
hsa-miR-219b-3p	-1.62604912374266	6.147832706672	0.999999999999995
hsa-miR-152-3p	-0.600589851232741	10.2667452705029	0.999999999999995
hsa-miR-8072	1.60388301060436	6.03416206542733	0.999999999999995
hsa-miR-146b-5p	0.286184667468798	14.9713517481497	0.999999999999995
hsa-miR-142-5p	-0.684575943202054	11.2077303777223	0.999999999999996
hsa-miR-181a-2-3p	-1.23763200533129	8.54973546826013	0.999999999999996
hsa-miR-23b-5p	-1.58256424412321	7.83299129558212	0.999999999999996
hsa-miR-30a-3p	0.183744272078607	9.23679937217119	0.999999999999996
hsa-miR-409-5p	-1.67534786216265	5.82690149196799	0.999999999999997
hsa-miR-196b-5p	0.264360416367348	10.5014789403789	0.999999999999997
hsa-miR-155-5p	1.63242963343388	6.09655122964838	0.999999999999997
hsa-miR-30c-2-3p	1.65130356107384	7.27335467143492	0.999999999999998
hsa-miR-744-3p	-1.58977450080295	6.6055105529732	0.999999999999998
hsa-miR-378d	-1.60571375884702	8.21627169693949	0.999999999999998
hsa-miR-3714	1.90093404394957	5.82760322499037	0.999999999999998
hsa-miR-1301-3p	-0.625434905213618	10.9944688011725	0.999999999999998
hsa-miR-28-5p	0.258711328537244	9.15302378605481	0.999999999999998
hsa-miR-1287-5p	1.6513477140349	7.37402012357429	0.999999999999998
hsa-miR-655-3p	-1.64762897160389	5.85038516835351	0.999999999999999
hsa-miR-361-3p	0.106470311237463	12.4905910493233	0.999999999999999
hsa-miR-4532	-1.69725575179321	8.75383886209902	0.999999999999999
hsa-miR-7977	1.65075229086089	7.12070694447114	0.999999999999999
hsa-miR-26b-3p	-2.23864517295057	6.8724989942965	0.999999999999999
hsa-miR-504-3p	-2.14962713238353	6.86835347336341	0.999999999999999
hsa-miR-199b-5p	1.73561589309803	7.4355666427509	0.999999999999999
hsa-miR-4683	-1.56712787798239	6.9226606821358	0.999999999999999
hsa-miR-504-5p	-1.5596569866409	9.86936233929104	0.999999999999999
hsa-miR-2278	-1.72755344418122	7.19680901044195	0.999999999999999

hsa-miR-6862-5p	1.64331899559692	6.00645051691554	0.999999999999999
hsa-miR-18b-5p	0.187024968728128	9.64425260024551	0.999999999999999
hsa-miR-376a-5p	-2.23285701325168	5.90967705429386	0.999999999999999
hsa-miR-454-3p	1.64985213044012	10.7394488771049	0.999999999999999
hsa-miR-1254	0.291712880476492	9.03785272650124	0.999999999999999
hsa-miR-1180-3p	-0.224360782331802	12.4984625653563	0.999999999999999

Annex 7: Table S8- Log Fold Change of levels of miRs between EVs released by drug-sensitive (NCI-H460) cells and EVs released by their MDR (NCI-H460/R) counterparts.

	logFC	logCPM	PValue
hsa-miR-671-5p	11,0804889	13,35444522	1,27E-16
hsa-miR-320b	9,40107166	12,50109093	6,83E-10
hsa-miR-320c	6,786997984	12,24835296	4,68E-08
hsa-miR-320a	5,489028663	16,19139241	4,23E-07
hsa-miR-3180-3p	8,543045172	10,81684785	2,60E-06
hsa-miR-4443	8,116505732	11,0810235	3,77E-06
hsa-miR-378a-3p	9,044631763	14,36207624	5,50E-06
hsa-miR-423-3p	9,123621413	14,06155751	1,28E-05
hsa-miR-320d	7,937260766	10,13985397	1,73E-05
hsa-miR-423-5p	7,952932678	14,06860713	3,20E-05
hsa-miR-92a-1-5p	7,125696967	10,34807306	0,00015478
hsa-miR-19b-3p	9,399111206	19,22619255	0,00017215
hsa-miR-3180	7,032389598	9,110362989	0,000201776
hsa-miR-185-5p	7,734533298	14,09032894	0,000225865
hsa-miR-1908-5p	6,53965768	9,259029421	0,000472329
hsa-miR-486-5p	7,598378068	13,25643674	0,000708219
hsa-miR-19a-3p	7,862604174	18,25830255	0,000893399
hsa-miR-1307-3p	6,704747197	12,76089353	0,000914146
hsa-miR-769-5p	5,93639408	10,8319817	0,001163992
hsa-miR-22-3p	6,648104329	12,93514731	0,00128372
hsa-miR-17-3p	6,758154387	13,81074234	0,001746639
hsa-miR-125a-5p	6,412744448	13,72810261	0,001930507
hsa-miR-629-5p	5,850823139	10,41260937	0,007745956
hsa-let-7e-5p	5,527565471	13,840469	0,014278219
hsa-miR-452-5p	5,251190146	12,35364456	0,014994737
hsa-miR-185-3p	5,11139897	7,164217737	0,020007031
hsa-miR-193b-5p	4,742882842	8,818482945	0,0290672
hsa-miR-210-3p	4,938555823	12,80921043	0,047999248
hsa-miR-378c	4,49477315	9,392496067	0,064515655
hsa-miR-92a-3p	4,748930269	15,84682458	0,069477422
hsa-miR-30d-5p	4,75891684	15,21143001	0,083690376
hsa-miR-597-5p	4,23021849	7,240449839	0,098155523
hsa-miR-1307-5p	3,360428042	11,01389375	0,108909857
hsa-miR-146b-5p	4,235792375	14,97135175	0,110049025
hsa-miR-125b-5p	4,27895375	13,91042961	0,142248515
hsa-miR-769-3p	3,908559844	8,249039379	0,170885058
hsa-miR-133a-3p	-4,418328764	6,6938211	0,17370883
hsa-miR-126-3p	4,287234217	16,88771328	0,174384709
hsa-miR-23a-5p	3,932871178	9,18920897	0,176438577
hsa-miR-1180-3p	3,937131164	12,49846257	0,185974676
hsa-miR-21-5p	1,762674166	17,0144354	0,190948937
hsa-miR-193b-3p	3,93918263	13,21641037	0,197104304
hsa-miR-2278	3,945703889	7,19680901	0,204396085
hsa-let-7b-5p	-1,073785452	14,63317092	0,245703187
hsa-miR-296-3p	3,473102209	8,786358318	0,270833043
hsa-miR-19b-1-5p	3,48868941	10,22892244	0,281510972
hsa-miR-20a-3p	3,492735192	9,998284195	0,283935033
hsa-miR-550a-3p	3,51325279	10,54056985	0,284474028
hsa-miR-373-3p	-4,050747335	6,174490852	0,300614275

hsa-miR-652-3p	3,517363862	11,82885634	0,300893494
hsa-miR-1306-3p	3,521537271	6,953646198	0,304217865
hsa-miR-4674	-4,005555984	6,71637378	0,305804941
hsa-miR-151a-5p	3,528267637	12,07299448	0,309916993
hsa-miR-6769b-5p	-3,454538649	5,987518856	0,317831957
hsa-miR-219b-3p	-3,207747985	6,147832707	0,330012702
hsa-let-7a-5p	3,55129724	15,31364297	0,333381217
hsa-miR-223-3p	-3,456834208	14,36036238	0,348442105
hsa-let-7i-5p	-3,319414257	16,44669531	0,35825866
hsa-miR-181a-5p	-1,160912003	14,98796356	0,4118
hsa-miR-372-3p	-3,50585369	5,893973514	0,462879161
hsa-miR-29c-5p	2,942430128	10,00465781	0,517155592
hsa-miR-106b-3p	2,945479907	11,14385153	0,518603107
hsa-miR-1273h-3p	2,945682097	7,302518319	0,518700235
hsa-miR-6087	0,90623864	12,34500575	0,520788988
hsa-miR-500a-3p	2,95929375	9,013893444	0,52559904
hsa-miR-296-5p	2,961490033	9,462302537	0,526783917
hsa-miR-7641	2,964514905	8,036668748	0,528451518
hsa-miR-33b-5p	2,966659366	10,5013824	0,529659749
hsa-miR-1296-3p	2,972830653	6,673737302	0,533264241
hsa-miR-1254	2,978924439	9,037852727	0,537023508
hsa-miR-193a-3p	2,983855245	7,147266757	0,540224641
hsa-miR-186-5p	2,985710374	11,77172476	0,541468555
hsa-miR-3687	2,996283494	8,773221344	0,549013292
hsa-miR-3182	2,999122647	9,388608777	0,551183268
hsa-miR-103a-3p	3,003986416	15,10389606	0,555058412
hsa-miR-375	3,009767384	12,76578763	0,559945849
hsa-miR-127-3p	3,022296695	6,077951389	0,5717579
hsa-miR-7-5p	0,740223831	13,38268703	0,589188952
hsa-miR-374c-3p	3,046545274	5,911043775	0,601051779
hsa-miR-7704	-0,610165586	9,463400143	0,642070289
hsa-miR-6133	-3,060599378	5,826679996	0,667539364
hsa-miR-17-5p	1,60683407	17,67974643	0,774500237
hsa-miR-3140-3p	-0,631285119	6,564924718	0,813793631

Annex 8: Table S9- Log Fold Change of miRs expression between drug-sensitive (K562) cells and EVs derived from their MDR (K562Dox) counterparts.

ensembl_transcript_id	ensembl_gene_id	logFC	logCPM	PValue	description
ENST00000365512	ENSG00000202382	9,788721	7,714221	9,62E-17	
ENST00000364232	ENSG00000201102	6,505432	7,027775	3,09E-16	
ENST00000545923	ENSG00000255652	8,845785	6,447058	8,31E-14	novel transcript
ENST00000384294	ENSG00000207021	7,375205	7,487893	2,29E-12	
ENST00000380913	ENSG00000146950	8,587122	6,586931	7,07E-11	shroom family member 2 [Source:HGNC Symbol;Acc:HGNC:630]
ENST00000368147	ENSG00000163554	8,468004	7,498571	4,63E-10	spectrin alpha, erythrocytic 1 [Source:HGNC Symbol;Acc:HGNC:11272]
ENST00000384168	ENSG00000206895	8,003519	6,452428	5,51E-10	
ENST00000366955	ENSG00000117724	6,607386	7,231118	1,52E-09	centromere protein F [Source:HGNC Symbol;Acc:HGNC:1857]
ENST00000384426	ENSG00000207155	7,848631	6,251165	3,71E-09	RNA, Ro-associated Y1 pseudogene 14 [Source:HGNC Symbol;Acc:HGNC:50877]
ENST00000365114	ENSG00000201984	8,021365	6,117704	8,48E-09	
ENST00000444527	ENSG00000248522	9,080911	6,632479	1,17E-08	SET binding factor 1 pseudogene 1 [Source:HGNC Symbol;Acc:HGNC:31098]
ENST00000391267	ENSG00000212569	9,792009	8,318699	1,5E-08	
ENST00000408566	ENSG00000221493	8,524349	8,752225	2,39E-08	microRNA 320c-1 [Source:HGNC Symbol;Acc:HGNC:35248]
ENST00000365274	ENSG00000202144	8,208311	12,78004	2,87E-08	
ENST00000363964	ENSG00000200834	9,962699	9,892849	3,28E-08	
ENST00000459041	ENSG00000238516	9,817816	8,711319	3,72E-08	
ENST00000390136		8,590325	7,906389	6,2E-08	
ENST00000439118	ENSG00000198885	8,65205	6,451953	2,41E-07	ITPRIP like 1 [Source:HGNC Symbol;Acc:HGNC:29371]
ENST00000376335	ENSG00000043355	7,536214	5,880743	2,65E-07	Zic family member 2 [Source:HGNC Symbol;Acc:HGNC:12873]
ENST00000528284	ENSG00000131626	7,234733	7,320979	3,59E-07	PTPRF interacting protein alpha 1 [Source:HGNC Symbol;Acc:HGNC:9245]
ENST00000385302	ENSG00000208037	6,405428	14,54366	4,13E-07	microRNA 320a [Source:HGNC Symbol;Acc:HGNC:31632]
ENST00000390209	ENSG00000211543	8,755337	10,04517	6,68E-07	microRNA 320b-1 [Source:HGNC Symbol;Acc:HGNC:35247]
ENST00000440492	ENSG00000233975	8,185327	5,796178	1,18E-06	long intergenic non-protein coding RNA 2574 [Source:HGNC Symbol;Acc:HGNC:537
ENST00000384198	ENSG00000206925	9,194113	10,11205	1,25E-06	
ENST00000580842	ENSG00000264070	6,801929	7,241109	1,64E-06	DND microRNA-mediated repression inhibitor 1 pseudogene 1 [Source:HGNC Syml
ENST00000423985	ENSG00000225469	6,784491	5,004011	1,9E-06	MAGE (Melanoma Associated Antigen) family pseudogene
ENST00000408479	ENSG00000221406	7,232095	8,488314	2,18E-06	microRNA 320b-2 [Source:HGNC Symbol;Acc:HGNC:35256]
ENST00000585052	ENSG00000265483	7,940962	9,03636	2,32E-06	microRNA 4443 [Source:HGNC Symbol;Acc:HGNC:41830]
ENST00000523153	ENSG00000253667	6,705228	4,997868	2,4E-06	ESF1, nucleolar pre-rRNA processing protein, homolog (S. cerevisiae) (ESF1) pseud
ENST00000365617		10,06181	13,95241	3,76E-06	
ENST00000411370	ENSG00000223302	4,839795	7,475078	3,93E-06	
ENST00000362177	ENSG00000199047	8,809389	12,93135	5,38E-06	microRNA 378a [Source:HGNC Symbol;Acc:HGNC:31871]
ENST00000365403	ENSG00000202273	7,764483	10,42127	6,01E-06	
ENST00000363110	ENSG00000278320	6,885252	8,53649	6,3E-06	
ENST00000390762	ENSG00000212051	5,989468	8,478874	8,93E-06	microRNA 320c-2 [Source:HGNC Symbol;Acc:HGNC:35387]
ENST00000408154	ENSG00000221081	6,980482	6,697315	1,13E-05	microRNA 320d-2 [Source:HGNC Symbol;Acc:HGNC:35388]
ENST00000533173	ENSG00000187954	6,740006	8,047449	1,32E-05	cysteine and histidine rich 1 [Source:HGNC Symbol;Acc:HGNC:17806]
ENST00000445946	ENSG00000227268	4,092859	5,70493	1,44E-05	killin, p53 regulated DNA replication inhibitor [Source:HGNC Symbol;Acc:HGNC:37
ENST00000365484	ENSG00000202354	10,09529	16,11876	1,48E-05	RNA, Ro-associated Y3 [Source:HGNC Symbol;Acc:HGNC:10243]
ENST00000588682	ENSG00000176170	9,336556	7,111059	1,56E-05	sphingosine kinase 1 [Source:HGNC Symbol;Acc:HGNC:11240]
ENST00000364685	ENSG00000201555	8,757864	10,77019	1,58E-05	
ENST00000384358	ENSG00000207086	7,542686	10,42068	2,61E-05	
ENST00000201031	ENSG00000087510	5,191374	5,349667	2,79E-05	transcription factor AP-2 gamma [Source:HGNC Symbol;Acc:HGNC:11744]
ENST00000363120	ENSG00000199990	7,887923	12,32745	3,38E-05	vault RNA 1-1 [Source:HGNC Symbol;Acc:HGNC:12654]
ENST00000364613	ENSG00000201483	7,590769	7,581196	3,66E-05	
ENST00000252506	ENSG00000130222	6,232031	5,345258	3,78E-05	growth arrest and DNA damage inducible gamma [Source:HGNC Symbol;Acc:HGNC
ENST00000264039	ENSG00000063660	6,748053	5,726206	6,16E-05	glypican 1 [Source:HGNC Symbol;Acc:HGNC:4449]
ENST00000609386	ENSG00000119906	7,331803	5,244514	8,17E-05	SMC5-SMC6 complex localization factor 2 [Source:HGNC Symbol;Acc:HGNC:17814]
ENST00000365645	ENSG00000202515	7,089037	9,640322	8,94E-05	vault RNA 1-3 [Source:HGNC Symbol;Acc:HGNC:12656]
ENST00000201586	ENSG00000088002	6,851716	8,070273	9,75E-05	sulfotransferase family 2B member 1 [Source:HGNC Symbol;Acc:HGNC:11459]
ENST00000362710	ENSG00000199580	6,082051	11,74083	0,000145	
ENST00000390895		6,624969	13,17984	0,000145	
ENST00000363220	ENSG00000200090	6,468269	12,42303	0,000146	
ENST00000422488	ENSG00000234715	7,026251	5,999432	0,000151	
ENST00000382082	ENSG00000168263	8,278439	5,949427	0,000178	potassium voltage-gated channel modifier subfamily V member 2 [Source:HGNC S
ENST00000362540	ENSG00000199410	8,29206	11,87101	0,000208	
ENST00000390225	ENSG00000211580	6,051649	9,356991	0,000234	microRNA 769 [Source:HGNC Symbol;Acc:HGNC:33138]
ENST00000363421	ENSG00000200291	8,343009	13,37358	0,000242	
ENST00000385288	ENSG00000208023	7,722549	12,6733	0,000262	microRNA 185 [Source:HGNC Symbol;Acc:HGNC:31556]
ENST00000581869	ENSG00000198795	6,62663	9,526744	0,000349	zinc finger protein 521 [Source:HGNC Symbol;Acc:HGNC:24605]
ENST00000249842	ENSG00000129009	5,68765	4,62136	0,000379	immunoglobulin superfamily containing leucine rich repeat [Source:HGNC Symbol;
ENST00000365241	ENSG00000202111	7,309988	12,33997	0,000385	vault RNA 1-2 [Source:HGNC Symbol;Acc:HGNC:12655]
ENST00000224605		3,841405	6,182448	0,000387	
ENST00000452924		5,323744	4,524116	0,000431	
ENST00000554976	ENSG00000042088	7,279855	5,581108	0,00045	tyrosyl-DNA phosphodiesterase 1 [Source:HGNC Symbol;Acc:HGNC:18884]

ENST00000384673	ENSG00000207404	6,422377	9,678124	0,000548	
ENST00000390157	ENSG00000211491	6,39839	6,516825	0,000573	microRNA 320d-1 [Source:HGNC Symbol;Acc:HGNC:35386]
ENST00000405846	ENSG00000132975	5,995288	4,950875	0,00059	G protein-coupled receptor 12 [Source:HGNC Symbol;Acc:HGNC:4466]
ENST00000363564	ENSG00000200434	3,570418	13,246	0,000596	RNA, 5.8S ribosomal pseudogene 2 [Source:HGNC Symbol;Acc:HGNC:41956]
ENST00000309575	ENSG00000175040	3,6255	6,13646	0,000647	carbohydrate sulfotransferase 2 [Source:HGNC Symbol;Acc:HGNC:1970]
ENST00000428177	ENSG00000065970	5,168065	4,446376	0,000714	forkhead box J2 [Source:HGNC Symbol;Acc:HGNC:24818]
ENST00000579470		5,662571	8,366716	0,000732	
ENST00000456105	ENSG00000234996	3,717269	7,776698	0,001125	
ENST00000377403	ENSG00000049239	6,416599	5,272242	0,001159	hexose-6-phosphate dehydrogenase/glucose 1-dehydrogenase [Source:HGNC Sym
ENST00000519280	ENSG00000253496	8,101075	6,149181	0,001166	novel transcript
ENST00000435173		5,285688	5,993185	0,001252	
ENST00000506028	ENSG00000095587	7,32618	5,384581	0,001253	tolloid like 2 [Source:HGNC Symbol;Acc:HGNC:11844]
ENST00000381020	ENSG00000165556	5,227201	5,618101	0,001354	caudal type homeobox 2 [Source:HGNC Symbol;Acc:HGNC:1806]
ENST00000489408	ENSG00000197385	7,005294	11,3221	0,00166	zinc finger protein 860 [Source:HGNC Symbol;Acc:HGNC:34513]
ENST00000433750	ENSG00000132330	6,503983	4,839328	0,001733	selenocysteine lyase [Source:HGNC Symbol;Acc:HGNC:18161]
ENST00000251296	ENSG00000117154	6,343556	6,04249	0,001739	immunoglobin superfamily member 21 [Source:HGNC Symbol;Acc:HGNC:28246]
ENST00000342972	ENSG00000187601	7,122888	5,388066	0,001746	MAGE family member H1 [Source:HGNC Symbol;Acc:HGNC:24092]
ENST00000408966	ENSG00000221990	6,379344	5,308486	0,001787	EXOC3 antisense RNA 1 [Source:HGNC Symbol;Acc:HGNC:25175]
ENST00000420866	ENSG00000231453	5,078924	7,077154	0,002004	long intergenic non-protein coding RNA 1305 [Source:HGNC Symbol;Acc:HGNC:276
ENST00000319363	ENSG00000177663	5,076003	5,469375	0,002028	interleukin 17 receptor A [Source:HGNC Symbol;Acc:HGNC:5985]
ENST00000529192	ENSG00000180423	7,246905	5,793915	0,002048	harbinger transposase derived 1 [Source:HGNC Symbol;Acc:HGNC:26522]
ENST00000546283	ENSG00000115286	5,30919	7,660934	0,00208	NADH:ubiquinone oxidoreductase core subunit S7 [Source:HGNC Symbol;Acc:HGN
ENST00000362552	ENSG00000199422	6,431225	9,499851	0,002288	vault RNA 3-1, pseudogene [Source:HGNC Symbol;Acc:HGNC:23027]
ENST00000365589	ENSG00000202459	4,957173	8,137324	0,002345	
ENST00000408108		7,363996	11,90413	0,002482	
ENST00000362105	ENSG00000198975	-1,898225	11,68855	0,002504	microRNA let-7a-2 [Source:HGNC Symbol;Acc:HGNC:31477]
ENST00000252999	ENSG00000130702	2,963969	5,780166	0,002544	laminin subunit alpha 5 [Source:HGNC Symbol;Acc:HGNC:6485]
ENST00000506382	ENSG00000248767	5,751019	5,308852	0,002737	
ENST00000364228	ENSG00000201098	7,872374	16,53687	0,002809	RNA, Ro-associated Y1 [Source:HGNC Symbol;Acc:HGNC:10242]
ENST00000562272	ENSG00000166851	5,323414	4,867807	0,002843	polo like kinase 1 [Source:HGNC Symbol;Acc:HGNC:9077]
ENST00000426556	ENSG00000223498	-2,284172	6,115996	0,002955	novel pseudogene
ENST00000555923	ENSG00000071537	5,104969	4,459572	0,003054	SEL1L, ERAD E3 ligase adaptor subunit [Source:HGNC Symbol;Acc:HGNC:10717]
ENST00000263233	ENSG00000102003	5,628612	5,974491	0,003202	synaptophysin [Source:HGNC Symbol;Acc:HGNC:11506]
ENST00000367321	ENSG00000120254	3,360445	5,247064	0,003242	methylenetetrahydrofolate dehydrogenase (NADP+ dependent) 1 like [Source:HGI
ENST00000581458	ENSG00000265735	5,572762	8,519733	0,003339	RNA, 7SL, cytoplasmic 5, pseudogene [Source:HGNC Symbol;Acc:HGNC:10040]
ENST00000552061	ENSG00000257298	8,128443	6,966096	0,003358	novel transcript, sense intronic to LIMA1
ENST00000364357		5,005241	12,58756	0,003626	
ENST00000587527	ENSG00000267409	4,898545	4,580842	0,00377	novel transcript
ENST00000370509	ENSG00000143162	5,725336	5,91846	0,004065	cellular repressor of E1A stimulated genes 1 [Source:HGNC Symbol;Acc:HGNC:2351
ENST00000522557	ENSG00000124097	4,752007	4,535828	0,004086	high mobility group box 1 pseudogene 1 [Source:HGNC Symbol;Acc:HGNC:4993]
ENST00000294244	ENSG00000168005	3,775963	5,698047	0,004213	spindlin interactor and repressor of chromatin binding [Source:HGNC Symbol;Acc:I
ENST00000365304	ENSG00000202174	3,901844	12,64329	0,004367	RNA, 5.8S ribosomal pseudogene 5 [Source:HGNC Symbol;Acc:HGNC:41959]
ENST00000406019	ENSG00000220557	4,898639	4,391188	0,004691	high mobility group box 1 pseudogene 13 [Source:HGNC Symbol;Acc:HGNC:13318]
ENST00000385077	ENSG00000284107	7,448526	16,02821	0,004818	microRNA 19b-2 [Source:HGNC Symbol;Acc:HGNC:31576]
ENST00000417586	ENSG00000227370	6,868242	5,041676	0,005205	chromosome 6 open reading frame 108 (C6orf108) pseudogene
ENST00000373115	ENSG00000122863	2,888887	6,351086	0,005245	carbohydrate sulfotransferase 3 [Source:HGNC Symbol;Acc:HGNC:1971]
ENST00000541473	ENSG00000187049	6,519981	4,844425	0,005417	transmembrane protein 216 [Source:HGNC Symbol;Acc:HGNC:25018]
ENST00000369150	ENSG00000178096	6,100167	4,834959	0,005925	bolA family member 1 [Source:HGNC Symbol;Acc:HGNC:24263]
ENST00000587077	ENSG00000178904	7,011168	5,216202	0,005934	dpy-19 like C-mannosyltransferase 3 [Source:HGNC Symbol;Acc:HGNC:27120]
ENST00000261609	ENSG00000128731	5,038357	5,769292	0,006105	HECT and RLD domain containing E3 ubiquitin protein ligase 2 [Source:HGNC Symb
ENST00000578504	ENSG00000264012	5,461862	4,688461	0,006185	novel transcript, antisense to GATA6
ENST00000565286	ENSG00000259892	5,178454	4,497913	0,006345	amyloid beta (A4) precursor protein-binding, family A, member 2 (APBA2) pseudo
ENST00000385230	ENSG00000207965	5,62592	8,954588	0,006427	microRNA 629 [Source:HGNC Symbol;Acc:HGNC:32885]
ENST00000344575	ENSG00000188763	5,116375	6,067478	0,006548	frizzled class receptor 9 [Source:HGNC Symbol;Acc:HGNC:4047]
ENST00000311910	ENSG00000215168	4,504779	6,766667	0,006802	novel pseudogene
ENST00000571422	ENSG00000262539	5,059648	6,115832	0,007025	dead end homolog 1 (zebrafish) (DND1) pseudogene
ENST00000608531	ENSG00000143429	3,103776	4,471798	0,007671	LSP1 pseudogene 4 [Source:HGNC Symbol;Acc:HGNC:53915]
ENST00000373012	ENSG00000185668	4,996794	6,074771	0,008051	POU class 3 homeobox 1 [Source:HGNC Symbol;Acc:HGNC:9214]
ENST00000598446	ENSG00000256087	5,475238	4,606141	0,008114	zinc finger protein 432 [Source:HGNC Symbol;Acc:HGNC:20810]
ENST00000417346	ENSG00000218018	5,217978	4,588933	0,008129	
ENST00000289746	ENSG00000129910	3,134765	5,703803	0,008168	cadherin 15 [Source:HGNC Symbol;Acc:HGNC:1754]
ENST00000410504	ENSG00000222436	4,412181	4,381048	0,008497	RNA, 7SK small nuclear pseudogene 278 [Source:HGNC Symbol;Acc:HGNC:46002]
ENST00000576738	ENSG00000262585	5,731567	4,903023	0,009004	long intergenic non-protein coding RNA 1979 [Source:HGNC Symbol;Acc:HGNC:528
ENST00000440542	ENSG00000226887	-2,305502	4,668921	0,009157	endogenous retrovirus group MER34 member 1, envelope [Source:HGNC Symbol;A
ENST00000492383	ENSG00000114353	4,844699	4,622113	0,009797	G protein subunit alpha i2 [Source:HGNC Symbol;Acc:HGNC:4385]
ENST00000342213	ENSG00000176435	4,622024	5,239899	0,00998	C-type lectin domain containing 14A [Source:HGNC Symbol;Acc:HGNC:19832]

ENST00000577275		5,705333	12,53018	0,010124	
ENST00000548943	ENSG00000257611	5,732908	4,903169	0,010286	thyroid hormone receptor interactor 11 (TRIP11) pseudogene
ENST00000468491	ENSG00000067840	4,894339	4,924763	0,010294	PDZ domain containing 4 [Source:HGNC Symbol;Acc:HGNC:21167]
ENST00000471086	ENSG00000244642	4,993363	6,989789	0,01074	RNA, 7SL, cytoplasmic 396, pseudogene [Source:HGNC Symbol;Acc:HGNC:46412]
ENST00000565336	ENSG00000260464	4,315967	11,50734	0,010952	novel transcript
ENST00000434152	ENSG00000130203	5,692073	4,60141	0,011736	apolipoprotein E [Source:HGNC Symbol;Acc:HGNC:613]
ENST00000531479	ENSG00000254443	6,425319	6,499689	0,011918	novel transcript
ENST00000596009	ENSG00000268949	4,578662	4,629453	0,012512	mitochondrial ribosomal protein S17 pseudogene 1 [Source:HGNC Symbol;Acc:HG
ENST00000448907	ENSG00000162374	5,025379	5,03403	0,012661	ELAV like RNA binding protein 4 [Source:HGNC Symbol;Acc:HGNC:3315]
ENST00000217260	ENSG00000101282	5,378819	4,660325	0,013062	R-spondin 4 [Source:HGNC Symbol;Acc:HGNC:16175]
ENST00000270458	ENSG00000142408	4,101689	7,787682	0,013308	calcium voltage-gated channel auxiliary subunit gamma 8 [Source:HGNC Symbol;A
ENST00000477973	ENSG00000163602	-1,626981	7,362049	0,013322	RING1 and YY1 binding protein [Source:HGNC Symbol;Acc:HGNC:10480]
ENST00000489501	ENSG00000078295	-4,863305	4,802648	0,0135	adenylate cyclase 2 [Source:HGNC Symbol;Acc:HGNC:233]
ENST00000429007	ENSG00000232131	2,572122	4,489652	0,013706	NCOA7 antisense RNA 1 [Source:HGNC Symbol;Acc:HGNC:40954]
ENST00000423021	ENSG00000236567	5,051401	5,585892	0,014235	transcription factor 3 pseudogene 1 [Source:HGNC Symbol;Acc:HGNC:49742]
ENST00000362808		4,723263	14,13542	0,014505	
ENST00000403084	ENSG00000184113	-2,327099	5,221263	0,014974	claudin 5 [Source:HGNC Symbol;Acc:HGNC:2047]
ENST00000579179		4,955634	5,10985	0,015053	
ENST00000400490	ENSG00000158828	5,643174	4,948159	0,015607	PTEN induced kinase 1 [Source:HGNC Symbol;Acc:HGNC:14581]
ENST00000384907	ENSG00000207639	5,223971	12,01219	0,015658	microRNA 193b [Source:HGNC Symbol;Acc:HGNC:32087]
ENST00000449073	ENSG00000237751	4,908147	6,859909	0,015739	long intergenic non-protein coding RNA 1143 [Source:HGNC Symbol;Acc:HGNC:494
ENST00000380495	ENSG00000149926	4,405025	4,556881	0,016041	family with sequence similarity 57 member B [Source:HGNC Symbol;Acc:HGNC:252
ENST00000433670	ENSG00000130508	4,403392	4,337501	0,016041	peroxidasin [Source:HGNC Symbol;Acc:HGNC:14966]
ENST00000372443	ENSG00000156113	6,311117	5,336589	0,016044	potassium calcium-activated channel subfamily M alpha 1 [Source:HGNC Symbol;A
ENST00000382713	ENSG00000206052	2,970611	5,526113	0,016469	docking protein 6 [Source:HGNC Symbol;Acc:HGNC:28301]
ENST00000457543	ENSG00000236609	2,75534	6,785326	0,016771	zinc finger protein 853 [Source:HGNC Symbol;Acc:HGNC:21767]
ENST00000593685	ENSG00000105204	5,727923	6,008332	0,016992	dual specificity tyrosine phosphorylation regulated kinase 1B [Source:HGNC Symb
ENST00000455228	ENSG00000227744	5,815324	5,138385	0,017419	long intergenic non-protein coding RNA 1940 [Source:HGNC Symbol;Acc:HGNC:527
ENST00000277541	ENSG00000148400	2,806286	6,736627	0,017426	notch 1 [Source:HGNC Symbol;Acc:HGNC:7881]
ENST00000219837	ENSG00000103550	-4,536695	4,665165	0,017542	lysine rich nucleolar protein 1 [Source:HGNC Symbol;Acc:HGNC:34404]
ENST00000255416	ENSG00000133055	3,319923	4,617549	0,017611	myosin binding protein H [Source:HGNC Symbol;Acc:HGNC:7552]
ENST00000583743	ENSG00000264397	3,488967	6,263864	0,017706	microRNA 3180-5 [Source:HGNC Symbol;Acc:HGNC:38969]
ENST00000407803	ENSG00000219074	4,738882	4,533545	0,018085	superoxide dismutase 1 pseudogene 1 [Source:HGNC Symbol;Acc:HGNC:45134]
ENST00000296839	ENSG00000164379	4,772085	5,996936	0,018094	forkhead box Q1 [Source:HGNC Symbol;Acc:HGNC:20951]
ENST00000424737	ENSG00000225920	-2,564755	4,87823	0,018115	ribosomal modification protein rimK like family member B pseudogene 2 [Source:
ENST00000371741	ENSG00000158445	3,930356	5,078499	0,018307	potassium voltage-gated channel subfamily B member 1 [Source:HGNC Symbol;Ac
ENST00000602865	ENSG00000269896	5,14046	4,565177	0,018561	
ENST00000246841	ENSG00000126500	3,016711	5,152674	0,018819	fibronectin leucine rich transmembrane protein 1 [Source:HGNC Symbol;Acc:HGN
ENST00000283426	ENSG00000153404	4,473049	4,791921	0,019331	pleckstrin homology and RhoGEF domain containing G4B [Source:HGNC Symbol;A
ENST00000321895	ENSG00000177352	-4,584851	4,865201	0,019533	coiled-coil domain containing 71 [Source:HGNC Symbol;Acc:HGNC:25760]
ENST00000237841	ENSG00000118976	3,613515	4,719677	0,020345	OTUD4 pseudogene 1 [Source:HGNC Symbol;Acc:HGNC:33912]
ENST00000514701	ENSG00000171444	2,298427	5,138058	0,020916	MCC, WNT signaling pathway regulator [Source:HGNC Symbol;Acc:HGNC:6935]
ENST00000428285	ENSG00000233993	5,816288	5,240377	0,020943	
ENST00000295727	ENSG00000163497	4,886759	5,430413	0,021127	FEV, ETS transcription factor [Source:HGNC Symbol;Acc:HGNC:18562]
ENST00000257359	ENSG00000134917	4,973548	10,67439	0,021235	ADAM metallopeptidase with thrombospondin type 1 motif 8 [Source:HGNC Symb
ENST00000312655	ENSG00000175155	4,223449	4,605934	0,021469	yippee like 2 [Source:HGNC Symbol;Acc:HGNC:18326]
ENST00000585470	ENSG00000267675	4,515442	4,529208	0,021846	novel transcript
ENST00000563701	ENSG00000261079	5,314151	4,856972	0,022837	novel transcript
ENST00000263238	ENSG00000115091	5,049958	5,042466	0,02378	ARP3 actin related protein 3 homolog [Source:HGNC Symbol;Acc:HGNC:170]
ENST00000298310	ENSG00000165525	4,256849	4,556908	0,024094	nuclear export mediator factor [Source:HGNC Symbol;Acc:HGNC:10663]
ENST00000296847		5,188806	4,82398	0,024264	
ENST00000377698	ENSG00000137124	-5,288311	5,136814	0,02439	aldehyde dehydrogenase 1 family member B1 [Source:HGNC Symbol;Acc:HGNC:40
ENST00000443490	ENSG00000197182	-3,611743	4,667013	0,024686	MIRLET7B host gene [Source:HGNC Symbol;Acc:HGNC:37189]
ENST00000584923	ENSG00000263934	4,447797	5,469303	0,024972	small nucleolar RNA, C/D box 3A [Source:HGNC Symbol;Acc:HGNC:33189]
ENST00000397752	ENSG00000105976	5,305723	4,83745	0,025311	MET proto-oncogene, receptor tyrosine kinase [Source:HGNC Symbol;Acc:HGNC:7
ENST00000222374	ENSG00000105767	4,875105	4,973325	0,02563	cell adhesion molecule 4 [Source:HGNC Symbol;Acc:HGNC:30825]
ENST00000517562	ENSG00000253250	3,164889	5,820477	0,02596	chromosome 8 open reading frame 88 [Source:HGNC Symbol;Acc:HGNC:44672]
ENST00000586394	ENSG00000267274	6,05086	4,964816	0,026438	novel transcript, sense overlapping with ZNF700
ENST00000585593	ENSG00000267122	5,349084	5,413176	0,026752	novel transcript, antisense to DOT1L
ENST00000428234	ENSG00000233007	5,190364	5,036725	0,027515	UBTF like 11 (pseudogene) [Source:HGNC Symbol;Acc:HGNC:50288]
ENST00000551654	ENSG00000197376	5,075684	4,527351	0,027781	biorientation of chromosomes in cell division 1 like 2 (BOD1L2) pseudogene
ENST00000581760		5,538301	6,137854	0,028001	
ENST00000418112	ENSG00000233951	4,869748	5,009144	0,028097	regulator of chromosome condensation 2 pseudogene 3 [Source:HGNC Symbol;Ac
ENST00000465915	ENSG00000163870	-4,475296	4,593273	0,028142	transmembrane protein adipocyte associated 1 [Source:HGNC Symbol;Acc:HGNC:3
ENST00000509211	ENSG00000254186	-2,09057	4,674802	0,028327	novel transcript
ENST00000481577	ENSG00000239344	-3,379981	5,109559	0,028351	ribosomal protein S6 (RPS6) pseudogene

ENST00000569046	ENSG00000259781	4,343739	4,665772	0,028375	high mobility group box 1 pseudogene 6 [Source:HGNC Symbol;Acc:HGNC:4998]
ENST00000182096		-2,175404	5,410245	0,028824	
ENST00000421770	ENSG00000226411	-4,449592	4,508662	0,029324	phosphorylase kinase, gamma 1 (muscle) (PHKG1) pseudogene
ENST00000229812	ENSG00000112079	4,347777	5,481337	0,02942	serine/threonine kinase 38 [Source:HGNC Symbol;Acc:HGNC:17847]
ENST00000265271	ENSG00000091009	4,536252	4,935879	0,0295	RNA binding motif protein 27 [Source:HGNC Symbol;Acc:HGNC:29243]
ENST00000577570		4,548174	9,333089	0,030098	
ENST00000234198	ENSG00000115844	4,376848	6,086856	0,030202	distal-less homeobox 2 [Source:HGNC Symbol;Acc:HGNC:2915]
ENST00000268489	ENSG00000140836	4,538935	5,466864	0,030809	zinc finger homeobox 3 [Source:HGNC Symbol;Acc:HGNC:777]
ENST00000268489	ENSG00000140836	4,538935	5,466864	0,030809	zinc finger homeobox 3 [Source:HGNC Symbol;Acc:HGNC:777]
ENST00000272286	ENSG00000143921	4,598307	4,70435	0,03094	ATP binding cassette subfamily G member 8 [Source:HGNC Symbol;Acc:HGNC:138
ENST00000587491	ENSG00000129657	-3,324201	5,001744	0,031664	SEC14 like lipid binding 1 [Source:HGNC Symbol;Acc:HGNC:10698]
ENST00000513405	ENSG00000251226	3,043659	4,739713	0,031676	novel transcript
ENST00000588238	ENSG00000167671	4,191676	4,48675	0,031843	UBX domain protein 6 [Source:HGNC Symbol;Acc:HGNC:14928]
ENST00000491712	ENSG00000197694	-3,991528	4,300334	0,031843	spectrin alpha, non-erythrocytic 1 [Source:HGNC Symbol;Acc:HGNC:11273]
ENST00000367996	ENSG00000158859	4,723771	6,438386	0,03386	ADAM metallopeptidase with thrombospondin type 1 motif 4 [Source:HGNC Symb
ENST00000377122	ENSG00000078114	3,075285	4,854571	0,034027	nebulette [Source:HGNC Symbol;Acc:HGNC:16932]
ENST00000602918	ENSG00000256092	4,566689	4,991172	0,034268	novel transcript
ENST00000304883	ENSG00000169836	4,464532	6,127499	0,034349	tachykinin receptor 3 [Source:HGNC Symbol;Acc:HGNC:11528]
ENST00000491240	ENSG00000102317	4,611978	6,929671	0,034702	RNA binding motif protein 3 [Source:HGNC Symbol;Acc:HGNC:9900]
ENST00000302787	ENSG00000168924	4,736965	5,0952	0,03493	leucine zipper and EF-hand containing transmembrane protein 1 [Source:HGNC Sy
ENST00000562782	ENSG00000261546	4,309398	4,35856	0,035629	novel transcript, antisense to ACSF3
ENST00000431382		3,97246	4,387931	0,035983	
ENST00000312233	ENSG00000174332	3,552361	4,8004	0,036299	GLIS family zinc finger 1 [Source:HGNC Symbol;Acc:HGNC:29525]
ENST00000377648	ENSG00000116273	4,951372	4,729863	0,036386	PHD finger protein 13 [Source:HGNC Symbol;Acc:HGNC:22983]
ENST00000607318	ENSG00000272435	4,548549	13,03113	0,036389	RNA, 5S ribosomal pseudogene 357 [Source:HGNC Symbol;Acc:HGNC:43257]
ENST00000487065	ENSG00000118007	4,56094	4,37028	0,036716	stromal antigen 1 [Source:HGNC Symbol;Acc:HGNC:11354]
ENST00000363865		5,166416	14,01759	0,037716	
ENST00000276571	ENSG00000147571	4,255187	4,907319	0,038174	corticotropin releasing hormone [Source:HGNC Symbol;Acc:HGNC:2355]
ENST00000268182	ENSG00000140575	-5,036292	4,948317	0,038702	IQ motif containing GTPase activating protein 1 [Source:HGNC Symbol;Acc:HGNC:6
ENST00000376495	ENSG00000165312	4,317891	5,163365	0,038735	OTU deubiquitinase 1 [Source:HGNC Symbol;Acc:HGNC:27346]
ENST00000419932		2,458114	13,14453	0,039736	
ENST00000278947	ENSG00000149575	4,553259	4,396266	0,039758	sodium voltage-gated channel beta subunit 2 [Source:HGNC Symbol;Acc:HGNC:105
ENST00000314134	ENSG00000181830	4,447545	4,651022	0,040528	solute carrier family 35 member C1 [Source:HGNC Symbol;Acc:HGNC:20197]
ENST00000516507	ENSG00000252316	3,921265	17,58386	0,040687	RNA, Ro-associated Y4 [Source:HGNC Symbol;Acc:HGNC:10244]
ENST00000535362	ENSG00000259009	4,680954	4,463367	0,041103	tetrapeptide repeat homeobox 2, pseudogene [Source:HGNC Symbol;Acc:HGNC:32
ENST00000362645	ENSG00000199515	4,555166	9,141192	0,041269	
ENST00000578683	ENSG00000264803	4,303346	7,562282	0,041682	microRNA 378c [Source:HGNC Symbol;Acc:HGNC:38374]
ENST00000498027	ENSG00000162909	4,005195	4,4274	0,042174	calpain 2 [Source:HGNC Symbol;Acc:HGNC:1479]
ENST00000412427	ENSG00000204362	2,037267	5,172129	0,042307	novel transcript
ENST00000364294	ENSG00000201164	4,709175	12,88239	0,042425	RNA, U4 small nuclear 36, pseudogene [Source:HGNC Symbol;Acc:HGNC:46972]
ENST00000516594		5,331163	14,31278	0,042511	
ENST00000579913	ENSG00000214425	4,129832	4,454994	0,043069	leucine rich repeat containing 37 member A4, pseudogene [Source:HGNC Symbol;/
ENST00000328914	ENSG00000164916	3,007122	7,273575	0,043129	forkhead box K1 [Source:HGNC Symbol;Acc:HGNC:23480]
ENST00000562061	ENSG00000261081	4,63508	4,508939	0,043146	amyloid beta (A4) precursor protein-binding, family A, member 2 (APBA2) pseudo
ENST00000411317		4,544928	6,807402	0,043479	
ENST00000360184	ENSG00000197102	3,287178	7,200479	0,043926	dynein cytoplasmic 1 heavy chain 1 [Source:HGNC Symbol;Acc:HGNC:2961]
ENST00000263620	ENSG00000116017	4,313512	5,442201	0,04454	AT-rich interaction domain 3A [Source:HGNC Symbol;Acc:HGNC:3031]
ENST00000467614	ENSG00000230626	2,254969	5,003327	0,044556	novel protein similar to mitogen-activated protein kinase kinase 2 MAP2K2
ENST00000549319	ENSG00000136630	-4,280392	4,51127	0,044573	H2.0 like homeobox [Source:HGNC Symbol;Acc:HGNC:4978]
ENST00000570843	ENSG00000261889	4,697183	9,522371	0,044775	novel transcript
ENST00000328504	ENSG00000185594	4,903764	5,11035	0,044782	spermatogenesis associated 8 [Source:HGNC Symbol;Acc:HGNC:28676]
ENST00000439075	ENSG00000236548	4,176867	6,710525	0,045204	RNF217 antisense RNA 1 (head to head) [Source:HGNC Symbol;Acc:HGNC:50866]
ENST00000397098	ENSG00000146540	4,239526	5,102923	0,045238	chromosome 7 open reading frame 50 [Source:HGNC Symbol;Acc:HGNC:22421]
ENST00000504490	ENSG00000251441	4,117005	4,640153	0,046708	regulator of telomere elongation helicase 1 pseudogene 1 [Source:HGNC Symbol;A
ENST00000362735	ENSG00000199605	4,92861	8,379832	0,046874	RNA, Ro-associated Y4 pseudogene 24 [Source:HGNC Symbol;Acc:HGNC:42474]
ENST00000366923	ENSG00000136628	-4,517309	5,22527	0,047024	glutamyl-prolyl-tRNA synthetase [Source:HGNC Symbol;Acc:HGNC:3418]
ENST00000471389	ENSG00000140718	4,42111	4,687417	0,048127	FTO, alpha-ketoglutarate dependent dioxygenase [Source:HGNC Symbol;Acc:HGNC
ENST00000257552	ENSG00000135097	1,574451	7,210172	0,048598	musashi RNA binding protein 1 [Source:HGNC Symbol;Acc:HGNC:7330]
ENST00000256509	ENSG00000134121	4,015018	4,588633	0,048712	cell adhesion molecule L1 like [Source:HGNC Symbol;Acc:HGNC:1939]
ENST00000269389	ENSG00000141574	4,553737	4,938336	0,048906	secreted and transmembrane 1 [Source:HGNC Symbol;Acc:HGNC:10707]
ENST00000559466	ENSG00000188681	3,637907	4,709792	0,048912	tektin 4 pseudogene 2 [Source:HGNC Symbol;Acc:HGNC:40046]
ENST00000559466	ENSG00000188681	3,637907	4,709792	0,048912	tektin 4 pseudogene 2 [Source:HGNC Symbol;Acc:HGNC:40046]
ENST00000602323	ENSG00000215386	3,989988	5,357761	0,049016	mir-99a-let-7c cluster host gene [Source:HGNC Symbol;Acc:HGNC:1274]
ENST00000577708	ENSG00000264063	4,30271	6,747323	0,049106	microRNA 3687-2 [Source:HGNC Symbol;Acc:HGNC:50835]
ENST00000591924	ENSG00000141429	4,536573	7,689395	0,049125	polypeptide N-acetylgalactosaminyltransferase 1 [Source:HGNC Symbol;Acc:HGNC
ENST00000264828	ENSG00000080573	3,62806	5,826723	0,04971	collagen type V alpha 3 chain [Source:HGNC Symbol;Acc:HGNC:14864]
ENST00000362002	ENSG00000198881	4,734088	5,011276	0,049746	ankyrin repeat and SOCS box containing 12 [Source:HGNC Symbol;Acc:HGNC:1976